The Nummulitique: carbonate deposition in a foreland basin setting; Eocene, French alps

Zoë Rebecca Sayer

The Nummulitique: Carbonate Deposition in a Foreland Basin Setting; Eocene, French Alps

Zoë Rebecca Sayer

A thesis submitted in partial fulfilment of the degree of Doctor of Philosophy at the Department of Geological Sciences, University of Durham. 1995.

Frontispiece

Entrevaux and the Nummulitique

No part of this thesis has been previously submitted for a degree in this or any other university. The work described in this thesis is entirely that of the author, except where reference is made to previous published or unpublished work.

Abstract

The Eocene Nummulitique (Lutetian to Priabonian) has been studied in the external chains of the French Alps in Haute Savoie and Haute Provence. The Nummulitique unconformably overlies the Mesozoic passive margin succession and represents the onset of sedimentation in the Alpine Foreland Basin which formed due to lithospheric flexure caused by the advance of the Alpine orogeny. The base of the formation is marked by a regional erosional unconformity that developed during subaerial exposure of the Alpine foreland. The Nummulitique may be divided into two informal members: the lower Infranummulitique, a succession of terrigenous carbonates, and the overlying Nummulitic Limestone, a shallow marine carbonate ramp succession.

The Infranummulitique is composed of terrigenous carbonates thought to have been derived from the uplifted and eroding foreland which were redeposited in local depocentres due to the topography on the erosion surface. The Infranummulitique can be divided into four facies associations: i) a lenticular conglomerate/nodular marl deposited from ephemeral streams, ii) a sheet conglomerate deposited in a marginal marine fan delta, iii) a *Cerithium* marl deposited in a brackish water coastal plain/lagoon and iv) a *Microcodium* wackestone deposited from coastal marine channels.

The Nummulitic Limestone is marked by the appearance of the first fully marine foraminifera and a change from terrigenous to autochthonous carbonate sedimentation on a low-energy ramp dominated by larger benthonic foraminifera. The inner-ramp is represented by the deposition of bioclast shoals (packstones and grainstones) dominated by either calcareous red algae, *Nummulites* or peloids. The middle-ramp is dominated by mud-rich wackestones with a fauna of flat foraminifera, with local winnowed accumulations attributable to storm reworking. The outer ramp and basin are represented by mudstones and marls with a sparse benthos.

The Nummulitique shows a marked cyclicity within an overall deepening upwards succession which is interpreted to be the combined effects of tectonic basin subsidence and high-frequency (4th order) eustatic sea-level variations. As the basin developed, the eustatic signature producing the small-scale cyclicity was successively overprinted by accelerating basin subsidence which controlled the stratigraphy of the underfilled foreland basin. Initially, the carbonate productivity is able to keep pace with the relative sea-level changes and the ramp prograded into the basin. The combination of accelerating subsidence rates and nutrient and detrital influx from the approaching orogenic wedge reduced the carbonate productivity and the ramp drowned, leading to pelagic marl deposition.

The drowning surface and small-scale cyclicity have been used to correlate between measured sections within each field area, but problems occur in correlating between areas due to the migration of the foreland basin producing a diachronous sedimentary succession, which shows a similar development around the Alps, regardless of the age of the sediments. This diachroneity is evident in the two study areas with similar sediments, cycles and key surfaces developed at different stages of the basin development. The similarity in the successions demonstrates that the early sedimentation in the French Alpine Foreland Basin was controlled primarily by flexural subsidence.

Acknowledgements

Firstly, thanks must go to Maurice Tucker for his supervision and signature (despite being the most difficult person in the department to find) and to Hugh Sinclair for all his Alpine input and for still providing invaluable supervision despite leaving Durham for the lures of Birmingham. Thanks also to Dick Swarbrick for reading the draft version of this thesis and helping me on the job front, and to NERC for providing me with the funds for the project.

Help was gratefully received from Dan Bosence, Pamela Hallock, Owen Green and Dick Moody on the identification and interpretation of my algae and forams. Big thanks to the other Alpine workers: Jo Lihou for useful discussions and reprints, Steve Moss for the loan of various theses, and especially Trey Meckel for his enthusiastic emails in what would otherwise have been a desert of discussion.

To the technical support in Durham: Karen's normatone and kroy, George and Julie's thin-section making expertise, Dave Asbery's petty cash box and car keys, Carol, Lynne and Claire for fending off phone calls and Dave Stevenson for putting up with my PC problems.

Big thanks to mum and dad, who had the foresight to move to the Alps in 1986 thereby providing me with an invaluable taxi service between field areas and a refuge during bouts of french food poisoning.

And to the Durham postgrads:

My various housemates over the years: Jane and Charlotte (of the ELC), Debbie, Simon, Jon, Michelle, Sarah, Kate and Si for putting up with me and the cat.

Thanks to Paul, Billy, Sue, Jane, Bole, Mikey and the rest of the "old crowd" for introducing me to the delights of Durham's social life and the gossip potential of the coffee room.

To the "new kids" and the rest: Wayn-ee, Pricer, Bouncy, Jo, Jimber, Molly, Ziad, Gayle, Alwyn, Si, Angus, Caroline, Matt and anyone else I may have inadvertantly forgotten for helping keep the traditions of beer o'clock and the spontaneous sesh alive.

Thanks also to Whisky for being cute and furry and making sure I got up early every morning by her incessant miaowing.

Finally, a huge thanks to Ed for saving me from an enforced midnight swim in Eriboll and for always being there despite the occasional bad mood while writing up.

Contents

Chapter 1

Introduction

1.1. Aims

The Nummulitique was deposited on the distal margin of the peripheral Alpine Foreland Basin in Switzerland and France. Due to the sensitivity of carbonates to small-scale fluctuations in relative sea-level, the Nummulitique provides a prime opportunity to document the changing carbonate system during the early subsidence of the foreland basin and to interpret the variations in relative sea-level.

Previous studies on the Nummulitique have been concentrated on mapping its distribution, palaeontology and biostratigraphy (Herb, 1988; Campredon, 1977; Pairis and Pairis, 1975; Pairis, 1988; Bodelle, 1971). Crampton (1992) carried out a study of the facies and foreland basin subsidence in eastern Switzerland and the Champsaur, but detailed sedimentological study of the French Nummulitique is so far lacking from the literature.

The aims of this study were:

i) to carry out a detailed sedimentological study of the Nummulitique in order to determine the constituent microfacies of the formation based on the exposure in two field areas; Haute Savoie and Haute Provence, and to produce a model of the depositional environments,

ii) to use the microfacies and cyclicity within the formation to determine the development of the carbonate succession, to interpret the relative sea-level variations with the aid of foraminiferal palaeoecology and to assign a sequence stratigraphic framework,

iii) to determine the controls on relative sea-level variations and carbonate deposition during early foreland basin subsidence.

The work was carried out in two field seasons using sedimentary section measurement (1:100 scale), documentation of field relationships and sample collection. The samples were studied in thin section and a microfacies analysis carried out for each field area based on the depositional texture and the bioclastic content. The microfacies and facies associations were assigned relative water depths based on the palaeoecology of large benthonic foraminifera.

The measured sections and the microfacies analysis are presented in the appendices.

1.2. Thesis Outline

Chapter 1: Introduction to the French Nummulitique and its constituent members, the Infranummulitique and the Nummulitic Limestone. The stratigraphic terminology used in the thesis is defined in order to be able to compare this work with previous studies in the literature. The regional geology of south-east France is discussed, with the location and geological setting of the two field areas. The remainder of the chapter deals with aspects of foreland basin development, introducing modelling carried out by previous workers, the development and stratigraphy of the Alpine Foreland Basin and the occurrence of carbonates in foreland basins.

Chapter 2: The dominant bioclasts used in the microfacies study are introduced and identified to genus level. The use of large benthonic foraminiferal palaeoecology in palaeoenvironmental interpretation is reviewed along with a summary on the controls on the growth and development of calcareous red algae. The age of the Nummulitique is discussed, based on previous biostratigraphical studies, and an east-west younging trend is seen in both field areas.

Chapter 3: Outline of the sedimentological study of the Infranummulitique, representing early terrigenous carbonate deposition in localised depocentres. The unit is divided into four facies associations which are described in detail and the probable depositional environments discussed.

Chapters 4 and 5: Results of the microfacies studies of the Nummulitic Limestone in Haute Savoie (Chapter 4) and Haute Provence (Chapter 5). The microfacies are described and interpreted, and the facies associations seen in the field are discussed in terms of a carbonate ramp depositional environment.

Chapter 6: The basal unconformity and its formation are discussed in terms of the features on the unconformity surface, the overlying sediments and the depth of erosion and stratigraphic gap in the two field areas. Possible mechanisms for producing the unconformity proposed.

Chapter 7: The chapter starts with a summary of the controls on carbonate deposition and carbonate sequence stratigraphy. The sequence stratigraphy of the Nummulitique is outlined, based on the studies in the previous chapters and the problems of the diachroneity of foreland basin stratigraphy is highlighted. The small-scale cyclicity of the formation is discussed for both field areas and is used to determine the magnitude,

time-scale and possible causes of relative sea-level variations during the Eocene in the French Alpine Foreland Basin. Possible factors contributing to the drowning of the carbonate ramp are suggested. The relative sea-level variations and subsequent cyclicity is used to correlate between the measured sections and to determine the development of the Nummulitique in each field area. Finally, the implications for the development of the French Alpine Foreland Basin are discussed.

Chapter 8: Outline of the spatial and temporal variations in the Tertiary sedimentation around the Alpine Arc, putting the two study areas in the context of the foreland basin as a whole. The diachroneity of the development and migration of the foreland basin are discussed, and the use of the Nummulitique as an indicator of marine transgression and relative sea-level variations is summarised. The end of the chapter lists the principle conclusions of the thesis.

1.3. Stratigraphic Terminology

As a result of extensive literature dealing with the Tertiary carbonate deposits in different areas in France, the nomenclature relating to these sediments is highly variable. In order to maintain consistency within this thesis and to be able to compare the different stratigraphic units encountered with those in the literature, I have defined a terminology (Table 1.1) relating to the various units, which is outlined below along with the equivalent names encountered in the literature.

1.3.1. The Nummulitique

The Nummulitique is the name given to the carbonate sediments directly overlying the unconformity at the top of the Mesozoic passive margin succession and which have been interpreted as recording the onset of foreland basin subsidence (Allen et al., 1991). The term Nummulitique was used to describe the Alpine nummulite-rich limestones and associated sediments by Boussac (1912), and the term has similarly been used by Fujiwara and Pairis (1969) in the St Auban area of Provence and by Crampton (1992) in the Champsaur. In this thesis, the Nummulitique has been divided into two informal members - the basal Infranummulitique and the overlying Nummulitic Limestone.

Thesis terminology	**Literature terminology**	**References**
Nummulitique		Boussac, 1912
Infranummulitique	Couches Infranummulitiques	Bodelle, 1971
	Conglomerats Infranummulitiques	Thome, 1987
	Formations à *Microcodium*	Bodelle and Campredon, 1968; Bodelle, 1971; Campredon, 1977
	Formation à *Microcodium*	Fujiwara and Pairis, 1969
Lenticular conglomerate, Sheet conglomerate	Poudingues d'Argens	Apps, 1987; Thome, 1987; Evans and Mange-Rajetsky, 1991
	Couches à *Microcodium*	Campredon, 1966, 1977
	Couches conglomeratiques	Bodelle and Campredon, 1968
	Conglomerat de base	Collet and Lillie, 1938
	Assises conglomeratiques	Pairis and Pairis, 1975; Pairis, 1988; Pairis et al., 1992
top sheet c/g	Morte de l'Homme member	Apps, 1987
***Cerithium* marl**	Morte de l'Homme member	Apps, 1987
	Couches à Cérithes	Collet and Lillie, 1938; Weidmann et al., 1991
	Couches à *Cerithium diaboli*	Campredon, 1966; Bodelle, 1971
	Couches à Cérithes et Pulmonés	Campredon, 1977
	Couches de Diablerets	Weidmann et al., 1991
	Diablerets layers	Gorin et al., 1989
***Cerithium* marl and *Microcodium* wackestone**	Formation Brune	Pairis and Pairis, 1975; Pairis, 1988; Pairis et al., 1992
Nummulitic Limestone	Calcaire Nummulitique	Bodelle, 1971
	Calcaires Nummulitiques	Thome, 1987; Pairis et al., 1992; Evans and Mange-Rajetsky, 1991
	Calcaires à petites nummulites	Charollais et al., 1977; Lateltin and Müller, 1987; Chaplet, 1989
	Calcaires et grès à Nummulites et Discocyclines	Collet and Lillie, 1938
	Scaffarels member	Apps, 1987
	Calcaires	Campredon, 1977
	Nummulitique marin basal	Fujiwara and Pairis, 1969
Basal clastics	Formation Grise	Pairis and Pairis, 1975; Pairis et al., 1992
	Faciès gréso-conglomeratiques	Lateltin and Müller, 1987
Ramp carbonates	Calcaires Blancs	Pairis and Pairis, 1975; Pairis et al., 1992
	Faciès calcaire récifale à algues	Lateltin and Müller, 1987

Table 1.1: Summary of the stratigraphic terminology used in this thesis and the corresponding terms in the literature.

1.3.2. The Infranummulitique

The term Infranummulitique is used to describe the terrigenous carbonate sediments occurring directly above the Mesozoic substratum, which were deposited prior to the marine transgression in the basin. They are sporadically distributed, occurring in morphological lows on the unconformity, and represent alluvial and marginal marine sedimentation (Chapter 3). The sediments have been variously referred to in the literature as the "Couches Infranummulitiques" (Bodelle, 1971), or the "Conglomerats Infranummulitiques" (Thome, 1987), indicating their position below the nummulitic limestones, and the "Formations à *Microcodium*" (Bodelle and Campredon, 1968; Bodelle, 1971; Campredon, 1977) or "Formation à *Microcodium*" (Fujiwara and Pairis, 1969) after the common occurrence of *Microcodium* within these sediments. The Infranummulitique can be divided into a number of constituent facies dominated either by conglomerate or marl.

1.3.2.1. The conglomerates

In this thesis, the conglomeratic facies have been named according to the geometries observed in the field, either lenticular or massive, sheet-like conglomerates. These distinctions are rarely made in the literature and the conglomeratic beds and associated fine-grained sediment are generally grouped together under a collective name. In Haute Provence, the conglomerates are variously termed "Couches à *Microcodium*" (Campredon, 1966, 1977), "Couches Conglomeratiques" (Bodelle and Campredon, 1968), or the "Poudingues d'Argens" (Apps, 1987; Thome, 1987; Evans and Mange-Rajetsky, 1991), named after the lenticular conglomerate / nodular marl succession encountered at Argens. The term "Poudingues d'Argens" usually encompasses all conglomeratic facies found in the area, but Apps (1987) only uses it for what she describes as alluvial sediments, with the "Morte de l'Homme Member" of the "Calcaires Nummulitiques Formation" describing the overlying "marine" sediments of bored conglomerate and the Cerithium Marl (see below). This is somewhat confusing, as some of the sediments she has called "Poudingues d'Argens", such as those found at Peyresq, also contain evidence of marine influences such as rare foraminifera and extensively bored Cretaceous clasts (Section 4.4) and therefore the boundary between the "Poudingues d'Argens" and the "Morte de l'Homme Member" at Peyresq is difficult to determine.

In Haute Savoie, the conglomerates are less widespread and are known as the "Conglomerat de base" (Collet and Lillie, 1938) and the "Assises Conglomeratiques" (Pairis and Pairis, 1975; Pairis, 1988; Pairis et al., 1992).

1.3.2.2. Cerithium *marl*

The *Cerithium* marl overlies either the conglomeratic facies of the Infranummulitique or the Mesozoic substratum and is dominated by gastropods of the genus *Cerithium* from which its name is derived. It corresponds to the upper, fine-grained part of the "Morte de l'Homme Member" (Apps, 1987) and is described in the literature as the "Couches à Cérithes" (Collet and Lillie, 1938; Weidmann et al., 1991), "Couches à *Cerithium diaboli*" (Campredon, 1966; Bodelle, 1971), "Couches à Cérithes et Pulmonés" (Campredon, 1977), "Formation Brune" (Pairis and Pairis, 1975; Pairis, 1988; Pairis et al., 1992), "Couches de Diablerets" (Weidmann et al., 1991) and "Diablerets Layers" (Gorin et al., 1989). The term "Formation Brune" also encompasses the *Microcodium* wackestone described in this thesis.

1.3.3. The Nummulitic Limestone

The Nummulitic Limestone is the term used to describe the marine sediments characterised by abundant larger benthonic foraminifera (*Nummulites, Amphistegina, Operculina, Discocyclina*) and coralline red algae that overlie the Infranummulitique or the Mesozoic substratum where the Infranummulitique is absent (Chapters 4 and 5). Its base is defined as the first appearance of large foraminifera visible in the field and the top as the last occurrence of foraminifera seen in the field, which commonly coincides with the present erosion surface. The Nummulitic Limestone corresponds to the "Calcaire Nummulitique" (Bodelle, 1971), "Calcaires Nummulitiques" (Thome, 1987; Evans and Mange-Rajetsky, 1991; Pairis et al., 1992), "Calcaires à petites nummulites" (Charollais et al., 1977; Lateltin and Müller, 1987; Chaplet, 1989), "Calcaires et Grès à Nummulites et Discocyclines" (Collet and Lillie, 1938), the "Scaffarels Member" of the "Calcaires Nummulitiques Formation" (Apps, 1987), the "Calcaires" (Campredon, 1977) and the "Nummulitique marin basal" (Fujiwara and Pairis, 1969). It has been subdivided to a certain extent into the "Formation Grise" (Pairis and Pairis, 1975; Pairis et al., 1988) or "Faciès gréso-conglomeratiques" (Lateltin and Müller, 1987), which correspond to the basal clastic facies association in this thesis, and the "Calcaires Blancs" (Pairis and Pairis, 1975; Pairis et al., 1992) or "Faciès calcaire récifale à algues" (Lateltin and Müller, 1987), corresponding to the overlying pure carbonates.

The older "Calcaires à grandes nummulites" (Pairis and Pairis, 1975; Lateltin and Müller, 1987; Chaplet, 1989; Pairis et al., 1992) are not included in the term Nummulitic Limestone as they were deposited prior to the deposition of the Infranummulitique. They are only dealt with briefly in this thesis and are simply referred to as limestone containing large *Nummulites*.

1.3.4. The Globigerina Marl

The Globigerina marl occurs above the Nummulitic Limestone and is not dealt with in this study. The term has been used to encompass all the relatively deep water formations that were deposited during the starved basin phase of sedimentation. In Haute Savoie, this includes the "Marnes à Foraminifères" (Charollais et al., 1977, 1980; Chaplet, 1989; Pairis, 1988; Pairis et al., 1992) or "Schistes à Globigerines" (Collet and Lillie, 1938; Pairis and Pairis, 1975) characterised by a planktonic foraminiferal assemblage and which pass into the overlying "Schistes à Meletta" (Charollais et al., 1980) or " Marnes à Meletta" (Pairis et al., 1992), containing fish scales, and eventually into the turbiditic flysch of the Taveyannaz and Val d'Illiez Sandstones. In Haute Provence, Bodelle (1971) described the basal beds of the Marls as the "Calcaires argilo-sableux" which pass up into the "Marnes nummulitiques". Other workers have described the Globigerina marl as the "Marnes bleues" (Apps, 1987; Evans and Mange-Rajetsky, 1991) or simply as "Marnes" (Fujiwara and Pairis, 1969; Campredon, 1977). The Globigerina marl passes up into the turbiditic flysch of the Annot Sandstone.

1.4. Field Areas and Regional Geology

1.4.1. Regional Geology

The geology of south-east France is governed by a series of major structural events, including the Hercynian orogeny, which produced major NE-SW (and minor SE-NW) structural lineaments reactivated during later deformations (Apps, 1987), the breakup of Pangea and the collision of the African and European plates (Debrand-Passard, 1984). Fig. 1.1 shows a summary of the main events and the resultant sedimentary succession.

Western Europe became emergent during the Upper Carboniferous and was probably mountainous at the end of the Westphalian, subsequent erosion causing a peneplaining of this topography (Debrand-Passard, 1984).

The Permian saw the onset of a major extensional phase of tectonism, lasting until the Cretaceous which led to the break-up of Pangea and the establishment of the Tethyan Ocean. The Permian is represented by continental sedimentation of red beds with associated rhyolitic volcanism (Kerkhove, 1979) outcropping in the Barrot Dome and Argentera Massif in Haute Provence. It does not outcrop in Haute Savoie.

Extension continued during the Triassic with diachronous sedimentation representing the advance of the marine transgression from the NE (Debrand-Passard,

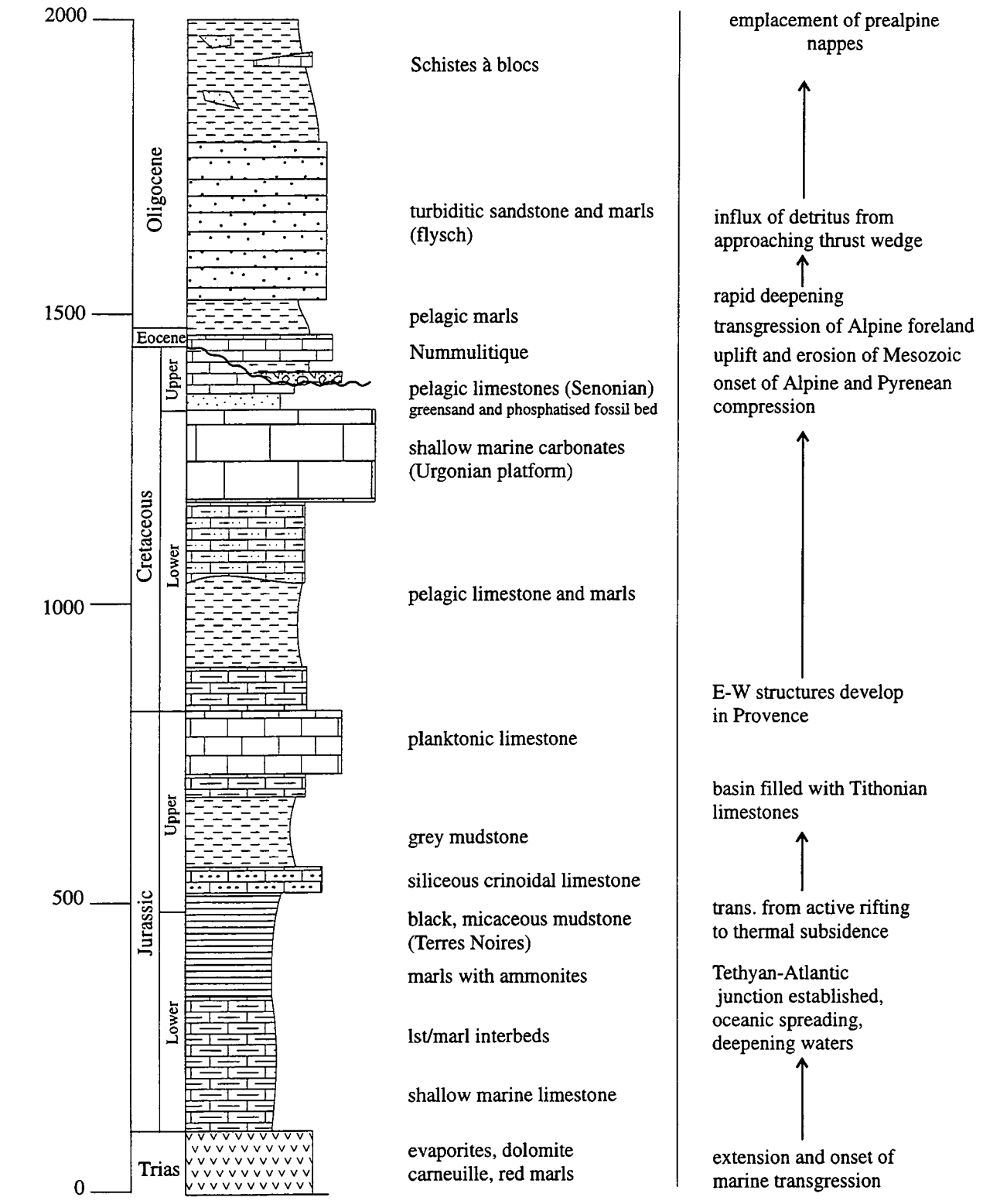

Fig. 1.1: Sedimentary succession of the Mesozoic and Tertiary formations encountered in the French Alps with the major events affecting sedimentation. Thicknesses are approximate. Based on Delamette (1993, fig. 46) with additional data from Debrand Passard (1984), Detraz et al. (1986) and Kerkhove (1979).

1984; Trümpy, 1980). This transgression led to the deposition of thick, shallow marine carbonates (Muschelkalk) in the Helvetic Realm (Trümpy, 1980), which pass into lagoonal and continental facies (dolomites, red marls, carneuille). During the Carnian, evaporite deposition occurred all around the subalpine chains (Debrand-Passard, 1984), dominated by anhydrite, but with halite deposition in the Jura and Rhône Valley (Trümpy, 1980) which later acted as an important décollement horizon during Alpine deformation (Guellec et al., 1990). The Triassic outcrops locally in the Annes and Sulens klippen in Haute Savoie and the Barrot Dome in Haute Provence.

The Jurassic saw the establishment of the Tethyan-Atlantic junction, the break-up of the carbonate platform and the onset of oceanic spreading (Trümpy, 1980; Tricart, 1984) with associated passive margins around Tethys (Wooler et al., 1992). This led to a deepening of the area with a transition from shallow marine carbonates to shales and limestone/marl interbeds (Debrand-Passard, 1984) with olistostromes containing mafic and ultramafic material indicating active faulting (Tricart, 1984). The transition from active rifting to thermal subsidence occurred in the Middle Jurassic and large carbonate platforms were established in Haute Provence, with dolomitisation occurring in the SE of the basin around Nice (Debrand-Passard, 1984). Strong subsidence led to the deposition of black, deep water marls (Terres noires) over much of the basin (Kerkhove, 1979; Detraz et al., 1986) after which the basin filled with the deposition of thick bedded Tithonian limestones in Haute Savoie and Haute Provence (Kerkhove, 1979).

During the Lower Cretaceous east-west structures developed in Provence due to the rotation of the Iberian peninsula (Debrand-Passard, 1984; Apps, 1987), reactivating Hercynian faults and leading to the deposition of pelagic sediments. In Haute Savoie, the Lower Cretaceous is represented by pelagic limestones and marls persisting through the Hauterivian (Huggenberger and Wildi, 1991; Detraz et al., 1986) until the establishment of the Urgonian limestone platform which prograded from NW to SE during the Lower Barremian to Lower Aptian (Chaplet, 1992). The Urgonian platform is overlain by greensands and a condensed section represented by a phosphatised fossil bed indicating deep waters with corresponding low sedimentation rates.

The Upper Cretaceous is marked by the onset of Alpine compression due to the collision of the African and European plates (Dewey et al., 1989). In Haute Savoie a slight shallowing is marked by the deposition of the pelagic, thin-bedded limestones of the Senonian (Detraz et al., 1986), equivalent to the Swiss Seewen and Wang Formations (Turonian to Maastrichtian). Southern France saw the development of Pyrenean compression and associated structures (Lemoine and Graciansky, 1988; Apps, 1987) with marly flysch deposited in the North Pyrenean Basin (Debrand-

Passard, 1984). In the subalpine chains of Haute Provence and the Alpes Maritimes, monotonous bedded pelagic limestones were deposited in the north passing into neritic platform carbonates in the south around Nice (Roure, 1980). In the Penninic and Austro-alpine realms in Switzerland, southerly derived flysch sedimentation had commenced (Schlieren, Sardona and Helminthoid Flysch; Trümpy, 1980).

Compression continued during the Palaeocene and Early Eocene, with much of SE France being emergent. Compression-related lateral extensional structures in the foreland of the developing mountain belt (Hancock and Bevan, 1987) initiated a series of grabens in the European Plate (Rhine, Rhône and Bresse Grabens) and extension reached a maximum during the Eocene, with volcanism occurring in the Rhine Graben (Illies, 1977; Ziegler, 1988). Transgression began in eastern Switzerland with the initiation of the Alpine Foreland Basin during the Thanetian (Lihou, 1995) and an early phase of marine transgression occurred during the Ypresian in France and Western Switzerland (Debrand-Passard, 1984; Herb, 1988), with the main marine incursion and development of the foreland basin in France starting in the Lutetian and progressing westward during the Bartonian and Priabonian (Bodelle, 1971; Campredon, 1977; Apps, 1987; Pairis, 1988).

A phase of E-W extension initiated during the Bartonian (Debrand-Passard, 1984) which reached a maximum during the Oligocene, reactivating older faults and affecting the Alpine foreland as well as the European graben systems. A phase of volcanism occurred in the Alps producing andesitic material in the foreland flysch (Trümpy, 1980).

The end of the main Alpine compression occurred during late Miocene times, with the infilling of the foreland basin and the deposition of the Molasse eroded from the uplifting mountain belt (Pfiffner, 1986), which ceased during the Mid-Late Miocene. since when the area has been emergent and erosional.

1.4.1. Haute Savoie

The Haute Savoie field area is located in the subalpine chains NW of Chamonix (Fig. 1.2) and includes the NE end of the Thônes Syncline (Bornes and Aravis Massifs) and the Massif de Platé (Fig. 1.3). The foreland basin sediments studied lie unconformably above the Mesozoic passive margin succession which consists of Valanginian to Senonian sediments. The Jurassic outcrops locally in the southern end of the Arve valley, but is never overlain directly by the Tertiary succession. The Triassic and Jurassic are present in the Annes and Sulens klippen, which are the erosional remnants

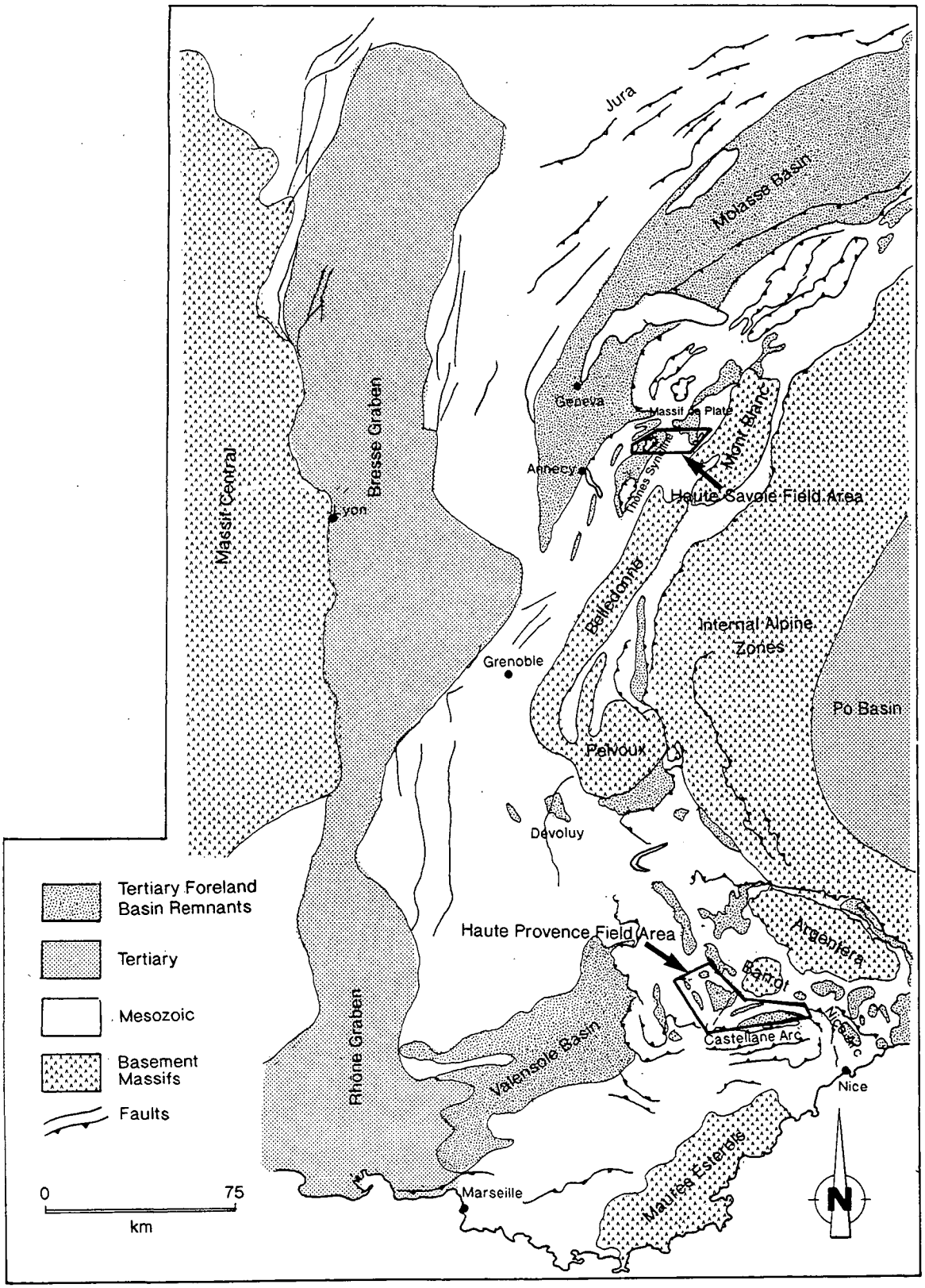

Fig. 1.2: Simplified map of the Alps of SE France, showing the location of the two study areas, the Tertiary foreland basin sediments and the crystalline massifs. After Debrand Passard (1984, map G1).

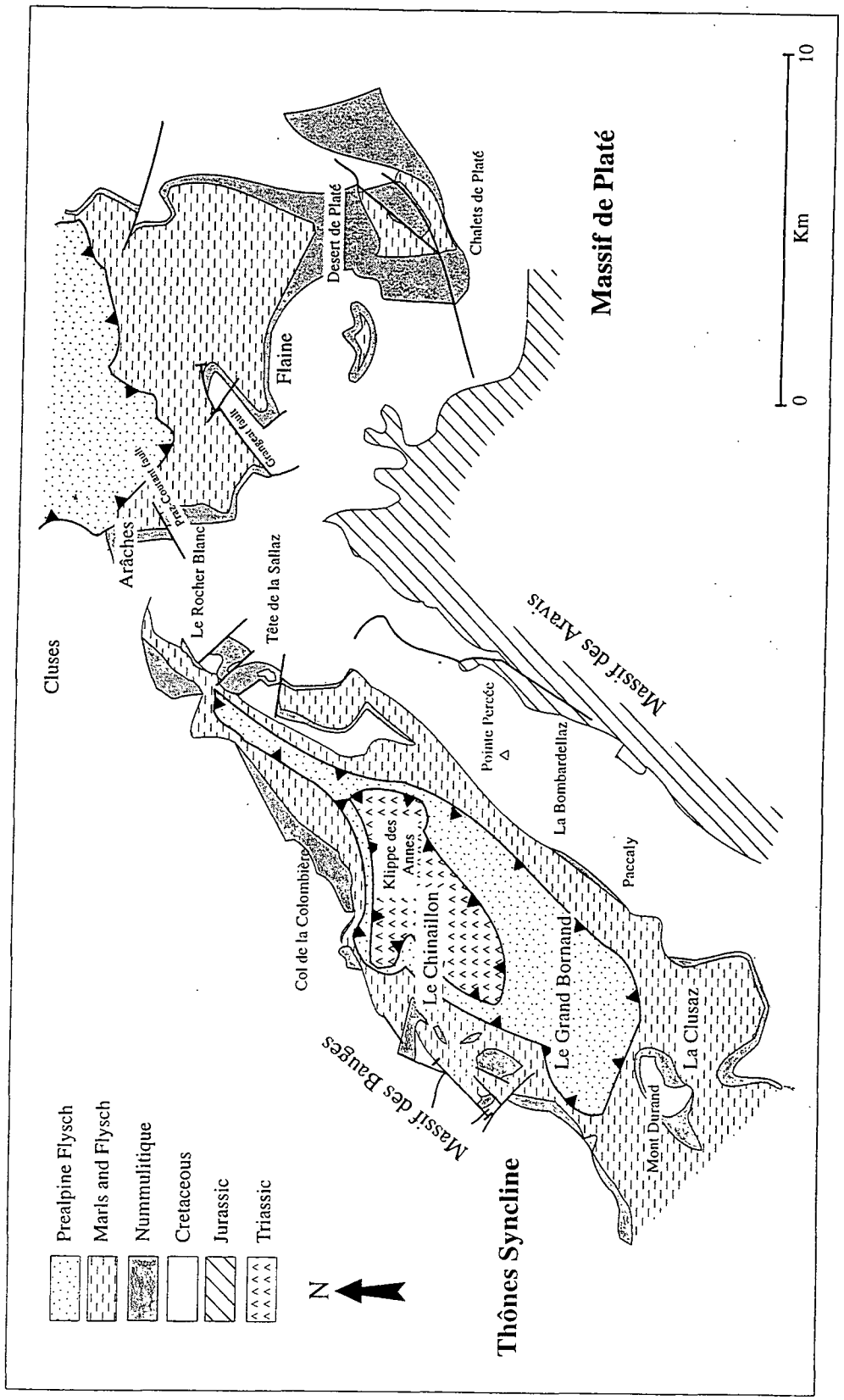

Fig. 1.3: Geological map of the Haute Savoie study area showing the outcrop of the Nummulitique in the Thônes Syncline and the Desert de Platé.

of a prealpine thrust nappe which overrode the Bornes and Aravis Massifs.

The Mesozoic substratum and its Tertiary cover have been caught up in the later stages of Alpine deformation, and a brief structural history of the area is given below.

The structure of the area has been governed by four major events (Chaplet, 1989): i) post-Upper Cretaceous emergence and faulting; ii) Eocene/Oligocene extension; iii) Lower Oligocene to Middle to Upper Miocene S-N compression and iv) a late SE-NW compression from the Upper Miocene to the Quaternary. Each of these stages reactivates earlier structures (Pairis and Pairis, 1978).

The early post-Upper Cretaceous emergence and faulting marks the onset of Alpine compression (Debrand-Passard, 1984) with associated faulting producing a conjugate strike-slip system (pre-Lutetian), with dextral faults striking 170° and sinistral faults striking 050° (Chaplet, 1989). These produced a series of palaeovalleys on the Mesozoic erosion surface (Pairis and Pairis, 1978) which affected the facies distribution during the early stages of marine transgression in the Eocene (Chapter 3).

Extension, synchronous with foreland basin sedimentation, occurred at the Eocene/Oligocene boundary, enhancing the subsidence of the nummulitic basin and reactivating the pre-Lutetian faults (Chaplet, 1989), producing slumps and deformation structures in the marls and sandstones (La Balacha, Massif de Platé).

After the basin filled with the detrital sediments of the marls and Taveyannaz Sandstone a major phase of S-N compression occurred during the Oligocene to Middle to Upper Miocene, produced by a southerly compression, carrying the cover to the NW (Pairis and Pairis, 1978; Chaplet, 1989). This produced most of the structural configuration seen in the area today, and was associated with basement shortening in the Belledonne Massif (Chaplet, 1989). This deformation led to the thrusting of prealpine nappes over the Tertiary foreland basin fill (Annes and Sulens klippen) and the emplacement of the Aravis and Bornes nappes (Chaplet, 1992). This phase also produced the folding and faulting of the Mesozoic and Tertiary seen in the eastern cliffs of the Arve valley, producing the Cluses anticline and reactivating the pre-Lutetian faults (Grangeat and Praz-Coutant Faults; Pairis and Pairis, 1978). The end of the tangential deformation saw the emplacement of the Bornes Massif over the Jura domain (Chaplet, 1989).

The final SE-NW compression occurred from the Upper Miocene to the Quaternary (Chaplet, 1989) producing folds oriented NE-SW (axes striking 20-30°), including the Thônes Syncline. Older faults were again reactivated.

This series of tectonic events produced the present structures seen in Haute Savoie and led to the cannibalisation of the foreland basin fill by the developing Alpine orogeny.

1.4.2. Haute Provence

The field area is centred on the village of Annot in the Var valley of Haute Provence (Fig. 1.2) and includes several of the synclines comprising the Castellane Arc in the southern subalpine chains (Fig. 1.4). The Tertiary sediments unconformably overlie the Mesozoic substratum which consists of sediments of Jurassic (Bathonian) to Upper Cretaceous (Senonian) age. As a result of its position in SE France, the area has been affected by both Alpine and Pyrenean tectonism since the Upper Cretaceous, producing a relatively complicated interaction of structures, the origin of which is often difficult to determine (Apps, 1987). The main tectonic events are: i) Late Cretaceous to Early Eocene Pyrenean compression; ii) Alpine compression dominant during the Eocene; iii) Oligocene extension and iv) Miocene compression (Roure et al., 1992; Apps 1987; Tempier, 1987).

The N-S Pyrenean compression occurred during the Late Cretaceous and Early Eocene due to the collision of Europe and Iberia. This compression produced a series of E-W trending folds in Provence and Languedoc (Roure et al., 1992), reworking Hercynian structures in a strike-slip motion and causing the initial uplift of the Barrot Dome (Apps, 1987).

The Alpine compression started to affect Haute Provence during the Eocene and was the dominant control on the geometry and subsidence of the nummulitic basin (Apps, 1987) that developed after a period of Late Cretaceous to Early Eocene emergence and deformation. This produced kinking and disharmonic folding of the Cretaceous sediments (Hamiti, 1994) prior to a peneplaining of the area through Early Eocene erosion (Apps, 1987).

The combined effects of the two orogenies produced the configuration of the Castellane Arc (Apps, 1987), which has both E-W and NW-SE trending synclines, the exact age of which is difficult to determine (Siddans, 1979). The advance of the Alpine orogeny from the east caused the onset of subsidence of the nummulitic basin which is attributed to lithospheric flexure (Hamiti, 1994).

An extensional phase occurred at the Eocene/Oligocene boundary, thought to be due to the stress field affecting Haute Savoie and much of the European foreland at that time (Tempier, 1987) with a principal stretching direction of 110° associated with the developing rift systems of the Rhine and Bresse grabens. This produced extensional faulting synchronous with the deposition of the marls which resulted in dramatic thickness variations across the faults as seen at St Benoit, East of Annot (Fig. 1.5).

After the shallow marine deposition of the Nummulitique, the basin subsequently filled with pelagic marls and the turbiditic Annot Sandstone during the Oligocene, and the emplacement of the Alpine nappes occurred shortly after the

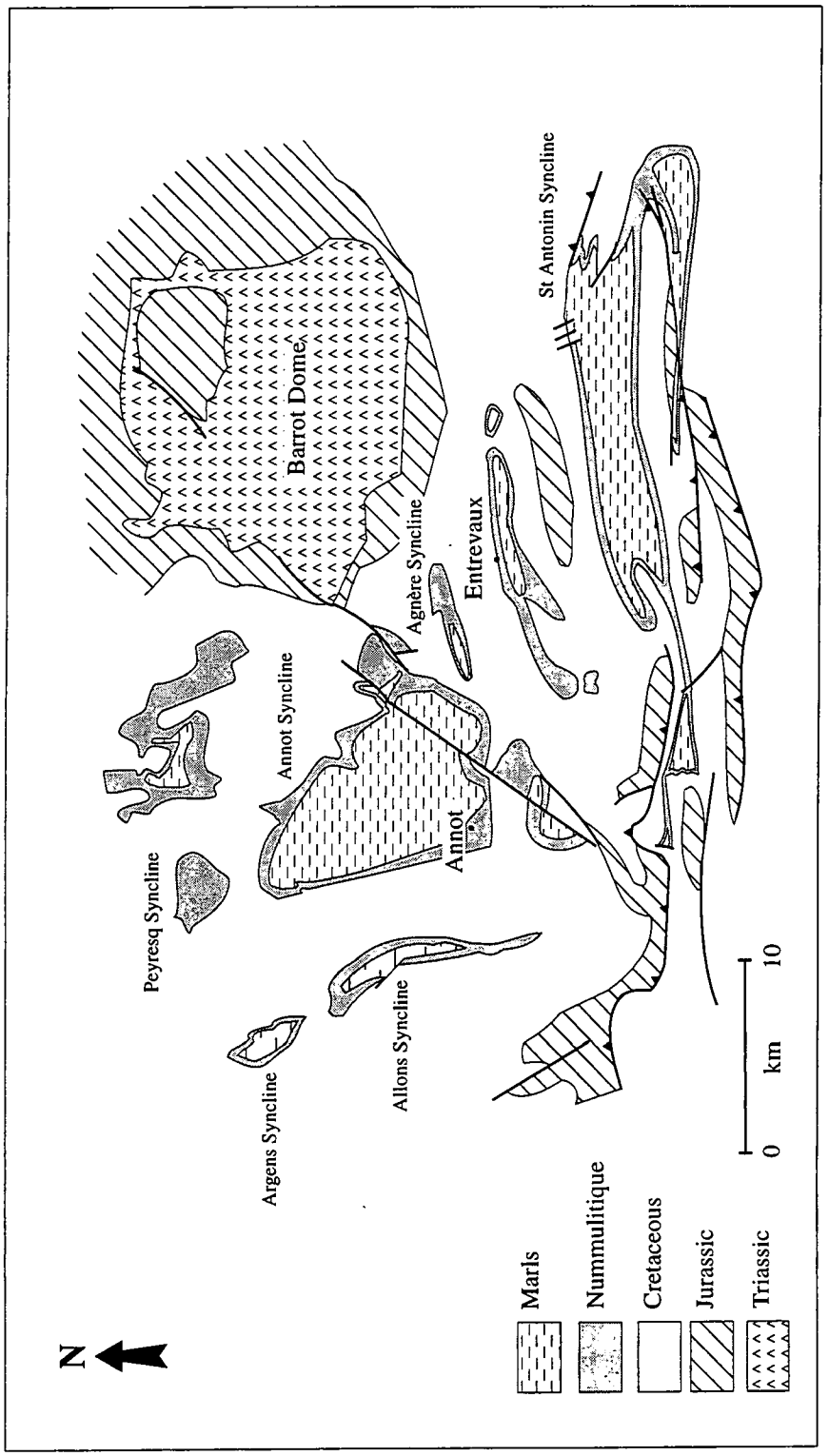

Fig. 1.4: Geological map of the Haute Provence study area showing the distribution of the Nummulitique, which is restricted to a series of E-W or SE-NW trending synclines. The substratum is dominantly Upper Cretaceous marl.

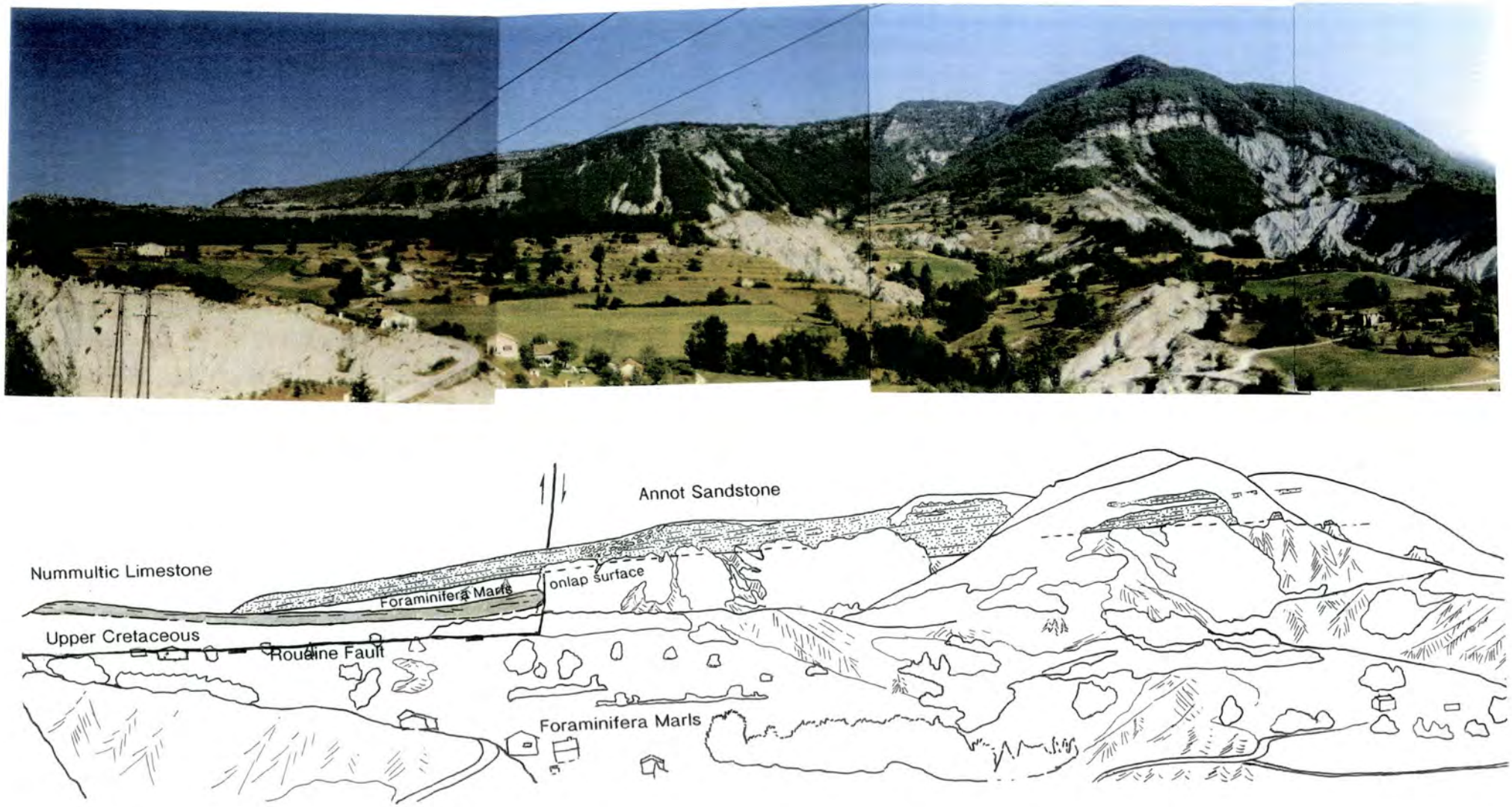

Fig. 1.5: Photograph and line drawing demonstrating the thickness variation across the Rouaine Fault, Haute Provence due to synsedimentary extensional fault reactivation during marl deposition.

deposition of the Annot Sandstone. This resulted in the plastic deformation of the uppermost beds of the sandstones during emplacement of the nappes (Hamiti, 1994). Early workers attributed the nappe emplacement to gravity gliding from an uplifted region to the east (Tempier, 1987; Apps, 1987; Siddans, 1979) but Hamiti (1994) suggested that it is more likely to be the result of the development of an accretionary wedge due to the advance of the Alpine thrust sheets from the east.

A final Miocene to Pliocene phase of tectonism produced localised depocentres within the foreland basin within which the Molasse was deposited (Siddans, 1979; Tempier, 1987).

This combination of the effects of the Alpine and Pyrenean orogenies led to the present day structures, with many of the synclines probably existing since the onset of compression, though the exact dating is unsure (Siddans, 1979). The late Tertiary advance of the Alpine thrust wedge caused the emplacement of the subalpine nappes from the east and the deformation of the Tertiary sediments of the nummulitic basin.

1.5. Foreland Basins: an Introduction

Foreland basins can be defined as the sedimentary basins that develop between the front of a developing orogenic belt and its adjacent craton (Allen et al., 1986). They occur in a collisional setting (Fig. 1.6) due to either continent-continent collision (peripheral foreland basins) or related to the development of a thrust wedge in front of an Andean-type magmatic arc (retro-arc foreland basins, (Dickinson, 1974) or retro foreland basins (Crampton and Allen, submitted)). Foreland basins are formed due to the flexure of the lithosphere during the loading of the underriding collisional plate by the advancing thrust wedge; this is thought to occur via a continuous process rather than episodic loading (Sinclair et al., 1991). They act as depocentres for sediment shed from both the foreland and the advancing orogenic wedge and the stratigraphy produced reflects the development of the basin through time. Foreland basins are elongate parallel to the orogenic belt and have a characteristic asymmetric cross-sectional profile, deepest proximal to the thrust load and shallowing towards the distal cratonic margin (Fig. 1.6). Foreland basins typically undergo three stages of development reflected in their stratigraphy (Allen et al., 1991):

1) initial uplift and erosion on the foreland,

2) an underfilled stage, characterised by deep-water (flysch) sedimentation and

3) a final overfilled stage characterised by shallow marine and alluvial (molasse) sedimentation.

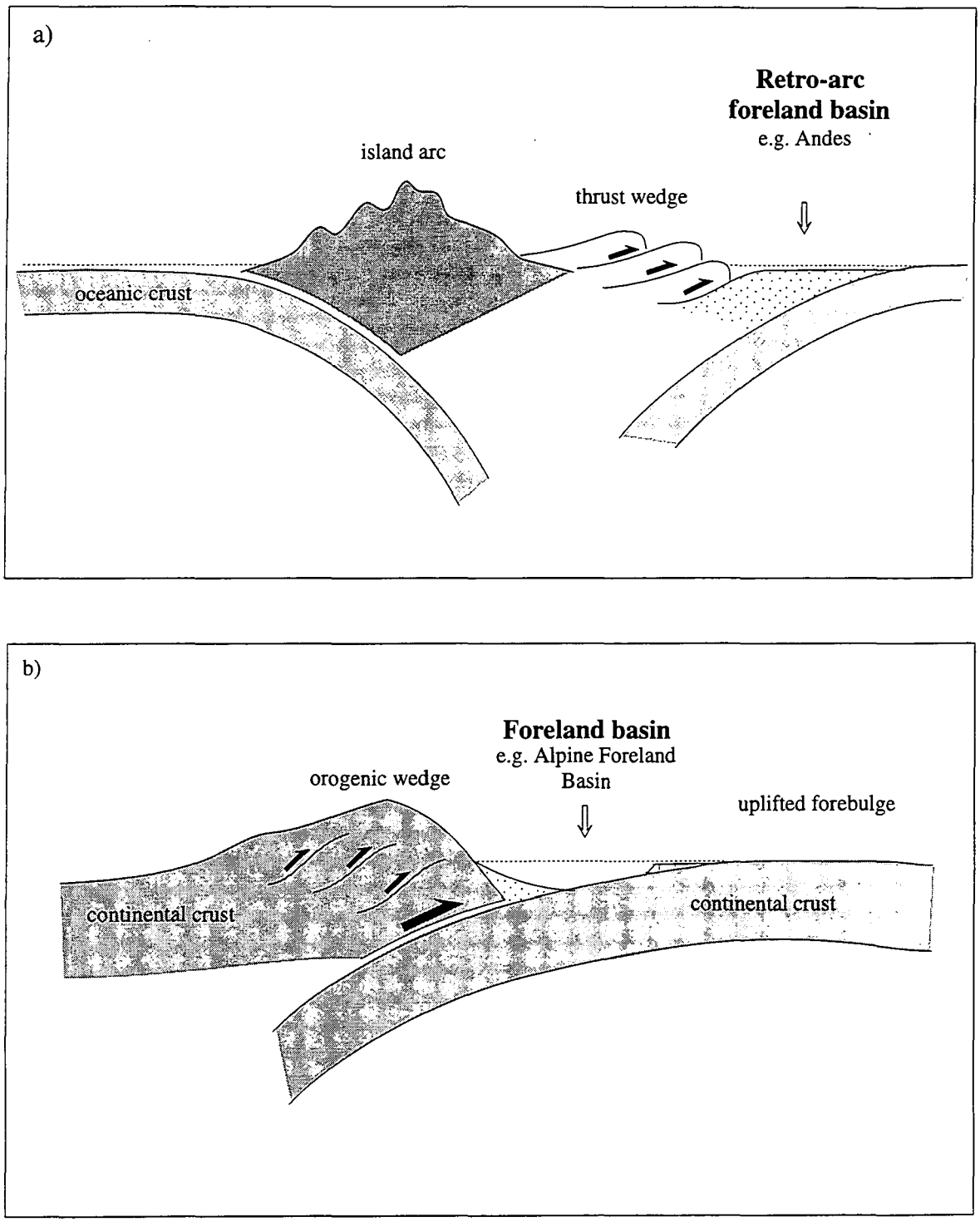

Fig. 1.6: The development of a) a retro-arc foreland basin (e.g. Andes) and b) a peripheral foreland basin (e.g. Alps). After Dickinson (1974).

Table 1.2: Foreland basins: location, age of formation, underfilled and overfilled sedimentation and geometry.

Basin	Location	Age	Underfilled Stage	Overfilled Stage	Geometry	References
Alpine FB	France, Switzerland	Upper Cretaceous - Miocene	terrigenous carbonate carbonate ramp pelagic marls turbiditic sandstones	delta sandstones fluvial sandstones lacustrine sediments alluvial fan c/gs	narrow, deep arcuate	Herb (1988) Homewood et al. (1986) Allen et al. (1991) Sinclair et al. (1991) Lihou (1995)
Pyrenean FB	North Spain	Upper Cretaceous - Oligocene	red beds carbonate platform coral reefs deltaic clastics pelagic marls turbiditic sandstones	delta sandstones alluvial fan c/gs alluvial plain facies	?	Burbank et al. (1992) Puidefabregas et al. (1986) Hirst and Nichols (1986) Cabrera et al. (1986)
Appalachian Basin	Eastern USA	Mid-Ordovician - Permian (?)	extensive carbonate ramp slope carbonates anoxic basin muds submarine fan clastics	delta and coastal plain clastics shallow molasse coal	broad, shallow, multi-stage	Read (1980) Tankard (1986) Bradley and Kusky (1986) Quinlan and Beaumont (1984)
Alberta Basin	Western Canada	Upper Jurassic - Eocene	cyclic clastics	clastics shale coal	multistage	Beaumont (1981) Hart and Plint (1993) Plint et al. (1993)
Appennines	Italy	Oligocene - Quaternary	turbidite clastics	?	narrow, deep	Ricci Luchi (1986)
Sevier	Idaho, Wyoming, Utah, USA	Cretaceous		?		Jordan (1981)

Table 1.2: Foreland basins: location, age of formation, underfilled and overfilled sedimentation and geometry.

Basin	Location	Age	Underfilled Stage	Overfilled Stage	Geometry	References
Timor Trough	Indonesia, Australia	Late Miocene - Present	reef carbonates pelagic ooze turbidite clastics	n/a	100km wide 6km amplitude	Veevers et al. (1978)
Marathon-Ouachita Foreland	West Texas, Southern New Mexico	Carboniferous - Permian	carbonate platform conglomerates fine siliciclastics shales	?	composite	Yang and Dorobek (1995) Dorobek (1995)
Oman Mountains	Oman	Upper Cretaceous	Fe chemical seds concretionary lsts marls and debrites clastic turbidites	?	broad, shallow	Robertson (1988)
Papua New Guinea	Indonesia, Australia	Mid Oligocene - Pliocene	slope limestones and reefs pelagic ooze turbidite clastics	n/a	broad	Pigram et al. (1989)

The stages of development will be discussed further in Section 1.6 with reference to the Alpine Foreland Basin. Table 1.2 lists some of the foreland basins developed around the world.

The geometry and fill of a foreland basin are controlled by a number of factors including the strength or effective elastic thickness of the lithosphere, the topographic slope of the mountain belt, the effects of erosion and sedimentation (transport coefficient) and the rate of thrust tip advance (Sinclair et al., 1991). These factors have been applied in a number of models trying to reproduce the observed stratigraphy within foreland basins. The earlier models reproduced the stratigraphy by applying loads at separate time-steps on to a lithospheric plate that behaved either elastically (Jordan, 1981) or viscoelastically (Beaumont, 1981; Quinlan and Beaumont, 1984). This produced the observed forebulge uplift and erosion and subsequent onlap of the basin fill, but failed to take into account the effects of a continuous process with load redistribution by erosion and sediment transportation. These factors were included in the diffusion modelling carried out by Sinclair et al. (1991) and Crampton (1992) on the Swiss Molasse basin of the Alps.

These models have shown the following controlling effects:

a) Lithospheric strength controls the width and depth of the basin, with a weak lithosphere (low effective elastic thickness) producing a narrow, deep basin with a low flexural wavelength (e.g. Apennines) and a stronger lithosphere leading to a broad, shallow basin (e.g. Appalachians). These two geometries reflect the bimodality of the effective elastic thickness of continental lithosphere (Watts, 1992),

b) Erosion and sedimentation transport coefficient controls the rate of infilling of accommodation space created within the basin, with a high coefficient promoting overfilling of the basin,

c) Topographic slope angle affects the rate of growth of the thrust load and sedimentary supply into the basin and also the movement of the thrust wedge, which will not move horizontally until the critical taper is reached (Davis et al., 1983),

d) the rate of thrust tip advance also controls the load increase and the rate of fill of the basin with a rapid rate of advance creating an underfilled basin and *vice versa.*

1.6. The Alpine Foreland Basin: Development and Stratigraphy

The Alpine Foreland Basin occurs to the north and west of the main Alpine massifs and stretches from Austria in the east to Haute Savoie, France, where it arcs

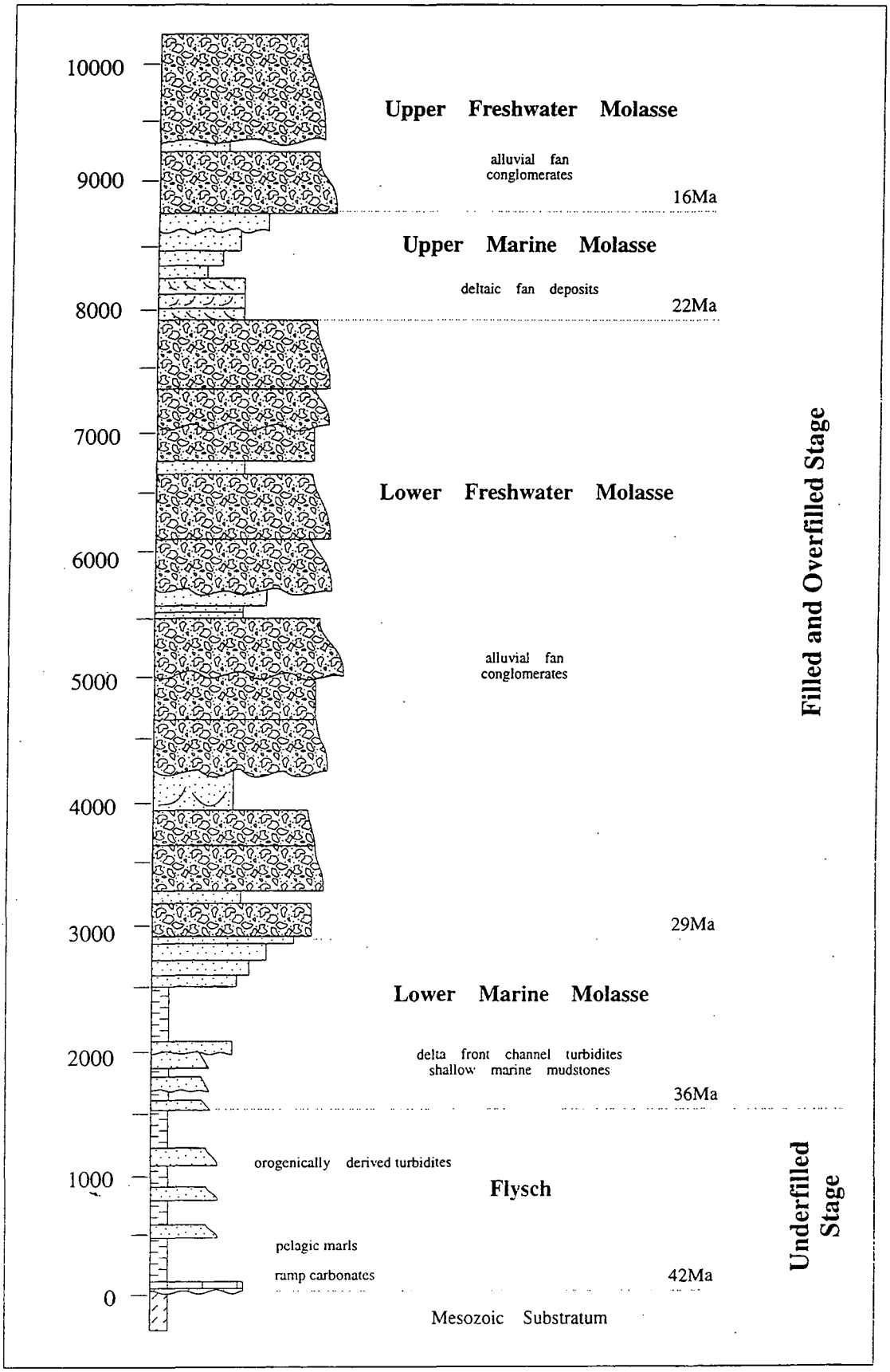

Fig. 1.7: Summary log through the sediments of the Alpine foreland basin fill, showing the characteristic coarsening upwards succession as the orogenic wedge approaches. Average thicknesses and ages are from Sinclair et al. (1991).

round to meet the Mediterranean at Nice, mimicking the arcuate nature of the Alpine chain. The basin was formed by loading of the European lithosphere due to the advance of the Alpine thrust wedge from the south and east formed during the collision of the European and African continents (Dewey et al., 1989). This led to the flexure of the Mesozoic passive margin which became unconformably overlain by the foreland basin fill (Fig. 1.7) before being incorporated into the Helvetic thrust nappes.

The basin development has been documented from the stratigraphy of the sedimentary fill. It appears to have initiated in eastern Switzerland during the Late Cretaceous and Early Tertiary (Lihou, 1994), and progressed westward through Switzerland during the Ypresian and Lutetian as the thrust wedge advanced (Crampton, 1992; Herb, 1988), producing a characteristic younging of the sediments from east to west and from south to north, and a corresponding increasing stratigraphic gap at the unconformity between the passive margin sediments and the foreland basin fill (Allen et al., 1991; Herb, 1988).

The oldest basin fill sediments in western Switzerland and the Alpes Maritimes, France, were deposited during the Lutetian (Campredon, 1971; Herb, 1988) indicating that the onset of subsidence occurred later in France than in Switzerland. A similar younging westward trend is seen in France (Bodelle, 1971; Campredon, 1977; Pairis, 1988), with the onset of sedimentation in the two study areas occurring in the Upper Eocene (Haute Provence - Bartonian, Haute Savoie - Priabonian).

The younging trend in the sediments and the increasing stratigraphic gap at the unconformity reflect the backstepping of the foreland basin fill over the foreland as the thrust wedge advanced. The stratigraphy corresponds to a typical foreland basin succession, demonstrating initial uplift and erosion of the forebulge, an early underfilled (flysch) phase of sedimentation and a final overfilled (molasse) phase.

1.6.1. Forebulge uplift

The uplift of the forebulge region due to lithospheric flexure is represented in the stratigraphy by an erosional unconformity between the Mesozoic passive margin sediments and the foreland basin fill (Allen et al., 1991). This has commonly been karstified, with the preservation of a palaeokarst which, in Switzerland and locally in France, may have an associated karst fill of iron-rich, pisolithic sediments (Siderolithique) representing terrestrial conditions (Herb, 1988). In France, subaerial conditions are indicated by terrigenous carbonate deposition (Infranummulitique) seen in Haute Savoie, Haute Provence and Dévoluy (Meckel et al., submitted) including alluvial conglomerates and palaeosols (Chapter 3; Bodelle, 1971; Apps, 1987; Delamette, 1993).

1.6.2. Underfilled (flysch) phase

The underfilled phase of foreland basin development occurs from the onset of marine transgression where the rate of creation of accommodation space outpaces the rate of sedimentation, producing a deepening-upwards sedimentary package (Sinclair and Allen, 1992). The factors governing the formation of the basin and the creation of accommodation space are discussed above (Section 1.5).

In the Alps, the underfilled phase is represented by flysch sedimentation (Trümpy, 1980; Homewood et al., 1986) dominated by turbiditic sandstones and hemipelagic mudrocks (Fig. 1.8). The sedimentary successions developed are similar around the Alps and regional and temporal variations are discussed in Chapter 8.

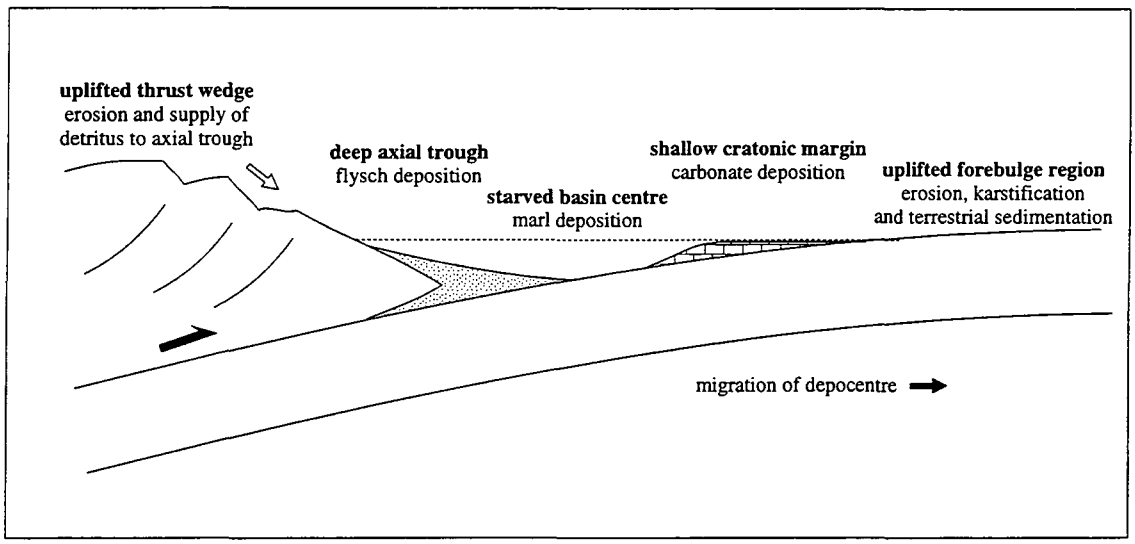

Fig. 1.8: Underfilled (flysch) stage of foreland basin development. The rate of creation of accommodation space related to subsidence outpaces sedimentation rates and the basin deepens. All detritus shed into the basin from the developing mountain belt is trapped in the deep axial trough (turbidite deposition), producing a starved basin centre (marl deposition), clear waters on the distal cratonic margin suitable for carbonate deposition and a region of forebulge erosion. The depocentre migrates over the foreland as the orogenic wedge approaches, causing a backstepping of facies and the vertical succession illustrated in Fig. 1.7.

The onset of transgression is represented by shallow-marine carbonate deposition (up to 70m nummulitic limestones and associated sediments), the restored location of which marks the position of the foreland basin at the onset of subsidence and which can be used to date the onset of subsidence at a given locality. As subsidence rates increase, accommodation space increases and the limestone platform is flooded and pelagic marl deposition (up to 400m) marks the development of a deep basin starved of detrital influx. As the orogenic wedge advances, there is a change from carbonate to siliciclastic sedimentation with the influx of orogen derived detritus (Sinclair and Allen, 1992) leading to turbidite deposition which shows a shallowing-

upwards trend (Meckel et al., submitted) as the accommodation space is reduced due to sedimentation rates now outpacing subsidence rates.

1.6.3. Overfilled (molasse) phase

The transition from an underfilled to an overfilled basin in the Alps is thought to be due to a slowing in the rate of thrust wedge advance and increased sediment influx due to increased exhumation of the mountain chain (Sinclair and Allen, 1992) rather than the transferral of the thrust load from attenuated passive margin lithosphere (low effective elastic thickness) to undeformed continental lithosphere (higher effective elastic thickness) as postulated by Watts (1992).

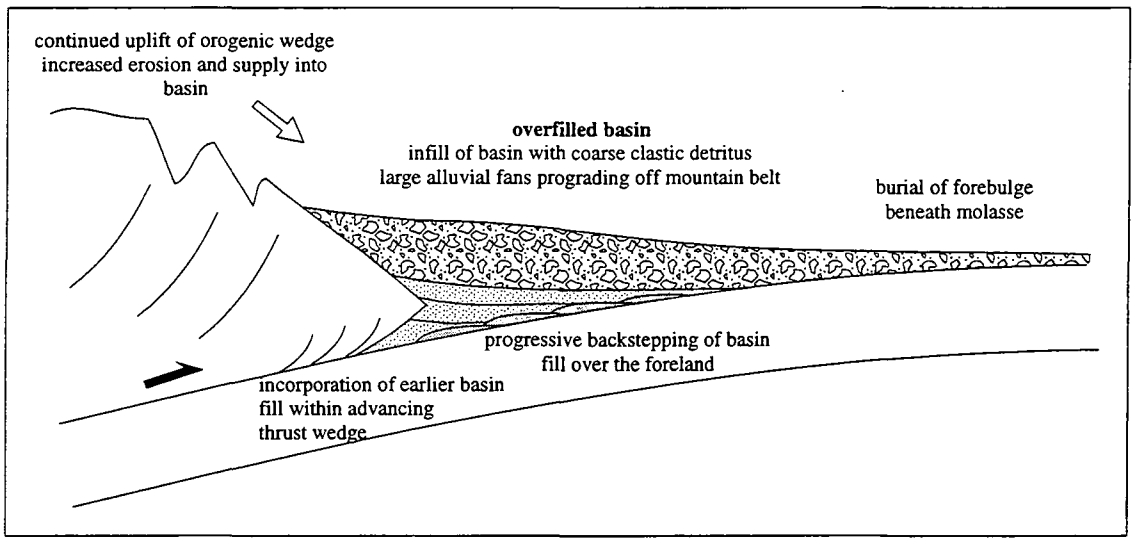

Fig. 1.9: Overfilled (molasse) stage of foreland basin development. Increased exhumation rates lead to a greater influx of detritus from erosion of the orogenic wedge, outpacing the creation of accommodation space and infilling the basin. The molasse is dominated by thick alluvial fans prograding off the advancing mountain front, burying the forebulge region. The earlier basin fill has begun to be incorporated into the thrust wedge, with the later sediments buried beneath the molasse.

The overfilled phase is represented by up to 7 km of shallow marine and continental siliciclastic sedimentation of the Molasse (Fig. 1.9), deposited in deltaic, fluvial, lacustrine and alluvial fan settings, supplied by material eroded from the uplifting Alpine chain (Trümpy, 1980; Homewood et al., 1986; Sinclair and Allen, 1992). The Molasse is dominantly present in Switzerland with smaller remnants present in localised basins in France (Siddans, 1979; Tempier, 1987).

1.7. Foreland Basin Carbonates

Carbonate platforms are a common feature in foreland basins around the world and throughout geological time, though their existence has been largely neglected in the literature, with most studies of foreland basin fills focusing on the overlying siliciclastics. This has left neglected the carbonates developed during the earliest stages of foreland basin subsidence and transgression and which, due to their sensitivity to sea-level variations, have the potential to tell us a great deal about the onset of foreland basin development. Table 1.3 gives some examples of foreland basin carbonates documented in the literature; the development of synorogenic carbonates has been discussed in detail by Dorobek (1995).

Carbonate platforms in foreland basins form on the distal cratonic margin of the basin adjacent to the uplifted forebulge region (Fig. 1.10).

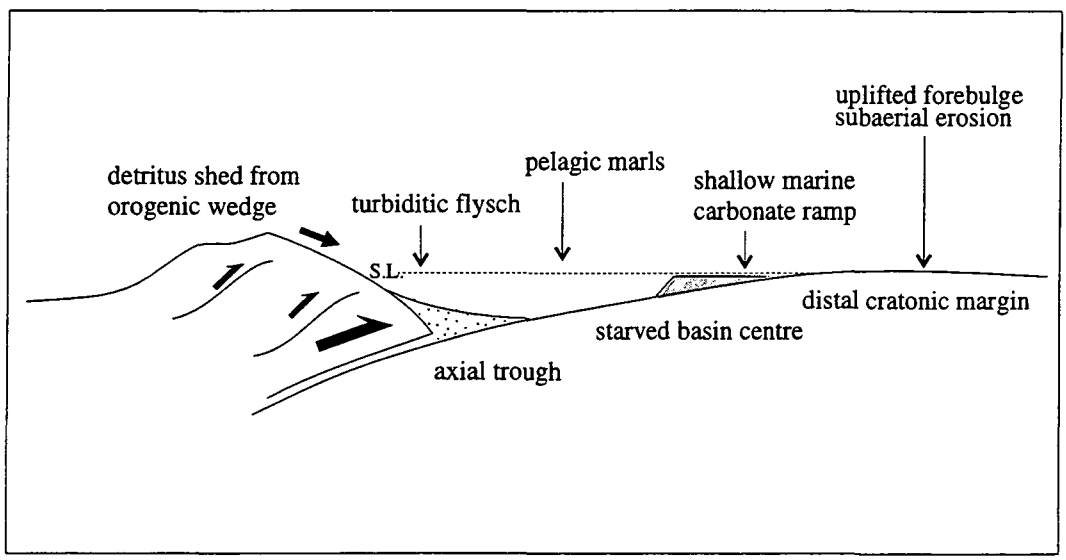

Fig. 1.10: The depositional environments in an underfilled foreland basin showing the locations of carbonate, marl and siliciclastic flysch depocentres.

They are typically homoclinal ramps, irrespective of the carbonate producing benthos, and this morphology is thought to reflect the shape of the flexed lithosphere (Dorobek, 1995). The carbonate ramps develop during the underfilled stage of basin development, when siliciclastic material shed from the advancing orogenic wedge is trapped in the proximal foredeep, thus preventing significant siliciclastic detritus reaching the carbonate system and reducing productivity. Though detritus may be shed from the uplifted forebulge area, this generally has a lesser effect on productivity, especially when the eroded substratum consists of a passive margin succession

Table 1.3: Occurrences of foreland basin carbonates showing age, facies, facies of alluvial, shallow and deep marine sediments and the climate at the time of deposition.

Basin	Age	Alluvial	Shallow Marine	Deep Marine	Climate	References
Alpine Foreland Basin (France, Switzerland)	Lower - Upper Eocene	terrigenous carbonate ephemeral stream c/gs, fan delta c/gs, coastal plain muds up to 35m *Infranummulitique*	CRA and large foram limestones progradational, bioclast shoals up to 70m *Nummulitic Lst*	pelagic marls with planktonic forams up to 400m *Globigerina Marls* *Schistes à Meletta*	subtropical	Crampton (1992) Allen et al. (1991) Lihou (1995) Bodelle (1971) Campredon (1977) Pairis (1988)
Pyrenean FB (N Spain)	Ypresian	red beds, channel ssts fenestral limestones algal laminites *Garumnian Fm* *Tremp Formation*	large foram limestones, delta clastics, algal and nummulitic limestone coral reefs, evaporites 100-200m *Cadi Formation* *Corones Sequence*	marls, calciturbidites and slope breccias up to 900m *Armancies Sequence*	subtropical to tropical	Puidefabregas et al. (1986) Burbank et al. (1992) Pedley (1994)
Papua New Guinea	Oligocene - Pliocene		epicontinental sea CRA-foram lsts, local mounds developed into rimmed platform with coral reefs 1000-1200m *Darai Limestone,* *Nipa Group* *Great Barrier Reef*	pelagic carbonates and shale, pinnacle reefs on highs *Pasca Reef*	tropical with increasing temperature	Pigram et al. (1989)

Table 1.3: Occurrences of foreland basin carbonates showing age, facies, facies of alluvial, shallow and deep marine sediments and the climate at the time of deposition.

Basin	Age	Alluvial	Shallow Marine	Deep Marine	Climate	References
Timor Trough (Sahul Shelf)	Pliocene - Quaternary		discontinuous reefs, calcarenites 30m	calcareous ooze 400m	tropical	Veevers et al. (1978)
Appalachian Basin (E USA)	Mid-Ordovician	(supratidal deposits) up to 100m *Blackford-Elway-Five Oaks Fms*	transgressive peloidal carbonates, downslope buildups, skeletal and fenestral carbonates, lime sand flats up to 300m *New Market Lst* *Mosheim Lst* *Trenton Group* *Black River Group*	black limestone and anoxic sediments 450-900m *Fetzer/Botetourt Fms* *Paperville Fm* *Utica Fm*	humid	Read (1980) Bradley and Kusky (1986)
Oman Mountains	Turonian - Campanian		ferrugineous crusts and nodules, concretionary limestones, Fe ooids *Muti Formation*	hemipelagic marl limestone debris-flows *Muti Formation*	hot and humid	Robertson (1988)
Great Slave Lake (Canada)	Proterozoic		microbial carbonates subtidal platform to basin assemblage *Pertei Group*	deep water microbialites *Pertei Group*	?	Sami and James (1993)

dominated by carbonates and shoal siliciclastics, the influx of which has little effect on the benthos (Dorobek, 1995). Thus, the shallow, clear waters adjacent to the forebulge are optimum sites for carbonate growth. As carbonate is produced dominantly by organisms reliant on photosynthesis, the maximum zone of carbonate productivity must necessarily fall within the photic zone, typically down to 50 - 100m depth

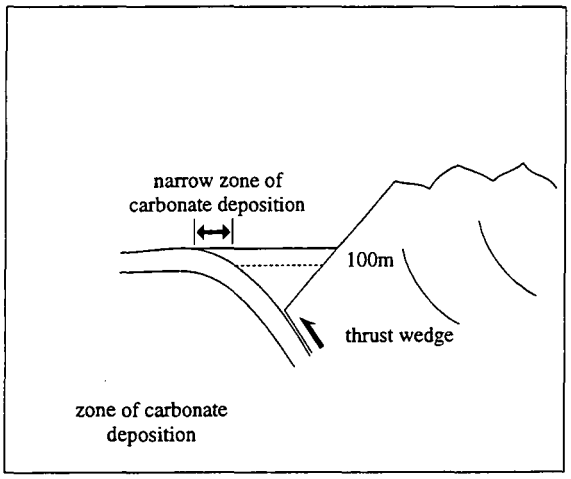

a) weak lithosphere (low Te), narrow zone for carbonate platform development.

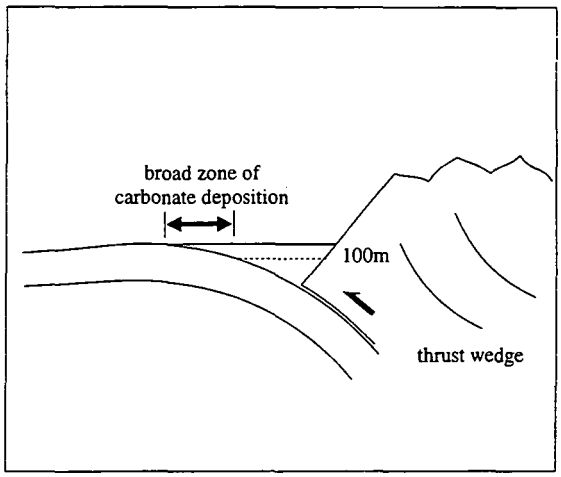

b) strong lithosphere (high Te), broader carbonate platform development.

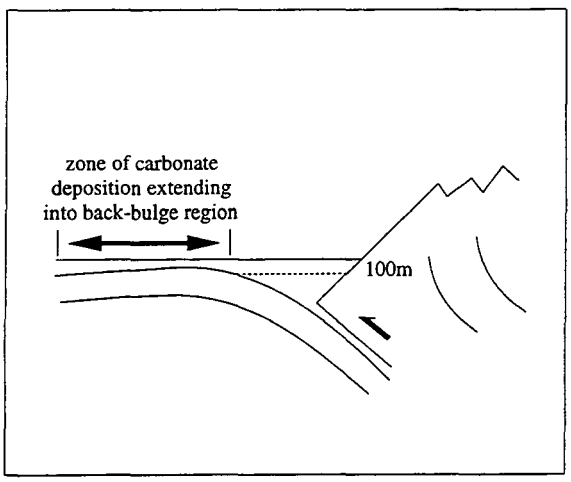

c) high initial sea-level - forbulge submerged, broad carbonate platform development extending into back-bulge region.

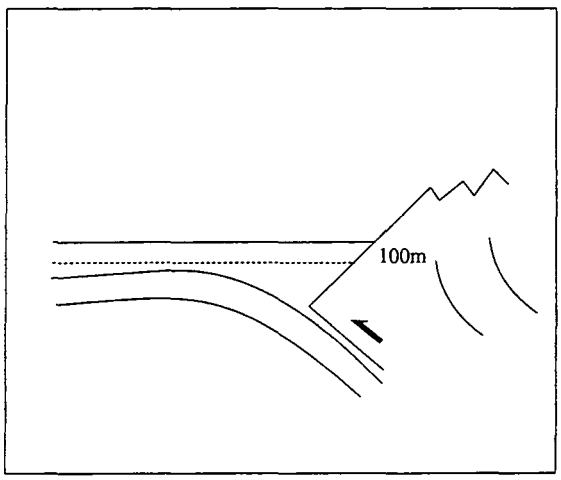

d) very high initial sea-level - forebulge crest submerged below 100m isobath, no carbonate deposition.

Fig. 1.11: Intersection of the 100m isobath with the foreland basin flexural profile as the limit of carbonate deposition (Dorobek, 1995), showing how the flexural geometry produced by weak (a) and strong (b) lithospheric plates and high initial sea-levels (c,d) affect the distribution of carbonates flanking the forebulge.

(Schlager, 1981). This is an important governing factor in platform development, and particularly so in foreland basins where continually increasing rates of subsidence

during basin development lead to a given point on the foreland subsiding to depths often far in excess of this limit. Dorobek (1995) proposed that the limit of carbonate platform development in foreland basins can be approximated to the intersection of the flexural profile of the basin with the 100m isobath (Fig. 1.11). Therefore the theoretical extent of development of the platform is governed by factors controlling this intersection, such as the strength of the flexed lithosphere and eustatic sea-level variations. For instance, in a basin with initial low sea-level and a weak lithosphere, the 100m isobath will meet the flexural profile relatively close to the uplifted forebulge, leading to a narrow platform being developed compared to a basin with a stronger lithosphere (Fig. 1.11a, 1.11b). In basins with an initial high sea-level, the entire forebulge region may be submerged and can act as a site of carbonate deposition producing a broad platform extending into the back-bulge region (Fig. 1.11c) or the crest of the forebulge may occur below the 100m isobath and so carbonate deposition is precluded (Fig. 1.11d).

The rate of creation of accommodation space controls the stratal geometry of a carbonate platform. During the early stages of basin subsidence, where rates of subsidence are lower than the carbonate productivity rates, the carbonate platform flanking the forebulge can aggrade up to sea-level (Fig. 1.12a) and even prograde to a certain extent (Fig. 1.12a) into the basin (Chapter 7; Allen et al., 1991; Lihou, 1995). As the orogenic wedge advances, the rate of subsidence at a given point increases and the rate of creation of accommodation space outpaces carbonate productivity. This can have two effects: a backstepping of the carbonate ramp over the foreland (Fig. 1.12c) into zones of higher productivity (e.g. Swiss Alps: Crampton, 1992; Lihou, 1995), or a complete drowning of the carbonate platform (Fig. 1.12d) with an abrupt transition into deep water facies (seen in the transition from the Nummulitic Limestone to pelagic marls in France (Chapter 7) and the burial of pinnacle reefs on the Sahul Shelf (Dorobek, 1995)). Though tectonism is the main driving force for platform termination, carbonate productivity may also be influenced by climate, turbidity, nutrient supply, oxygenation, siliciclastic supply, benthos type and eustatic sea-level variations. These factors are discussed further with reference to the Nummulitique in Chapter 7.

1.7.1. Effects of intrabasinal structures on sedimentation

Though the overall geometry of a foreland basin is the dominant control on the distribution of the sedimentary fill, the facies distribution, especially within the carbonates, may be affected by compressional or extensional intrabasinal structures related to flexural extension or in-plane stresses into the foreland region (Cloetingh, 1988; Bradley and Kidd, 1991; Dorobek, 1995).

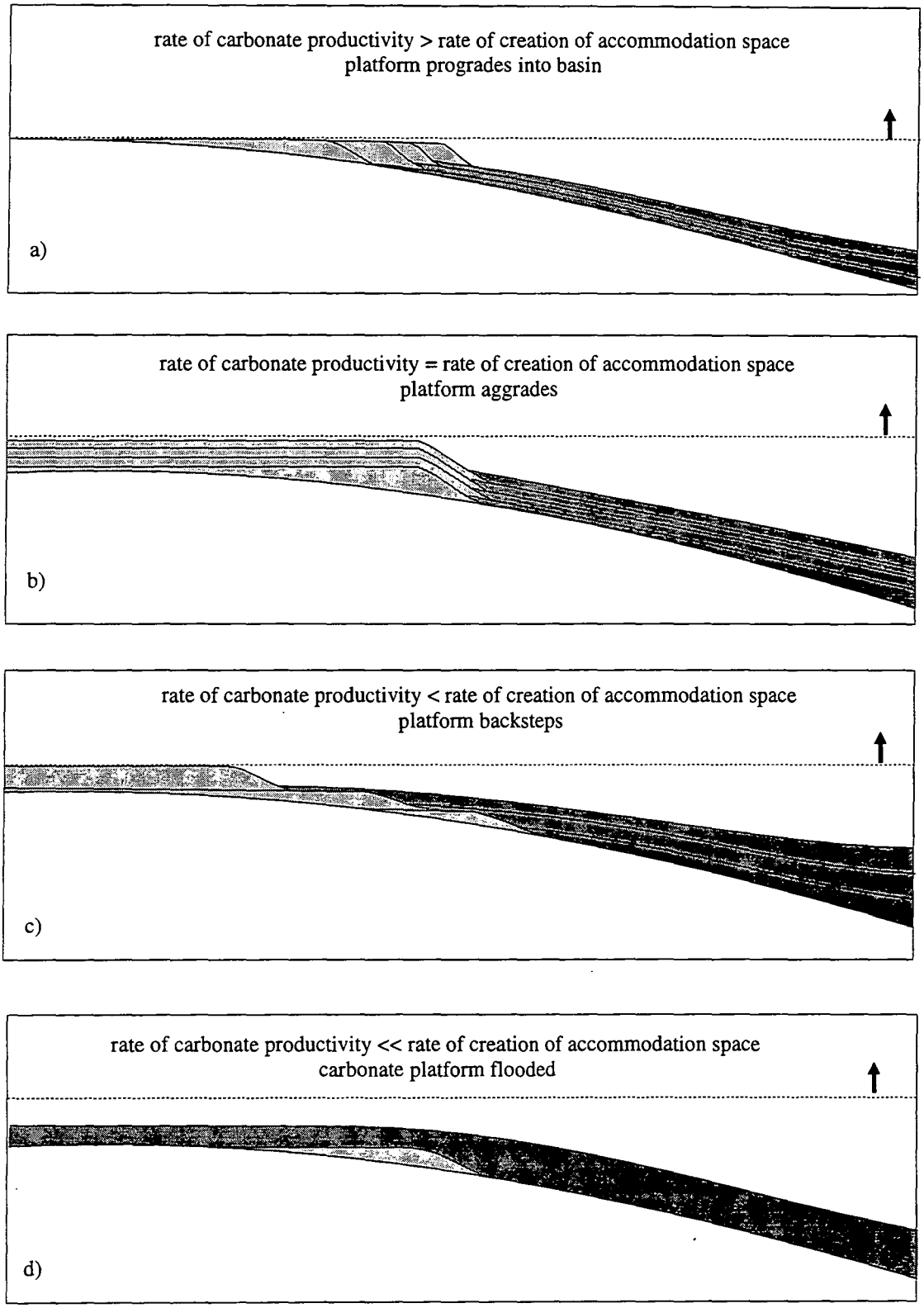

Fig. 1.12: Variations in stratal geometries produced in carbonates with varying rates of creation of accommodation space (vertical arrow): a) progradation into the basin, b) aggradation up to sea-level, c) backstepping over the foreland and d) platform flooding.

Extensional faulting related to inelastic deformation of the upper crust during lithospheric flexure occurs in a number of foreland basins and has been described from the Taconic Foreland by Bradley and Kidd (1991). This flexural extension during collision produces normal faults striking parallel to the deformation front (Fig. 1.13), with the faults typically showing four stages of development:

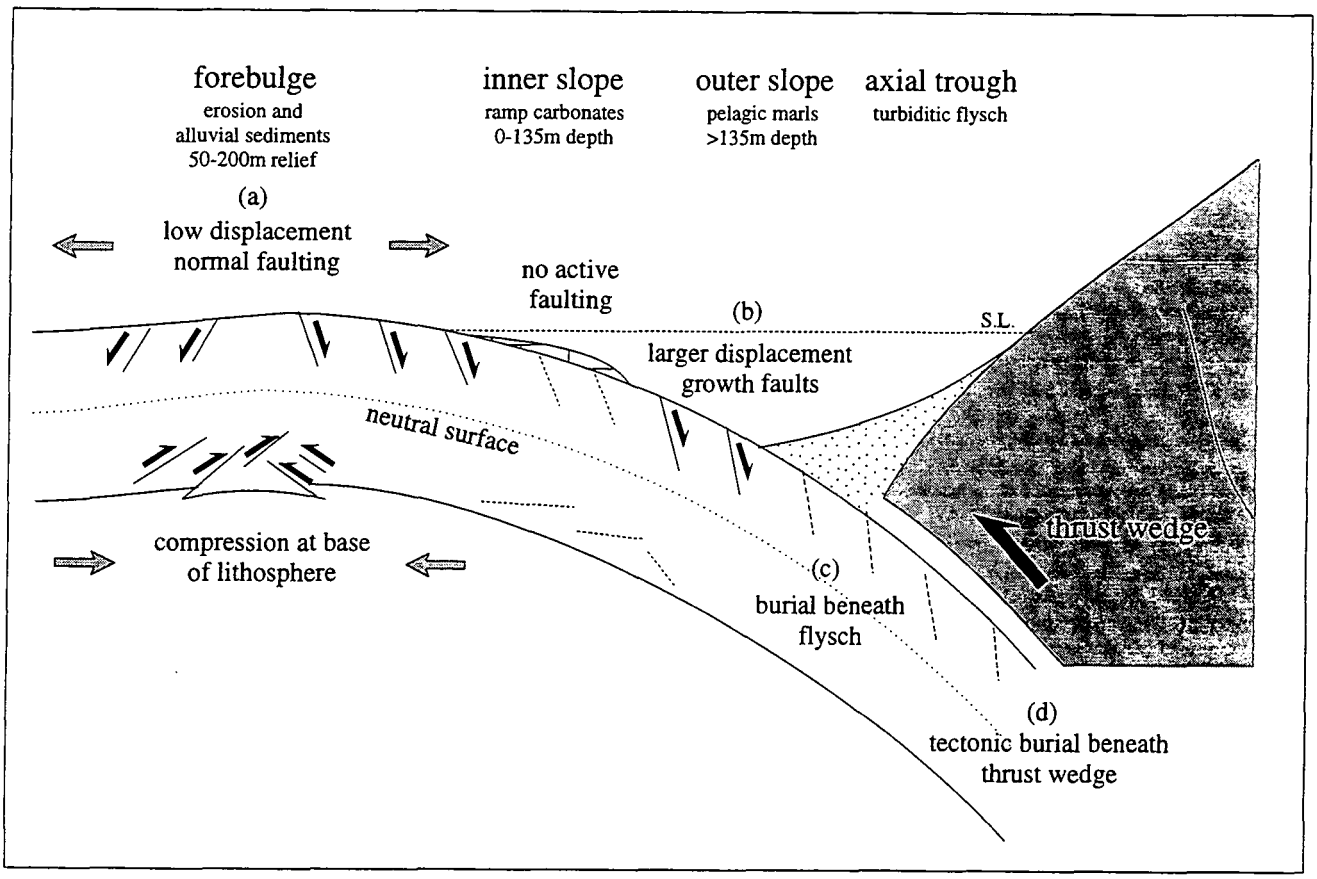

Fig. 1.13: Extensional deformation of the foreland area due to lithospheric flexure, producing normal faults striking parallel to the deformation front showing the four stages of development. After Bradley and Kidd (1991), height of forebulge from Crampton and Allen (submitted), water depths based on Racey (1990, fig. 7.4).

a) early, low-displacement normal faults occurring far into the foreland of the deformation front,

b) major growth faulting occurring on the outward slope of the flexed plate as subsidence rates increase,

c) burial beneath flysch or molasse sediments and

d) tectonic burial beneath the deformation front.

The first two stages of fault development can strongly affect the sedimentary fill of the basin, with thickness and facies variations occurring across faults.

Other brittle fractures may occur at a high angle to the deformation front, with some strike-slip movement, described by Hancock and Bevan (1987). These are a feature of many forelands and are thought to be due to the transmission of tensional in-plane stresses far into the foreland (500 km or more) produced by indentation tectonics causing the lateral escape of material as the deformation front advances (Fig. 1.14).

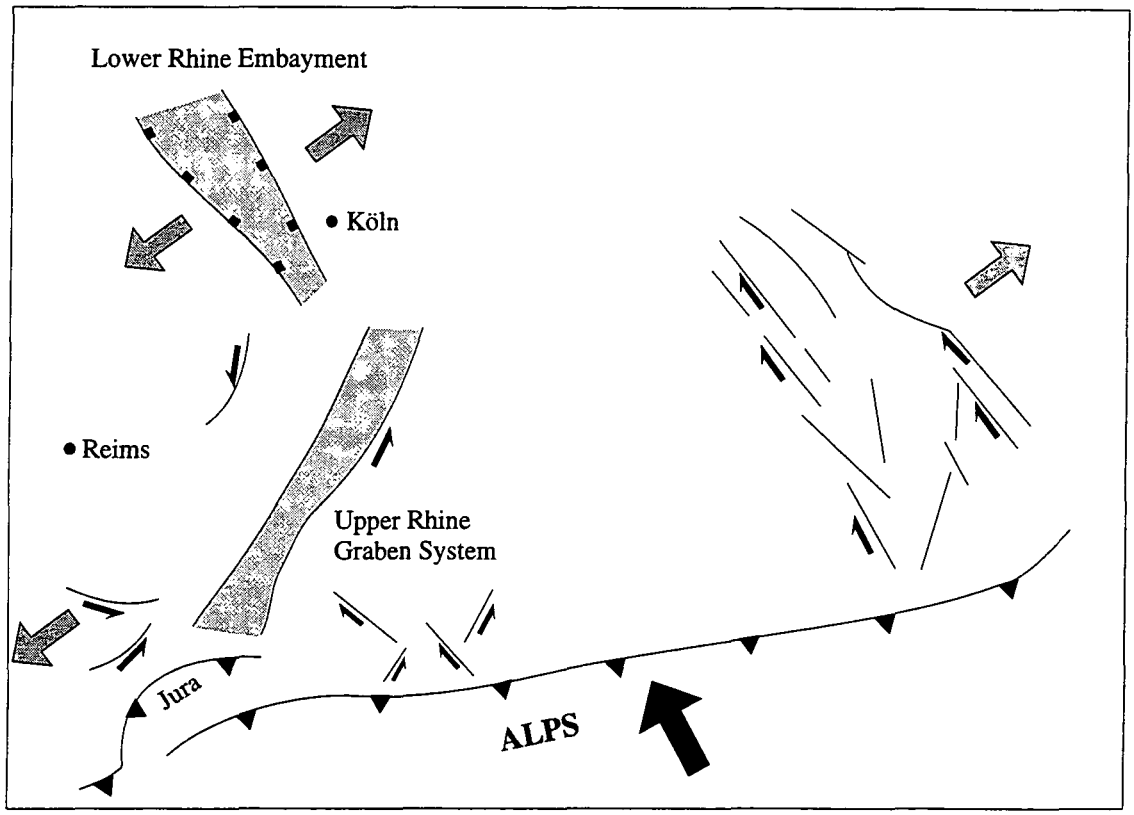

Fig. 1.14: Schematic map of structures due to lateral extension of the Alpine foreland in Switzerland, France and Germany. Note the high angle of the extensional structures with respect to the Alpine deformation front. After Hancock and Bevan (1987, fig. 1c).

In-plane stresses can also produce compressional structures such as thrust slices in advance of the main deformation front; these have been described from the Champsaur by Crampton (1992), and low-amplitude folding occurs in Provence (Apps, 1987). They may reactivate pre-existing basement structures (Dorobek, 1995), with several phases of structural inversion along faults occurring as the stress field in the foreland evolves with the approaching thrust wedge. Fluctuations in in-plane stresses are particularly noticeable in the forebulge region (Cloetingh, 1988) where they may modify the relative sea-level curve (Chapter 7) by affecting the height of the forebulge. The effects of in-plane stresses may be important in the development of the pre-Nummulitic structures, though a detailed structural study would be necessary in order to determine the controlling tectonics.

The varying structural relief produced by any one or more of these structural styles affects the depositional patterns of the sediments of the underfilled phase of foreland basin evolution, but they become buried by the steady-state/overfilled phase (Bradley and Kidd, 1991). Structural lows during the early subsidence of the forebulge region can act as depocentres for alluvial/fluvial sedimentation with the corresponding, eroding highs providing a source for the terrigenous material (Pairis and Pairis, 1975; Apps, 1987; May et al., 1995). During early transgression the facies distribution within the carbonates and/or shallow marine sands is complicated by pre-existing structural relief within the basin, with highs providing sites for preferential shoal or reef development (Crampton, 1992; Dorobek, 1995) and the corresponding lows filling with more basinal or allochthonous sediments.

Chapter 2

Palaeoecology and Biostratigraphy of the Nummulitique

2.1. Introduction

The Nummulitique is characterised by the presence of abundant larger benthonic foraminifera dominated by the genus *Nummulites* from which its name has been derived. During the Eocene, reef communities were still recovering from the late Cretaceous extinctions, and reef-building corals did not proliferate until the Miocene (Bryan, 1991). Instead, foraminifera and algae tended to dominate in "reefal" environments, forming extensive banks, with sufficient relief to be able to identify between fore- and back-reef environments. Such foraminiferal buildups have been documented from the Tertiary of Oman (Racey, 1990), Tunisia (Moody, pers. comm.), Egypt (Aigner, 1982, 1983, 1985) and Switzerland (Crampton, 1992), with monospecific accumulations showing abundant evidence of wave reworking and winnowing. The French Nummulitic Limestone post-dates the extinction of the large bank-building foraminifera and is dominated by smaller forms, but the facies show similar characteristics to the sediments described above, forming low relief bioclastic accumulations, which are discussed in Chapters 4 and 5. In this study, the foraminifera along with coralline red algae (CRA) have been used to assist in the microfacies analysis and environmental interpretation of the carbonate ramp. This chapter introduces the principal fossils present and their use in interpreting the depositional environment, and discusses the biostratigraphic dating of the formation based on the available literature. It is assumed that the reader has a basic understanding of palaeontological classification the palaeontology of foraminifera and calcareous algae. Names in italics denote the generic level of classification and names in normal text denote the family.

2.2. Larger Benthonic Foraminifera and their use as Environmental Indicators.

2.2.1. *Nummulites* and *Operculina*

Nummulites (Fig. 2.1) and *Operculina* (Fig. 2.2) are epifaunal, free-dwelling, rotaline foraminifera preferring a muddy substrate. They are characteristic of normal-

marine salinities (Blondeau, 1972), though *Operculina* can tolerate slightly hypersaline conditions, and warm waters (25°C ± 3°). The flattest Nummulitids occur on the deep

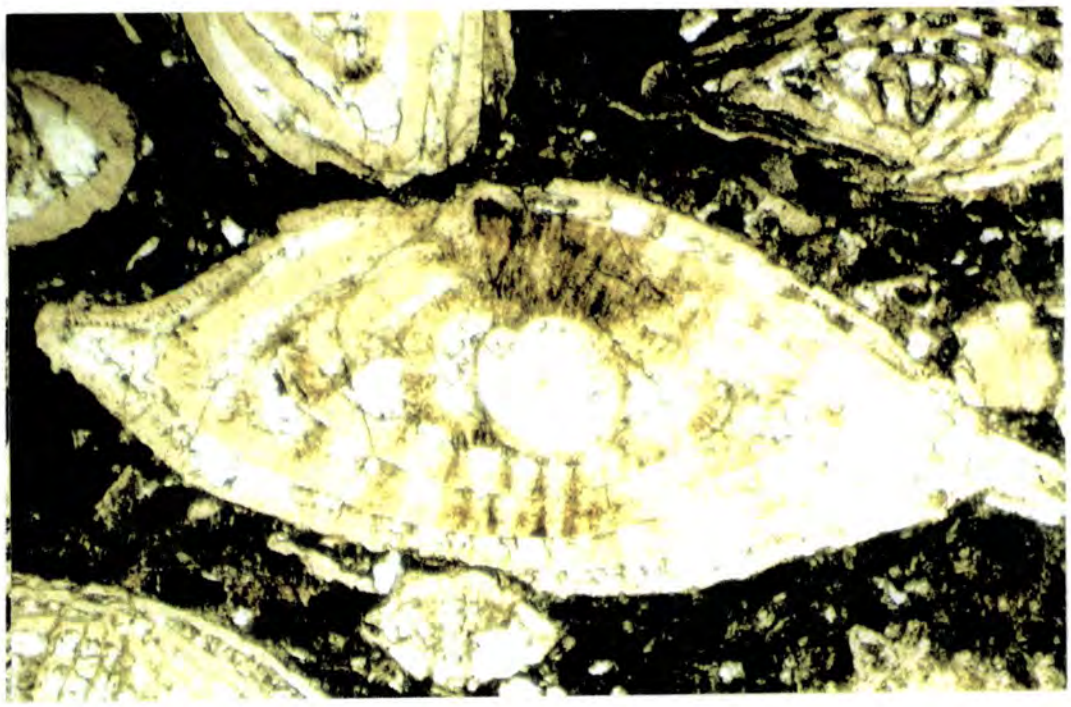

Fig. 2.1: Nummulites, showing initial large proloculus (A-form) and internal chambers infilled with calcite cement. Field of view 3x1.9mm.

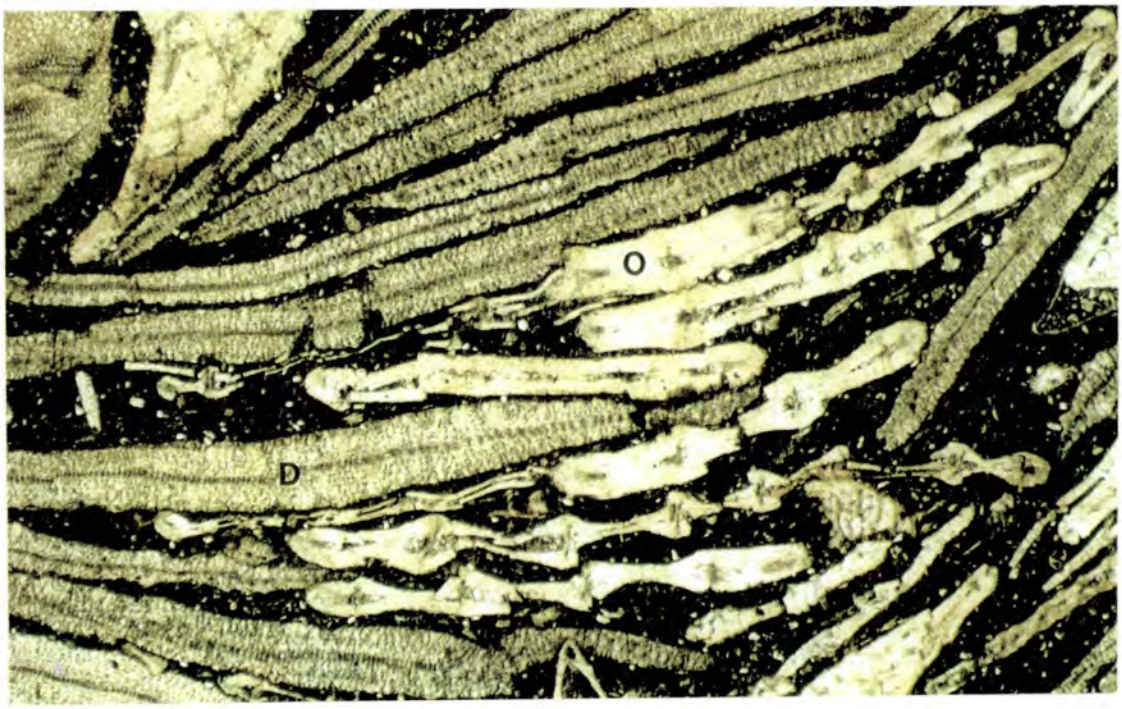

Fig. 2.2: Packstone containing Operculina (O) and Discocyclina (D). Field of view: 6x3.7mm.

shelf within the photic zone (down to 130m; Hallock and Glenn, 1986; Murray, 1991) with the more robust forms inhabiting fore-reef shoals, back-reef areas and possibly forming banks (Racey, 1989; Ghose, 1976). Shallower Eocene ramps are represented by *Nummulites* - Rotaliid - *Operculina* shoals (Hallock and Glenn, 1986).

2.2.2. *Discocyclina*

Discocyclina (Figs 2.2, 2.3) is a typical fore-reef rotaline foraminifera, forming banks and offshore bars (Racey, 1990; Ghose, 1986) and existed from the Palaeocene to the Early Oligocene. The large, flat forms are common in deeper waters (up to 200m, Hallock and Glenn, 1986) on the outer ramp. An abundance of *Discocyclina* is indicative of proximity to a reefal environment (Racey, 1990).

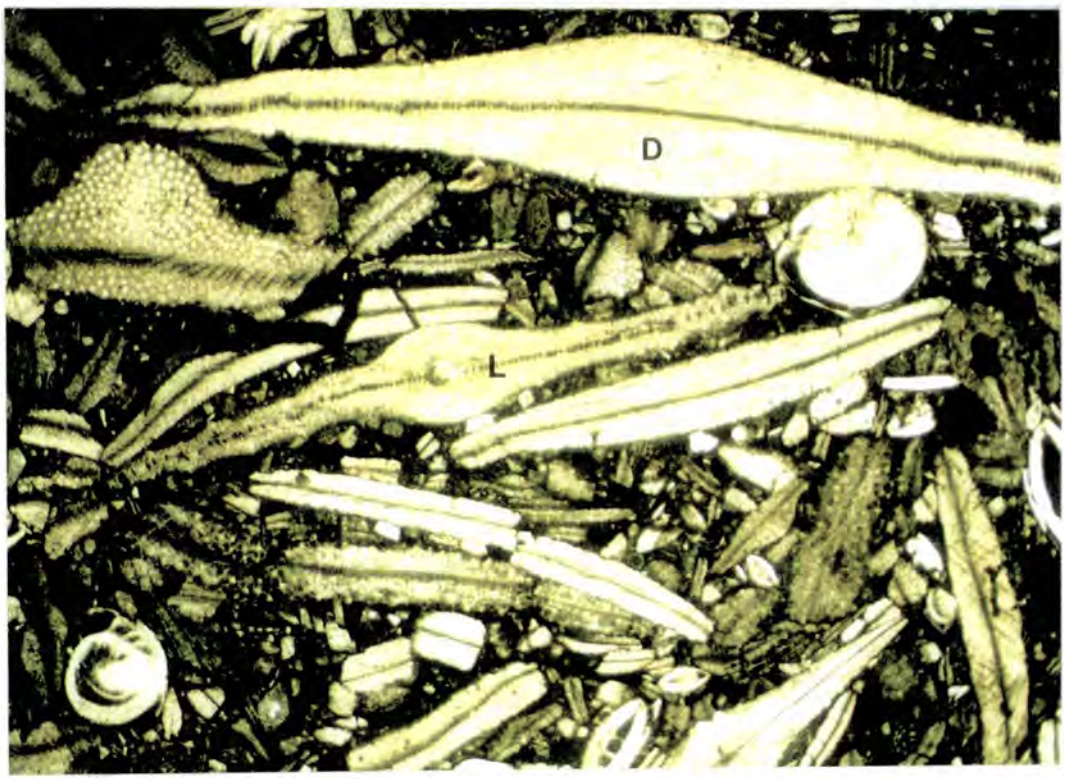

Fig. 2.3: Packstone containing inflated Discocyclina (D) and Lepidocyclina (L), recognisable by its inflated polar region. Field of view 12x7.2mm.

Lepidocyclina (Upper Eocene to Miocene) is also present, occurring along with *Discocyclina* and is recognisable by its inflated polar regions (Fig. 2.3).

2.2.3. *Amphistegina*

Amphistegina (Fig. 2.4) appeared during the Palaeocene and is rotaline, epifaunal and free-living, preferring a coarse carbonate-sand substrate. It typically lives in temperatures greater than 20°C but can tolerate temperatures as low as 14°C

(Murray, 1991). It is adapted to high energy conditions and thick-shelled, robust forms

Fig. 2.4: Small Amphistegina (A) showing asymmetry about the equatorial axis. Field of view 3x1.9mm.

are common in reefs and among algae and sea-grasses down to depths of 35m (Racey, 1990). Flatter species occur on the open shelf down to 130m (Hallock and Glenn, 1986). *Amphistegina* does not occur in restricted lagoons or deep waters.

2.2.4. Miliolidae

The Miliolidae (Fig. 2.5) are porcellanous and have existed since the Jurassic. They are epifaunal and free-living or occur clinging to plants and can live in normal marine to hypersaline conditions (32 - 65‰; Murray, 1991), tolerating cold to warm waters. They are typical of inner-shelf zones (Ghose, 1986) and are widely reported from back-reef lagoons. They are common in depths of between 6 and 9m and can be found in banks, near-shore shelves and intertidal areas. An abundance and low diversity of Miliolidae can indicate a protected environment, especially if associated with micritised bioclasts (Racey, 1990), though it must be noted that they are equally abundant in normal salinities and the associated bioclasts must be considered before assuming restricted conditions.

Fig 2.5: Algal limestone containing diverse Miliolidae (M). Note the porcellanous tests composed of dense micrite. Field of view 6x3.7mm.

2.2.5. Alveolinidae

Alveolinidae (Fig. 2.6) are also porcellanous and appeared in the Lower Cretaceous. They are characteristic of the inner ramp (Buxton and Pedley, 1989), inhabiting lagoons and protected embayments. They are capable of tolerating hypersaline conditions (up to 65‰) but are also common in normal-marine salinities.

2.2.6. Orbitolinids

The rotaline Orbitolinids (Lower Cretaceous to Upper Eocene; Fig. 2.7) are characteristic of shallow, warm waters (Loeblich and Tappan, 1964). During the Lower and Middle Cretaceous, the Orbitolinids were typical of the outer-platform and were used to subdivide shelf sediments (Flügel, 1982; Sartorio and Venturini, 1988). In the Palaeocene and Lower to Middle Eocene, the Orbitolinids and other Textulariina occurred with the Miliolidae on the shallow inner-platform (Sartorio and Venturini, 1988).

Fig. 2.6: Alveolinid, showing the micritic test and internal chambers infilled with calcite. Field of view 3x1.9mm.

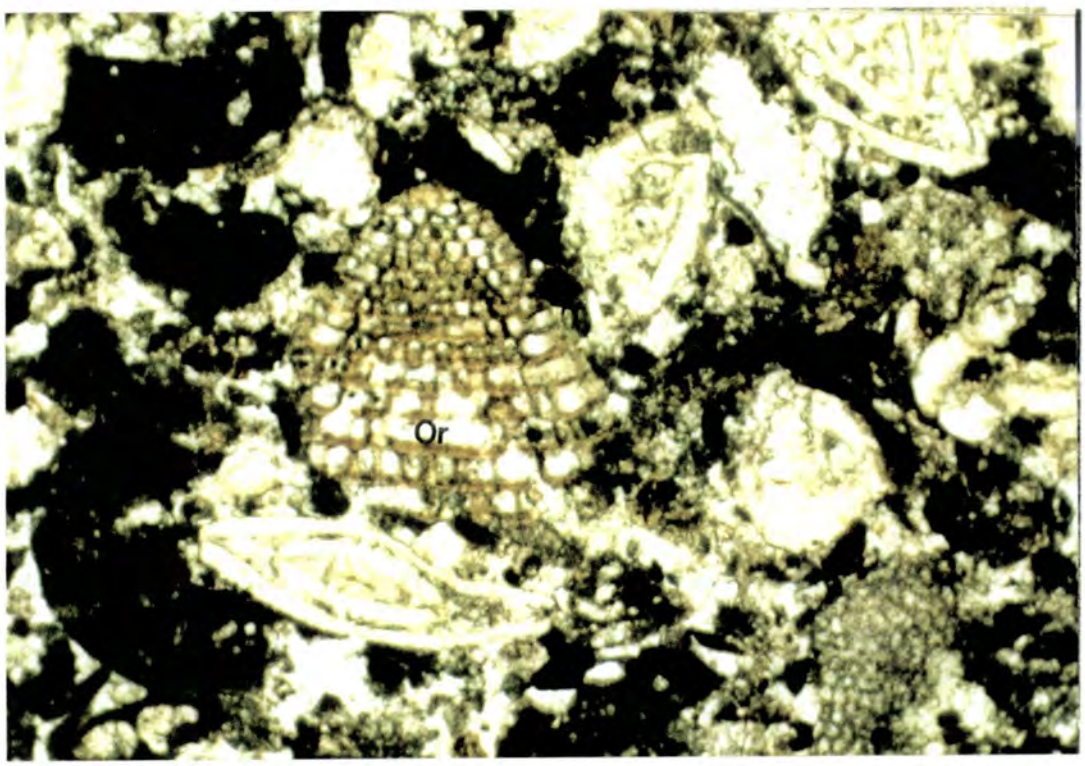

Fig. 2.7: Foraminifera packstone containing a conical Orbitolinid (Or). The test is slightly reddened and the internal chambers infilled with calcite. Field of view 3x1.9mm.

2.2.7. The use of larger foraminifera as environmental indicators

As has already been demonstrated above, a particular genus of foraminifera can be indicative of a certain environmental setting (for example, Alveolinids and Miliolids representing a protected lagoon). Others, however, can occur in a number of environments (*Nummulites, Discocyclina, Amphistegina*) but they commonly show a distinct change in size and shape within a given genus, or even species, in moving from one setting on the carbonate ramp to another (Hallock and Glenn, 1985, 1986;

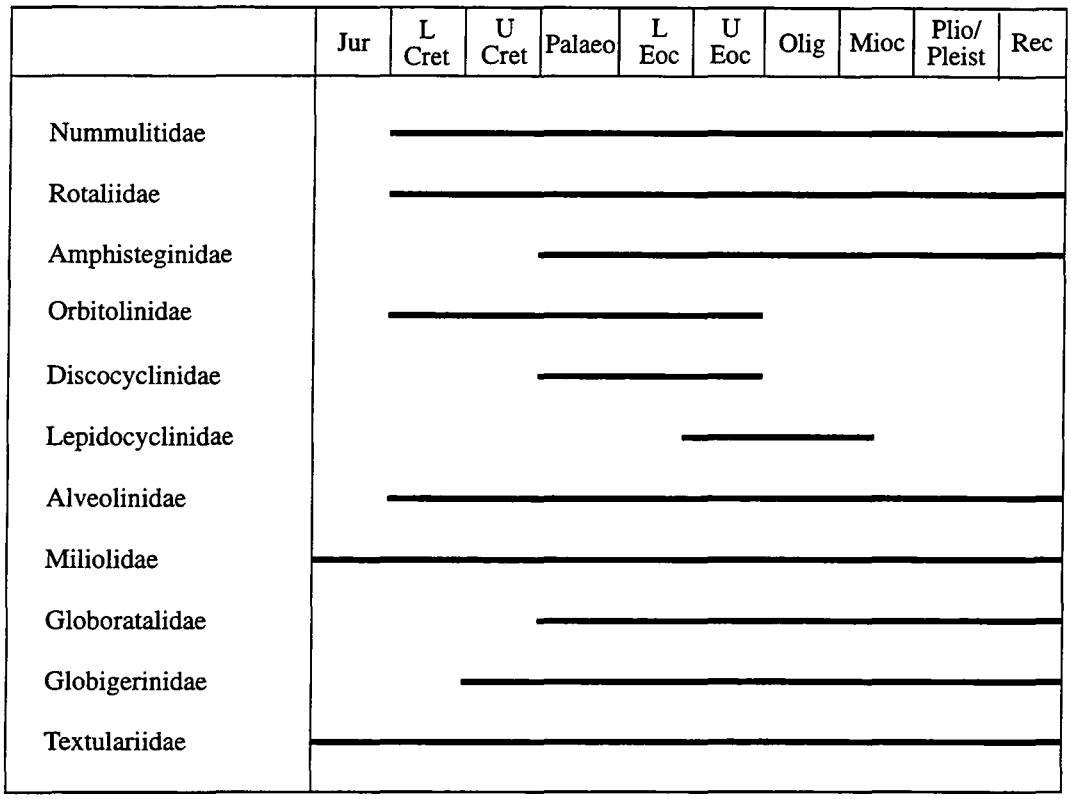

Fig. 2.8: Distribution in geological time of the main groups of foraminifera encountered in the Nummulitique (Loeblich and Tappan, 1964).

Hallock, 1979; Hottinger, 1983; Racey, 1990). This is governed by a number of external factors including light intensity, water energy, temperature, salinity and water depth. A brief discussion of the effects of these factors on the foraminifera follows, with an indication as to how this can be used in the palaeoenvironmental reconstruction of larger foraminifera bearing limestones.

2.2.7.1. Light intensity

Many large benthonic foraminifera are dependent on algal symbionts for photosynthesis, especially when nutrient supplies are scarce. This requirement restricts them to within the photic zone (up to 130m; Hottinger, 1983; Hallock and Glenn, 1986). In very shallow settings, the light intensity may be such that it would be

harmful to the organism and its symbionts, and the test thickness of foraminifera living in these environments tends to be greater in order to prevent the penetration of too much harmful radiation. Conversely, in low light environments, the foraminifera tend to develop thin, fragile tests which are advantageous in allowing as much light radiation to penetrate the test as possible. The tests of porcellanous foraminifera are more resistant to light penetration, and porcellanous forms tend to dominate over rotaline forms in environments with a high light intensity.

2.2.7.2. Water energy

This produces similar results to the effects of light intensity and the two factors are linked. Shallow waters, with a high wave energy, tend also to be those with the highest light intensity and the thick test developed helps to protect the symbionts not only from light penetration, but also to protect the organism itself from being damaged in a turbulent environment (Hallock and Glenn, 1986). A high water energy also promotes the development of a more robust shape able to withstand wave energy, as is demonstrated by *Nummulites* and *Amphistegina*. In lower energy conditions, flatter forms with thin tests dominate the fauna.

2.2.7.3. Water depth

The effects of light intensity and water energy along with the presence or absence of nutrients serve to promote a trend in test shape and size variations with depth. Shallow, light and high energy waters tend to be dominated by robust, thick-shelled foraminifera as described above. In waters with sufficient light and available nutrients, individuals will tend to mature fairly rapidly and reproduce at a relatively small size (Hallock and Glenn, 1986). In more stressed conditions, they grow more slowly and mature at a larger size and in some cases, particularly when shallow-water forms have been washed down-slope into nutrient-poor waters, giant individuals may develop as conditions are suitable to sustain growth but not to reach reproductive maturity. Therefore, the size of a given genus or species, as well as its shape, can be characteristic of water depth. This trend was noted by Hottinger (1983) in the Gulf of Aqaba, where small, robust, thick-shelled forms occur in shallow waters and large, flat, thin-shelled forms in deeper waters.

This can only be used as a factor for determining relative depth within a given genus as different genera attain different sizes and shapes at varying positions on the carbonate ramp. This is shown by the fact that *Discocyclina* is generally characteristic of deeper waters than *Nummulites* (Buxton and Pedley, 1989) and so robust forms of *Discocyclina* will be indicative of a position further down the ramp than the equivalent shape of *Nummulites*.

Water depth indications can also be misleading when cryptic conditions occur. This is due to the main controls on changes in morphology with depth being due to light intensity, nutrient availability and water energy. It must therefore be noted that low light, nutrient and water energy conditions, normally associated with an outer-ramp setting, can also occur in a sheltered, shallow-water environment, such as a lagoonal setting, protected from light and wave intensity by reefs or shoals. This environment will also be conducive to the development of flat, thin-shelled forms which would otherwise be assigned to an outer-ramp position. It is therefore important to consider the other bioclasts present in the sediment in order to be able to differentiate between these two settings.

2.2.7.4. Substrate

This is closely related to water turbulence (Hallock and Glenn, 1986) and may strongly affect the distribution of some groups (Racey, 1990), though others, especially smaller forms such as *Amphistegina*, are relatively unaffected (Hottinger, 1983).

Hard substrates (which are often laterally discontinuous) are colonised by sessile organisms such as corals and bryozoans and tend to be dominated by encrusting and free-living foraminifera (Hottinger, 1983; Hallock and Glenn, 1986; Racey, 1990).

Soft, low-energy substrates are dominated by sediment dwellers (Hallock and Glenn, 1986). Racey (1990) has noted for the Seeb Limestone in Oman, that the greatest abundance of foraminifera occurred on a muddy substrate as the presence of organic matter in the mud served as a supply of nutrients. Sandy substrates had the lowest abundance due to the instability of the substrate and a lack of nutrients.

Of the foraminifera present in the Nummulitique, only *Amphistegina* favours mud-free sands.

2.2.7.5. Salinity

Most modern, rotaline foraminifera are stenohaline, tolerating salinities of 30-45‰ (Blondeau, 1972; Hallock and Glenn, 1986; Racey, 1990). Porcellanous forms (miliolids and alveolinids) can survive in salinities of up to 65‰ (Murray, 1991). However, they are also common in normal-marine conditions, but an abundance and low diversity in conjunction with a lack of rotaline forms can indicate hypersaline conditions.

2.2.7.6. Use as environmental indicators

In general, small, robust, thick-shelled foraminifera (Fig. 2.9) are indicative of high-energy, shallow-marine environments, with high light intensity and sufficient nutrients, though it must be noted that too many nutrients may induce environmental stress on the foraminifera (Hallock and Schlager, 1986). Large, flat, thin-shelled foraminifera suggest a lower-energy environment, with a lower light intensity and fewer nutrients. Giant foraminifera develop when nutrient supply is sufficient to sustain growth, but does not promote reproduction. This typically involves shallow-water forms that have been washed into deeper ramp environments.

An abundance and diversity of rotaline foraminifera indicate a marine environment of normal salinity and a muddy substrate. A lack of rotalines and a high

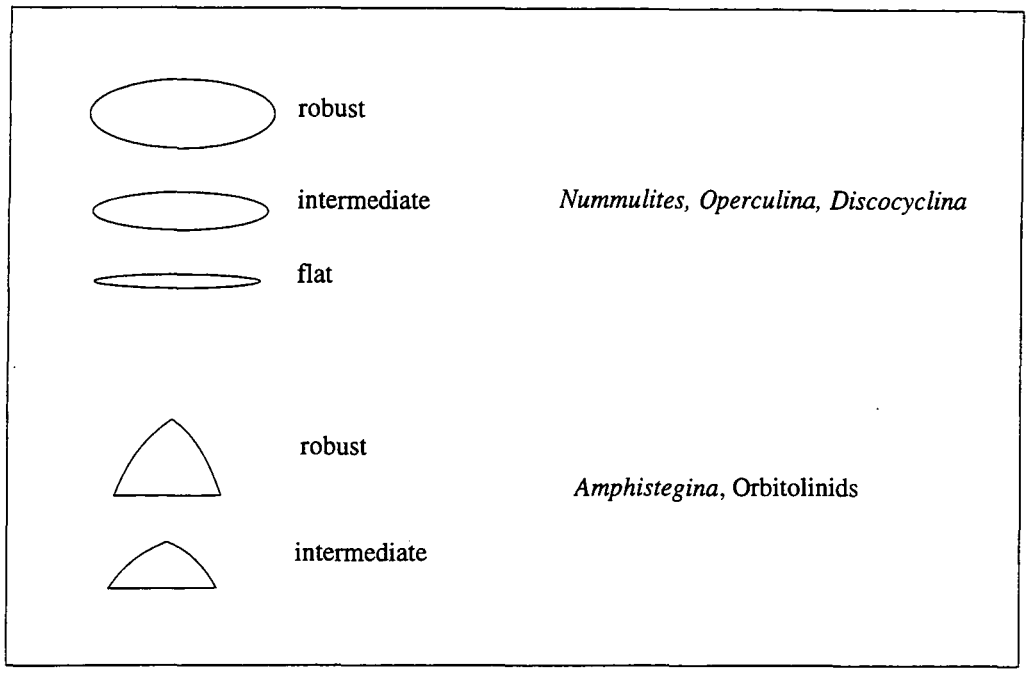

Fig. 2.9: Terminology used in the thesis to describe the forms of rotaline foraminifera.

abundance but low diversity of miliolids and alveolinids may be indicative of hypersaline conditions.

Therefore, the relative position of a facies on the carbonate ramp can be predicted by the presence, size and shape of a given genus, as demonstrated in Fig. 2.10. However, effects such as the presence of cryptic conditions (e.g. low light but shallow water depths) and the reworking of bioclasts down the ramp must also be taken into account in reconstructing the palaeoenvironments of larger foraminifera-bearing limestones.

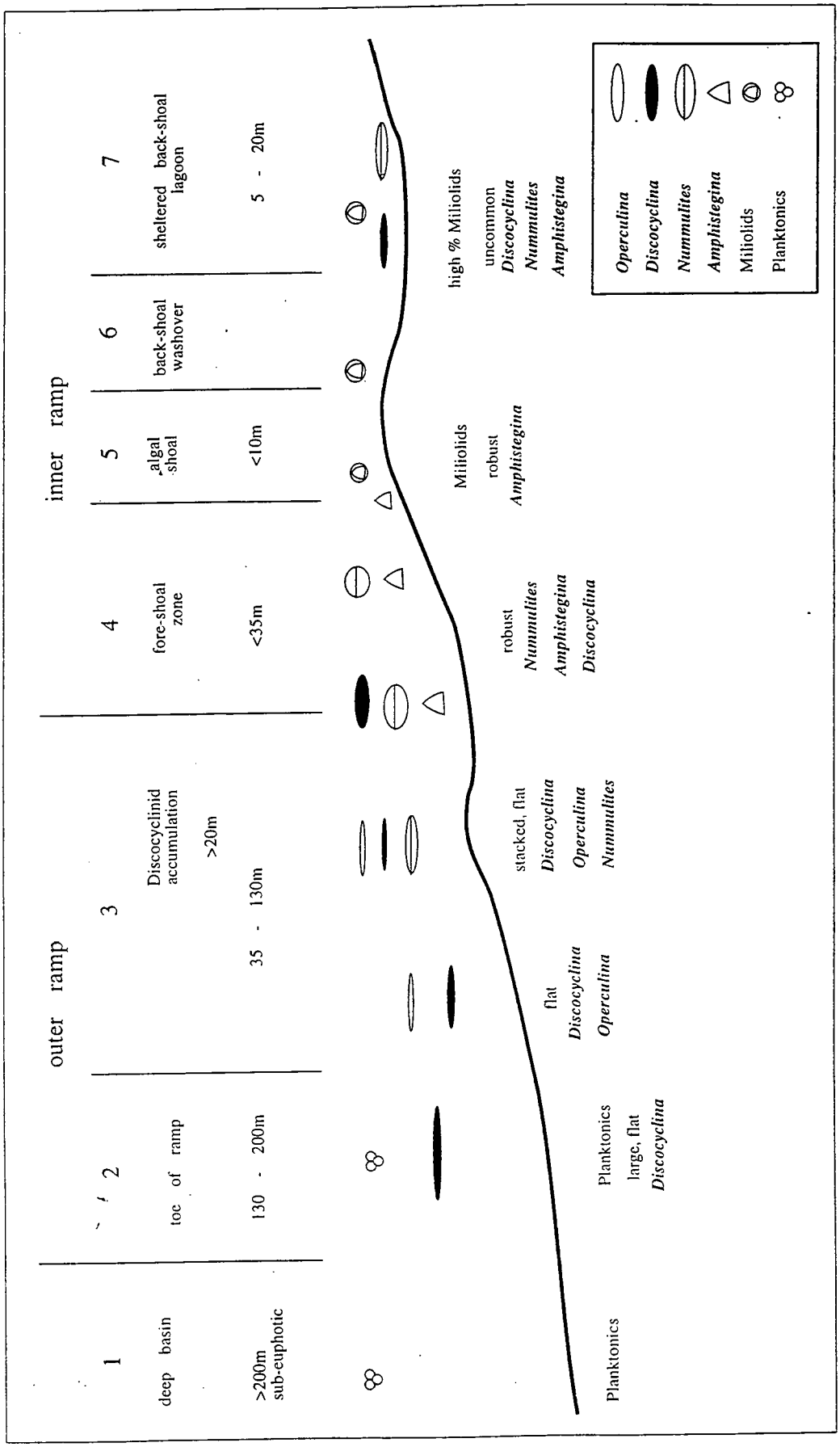

Fig 2.10: Distribution of foraminifera with depth in a carbonate ramp setting. Based on Hallock and Glenn (1986).

2.3. Red Algae

The Nummulitique, especially in Haute Savoie, contains abundant red algae (up to 50% of the sediment) in the form of crusts, rhodoliths and abraded debris. The dominant algae are the calcareous red algae (CRA), of which a number of genera have been identified (*Lithothamnium, Lithophyllum, Archaeolithothamnium, Mesophyllum).* Also present, in much smaller amounts, are the originally aragonitic Squamariacea.

The environmental interpretations based on these red algae have been derived from the available literature on both Recent and fossil forms, their distribution and morphology. Workers on the Miocene algal limestones (Bosence and Pedley, 1982; Bosence, 1985) have observed that the palaeoenvironments within these limestones are comparable with present day algal ridges and gravels (Coralligène of the Mediterranean; the Upper Coralline Algal Limestone, Malta). As little is known about Eocene algal growth habits and whether they were similar to those of the present day, a uniformitarian approach has been adopted in order to try and confirm the approximate depth zonations using the larger benthonic foraminifera as described above. In order to carry out this approach, identification has been attempted on a generic level (figs 2.11, 2.12, 2.13, 2.14) A summary of the main controls on the distribution of the algae present is outlined below.

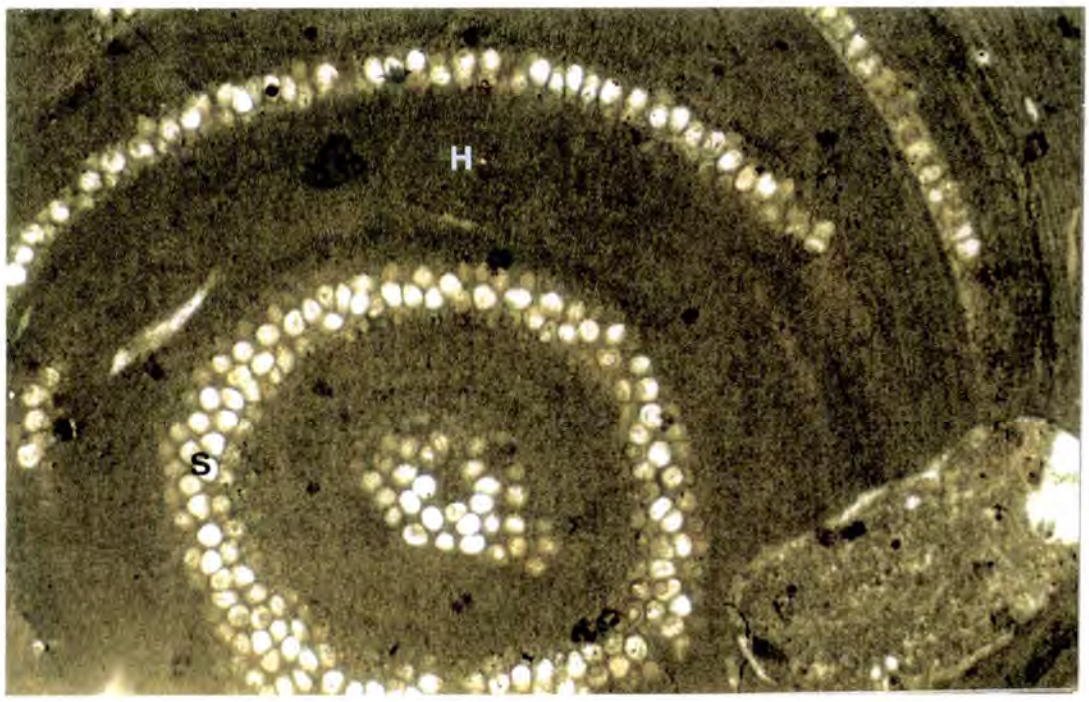

Fig. 2.11: Archaeolithothamnium, showing the characteristic sporangial sori (S) and multilayered hypothallium (H). Field of view 3x1.9mm.

2.3.1. Calcareous red algae (CRA)

Calcareous red algae occur in a variety of environments ranging from polar to tropical waters with normal-marine salinities and at depths from intertidal down to 200m (Johnson, 1961; Adey and McIntyre, 1973; Ghose, 1977). This wide range of depths and temperatures means that an environmental interpretation cannot be determined solely from the presence of these algae unless identification is carried out at least to a generic level.

The distribution of CRA is controlled by a number of external, physical factors including temperature, light, water depth, water agitation, substrate character, salinity and water clarity (Johnson, 1961). These factors are closely related and it is often not possible to distinguish between the effects. For instance, depth distribution is linked to light intensity, water clarity and temperature effects and substrate character is closely related to water agitation. This may result in a mistaken environmental interpretation as typically temperate forms can also be found in deep settings in sub-tropical or tropical waters (Adey and McIntyre, 1973).

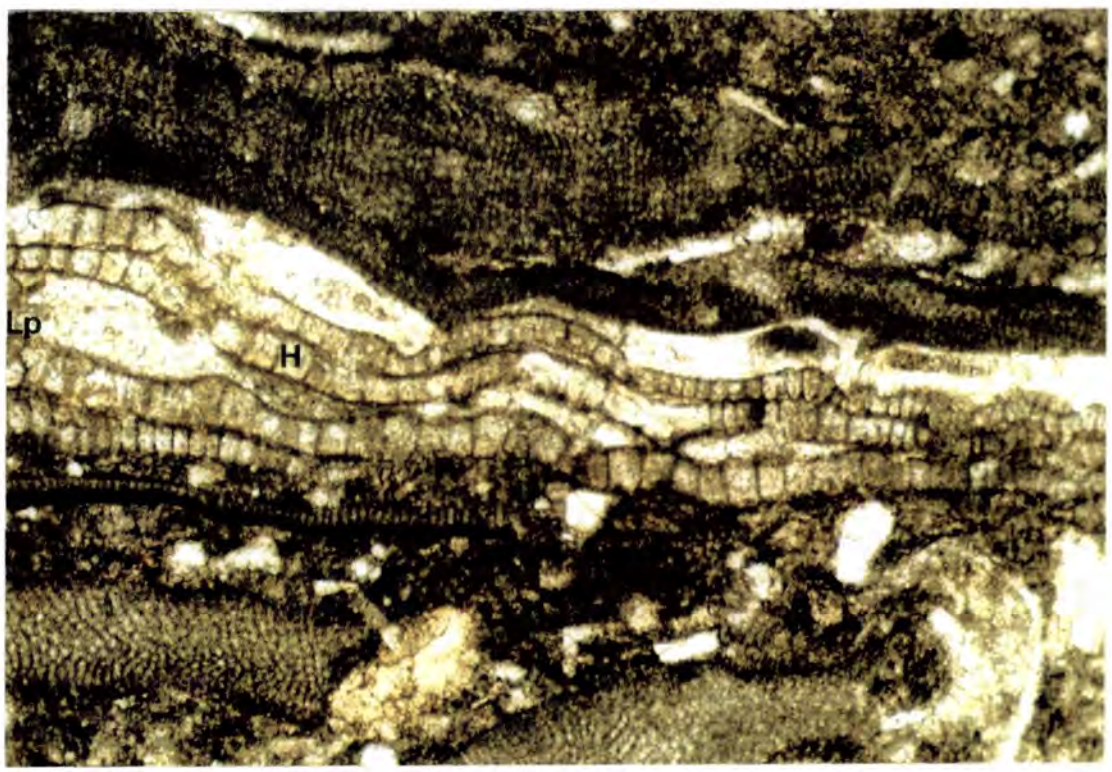

Fig. 2.14: Lithoporella encrustation (Lp) showing the typical large hypothallial cells (H). Field of view 1.3x0.8mm.

Fig. 2.12: Encrustations of Lithothamnium, showing multipored conceptacles (C) and the multilayered hypothallium (H).

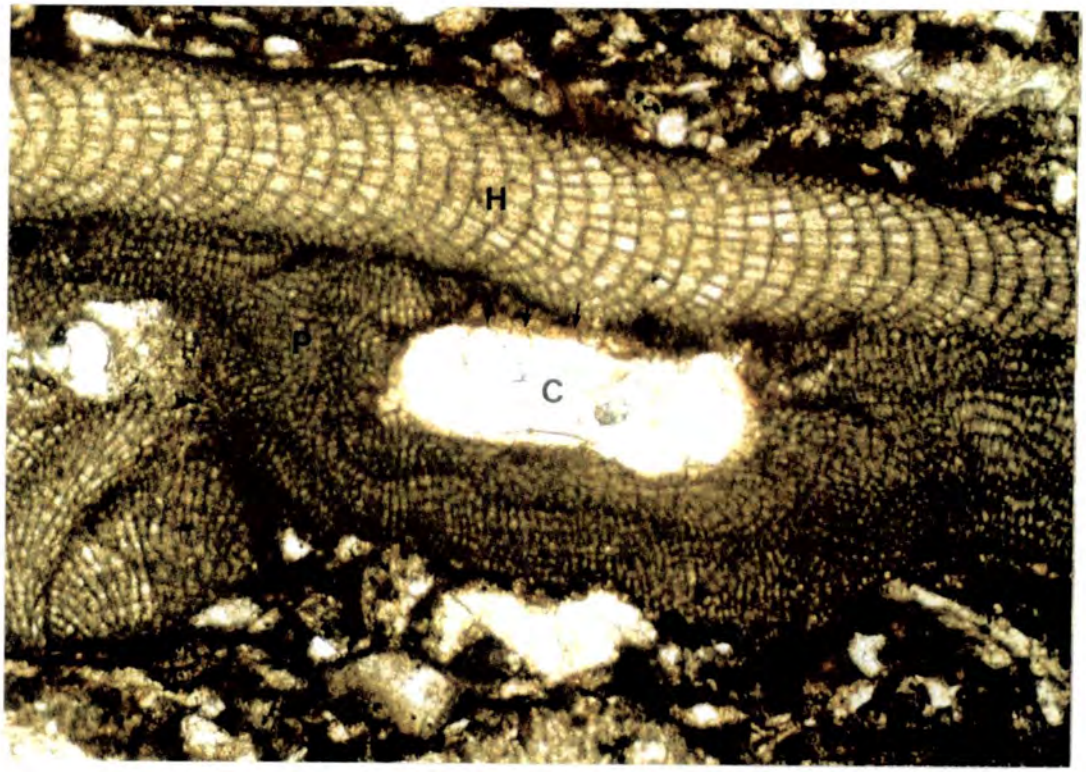

Fig. 2.13: Single crust of Mesophyllum, showing a thick perithallium (P) with multipored conceptacle (C) and coaxial hypothallium (H). Field of view 1.3x0.8mm.

2.3.1.1. Temperature

Temperature is important in controlling the geographical distribution of CRA (Fig. 2.15) and, to a certain extent, depth zonation (Johnson, 1961). A variation in the genera and species present has been observed with latitude by many workers (Johnson, 1961; Adey and MacIntyre, 1973; Wray, 1977; Bosence, 1985) with some forms restricted to warm, tropical and sub-tropical waters (*Lithoporella, Mesophyllum, Archaeolithothamnium, Tenarea*) and others to temperate and polar regions (*Leptophytum*). Other forms (*Lithothamnium, Lithophyllum*) are universally distributed on a generic level, with geographical zonation only occurring at a specific level. Specific identification has not been attempted in this study.

Of the genera identified within the Nummulitique, *Lithophyllum* and *Lithothamnium* are widely distributed in Recent sediments, and *Archaeolithothamnium* and *Mesophyllum* occur in warm water environments.

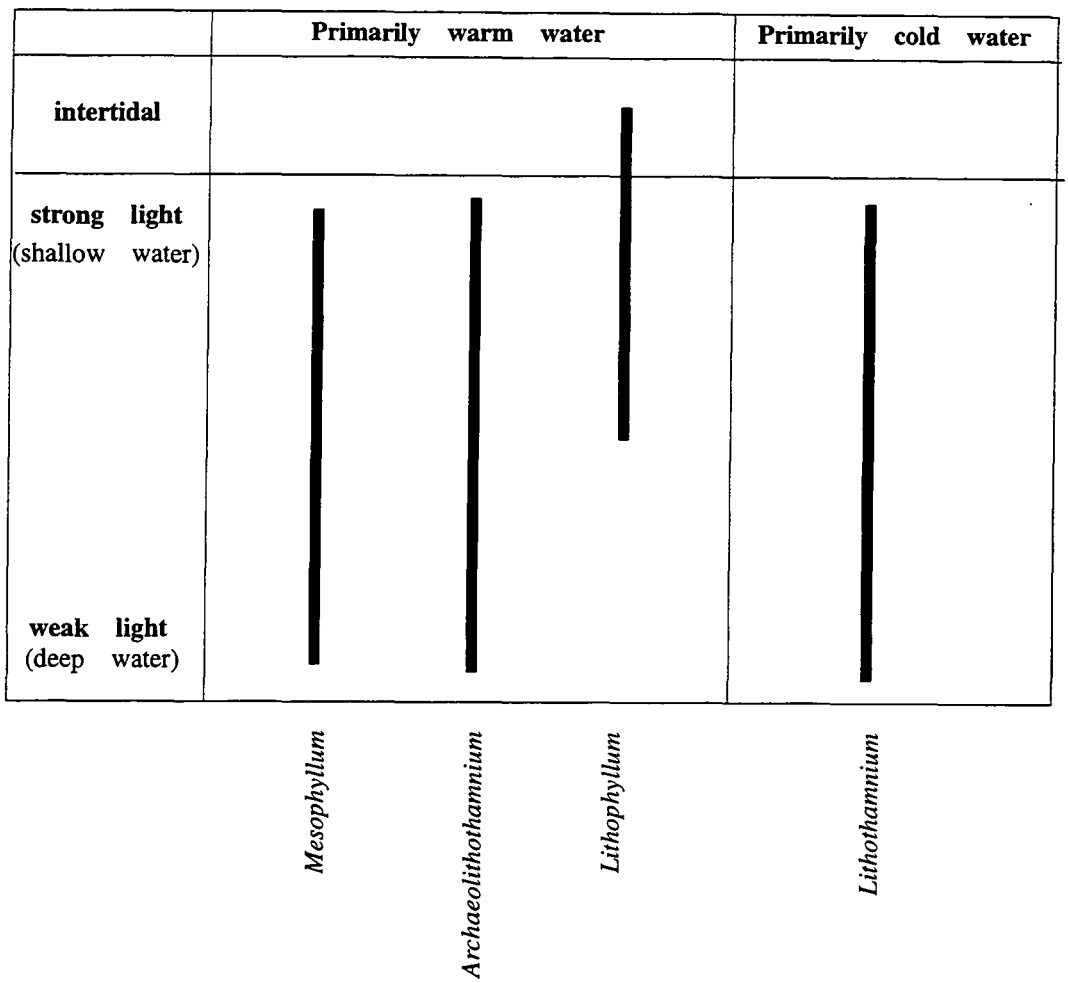

Fig. 2.15: Distribution with light, and therefore depth, of the principal genera of CRA in the Nummulitique (after Wray, 1977).

2.3.1.2. Light

Light is an important controlling factor, as, being plants, algae depend on light to carry out their basic metabolism via photosynthesis (Johnson, 1961). The toleration of light intensity varies (Fig. 2.15), with some species able to tolerate some subaerial exposure and others living towards the limit of the photic zone (Johnson, 1961; Ghose, 1977). However, the greatest development of algae occurs between low-tide level and 25m in agitated waters (Johnson, 1961).

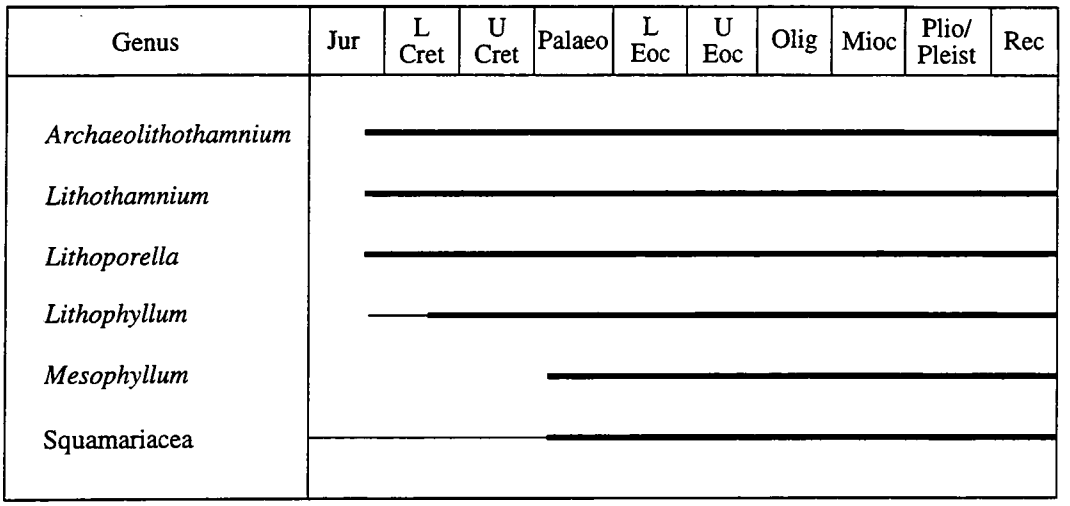

Fig. 2.16: Distribution in geological time of the main groups of calcareous algae encountered in the Nummulitique (after Wray, 1977).

2.3.1.3. Water Circulation

Water circulation promotes growth and the best development of algae occurs in waters with slight wave action and good circulation (Johnson, 1961). Water agitation also affects the growth form of a given genus of algae and this may even occur on a specific level.

High-energy, usually shallow-water (low tide to 30m) environments are characterised by densely branching, rounded heads of algae (Johnson, 1961; Bosence, 1985). This is seen at Bikini Atoll where dense, algal crusts form a narrow rim which serves to protect the rest of the reef from intense wave action. The more protected, but still agitated zone is dominated by encrusting forms with free nodules and a looser network of branches.

Low-energy environments, such as lagoons and deep water, are characterised by open, delicately branching frameworks and crusts (Bosence and Pedley, 1982; Bosence, 1985).

2.3.1.4. Substrate

Most crustose corallines prefer a hard, rocky substrate to which they are firmly attached (Johnson, 1961), though they can also grow on firm sand and attached to other organisms such as sea-grasses, coral and shell fragments. Rhodoliths and free-living corallines tend to develop on soft substrates (Adey and MacIntyre, 1973) providing there are skeletal fragments large enough to initiate algal growth.

2.3.2. Squamariacea

The Squamariacea (Fig. 2.17) are also red algae, but were originally composed of aragonite rather than calcite, though some forms may undergo calcification. They exhibit similar growth forms to CRA and living forms mainly occur in tropical and subtropical regions. Their typical depth range is from low tide level to a few metres, and they have been described from depths down to 30 - 50m in the Caribbean (Wray, 1977). Most Squamariacea need a firm substrate and occur as sheet-like crusts. Articulated forms have been found on soft substrates in the Mediterranean (Wray, 1977).

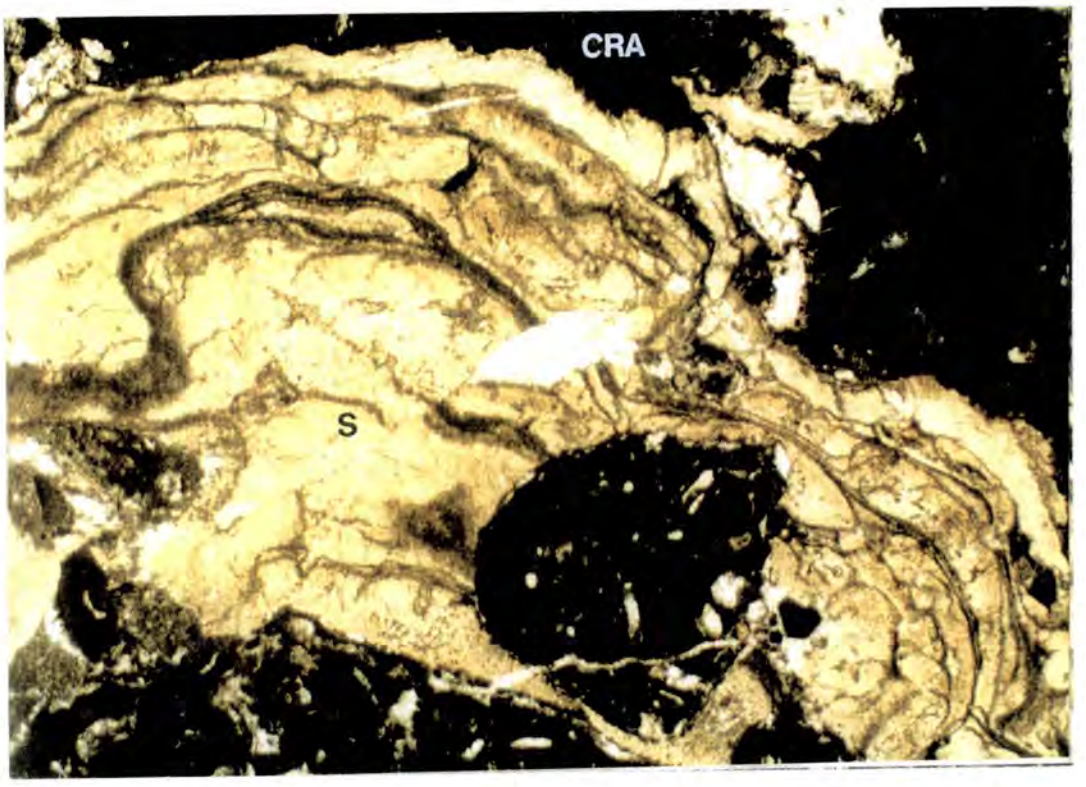

Fig. 2.17: Multiple encrustation of a Squamariacea (S), showing the characteristic creamy colour in thin section contrasting with the black micrite of the originally calcitic CRA. Field of view 2x3.7mm.

In thin section they are distinct from CRA in that they are a clear, creamy colour as opposed to the opaque micritic appearance of the CRA. In the

Nummulitique, they can be seen to have grown, associated with CRA, in multilayered crusts and rhodoliths.

2.3.3. Rhodoliths

Rhodoliths are a further form in which red algae can occur (Fig. 2.18). Bosence (1983) defined rhodoliths as "nodules and unattached branched growths with a nodular form composed principally of coralline algae". They occur in the same wide range of environments as the crustose CRA, as they are controlled by the factors needed for algal growth described above. They typically occur in depths of less than 100m, but have been described from depths down to 220m (Bosellini and Ginsburg, 1971; Bosence, 1983).

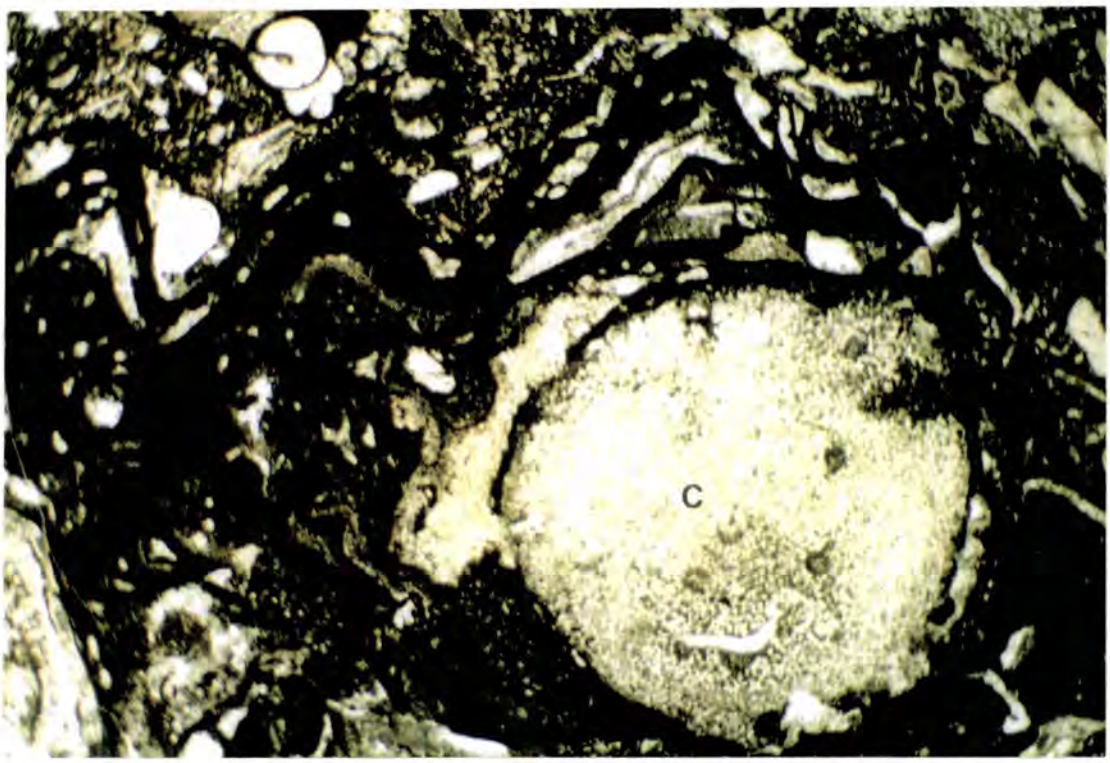

Fig. 2.18: Rhodolith, showing multiple encrustations of CRA around a coral fragment (C). Field of view 12x7.2mm.

Rhodoliths can form in relatively soft sediment, providing there are sufficiently large fragments on which algal growth can nucleate, and that the water agitation is able to turn the rhodolith in order to promote continued growth on all sides of the nodule (Bosence, 1983). Once established, however, a rhodolith bottom can support itself through fragmentation and further growth (Adey and MacIntyre, 1973).

Temperate and polar rhodoliths occur as maerl (algal gravels and unattached algae) which form in depths down to 27m in clear, sheltered waters as around the modern coasts of Britain and France (Adey and MacIntyre, 1973; Bosence, 1983).

Deeper water rhodoliths in modern seas are commonly dead, relict algal nodules and are interpreted to have formed during times of lower sea-level (Bosence, 1983). In the tropics, rhodoliths occur in a reefal environment in the fore-reef zone, on reef flats and in reef channels (Bosence, 1983; Johnson, 1961) and in back-reef sea-grass beds (Bosellini and Ginsburg, 1971).

Rhodolith morphology is controlled primarily by water agitation, with delicate, branching rhodoliths occurring in sheltered environments with little water agitation, and dense, ball-like forms in higher energy, agitated waters (Bosence, 1983; Bosellini and Ginsburg, 1971).

2.4. Biostratigraphic Dating of the Nummulitique

2.4.1. Infranummulitique

In both field areas, the Infranummulitique occurs above the Upper Cretaceous limestones (Senonian) and below the marine Nummulitic Limestone. However, due to the lack of fauna in the lower, conglomeratic units of the member, precise dating is difficult. Due to the diachroneity of the Nummulitique around the Alpine Arc, the chronostratigraphy of the two field areas studied will be considered separately.

2.4.1.1. Haute Savoie

The substratum in Haute Savoie consists dominantly of Senonian micrites, which have been dated as Coniacian to Upper Maastrichtian (Chaplet, 1989). The contact between the Infranummulitique and the substratum is erosional and represents a sufficient time gap which permitted uplift of the Cretaceous and subsequent erosion under subaerial conditions (Chapter 6). Therefore, the maximum time period possible for the deposition of the Infranummulitique sediments occurs between the top Maastrichtian and the Upper Priabonian of the overlying Nummulitic Limestone. The probable ages of the individual units encountered in the area are discussed below and are shown in the chronostratigraphic diagram in Fig. 2.19.

Sheet conglomerates and *Microcodium* wackestone

The first deposits of the Infranummulitique in Haute Savoie are sheet conglomerates and *Microcodium* wackestone (Chapter 3). The sheet conglomerates contain a very sparse fauna (bivalve fragments) which cannot be dated. However, they do contain clasts of a limestone containing large *Nummulites*. This limestone outcrops *in situ* at Arâches, preserved in a faulted graben and its fauna has been dated as Middle Lutetian to Biarritzian (Pairis and Pairis, 1975; Chaplet, 1989). Thus, the sheet conglomerates necessarily post-date this earlier transgression in order for uplift and

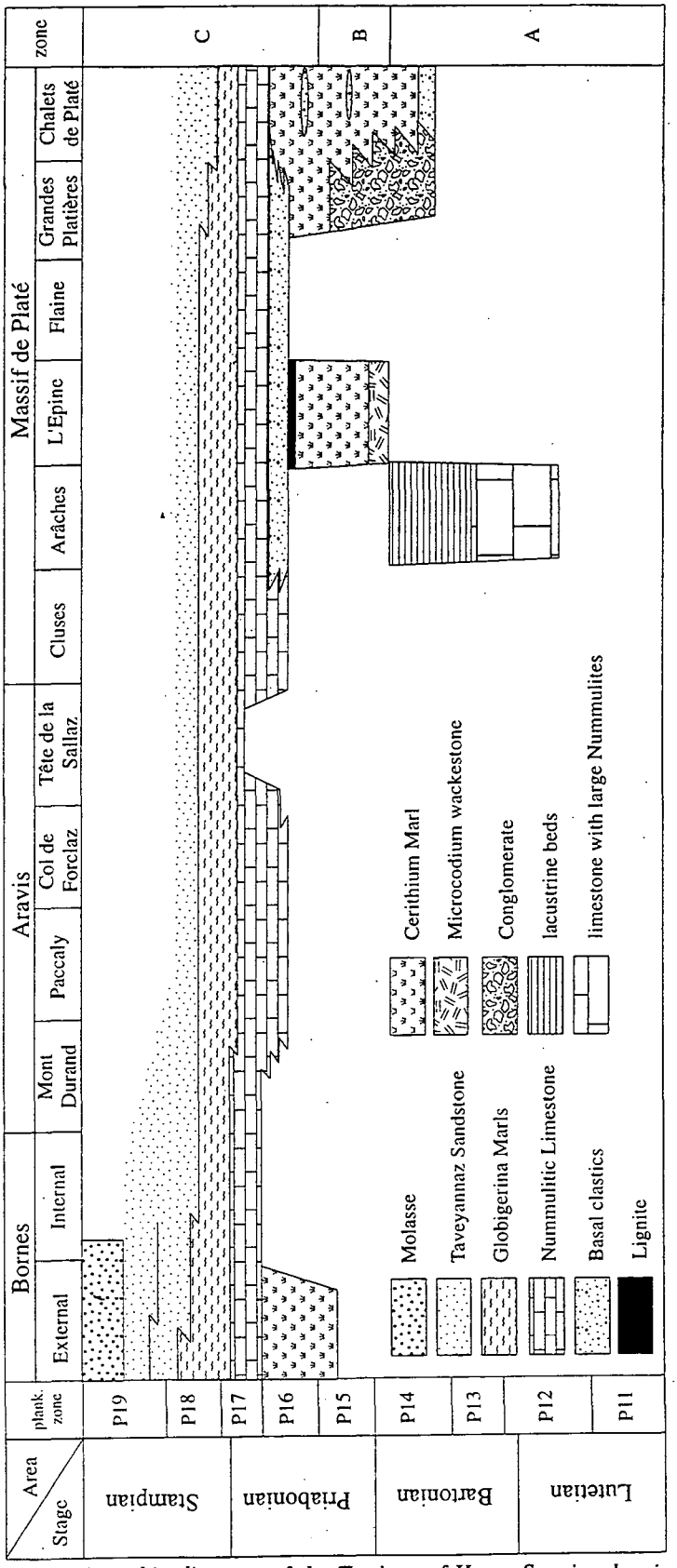

Fig. 2.19: Chronostratigraphic diagram of the Tertiary of Haute Savoie, showing the distribution in time and space of the facies encountered during basin development. Note the deposition of the Infranummulitique in depositional lows which were subject to the earliest stages of transgression, and the blanketing of this effect by the Nummulitic Limestone. There is an overall younging of all facies from east to west. Data from Pairis and Pairis (1975), Debrand Passard et al. (1984), Pairis (1988), Lateltin and Müller (1987), Chaplet (1989), Weidmann et al. (1991).

erosion of the sediment to have occurred. Similarly, the *Microcodium* wackestone contains clasts of micrite that contain charophytes, which are thought to have been eroded from the Lutetian to Priabonian lacustrine deposits described by Pairis and Pairis (1975) that overlie the limestone with large *Nummulites*. Therefore the oldest possible age for the sheet conglomerates and *Microcodium* wackestone is Late Biarritzian (Late Bartonian) to Priabonian, i.e. significantly younger than the Upper Lutetian age proposed by Pairis (1988).

***Cerithium* marl**

The *Cerithium* marl overlies the conglomerates and contains an abundant fauna of gastropods (including *Cerithium diaboli* which is typically Priabonian), bivalves and some vertebrate remains which have been used to constrain its age. Pairis (1988) originally placed the *Cerithium* marl as basal to Upper Bartonian, based on the relationship with the Nummulitic Limestone. Weidmann et al. (1991) discovered several species of mammal teeth of the genus *Palaeotherium* within the marls which they used to constrain further the biostratigraphy. They were able to obtain a more precise date on the unit due to the co-existence of species of *Palaeotherium* that characteristically occur around the "Grande Coupure"; a major boundary in mammalian biostratigraphy that occurred at the Eocene/Oligocene boundary. The presence of these species indicates a Priabonian age for the marl, and the co-existence of species points more precisely to an Upper Priabonian age for the top beds of the *Cerithium* marl (MP 20, St Capraise level).

Age of the Infranummulitique

Based on the data outlined above, the age of the Infranummulitique can be constrained by the dates of the two marine transgressions in the area that resulted in the deposition of Nummulitic Limestone. The lowest limit of the basal beds occurs above the Lutetian to Upper Bartonian transgression, and the top of the *Cerithium* marl is dated as Upper Priabonian, which corresponds with the subsequent transition into Upper Priabonian Nummulitic Limestone.

2.4.1.2. Haute Provence

Again, a problem is encountered in defining the age of the sediments due to the lack of fauna in the basal part of the member, and that present in the upper part evolving too slowly to provide an accurate age for the sediments (Bodelle, 1971). The probable ages of the individual units are shown in Fig. 2.20.

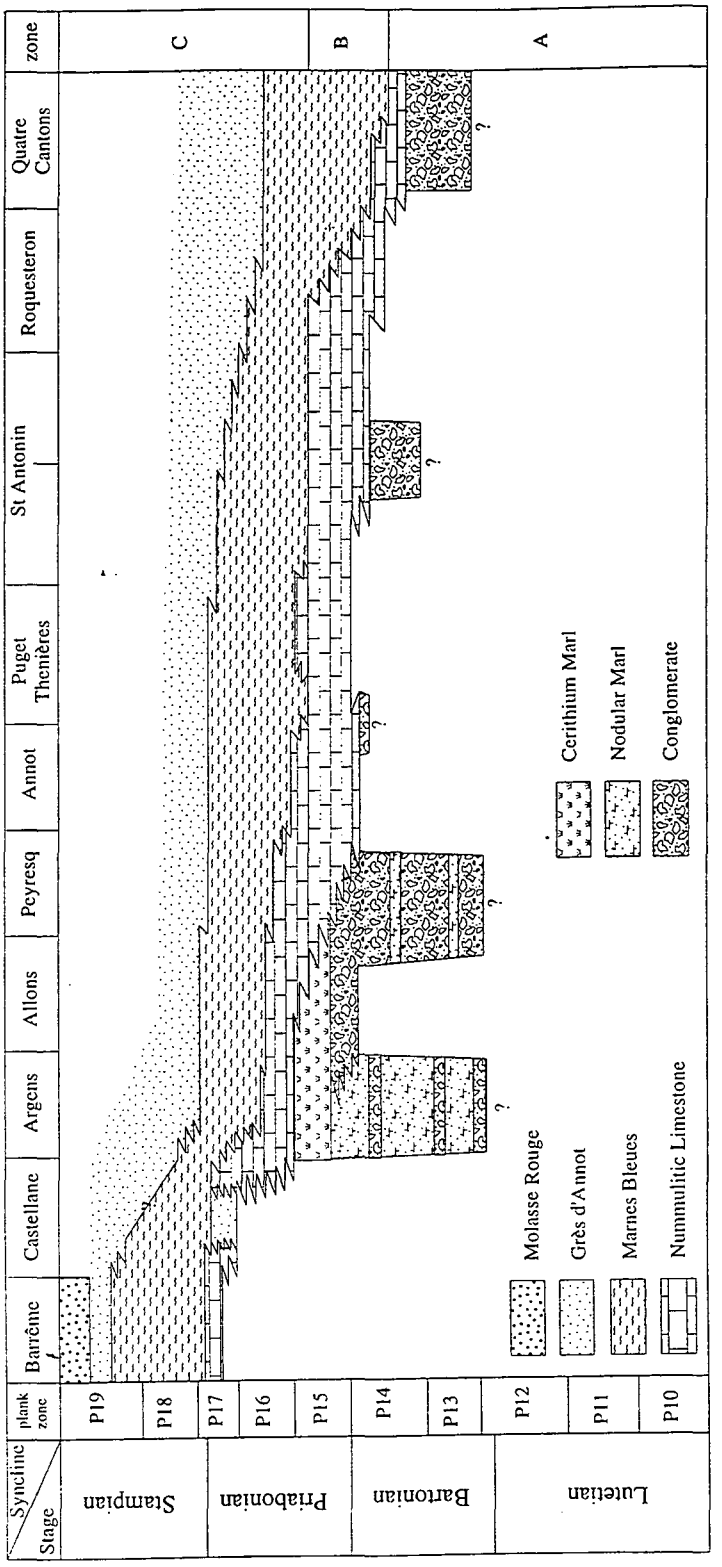

Fig. 2.20: Chronostratigraphic diagram of the Tertiary of Haute Provence, showing the distribution of the facies present. The Infranummultique is developed in depositional lows subject to the early stages of transgression, with the younger Cerithium marls deposited contemporaneously with the Nummulitic Limestone. There is a marked younging of the facies from east to west and the succession as a whole is older than that encountered in Haute Savoie. Data from Bodelle (1971), Bodelle and Campredon (1968), Campredon (1977), Mougin-Grosso and Pairis (1973), Apps (1987), Thomes (1987).

Lenticular conglomerates

The lenticular conglomerate/nodular marl facies association at Argens overlies the Maastrichtian sediments of the Upper Cretaceous. The uppermost sediments in the unit are thought to be of a similar age to the overlying Nummulitic Limestone (Apps, 1987), i.e. Upper Lutetian to Priabonian. Therefore, the maximum age range for the deposition of the lenticular conglomerate unit would be Upper Maastrichtian to Upper Lutetian. However, there must have been a sufficient time gap between the deposition of the Upper Cretaceous and the Infranummulitique for uplift, erosion and redeposition of Cretaceous clasts. Considering this and the transition to the overlying Nummulitic Limestone, the sediments were probably deposited during the Lower to Middle Eocene.

Massive conglomerates

The massive conglomerates at Peyresq also contain a very sparse fauna. However, a heavily abraded *Nummulites* was found in the matrix at the base of the unit, which indicates that deposition necessarily occurred during the Eocene, and considering the transitional relationship with the overlying Nummulitic Limestone, probably during the Lutetian to Bartonian.

***Cerithium* marl**

The *Cerithium* marl contains a more diverse fauna of molluscs and some vertebrate remains. The transitional relationship with the overlying Nummulitic Limestone suggests that deposition occurred just prior to the deposition of the marine beds (Apps, 1987), i.e. Upper Lutetian to Priabonian in the eastern synclines, and Priabonian to the west (Bodelle, 1971). A *Palaeotherium* tooth was discovered in the cover of the Argentera massif further east which was dated as Bartonian (Weidmann et al., 1991) and the marl contains *Cerithium diaboli* which is typically Priabonian (Bodelle and Campredon, 1968).

Age of the Infranummulitique

The age of the basal conglomerates is uncertain, but deposition must have taken place post-Maastrichtian due to the uplift and erosion of sediments of that age forming the substratum in the area. The massive conglomerates at Peyresq can be better constrained as being deposited during the Eocene, and this age also seems likely for the lenticular conglomerates at Argens, taking into consideration the transition with the overlying *Cerithium* marl, dated as Lutetian to Priabonian.

2.4.2. Nummulitic Limestone

2.4.2.1. Haute Savoie

Biostratigraphical studies of the area have placed the Nummulitic Limestone as Upper Priabonian, based on their faunal content and relationship with the Infranummulitique. The species of *Nummulites* encountered in the formation and identified by Pairis and Pairis (1975) and Lateltin and Müller (1987) are shown in Fig. 2.21 along with their geological distribution (Schaub, 1981; Pairis, 1988). A slight younging is seen from the southern end of the Desert de Platé to the Thônes Syncline, with the older *Nummulites brongniarti, N. striatus* and *N. praefabianii* being absent from the Thônes Syncline sections (Lateltin and Müller, 1987).

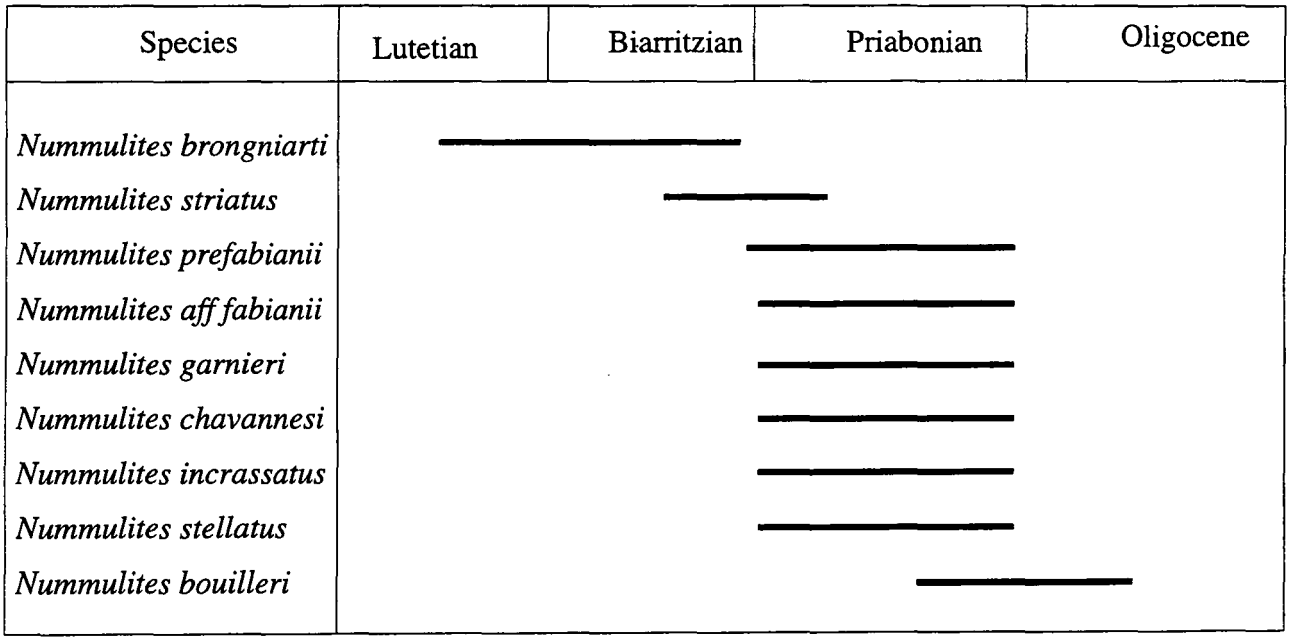

Fig. 2.21: Geological ranges of the species of Nummulites encountered in the Nummulitic Limestone in the Massif de Platé and the Thônes Syncline, Haute Savoie (Pairis and Pairis, 1975; Lateltin and Müller, 1987). Age data from Pairis (1988) and Schaub (1981).

Pairis (1988) has shown an overall younging of the stratigraphy across the area from east to west. This trend is shown in Fig. 2.19, which combines his data with that published by Debrand-Passard (1984), Pairis and Pairis (1975), Lateltin and Müller (1987), Chaplet (1989) and Weidmann et al. (1991).

The preserved remnants of the earlier transgression at Arâches and Le Rocher Blanc contain an Upper Lutetian (Biarritzian) assemblage (Pairis and Pairis, 1975; Schaub, 1981; Pairis, 1988; Chaplet, 1989) which is illustrated in Fig. 2.22. This early limestone is separated from the Priabonian limestone by a succession of Lutetian to Priabonian lacustrine sediments (Pairis and Pairis, 1975).

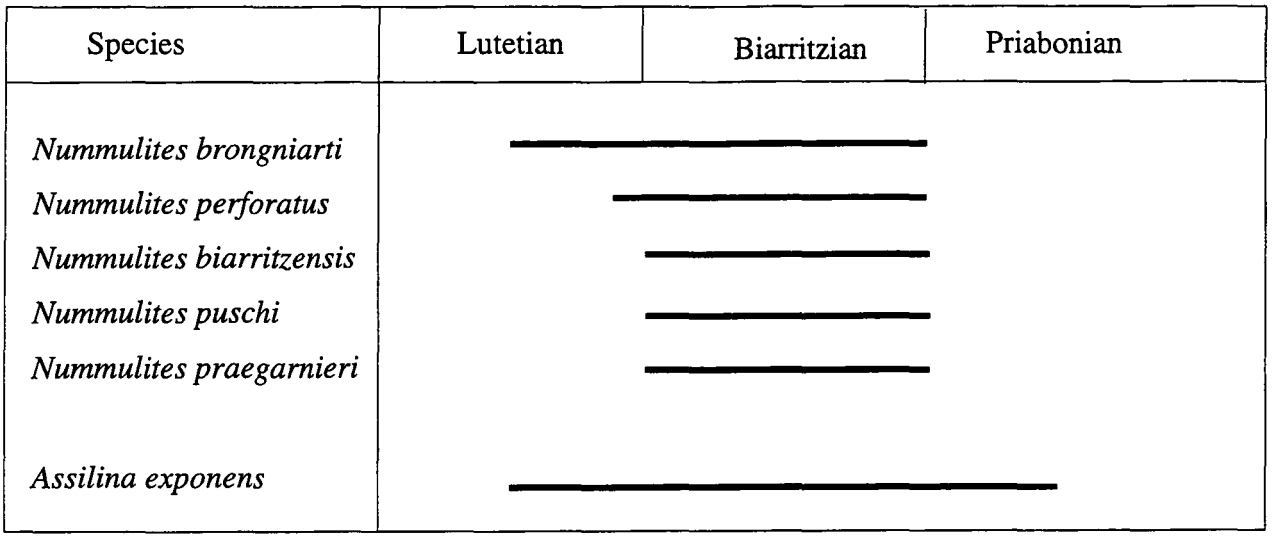

Fig. 2.22: Geological ranges of the species of Nummulites and Assilina encountered in the lower Nummulitic Limestones at Arâches, Massif de Platé (Pairis and Pairis, 1975). Age data from Pairis (1978) and Schaub (1981).

The overlying Globigerina Marls have been dated as Upper Priabonian to Lower Oligocene on the basis of benthonic and planktonic foraminiferal assemblages and palynological associations, with the majority of the formation occurring in the Lower Oligocene (Collet and Lillie, 1938; Charollais et al., 1980).

2.4.2.2. Haute Provence

Biostratigraphical studies (Bodelle, 1971; Mougin Grosso and Pairis, 1973; Campredon, 1977) have placed the Nummulitic Limestones in the Upper Lutetian to Priabonian based on the foraminiferal assemblage. Bodelle (1971) divided the assemblage into three zones, with Zone A corresponding to the Lower Lutetian, Zone B to the Bartonian and Zone C to the Priabonian.

In general a younging is seen from south to north and from east to west (Campredon, 1977), with the thicker Zone B sections occurring in the south and east (Fig. 2.20). Zone A is not encountered in the study area. In the study areas, the St Antonin sections have the thickest Zone B successions, and it is seen to be still present at the base of the limestone in the Annot and Agnère Synclines. The limestone in the more northern Allons and Argens Synclines occurs within Zone C, i.e. Priabonian. The top of the formation has been dated as Priabonian across the entire study area. The species of *Nummulites* identified in the succession (Bodelle, 1971; Mougin Grosso and Pairis, 1973; Campredon, 1977; Thomes, 1987) are shown in Fig. 2.23. along with their geological distribution (Schaub, 1981).

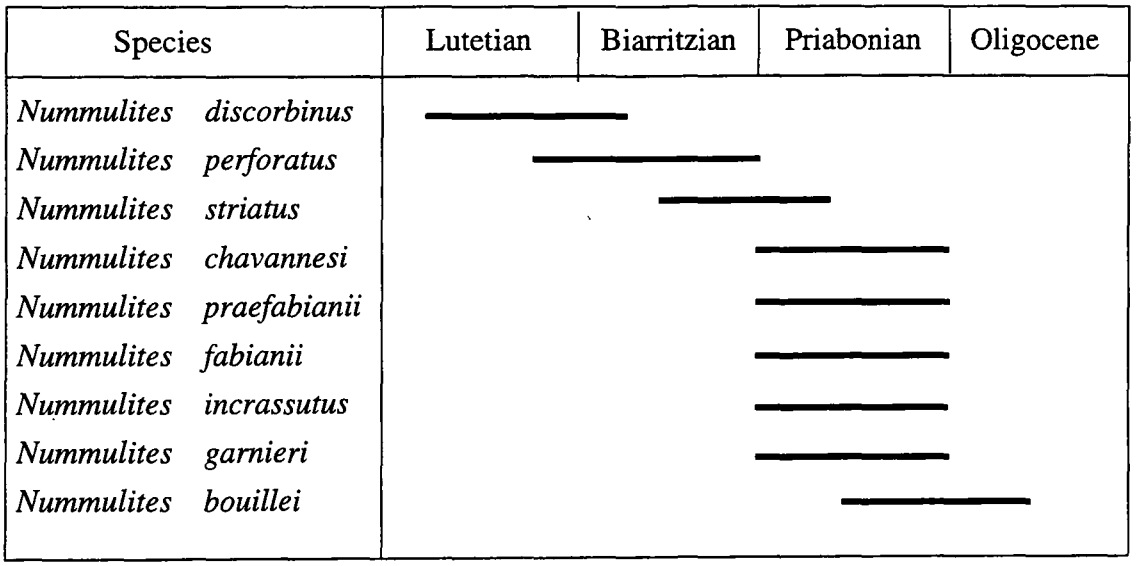

Fig. 2.23: Geological ranges of the species of Nummulites encountered in the Nummulitic Limestone in Haute Provence (Bodelle, 1971; Mougin Grosso and Pairis, 1973; Campredon, 1977). Age data from Pairis (1988) and Schaub (1981).

The base of the Marnes Bleues has been dated as Upper Eocene across the whole area and there is no evidence for the marls extending into the Oligocene (Bodelle, 1971). However, Campredon (1977) has dated the top of the marls in the Annot and Puget-Thenières Synclines as occurring just above the Eocene/Oligocene boundary, with the majority of the succession occurring in the Upper Eocene.

Chapter 3

The Infranummulitique

3.1. Introduction

The Infranummulitique is the term given to the coarse-grained, allochthonous carbonates that were deposited beneath the Nummulitic Limestone. The Infranummulitique has been studied previously by Pairis and Pairis (1975), Bodelle (1971), Campredon (1977), and Apps (1987) in terms of sediment descriptions, distribution and stratigraphy. This study has integrated the existing literature with additional field study in order to refine the facies analysis and new interpretations of the depositional environments are presented. Sedimentary section measurement has revealed the cyclicity within the sediments, which has been used to determine the relative sea-level variations during the deposition of the Infranummulitique (Chapter 7). This analysis has been carried out in order to be able to gain a more complete understanding of the controls on sedimentation during the onset of subsidence of the basin, and to put the sediments of the Infranummulitique into the overall context of the developing Alpine Foreland Basin.

The Infranummulitique is of particular interest in that field studies by the above workers have shown that its localised distribution (Figs 3.1, 3.2) is due to topographic and structural lows in the substratum which are thought to have been the first areas affected by the transgression during early basin subsidence. This limited distribution is interpreted to represent depositional rather than erosional remnants (Apps, 1987) and therefore the distribution and facies of the Infranummulitique can provide an insight into the inherent topography on the surface of the Mesozoic substratum at the time of deposition. The Infranummulitique can be divided into four characteristic units dominated by coarse and fine-grained terrigenous carbonates. This chapter outlines the facies associations and depositional environments of the four units and suggests a depositional model for this early phase of foreland basin sedimentation.

3.2. Lenticular Conglomerate/Nodular Marl

The lenticular conglomerate/nodular marl facies association is only encountered in Haute Provence. Thick successions are not commonly developed, though a vertical section 40m thick is developed on the road to Argens (Log P1).

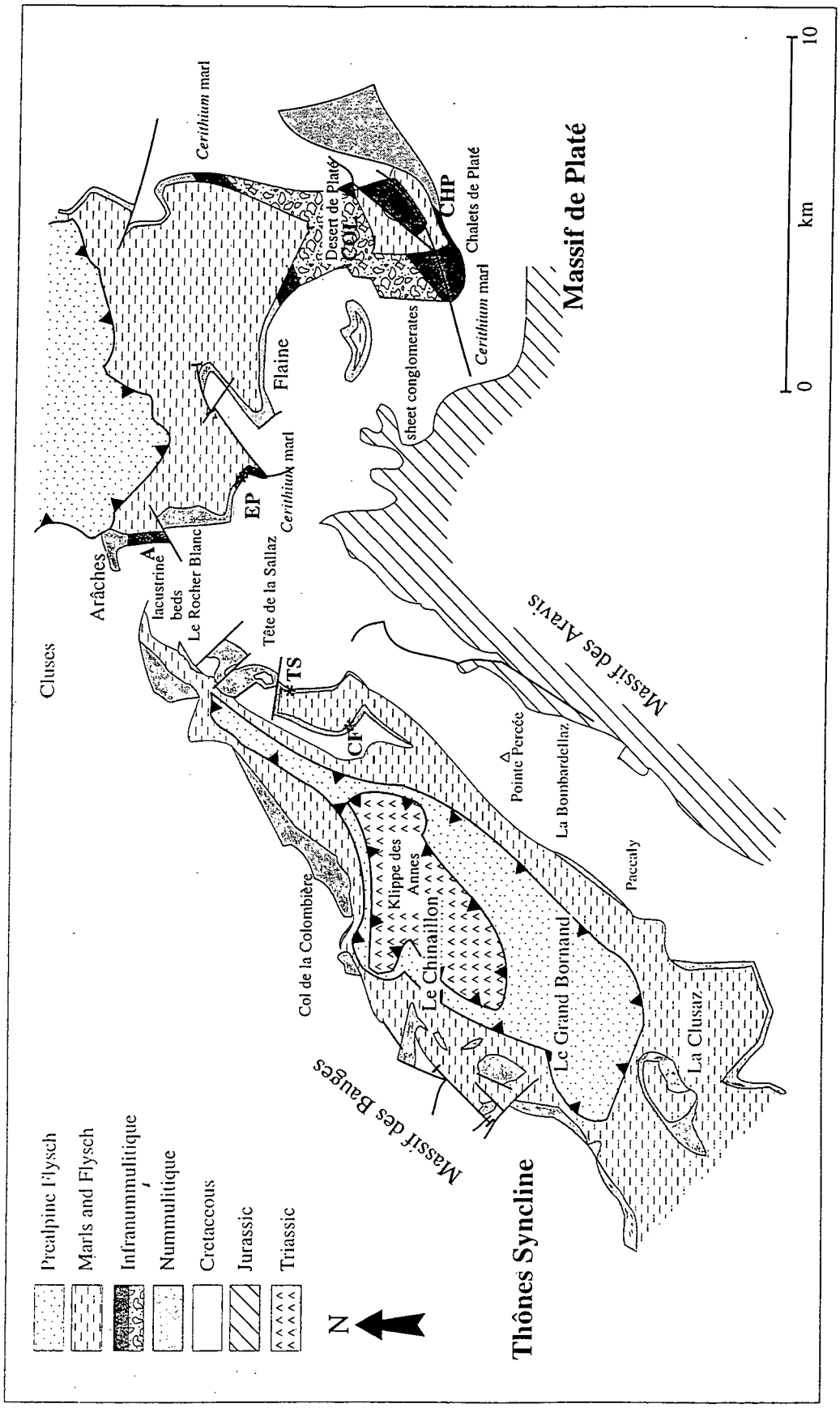

Fig. 3.1: Map of the Massif de Platé showing the approximate present day limits of the facies of the Infranummulitique. Note the influence of pre-existing faulting on the facies distribution. After Pairis and Pairis (1975).

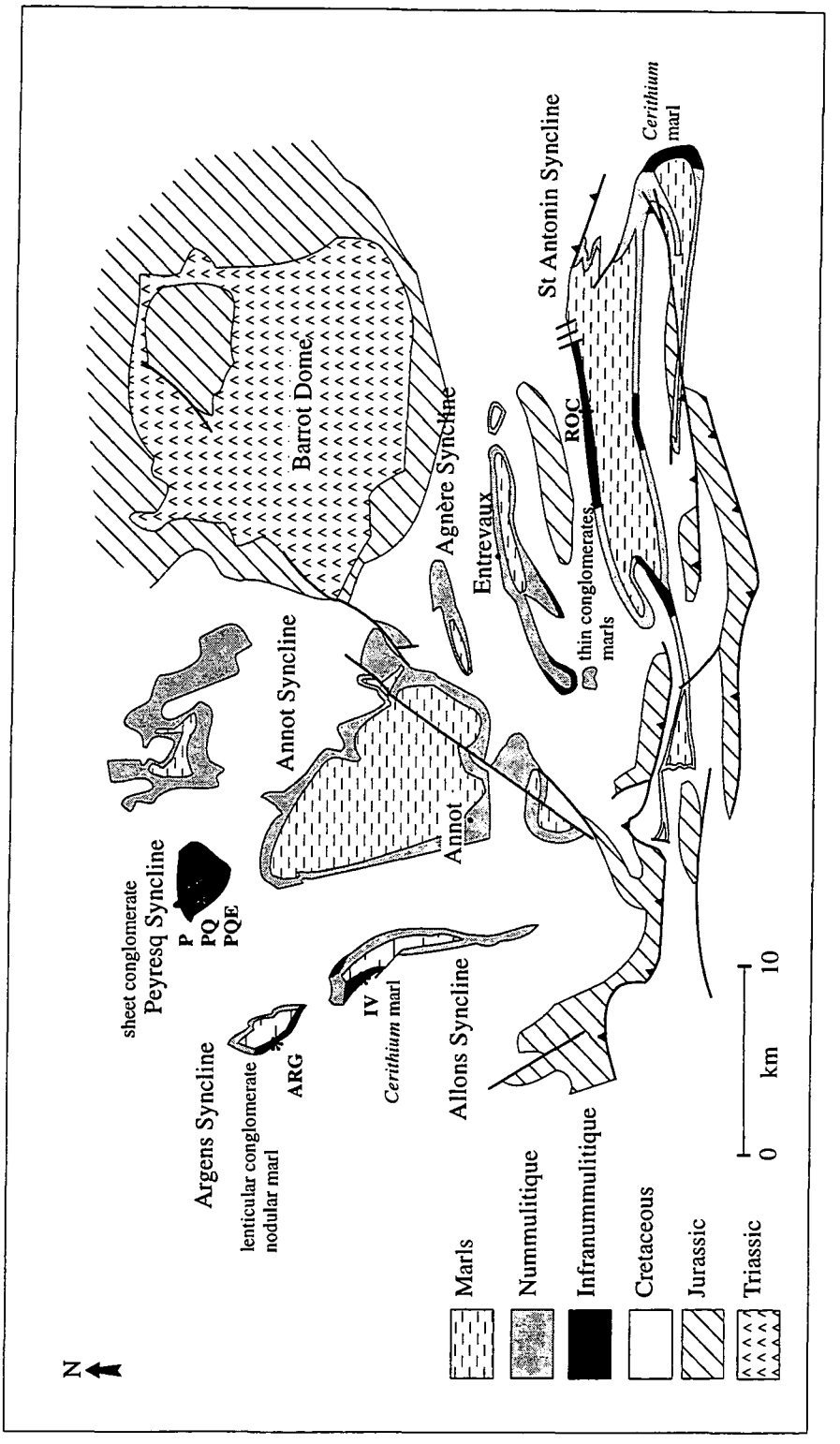

Fig. 3.2: Map of the Castellane Arc showing the present day distribution of the facies of the Infranummulitique, controlled by the synclines thought to segment the basin. Data from Bodelle (1971), Campredon (1977), Apps (1987), Thomes (1987).

The basal contact is not seen, due to the fissile nature of both the nodular marls and the Cretaceous substratum in the area. The succession at Argens is dominated by fine-grained facies, constituting up to 80% of the section, with the remainder consisting of isolated, lenticular conglomerate bodies. Each facies will be considered individually and a palaeoenvironmental interpretation has been based on the individual nature and relationships of the two facies in the field.

3.2.1. Nodular marls

The succession is dominated by white, pale buff or grey (rarely red or green), fissile marls containing rounded to elongate, hard nodules (Fig. 3.3). Nodules are abundant, but their distribution is irregular, with horizons occurring enriched in nodules relative to the rest of the succession.

Fig. 3.3: Photograph of the nodular marls at Argens. Scale=30cm.

In thin section (Fig. 3.4) the sediment dominantly consists of a dark micrite with lithic grains (5-50%) of spicular Senonian micrite and chert. The soft micrite clasts are sub-rounded to well rounded, whereas the more resistant chert is angular. The clasts reach a maximum size of 4mm. The proportion of lithics present in the sediment decreases towards the top of the succession.

The matrix contains patches of coarser-grained calcite. These tend to be round to irregular and show two phases of calcite growth. The first is a coarse micrite, occurring around the edges, and the second is a calcite spar occurring in the centre of

the patch or infilling fractures. The calcite spar does not occur in all the patches present in a section and is therefore interpreted as a second phase of precipitation rather than a coarsening away from the boundaries of a single phase of cement generation. The calcite may also have undergone a partial or, rarely, total replacement by chert. This can be fine-grained microcrystalline or chalcedonic radial quartz. The two growth forms can be seen to grade into one another and are therefore interpreted as being from the same phase of precipitation. The replacement by chert appears to start in the centre of the calcite patches, replacing the coarser calcite spar before the micrite. Individual calcite grains are present in the matrix.

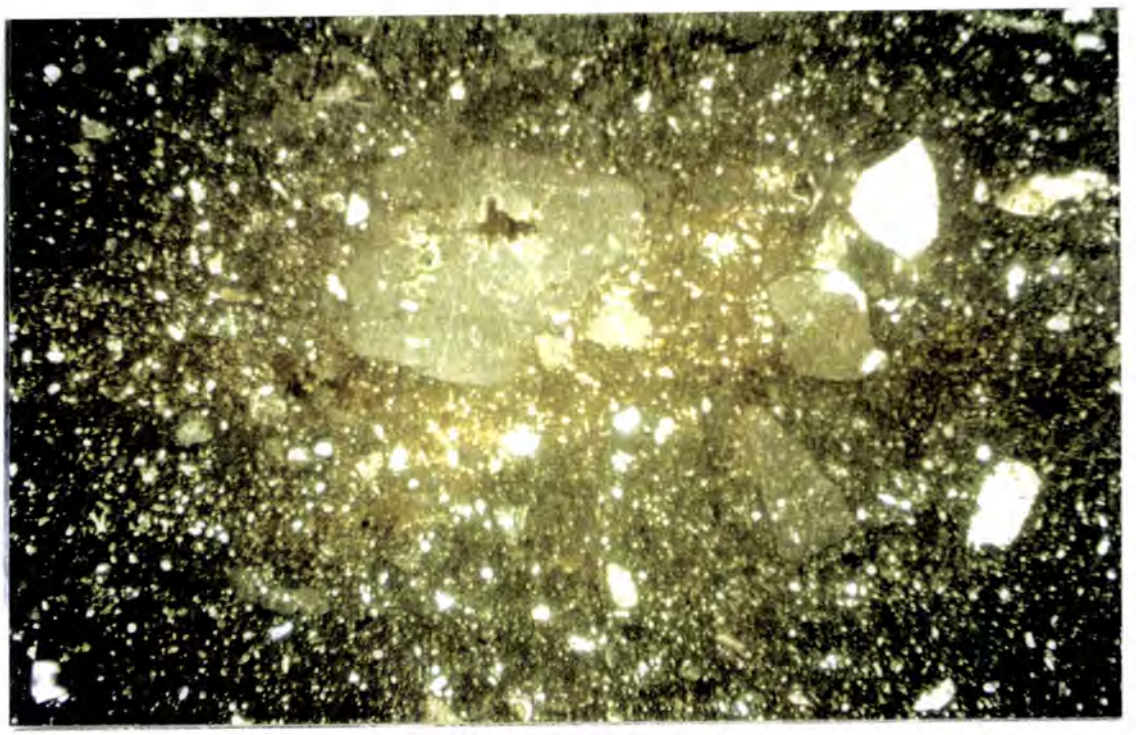

Fig. 3.4: Thin section of the nodular marls showing patches of coarse calcite, calcite rhombs, lithic grains and dense micritic matrix. Field of view 3x1.9mm.

Bioclasts include crystals of *Microcodium*, which are generally fragmented and consist of clear or pale brown calcite. Small Textulariids may be present towards the base of the succession, but are not common. Small amounts of organic debris may also be present in the form of thin seams cutting through the matrix or, more commonly, as fine debris. They may also be associated with patches of framboidal pyrite starting to nucleate in the matrix. Other grains include sand-grade, angular quartz and rare glauconite, which float in the micrite matrix.

The nodular appearance of the matrix persists into thin section, with the sediment cut by irregular fractures. These tend to be anastomosing, breaking up the sediment and may be associated with lithic grains or patches of calcite present in the

matrix. Towards the top of the section, the matrix around the nodules is reddened, and lithic clasts may also exhibit reddened rims.

3.2.2. Lenticular conglomerates

The conglomerates may be massive or show crude bedding and cut down into the underlying marls with their thickness varying from 0.5m to 3m. They are lenticular in shape, with a concave-up erosive base and flat tops (Fig. 3.5). The top tends to fine slightly before passing up into the overlying marls.

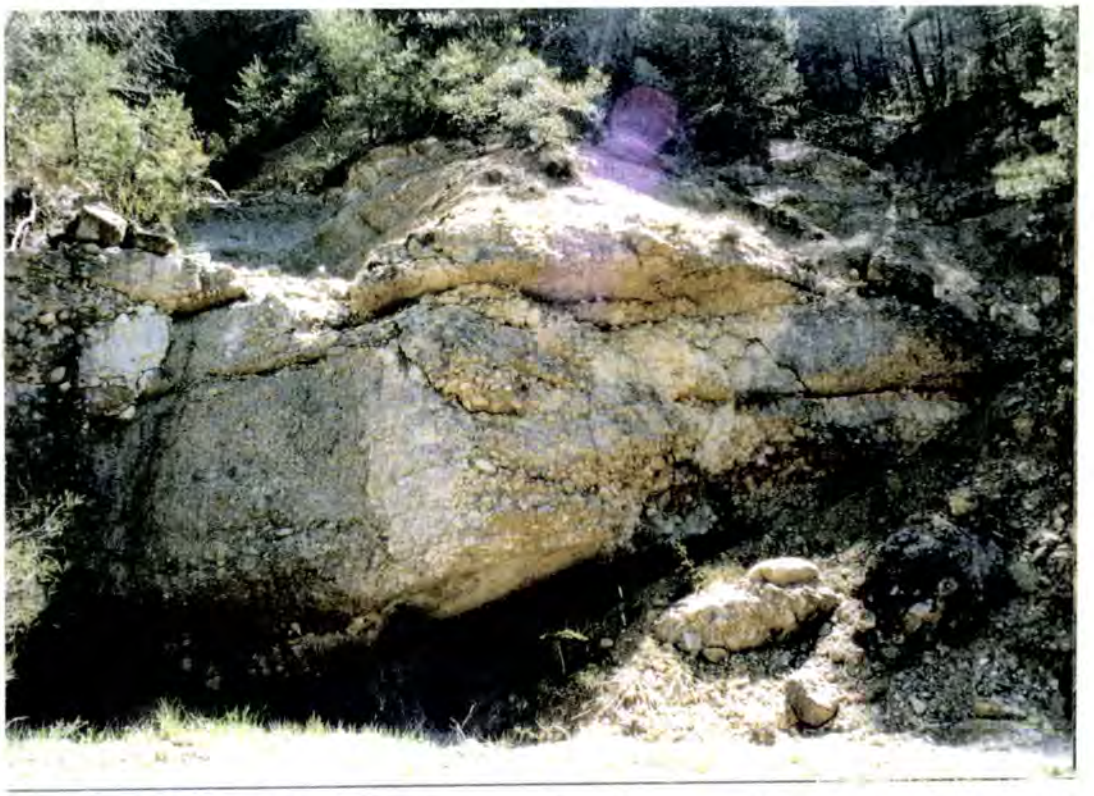

Fig. 3.5: 4m thick, crudely bedded conglomerate channel at Argens. Note the erosive nature of the base of the bed (concave upwards) and the bedding developing towards the top of the unit.

The clasts are composed of Cretaceous micrite and chert. They are angular to well rounded and pebble to cobble size, with a maximum diameter of 1m. Sorting is very poor and there is no imbrication (Fig. 3.6). The surfaces of the clasts may be reddened and encrusted by *Microcodium*. The matrix is a fine-grained, fissile lime mud, similar to the surrounding marls. It is white or red-brown, with reddening occurring around the clasts. This colouring is sporadic and may not occur throughout a conglomerate body.

The conglomerates occur in discrete units, each unit starting with a thick, erosively based lenticular conglomerate body which is commonly bedded and has an irregular base. The base can cut down into the underlying marls by up to 4m. The marls directly underlying the conglomerate lenses tend to be grey rather than white.

The larger clasts in the base of these lenses can be seen to sink into the marls. The conglomerate lenses are overlain by interbeds of conglomerate and nodular marl which thin and fine upwards. The bases of the conglomerates may still be erosive, but not as marked as the basal unit in each cycle.

In the thinner successions (Ivoire, Amirat, La Rochette) this cyclicity is not developed and the beds tend to have flat bases and tops. However, there are similarities in the composition with that of the Argens conglomerates; reddening of the clasts and the presence of a white marly matrix.

Fig. 3.6: Close up of the Argens conglomerates showing poor sorting, lack of imbrication and reddening of the matrix and some clasts. The basal clasts sink in to the underlying marls. Scale=14cm.

3.2.3. Interpretation

This facies association represents periodic influxes of coarse conglomeratic material occurring during high-energy events in an otherwise low-energy depositional environment. The presence of *in situ Microcodium* indicates continental deposition (Esteban and Klappa, 1983). *Microcodium* is an organic precipitate of calcite with characteristic prismatic crystals, which is caused by a symbiotic relationship between plant roots and fungi (Klappa, 1978). The association of *Microcodium* with roots suggests that there was significant soil cover for plants to exist. *Microcodium* typically occurs at stratigraphic intervals (Eocene to Recent) where continental deposition was accompanied by a lime substrate. This suggests that the nodular marls represent the

development of a palaeosol during the exposure of the Mesozoic substratum, which consists almost exclusively of carbonates.

The marls exhibit very similar features to the "chalky" and "nodular" calcrete horizons (Fig. 3.7) of Esteban and Klappa (1983).

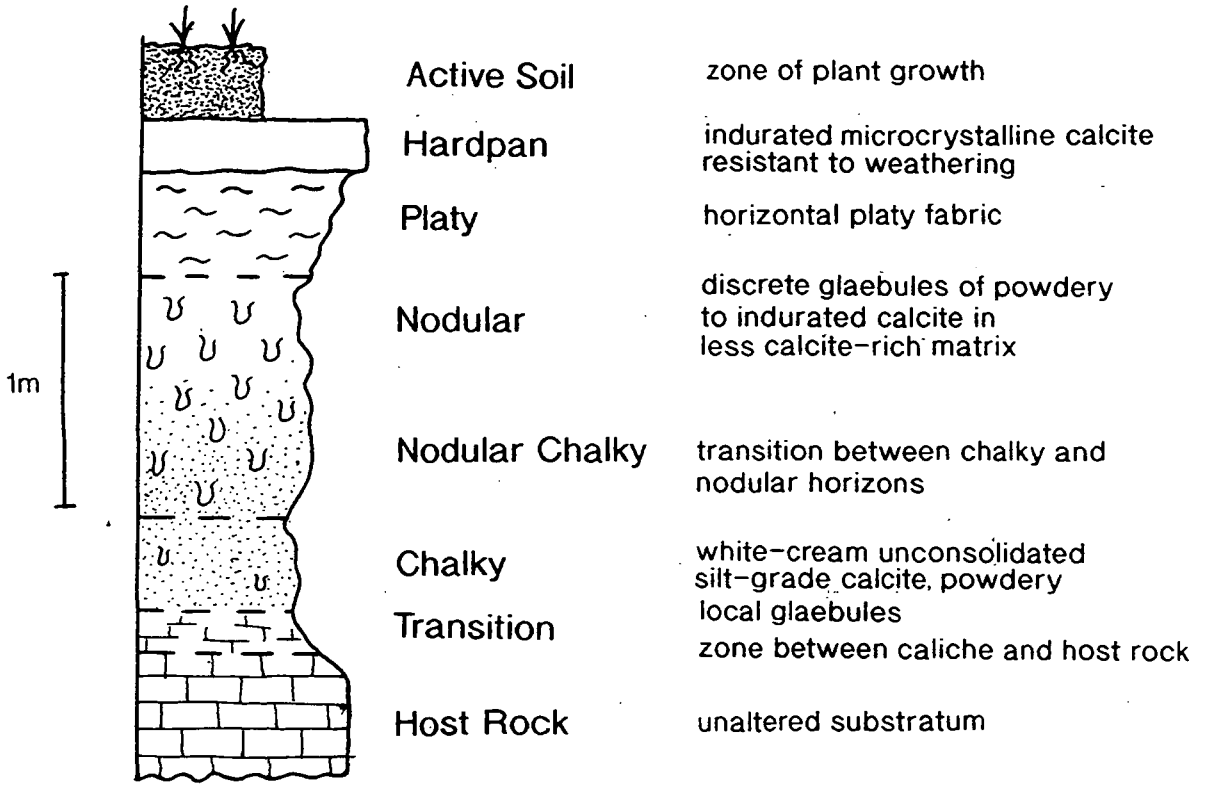

Fig. 3.7: Simplified diagram of the horizons constituting a calrete profile. From Esteban and Klappa (1983).

The more mature "platy" calcrete and hardpan horizons are not evident at Argens, suggesting that the palaeosol profiles are immature. Apps (1987) identified six calcrete profiles at Argens, with only two reaching a mature stage of development. The microfabric of the nodular marls corresponds to an alpha calcite fabric (Wright and Tucker, 1991), characterised by a dense micritic matrix, nodules, fractures, calcite rhombs and floating grains (Fig. 3.8). The development of calcrete profiles, and particularly alpha fabrics, generally occurs in arid to semi-arid regions which promote $CaCO_3$ precipitation. The prime control on development is the saturation of vadose and phreatic waters with $CaCO_3$ (Wright and Tucker, 1991). In arid environments, this occurs due to evaporation and transpiration of sediment fluids, but in areas where the substratum consists entirely of carbonate rocks, there may be enough carbonate in the system for the required saturation to be reached without significant fluid loss, i.e. in less arid conditions, which is believed to have been the case in Provence.

Apps (1987) has described the Argens marls as gley to pseudogley soils, which typically develop in areas with a relatively high water table, with the colour mottling

and nodules indicative of seasonally high rainfall. Gley-type soils occur in the Moist Mid-latitude zone of Mack and James (1994), between latitudes of 30° and 60°, though they state that gley soils characteristically lack calcitic horizons. In Provence, this can be explained by the high proportion of carbonate in the substratum.

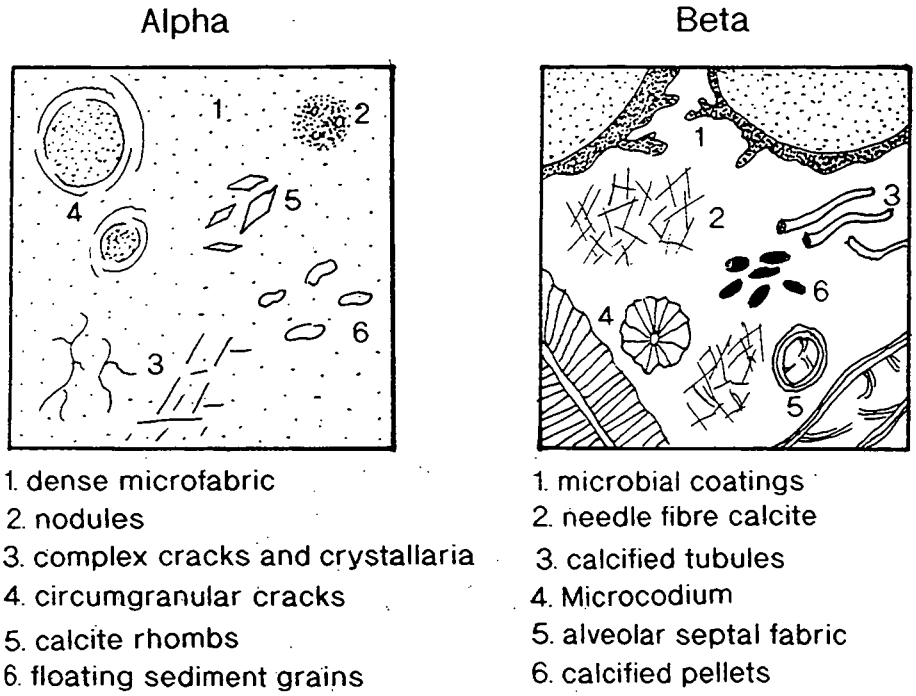

Fig. 3.8: Diagrams showing the characteristic features of the alpha and beta calrete microfabrics described by Wright and Tucker (1991).

The presence of conglomerates cutting through the soils indicate local high energy influxes of detritus. The presence of reddened clasts and matrix and *in situ Microcodium* encrustations in the conglomerates indicate that they were also deposited and/or reworked in a subaerial environment.

The lenticular nature of the conglomerates with erosive bases, crude internal stratification and transitional or reworked tops is indicative of channelised flow. The coarse clast size (pebble to cobble) would require high transport velocities, possibly occurring during high rainfall producing floods and/or ephemeral streams. The poor sorting and presence of fines suggests that the conglomerates represent deposition from coarse-grained, channelised flows (Miall, 1977), with the clasts transported by bedload traction. Each channel deposit represents waning flow from erosion at the base to reworking of the top of the deposit. The channels were probably produced by the development of ephemeral streams on an alluvial plain. The succession, dominated by fine-grained sediment with periodic coarse-grained influxes, is similar in texture to the Lower Devonian Ridgeway Conglomerate of the Old Red Sandstone

in South Wales (Ekes, 1993). The lack of sand in the system probably reflects the lack of sandstones in the exposed substratum.

The source area is interpreted to be local due to the limited clast lithologies and the Cretaceous marls are friable and would not withstand significant transportation without disintegration. A short transport distance would also be round the soft micritic clasts but not chert clasts.

The fining and thinning upwards of the conglomerate beds indicates a gradual decrease in the flow, with eventual abandonment of repeatedly used channels and a return to marl deposition. This may be due to either periodic rejuvenation of the source area by tectonic processes after which supply into the depocentre is cut off, or by the migration of channels across the alluvial plain, with the profile developed representing channel evulsion and abandonment. However, due to the lack of lateral exposure of this facies it is not possible to say with confidence which of the processes occurred.

3.3. Sheet Conglomerates

The sheet conglomerate facies is more widely distributed than the lenticular conglomerate/nodular marl, occurring both in Haute Provence (Peyresq, Le Ruch) and Haute Savoie (Desert de Platé). The succession is dominated by massive to bedded, laterally continuous, sheet-like conglomerate bodies, up to 30m thick and interbedded with a minor amount of fine-grained sediment (marl, calcareous sandstone). The thickest vertical sections occur in Provence, where the topography on the surface of the Mesozoic is more pronounced. Significant lateral variations in thickness occur due to variations in the underlying topography; the conglomerates are deposited in depositional/structural lows and thin towards the corresponding highs.

3.3.1. Haute Provence

The sheet conglomerates have been studied at Peyresq (Logs P2, P3, P4), where they form steep, laterally continuous cliffs up to 30m high.

The base of the conglomerates is planar and erosive, overlying marine micrites of the Upper Cretaceous, with iron precipitation occurring in burrows cutting into the erosion surface. The conglomerate is monomict, consisting of pale buff to grey clasts of Cretaceous micrite. The clasts are well rounded and poorly sorted, with a maximum a-axis length of 0.5m. A crude coarsening upwards profile can be seen in the basal 30cm of the unit passing up into generally structureless conglomerates but which may locally exhibit large-scale cross bedding (Fig. 3.9).

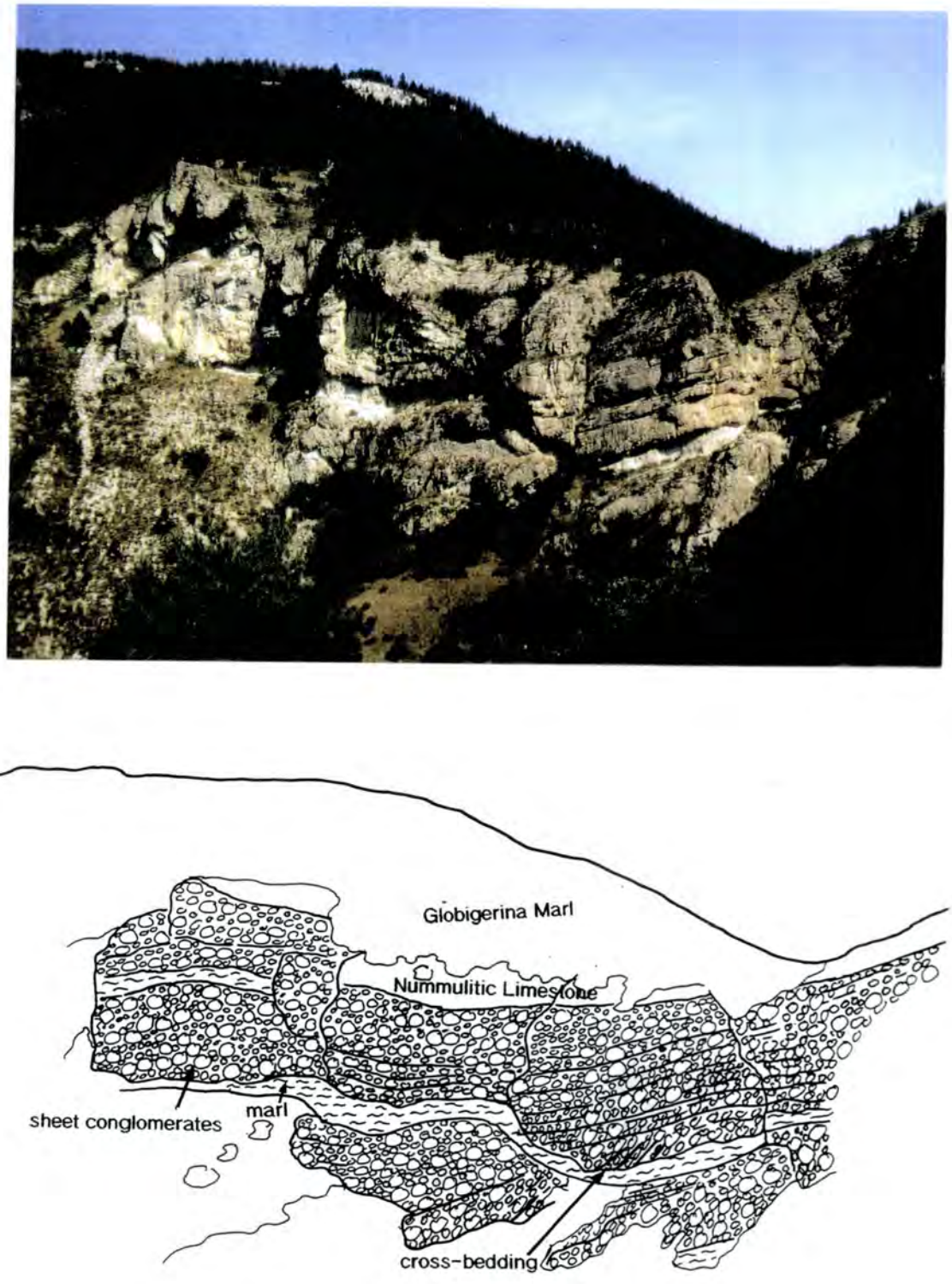

Fig. 3.9: Photograph and line drawing of the Peyresq conglomerates. Note the more massive conglomerates at the base of the succession passing up into thinner beds higher up the section. Erosive bed bases occur throughout the succession and two horizons of fine-grained sediment occur. View looking east towards the village of Peyresq.

Higher up in the section the conglomerates are bedded on a metre scale, with up to 20 cm thick lenses of finer material occurring between individual beds. The bed bases are commonly erosive, with a concave upwards profile and can be seen to cut down into the underlying sediment. This is most marked in the more marl-rich sections to the east. Imbrication of the clasts is uncommon, but, where present tends to occur towards the base of the beds and is due to the alignment of the intermediate b-axis of the clasts giving an E-W flow direction. Cross bedding may also occur at the base of the beds, marked by variations in clast size and again indicating an E-W flow direction (Fig. 3.10).

Fig. 3.10: Small-scale cross-bedding with variations in clast size marking the foresets. Scale=1m.

There is no evidence of *in situ Microcodium* encrustation of the clasts and *Lithophaga* borings occur throughout the facies on all sides of the clasts (Fig. 3.11), some with the bivalve in place, with other, smaller borings thought to be due to the action of Polychaete worms.

The matrix (Fig. 3.12) consists of a calcareous lithic arenite with 60% lithic grains (micrite) and 20% angular quartz and chert in a dark micrite. The matrix also contains fragments of reworked *Microcodium* which is dark brown and heavily abraded. Rare glauconite and abraded foraminifera (*Nummulites*) may also be present.

The conglomerate units (4 to 6m thick) are separated by fine-grained, nodular sediments (marls and fine-grained sandstone). The fine units are up to 6m thick and

Fig. 3.11: Borings on a clast surface. Both Lithophaga *(L) and Polychaete worm (P) borings are present. The* Lithophaga *borings still have the bivalve in place.*

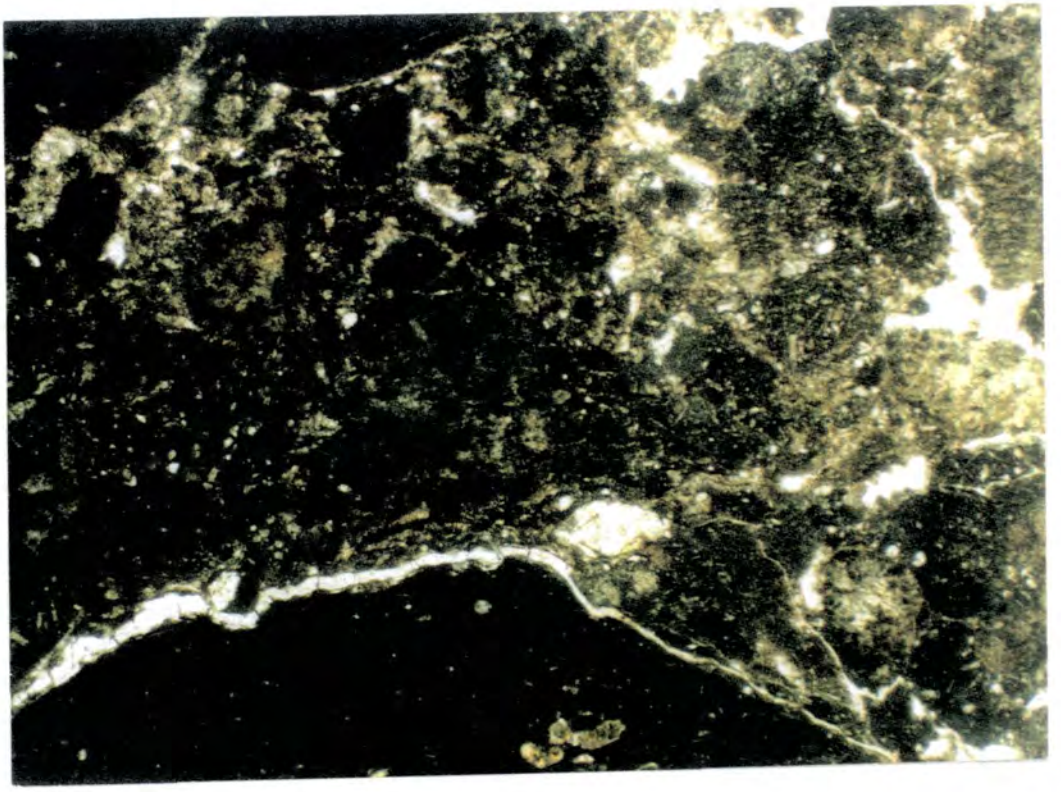

Fig. 3.12: Thin section photomicrograph of the matrix to the conglomerates dominated by lithic grains. Also present are Microcodium *fragments, an abraded Nummulites, quartz and micrite. Scale: 6x3.5mm*

increase in thickness towards the east.

The marls have a similar texture to those seen at Argens (lenticular conglomerate/ nodular marl facies) and are white to grey in colour with abundant nodules (Fig. 3.13).

Fig. 3.13: Nodular marls exposed at Peyresq Quarry.

In addition, they are also extensively bioturbated. Coarser, sandy beds with extensive bioturbation (Fig. 3.14) and conglomeratic pockets occur throughout the marls.

In thin section (Fig. 3.15), the marls consist dominantly of micrite (60-80%), with planktonic foraminifera and sponge spicules. Lithic grains may be present towards the base of the facies association and patches of coarser calcite have developed in the micrite. Bioclasts include reworked *Microcodium*, Textulariids and echinoderm fragments. Glauconite may also be present.

Replacement of the calcite patches by fine-grained and radial chert is common throughout the facies.

Fig. 3.14: Bedding surface in the nodular marls, showing the intense bioturbation in the sediment.

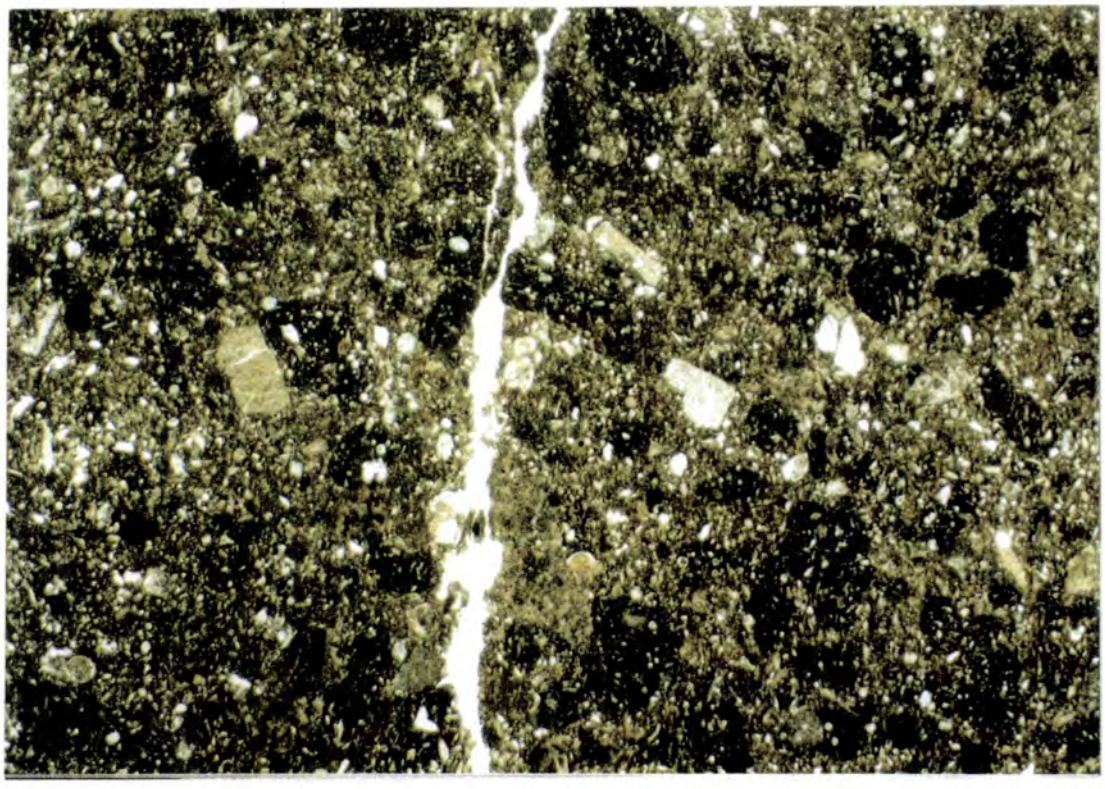

Fig. 3.15: Thin section of the Peyresq nodular marls showing the high proportion of micrite and the presence of marine bioclasts. Scale: 12x7.5mm.

3.3.2. Haute Savoie

The sheet conglomerates outcrop in the Desert de Platé and have been studied at Col du Colonney (Log S11). They are much thinner then those encountered in Haute Provence, only reaching a maximum thickness of 6m. The base of the conglomerates is erosive and commonly concave-upwards and can be seen cutting down into the underlying Senonian micrites (Fig. 3.16).

Fig. 3.16: The Desert de Platé, Haute Savoie, showing the erosive nature of the base of the conglomerates. The unit is much thinner than that developed in Haute Provence. View looking west from Grandes Platières.

The conglomerate is polymict, consisting of clasts of Senonian micrite, chert and limestone with large *Nummulites* (Fig. 3.17). The clasts are rounded to sub-angular, with the chert clasts tending to be more angular. The chert clasts are clearly visible as they stand out in relief from the erosion surface of the conglomerates. The conglomerate is moderately sorted with a dominant clast size range of 2-10cm, The maximum clast size is 30cm.

The clasts have been bored throughout the sheet conglomerates The borings are dominantly *Lithophaga*, and the intensity of the borings increases upwards. Some alignment of the clasts is seen, however, as this is sub-parallel to a pressure dissolution cleavage, it is thought to be tectonic in origin. There is no evidence of cross-bedding.

The conglomerate contains lenses of, and is interbedded with up to 0.5m of coarse-grained calcareous sandstone, with the two facies passing laterally into one another over a relatively short distance. The sandstone contains pockets of conglomerate and is bioturbated, with the burrows infilled with coarser material from the overlying bed, which may be slightly reddened (Fig. 3.18). The sandstone may also contain black bivalve shells which are generally fragmented. The fine-grained facies are laterally discontinuous as they are commonly cut by the overlying channel conglomerates.

Fig. 3.17: Close-up of the Platé conglomerates showing the different clast types: chert (C), Senonian micrite (S) and Nummulitic Limestone (N). Note also the presence of Lithophaga *borings in some clasts. The clasts are tightly packed in a coarse, dark matrix.*

Pairis and Pairis (1975) have described the conglomerates (their "Assises Conglomeratiques") from a number of other localities on the Desert de Platé also showing the erosive and downcutting nature of the contact with the substratum and also the presence of *Microcodium* in the basal parts of the succession and encrusting the Mesozoic substratum.

3.3.3. Interpretation

The sheet conglomerates, at least in Provence, are compositionally and texturally similar to the lenticular conglomerates and are therefore interpreted to have originated from a similar source, i.e. a local structural / depositional high undergoing

erosion. The difference in composition between the Provence and Savoie conglomerates is due to the greater number of rock types exposed at the surface in

Fig. 3.18: Bioturbated sandy limestone interbedded with the coarse conglomeratic facies. The burrows are infilled with the coarser-grained matrix to the conglomerates. Scale=5cm.

Savoie and undergoing erosion due to the effects of the faulted topography. However the similarity in texture and sedimentary processes allows the two areas to be interpreted as the same type of depositional system. In Savoie, the Senonian micrites represent the underlying Mesozoic substratum in the area, which may contain chert. Chert is also present in the Lutetian-Priabonian lacustrine beds encountered at Arâches. The limestone with large *Nummulites* can also be seen *in situ* at Arâches, preserved in a faulted graben (Pairis and Pairis, 1975) and representing an earlier, Lutetian, phase of marine transgression, based on the faunal content of the limestone (see Chapter 2 for biostratigraphy). The clast reworking indicates that the Savoie conglomerates post-date the earlier marine transgression and that the two events were separated by a relative sea-level fall and subsequent erosion. There is no evidence of an earlier transgression in Provence.

The concave-upwards nature of the base of the conglomerate beds indicates that, like the lenticular conglomerates, the sheet conglomerates were deposited from bedload traction during channelised flow. However the high proportion of coarse detritus and the lateral extent of the conglomerate facies suggests that the source area was providing the site of deposition with an abundant supply of clastic material. The

lateral continuity of the conglomerates is thought to be due to channel amalgamation and lateral migration, indicated by the large-scale cross-bedding at the base of the unit at Peyresq.

The presence of reworked *Microcodium* indicates proximity to vegetated land. However, the presence of *Lithophaga* and Polychaete borings indicates a marine influence evidence for which is also present in the matrix and fine-grained facies in the form of glauconite and foraminifera (*Nummulites*, Textulariids). Therefore the sheet conglomerates do not represent terrestrial alluvial fan deposition as indicated by Apps (1987).

The similarity in texture between the alluvial channels of the lenticular conglomerates and the sheet conglomerate channels suggests that similar depositional processes occurred. However, for the sheet conglomerates, the supply from the source area was much greater producing amalgamated channels in a sheet-like configuration, dominated by pebble- to cobble-grade sediments. The sediments were deposited in a marine environment leading to borings on clast surfaces, and a sparse marine fauna developing. The combination of alluvial-type processes and a marine influence indicates that the sheet conglomerates were deposited in a fan delta setting, where a coarse-grained alluvial fan meets the sea, though the presence of *Microcodium* encrustations at the base of the unit in Savoie suggests that the conglomerates may initially have been continental in some localities.

The distribution of the conglomerates seems to be influenced by the topography of the Mesozoic erosion surface. At Peyresq and further east towards Le Ruch, the conglomerates can be seen to thin over the topographic highs on the erosion surface. On the Massif de Platé, Pairis and Pairis (1975) have shown that the conglomerates outcrop along the axis of a depositional low between the Croix Fer and Praz Coutant Faults, though this study was not able to confirm this. The conglomerates are not present elsewhere in the region indicating that deposition was laterally restricted.

The sheet conglomerates are interbedded with fine-grained facies. In Savoie, these are coarse-grained calcareous sandstones with bivalve shells and bioturbation. The grainsize and the presence of pockets of conglomerate indicate that deposition was still occurring under fairly high energy conditions, with bioturbation probably indicating pauses in or a slowing of the sedimentation rate. The presence of reddened material in these burrows also indicates a slower rate of sedimentation a with the possibility of subaerial exposure. However, there are no desiccation cracks or soil profiles developed and so the sandstones probably remained beneath water, but very close to vegetated land (reworked *Microcodium*).

In Provence, the similarity of the marls to the nodular marls encountered at Argens suggests that pedogenic processes probably played a part in reworking the fine-grained sediments. However, the presence of glauconite and foraminifera within the marls suggests that they were also under marine influence. Therefore, the marls are interpreted as fine-grained sedimentation occurring within the marine realm which have undergone periodic exposure producing immature calcrete profiles.

The presence of a greater thickness of sheet conglomerates in Haute Provence is probably indicative of a greater relief on the topography in comparison with Haute Savoie. This corresponds to the development of laterally restricted sub-basins which markedly influenced the facies distribution of the Infranummulitique and could have served to trap the sediment within the basins rather than allowing some sediment bypass which could have occurred in the more open horst/graben topography of Savoie.

The sheet conglomerates are interpreted as having been deposited in fan deltas occurring where the alluvial fans met the sea. Deposition occurred from bed-load traction during high-energy channelised flow, sourced locally and with subsequent marine reworking (borings). Lateral migration of individual channels has produced amalgamated sheet-like geometries. In between influxes of coarse detritus, fine-grained sediment was deposited that was subject to periodic exposure, preserved either as lenses within the conglomerate bodies or as laterally continuous beds separating the conglomeratic units.

3.4. *Microcodium* Wackestone

This facies has only been found at L'Epine (Log S14) in the Massif de Platé, Haute Savoie where a 7m thick succession occurs between the Mesozoic substratum and the *Cerithium* marl. This consists of two massive, lenticular beds (Fig. 3.19) the upper of which has a concave upwards base that cuts down into the underlying sediment by 2m. The rock is grey to buff and featureless in the field with no observed sedimentary structures or grainsize variations.

In thin section (Fig. 3.20), the sediment is a wackestone consisting of bioclasts and clastic debris in a dark micrite matrix. The dominant bioclasts are clear to pale brown, abraded fragments of *Microcodium* (20%). Other bioclasts include well preserved foraminifera (*Nummulites*, Textulariids) and abraded fragments of echinoderms and bivalves. Lithic grains and quartz are present in the matrix along with patches of coarser micrite which are thought to be burrows. Pyrite occurs in the matrix and is particularly associated with lithic grains and darker, more organic-rich

patches of micrite. The *Microcodium* fragments have undergone partial replacement of the calcite by fine-grained and radial chert.

The base of the unit is erosive and marked by a conglomerate 0.8m thick. The conglomerate is poorly sorted and consists of sub-rounded to angular clasts in a lime

Fig. 3.19: Field photograph showing the channels in the Microcodium *wackestone at L'Epine. The top channel cuts down 2m into the underlying bed.*

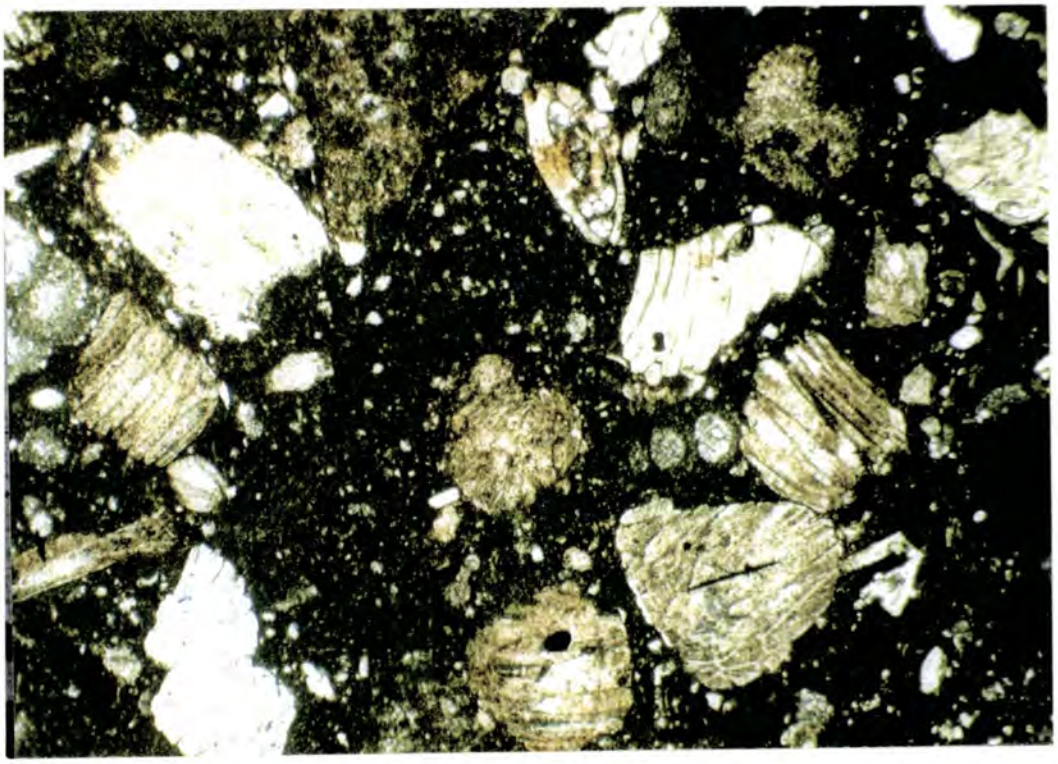

Fig. 3.20: Thin section photomicrograph of the Microcodium *wackestone at L'Epine. Reworked fragments of* Microcodium *float in a dark, micrite matrix with quartz, echinoderm fragments and foraminifera. Scale: 3x1.9mm.*

mud matrix. The matrix also contains small lithic grains, quartz, reworked *Microcodium*, *Nummulites*, Textulariids, bivalves and echinoid fragments. Three rock types are represented in the lithic clasts: i) Senonian micrite, which is the dominant clast type and forms the substratum in the area; ii) Miliolid peloidal grainstone with Textulariids and echinoid plates in a clear calcite cement; iii) micrite containing charophytes. The conglomerate passes up abruptly into the wackestone.

3.4.1. Interpretation

The presence of well preserved *Nummulites* and Textulariids indicates that deposition occurred in a marine environment. However, the abundance of reworked *Microcodium* fragments indicates that this environment was close to an exposed land surface.

The lithic grains present show that Senonian micrites were the dominant rock-type exposed, with the Miliolid-peloidal grainstone indicating exposure of the older Urgonian limestone. The presence of clasts of micrite containing charophytes, which can be seen to outcrop in situ at Arâches (Log S15), is likely to be due to the erosion of the Lutetian to Priabonian lacustrine sediments which occur above the limestone with large *Nummulites* deposited during an earlier Lutetian transgression (Pairis and Pairis, 1975). These clasts indicate that the *Microcodium* wackestone post-dates the Lutetian transgression (see also Section 3.3.2).

The lack of winnowing, preserving a high proportion of fine-grained sediment implies that deposition occurred in a relatively low-energy environment, and the lenticular bedforms indicate that deposition was from channelised flow. The succession at L'Epine was deposited in a narrow graben produced by the La Grangeat and Bellegarde faults (Pairis and Pairis, 1975) and the sediments represent an early transgression within this graben.

The sediment was probably sourced locally from exposed, vegetated ground that was encrusted by *Microcodium*. The sediments were transported via relatively low energy channel systems (low relief between source and depocentre) and deposited in a marine environment. The relationship between the *Microcodium* wackestone and the overlying *Cerithium* marl suggests that the *Microcodium* wackestone was deposited in a coastal environment but without the restricted, brackish conditions that developed during the deposition of the *Cerithium* marl. The *Microcodium* wackestone passes up abruptly into the organic-rich beds of the *Cerithium* marl.

3.5. *Cerithium* Marl

The *Cerithium* marl occurs between the conglomeratic or *Microcodium*-rich facies of the Infranummulitique and the marine Nummulitic Limestone. It is relatively widespread, occurring on the Massif de Platé and the Massif des Bornes (Gorin et al., 1989) in Haute Savoie and stretches from the Trucco region of the Alpes Maritimes in Italy (Campredon, 1977) to near Castellane in Haute Provence (Bodelle, 1971). Distribution is not continuous but, like the underlying conglomerates, is of limited lateral extent that was controlled by pre-existing structures in the substratum. The *Cerithium* marl was deposited in the structural / depositional lows which acted as depocentres for the continental and marginal marine conglomeratic facies (Pairis and Pairis, 1975; Apps, 1987). The thickness of the *Cerithium* marl is highly variable, from less than 1m at Argens (Thome, 1987) to more than 30m at Chalets de Platé on the Desert de Platé. The *Cerithium* marl has been studied at four localities; L'Épine (Log S14), Col du Colonney (Log S11) and Chalets de Platé in the Massif de Platé, Haute Savoie, and at Ivoire (Log P5) in the Argens Syncline in Haute Provence.

The *Cerithium* marl derives its name from the abundance of the *Cerithium* genus of gastropod within the facies (Fig. 3.21).

Fig. 3.21: The marl contains abundant high-spired gastropods of the genus Cerithium *(C). Scale=5cm.*

The marl is buff to dark brown, depending on the amount of organic material present in the sediment, and is generally laminated and highly friable, with abundant bioturbation. The gastropods may reach relatively large sizes, with basal diameters up to 3cm. Small spine-like protruberences are preserved on the shells indicating that abrasive processes were minimal during deposition. Bivalves are also common, including oysters, smooth and ribbed-shelled varieties. The molluscs present may form *in situ* shelly accumulations (Fig. 3.22).

Fig. 3.22: Shelly horizon with in situ infaunal bivalves and abundant mollusc debris. Scale=40cm.

Weidmann et al. (1991) have described vertebrate remains from the *Cerithium* marl which have been used to constrain the age of the sediment. On the Desert de Platé these remains include sharks teeth (*Caracharias*), reptile and mammal bones, mammal teeth (*Palaeotherium*), crocodile teeth and turtle shells. Fish teeth have also been found at the contact with the underlying sheet conglomerates. The most important of these in terms of biostratigraphy are several species of *Palaeotherium* teeth, which have been dated as Upper Priabonian. Similar teeth from the *Cerithium* marl on the cover of the Argentera Massif in Provence has been dated as Bartonian by the same workers.

In thin section (Fig. 3.23), the marl can be seen to have a dark micritic matrix with fragments and seams of organic debris. In addition to the molluscs described above, bioclasts present are echinoid fragments, miliolids and other skeletal debris.

Microcodium is uncommon and abraded. Clastic content varies between localities, with the most quartzitic sections occurring on the Desert de Platé. All sections contain angular to subrounded, silt- to sand-grade quartz, with the larger grains tending to be more rounded. Lithic grains may also be present, but are uncommon except at Col du Colonney, where they constitute 15% of the sediment. Two sediment types are represented in the lithic grains: i) a micrite with calcispheres, reworked from the Senonian substratum, and ii) a fine-grained miliolid-peloidal grainstone with Textulariids, echinoid plates and bivalve fragments in a clear calcite cement, thought to be reworked from the Urgonian limestones.

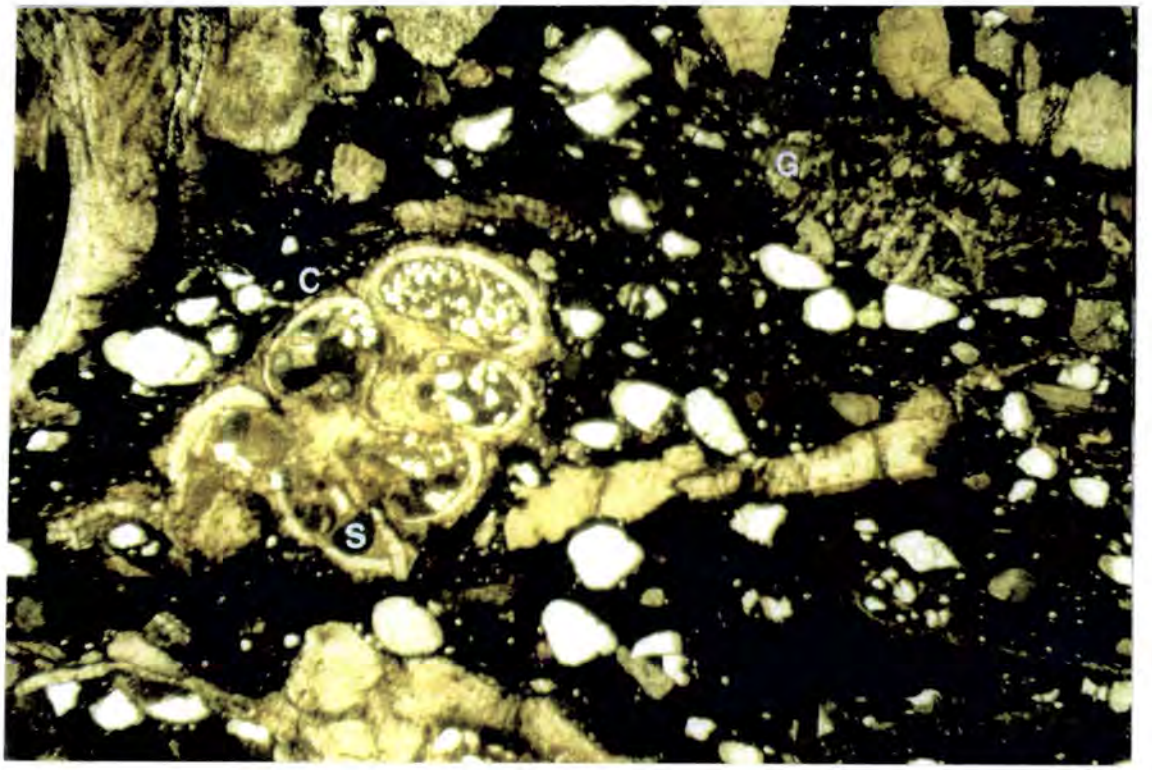

Fig. 3.23: Thin section of the Cerithium *marl showing the abundance of molluscs and lithic grains: Senonian micrite (S), miliolid-peloidal grainstone (G). Field of view 12x7mm.*

Pyrite occurs in all samples, commonly associated with the lithoclasts (especially the Senonian micrite) and organic-rich seams in the matrix. Many of the molluscs (gastropods and smooth-shelled bivalves) have undergone alteration of the originally aragonitic shell to calcite, destroying the internal structure. This has not occurred with the oysters and some of the ribbed-shelled bivalves which were originally calcite. The calcite may rarely have undergone partial replacement by fine-grained and/or radial chalcedonitic chert.

The organic content of the marl is relatively enriched at some localities (L'Epine, Chalets de Platé, Ivoire). The marls at these localities are much darker and a

lignite seam 1m thick is developed at L'Epine, capping the marl (Fig. 3.24). The organic content decreases during the transition into the Nummulitic Limestone.

Fig. 3.24: Coal seam developed at the top of the Cerithium *marl at L'Epine passing up into lenticular, marine sandy limestones. Ford Escort for scale.*

The two sections observed on the Desert de Platé (Col du Colonney, Chalets de Platé) contain a high proportion of clastic detritus and have much thicker section of the facies. The high supply of clastic detritus leads to the development of flat-bedded to lenticular calcareous sandstones which are interbedded with the *Cerithium* marl The sandstone bodies may cut down into the underlying marls or contain small-scale cross-bedding. At Chalets de Platé, the marl is also interbedded with marine, organic-rich lime mudstones containing *Nummulites*. The thicker sections also show a marked cyclicity, with the development of shelly accumulations with in situ bivalves and gastropods, commonly associated with an increased supply of clastic detritus and bored lithoclasts.

3.5.1. Interpretation

The high proportion of fine-grained sediment and the good preservation of the bioclasts indicate a low-energy depositional environment. The fauna present indicates a confined marine to brackish-water environment (Pairis and Pairis, 1975; Gorin et al., 1989; Weidmann et al., 1991), though the presence of corals at some localities, echinoids and *Lithophaga* borings suggests that the sediment was subject to periodic

marine influences. Three of the species of *Palaeotherium* encountered are thought to have inhabited coastal swamps (Weidmann et al., 1991).

The presence of preserved organic matter, to the extent of metre thick coal seams being developed, indicates that dysaerobic conditions occurred, though the abundance of bioturbation throughout the unit indicates that this was not the case during the whole period of deposition of the *Cerithium* marl. Gorin et al. (1989) carried out geochemical analyses on the organic content of the *Cerithium* marl in the Bornes Massif which showed that the original kerogen was intermediate between types II and III and was therefore indicative of marine conditions with a considerable continental influence. Their analyses showed that the environment was subject to strong reducing conditions, which is also indicated by the amount of pyrite within the sediment. However the variation in the colour of the sediment and the degree of bioturbation indicates that the sediment was not subject to reducing conditions throughout its deposition and that conditions also varied between localities.

On the Desert de Platé the higher proportion of clastic detritus is indicative of the waning supply from the source area that fed the underlying coarse-grained fan delta system. Sand-grade detritus is fairly constant throughout the *Cerithium* marl, and horizons of coarser, pebble-grade, clastic influx indicates periodic rejuvenation of the source area, either through active faulting or sea-level variations, supplying detritus to the marginal marine realm where the clasts were subsequently bored. Where higher energy conditions produce an increase in the amount of sand supplied to the system, we see the development of sand bodies interbedded with the underlying marls (Chalets de Platé, Col du Colonney; Log S11).

The *Cerithium* marl is interpreted as having been deposited in a brackish water coastal setting that was subject to periodic marine influences. The fact that the marl is confined to narrow grabens in Haute Savoie (Pairis and Pairis, 1975) and to synclinal sub-basins in Haute Provence (Apps, 1987) could explain the restriction of the water circulation and the subsequent development of local anoxic, reducing conditions. The reduced salinity of the environment is due to the continuing supply of waters via fresh-water systems from the uplifted foreland.

Due to its relationship with the underlying conglomerates and the overlying marine Nummulitic Limestone, the *Cerithium* marl is interpreted as having been deposited during the earliest stages of the marine transgression over the previously exposed foreland, with the first stages of the transgression restricted to structural lows. The *Cerithium* marl passes up into the marine sandy limestone or peloidal shoals of the basal Nummulitic Limestone which are thought to protect the coastal area from wave action and winnowing and which may also restrict water circulation producing anoxic and reducing conditions.

The contact with the overlying Nummulitic Limestone is generally abrupt and marked by a thin conglomerate at the base of the marine beds marking a transgressive lag deposit. At Ivoire (Allons Syncline) the succession is transitional between the two units; organic-rich *Cerithium* marl passes upwards into paler, less organic beds, still containing a brackish water fauna and with abundant bioturbation indicating the end of anoxic reducing conditions. An increase in the marine influence is marked by the appearance of horizons with small, delicate corals (coral wackestone microfacies, Section 5.3.4) indicating that conditions were still low-energy, but that the environment now had normal marine salinities. Coral growth is periodically halted, either by a return to more brackish conditions or by influxes of mud into the system. As the transgression continues and the marine conditions start to dominate, the succession passes up into the peloidal facies association of the Nummulitic Limestone (Section 5.4.5.1).

The marl was deposited during the early stages of transgression in a vegetated coastal setting, with clastic detritus sourced from the uplifted foreland and with restriction occurring due to the lateral confines of the depocentres and the presence of offshore shoals. As the transgression continued, organic matter became scarcer and marine influences started to predominate, leading to corals colonising the sediment, though still in low-energy conditions. The marl finally passes upwards into the basal beds of the Nummulitic Limestone, commonly with a submarine erosion surface and transgressive lag separating the two units.

3.6. Depositional Model

Due to the lack of reliable age data for the lower units of the Infranummulitique, the exact relationships between the different depositional systems are difficult to determine. Also, the spatially restricted depocentres add to this problem in that not all of the facies encountered are present at any given locality. However, it is possible to build up a picture of the depositional system across an area, with the two field areas representing equivalent systems, and the development of this system during the onset of the nummulitic transgression.

The Infranummulitique represents terrigenous deposition of carbonate eroded from local highs, where the Mesozoic substratum had been exposed prior to the subsidence of the foreland basin. As has already been discussed, the Infranummulitique is not thought to have been deposited over the whole of the area, but was confined to structural lows which provided local depocentres for

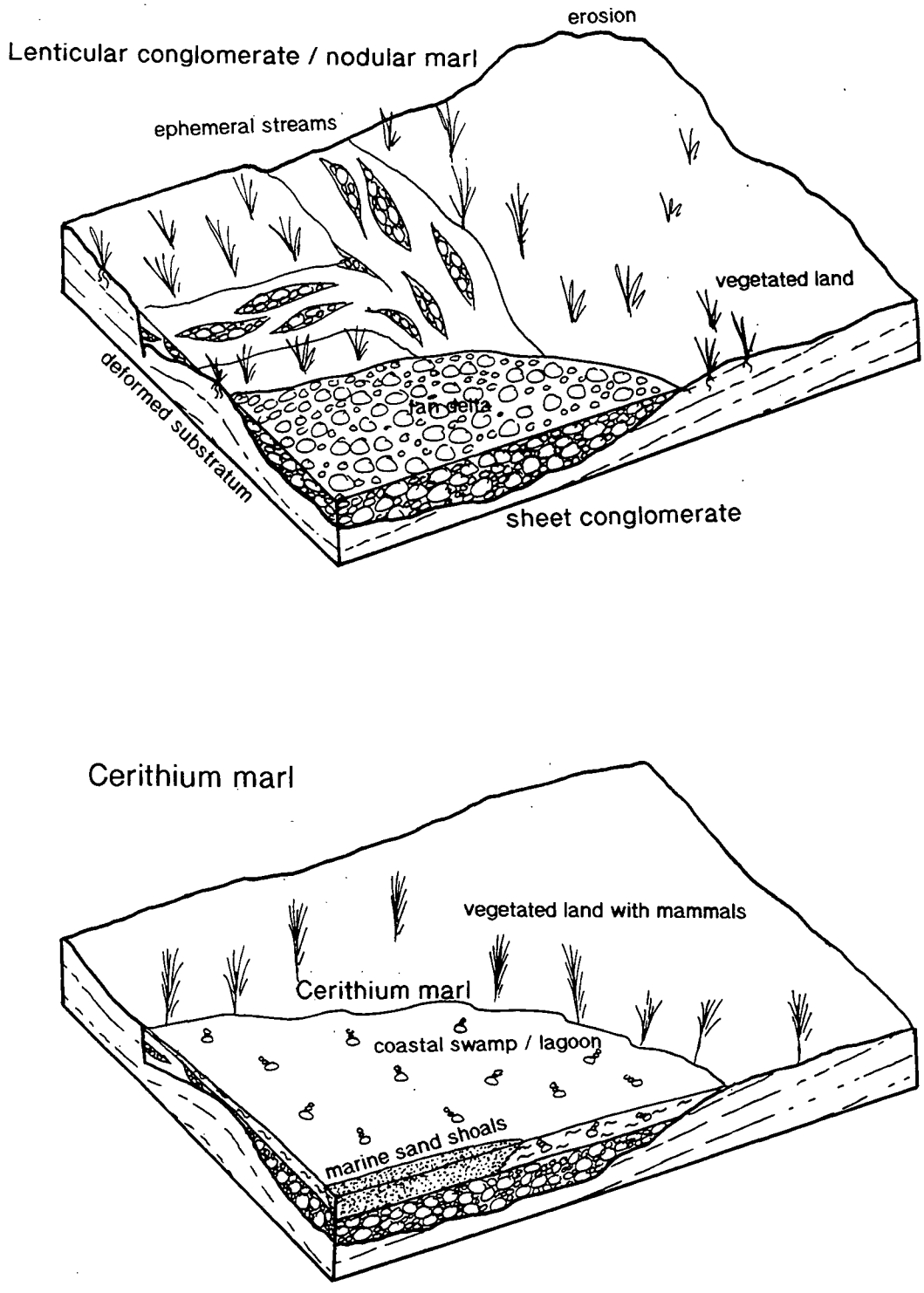

Fig. 3.25: Depositional model of the Infranummulitique based on sedimentary sections measured in Haute Savoie and Haute Provence.

the eroded detritus (Pairis and Pairis, 1975; Apps, 1987). This detritus was then deposited in an alluvial or marginal marine environment producing the facies described above (Sections 3.2 to 3.5) and illustrated in Fig. 3.25.

The earliest deposits, in that they occur between the Mesozoic substratum and the datable *Cerithium* marl, were the lenticular and sheet conglomerate facies. The exact timing of these two systems is unknown, so it is impossible to say accurately whether they were contemporaneous.

The alluvial system (lenticular conglomerate/nodular marl facies association) was sourced by local uplifted highs, which provided the well-rounded clasts of Upper Cretaceous micrite, which could not have withstood significant transportation. This coarse material was then periodically transported into the depocentres and deposited by channelised flows, thought to be due to the development of ephemeral streams. Due to the lack of lateral continuous exposure it is not possible to say how widespread the braid plains were, but they are thought to have been laterally restricted due to the size of the depositional lows. Coarse terrigenous influx was not constant as the sedimentary sections are dominated by fine-grained, nodular marls which have been reworked by pedogenic processes. These marls are thought to have been deposited either as overbank deposits to the ephemeral stream system, or as palustrine sediments.

The alluvial system fed a marginal marine fan delta (sheet conglomerates), dominated by channelised flow and reworked by marine processes. There is a much higher proportion of coarse terrigenous carbonate, still thought to have been sourced locally. The reduction in the amount of fine sediment preserved could be due to the winnowing effects produced by marine reworking, though fine horizons were periodically preserved, especially in Provence (Peyresq) indicating periodic waning of marine influences. The alluvial and fan delta systems were probably contemporaneous, as there is no evidence for the fan delta sediments having been preceded by alluvial deposition or for conglomeratic marginal marine sediments overlying the continental deposits at Argens, which instead passes up into the marginal marine *Cerithium* marl.

The *Cerithium* marl and *Microcodium* wackestone mark the advance of the transgression over the area, with a fauna representing deposition in marine or brackish waters (*Cerithium*, Textulariids, Miliolids) close to vegetated land (mammal remains, *Microcodium*). The *Cerithium* marl represents brackish, lagoonal sedimentation, with the environment probably protected by the offshore shoals of the basal beds of the Nummulitic Limestone; quartzitic shoals in Haute Savoie, peloidal or nummulitic shoals in Haute Provence. The marls experienced local anoxia (coal deposition) and

marine incursions (bored clasts) with terrigenous supply waning but still evident overlying the fan deltas.

The Cerithium marl is the uppermost unit of the Infranummulitique above which fully marine conditions developed with the deposition of the Nummulitic Limestone (Chapters 4 and 5).

Chapter 4

The Nummulitic Limestone - Haute Savoie

4.1. Introduction

The Nummulitic Limestone in Haute Savoie has been studied in the north-eastern part of the Thônes Syncline and the Massif de Platé. The succession was analysed by the measurement of sedimentary sections, which are shown in Appendix 1, and detailed microfacies analysis of samples collected in the field (Appendix 2). This chapter deals with the distribution and thickness variations of the limestone within the field area, the characteristic microfacies and the development of the carbonate ramp.

4.2. Distribution and Thickness Variations

4.2.1. The Thônes Syncline

The Nummulitic Limestone outcrops along the limbs of the Thônes Syncline, which is oriented SW-NE (Fig. 4.1). The Tertiary formations occur topographically below the Cretaceous passive margin succession, which forms the major topographic features in the area.

The outcrop of the Nummulitic Limestone is best along the north-western limb of the syncline. In the area studied, NE of the town of Thônes, the limestone varies in thickness from 24m to 60m between the basal unconformity and the overlying Globigerina Marls, with the thinner sections occurring over structural highs in the substratum (Lateltin and Müller, 1987). The Nummulitic Limestone directly overlies the Mesozoic substratum which generally consists of Senonian micrites.

In the axis of the syncline, the formation outcrops around the Mont Durand anticline to the west of La Clusaz. This structure appears to have formed a pre-existing structural high in the substratum (Charollais et al., 1977) resulting in a greater level of erosion of the substratum, which consists of black shales on the northern limb and Urgonian limestones on the southern limb.

On the south-eastern limb of the Thônes Syncline, the Nummulitic Limestone is much thinner, only attaining a maximum thickness of 24m at Tête de la Sallaz at the NE

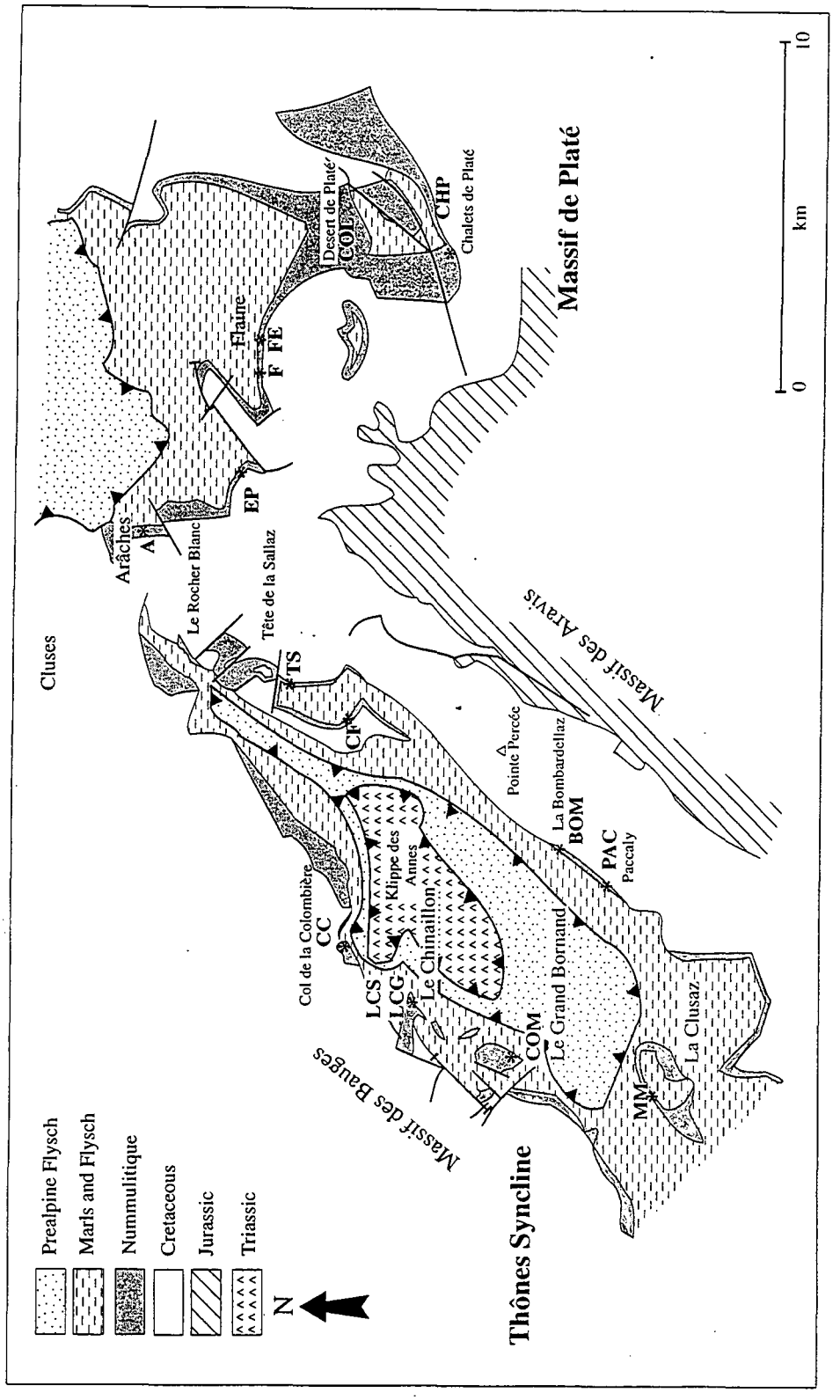

Fig. 4.1: Map of the Thônes Syncline and the Massif de Platé showing the outcrop of the Nummulitic Limestone and the location of measured sections (MM=Meubles Montagnardes; COM=La Communaille; LC=Le Chinaillon; CC=Col de la Colombière; PAC=Paccaly; BOM=La Bombardellaz; CF=Col de Forclaz; TS=Tête de la Sallaz; A=Arâches; EP=L'Epine; F=Flaine; FE=East Flaine; COL=Col du Colonney; CHP=Chalets de Platé).

tip of the structure. Further south around La Bombardellaz and Paccaly, the limestone is only 10m to 15m thick, and it then thins dramatically towards Col de l'Ouettaz, where it is absent altogether, with the Globigerina Marls directly overlying the Cretaceous micrites. In general, these sections show a more basinal facies association. The limestone reappears towards St Marto (2.5m) and thickens towards Col de Forclaz (4m) until prolific development is seen at Tête de la Sallaz.

4.2.2. Massif de Platé

The Massif de Platé is separated from the Thônes Syncline by the Arve valley. The Nummulitic Limestone outcrops at the top of the plateau formed of folded and thrust Cretaceous strata (Pairis et al., 1992). On the Desert de Platé, in the south of the Massif, the Nummulitique Formation forms the present day surface of erosion and is heavily karstified. Thicknesses are very variable, thought to be due to the continued effects of the palaeo-topography on the unconformity which provided the depocentres for the Infranummulitique (Pairis and Pairis, 1975). The maximum thickness encountered is at Vernant, where the limestone reaches 110m thick (Pairis and Pairis, 1975). A dramatic thinning is seen towards East Flaine, where the limestone is only 15m thick, before thickening again to 70m at Les Grandes Platières.

Further north, the Nummulitic Limestone outcrops as cliffs around the edge of the plateau, with the Globigerina Marls and Taveyannaz Sandstone forming the erosion surface. Thicknesses here vary from 80m at l'Epine to 15m at Balme (Pairis and Pairis, 1975).

The preserved remnants of an earlier transgression, represented by a thin limestone containing large *Nummulites* and *Assilina*, outcrop at Arâches and Le Rocher Blanc (Pairis and Pairis, 1975; Chaplet, 1989). This limestone has not been studied in detail due to inaccessibility, but is mentioned due to its implications for the early relative sea-level variations during the deposition of the formation (Chapter 7).

4.3 Basal Detrital Facies

These facies, which are the last sediments containing detrital input from the uplifted foreland region, occur at the base of the Nummulitic Limestone, directly overlying the Infranummulitique or the Mesozoic substratum. They are the most widely spread detrital deposits (c.f. Infranummulitique), being absent only from local highs. Their thickness varies from a few tens of centimetres to 6m and they commonly infill the

underlying karst surface marking the top of the Senonian, smoothing out the pre-existing topography. Four main facies can be distinguished (Table 4.1).

Facies	Features	Samples
Breccio Conglomerate SCg	Q, Gl, Li	
Quartzitic Wackestone SWq	Q, Gl, Li N, A, M, T, E, B, G Xb, Xl, M	LCS1, CC1, CC54, CC55, CC56, PW6, VAC7, F1, FE1
Quartzitic Grainstone SGq	Q, Gl, Li, E, B, (N, A) Xb, Xl, M	EP4, MM1, PAC8, FE2, FE3, F3 LCG19, BOM1
Quartz Arenite SQ	Q M	PAC1

Key to Features

Clastic Components	Bioclasts	Sedimentary Structures
Q = quartz	N = *Nummulites*	Xb = cross-bedding
Gl = glauconite	A = *Amphistegina*	Xl = cross-lamination
Li = lithic grains	M = Miliolid	M = massive
	E = echinoid	
	B = bivalve	
	G = gastropod	
	Sh = shell hash	

Table 4.1: Basal detrital facies of the Haute Savoie Nummulitic Limestone, showing dominant detrital clasts, bioclasts, sedimentary structures and sample collected of each facies.

4.3.1. Breccio-conglomerate (SCG)

The breccio-conglomerate occurs directly above the erosional unconformity where the Infranummulitique is absent and it marks the base of the marine beds. Where the Infranummulitique occurs between the Mesozoic and the Nummulitic Limestone, a thin breccio-conglomerate is commonly present at the base of the sandy marine limestones (Section 4.3.2). It varies in thickness, usually only reaching a few centimetres to tens of centimetres, but attains 1m at Col du Colonney. The breccio-conglomerate is absent from palaeo-highs, which may be recognised by the absence of the basal cycles of the Nummulitic Limestone (Chapter 7).

The breccio-conglomerate is characterised by the presence of angular to rounded clasts of the substratum (Fig. 4.2). These are composed of Senonian micrite, greensand and rarely chert. The clasts generally have long axes of 1-3 cm and rarely reach sizes of more than 10 cm. The largest clast sizes occur over the former karst surfaces, and where

Fig. 4.2: Basal breccio-conglomerate boulder from Le Chinaillon, showing the contact with the Senonian (S) and subangular to rounded clasts of Cretaceous micrites with borings (B) and local reddening (R) in a calcarenite matrix.

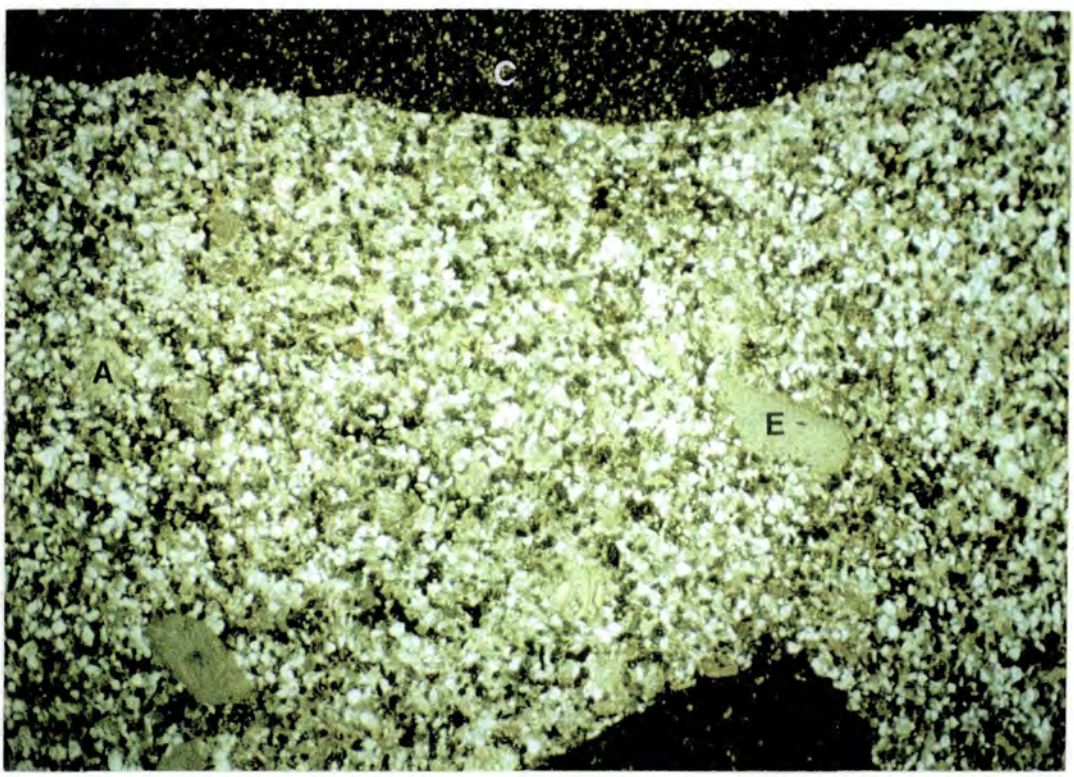

Fig. 4.3: Thin section of the basal breccio-conglomerate showing clasts of Senonian micrite (C) floating in matrix with quartz, glauconite, echinoid plates (E) and abraded Amphistegina (A). Scale 12x7mm.

the conglomerate overlies the Infranummulitique, the clasts tend to be more rounded. The breccio-conglomerate is matrix-supported, with the clasts floating in a matrix of sandy limestone (Fig. 4.3), and is generally structureless and poorly sorted. Both the clasts and the surface of the underlying Mesozoic may be bored. Locally the clasts may be reddened. At Col du Forclaz, the breccio-conglomerate is unusual in that it consists entirely of small, angular chert clasts in a calcarenite matrix.

4.3.2. Sandstones and sandy limestones

The sandstones and sandy limestones contain the first large benthonic foraminifera encountered in the succession (*Nummulites, Amphistegina*, Miliolids and Textulariids), though the faunal content varies between localities. Other bioclasts include pectinid bivalves and thick-shelled oysters, echinoids and low-spired gastropods. A shelly horizon occurs at Flaine, consisting of low-spired gastropods and bivalves. Reworked Mesozoic clasts are common.

The facies are generally flat-bedded, though centimetre- to decimetre-scale cross-bedding may occur (Fig. 4.4), with the base of the cross-beds commonly convex-upwards (trough cross-sets).

Fig. 4.4: Planar cross-bedding in coarse, quartzitic grainstones at La Bombardellaz.

Lenticular sandy limestones with large-scale cross-beds occur locally between the Mesozoic and the Nummulitic Limestone (Fig. 4.5).

Fig. 4.5: Sandy grainstone shoal with large-scale cross-bedding at Col de la Forclaz. "Scale" = 1.6m.

The sandstones can be divided into three constituent microfacies based on the proportions of quartz, matrix and cement present.

4.3.2.1. Quartzitic wackestone (SWq)

This facies (Fig. 4.6) contains 15-35% detrital quartz. The grains are angular to subangular and fine sand-grade (0.1-0.3mm). Sorting is generally poor, though some samples show a bimodal grain-size distribution with larger, rounded grains, of a similar size to the bioclasts (up to 1.5mm). Glauconite (0-15%) is the same size and shape as the quartz grains. Lithic grains (0-5%) consist of subrounded clasts of Senonian micrite and greensand (0.5-2mm diameter).

The matrix is an organic-rich micrite, with bioturbation causing concentration of quartz grains and bioclasts and producing mottling of the micrite. Some samples contain a high proportion of skeletal hash.

Bioclasts (0-70%) include rotaline and porcellanous foraminifera, algae, bivalves, echinoderms and fragments of *Cerithium* gastropods. The most common foraminifera are

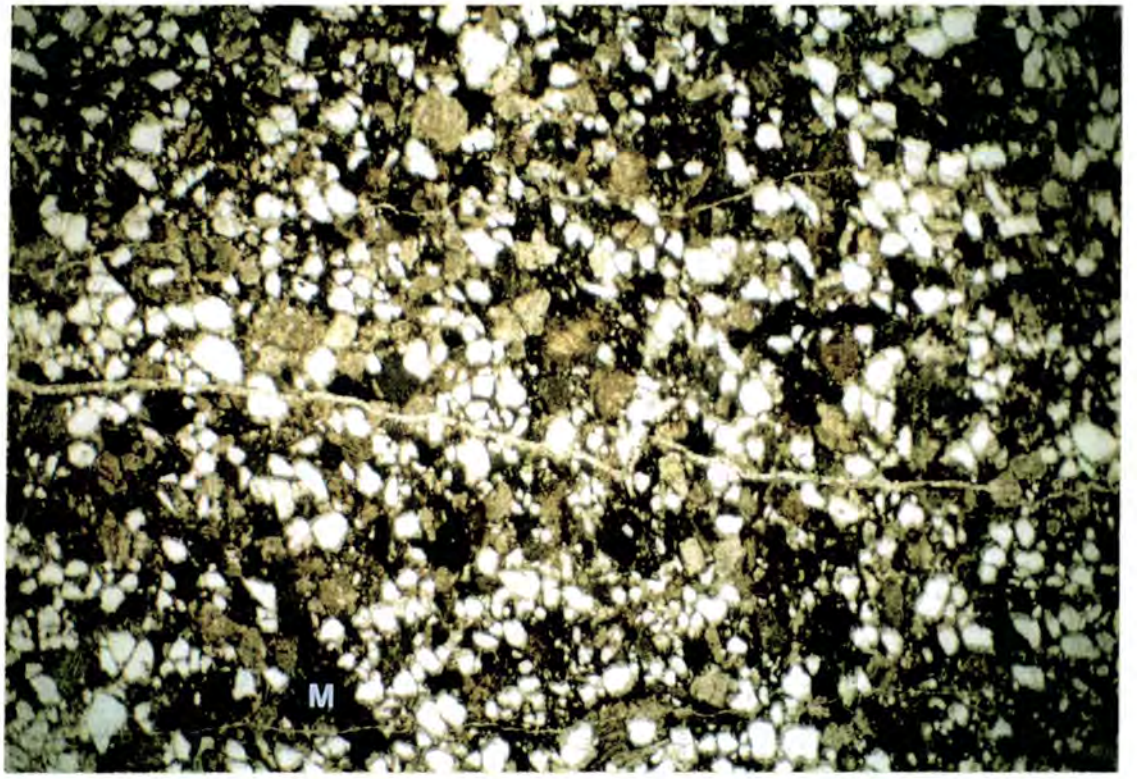

Fig. 4.6: Thin section of the quartzitic wackestone microfacies. The sediment consists of quartz, lithic grains, glauconite and skeletal fragments in a calcareous mud matrix (M). Scale 12x7mm.

small, robust forms of *Amphistegina* and *Nummulites* which constitute up to 20% of the sediment and are heavily abraded,and Miliolids and Textulariids (up to 5%). Fragments of CRA may contribute to the skeletal debris but are generally uncommon. *Cerithium* gastropod fragments occur where the facies overlies the Infranummulitique. The skeletal hash consists of fine sand-grade, angular fragments of the above bioclasts.

4.3.2.2. Quartzitic grainstone (SGq)

This microfacies (Fig. 4.7) is characterised by the lack of fine-grained material and the development of a calcite cement (35-50%). Fine to medium sand-grade quartz constitutes 15-60% of the sediment and is angular to subangular. Sorting is moderate to poor, with outsized, rounded grains producing a bimodal distribution in some samples. Glauconite is the same order of size as the quartz. Lithic grains (0-30%) are angular to subrounded with a large grain-size variation from fine sand- to pebble-grade. The largest clasts occur in those grainstones forming the matrix to the breccio-conglomerate facies. The bioclasts (0-50%) are dominantly sand-grade skeletal fragments of echinoderms, bivalves, bryozoans and rotaline foraminifera. Heavily abraded *Amphistegina* may be

present, although they are very uncommon. Matrix, where present, makes up less than 5% of the sediment and is a dark, fine-grained micrite.

Fig. 4.7: Thin section of quartzitic grainstone microfacies showing quartz grains in a calcite cement. Note the absence of skeletal and lithic debris and the large size of the quartz compared to the quartz wackestone. Scale 12x7mm.

Several forms of cement are present (Fig. 4.8).

1) Isopachous Fringe This is the earliest cement and is very fine-grained, occurring as a fine rim around the quartz grains and bioclasts.

2) Calcite Mosaic: This is the most abundant cement, infilling the interstices between the grains. The crystal size is fairly uniform throughout the samples, though a slight coarsening away from the grain boundaries can occur.

3) Syntaxial Overgrowth: This is associated with the echinoderm fragments, growing in optical continuity with the bioclast. Where the overgrowth encompasses more than one grain, a poikilotopic texture is produced.

4.3.2.3 Quartz arenite (SQ)

This facies (Fig. 4.9) only occurs at Paccaly on the eastern side of the Thônes Syncline. In hand specimen it is white with a sugary texture and is therefore very distinct from the above grey, sandy limestones. In thin section, it can be seen to consist entirely of

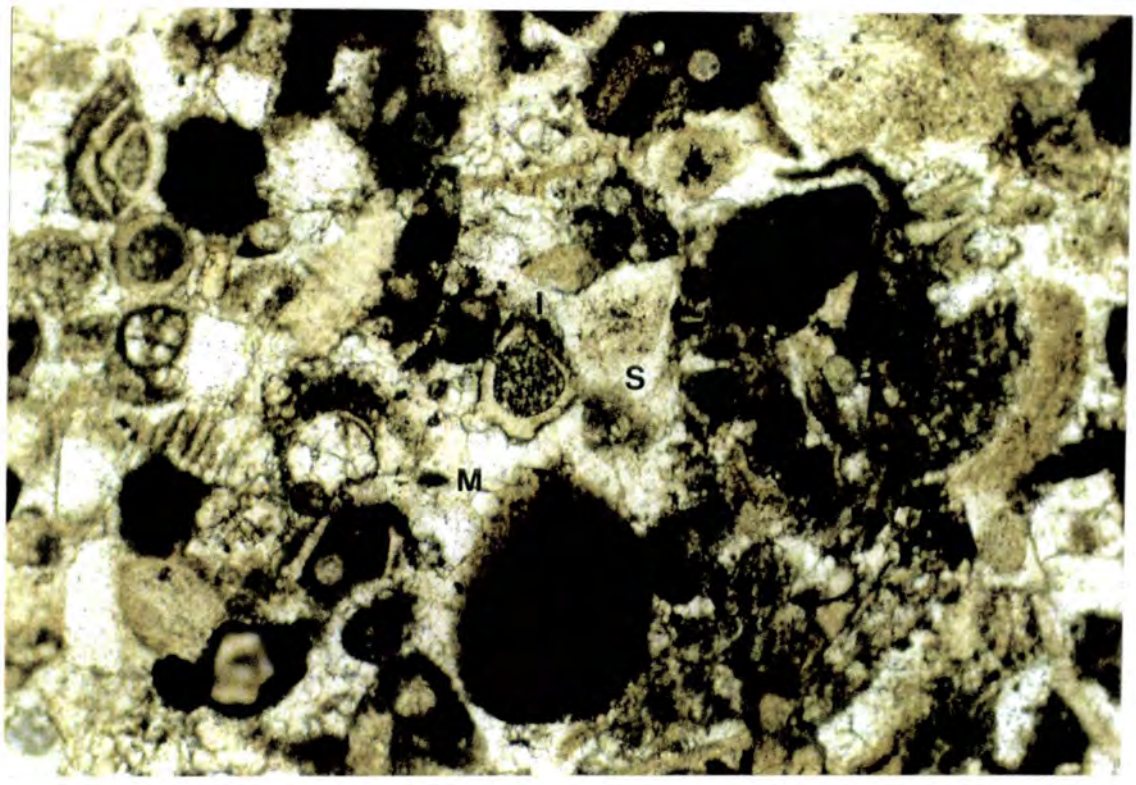

Fig. 4.8: Photomicrogaph showing the different cements in the quartz grainstone; isopachous rim (I), calcite mosaic (M) and syntaxial overgrowth around echinoid plates (S). Scale 3x1.7mm.

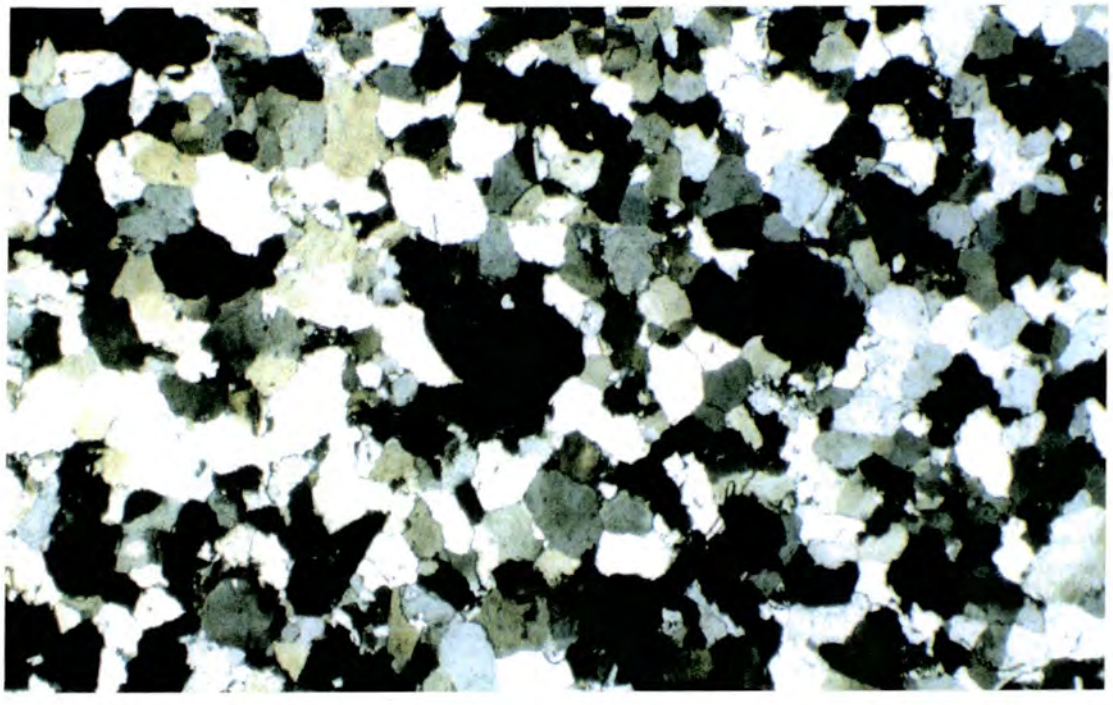

Fig. 4.9: Photomicrograph of the quartz arenite seen at Paccaly. The closely interlocking texture of the quartz is interpreted to be due to the presence of quartz overgrowth cement. Scale 6x3.5mm.

interlocking quartz grains with moderate sorting. Though original grain boundaries are difficult to distinguish, the interlocking texture is thought to be due to the development of an extensive quartz overgrowth cement around the grains.

4.3.3. Interpretation

The nature of the fauna and the bored Mesozoic clasts shows that the sandstones and breccio-conglomerate were deposited in a marine environment. The Cerithiids, typically brackish water indicators, have been reworked from the underlying Infranummulitique during the early stages of the transgression, as they are only present in the sandstones overlying the *Cerithium* marl facies. The sandstones and sandy limestones represent the first evidence of the marine transgression in the formation and the high proportion of quartz present in the sediments indicates that clastic source areas were still active with only the fine detritus reaching the marine realm.Pure carbonate sedimentation had not yet commenced, though the benthos had begun to be established

The base of the sandstones is erosive, reworking the exposed surface of the Mesozoic substratum to create the basal breccio-conglomerate. The reddened clasts indicate a period of subaerial exposure prior to transgression and the angularity and composition of the Senonian clasts suggests that they have been redeposited close to their source. The clasts are interpreted as reworked fragments eroded from the underlying karst surface; the more rounded clasts are thought to have been transported further from their source. The basal breccio-conglomerate is interpreted as a transgressive lag occurring above the previously exposed Mesozoic substratum (Thônes Syncline) or above the marine transgression surface separating the Infranummulitique and the Nummulitic Limestone (Desert de Platé). The deposition of this lag and the angularity of most of the clasts indicate that transgression was fairly rapid.

Cross-bedding and cross-lamination in the sandstones indicate that deposition occurred under the action of marine currents, though the presence of both matrix-rich and cemented sandstones suggests that water energies were variable. The quartzitic wackestones represent the lower energy conditions, with reworking abrading the bioclasts and producing cross-bedding and cross-lamination, but not removing all the fine-grained material. In the higher energy zones, the quartzitic grainstones dominate, with local quartz arenites, and the virtual absence of rotaline foraminifera suggests shallow, highly agitated waters. The sandstones are thought to represent shallow-water, offshore shoals and bars reworked by continual wave and current action, deposited after a rapid transgression over the exposed substratum and/or the coastal Infranummulitique.

4.4. Nummulitic Limestone Microfacies

The Nummulitic Limestone represents deposition in a carbonate ramp setting. There is no evidence for significant slopes being present during the deposition of the limestone (no turbidites, slumps or slope breccias) and the gradational transitions between facies indicates that the ramp was homoclinal. The benthos was dominated by larger benthonic foraminifera and calcareous red algae, which have been used to assign the microfacies to relative positions on the ramp and to discuss the relative water depths during the deposition of the sediments. The succession can be divided into 20 constituent microfacies (Table. 4.2) based on the depositional texture (classification of Dunham, 1962) and bioclastic content of the sediment.

Microfacies	Features	Samples
Mudstone **SM**	T, (R, A) Q, Org, Bio	BOM2, BOM3, BOM4, BOM5, BOM6, PAC2, VAC6, EP9, F12, PW4, PW7, PW8, LCS2
Foraminifera Mudstone **SMf**	N, D, O, A Q, Sh, Py, Bio	PAC3, PAC5
Algal Mudstone **SMa**	A, Br, M, R Bio, Q, Sh	LCG53, FE5, CC61
Skeletal Mudstone **SMsk**	N, M, T, R, Bio	TS4, TS5, CC76, LCG27, MM12, FE4, F4, CHP4,
Discocyclina/Operculina **Wackestone** **SWdo**	D, O, (N, A, R) Q, Sh	COM10, LCG26, PAC7
Nummulite Wackestone **SWn**	N, A, M, CRA, R Q, Sh., Bio, St	CC57, CC58, CC59, PAC4, PAC6, LCG36, LCG37, LCG38, LCG42, LCS3, LCS5, COM5, COM15, COM17, COM18, COL6
Skeletal Wackestone **SWsk**	CRA, Br, S, M, T, N, A, (D) Sh, Bio	CC72, CC77, COM2, COM3, COM7, COM8, COM16, LCS9, LCG49, MM9, MM10, MM11, TS2, VAC5, F6, F8, F10
Coral Wackestone **SWc**	C, CRA, R, A, (D) Q, Sh, Bio	LCS8, F5

Table 4.2: Constituent microfacies of the Nummulitic Limestone of Haute Savoie, showing dominant bioclasts, detrital grains, textures and samples collected of each microfacies

Microfacies	Features	Samples
Foraminifera Packstone **SPf**	D, O, N, A, (R) Sh	LCG28, LCS14, TS7, COM4
Nummulite Packstone **SPn**	N, A, (D, O), M, T, R, Br Org, Bio	LCG21, LCG33, PW9, CC2, CC56, COM13
Foralgal Packstone **SPfa**	N, A, CRA, D, O, T, (M), R Q	MM3, MM4, LCG32, F11
Nummulite-Algal Packstone **SPna**	N, A, CRA, R, M, T, (Pl) Q, (Gl)	LCS6, LCS15, LCS16, CC71, MM6, LCG22, LCG29, LCG44
Stacked Discocyclinid Packstone **SPd**	D, O, N, A, Q, (Gl), S t	LCS10, LCG25, COM6, CC63, TS6
Mollusc Packstone **SPm**	B, G, M, Q, Sh, Org	F2, LCS4
Algal Packstone **SPa**	CRA, R, N, A, (D), M, T Q, Sh	CC68, CC73, CC74, CC75, LCS13, MM2, MM8, LCG23, LCG43, LCG45, LCG48, LCG50, COM9, COM14, VAC2, VAC3, VAC4
Algal-Debris Packstone **SPad**	CRA, N, A, (D), M, T Sh	MM5, MM7
Algal Boundstone **SBa**	CRA, C, S, Br, M, T, (N, A, D), Sh	LCG34, LCG35, LCG39, LCG41, LCS11, CC65, CC66, CC70, F9
Coralgal Pack-Boundstone **SBc**	C, CRA, M, (N, A, D), Sh, Bor	CC67, CC69, COM11, COL7
Algal Grainstone **SGa**	CRA, R, (N, A) Bor	LCG47, MM13, COM12
Skeletal Grainstone **SGsk**	CRA, R, N, A, D, M, T Q, Gl	LCG46, LCG51, F7

Key to features

Foraminifera	**Other Bioclasts**	**Clastic components**	**Textures**
N = *Nummulites*	CRA = algae	Q = quartz	Bio = bioturbation
D = *Discocyclina*	C = coral	Gl = glauconite	St = bioclast stacking
O = *Operculina*	S = serpulid	Sh = skeletal hash	Bor = borings
A = *Amphistegina*	Br = bryozoa	Py = pyrite	( ) = rare
M = Miliolid	G = gastropod	Org = organic debris	
T = Textulariid	B = bivalve		
Pl = planktonics	R = reefal organisms		

Table 4.2: Constituent microfacies of the Nummulitic Limestone of Haute Savoie, showing dominant bioclasts, detrital grains, textures and samples collected of each microfacies.

4.4.1. Marl

This facies (Fig. 4.10) is a fine-grained, argillaceous lime mudstone with a small percentage of silt-grade quartz. The first major occurrence of pelagic foraminifera occurs in this facies, along with agglutinating foraminifera, some small *Nummulites* and *Discocyclina*. The rock is fissile and can contain fish-scale horizons. The base is gradational with the transitional beds (2-10 m) commonly showing bioturbation.

Interpretation: The marl represents pelagic deposition in very low-energy. deep, basinal waters and is only dealt with briefly in this study.

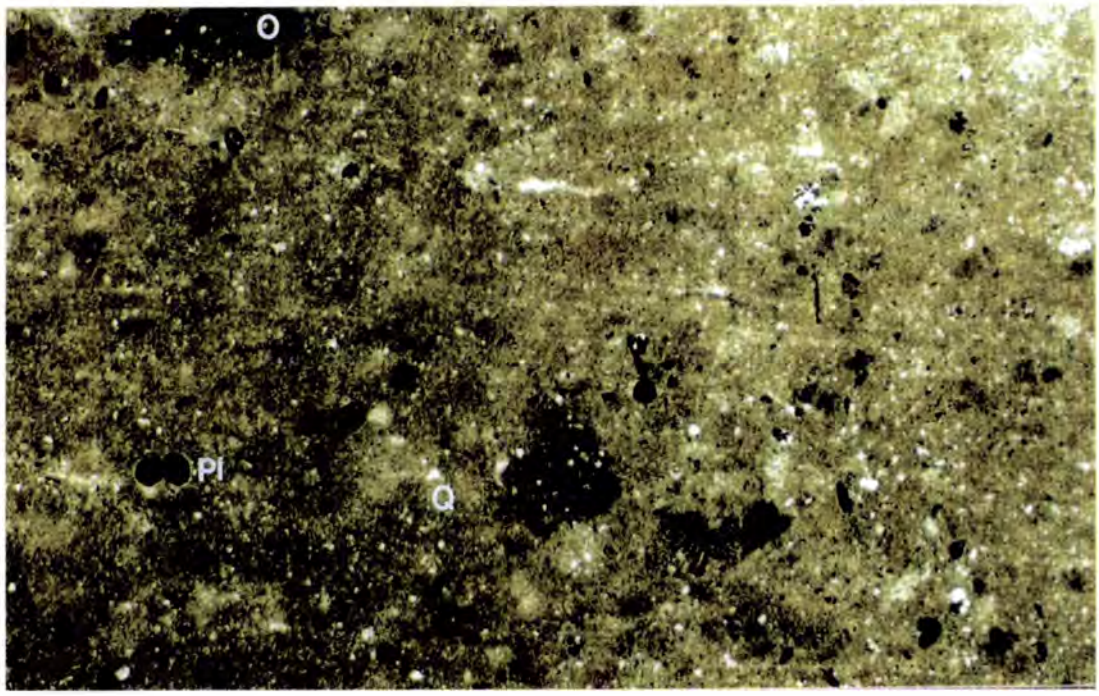

Fig. 4.10: Photomicrograph of the marl, showing laminae with concentrations of organic material (O), planktonic foraminifera (Pl) and silt-grade quartz (Q). Scale 6x3mm.

4.4.2. Mudstone (SM)

This microfacies (Fig. 4.11) contains 65-90% matrix, which is an organic-rich, brown micrite with rare silt-grade quartz. Bioturbation produces mottling and introduces shell debris. Some glauconite and silt-grade quartz occurs, more common in the samples taken from the top of the formation. Bioclasts include fragments of calcareous red algae (0-5%), bryozoans and corals (0-10%), bivalves and echinoderms. Foraminifera are rare (less than 5%) and, where present, are *Amphistegina* and Textulariids.

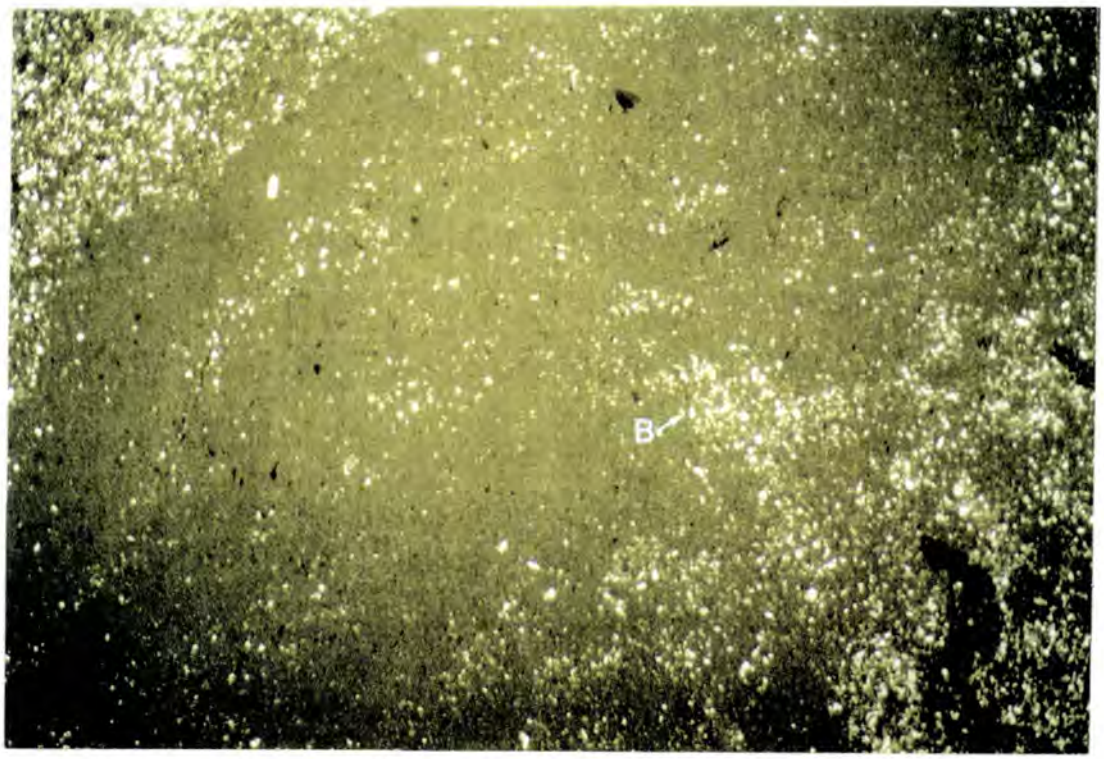

Fig. 4.11: Photomicrograph of the mudstone microfacies (SM). This clearly shows the effects of bioturbation concentrating planktonic foraminifera (B) and disrupting the original laminae, which are preserved in the centre of the photograph. Scale 12x7.2mm.

Interpretation: This represents deposition in very low-energy, basinal waters. The presence of silt-grade quartz indicates slight detrital influx and glauconite is deposited during very low sedimentation rates. The preservation of planktonic foraminifera (Globigerinids, Globoratalids) suggests a deep, very low-energy setting. Fragments of bioclasts and rotaline foraminifera (*Amphistegina*) have been washed into the basin from shallower water environments. The sediment was well oxygenated as shown by extensive bioturbation producing mottling and reworking the bioclasts.

4.4.3. Foraminiferal mudstone (SMf)

This microfacies (Fig. 4.12) contains more than 95% matrix, consisting of micrite with calcispheres, shell hash and a low percentage of silt-grade quartz. Bioturbation is common, producing mottling and local grain-size variations. Bioclasts (5%) include large, flat *Nummulites*, *Discocyclina* and *Operculina* and robust *Amphistegina*. The tests may be infilled with pyrite.

Interpretation: This facies was deposited in a very low-energy environment, unaffected by material derived from the shallow water shoal areas. Large, flat *Nummulites*

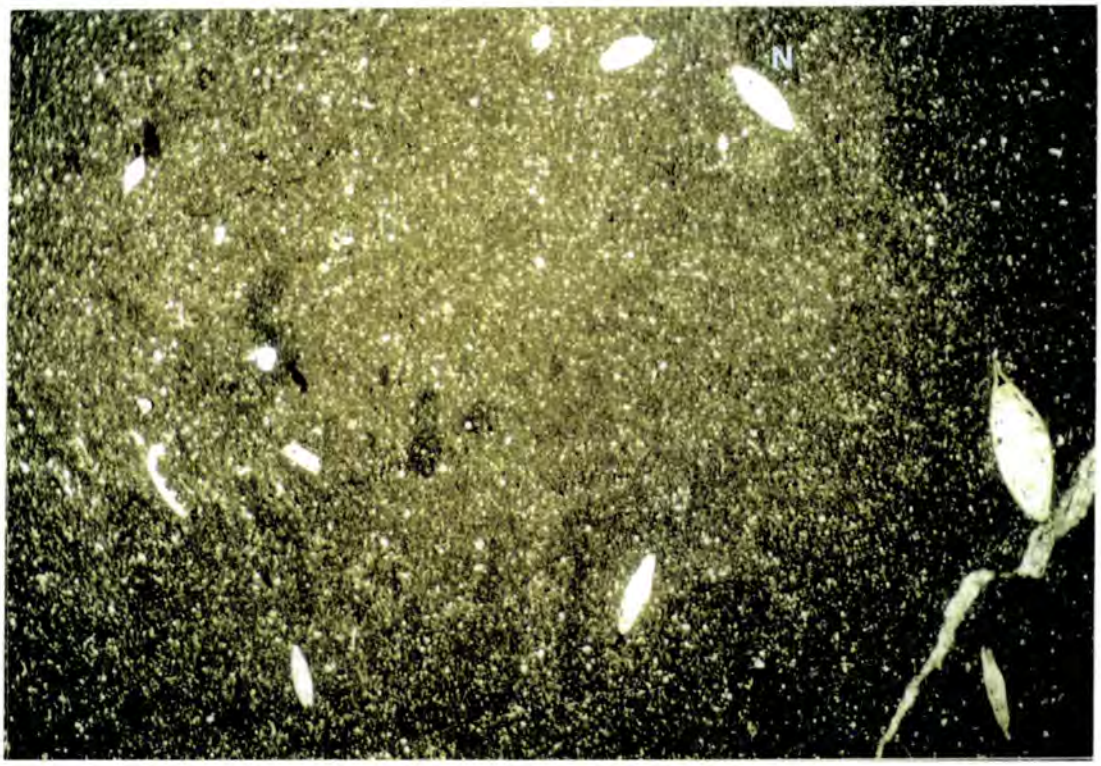

Fig. 4.12: Photomicrograph of the foraminiferal mudstone microfacies (SMf). Note the high proportion of micritic matrix and the elongate Nummulites (N). Scale 12x7mm

and *Operculina* are also indicative of deep, low nutrient waters from towards the outer part of the carbonate ramp. Any robust foraminifera present have been washed down from shallower environments.

4.4.4. Skeletal mudstone (SMsk)

This microfacies (Fig. 4.13) is characterised by a high proportion of micrite (70-90%). The bioclasts are small, intermediate *Nummulites* (1%), flat and spherical Miliolids (2%) and Textulariids (1%), none of which have been abraded. In addition, up to 15% of abraded fragments of reefal organisms are present. The sediment is reworked by bioturbation.

Interpretation: The high mud content indicates that the environment of deposition was low energy and the low proportion of bioclasts indicates that most samples of this microfacies were deposited in unfavourable conditions with low light and nutrient levels. The replacing of flat forms by intermediate *Nummulites* indicates that this is probably a shallower-water setting than the mudstone and foraminiferal mudstone microfacies. The

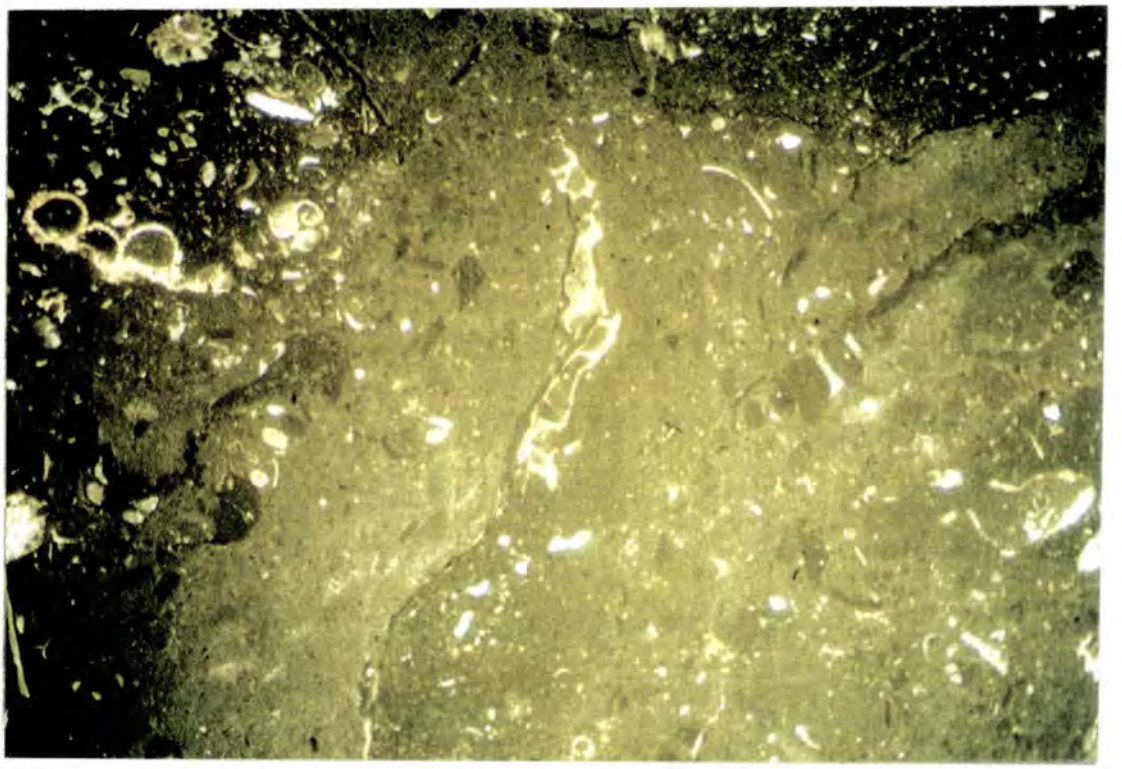

Fig. 4.13: Skeletal mudstone microfacies (SMsk). The abundance of reefal debris suggests proximity to a rhodolith shoal. Scale 12x7mm.

preservation of the bioclasts indicates that little transportation has occurred and that they are *in situ.*

4.4.5. Algal mudstone (SMa)

The bioclasts present in this microfacies (Fig. 4.14) are dominated by fragments of CRA (10%) and bryozoans (5%). Other bioclasts include serpulid worm tubes, echinoderm and coral fragments and Miliolids. CRA are present either as thin algal crusts, encrustations on other bioclasts or abraded fragments. The matrix (45-90%) consists of an organic-rich, dark brown micrite with mottling due to bioturbation and up to 15% silt-grade quartz.

Interpretation: This microfacies represents deposition in low-energy waters. The high proportion of CRA and bryozoans and the presence of serpulids and corals suggests that the mudstone was deposited in a inner-ramp setting. The presence of thin CRA crusts indicates little water agitation. The absence of rotaline foraminifera indicates that this is a shallow-water sediment.

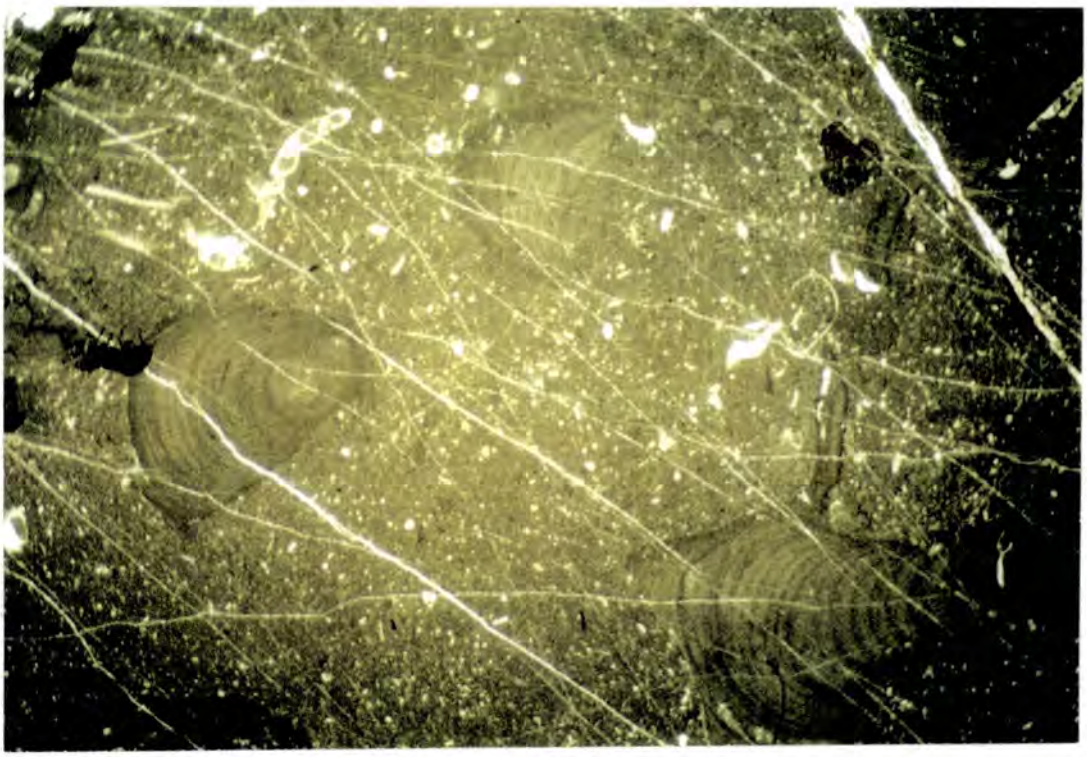

Fig. 4.14: Algal mudstone microfacies (SMa), showing abraded fragments of CRA in a micritic matrix. Scale 12x7mm.

This microfacies is interpreted as a back- or inter-shoal mud, sheltered from agitated waters by algal shoals, leading to the preservation a high proportion of micrite and a favourable environment for sediment dwellers to rework the sediment.

4.4.6. Nummulite wackestone (SWn)

This microfacies (Fig. 4.15) is dominated by larger *Nummulites* (up to 30%) and *Amphistegina* (up to 25%) in a high proportion of micritic matrix (55-80%). They are intermediate to robust and generally well preserved, with the larger forms tending to be more abraded. They locally occur in clusters, probably concentrated by bioturbation. Both A- and B-forms are present. CRA constitute up to 15% of the sediment and are associated with bryozoans (2%), coral fragments (up to 5%), serpulids and bivalve and echinoderm fragments. These bioclasts are generally fragmented and abraded, though well-preserved, possibly *in situ* rhodoliths occur. Miliolids are present in most samples and may reach up to 10% abundance.

The matrix is a dark micrite with skeletal debris of foraminifera and molluscs. Quartz is present as angular grains (2-10%) and may be concentrated in burrows. Bioturbation is also evident in mottling in the sediment and alignment of the bioclasts.

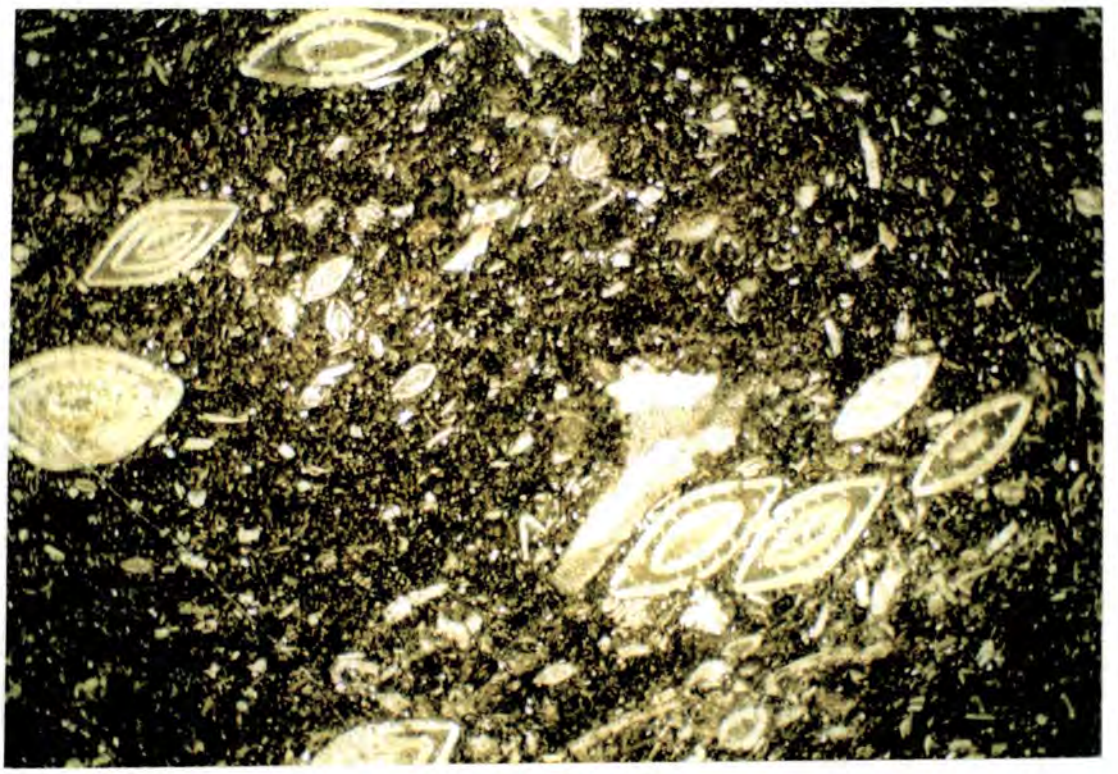

Fig. 4.15: Nummulite wackestone microfacies (SWn). Note the higher proportion of bioclasts compared to the mudstones, dominated by ovoid Nummulites with relatively thin tests and a high proportion of micrite. The lack of abrasion of the foraminifera indicates a lack of transportation. Scale 12x7mm.

Interpretation: The dominance of intermediate to robust *Nummulites*, *Amphistegina,* Miliolids and *in situ* CRA implies a position proximal to the algal banks from which the skeletal debris has been derived. The high proportion of matrix and shape of the foraminifera suggest deposition below FWWB, with the skeletal debris washed in by storm events and down-ramp currents which also caused abrasion of the foraminifera tests. The existence of both A- and B-forms implies that conditions were favourable for reproduction and that water energies were not strong enough to remove the smaller A-forms. The presence of rhodoliths suggests there was sufficient water agitation, though probably periodic, to rotate the fragments to sustain CRA growth.

This microfacies represents a middle ramp deposit, below wave base but with intermittent high-energy events turning the rhodoliths and introducing debris from the inner ramp.

4.4.7. *Discocyclina/Operculina* wackestone (SWdo)

The dominant bioclasts in this microfacies (Fig. 4.16) are large (up to 10mm), well preserved, flat *Discocyclina* and *Operculina* (up to 10%), which may show some alignment and imbricated stacks. Other bioclasts include small, abraded fragments of echinoids and bivalves and rare inner-ramp debris (serpulids, corals, CRA constituting less than 2% of the sediment). Small, intermediate *Nummulites* and *Amphistegina* may be present (up to 10%), and are generally abraded. Undifferentiated skeletal debris constitutes up to 20% of the sediment, which is micrite supported (55-80%) with a minor amount of silt-grade quartz.

Fig. 4.16: Discocyclina/Operculina wackestone microfacies (SWdo), dominated by flat Discocyclina (D) and Operculina (O) with elongate Nummulites (N). There is a crude alignment of the bioclasts. Scale 12x7mm.

Interpretation: The presence of flat *Discocyclina* and *Operculina* in conjunction with a high proportion of matrix indicates a low-energy, deep water setting below FWWB, relatively unaffected by storms. Abraded *Nummulites* and *Amphistegina* have been washed down-ramp from shallower environments during storms along with a minor influx of reefal detritus. The stacking of the flat *Discocyclina* and *Operculina* is probably due to the reworking of the stacked Discocyclinid packstone microfacies (SPd). Abrasion

of the low energy, flat foraminifera is due to them being less able to withstand reworking by currents, in this case probably storm events.

This microfacies represents a low-energy, outer-ramp deposit with a minor influx of material washed in from shallower parts of the ramp during storms.

4.4.8. Skeletal wackestone (SWsk)

This microfacies (Fig. 4.17) is dominated by CRA, corals and bryozoans with some foraminifera. CRA (5-15%) are present as rhodoliths, thin crusts and abraded fragments and here is some encrustation of the skeletal debris. The algal crusts tend to be fragmented, but the rhodoliths are thought to be *in situ*, nucleating in the soft micrite around algal fragments and/or other skeletal debris. Corals (0-10%) are present as abraded fragments of the same order of size as the other bioclasts (2-10mm). Other binding organisms present are whole and fragmented bryozoans (1-10%), serpulid worm tubes (0-5%) and small, thin-shelled gastropods (0-5%). Larger foraminifera may be present (up to 10%) and include well preserved Miliolids and Textulariids, intermediate to robust, slightly abraded *Nummulites* and *Amphistegina* (maximum 5%) and rare inflated *Discocyclina*. The matrix (50-70%) is a dark micritic mud with silt-grade skeletal debris. Mottling and a clustering of the bioclasts can occur.

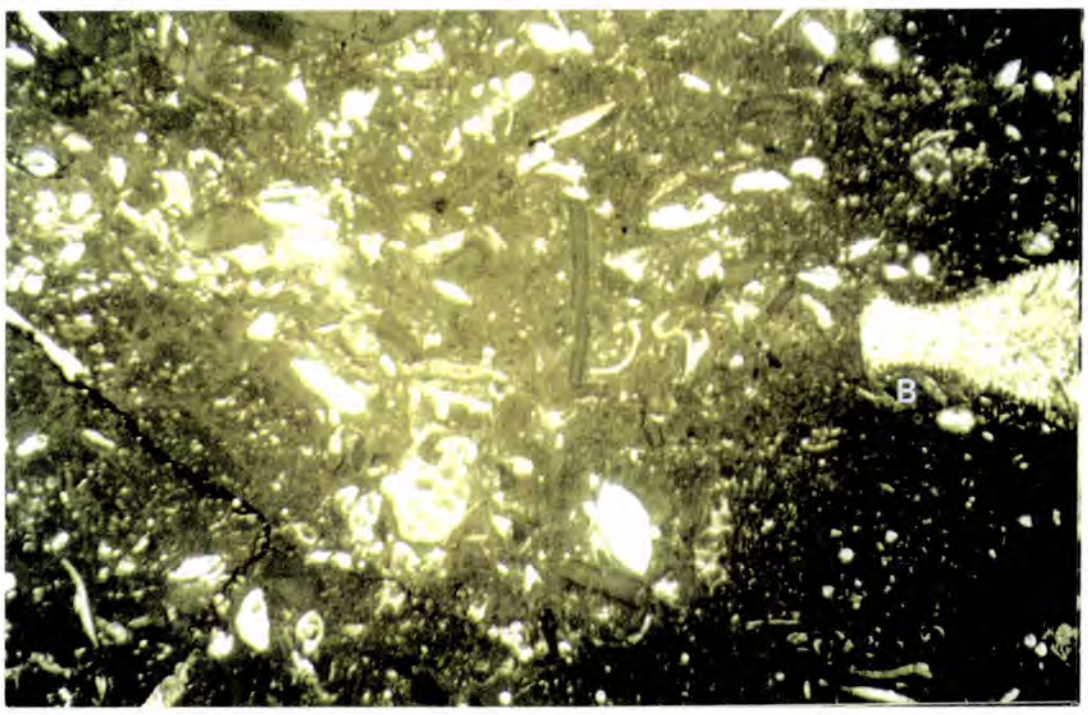

Fig. 4.17: Skeletal wackestone microfacies (SWsk) containing a high proportion of reefal debris including bryozoans (B) and CRA. Scale 12x7mm.

Interpretation: The dominance of reefal organisms implies a shallow-water environment proximal to the shoal areas. The high proportion of matrix indicates that it was still a low-energy environment with little winnowing. The low proportion of foraminifera suggests a relatively hostile environment for rotaline forms but conditions that are tolerated by porcellanous foraminifera i.e. relatively high light intensity. The shape of the rotaline foraminifera indicates a middle- to inner-ramp setting. The CRA appear to be colonising the sediment *in situ* (rhodolith growth and algal sheets). This would entail generally quiet conditions for the growth of the delicate crusts with intermittent water agitation turning the rhodoliths and fragmenting the fragile sheets. Abraded skeletal fragments are washed in from higher energy environments. Mottling of the sediment is due to bioturbation which may also create bioclast clusters.

This microfacies represents deposition in moderate-energy conditions on the inner-ramp with a constant supply of detritus washed in from the algal shoals.

4.4.9. Coral wackestone (SWc)

This microfacies (Fig. 4.18) is characterised by an unusually high proportion of solitary corals (15-30%).

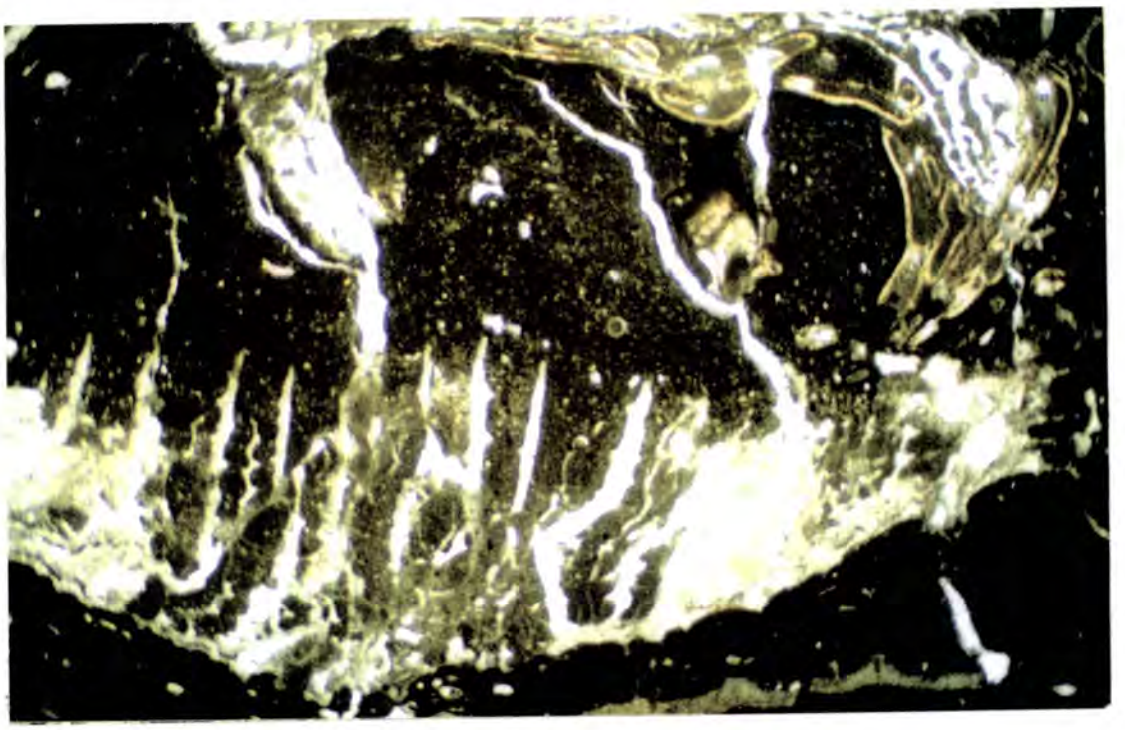

Fig. 4.18: Coral wackestone microfacies (SWc) showing flat, solitary corals in life position. The corals occur in several layers and are thought to be periodically killed off by influxes of lime mud sedimentation. Scale 12x7mm.

The corals may be both intact and fragmented and are commonly encrusted by CRA. The coral skeletons themselves have been pseudomorphed by a calcite cement. Other bioclasts are broken fragments of bryozoans and serpulids (2-10%) and rotaline foraminifera. Ovoid *Amphistegina* (2-5%) show little abrasion and rare *Discocyclina* may also be present. The matrix (50-60%) is micrite with fine-grained shell hash and quartz. Grains may be concentrated in patches indicating bioturbation of the sediment.

Interpretation: This is a low-energy depositional environment, as indicated by the high proportion of matrix. Much of the skeletal debris has been washed from the shoal areas, though the corals and foraminifera are thought to represent the *in situ* ramp fauna.

4.4.10. Foraminifera packstone (SPf)

This microfacies (Fig. 4.19) is dominated by larger benthonic foraminifera (35-45%) with a significant proportion (>15%) of flatter *Discocyclina* and *Operculina*. Inner-ramp bioclasts are rare and, where present, heavily abraded.

Fig. 4.19: Foraminifera packstone microfacies (SPf) containing a mixed foraminiferal assemblage with Discocyclina (D), Lepidocyclina (L) and Nummulites (N). All bioclasts show a high degree of abrasion indicating significant reworking. Scale 12x7mm

The matrix (40-50%) is micrite with a minor amount of silt- to sand-grade quartz. *Discocyclina* (10-25%) and *Operculina* (0-10%) are generally flat, though some inflated

Discocyclinids occur. They vary in size from 5 to 15mm diameter and there is some alignment of the flatter forms. The flatter forms tend to be less abraded than the inflated foraminifera. Small *Nummulites* (up to 20%) and *Amphistegina* (5%) are intermediate to robust and both intact and heavily abraded forms are present in the same sample.

Interpretation: The abundance of flat *Discocyclina* and *Operculina* implies an outer ramp setting, below FWWB, with slight *in situ* reworking producing some alignment of the bioclasts, though may indicate the life positions of the bioclasts. Robust *Nummulites* and *Amphistegina* are characteristic of a shallower-water environment and were probably washed into the sediment during storms, though the intermediate forms could represent the *in situ* fauna. The effects of storm reworking may also cause the abrasion of the bioclasts. This microfacies represents the in situ fauna and reworked shallow-water bioclasts deposited in an outer-ramp setting.

4.4.11. Nummulite packstone (SPn)

This microfacies (Fig. 4.20) is characterised by robust to intermediate *Nummulites* (10-30%) and *Amphistegina* (5 -25%).

Fig. 4.20: Nummulite packstone (SPn). This has a grain-supported texture with abundant bioclasts dominated by Nummulites and Amphistegina (A). The presence of dark, lime mud suggests that deposition is still below FWWB. Scale 12x7mm.

The foraminifera are small (2mm diameter) and have thick tests with both A- and B-forms commonly present. They are generally well preserved but may be slightly abraded. *Discocyclina* and *Operculina*, where present, are flat to inflated and highly abraded. Other bioclasts are Miliolids and Textulariids (up to 5% total) and debris of corals, serpulids, bryozoans and CRA (up to 5%), though bryozoans may occur in larger proportions (10%).

The matrix 15-50%) is a dark micrite which may be mottled and commonly contains organic-rich seams.

Interpretation: The preservation of abundant micrite implies deposition below FWWB, but the lower proportion in association with a higher concentration of bioclasts indicates a higher energy setting than the nummulite wackestone microfacies (SWn). The presence of robust *Nummulites* and *Amphistegina* indicates an inner-ramp environment and the abrasion of the bioclasts indicates agitated waters. The existence of two generations and a multi-specific assemblage of foraminifera indicate favourable conditions (muddy substrate and sufficient light and nutrients) and insufficient water-energy to remove the smaller A-forms. Bioturbation produces sediment mottling and concentration of bioclasts.

This microfacies represents deposition in a middle- to inner-ramp setting, with moderate water depth and agitation.

4.4.12. Foraminifera-algal packstone (SPfa)

This microfacies (Fig. 4.21) is dominated by rotaline foraminifera and CRA. CRA (10-25%) occur as branching forms and thin crusts with some rhodolith growth. The thin algal crusts may reach 50mm in length and fracturing appears to be due to compaction. Rhodoliths nucleate around skeletal debris and patches of micrite. They may be branched and reach up to 20mm diameter. *Nummulites* (5-20%) and *Amphistegina* (0-5%) are robust to intermediate, small (1mm diameter) and intact. *Discocyclina* (10-25%) and *Operculina* (0-5%) are flat to inflated, fairly abraded and fragmented and up to 10mm diameter where intact. Textulariids are present in all samples, but Miliolids are rare. Other bioclasts include a low proportion of skeletal debris (up to 5%) of bryozoans, corals and serpulids, and up to 10% echinoderm plates.

The matrix forms 20-40% of the sediment and is a dark, micrite with trace quartz.

Interpretation: The presence of flat *Discocyclina* and *Operculina* and thin crusts and branching calcareous red algae implies a low-energy setting with low light intensities. Robust to intermediate *Nummulites* suggest shallow depths. Therefore this microfacies represents a low-energy, dark environment with moderate water depths, though deep

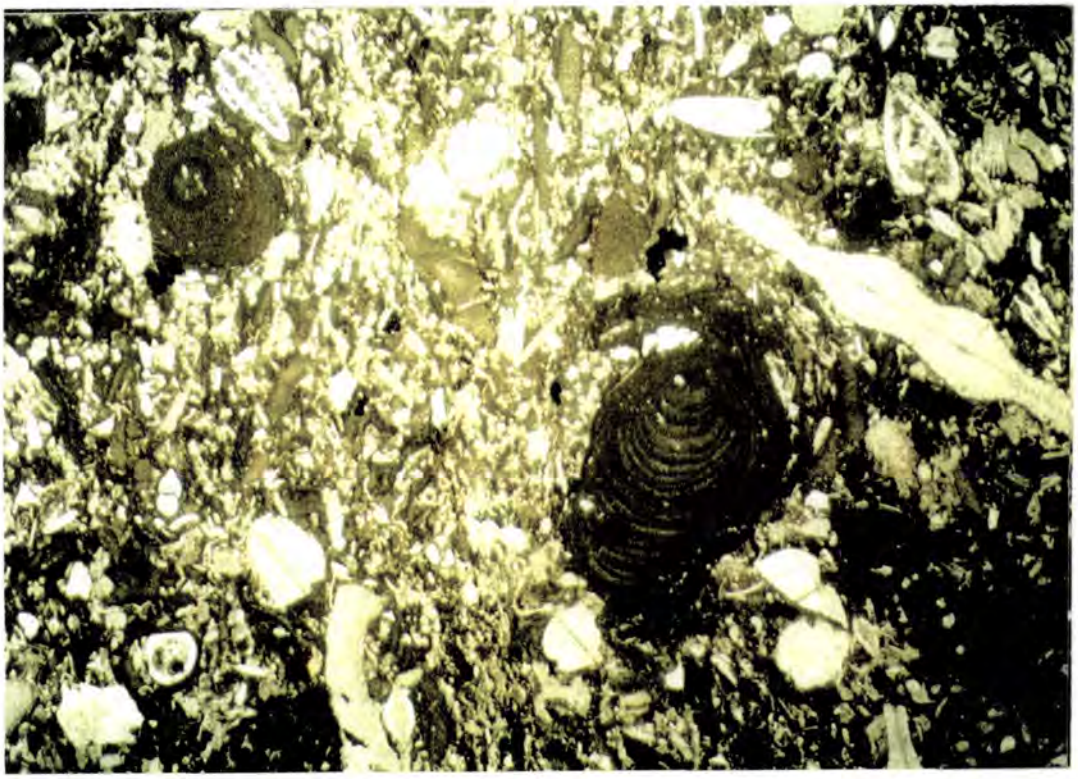

Fig. 4.21: Foraminifera-algal packstone microfacies (SPfa) containing abundant abraded bioclasts and a very low proportion of matrix indicating a high energy environment with significant reworking. Relatively unabraded CRA and foraminifera are present. Scale 12x7mm.

enough to prevent an abundance of Miliolids (i.e. >9 m depth). Some water agitation does occur; sufficient to turn the rhodoliths and fragment the CRA sheets and to winnow the sediment to some extent, causing local reworking of the bioclasts.

4.4.13. Nummulite-algal packstone (SPna)

This microfacies (Fig. 4.22) is characterised by robust, rotaline foraminifera, CRA and a significant proportion of inner-ramp bioclasts. *Nummulites* (7.5-25%) and *Amphistegina* (up to 7.5%) are small, robust and generally intact, with some abrasion. Both A- and B-forms are present. Calcareous red algae (10-20%) occur in various forms: rhodoliths, slightly branching forms and thin crusts. The rhodoliths are small and concentrically layered, forming around nuclei of skeletal debris (serpulids, algal fragments). The branching forms and algal crusts are generally fragmented. Other encrusting and inner-ramp bioclasts include bivalves, serpulids, bryozoans and solitary coral fragments. Miliolids and Textulariids are present in most samples (5%) and may

show some reddening of their tests and slight abrasion. Rare planktonic foraminifera may occur.

The matrix is a fine-grained micrite (35-45%) with 2-3% silt-grade quartz and trace glauconite.

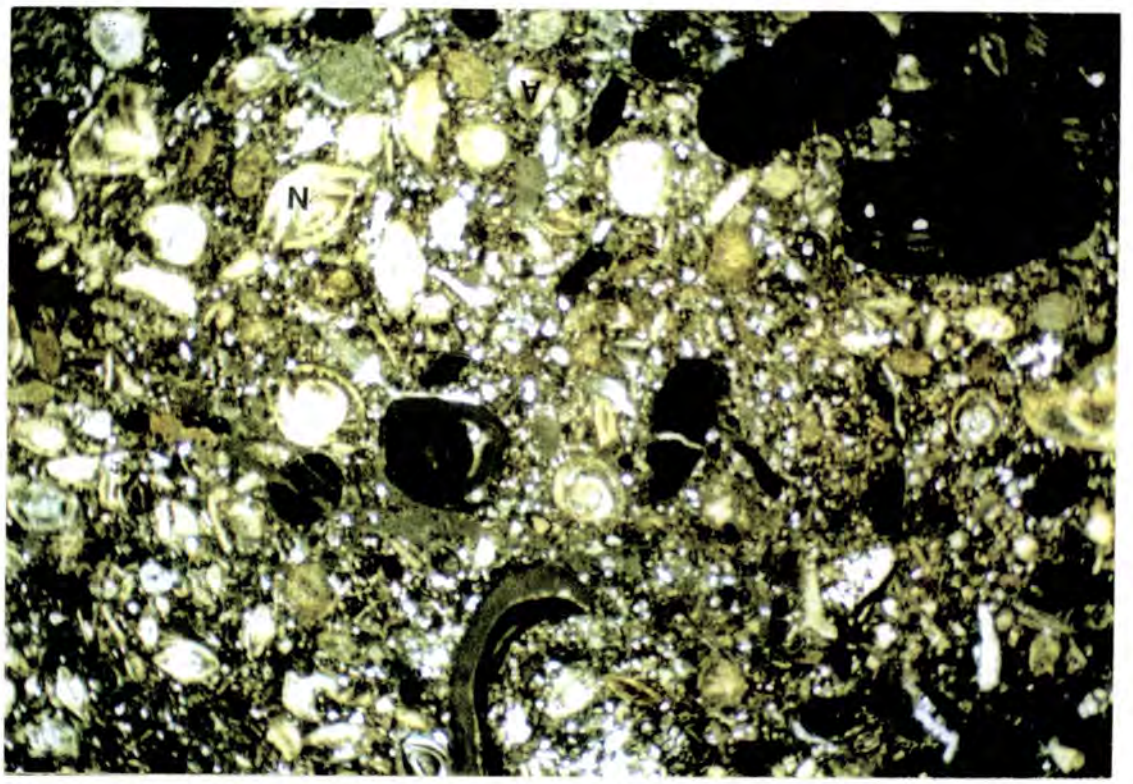

Fig. 4.22: Nummulite-algal packstone microfacies (SPna) containing small, robust Nummulites (N) and Amphistegina (A) with abraded reefal debris and CRA. The matrix consists of fine-grained skeletal hash and micrite. Scale 12x7mm.

Interpretation: The presence of robust foraminifera, abundant debris of encrusting organisms, Miliolids and CRA indicates a shallow, agitated waters, proximal to the shoal areas. This microfacies is a higher energy equivalent to the skeletal wackestone. The existence of two generations in a multi-specific foraminiferal assemblage implies sufficient light and nutrients to promote diversification and reproduction. Water agitation is insufficient to remove the smaller A-forms, though some abrasion occurs, and is sufficient to turn the rhodoliths and introduce skeletal debris into the sediment.

4.4.14. Stacked Discocyclinid packstone (SPd)

This microfacies (Fig. 4.23) is dominated by larger benthonic foraminifera, the majority of which are *Discocyclina* (20-40%). as flat, well preserved and ovoid, abraded

forms. They are up to 10mm in diameter and chaotically imbricated. *Nummulites* (5-15%) are intermediate or robust, with robust forms more abraded. They are stacked together with the *Discocyclina* and flat, well-preserved *Operculina* (2-10%). again A- and B-forms are present. *Amphistegina* (5%) are robust and well preserved. Other bioclasts are rare. The skeletal hash is composed almost entirely of foraminifera fragments. The matrix (25-65%) is a dark micrite with silt grade quartz (1-15%) and rare glauconite.

Fig. 4.23: Stacked Discocyclinid packstone microfacies (SPd) showing the dominance of flat Discocyclina (D) which are chaotically stacked indicating reworking, in situ, by oscillatory currents. Other foraminifera present are Operculina (O) and Nummulites (N). The high proportion of micrite indicates deposition below FWWB. Scale 12x7mm.

Interpretation: The flat, discoid nature of the *Discocyclina* and *Operculina* indicates deposition form low-energy, relatively deep waters. The presence of intermediate and robust *Nummulites* and *Amphistegina* implies a higher energy environment, but the degree of abrasion suggests that these have been transported into the area from shallower waters. The alignment and chaotic stacking of the foraminifera is thought to be the result of oscillatory currents (Racey, 1990), reworking and winnowing the sediment *in situ* and concentrating and re-orientating the foraminifera tests. The form of the foraminifera and good preservation indicate that this reworking occurred *in situ* on

the middle-ramp, below FWWB and is interpreted to be the result of storm events. Other sedimentary structures (ripples, cross-bedding and bioturbation) are rare (Fig. 4.24).

Fig. 4.24: Textures produced due to storm reworking by oscillatory currents and bioturbation encountered in the Disocyclinid packstone microfacies. Similar textures are also encountered in the Nummulite packstone microfacies encountered in Haute Provence (Section 5.3.10).

Flat forms of *Discocyclina* are also thought to be bank builders (Moody, pers. comm.). If this were the case, the *Discocyclina*-rich beds could represent low-relief foraminiferal banks. Similar foraminifera banks are seen in Egypt (Aigner, 1982, 1983) and many show cross-bedding and lamination, scour fills and reworking of the bioclasts by bioturbation. The beds described above are massive and interpreted to be middle-ramp para-autochthonous foraminifera accumulations.

4.4.15. Algal packstone (SPa)

This microfacies (Fig. 4.25) is dominated by CRA (25-50%), which are present in various forms: thin crusts, rounded fragments and branching growths. They are generally well preserved, but abraded fragments are also present. CRA also encrust reworked, skeletal debris, dominantly corals, bryozoans and serpulid worm tubes. Rotaline foraminifera are uncommon, but where present include robust, abraded *Nummulites* and *Amphistegina* (maximum 15%) and inflated, abraded *Discocyclina*. Miliolids and

Textulariids (0-10%) are well preserved and robust. There may be some reddening of the tests.

The matrix is composed of micrite (30-50%) with fine skeletal hash and up to 2% silt-grade quartz.

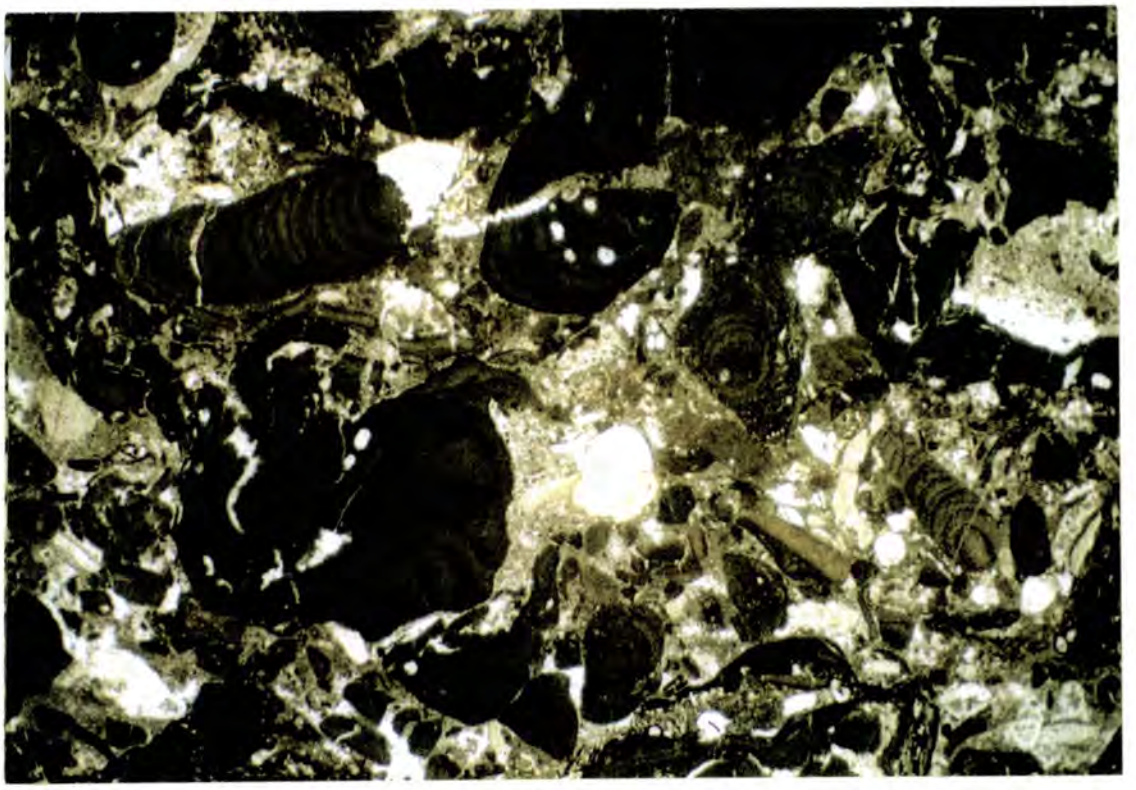

Fig. 4.25: Algal packstone microfacies (SPa) showing abundant fragments of branching CRA and abraded reefal detritus. Scale 12x7mm.

Interpretation: The CRA include both *in situ* forms (thin crusts and rhodoliths) and debris washed in from the main reef (abraded fragments). The form of the CRA indicates a low-energy environment allowing the development of delicate algal crusts, but with sufficient agitation, probably intermittent, to turn the rhodoliths. The preservation of micrite also indicates little water movement. The paucity of rotaline foraminifera indicates a high light intensity, which is also apparent by the relative abundance of Miliolids and Textulariids, whose test compositions make them more resistant to light penetration. Abrasion of the rotaline forms suggests that, where present, they have been transported or reworked *in situ*.

This microfacies represents a shallow-water, moderate-energy, inner-ramp environment, close to the shoals; either a fore- or back-shoal position, sheltered from water agitation by the relief of the algal shoals.

4.4.16. Algal debris packstone (SPad)

This microfacies (Fig. 4.26) contains a significant proportion of CRA (30%) in the form of sand-grade, abraded fragments. Other inner-ramp organisms are uncommon. Large foraminifera make up 10-15% of the sediment. *Nummulites* (5%) and *Amphistegina* (5%) are robust and well-preserved with both A- and B-forms present. *Discocyclina* (0-10%) are inflated to flat and generally heavily abraded. Intact Miliolids and Textulariids (5%) are present. The matrix (25-40%) is micrite with 5% skeletal hash.

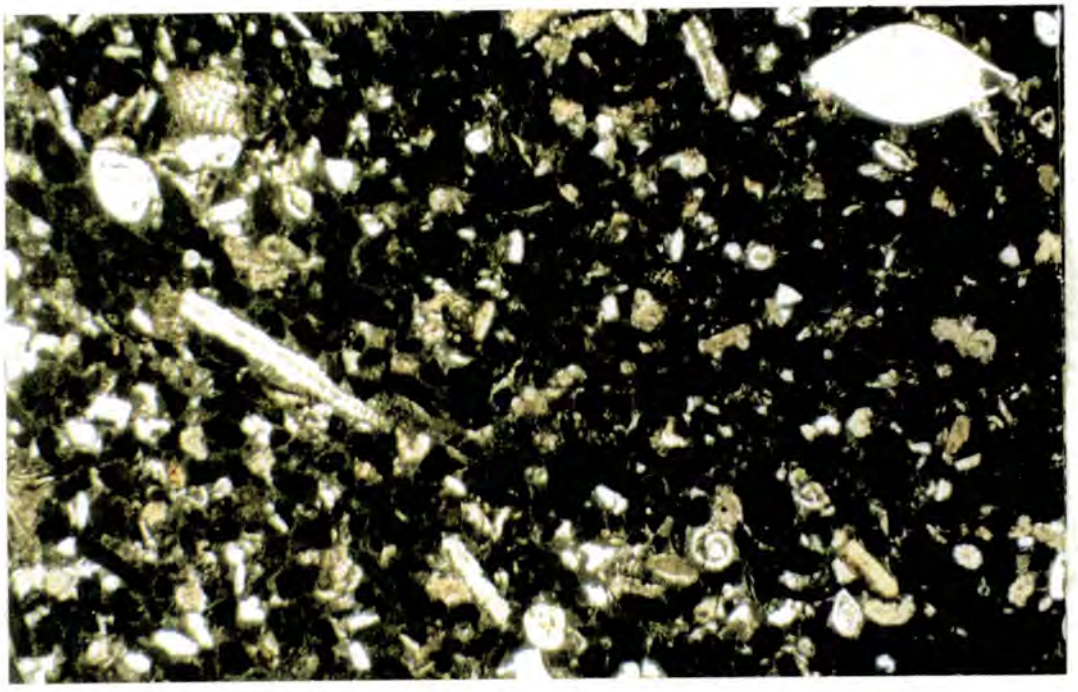

Fig. 4.26: Algal debris packstone microfacies (SPad) with abundant fine sand-grade fragments of CRA and in situ benthonic foraminifera. Scale 12x7mm.

Interpretation: The heavily abraded bioclasts suggests that they had been reworked and transported by high energy waters prior to deposition. The large foraminifera represent the *in situ* fauna from a middle- to inner-ramp setting. The nature of the skeletal debris indicates that it has been reworked from the shallow-water inner-ramp shoals (algal boundstone microfacies) and washed to a more distal ramp setting by storms and currents, which also serve to winnow the sediment to some extent and abrade the *in situ* fauna.

This microfacies represents a fore-bank washover deposit.

4.4.17. Algal boundstone (SBa)

This microfacies (Figs 4.27, 4.28) is characterised by a high proportion of densely branching CRA which constitute 25-65% of the rock.

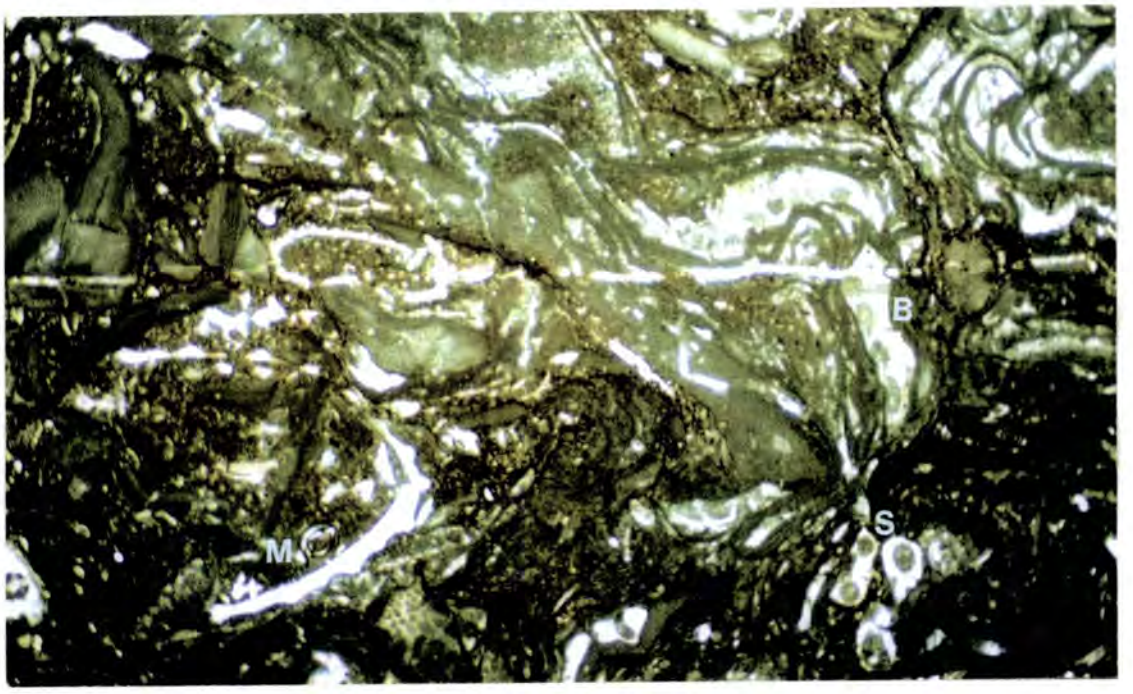

Fig. 4.27: Algal boundstone microfacies (SBa) showing multiple encrustations of CRA, bryozoans (B), and serpulids (S). Skeletal debris includes CRA and coral (C) fragments. Rotaline foraminifera have been replaced by the porcellanous Miliolids (M) which are able to tolerate a higher light intensity. Scale 12x7mm.

The CRA appear to bind the sediment together, with a minor contribution from corals (solitary and colonial, 10-15%), serpulids (1-2%) and bryozoans (2-10%). The algae may form rhodoliths, with a nucleus of coral or algal fragments or micrite. Other bioclasts are small, abraded, rotaline foraminifera (up to 15%; *Nummulites*, *Discocyclina*, *Amphistegina*), intact Miliolids and Textulariids (5-10%), bivalve fragments and echinoderm grains. Undifferentiated skeletal debris forms up to 15% of the sediment.

The matrix (up to 30%) is a dark micrite. Cement is rare and only reaches 10% in one sample.

Interpretation: The densely branching nature of the algae suggests that this is a high-energy environment, probably under the influence of wave action. The abrasion of the associated bioclasts supports this, as does the paucity of rotaline foraminifera, suggesting that the light intensity and water energy were too high for survival and

Fig. 4.28: Field photograph of an algal boundstone showing the massive mature of the rock and the presence of masses of branching CRA binding the sediment together.

proliferation. The presence of corals, in some localities starting to colonise the sediment, suggests normal salinities and light, clear waters, devoid of clastic detritus and suspended mud. The preservation of micrite is thought to be due to some binding of the sediment by the organisms, trapping the mud in interstitial cavities. Some micrite was probably produced by bioerosion.

This microfacies was deposited above FWWB under the influence of wave action causing considerable abrasion and reworking of the sediment. It represents the shallowest water depths encountered in the formation. The lack of an organic framework indicates that the facies does not represent true reef growth, and the sediments are thought to have been deposited as algal shoals and gravels on agitated inner-ramp areas.

4.4.18. Coralgal packstone-boundstone (SBc)

This facies (Figs 4.29, 4.30) is dominated by corals (30-50%) and algae (5-20%). Solitary corals are the most common, but colonial forms also occur. Both forms are either *in situ* or occur as abraded, reworked fragments. The internal structure has been replaced by calcite and the internal cavities are filled with micrite and/or cement. The CRA occur as binding masses encrusting the corals and bryozoans (10%) and commonly occur as

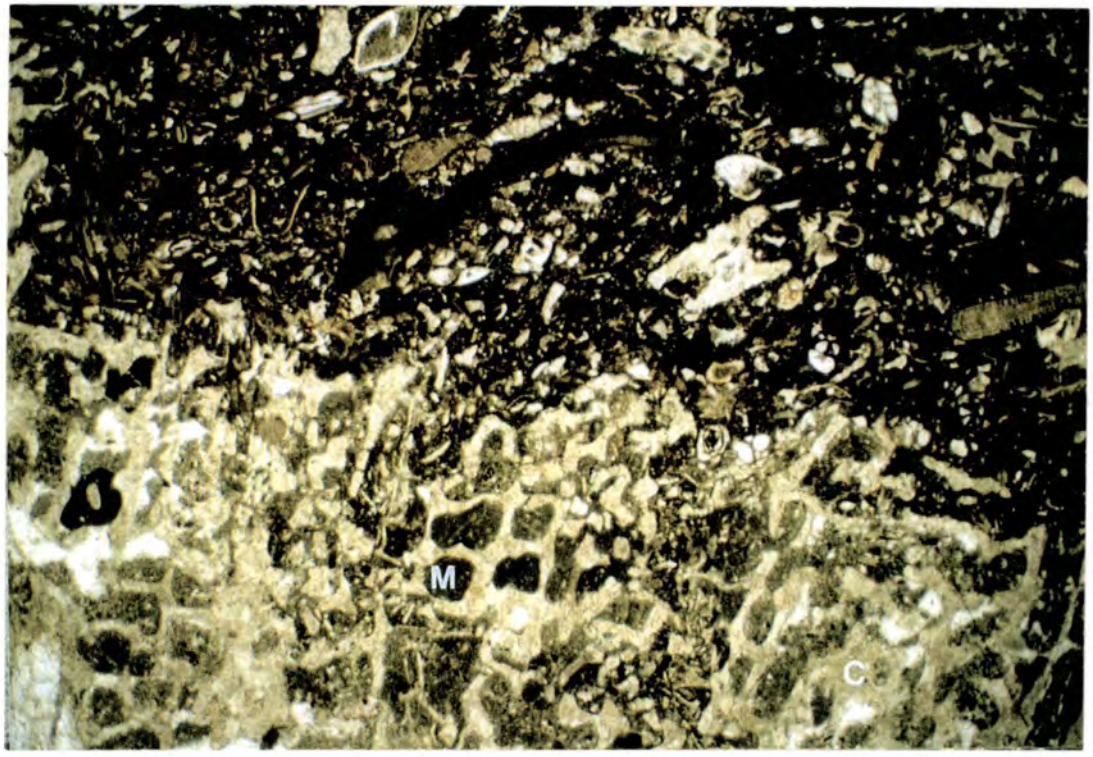

Fig. 4.29: Coral pack-boundstone microfacies (SBc) showing a section of a colonial coral, replaced by calcite, with the internal cavities infilled with cement (C) and micrite (M). The interstitial sediment is a micrite with abundant reworked debris from the surrounding shoal facies. Scale 12x7mm.

Fig. 4.30: Field photograph of a large colonial coral developed at Col de la Colombière within the coral pack-boundstone facies.

rhodoliths. Rotaline foraminifera are rare (<5%) and when present are *Nummulites*, *Amphistegina* or *Discocyclina*. They are generally well preserved, with slight abrasion. Miliolids are more common, forming up to 10% of the sediment, and are generally well preserved.

The matrix (10-30%) is a fine-grained micrite with silt-grade skeletal hash abraded from the bioclasts described above. Bioclasts may be bored.

Interpretation: This microfacies represents the development of patch reefs on the inner-ramp. The abundance of corals, especially the occurrence of colonial forms, indicates the existence of a relatively stable substrate. The abundance of micrite, low proportion of coarse skeletal debris and the presence of borings indicate that this microfacies may have been deposited in a lower energy environment than the algal boundstones, possibly forming small patch reefs in the quiet waters behind the algal banks. This microfacies is localised over pre-existing highs within the basin (Lateltin and Müller, 1987; Pairis and Pairis, 1975), located at Col de la Colombière, Meubles Montagnardes, Tête de la Sallaz and Col du Colonney.

4.4.19. Algal grainstone (SGa)

This microfacies (Fig. 4.31) is characterised by a grain-supported texture and the presence of a sparry calcite cement (15-40%), which is absent from most of the Nummulitic Limestone microfacies.

The dominant bioclasts are CRA, forming 25-45% of the sediment, as fragmented algal crusts and rhodoliths. Other bioclasts include corals and bryozoans and mollusc and echinoid fragments which are heavily abraded. Large foraminifera are scarce (5-10%).

The cement is a fine-grained calcite mosaic and a micrite matrix is also present in most samples, forming 5-20 % of the sediment.

Interpretation: The grainstone texture suggests a high-energy depositional environment with agitated waters which winnow the sediment removing most of the finer-grained material. The paucity of large foraminifera indicates high light intensity and/or high water energy which are unfavourable for survival. The dominance of algae and the debris of binding organisms indicates a close proximity to the algal banks. This microfacies was deposited in shallow, agitated waters, above FWWB, and represents a washover deposit.

4.4.20. Skeletal grainstone (SGsk)

This grainstone (Fig. 4.32) is characterised by a grain-supported texture and the presence of a drusy calcite cement (20-40%) which forms a fine-grained mosaic

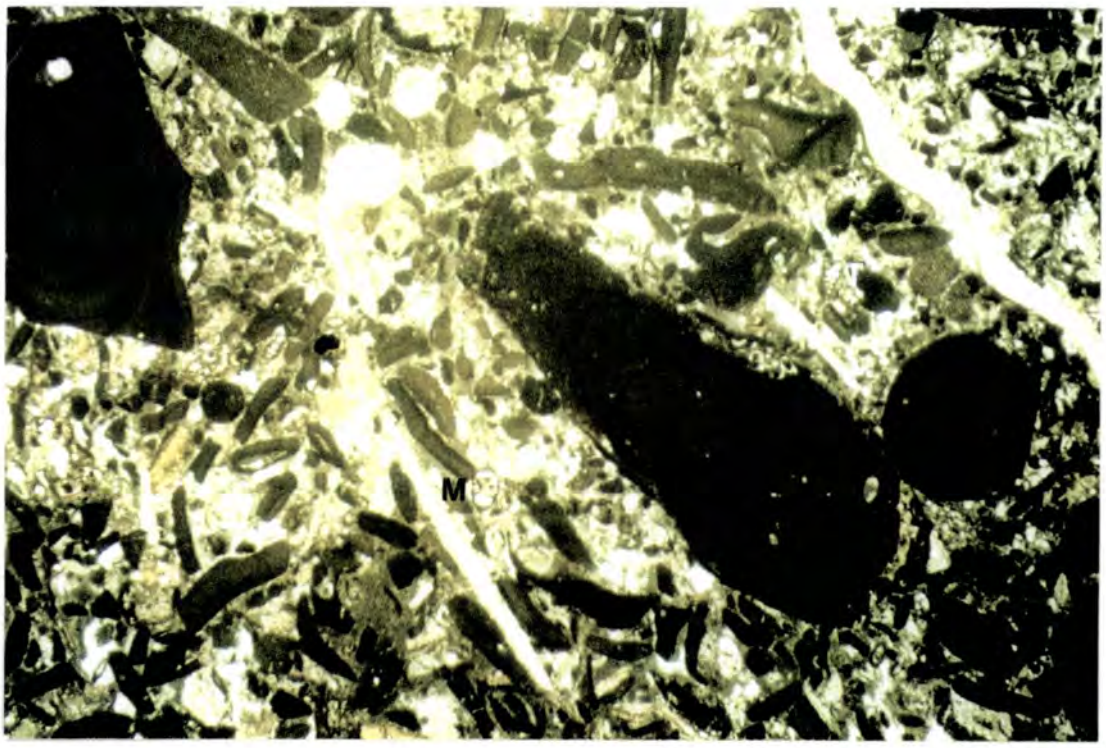

Fig. 4.31: Algal grainstone microfacies (SGa) showing abundant CRA in a calcite cement, all the fine material having been removed. Foraminifera present include Miliolids (M), Amphistegina (A) and Textulariids (T). Scale 12x7mm.

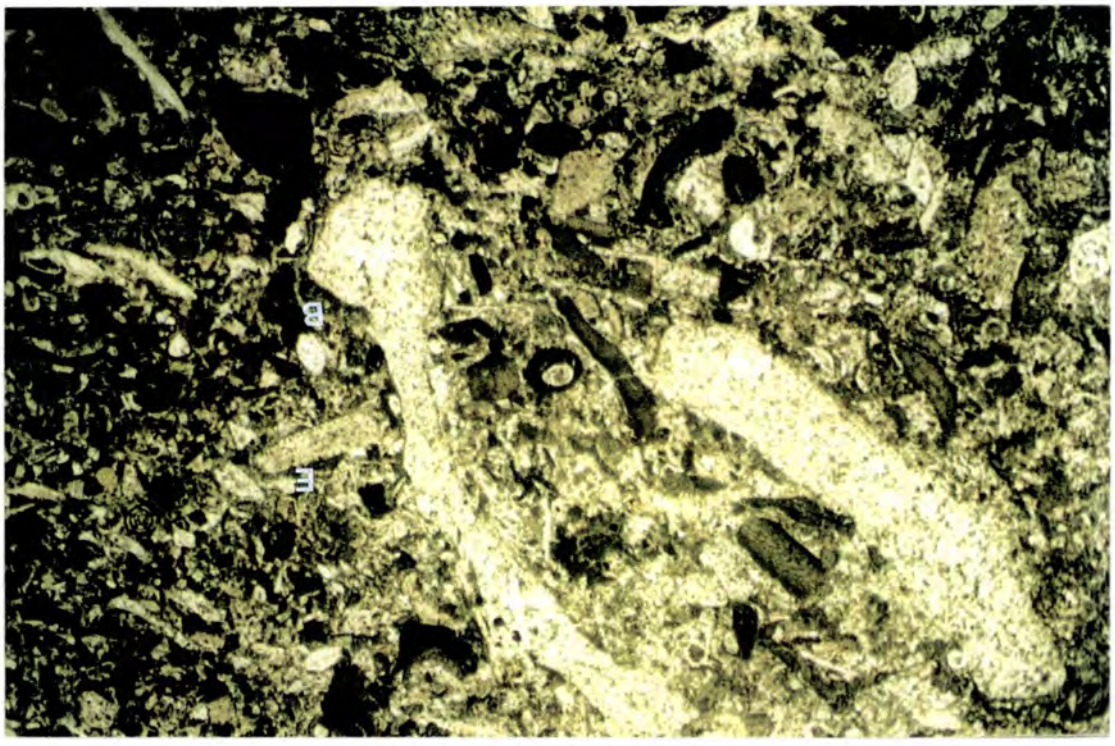

Fig. 4.32: Skeletal grainstone microfacies (SGsk) with abundant abraded skeletal debris including bivalves (Bi), echinoids (E) and CRA in a calcite cement. Scale 12x7mm.

coarsening away from grain boundaries. The bioclasts present are fragmented and heavily abraded and consist of binding organisms (25-30%) including CRA (10-25%), corals and bryozoans, with *Nummulites*, *Amphistegina* and *Discocyclina* (5-20%) and Miliolids and Textulariids (5-10%).

There is a small amount of matrix present (<10%) consisting of micrite with silt-grade quartz and glauconite.

Interpretation: This microfacies was deposited in a high-energy environment above FWWB with extensive winnowing due to wave action, removing most of the matrix and fragmenting and abrading the bioclasts. The nature of the bioclasts again suggests proximity to the algal shoals and this microfacies also represents a washover deposit.

4.5. Facies Associations

The microfacies described above occur in five principle facies association in the field representing deposition on different positions on the carbonate ramp, summarised in Table 4.3. In addition, these principle facies associations may be divided into sub-associations representing specific depositional settings within the inner-, middle- and outer-ramp respectively. The facies associations are discussed below, with a summary of the microfacies encountered in each association.

Facies Association	Dominant textures	Sedimentary structures	Dominant bioclasts	Interpretation
S0 **Quartzitic FA**	conglomerate sandy limestone mudstone SCG, SCm, SCw SQ, SM, SWn, SPm	cross-bedding lenticular bedding lamination	*Amphistegina* echinoids	**Initial Transgression** waning of clastic supply to the basin during transgression establishment of carbonate system establishment of benthos
S1a **Algal packstone FA**	packstone SPna, SPfa, SPa, SPad, SWsk	bioturbation	CRA *Nummulites* *Amphistegina* Miliolids	**Fore-shoal deposition** in situ ramp fauna and debris from algal shoal FA combination of foraminifera and CRA

Table 4.3: Facies associations encountered in the Nummulitic Limestone of Haute Savoie showing the dominant microfacies, sedimentary structures, bioclast content and environment of deposition.

Facies Association	Dominant textures	Sedimentary structures	Dominant bioclasts	Interpretation
S1b Boundstone FA	boundstone packstone SBa, SBc, SWsk, SMsk	massive bound by CRA	CRA rhodoliths corals bryozoans Miliolids	**Algal shoal** development of rhodolith shoals and gravels with local coral patch reefs colonisation and some binding of sediment by CRA, shallow water, above FWWB- favourable for porcellanous foraminifera but not rotaline
S1c Grainstone FA S1d Algal mudstone FA	grainstone mudstone SGa, SGsk, SWc, SMa, SWsk, SMsk	bioturbation	CRA bivalves corals bryozoans Miliolids	**Back-shoal** high energy winnowed shoals with abraded bioclasts and low-energy open marine protected lagoon, shallow water debris from shoal and *in situ* fauna
S2 Foralgal FA	packstone wackestone mudstone SWn, SPn, SPfa, SWsk, SMsk	bioturbation	*Nummulites Amphistegina Operculina Discocyclina*	**Middle ramp** deposition below FWWB ramp fauna dominated by rotaline foraminifera storm winnowing produces packstones
S2a Discocyclinid FA	packstone SPd	imbrication bioturbation	*Discocyclina Operculina Nummulites*	**Discocyclinid accumulation** para-autochthonous winnowed accumulation of lower-middle ramp foraminifera winnowing due to oscillatory currents thought to be storm reworking
S3 Mudstone FA	wackestone mudstone SWdo, SMf	bioturbation	*Operculina Discocyclina*	**Outer ramp** low-energy, deep water sedimentation dominated by large, flat foraminifera
S4 Marl FA	mudstone marl SPd, SWdo, SMf, SM	bioturbation lamination	*Discocyclina* Textulariids planktonics	**Transition to marl** deepening of basin and increase in amount of argillaceous and clastic influx; proportion and diversity of benthos decreases as water depth increases; sediment becomes more fissile

Table 4.3 (cont'd): Facies associations encountered in the Nummulitic Limestone of Haute Savoie showing the dominant microfacies, sedimentary structures, bioclast content and environment of deposition.

4.5.1. S0: Quartzitic facies association (SCG, SCm, SCw, SQ, SM, SWn, SPm)

As mentioned in Section 4.3, the base of the Nummulitic Limestone is marked by the presence of up to 6m of clastic facies (Fig. 4.33). Directly above the Mesozoic erosion surface and infilling the palaeokarst fissures, lies the breccio-conglomerate (SCG), which passes up gradationally into the basal detrital facies (SWq, SGq, SQ). In the thicker sandstone sections it can be seen that, moving up section, the facies pass from quartzitic wackestones (SWq) to the cleaner quartzitic grainstones (SGq) and even to quartz arenites (SQ) seen at Paccaly.

The fauna present within these facies is typically marine, consisting of oysters, pectinid bivalves, echinoids and small *Amphistegina*, the only genus of foraminifera in the succession able to tolerate a sandy substrate (Hottinger, 1983). Shelly horizons also occur within this facies association, as seen at Flaine, consisting of gastropods.

The only areas from which the quartzitic facies association is absent are the highs over which the algal facies association subsequently proliferates which include Tête de la Sallaz and La Communaille. La Communaille has a substratum consisting of Mid-Cretaceous greensand, clasts of which have been found in the transgressive lag at Le Chinaillon.

The quartzitic facies association is interpreted to represent the deposition of offshore sandy shoals, which reflect the waning supply of detritus from the clastic source as the area was flooded. The basal breccio-conglomerate represents a transgressive lag at the base of the succession, consisting of Cretaceous clasts reworked from the exposed and karstified substratum. This is thought to indicate a rapid flooding of the substratum (Crampton, 1992). The areas from which the facies association is absent are interpreted as being emergent at this stage and may have acted as a source areas for the clastic detritus. The decrease in micrite seen up-section suggests a shallowing upwards from relatively low-energy micrite-dominated sandstones into higher energy, and therefore more winnowed, rippled and cross-bedded facies.

The quartzitic facies association is bounded at the top by an abrupt transition into carbonate mudstone, representing a flooding prior to the onset of carbonate deposition. Above the mudstone, the carbonate factory is established, with the development of the characteristic benthonic foraminiferal assemblage encountered in the facies associations described below.

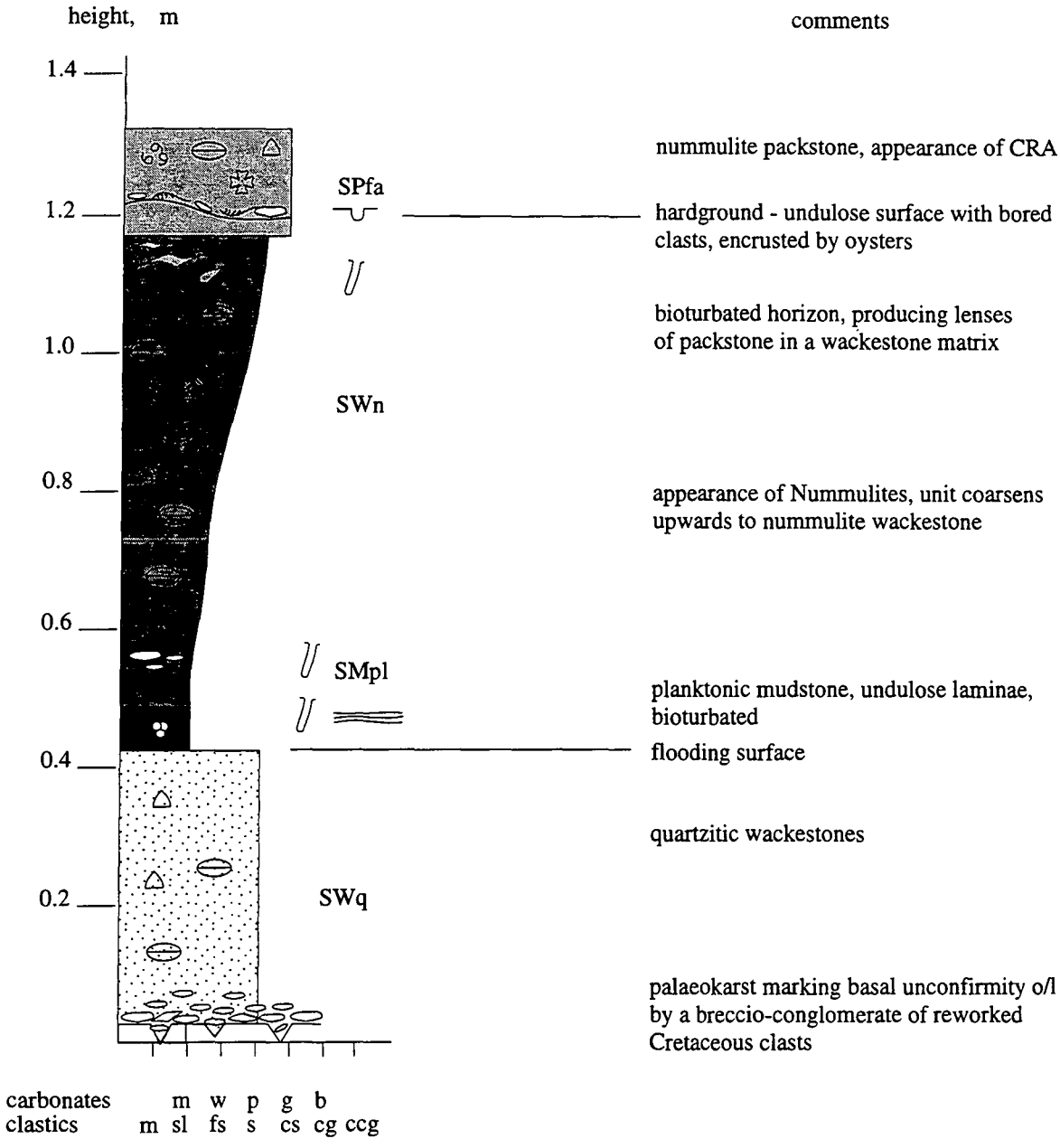

Fig. 4.33: Sedimentary log at Le Chinaillon (Superette) showing the initial transgression with the deposition of the basal clastics. The basal contact is marked by the breccio-conglomerate transgressive lag overlying a karstic erosion surface. The basal clastics here are represented by a quartzitic wackestone. The end of clastic supply into the basin is marked by a flooding surface at the top of the basal clastics and a transition to pure carbonate mudstone deposition and the establishment of the characteristic benthos.

4.5.2. S1: Algal facies association

The algal facies association (Fig. 4.34) is characterised by the shallowest-water facies in the succession. It can be divided into four sub-associations, dominated by algal packstones, boundstones, grainstones and mud- and wackestones.

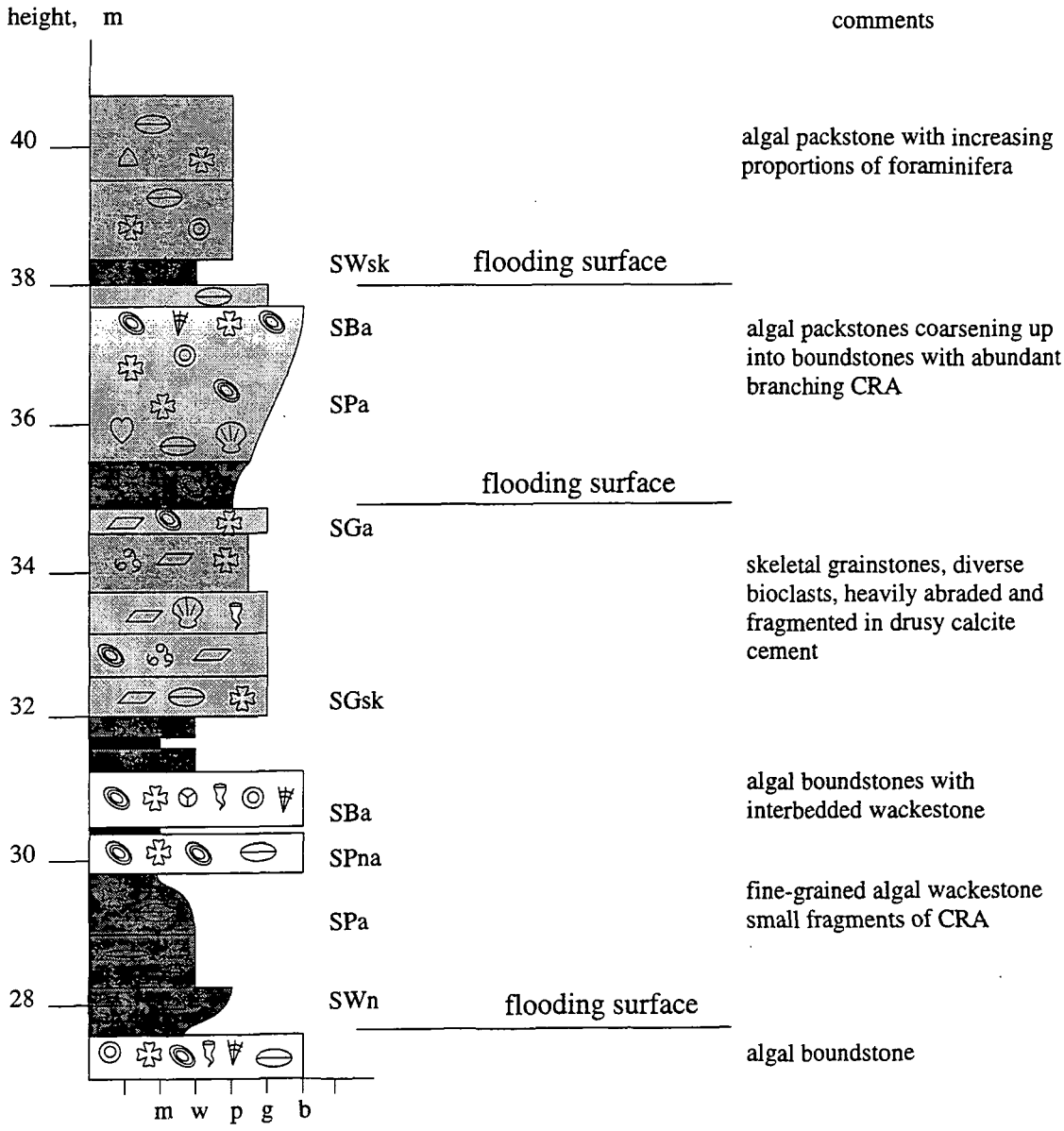

Fig. 4.34: Sedimentary log measured at Le Chinaillon (Gulley) showing the development of the algal facies association. The algal boundstones represent the development of algal shoals and gravels and are characterised by abundant rhodolith growth The facies association shows a marked cyclicity, with each cycle of shoal development separated by a flooding surface. Above the algal shoals, high energy wash-over deposits may be developed (SGsk, SGa), separating the algal shoals from the low-energy, protected lagoon (SM, SMsk).

4.5.2.a. S1a: Algal packstone association (SPna, SPfa, SPa, SPad, SWsk)

The algal packstone sub-association is dominated by grain-supported fabrics containing a marine fauna of CRA and benthonic foraminifera, with both A- and B-forms of *Nummulites* and *Amphistegina* present (SPna, SPfa). A significant proportion of fine micrite is still preserved as the matrix. The proportion of foraminifera decreases up-section, to be replaced by CRA, producing the algal packstone microfacies (SPa). The algae now encrust most of the skeletal fragments to form rhodoliths which may bind patches of the sediment.

The fauna present in this facies association represents both the *in situ* ramp fauna, with the onset of sediment colonisation by CRA (SPfa, SPna, SPa), and the detritus shed down-ramp from shallower waters in the form of heavily abraded algal fragments (SPad, SWsk). The sediments indicate sedimentation below FWWB, with a significant proportion of fine micrite preserved and unabraded foraminifera, with both generations present, representing the *in situ* slope assemblage. The algal-debris packstone and skeletal wackestone microfacies (SPad, SWsk) represent the debris washed down-ramp from the algal banks, in the form of abraded fragments dominated by CRA.

This facies association is interpreted to represent deposition on the lower inner-ramp, basinward of the boundstone sub-association.

4.5.2.b. S1b: Boundstone association (SBa, SBc, SWsk, SMsk)

This sub-association is dominated by massive algal boundstones (SBa) with coral development in some sections (SBc). The algal boundstone facies association is most extensively developed on faulted highs in the substratum (Lateltin and Müller, 1987), such as Col de la Colombière, Tête de la Sallaz and Meubles Montagnardes. The benthos is dominated by densely branching rhodoliths of CRA which bind patches of the sediment together, with minor contributions from solitary corals, bryozoans and serpulid worm tubes. Colonial corals are rare, only present at Col de la Colombière and Col du Colonney.

The boundstone sub-association is interpreted to represent the development of algal shoals and gravels under high-energy conditions dominated by rhodoliths with localised sediment binding; true reef growth is not thought to have occurred due to the lack of evidence for a biological framework composed of either corals or CRA. The existence of colonial corals at Col de la Colombière and Col du Colonney is thought to indicate local, immature patch reef development,

In the field the boundstone sub-association is laterally extensive for several hundred metres and is thought to represent discontinuous algal shoals and rhodolith

gravels, similar to those found in the present-day Mediterranean (Bosence, 1985) with the shoals locally providing sufficient relief to protect the landward areas from the action of waves and producing a low-energy, open-marine lagoon (Section 4.5.2.d).

4.5.2.c. S1c: Grainstone association (SGa, SGsk)

This sub-association consists of massive grainstones. The skeletal grainstone microfacies (SGsk) is dominated by heavily abraded skeletal debris, whereas the algal grainstone microfacies (SGa) still retains up to 20% micrite and contains well-preserves CRA. In vertical section the grainstones separate the boundstone sub-association from the algal mudstone sub-association.

This sub-association represents a high-energy setting as most of the fine-grained micrite has been removed. The grainstones are interpreted to represent winnowed accumulations of abraded skeletal detritus reworked from the boundstone sub-association by wave action and storms and redeposited in the back-shoal area above FWWB. The highest-energy setting is represented by the skeletal grainstone (SGsk), with sufficient soft sediment preserved in more sheltered areas allowing the growth of rhodoliths to produce the algal grainstone (SGa).

The vertical relationship of the facies seen in the field indicates that the grainstones represent high-energy washover deposits separating algal shoals from a protected back-shoal lagoon, where sufficient relief was developed.

4.5.2.d. S1d: Algal mudstone association (SWc, SMa, SMsk, SWsk)

This facies association is dominated by micritic sediments containing rare rotaline foraminifera (robust *Nummulites, Amphistegina*), Miliolids and Textulariids, calcareous red algae, as thin crusts and rhodoliths, and solitary corals.

This sub-association is thought to represent deposition in the sheltered areas developed behind the algal banks and winnowed shoals. This association is thought to have developed only when sufficient relief existed in the algal shoals, offering some protection from the main force of the waves. This phenomenon is restricted to Col de la Colombière and Tête de la Sallaz, where the algal mudstone facies association is commonly interbedded with the algal boundstone facies association.

The benthos present represents both the *in situ* inner-ramp fauna and flora and debris washed into a lagoonal environment from the algal shoals during storms. Rotaline foraminifera are rare due to the shallow waters and high light intensity and the foraminifera assemblage is dominated by diverse porcellanous forms. The remainder of the bioclasts present constitute bank detritus redeposited during storms and they

commonly form the nuclei for rhodolith growth. The fauna and flora suggest that these sediments were deposited in normal marine salinities as there is no evidence for hypersalinity (dolomite, evaporitic minerals, high abundance and low diversity of Miliolids). Though Miliolids are abundant, diversity is high and they occur along with rotaline foraminifera and CRA. This coupled with the high mud content suggests that the environment was protected from the main energy of the waves, but that circulation was not restricted producing an open-marine lagoon.

4.5.3. S2: Foralgal facies association (SWn, SPn, SPfa, SWsk, SMsk)

The foralgal facies association (Fig. 4.35) is characterised by micritic packstones and wackestones containing large benthonic foraminifera, the shape of which varies depending on the relative water depths. The foraminiferal assemblages present are generally diverse and both sexual and asexual generations coexist. Reworked skeletal debris may also be present.

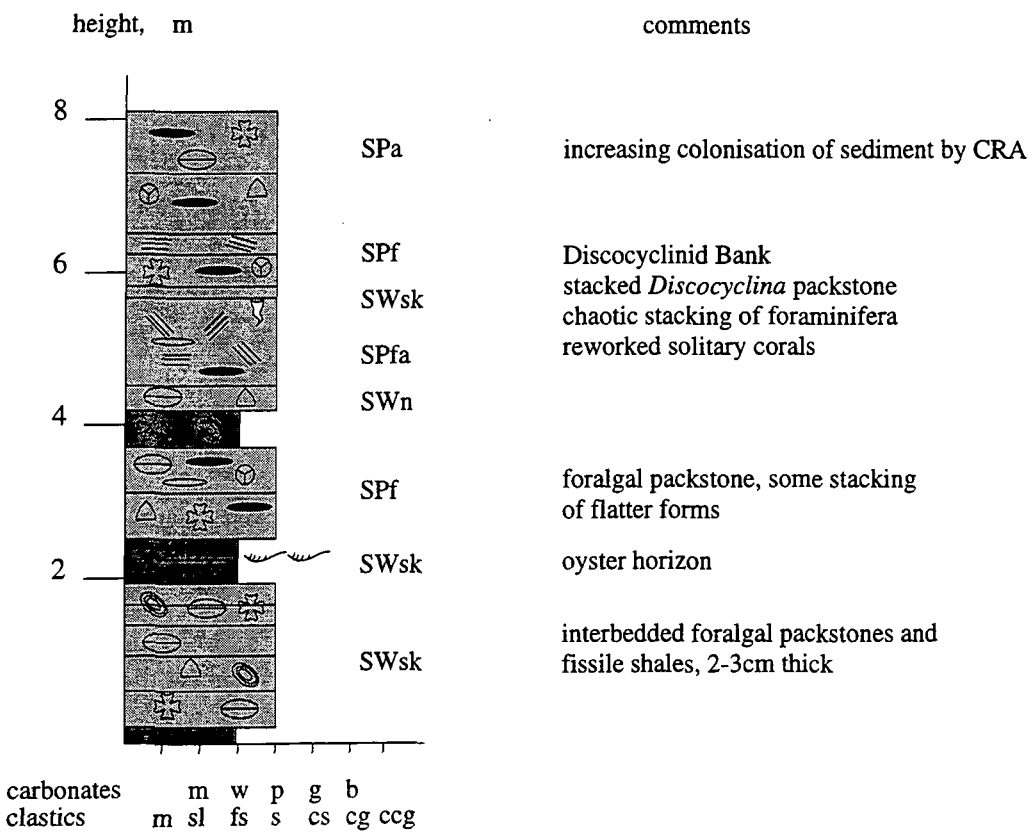

Fig. 4.35: Sedimentary log from La Communaille showing the foralgal facies association with the development of Discocyclinid accumulations (SPd) with chaotic imbrication. The facies show the middle-ramp faunal assemblage and the increasing colonisation of the sediment by CRA as the facies pass upwards into those of the inner-ramp.

The foralgal sub-association is interpreted to represent deposition in the middle-ramp setting. The bioclasts represent both the *in situ* ramp fauna and reworked debris washed in from shallower environments by down-ramp currents and storms. The position on the ramp is indicated by the foraminiferal assemblage as discussed in Section 2.1, with the upper middle-ramp dominated by small, robust to intermediate *Nummulites* and *Amphistegina* which are slightly abraded. Porcellanous foraminifera may also be present, indicating relatively shallow-waters, and skeletal debris is abundant, reworked from the inner-ramp. The lower middle-ramp is represented by a mixed foraminiferal assemblage, dominated by flat *Discocyclina* and *Operculina* and intermediate *Nummulites* and *Amphistegina*. Robust *Nummulites and Amphistegina* also occur, but they are heavily abraded and therefore interpreted as having been redeposited from shallower ramp environments. Detritus from the algal bank is uncommon lower down the ramp (foraminifera packstone microfacies, SPf).

4.5.3.a. S2a: Discocyclinid facies association (SPd)

This sub-association is dominated by the stacked Discocyclinid packstone microfacies (SPd) which occurs as discontinuous lenticular units, 0.2-1.3m thick. It is surrounded by the foralgal facies association described above.

Fig. 4.36: Field photograph of the chaotic imbrication of flat, middle-ramp foraminifera characteristic of the Discocyclinid sub-association. Scale=5cm.

The main body of the unit contains well-preserved, flat foraminifera (*Discocyclina, Operculina, Nummulites*) with a chaotic imbrication (Fig. 4.36). The units generally fine upwards, with CRA and solitary corals appearing at the top of the unit.

The packstones are interpreted to represent low relief, winnowed accumulations of middle- to outer-ramp foraminifera and reworked foraminiferal debris. The preservation of the foraminifera indicates that this reworking occurred *in situ* and so the banks can be interpreted as para-autochthonous accumulations (Racey, 1990). The chaotic imbrication is thought to be indicative of oscillatory currents (Racey, 1990), which, considering the position on the ramp as indicated by the foraminiferal assemblage, was probably due to storm reworking. Specific sedimentary structures such as those described by Aigner (1982, 1983) and Crampton (1992) cannot be distinguished, but some reworking by bioturbation is evident as higher concentrations of the micritic matrix.

4.5.4. S3: Mudstone facies association (SWdo, SMf)

This facies association (Fig. 4.37) is dominated by mud-rich wackestones and mudstones with only a small proportion of bioclasts dominated by large, flat *Discocyclina, Operculina, Nummulites* and *Amphistegina*, the proportion of which decreases up-section. Planktonic foraminifera and glauconite may also be present. Other skeletal debris is very rare. Rare, abraded, robust *Nummulites* and *Amphistegina* may be present.

The facies association is interpreted as representing deposition on the outer-ramp, with a sparse fauna, though bioturbation indicates that the sediments were oxygenated. Glauconite indicates low sedimentation rates. Rare skeletal debris and shallow-water foraminifera were brought into the environment by storms. Otherwise, the water energy was very low, allowing the preservation of abundant micrite. Alignment of the slope fauna may represent the *in situ* life position or may represent reworking by outer-ramp currents.

4.5.5. S4: Marl facies association (SPd, SWdo, Mf, M)

This represents the transition from the carbonate ramp to the overlying *Globigerina* Marls (Fig. 4.38) with an associated increase in argillaceous material. It is often badly exposed due to the fissile nature of the marls but, where it can be documented, the transition and facies association varies according to whether the locality represents a structural high with prolific algal bank development or a lower energy, more basinal setting.

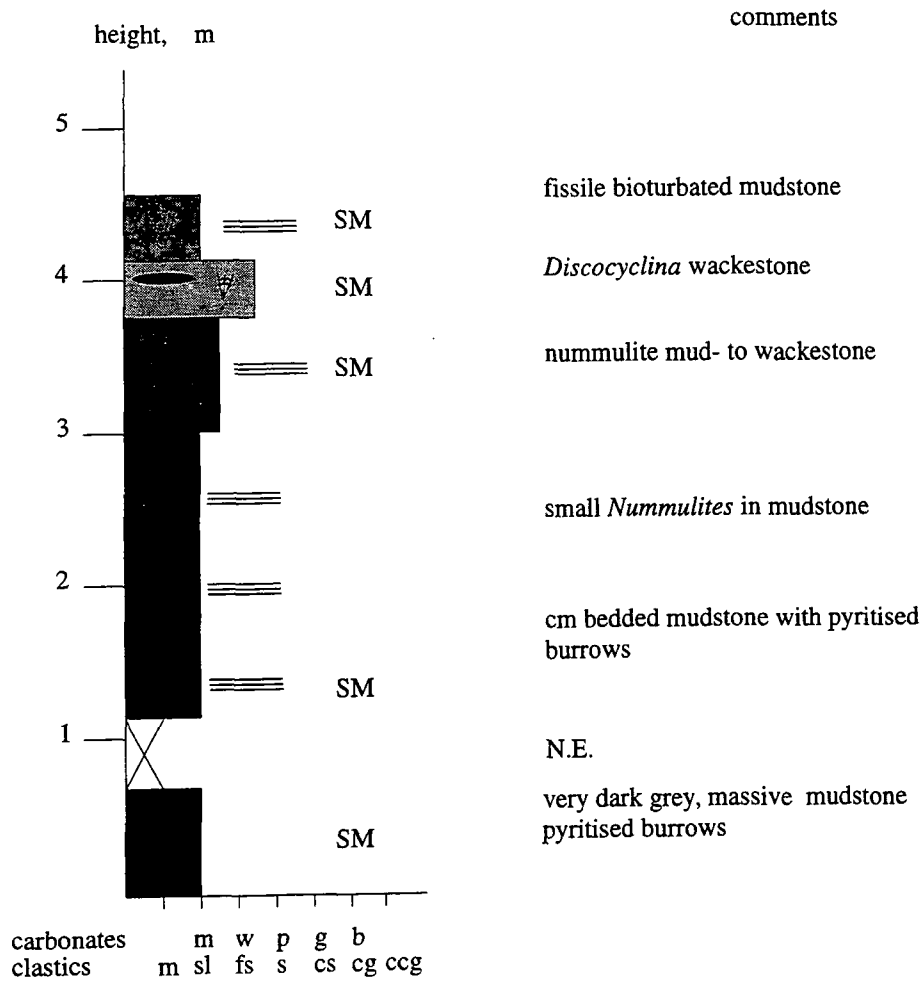

Fig. 4.37: Sedimentary log at La Bombardellaz showing the mud-rich sediments of the mudstone facies association, with a fauna dominated by flat, benthonic foraminifera.

The transition occurs over a vertical distance of 3m to 10m above the final shallowing-upwards unit of the carbonate ramp, usually represented by the algal facies association, but in more basinal settings by the foralgal facies association. A common feature of the transition is the reappearance of *Discocyclina/Operculina*- rich facies above the inner-ramp facies association (SPd, SWdo, SMf). These facies can show a stacking of the foraminifera, suggesting that foraminiferal accumulations were able to develop. In the transitional facies, these commonly have associated CRA, with the CRA disappearing up-section and the facies fine upwards into wackestones and mudstones, with an increasing clastic component. The proportion of planktonic foraminifera also increases. Some agglutinating forms may also be present, with tests composed of silt-grade quartz and micrite. Extensively bioturbated horizons imply that the sediments were oxygenated and

may indicate periodic decreases in sedimentation rate. The proportion of detrital, silt-grade quartz also increases up-section. In more basinal settings (e.g. La Bombardellaz) the transition is marked by an increase in the fissility of the sediment and a decrease in the amount of foraminifera.

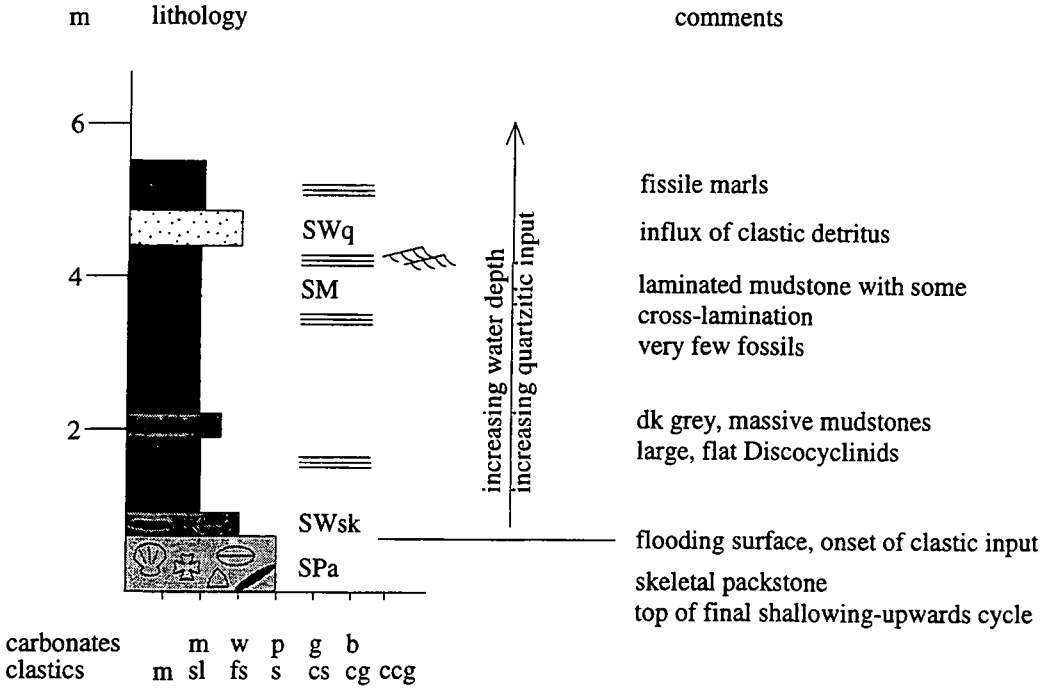

Fig. 4.38: Sedimentary log at La Vacherie showing the marl facies association representing the flooding of the carbonate ramp due to increasing flexural subsidence rates. The flooding is marked by an abrupt transition from inner- or middle-ramp facies to outer-ramp marls with an associated increase in quartzitic and argillaceous influx.

The abrupt change in the benthos from inner- or middle-ramp assemblages to middle- and outer-ramp fauna indicates that the marl facies association developed as the result of a flooding event which caused the transition from carbonate ramp deposition to pelagic marl deposition. The increase in the proportions of argillaceous material and detrital quartz marks the onset of siliciclastic influx from the advancing flysch.

4.6. Depositional Model

The Nummulitic Limestone in Haute Savoie was deposited in a carbonate ramp setting with no significant slope or break in slope noticeable from the sedimentary record (no slumps, turbidites or slope breccias). The ramp is dominated by a benthos of large benthonic foraminifera and calcareous red algae, the palaeoecology of which is outlined

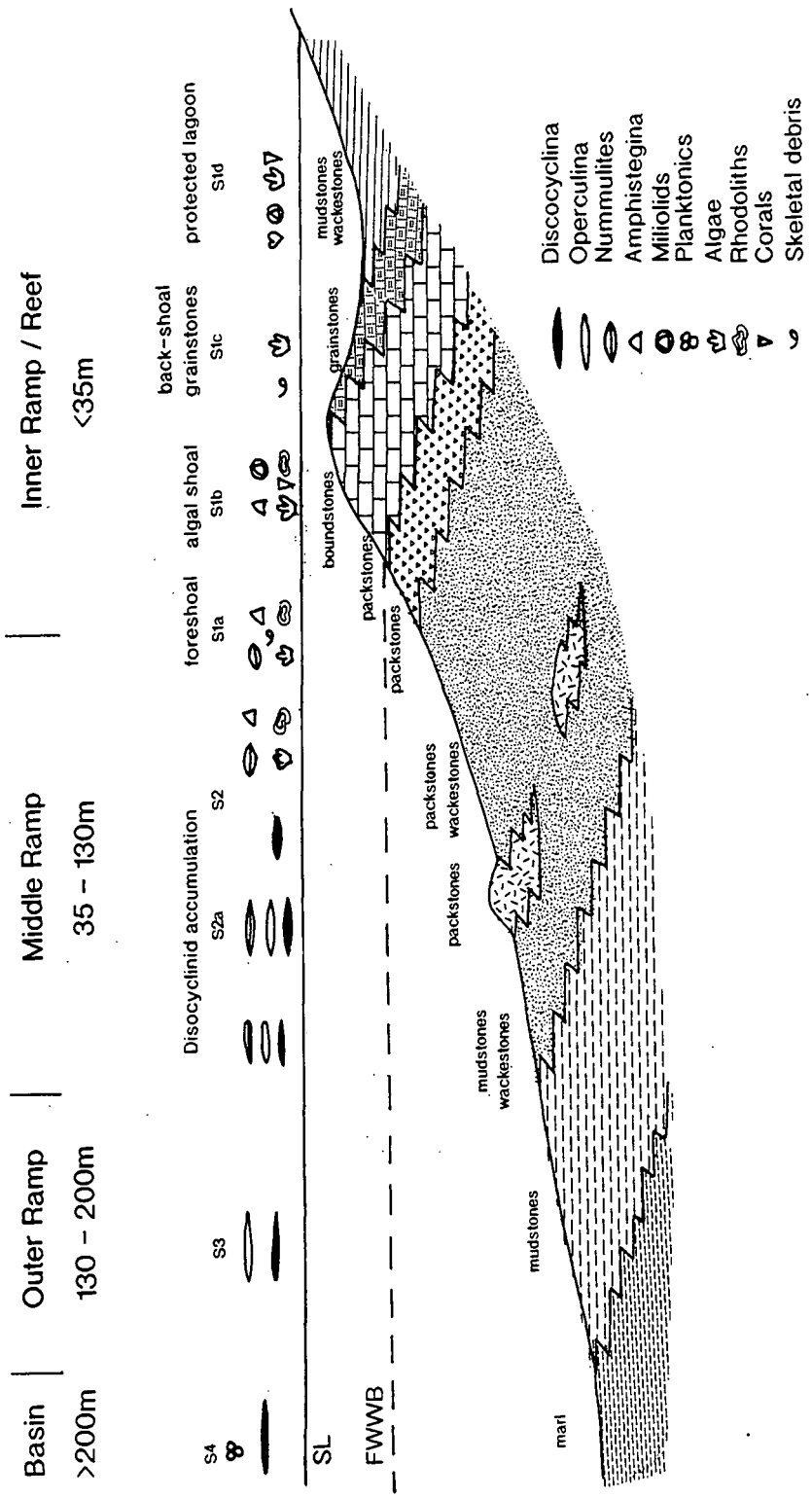

Fig. 4.39: Depositional environments of the Nummulitic Limestone carbonate ramp based on sections measured in Haute Savoie. The inner-ramp is represented by algal shoals which may form sufficient relief to be able to distinguish fore- and back-shoal facies. The middle-ramp is represented by micritic wackestones and packstones with local accumulations of flat foraminifera. The outer-ramp is dominated by mudstones and marls with a very sparse fauna.

in Chapter 2 and which was used in the microfacies analysis described above (Section 4.5). The sediments of the ramp can be divided up into those representing the inner-, middle-, and outer-ramp settings in terms of the changes in the nature of the benthos and the depositional texture of the sediment (Fig. 4.39).

The inner-ramp is dominated by facies association S1 which represents the development of rhodolith shoals and gravels (S1b), commonly occurring over depositional highs and deposited below FWWB in shallow water depths (10-50m; Racey, 1990). These are thought to form low relief, discontinuous features, with associated fore-bank washover deposits (S1a) passing down into the middle-ramp environment, high energy back-bank shoals (S1c) passing into low energy sheltered lagoonal settings (S1d) where relief is sufficient to provide protection from wave action.

The middle ramp environment (facies association S2) contains more mud-rich sediments and is interpreted to have been deposited below FWWB (50-100m), allowing preservation of the micrite. There is a variation in the benthos with increasing water depth, with the upper middle-ramp sediments containing *in situ* CRA and robust *Nummulites* and *Amphistegina*. The deeper lower middle-ramp environment is dominated by flatter *Nummulites*, *Discocyclina* and *Operculina* with very few CRA (reworked). *In situ* winnowing of these sediments by oscillatory storm currents removing much of the fine micrite produces local accumulations of flat foraminifera (S2a).

The outer ramp sediments(S3) contain a low proportion of bioclasts dominated by flat *Discocyclina* and *Operculina* and, as water depths increase, planktonic foraminifera. These sediments grade into the marl (S4), which represents the transition to starved basin deposition (>135m) and the final flooding of the carbonate ramp.

The clastic facies association (S0) occurs only during the initial transgression of the sea over the uplifted foreland / Infranummulitique and represents the waning of terrigenous supply into the basin prior to carbonate deposition. Therefore, this facies association is not considered to be part of the carbonate ramp *sensu stricto*, but is interpreted to have formed sandy offshore shoals in a marine environment.

Chapter 5

The Nummulitic Limestone - Haute Provence

5.1. Introduction

The Nummulitic Limestone has been studied in the Annot area of Haute Provence, illustrated in Fig. 5.1. This area has been segmented by compressional structures, producing a series of sub-basins in which the Tertiary rocks were deposited and have been preserved. The area was studied by the measurement of thirteen sedimentary sections (Appendix 1) and extensive thin section analysis (Appendix 2). This chapter deals with the microfacies encountered on the Provence Nummulitic carbonate ramp and the development of the ramp under the effects of the subsidence of the Alpine Foreland Basin.

5.2. Distribution and Thickness Variations

In southern France, from the Franco-Italian Alps north of Monte Carlo to the Allos area, the Nummulitic Limestone outcrops in a series of synclinal sub-basins (Fig. 5.1) caused by the combined effects of the Pyrenean-Provençal and Alpine orogenies which produce N-S and E-W oriented structures respectively (Apps, 1987). The synclines in the south of the field area (St Antonin, Entrevaux and Agnère Synclines) exhibit an E-W elongation, whereas the more northern structures have a NW-SE trend.

The Nummulitic Limestone outcrops as cliffs, forming relatively continuous ridges in the topography due to its resistance to weathering compared to the underlying limestone/marl interbeds of the Cretaceous and the overlying fissile Globigerina Marl. The limestone outcrops around the edges of the synclines, with the axial regions represented by the Globigerina Marl and the Annot Sandstone. It overlies either the Mesozoic substratum, in this area Middle and Upper Cretaceous marls and argillaceous sandstones, or the clastics of the Infranummulitique (Chapter 3).

The limestone shows a wide range of thickness variations, from 75m at Collongues (St Antonin Syncline) to less than 10m at Peyresq. The thicker limestone sections tend to be those directly overlying the thicker Infranummulitique successions, but there is also a geographical trend, with the southern, St Antonin syncline having a

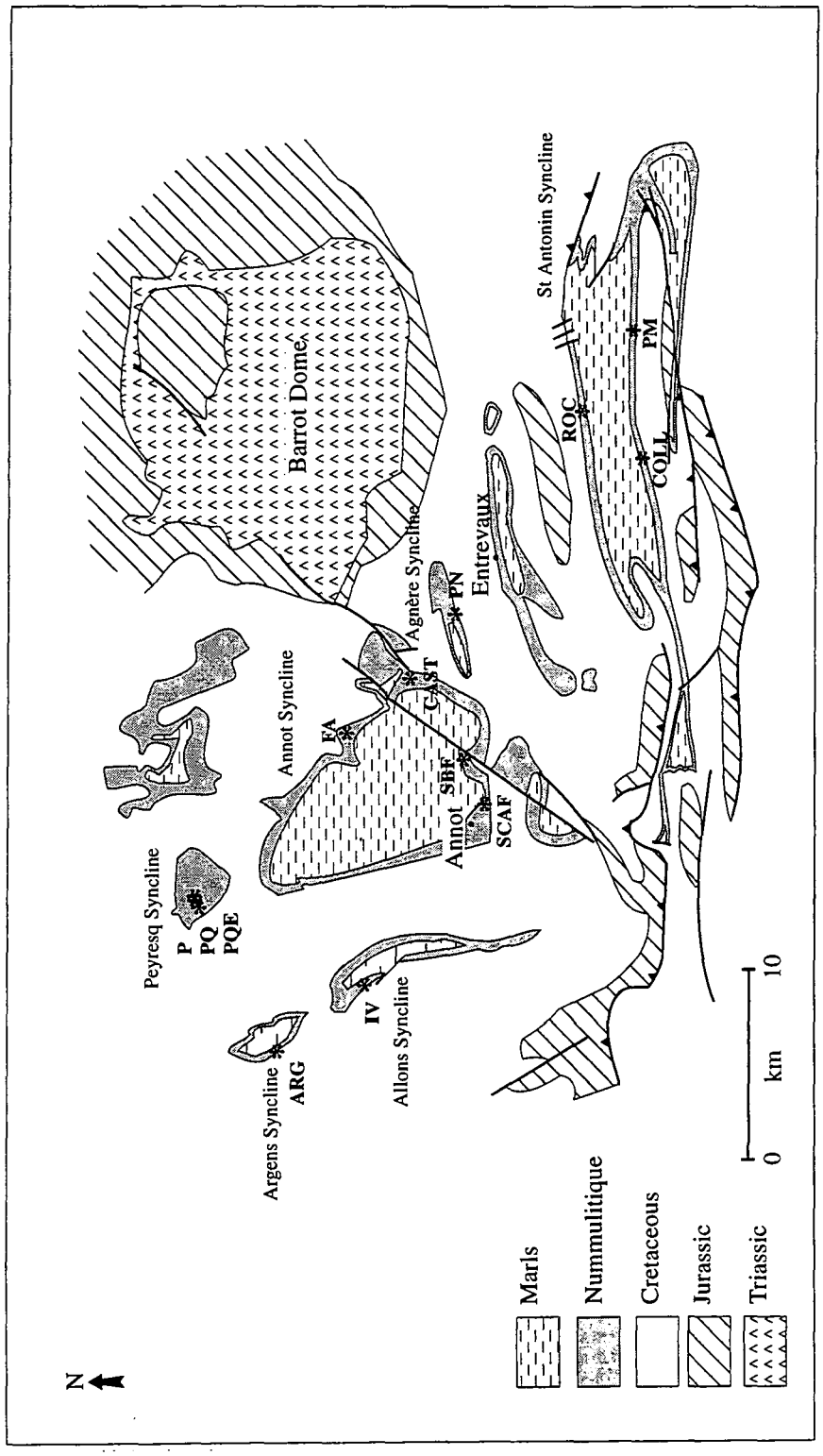

Fig. 5.1: Map of the Annot region in Haute Provence showing the outcrop of the Nummulitic Limestone in a series of synclinal sub-basins and the location of sections measured. (ARG=Argens; IV=Ivoire; P =Peyresq; FA=La Col du Fa; CAST=Castellet les Sausses; SBF=St Benoit Fault section; SCAF=Scaffarels; PN=Pont Noir; ROC=La Rochette; COLL=Collongues; PM=Pont au Miolans . PQ=Peyresq Quarry, PQE=Peyresq Quarry East)

much thicker overall succession. Local variations also occur due to the pre-existing topography of the erosion surface and structures in the substratum (Fig. 5.2).

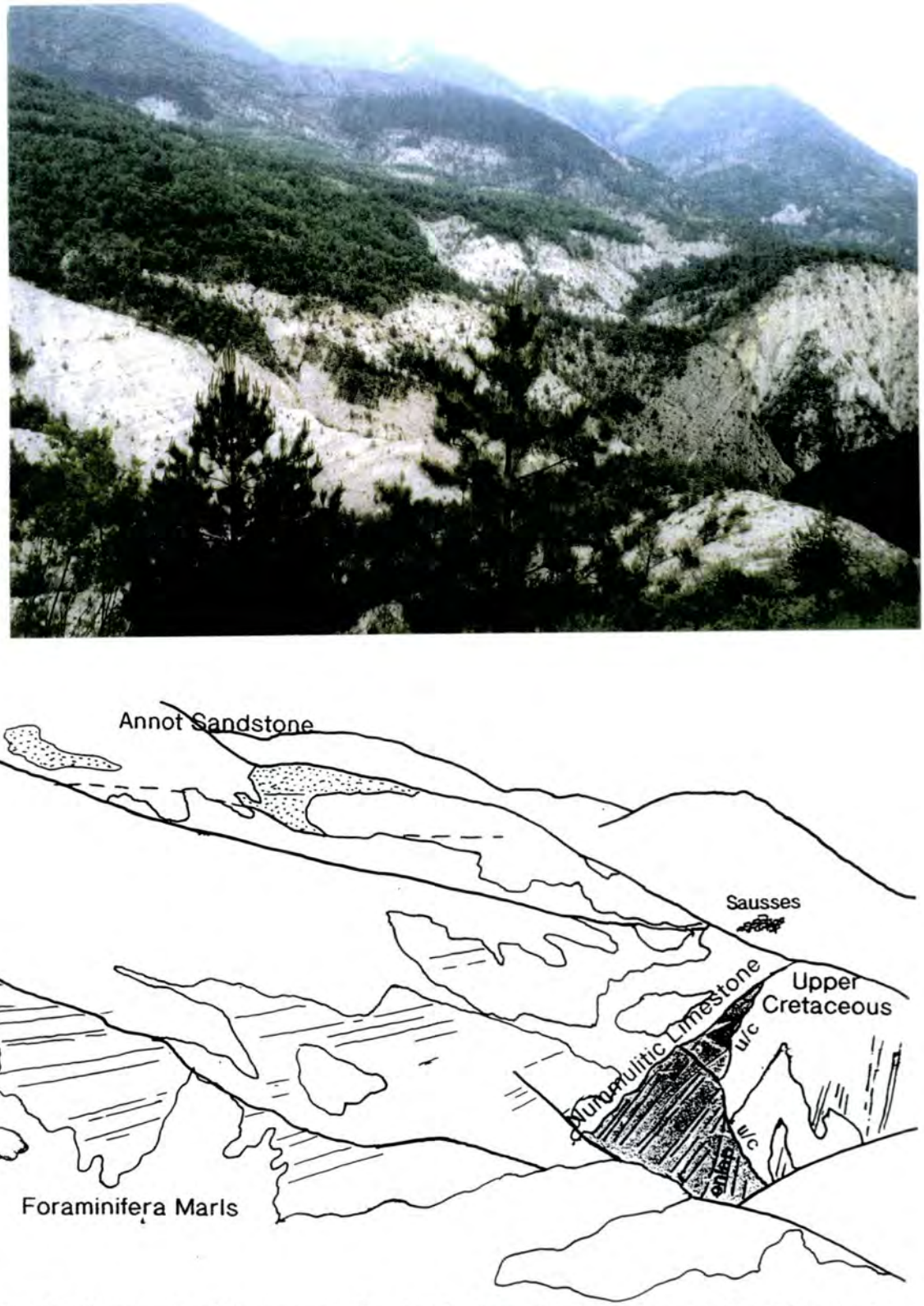

Fig. 5.2: Photograph and diagrammatic sketch of the Nummulitic Limestone to the NE of Castellet les Sausses showing the dramatic local thickness variations due to the infilling of pre-existing topography on the Cretaceous erosion surface.

5.3. Nummulitic Limestone Microfacies

The Nummulitic Limestone again represents deposition on a carbonate ramp dominated by large benthonic foraminifera. Unlike Haute Savoie, however, CRA are scarce. The succession has been divided up into 15 characteristic microfacies based on composition, texture and faunal content (Table 5.1.). These are described below using Dunham's (1962) classification.

Microfacies	Features	Samples
Organic siltstone **PSorg**	Org, Q, Lam	ROC2, ROC3
Peloidal mudstone **PMp**	Pel, (N, A, Pl) Q, Sh, Cem Lam, (XB)	PM9, PM10, PM17, COLL5, COLL8, COLL10, COLL11, COLL15
Skeletal mudstone **PMsk**	N, A, M, C, B, Sh, (Q, Gl) Bio	CAST2, CAST4, IV3, IV5, PM13, PM14, COLL12
Coral wackestone **PWc**	C, G, M, B, (Al, N) Q, Sh, Org Bor	IV1, IV4, I4
***Discocyclina-Operculina* wackestone** **PWdo**	D, O, N, (A, Or, M) Sh, Q, (G) Bio	ROC1, ROC4, ROC5, ROC6, ROC7, CAST8, PM20, SCAF4, SBF4, SBF5, COLL14
Peloidal wackestone **PWp**	Pel, (E, N) Sh, Q	IV13, IV14
Foraminifera-algal wacke-packstone **PWPfa**	CRA, C, N, D, O, Sh, (Q)	PN9, PN10
Foraminifera wackestone **PWPf**	N, A, Or, M, (D, O, Al) Sh, Q, Cem Bio	SBF1, SBF5, P12, P13, P14, P15, PM15, PM16, PM21 COLFA3, COLFA4, COLFA11, CAST6, COLL9, COLL13
Peloidal foraminifera wackestone **PWpf**	Pel, N, A, Or, (D, O), E, S Sh, Q Bio	PM11, PM19, IV9, IV10, IV12, SBF2, SBF3

Table 5.1: Constituent microfacies of the Nummulitic Limestone of Haute Provence, showing the dominant bioclasts, detrital grains, textures and the samples collected of each microfacies.

Nummulite packstone **PPn**	N, E, (A, Or, O) Bio, XB, St	COLFA2, FA1, FA2, CAST1, CAST7, IV15, IV16, A4, PM6, PM8, RC3
Foraminifera wacke-grainstone **PWGf**	N, A, Or, S, Pel Sh, Q, Cem	COLFA1, COLFA5, COLFA8, COLFA9, COLFA10, PM12, SCAF3
Foraminifera-algal pack-grainstone **PPGfa**	CRA, N, E, Pel, (A, D, M) Sh, Cem, (Q)	PN7, PN8, SCAF1
Microfacies	**Features**	**Samples**
Nummulite-Miliolid pack-grainstone **PPGnm**	N, M, Or, A, Pel, (D, O) Sh, Cem Bio	SCAF2, ROC9, COLFA6, COLFA7, CAST3, CAST5
Peloidal foraminifera grainstone **PGpf**	Pel, N, Or, M, R Cem	PN6, COLL7, IV7, PM2, PM5, PM7, RC3
Peloidal grainstone **PGp**	Pel, N, Or, M, R, (A, T) Cem, P, Bio?	RC4, A1, A2, A3, AL1, IV2, IV6, IV8, IV11, PM2, PM3, PM4, PM18, COLL1, COLL2, COLL3, COLL4, COLL6, ROC10

Key to features

Foraminifera	**Other bioclasts**	**Clastic + Diagenetic**	**Textures**
N = *Nummulites*	E = echinoid	Pel = peloids	Bio = bioturbation
A = *Amphistegina*	B = bivalve	Sh = skeletal debris	Bor = borings
Or = Orbitolinids	G = gastropod	Q = quartz	St = bioclast stacking
D = *Discocyclina*	S = serpulid	Py = pyrite	Lam = laminated
O = *Operculina*	C = coral	Gl = glauconite	XB = cross-bedding
M = Miliolids	CRA = red algae	Org = organic debris	
Al = Alveolinids	R = reefal organisms	Cem = cemented	
T = Textulariids			
Pl = planktonics			( ) = uncommon

Table 5.1 (cont'd): Constituent microfacies of the Nummulitic Limestone of Haute Provence, showing the dominant bioclasts, detrital grains, textures and the samples collected of each microfacies.

5.3.1. Organic siltstone (PSorg)

This microfacies is fine-grained and featureless in thin section (Fig. 5.3). It is dominated by a combination of micrite (35%) with a very fine-grained calcite microspar cement (20-35%). There are no body fossils present and the only bioclastic remains are organic debris (10-15%). Where the siltstone is laminated, the organic remains tend to be aligned along the laminae in addition to occurring within the matrix. The siltstone typically contains 20% angular, silt- to fine sand-grade quartz. There is no evidence for bioturbation.

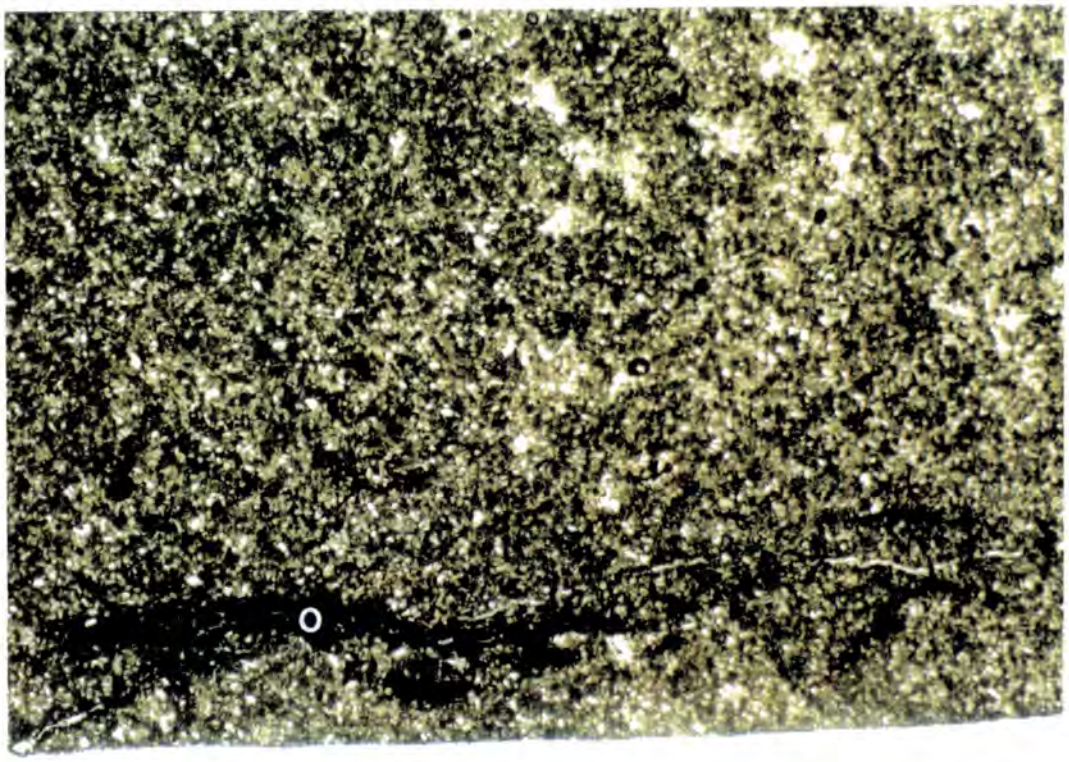

Fig. 5.3: Organic siltstone microfacies (PSorg) containing organic debris (O) and abundant silt-grade quartz in a micritic matrix. Scale 6x3.5mm.

Interpretation: The lack of bioclasts and bioturbation coupled with the abundance of preserved organic debris suggests that this microfacies was deposited in an oxygen depleted environment, affecting both the bottom waters and the sediments. The fine-grained nature of the sediment indicates a low energy environment. This indicates phases of deep, anoxic water in an outer-ramp setting, showing the first signs of clastic detritus influx of silt-grade quartz which is not seen throughout the rest of the formation.

5.3.2. Peloidal mudstone (PMp)

This microfacies (Fig. 5.4) is fine-grained and may be massive, laminated or rarely cross-bedded with echinoid plates marking the foresets in the field. The sediment is dominated by micrite (30-70%) with microspar replacing up to half of the micrite in some samples. Peloids (5-25%) are fine sand-grade and appear to be starting to disintegrate and are often difficult to distinguish from the micritic matrix. Body fossils consist mainly of fine skeletal debris (up to 35%) with rare *Nummulites* and *Amphistegina* (maximum 5%) and planktonic foraminifera. Silt-grade, angular quartz forms up to 15% of the sediment, with those samples higher in quartz thought to be closer to the source area.

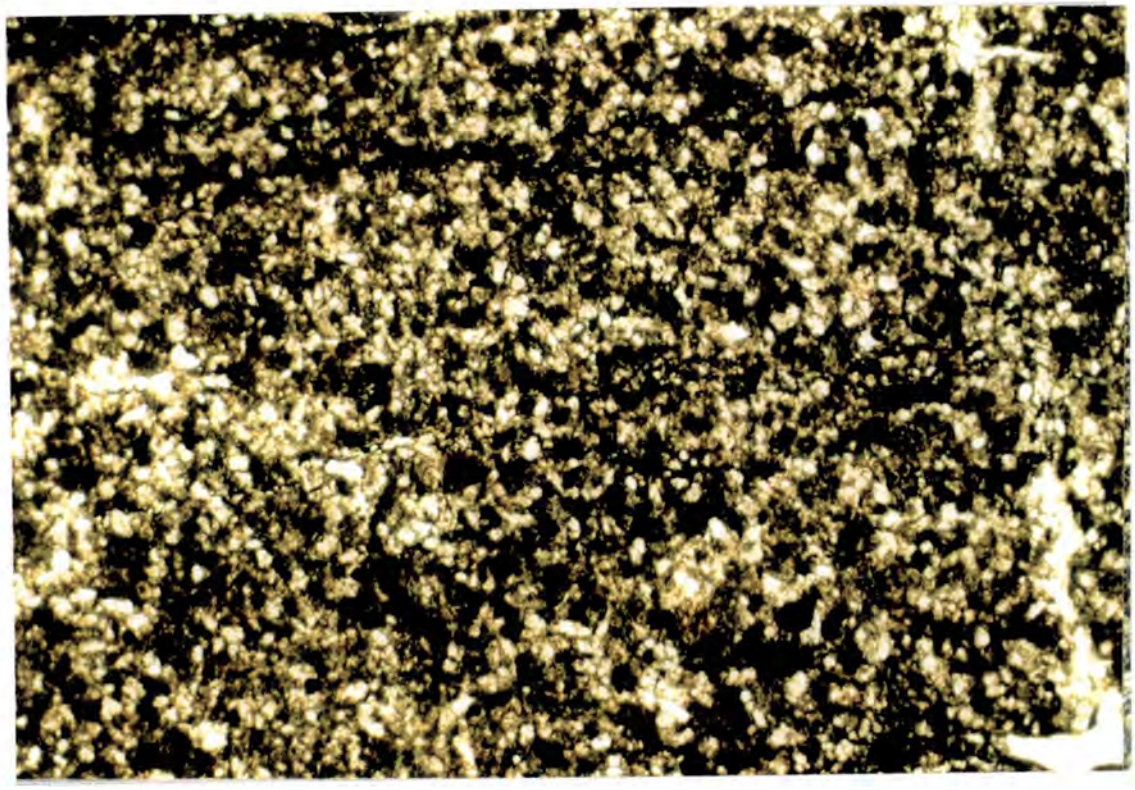

Fig. 5.4: Peloidal mudstone microfacies (PMp) containing dark peloids and quartz in a matrix of micrite and microspar. Scale 3x1.9mm.

Interpretation: The proportion of micrite and fine-grained detritus in this microfacies indicates a fairly low-energy depositional environment, though one in which rare cross-bedding could develop. The origin of the peloids is indeterminate, but in general they are deposited in restricted shallow-water settings; in view of their small grain-size, they would not require very high-energy currents for reworking. The presence of *Nummulites* and *Amphistegina* implies shallow water, in a middle- to inner-ramp setting, but the very low proportions suggest that this depositional environment was not conducive to survival and reproduction, possibly due to high light levels or restricted circulation.

5.3.3. Skeletal mudstone (PMsk)

This microfacies (Fig. 5.5) has a matrix composed of micrite (40-85%), fine-grained skeletal debris (5-30%) and rare quartz and glauconite. Some samples may have a fine-grained calcite cement occurring as patches forming up to 20% of the matrix and probably associated with bioturbation.

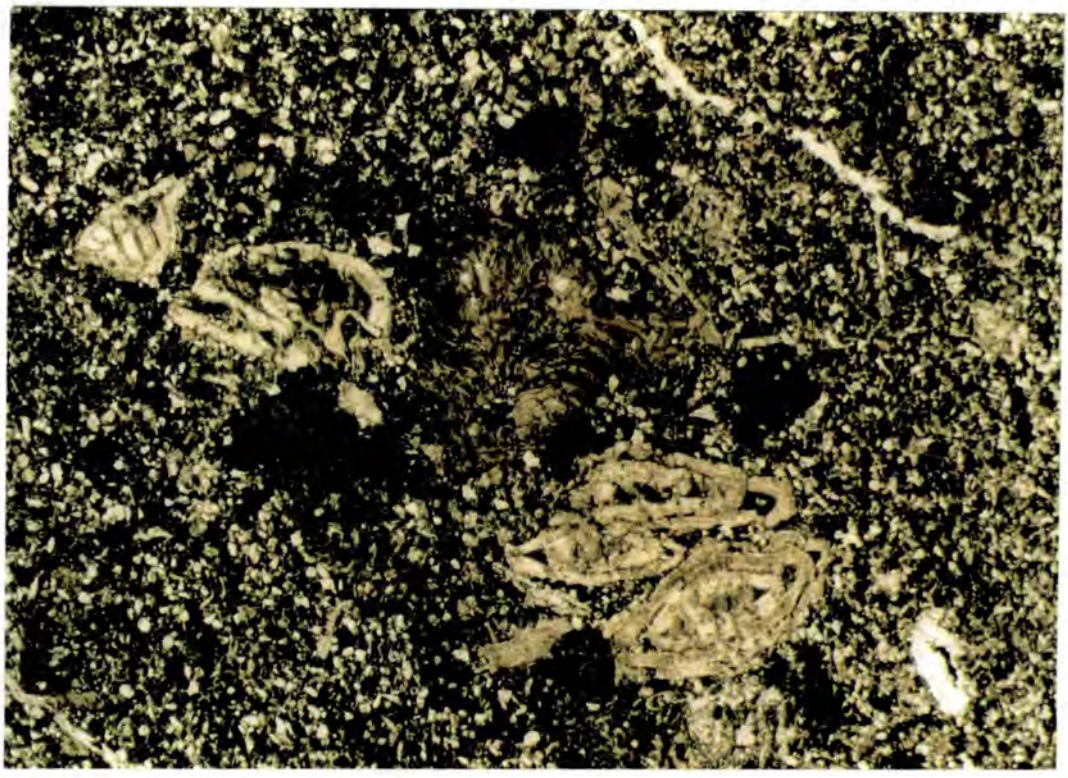

Fig. 5.5: Skeletal mudstone microfacies (PMsk) with Nummulites clustered in a burrow. The matrix is composed of micrite, skeletal hash and quartz. This sample has a high proportion of quartz due to the locality (Pont au Miolans) receiving a higher supply of clastic detritus than the rest of the area. Scale 6x3.5mm.

Bioclasts include larger foraminifera, coral and bivalve debris (0-5%) and echinoid fragments. Peloids may be present but are difficult to distinguish from the matrix. *Nummulites* (up to 10%) are small and flat, typically having a diameter of 2mm, but which may rarely reach 5mm. They are generally well preserved, with some post-depositional compactional deformation, though abraded individuals may also occur. *Amphistegina* (0-5%) are robust and heavily abraded. The foraminifera may be concentrated in burrows as well as distributed throughout the sediment indicating some introduction of material from overlying beds by bioturbation. Miliolids occur throughout the microfacies (2-5%) and may show a slight reddening of their tests.

Bioturbation is evident as bioclast clusters, sediment mottles, cement concentrations and visible burrows in the field.

Interpretation: The high proportion of matrix present in this microfacies indicates a low-energy depositional environment. The foraminifera are small and flat which suggests a middle-ramp setting. The assemblage is dominated by *Nummulites* and *Amphistegina* with no *Discocyclina* or *Operculina* so it is likely to have been deposited in the upper middle ramp, with skeletal debris washed down from the inner-ramp. The evidence for bioturbation indicates that the waters and surface sediments

were well oxygenated, and the burrows formed could have acted as fluid pathways during diagenesis.

5.3.4. Coral wackestone

This microfacies is characterised by a combination of brackish water *Cerithium* gastropods and a marine fauna dominated by corals and Miliolids (Figs 5.6, 5.7).

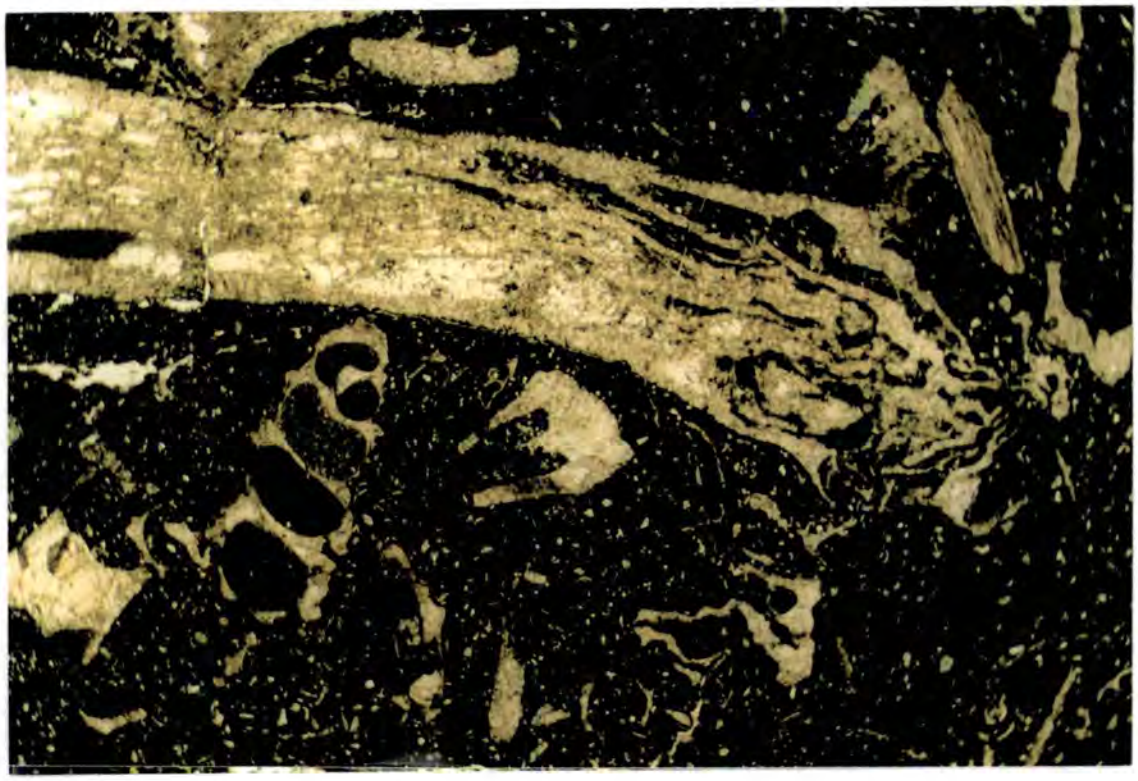

Fig. 5.6: Photomicrograph of the coral wackestone microfacies (PWc) consisting of elongate solitary corals (whole and fragmented), Cerithium gastropods and miliolids in a dark micrite. Scale 12x7.2mm.

The *Cerithium* are high spired, with the originally aragonitic shell replaced by a calcite mosaic. Small protuberances are still visible on the shells indicating that abrasive processes were negligible. The corals (20-30%) are solitary with calices of 4-5mm diameter and the length of the corals may be up to 30mm. The original aragonitic skeleton has been replaced by a calcite mosaic. The internal cavities are infilled with both micrite and calcite spar. The corals are generally intact and appear to be *in situ* in the field, though broken fragments also occur. Their margins are commonly bored. Miliolids (5-10%) are small (0.25-0.75mm diameters) and may have reddened tests. Both quinqueloculine and triloculine forms are present, but there is not a great diversity of forms. Rare Alveolinids also have reddened tests. Other bioclasts include rare *Nummulites* (away from the Infranummulitique boundary), bivalves and skeletal

debris. The matrix is a dark micrite (30-40%) with up to 5% silt-grade, angular quartz. There is no evidence of bioturbation in thin section.

This microfacies occurs between the Infranummulitique and the main marine beds of the Nummulitic Limestone.

Fig. 5.7: Field photograph of the coral wackestone (PWc) showing a horizon of small solitary corals in a muddy matrix. The corals occur in discrete horizons separated by micrite indicating periodic influxes of lime mud killing off the corals.

Interpretation: The combination of both brackish-water and marine faunas indicates that this microfacies was deposited very close to the palaeoshoreline. The coral wackestone represents a transitional stage between the brackish water *Cerithium* marls of the Infranummulitique (Section 3.6) and the fully marine Nummulitic Limestone, and was deposited during the earliest stages of the marine transgression.

The *Cerithium* gastropods could have been reworked from the underlying Infranummulitique, but the absence of abrasion suggests that this is not the case. It seems more likely that the brackish water *Cerithium* marls experienced a change in water chemistry due to the advance of the marine transgression. The marine fauna is dominated by a fairly low diversity of Miliolids suggesting that conditions could not yet sustain a varied marine fauna, but that there was no hypersalinity as conditions were suitable for coral growth. The presence of corals also indicates a relatively stable substrate.

Away from the boundary with the underlying Infranummulitique, the *Cerithium* disappear to be replaced by a marine fauna of *Nummulites*, Alveolinids, Miliolids and corals. The separation of the coral horizons by mud-rich layers, suggests that growth occurred during hiatuses in sediment supply. A low sedimentation rate is also evident in the presence of borings on the coral skeletons and slight reddening of the Miliolid tests. Sudden influxes of muddy sediment served to temporarily kill off the coral colonies. The lack of bioturbation and dark colour of the matrix suggests low oxygen levels during the deposition of some horizons, prohibiting colonisation of the sediment and promoting the preservation of organic matter.

The coral wackestone was deposited in a low energy, coastal environment during the early stages of marine transgression.

5.3.5. *Discocyclina/Operculina* wackestone (PWdo)

This is characterised by the abundance of foraminifera, in particular *Discocyclina* and *Operculina* (Fig. 5.8). *Discocyclina* (10%) occur both as flat and

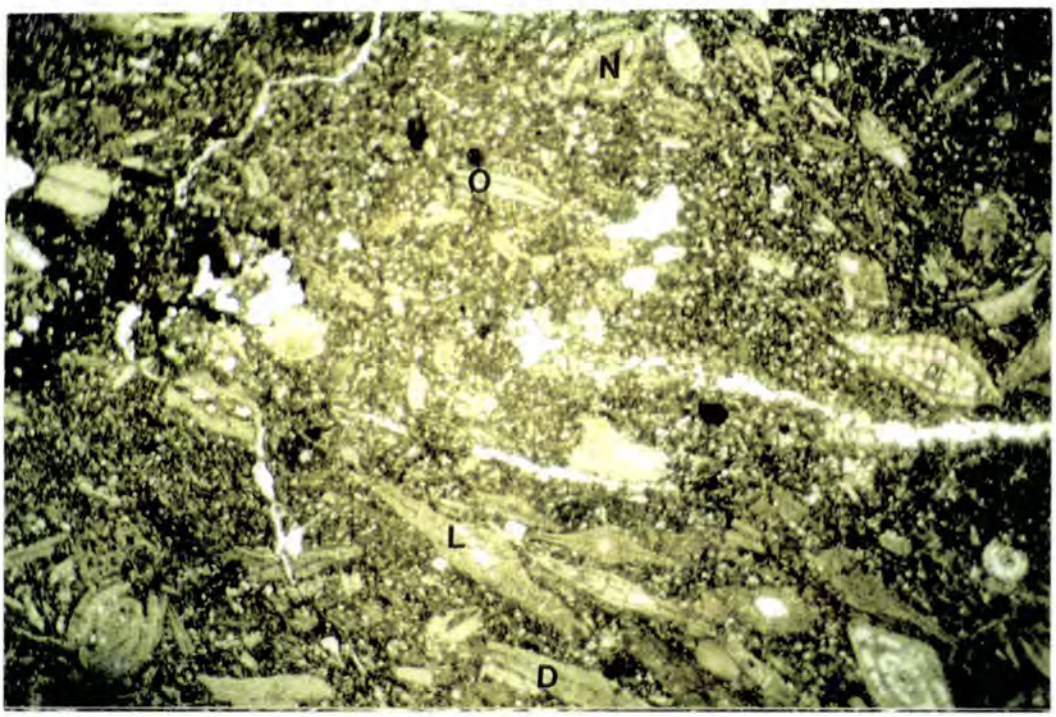

Fig. 5.8: Discocyclina / Operculina wackestone (PWdo) containing Discocyclina (D), Lepidocyclina (L), Operculina (O) and Nummulites (N) in a silty micrite. The bioclasts are crudely aligned and the benthos indicates an outer ramp setting. Scale 12x7mm.

inflated forms (*Lepidocyclina* may also be present) and generally have a diameter of 5mm, but may rarely reach up to 10mm. Both intact and abraded forms are present, the intact forms tending to be large, flat individuals with relatively thick tests.

Operculina (0-10%) are the same order of size and are flat with both thin and thick-tested forms present. They are typically fragmented and abraded, though rare intact forms can occur, showing compactional fracturing. *Nummulites* (5-15%) are intermediate to robust, abraded and small (up to 1.5mm diameter). Larger, flat forms also occur (4mm), with thinner tests, which are usually intact. *Amphistegina* and Orbitolinids are uncommon (<5%) and abraded. Other bioclasts include bivalve fragments, echinoid debris and rare Miliolids and Textulariids.

The matrix is a dark micrite (40-60%) with silt-grade, angular quartz (5%) and rare glauconite. Skeletal debris is fine sand-grade and consists dominantly of foraminifera debris (10-20%). An alignment of the larger foraminifera may occur but is not common. Mottling in the matrix and some concentration of bioclasts indicates bioturbation.

Interpretation: This microfacies generally occurs towards the top of the formation. The dominance of *Discocyclina* and *Operculina*, especially very large, flat forms in association with abundant micrite, indicates low-energy conditions, probably representing deposition in a deep, outer-ramp setting. *Nummulites* are also large and flat, with the robust abraded forms of *Nummulites*, *Amphistegina* and Orbitolinids due to the influx of shallow-water forms from higher up the ramp. The abundance of foraminiferal debris is probably due to the down-ramp transportation of shallow-water forms and also to *in situ* storm reworking of the sediment, concentrating the bioclasts. The effect of storms on the sediment may also produce the alignment of the foraminifera, though this may be due to bioturbation or reflect the life positions of the foraminifera.

5.3.6. Peloidal wackestone (PWp)

The dominant clasts in this microfacies (Fig. 5.9) are fine to medium sand-grade peloids (25-40%). The origin of the peloids is indeterminate, though the more angular grains are possibly micritised skeletal debris. The peloids are evenly distributed throughout the sediment and are associated with 10% skeletal debris. The matrix is a pale micrite (40-60%) with 2% silt-grade quartz and 5% calcispheres. Bioclasts other than skeletal debris are very uncommon, consisting of echinoid fragments and rare, small, intermediate *Nummulites*.

Interpretation: This appears to be a higher-energy equivalent to the peloidal mudstone. The peloids are coarser grained and there is a higher proportion of skeletal debris indicating a greater influence by marine currents. Some peloids appear to be micritised skeletal grains due to boring by micro-organisms. This could indicate a shallow, low-energy, protected environment. *In situ* bioclasts are uncommon which

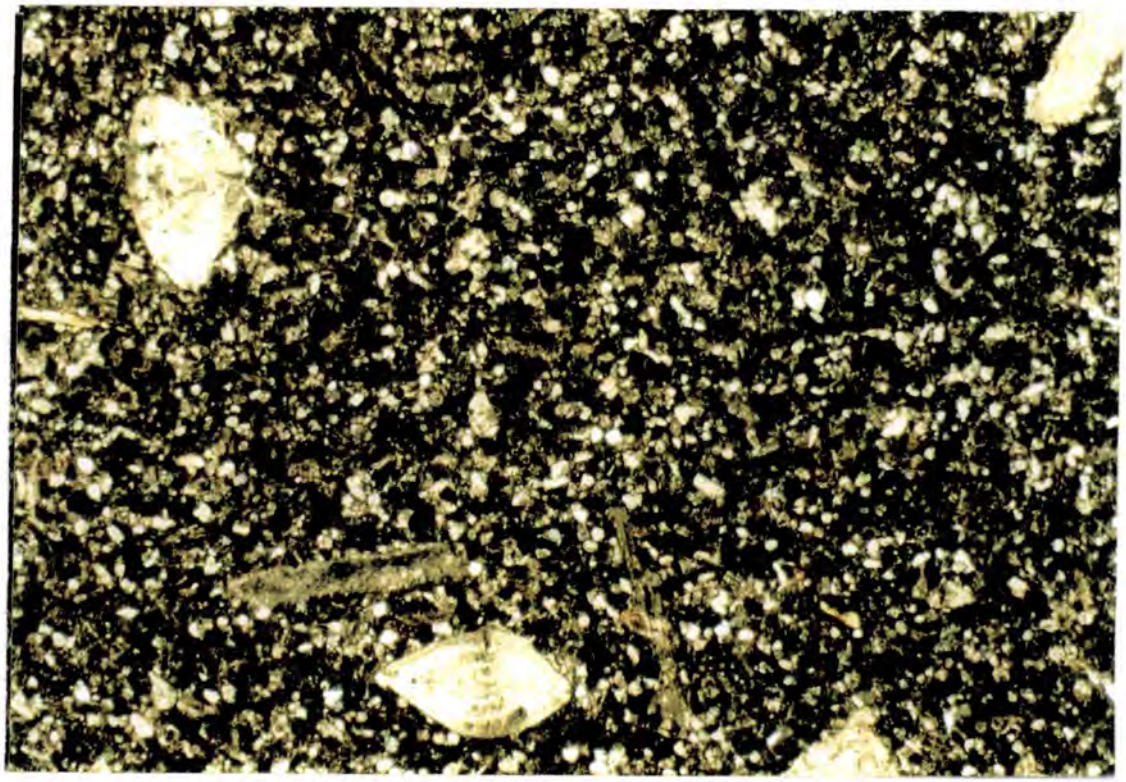

Fig. 5.9: Peloidal wackestone microfacies (PWp) with abundant black peloids and skeletal debris in a micritic matrix. Small, robust Nummulites are also present in this example. Scale 6x3.7mm.

could indicate restricted conditions or a high light intensity, reflected by the lack of rotaline foraminifera.

5.3.7. Foraminifera-algal wackestone (PWPfa)

This microfacies (Fig. 5.10) is one of the few in Haute Provence that contains calcareous red algae (CRA), which are localised to the Agnère and Annot synclines (Fig. 5.1). The CRA (10-20%) occur as abraded fragments, broken crusts on bioclasts and broken rhodoliths. Corals (0-5%) may also be present as fragments and are associated with the CRA.

The remainder of the bioclasts are foraminifera (20-25%). *Nummulites* (5%) are robust with thick tests and are normally well preserved, though may be mildly abraded. They are small, generally 1-2mm in diameter, and the internal chambers have been infilled with calcite. Some large, flat individuals may be present, reaching 8mm in diameter suggesting the presence of two generations. *Discocyclina, Lepidocyclina* and *Operculina* (5-10%) dominantly occur as broken fragments of inflated forms, of the same order of size as the *Nummulites*. A species of encrusting foraminifera is also present at Pont Noir (not identified). This foraminifera can be seen to bind patches of the sediment, and may itself be encrusted by CRA.

The matrix consists of a fine-grained micrite (40-50%) with abundant silt- to fine sand-grade skeletal debris (10-15%) dominated by foraminiferal fragments. There may also be silt-grade quartz present in small amounts.

It should be noted that there are no Orbitolinids or peloids present in this microfacies (c.f. Section 5.3.10).

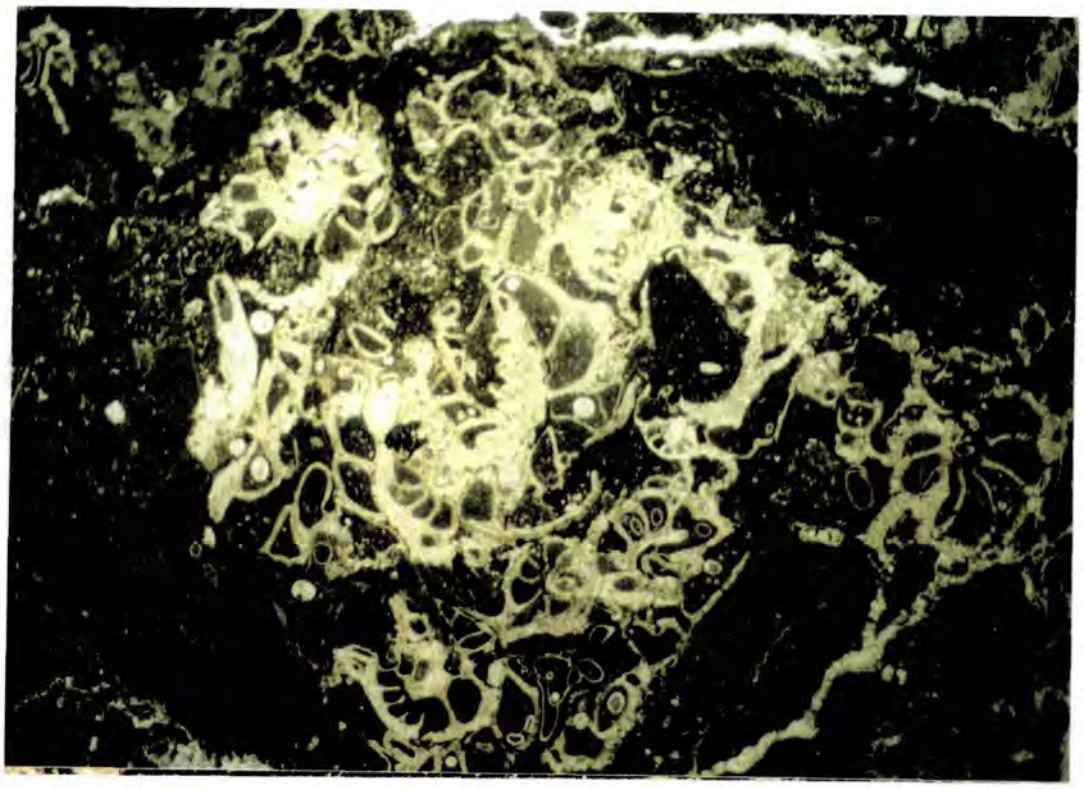

Fig. 5.10: Foraminifera-algal wacke-packstone (PWPfa) containing CRA and an encrusting foraminifera in a micritic matrix. Scale 12x7mm.

Interpretation: The presence of CRA and foraminifera indicates a shallow marine, possibly inner-ramp setting. The algae encrust bioclasts and occur as rhodoliths indicating the presence of nearby algal-rich sediments (not seen), though the degree of fragmentation indicates that the bioclasts underwent significant transportation prior to deposition. The algal fragments could be derived from local rhodolith gravels, which are thought to be of limited lateral extent, and there is no evidence for the development algal shoals similar to those observed in Haute Savoie (Section 4.5.2.).

Intact, robust *Nummulites* and abraded inflated Discocyclinids are indicative of a middle-ramp setting under the influence of currents reworking and abrading the more fragile bioclasts. The diversity of the fauna suggests a favourable environment, sufficient for foraminiferal reproduction producing the bimodal size distribution of the *Nummulites*.

5.3.8. Foraminifera wacke-packstone (PWPf)

This microfacies (Fig. 5.11) is characterised by a high proportion of micrite and a benthonic foraminiferal assemblage dominated by *Nummulites* and *Amphistegina*. *Nummulites* (5-20%) are intermediate to robust and two generations may be present. The robust A-forms have a diameter in the order of 2mm, whereas the flatter B-forms may reach up to 15mm diameter and show a higher degree of abrasion. *Amphistegina* (1-10%) are much smaller, only reaching a maximum diameter of 1mm. Orbitolinids may be common, forming up to 15% of the sediment and are the same order of size as the *Nummulites*. They tend to be fairly robust, with a high conical apex and are abraded. Other foraminifera which may be present in varying amounts are Miliolids (up to 10%), *Discocyclina*, *Operculina* and rare Alveolinids. The rotaline *Discocyclina* and *Operculina* tend to be heavily abraded and fragmented, whereas the porcellanous Miliolids and Alveolinids are well preserved. Echinoid plates (5%), bivalves and serpulids comprise the remainder of the bioclasts, occurring as abraded fragments of the same order of size as the foraminifera.

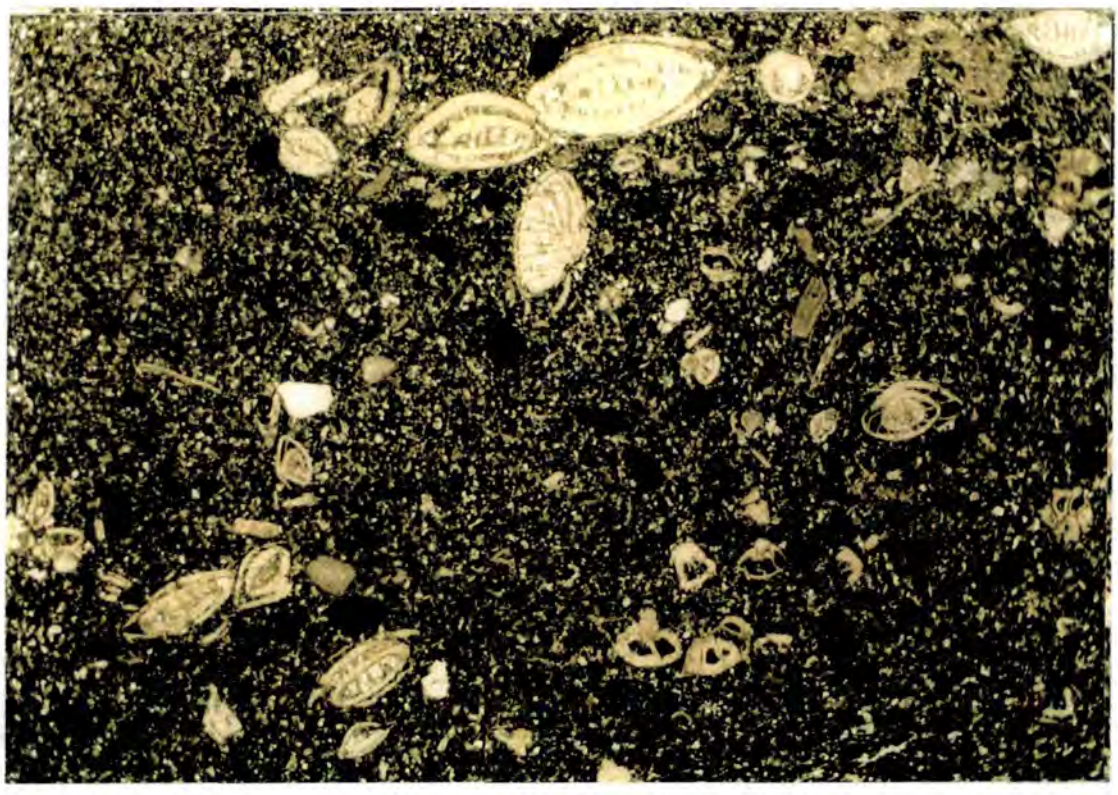

Fig. 5.11: Foraminifera wacke-packstone (PWPf) containing Nummulites and Amphistegina. Scale 12x7mm.

The matrix consists of micrite (30-60%) with up to 20% fine-grained skeletal debris. Silt-grade quartz may also be present and reaches 20% at one locality. This locality has a much higher input of clastic detritus compared to the rest of the study area. There may be up to 30% calcite cement, which occurs as patches in the

otherwise micritic matrix. This may be associated with bioturbation, which also produces a local preferred alignment of the foraminifera tests and clusters of bioclasts.

Interpretation: The high proportion of micrite indicates a low energy setting. probably below FWWB. The domination of the foraminiferal assemblage by *Nummulites* and *Amphistegina* and their shape imply a middle-ramp setting. The continued presence of *Discocyclina* and *Operculina* suggests a proximity to the lower ramp, but these have been reworked causing abrasion of the tests. Echinoid and serpulid fragments have probably been washed down-ramp from shallower areas.

This microfacies was deposited in a middle-ramp setting and represents the *in situ* ramp fauna.

5.3.9. Peloidal foraminifera wackestone (PWfp)

This has similar characteristics to the foraminifera wacke-packstone in addition to which it has 10-40% peloids (Fig. 5.12). The sediment has had a much lower influx of debris, with skeletal hash only reaching a maximum of 10% and being absent from many samples. There is also no cement development, the matrix being composed of micrite (35-50%) and peloids. Quartz is more abundant in localities with an overall higher supply of clastic detritus.

Fig. 5.12: Peloidal foraminifera wackestone (PWfp) with flat Nummulites and Operculina floating in a matrix of dark micrite and peloids. Scale 12x7mm.

The foraminiferal assemblage is dominated by *Nummulites* (5-20%) with lesser amounts of *Amphistegina* (0-10%) and Orbitolinids (0-5%). There may also be rare *Operculina* and *Discocyclina*, which are generally fragmented. The Nummulites are flat-intermediate and tend to be well preserved. Smaller, robust forms are also present which are more abraded. Other bioclasts are echinoid, bivalve and serpulid fragments. The bioclasts are distributed fairly uniformly throughout the sediment, with slight clustering indicating bioturbation. This also produces mottling in the micrite.

Interpretation: The lack of skeletal debris and an abundance of peloids suggest a lower energy environment, though the similarity of the foraminiferal assemblage to that in the foraminifera wacke-packstone indicates a similar position on the ramp in terms of light intensity and water depth. The fauna is generally *in situ*, with some reworking of the sediment abrading the smaller bioclasts. Bioturbation indicates that the sediment was oxygenated and a lack of cement suggests that there were no winnowing processes removing the fine micrite.

This microfacies is interpreted as having been deposited in a low energy, probably sheltered, middle-ramp setting. The lack of *Discocyclina* and *Operculina* preclude deposition on the lower middle-ramp.

5.3.10. Nummulite packstone (PPn)

Fig. 5.13: Nummulite packstone microfacies (PPn) illustrating the tightly packed nature of the sediment and the low proportion of micrite. Other bioclasts are rare in this microfacies. Scale 12x7mm.

This microfacies (Figs 5.13, 5.14) is dominated by well preserved *Nummulites* (20-40%) with both A- and B-forms present. The megalospheric A-form is dominant (>20:1). A-forms are robust and thick tested, with equatorial diameters ranging from 2-4mm. The chambers are infilled with calcite spar. B-forms are more elongate and diameters reach up to 10mm. Some samples contain a higher proportion of more abraded, smaller A-forms. Other foraminifera only make up 10% of the sediment and include *Amphistegina*, Orbitolinids and *Operculina*. There is usually only one of these genera present in any given sample and they tend to be much more abraded than the *Nummulites*. Echinoids (5%) occur as large plate fragments up to 9mm long, i.e. of the same order of size as the foraminifera, and may be bored. Fragments are very angular, suggesting that no rounding by abrasion or transportation has taken place. Both ribbed and smooth bivalves may be present (2-5%).

The matrix is dominantly micrite (20-25%) with peloids (10-20%) and a small amount of silt-grade quartz (1%). There is commonly a crude parallel alignment of the elongate bioclasts, which may be disrupted by bioturbation producing bioclast clusters and/or micrite-rich patches in the sediment. Organic debris can also occur along these 'horizons'.

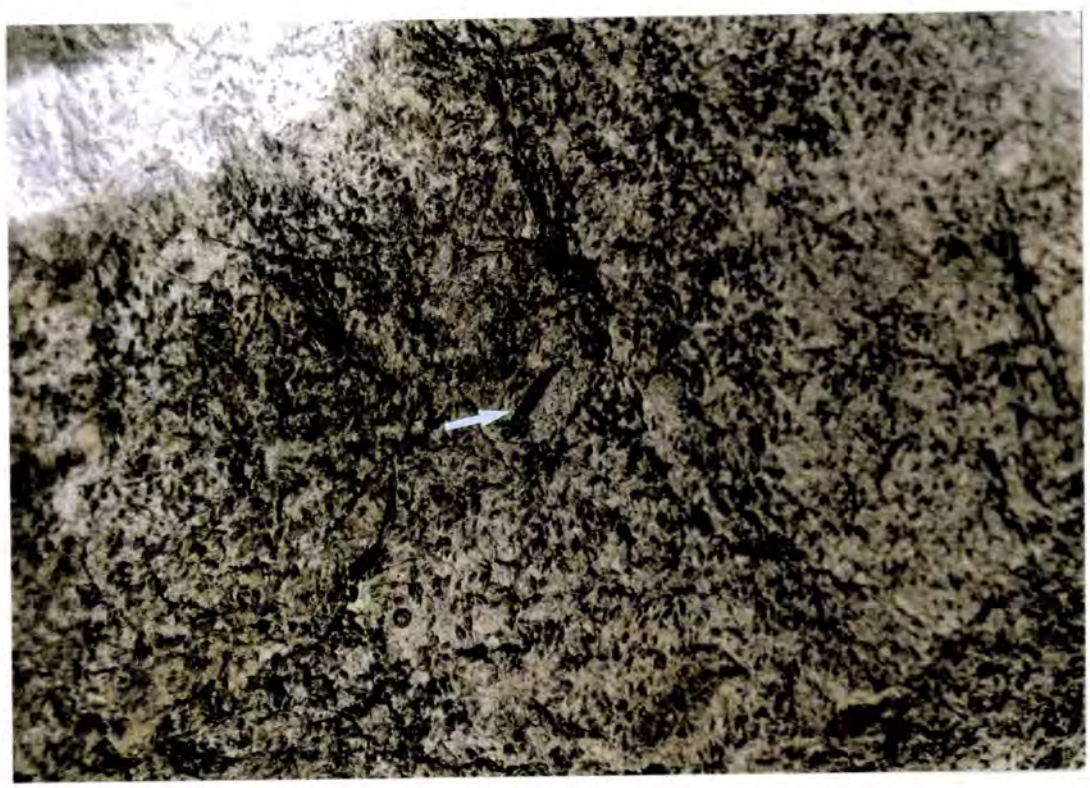

Fig. 5.14: Field photograph of the nummulite packstone showing the tightly packed texture and the dominance of A-forms. An elongate B-form is present in the centre of the field of view (2cm length).

Interpretation: The presence of a high concentration of an essentially monospecific *Nummulites* assemblage, along with excellent preservation of the fauna suggests that this microfacies could indicate the development of an autochthonous Nummulite build-up, similar to those described by Racey (1990), Aigner (1982, 1983, 1984) and Crampton (1992) from the Eocene around the world.

The shape and size of the foraminifera suggests a middle- to inner-ramp setting, with sufficient wave energy to winnow the sediment, removing most of the micrite, but too weak to transport the smaller A-forms. The boring of the echinoid plates and the presence of finer organic debris along laminae within the sediment suggests that this winnowing may have been sporadic, with intermittent, low-energy conditions producing the finer laminae and allowing boring by organisms.

This microfacies represents the *in situ* concentration of bioclasts leading to a para-autochthonous nummulite build-up in a lower inner-ramp setting.

5.3.11. Foraminifera wacke-grainstone (PWGf)

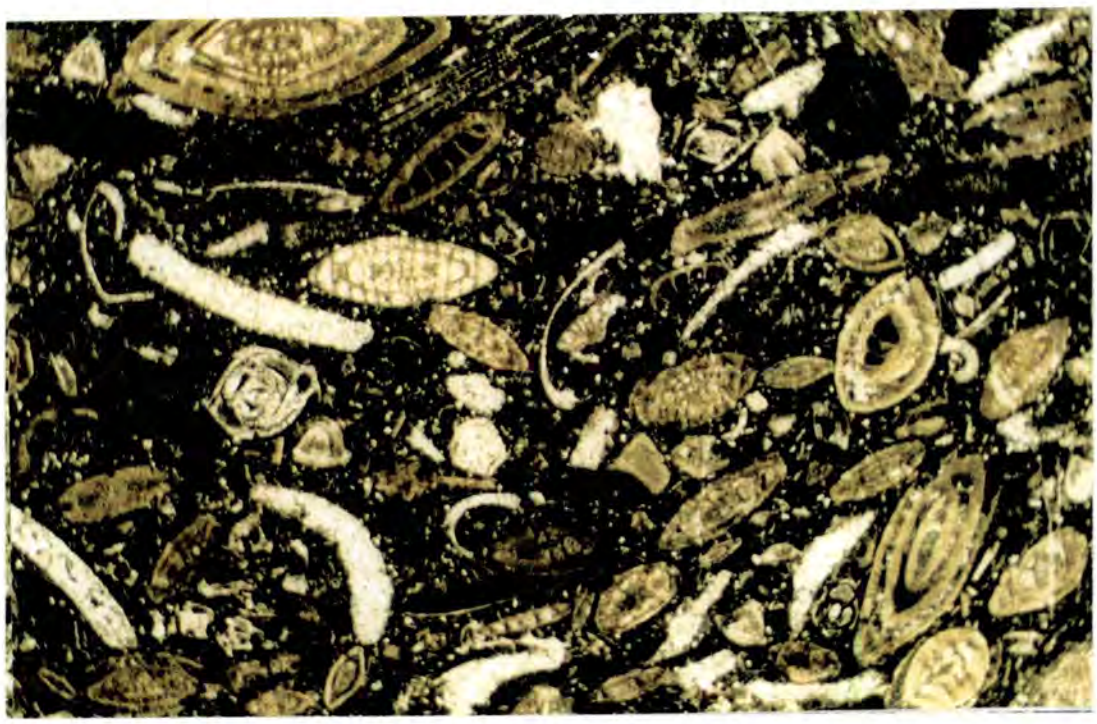

Fig. 5.15: Foraminifera wacke-grainstone (PWGf) containing Nummulites, Amphistegina, Miliolids, Orbitolinids and abundant peloids in a matrix containing both micrite and microspar. Scale 12x7mm.

This microfacies (Fig. 5.15) is characterised by the presence of both micrite (<30%) and a fine-grained calcite cement (10-30%). The foraminiferal assemblage is dominated by *Nummulites, Amphistegina* and Orbitolinids. *Nummulites* (up to 20%) are small (less than 2mm) and intermediate to robust. Two assemblages occur, with

differing degrees of abrasion: a well preserved, seemingly monospecific assemblage, and a more abraded, diverse assemblage. The more abraded forms tend to be more robust. *Amphistegina* (<10%) are smaller and more robust and tend to be more heavily abraded than the larger *Nummulites*. Orbitolinids (5%) are intermediate, and generally abraded. Miliolids form up to 5% of the sediment. No alignment of the foraminifera is seen in thin section. Other bioclasts present are abraded fragments of bivalves, echinoids, serpulids and skeletal debris.

Peloids are relatively abundant, forming 10-40% of the sediment. They are sand-grade and occur in the matrix with quartz grains of the same size (2%), micrite (<30%) and cement (10-30%). The micrite and cement are not evenly distributed throughout the slide, with patches occurring enriched in either micrite or cement. Areas enriched in cement usually contain a higher proportion of skeletal debris, which is indicative of bioturbation. Two types of cement are present: an initial fine-grained microspar occurring between the grains and a later, coarser calcite mosaic infilling the remaining pore spaces.

Interpretation: This microfacies contains a typical inner-ramp assemblage of small, robust foraminifera dominated by diverse rotaline forms. The microfacies represents both the *in situ* ramp fauna (well preserved bioclasts) that may be associated with the nummulite banks, and reworked bioclasts dominated by more abraded forms. The abundance of peloids indicates a shallow, inner-ramp setting with winnowing removing some of the fines and abrading the bioclasts. The sediment was well oxygenated and reworked by bioturbation producing the concentrations of peloids and bioclasts and allowing cementation in the micrite-poor areas.

5.3.12. Foralgal pack-grainstone (PPGfa)

This microfacies (Fig. 5.16) is characterised by the presence of CRA (10-20%), which mostly occur as angular fragments, some of which appear to have been reworked from branching masses. *Nummulites* (2-20%) are robust and generally have diameters less than 2mm. Orbitolinids are present (c.f. foraminifera algal wacke-packstone) forming up to 10% of the rock. Other foraminifera present are *Amphistegina, Discocyclina,* Miliolids and Textulariids. Encrusting foraminifera may also occur (Pont Noir section) The preservation of the foraminifera is variable, with both intact and heavily abraded forms present in the same sample. Echinoderm plates are relatively common, constituting 5% of the sediment. Other skeletal debris is negligible.

The matrix consists of silt- to fine sand-grade peloids (5-15%) in a dark micrite (30%). Most samples have a patchy distribution of the micrite and a fine-grained drusy calcite cement (15-45%). Some samples have been winnowed, with all

the fine material having been removed, allowing extensive cement formation. Quartz is rare.

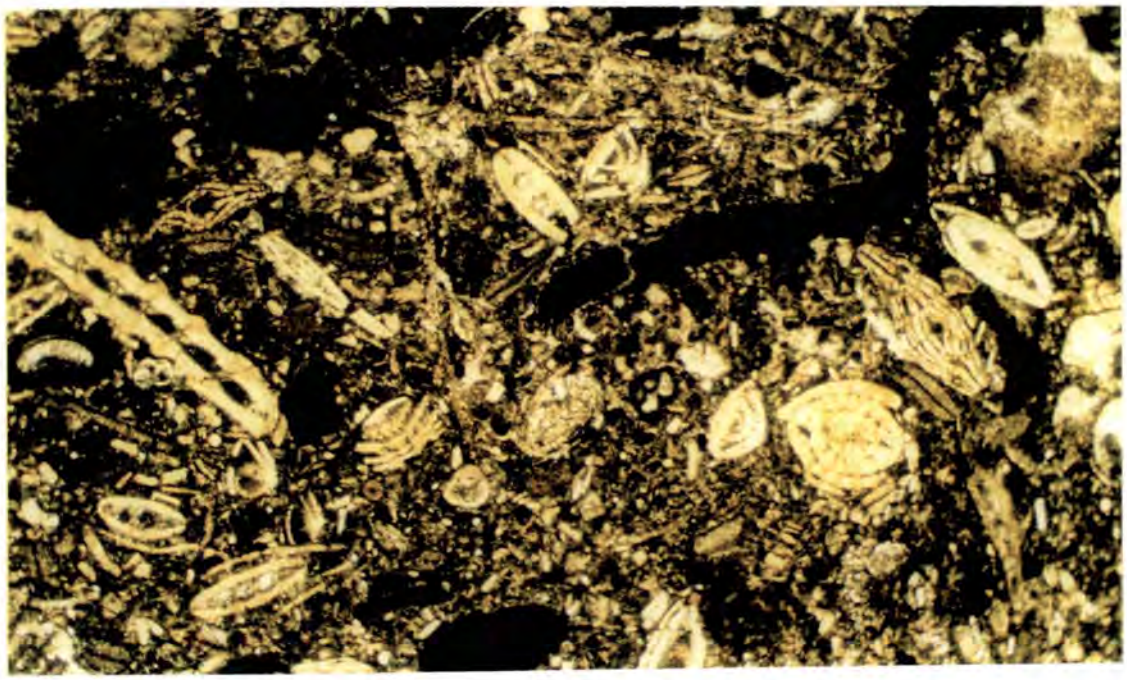

Fig. 5.16: Foraminifera-algal pack-grainstone (PPGfa) showing the presence of CRA, foraminifera and peloids in micrite and calcite microspar.

Interpretation: This microfacies is again localised to the Annot and Agnère Synclines and represents a higher energy equivalent to the foraminifera-algal wackestone. Again, the CRA have undergone significant transportation fragmenting the rhodoliths. In contrast to the wackestone, this microfacies contains both peloids and Orbitolinids indicating that it was deposited in an inner-ramp setting. This accounts for the higher water energies, causing winnowing of the sediment and the removal of micrite allowing subsequent cementation. The patchy distribution of the cement and micrite is probably due to bioturbation.

5.3.13. Nummulite-Miliolid pack-grainstone (PPGnm)

This microfacies is dominated by *Nummulites* and Miliolids (Fig. 5.17). The *Nummulites* (10-20%) are generally small, with diameters of less than 2mm but may rarely reach 4mm. They are intermediate to robust and usually have thin tests. Preservation is generally good, but tests may be mildly abraded. Miliolids (5-15%) are abundant and diverse, with sizes ranging from 0.25-2.5mm. The tests are very well preserved and larger forms are clearly visible in hand specimen. Other foraminifera present are Orbitolinids (10%), *Amphistegina* (≤5%) and rare *Operculina* and

Discocyclina, all of which are heavily abraded. The bioclasts occur in a micritic matrix (15-35%) with fine-grained skeletal debris (5-20%), quartz and peloids (5-10%) with a patchy distribution of microspar. The peloids are fine sand-grade and generally rounded. Some may be reworked lithic grains. Skeletal debris is dominantly composed of foraminifera fragments, with echinoid plates and broken serpulids.

The cement (10-30%) is present as two phases; an early, fine-grained isopachous fringe occurring around the bioclasts, and a later drusy calcite mosaic infilling the intergranular spaces. Mottling occurs in some samples due to bioturbation. Some cementation may be associated with the bioturbation.

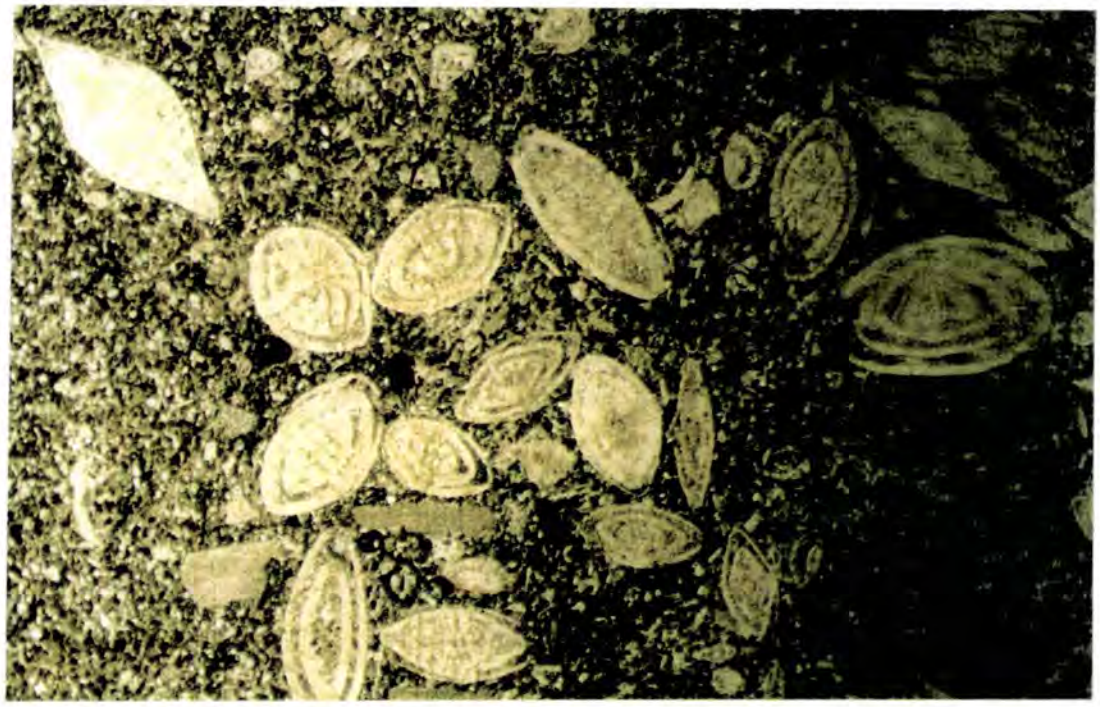

Fig. 5.17: Nummulite-miliolid pack-grainstone (PPGnm) with abundant Nummulites and Miliolids along with replaced bivalve fragments, echinoid spines, Amphistegina and Orbitolinids. The matrix is micritic, with patches of calcite spar. Scale 12x7mm.

Interpretation: The abundance and diversity of Miliolids indicates a shallow-water, normal-marine, inner-ramp environment. However, the presence of rotaline forms suggests that light intensities were not too high to affect their survival. Other bioclasts are typical of an inner-ramp setting. The sediment was deposited under the influence of winnowing currents, removing the micrite and leaving a residual, thin bioclastic lag.

5.3.14. Peloidal foraminifera grainstone (PGpf)

This microfacies is characterised by a high proportion of peloids and foraminifera in a sediment from which all fine-grained carbonate has been removed (Fig. 5.18). The peloids (15-35%) show a uniform grainsize distribution and are well rounded. Some are more pointed at one end and may be faecal pellets. Others may be small, rounded lithic grains, but the origin is generally uncertain.

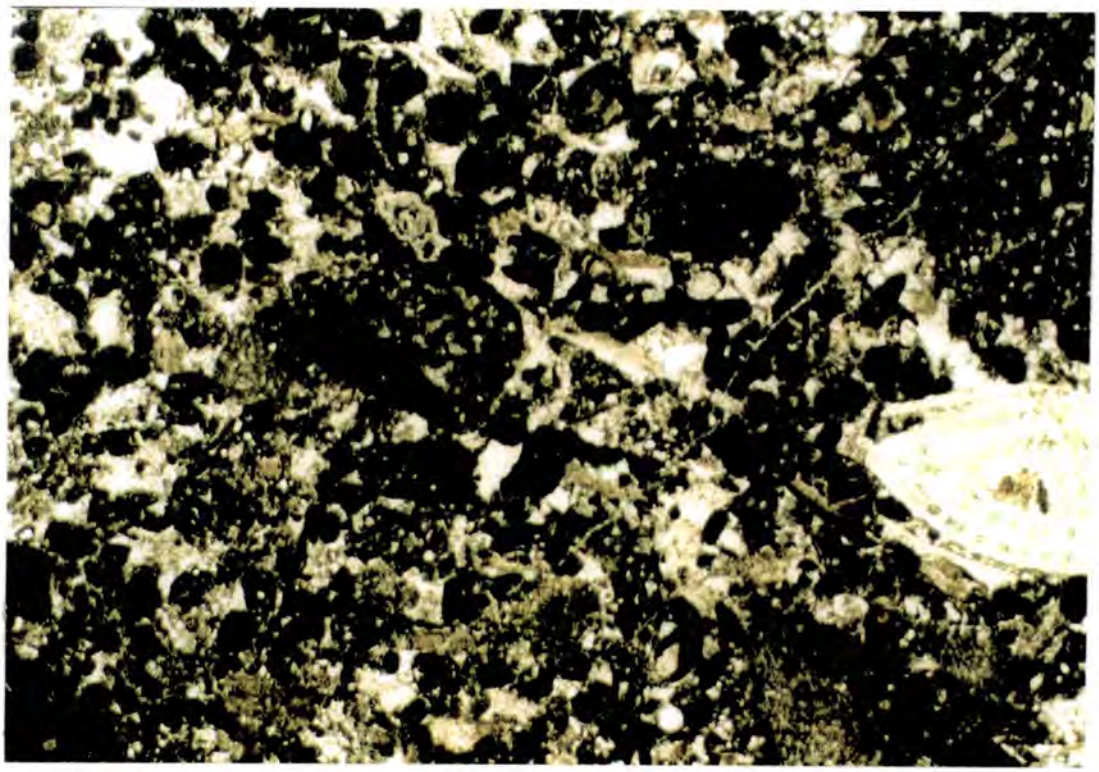

Fig. 5.18: Peloidal foraminifera grainstone (PGpf) showing the absence of micrite. Instead the peloids and Nummulites are packed into a clear calcite spar. Scale 6x3.5mm.

The foraminiferal assemblage is dominated by *Nummulites* (≤15%) and Orbitolinids (≤15%). *Nummulites* are small (1-3mm) and intermediate to robust with thick tests. The megalospheric A-form is dominant, but microspheric B-forms may also be present. They are generally well preserved, but may be slightly abraded. The Orbitolinids are "chinese hat"-shaped and occur both as abraded fragments and intact individuals of the same order of size as the *Nummulites*. Miliolids may form up to 5% of the sediment and a diversity of forms are present. They are small (0.5mm) and may be intact or abraded. Echinoids and/or serpulids may locally form up to 20% of the sediment. Otherwise, these bioclasts form a small proportion (10%) of the sediment, along with fragmented corals, bryozoans, echinoids, serpulids and rare CRA and encrusting foraminifera (Pont Noir section). The bioclasts show a uniform distribution, with no evidence of bioturbation or post-depositional compaction.

The cement occurs as two phases. The first phase is a fine-grained isopachous rim around the bioclasts and infilling smaller interstitial regions. The second phase infills the remaining pore spaces and is a coarser drusy calcite, showing a marked coarsening away from the grain boundaries. Syntaxial overgrowths occur associated with the echinoid plates.

Interpretation: The high proportion of peloids indicates an inner-ramp setting as do the shape and nature of the foraminifera and the abundance of serpulids, corals and bryozoans. The lack of fines indicates winnowing by marine currents, concentrating the bioclasts and allowing extensive cementation to occur. Layers of concentrations of bioclasts may represent winnowed lags due to the removal of fines. The lack of evidence for post-depositional compaction may indicate early marine cementation. This microfacies was deposited in a high-energy, inner-ramp setting, above FWWB.

5.3.15. Peloidal grainstone (PGp)

This microfacies consists of abundant peloids in a calcite cement (Fig. 5.19). Fragmented foraminifera make up less than 20% of the sediment. The peloids (20-40%) are fine to medium sand-grade, well sorted and vary from angular to rounded.

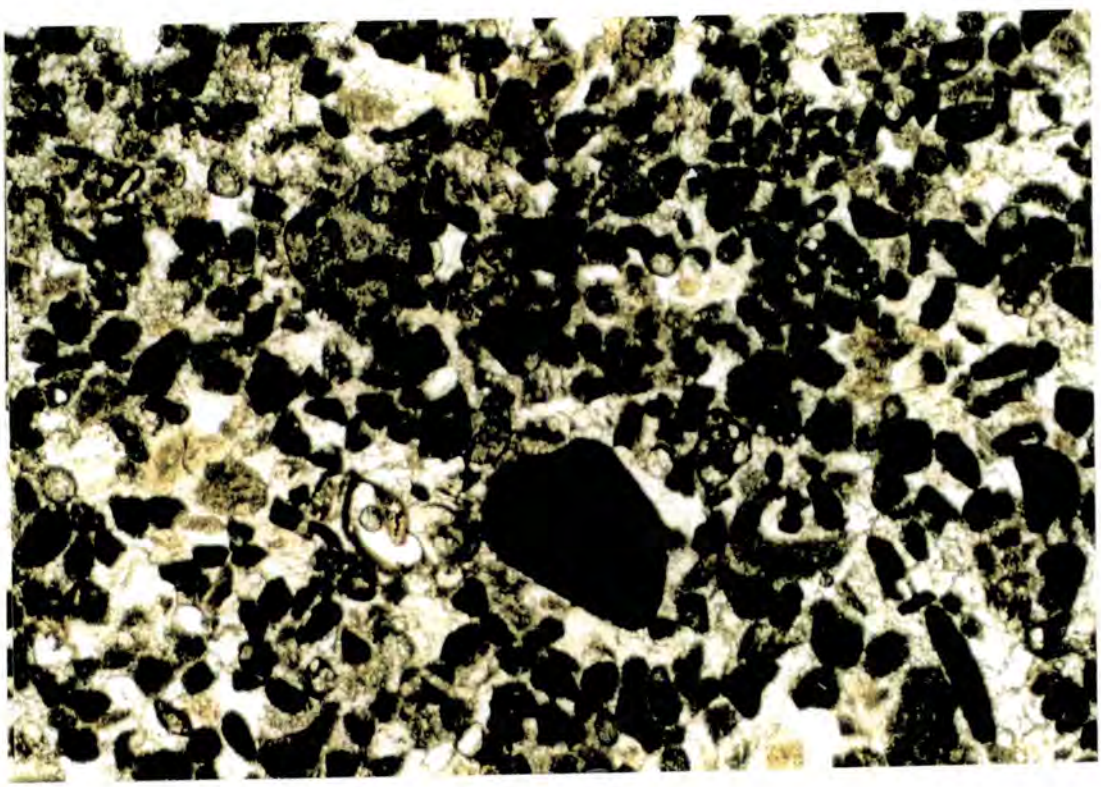

Fig. 5.19: Peloidal grainstone microfacies (PGp) dominated by dark peloids with rare Miliolids. Rotaline foraminifera are absent. Scale 3x1.9mm.

Their origin is generally indeterminate, though some may have originated as small lithic grains. The foraminifera consist dominantly of fragments of *Nummulites*, Orbitolinids and Miliolids with lesser proportions of *Amphistegina* and Textulariids. *Operculina* and *Discocyclina* are very rare. They occur as small abraded fragments which have not undergone micritisation and are therefore easily discernible from the micritic peloids. Other bioclasts include binding organisms, serpulids, bryozoans and corals, and echinoids, bivalves and other skeletal debris. The serpulids may be intact, but in general all bioclasts are fragmented and abraded.

The cement occurs in two phases and has a patchy distribution: an early isopachous fringe with a later drusy pore-filling cement.

Interpretation: The lack of foraminifera indicates a shallow-water environment with high light intensities. As most of the foraminifera occur as abraded fragments, this would suggest that they have been transported from their life position by wave action. The abundance of peloids implies a shallow, inner-ramp setting, as does the presence of serpulids, corals, bryozoans and echinoids. The lack of micritisation of the bioclasts indicates an open-marine setting and the complete removal of micrite indicates agitated conditions, though with insufficient energy to remove the peloids. There may be bioturbation as rare patches of micrite are present, which is thought to have been introduced from the overlying sediments. Patches devoid of bioclasts also indicate biogenic reworking of the sediment.

This microfacies represents an inner-ramp setting, probably occurring above FWWB.

5.4. Facies Associations

The microfacies described above occur in five typical facies associations, representing the different positions on the carbonate ramp (Table 5.2). These are outlined below, with a sedimentary log showing the vertical arrangement of the microfacies seen in the field.

5.4.1. P1: Peloidal Facies Association (PGp, PGpf, PMp, PMsk)

In some localities, especially in the St Antonin, Allons and Argens synclines peloidal grainstone deposits occur above the basal unconformity or Infranummulitique and below the nummulite accumulations. The facies association consists of a thickening-upwards succession dominated by peloidal grainstones, interbedded with wackestones and mudstones, illustrated in Fig. 5.20. In the field the peloidal facies association is generally flat bedded with local cross-bedding developed. The foresets

Facies Association	Dominant textures	Sedimentary structures	Dominant bioclasts	Interpretation
Peloidal FA **P1**	grainstone mudstone PGp, PGpf PMp, PMsk	cross-bedding shelly lags bioturbation cemented	peloids foraminifera echinoderms plant debris	**Peloidal shoal** High-energy deposition in a shallow-water environment, above FWWB, with current reworking and periodic events producing shell lags. Mudstones represent low-energy back-shoal areas.
Nummulitic FA **P2**	pack- grainstone packstone wackestone PPn, PWf PPGnm	cross-bedding bioturbation erosive bed bases lamination some cementation	*Nummulites* foraminifera echinoderms	**Nummulite shoal** High-energy, inner-ramp para-autochthonous nummulite accumulations. *In situ* winnowing by currents and storm events. Wackestones and miliolid-rich facies represent sheltered back-bank areas.
Algal FA **P3**	packstone wackestone PPGfa PWfa	binding organisms	CRA, rhodoliths encrusting foraminifera bryozoans corals, serpulids	**Algal shoal** Inner-ramp setting proximal to rhodolith shoal / gravel. Some colonisation by CRA and foraminifera.
Foraminiferal FA **P4**	wacke- packstone wackestone mudstone PWGf, PWPf, PWpf, PWp PWdo, PMp, PMsk	bioturbation lamination	*Nummulites* *Operculina* *Discocyclina* bivalves	**Middle-ramp** Lower-energy setting, below FWWB with some storm reworking
Mudstone FA **P5**	wackestone mudstone marl PWdo, PSorg, marl	lamination bioturbation	*Operculina* *Discocyclina* organics bivalves	**Outer-ramp / basin** Low-energy setting. Increasing water depths with alternation between oxic and anoxic conditions

Table 5.2: Facies associations encountered in the Nummulitic Limestone of Haute Provence showing microfacies encountered, sedimentary structures, bioclast content and environment of deposition.

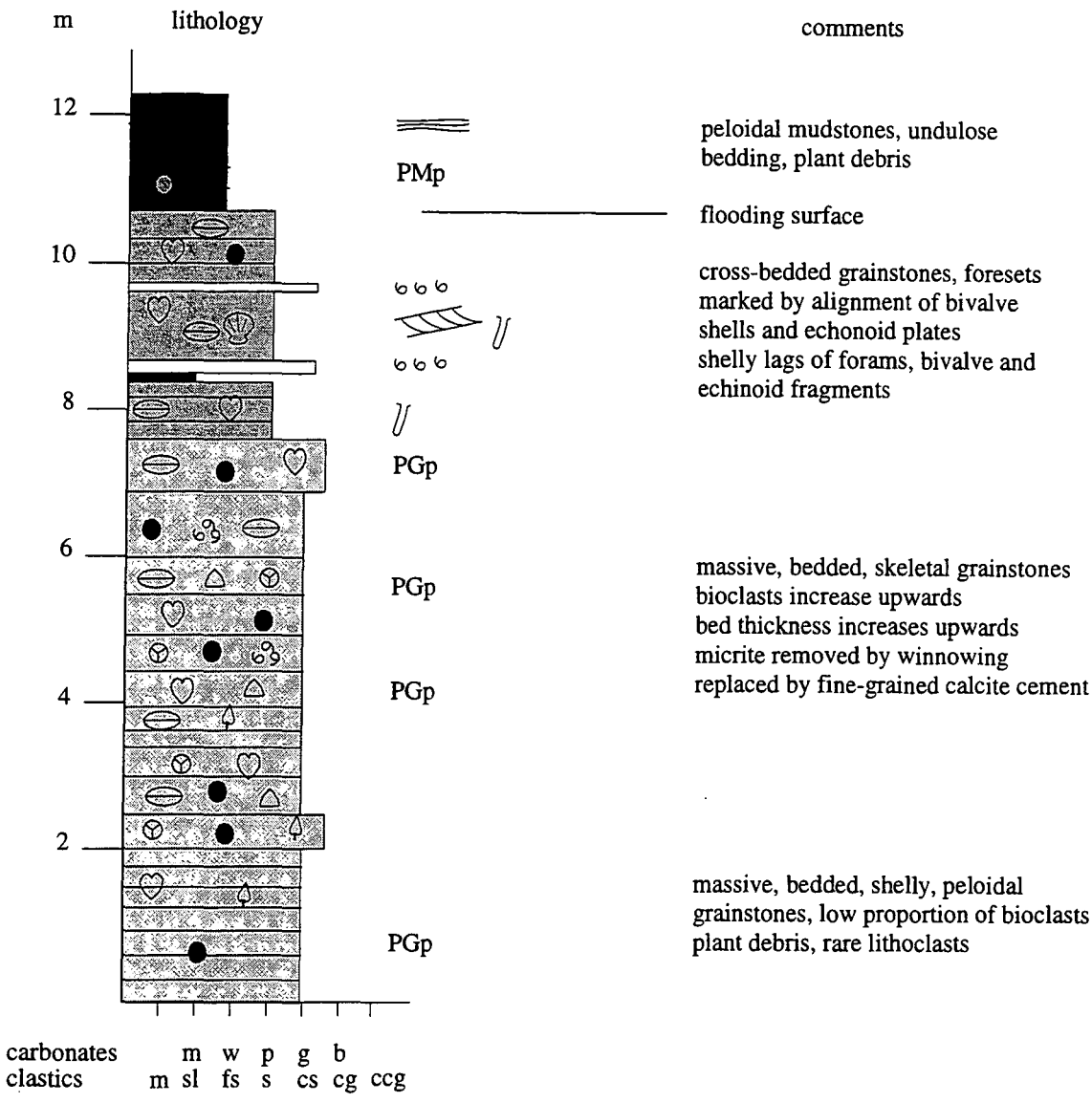

Fig. 5.20: Sedimentary log at Collongues (St Antonin Syncline) showing the development of the peloidal facies association (P1) deposited on the shallow inner-ramp. The sediments have been winnowed and cross-bedding is developed. Bedding thickens upwards. The succession terminates with a flooding surface overlain by calcareous mudstones rich in plant debris.

of the cross-bedded units are marked by reddening or an alignment of echinoid plates and/or flat foraminifera (Fig. 5.21).

The grainstones generally lack fossils, and the wackestones and mudstones contain a limited foraminiferal assemblage. Local accumulations of echinoid plates, serpulids or *Nummulites* may occur, though generally these fossils are uncommon.

As has been discussed in Section 5.4, the peloidal nature of the sediments indicates a shallow-water, inner-ramp setting. Peloids usually form in low energy areas, but, due to their small size, they can be easily transported to higher energy settings (Flügel, 1982), and they have been described from Recent sediments in the Bahamas, occurring in waters of 2-6m depth. This would explain the general lack of rotaline foraminifera seen in the purer peloidal grainstone facies, as these depths

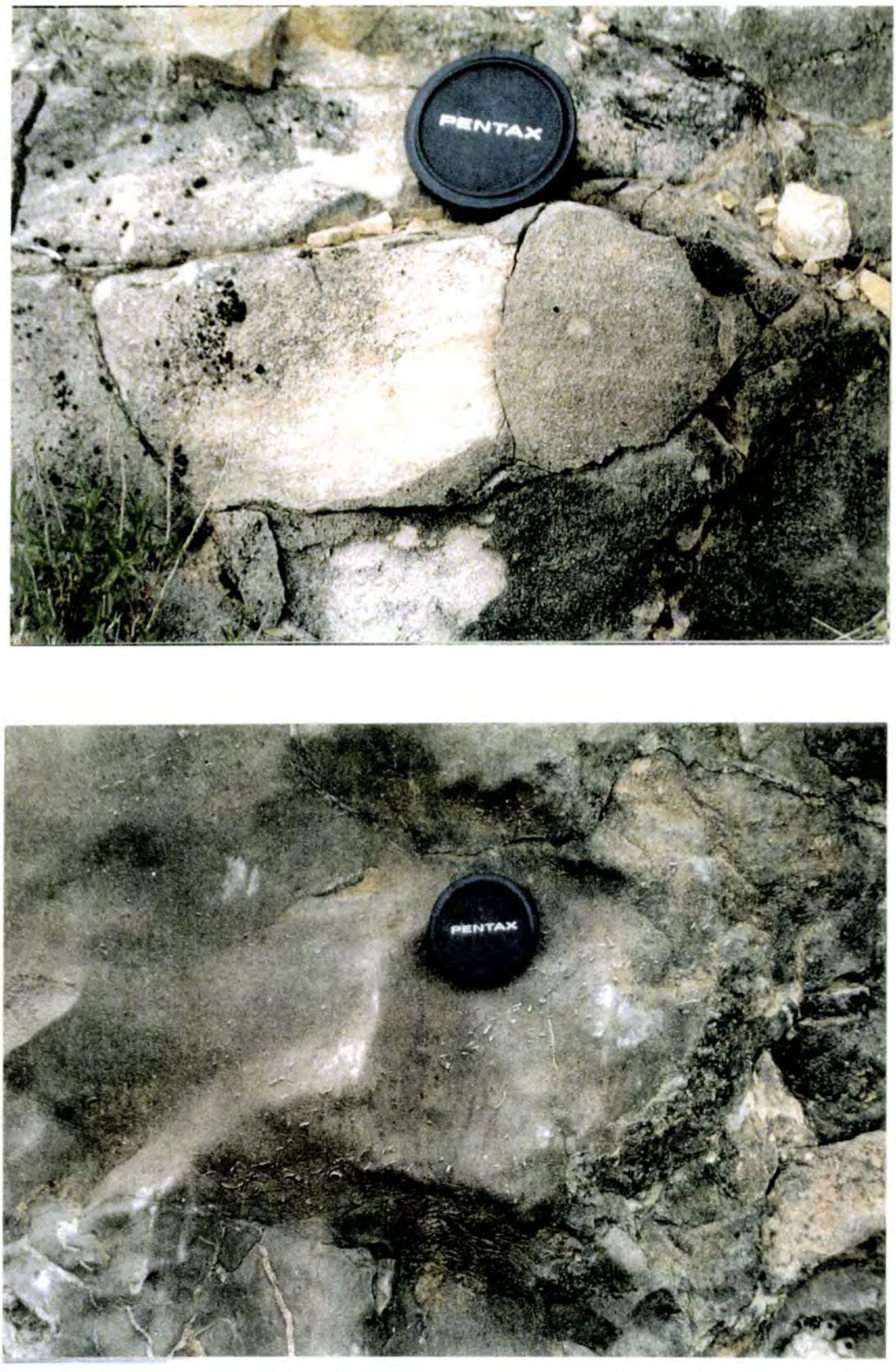

Fig. 5.21: Field photographs showing cross-bedding in the peloidal facies association at Collongues. The bedding planes and foresets are marked by the alignment of echinoid plates or reddening.

would have a high intensity of light radiation which is harmful to the organism and its algal symbionts (Hallock and Glenn, 1986).

The shallowest-water facies are represented by the peloidal grainstones (PGp), where bioclasts are present only as abraded detritus and wave action has removed all the fine micrite from the sediment. Slightly deeper conditions are marked by the appearance of low proportions of small, robust rotaline foraminifera, dominated by *Nummulites* and Orbitolinids (PGpf). Lower energy conditions are uncommon and are represented by the occurrence of peloidal and skeletal mudstones, where the fine grained matrix of the sediment has been preserved. These lower energy facies occur above the main peloidal grainstone deposits and represent either an increase in water depth or continued shallow-water conditions protected from wave action by relief built up by the grainstone accumulations. However, in the field there is no evidence for such relief and so the mudstones are interpreted as representing the termination of the peloidal facies by an increase in water depth allowing the proliferation of the foraminiferal assemblage and a transition to the nummulite bank facies association.

5.4.2. P2: Nummulitic Facies Association (PPn, PPGnm, PWf)

This facies association is characterised by monospecific accumulations of *Nummulites*. Both A- and B-forms are present, but there is a greater abundance of the smaller, megalospheric A-forms. The succession is dominated by *Nummulites*-rich packstones and grainstones with some wackestones and rare mudstones (Fig. 5.22).

In the field, the main body of the unit is represented by thick, massive beds of *Nummulites*-rich packstones and grainstones, with bed thicknesses generally of 1 to 2m. The beds may have slightly erosive bases and crude, large-scale cross-bedding may be evident, as is seen at Col du Fa and Collongues. The main body of the unit passes into Miliolid-rich grainstones (PPGnm), skeletal mudstones (PMsk) or foraminifera wackestones (PWf). Peloids may also be present within these microfacies.

The domination of the assemblage by A-forms could represent a "winnowed lag" due to the removal of the smaller A-forms from a higher energy zone. However, the general small size of the foraminifera leads to similar transport velocities for both A- and B-forms of 18-34 cms^{-1} (Aigner, 1983) and so the high energy residual build-ups dominated by the larger B-forms and the corresponding allochthonous lags of transported A-forms as described from Oman and Egypt (Racey, 1990; Aigner, 1984) may not occur.

The presence of cross-bedding and the dominance of high energy fabrics shows that the sediment has been reworked by marine currents. This has probably occurred *in situ* as the state of preservation of the nummulite tests suggests that they

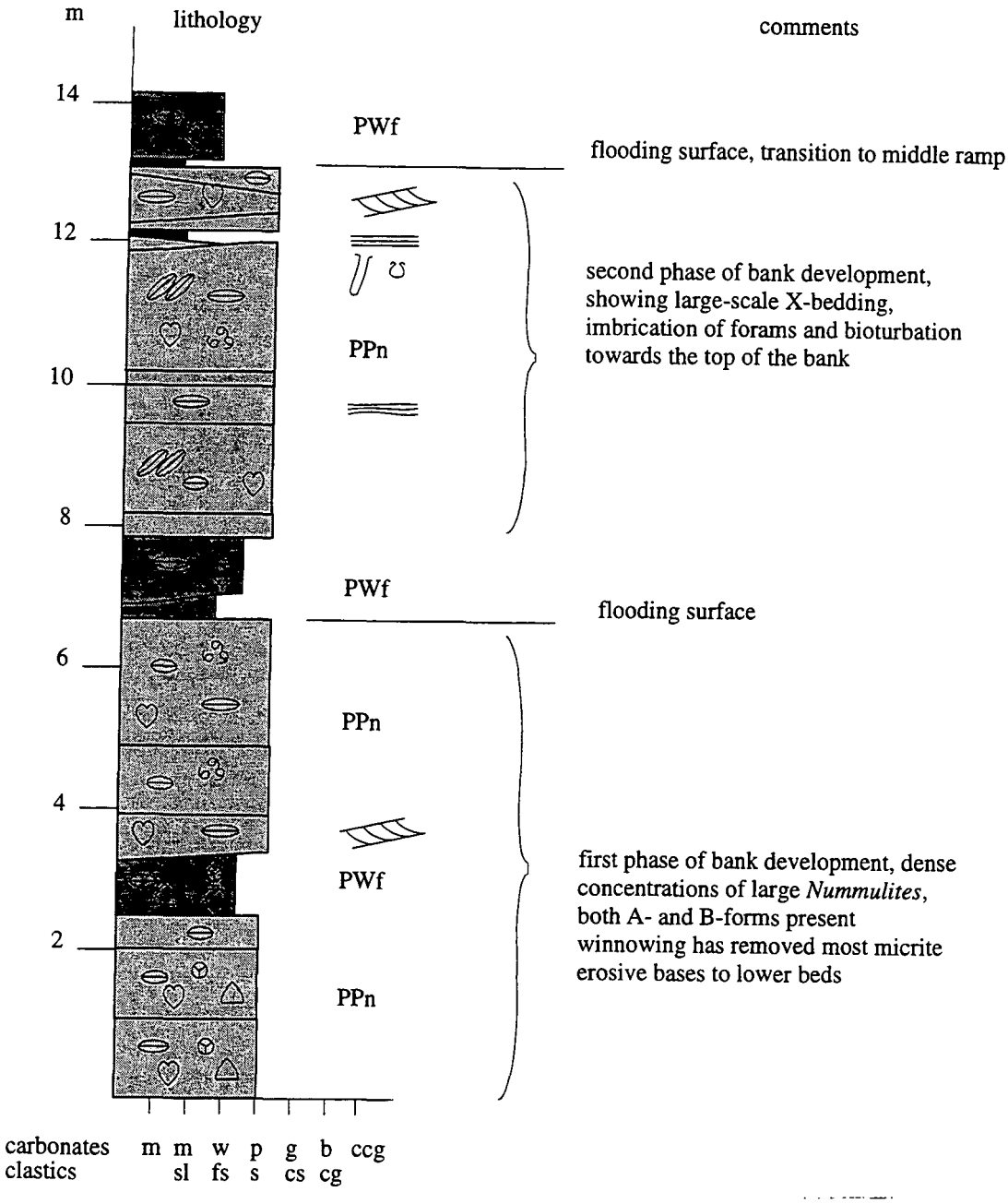

Fig. 5.22: Sedimentary log at Col du Fa (Annot Syncline) showing the nummulitic facies association (P2) representing two main phases of nummulite bank development on the inner-ramp. The body of the bank is represented by nummulite packstones with some large-scale cross-bedding and imbrication of the bioclasts due to current reworking. Towards the top of the second bank succession, cross-bedding becomes more developed suggesting that the bank had built up into higher-energy waters.

have not undergone transportation (also indicating that this is not an allochthonous A-form deposit). This *in situ* reworking has merely removed most of the fines and fragmented the more fragile bioclasts (breaking up echinoids into individual plates). The currents have reoriented the bioclasts producing a chaotic imbrication of the nummulite tests, which has been attributed to oscillatory currents (Aigner, 1983; Racey, 1990). Bioturbation also produces a realignment of the bioclasts, though the

two processes are generally distinguishable in the field due to the localised extent of individual burrows.

Though current reworking does occur, it is not to the same extent as occurs in the nummulite build-ups described by the above workers, as none of the sedimentary structures due to continual reworking they have described (scour and fill, erosive pockets, firmgrounds, ripples) are present. This suggests that reworking in the nummulite facies association was of lower energies, which would be possible due to the small size of the foraminifera compared with those typical of the nummulite accumulations in the literature. Intermittent low-energy periods lead to the boring of bioclasts, especially echinoid plates, and the settling out of organic debris along laminae, producing mudstones and wackestones.

This facies association may show a repetition of the nummulite bank, separated by lower energy back-bank facies. This facies association generally directly overlies the erosional unconformity above the Mesozoic substratum, suggesting that the nummulite banks were deposited at the onset of the marine transgression in the basin, though where the peloidal facies association is present the nummulite accumulations overlie this. They pass up into the middle-ramp facies association described below.

5.4.3. P3: Algal Facies Association (PPGfa, PWfa)

This facies association (Fig. 5.23) is localised to the Agnère Syncline and is only represented by the Pont Noir section.

The facies association is similar to that observed in Haute Savoie limestones (Section 4.5.2), in that it is characterised by the presence of abundant CRA, which are not observed elsewhere in the Provence field area, which develop boundstones with corals and encrusting foraminifera (not identified).

There is an up-section transition from the intermediate foraminifera dominated packstones and wackestones into sediments with an increasing abundance of CRA, forming crusts and rhodoliths, and also associated encrusting foraminifera, corals and serpulids.

This change in benthos is thought to represent the transition from middle-ramp foraminiferal limestones to the inner-ramp, with the shallowest ramp positions represented by algal boundstone development. The algal-rich facies again lack a distinct framework, and are interpreted as an algal shoal or rhodolith gravel produced by the accumulation of rhodoliths in a shallow-water setting, above FWWB, with sufficient wave agitation to turn the rhodoliths and remove much of the fine sediment.

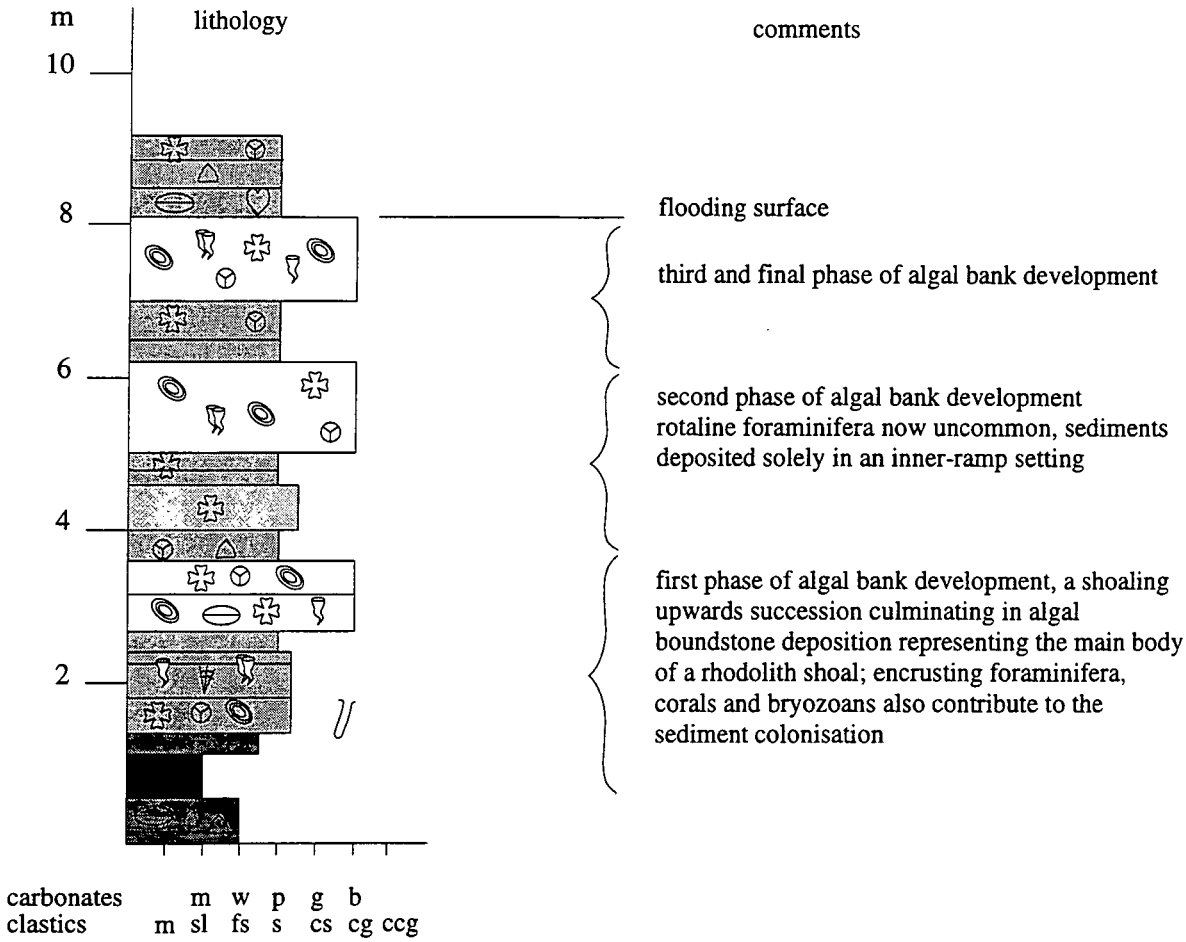

Fig. 5.23: Sedimentary log at Pont Noir (Agnère Syncline) showing the development of the algal facies association (P3), similar to that encountered in Haute Savoie and deposited in an inner-ramp setting. Three phases of algal shoal development have occurred, each shallowing-upwards cycle representing the main body of a rhodolith shoal.

5.4.4. P4: Foraminiferal Facies Association (PWGf, PWPf, PWpf, PWp, PWdo, PMp, PMsk)

This facies association is dominated mud-rich facies dominated by wackestones and mudstones (Fig. 5.24). All the microfacies contain relatively abundant foraminifera which change in character according to the water depth (see Chapter 2). Where the peloidal facies are present at the base of the formation, the occurrence of peloids generally persists throughout the succession (PWpf, PWp, PMp).

This facies association is interpreted to represent middle-ramp sedimentation with the lack of winnowing (c.f. inner-ramp facies associations) indicating a position below FWWB. However, the sediments are generally reworked by bioturbation producing concentration and some alignment of the bioclasts. The sediments show a variation in the foraminifera assemblage with increasing depth from facies dominated by robust *Nummulites, Amphistegina* and Orbitolinids in the upper middle-ramp, to wackestones and mudstones containing large, flat *Discocyclina* and *Operculina* in

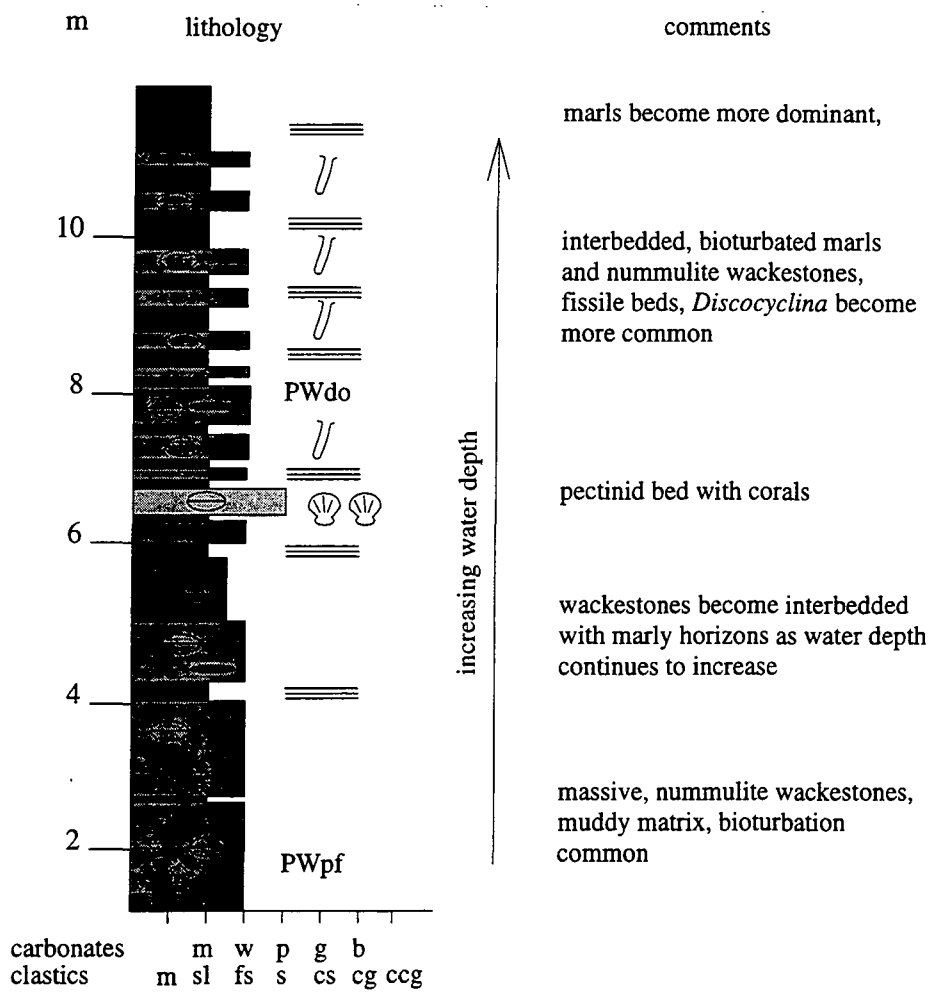

Fig. 5.24: Sedimentary log measured on the hanging wall of the Rouaine Fault near St Benoit (Annot Syncline) showing the foraminiferal facies association which was deposited in a middle-ramp setting. The facies are dominated by foraminiferal wackestones and mudstones, with the proportion of mudstones increasing with water depth. Bivalve accumulations may occur, possibly indicating a decrease in sedimentation rate.

deeper waters. The lower middle-ramp may also have accumulations of Discocyclinids, producing marly packstones containing chaotic stacking indicative of storm reworking.

5.4.5. P5: Mudstone Facies Association (PWdo, PSorg, marl)

This facies association is dominated by mudstone and marl sedimentation (Figs 5.25, 5.26) with a low diversity benthonic assemblage and an increase in the proportion of argillaceous and quartzitic detritus. Bioclasts include organic debris, deep water foraminifera (large, flat *Discocyclina*, *Operculina*), bivalves and skeletal debris. Bioturbation may occur.

The facies association is interpreted to represent outer-ramp deposition, in the greatest water depths encountered in the formation. The foraminiferal wackestones of the lower middle ramp (PWdo) become interbedded with fissile, argillaceous

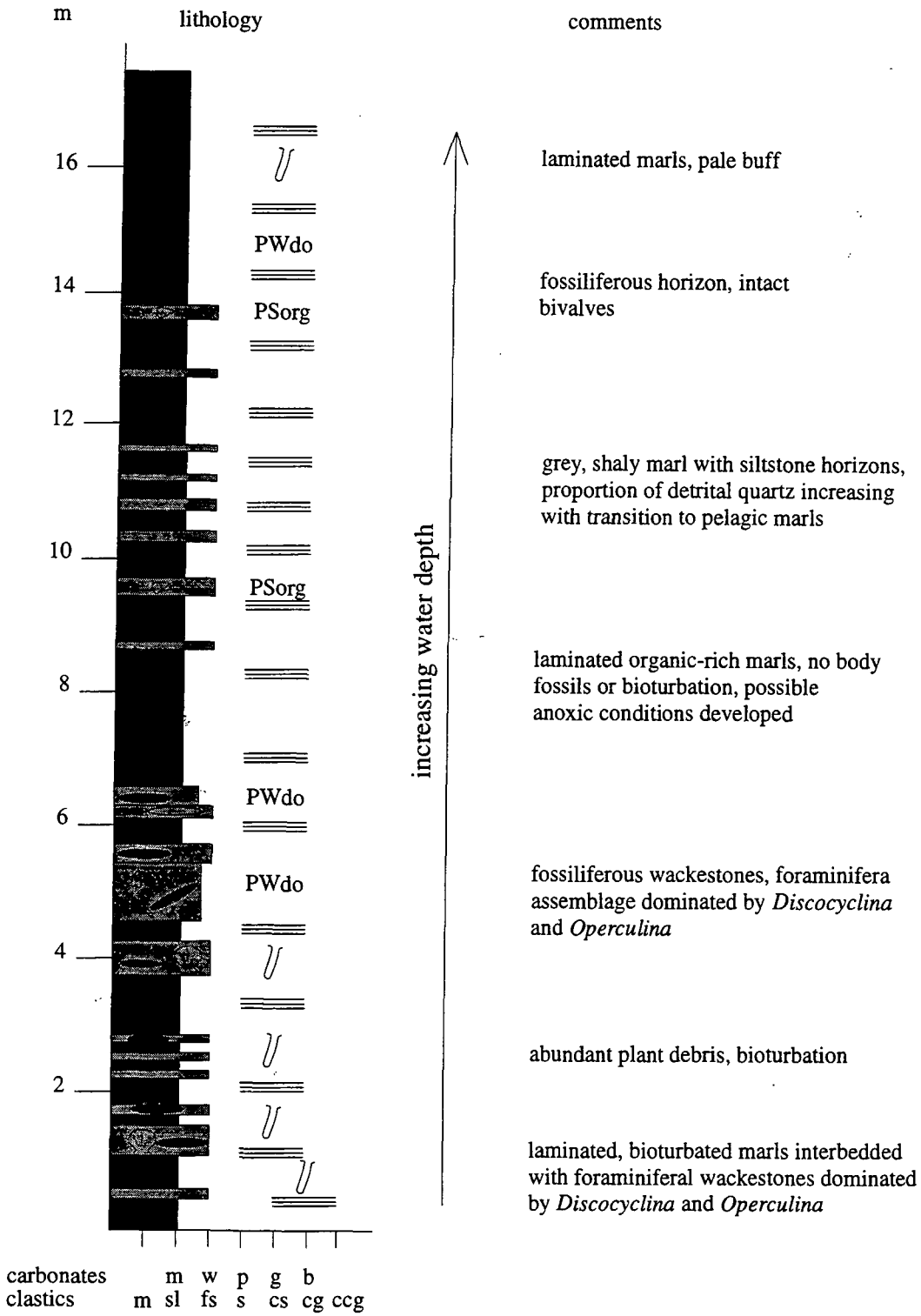

Fig. 5.25: Sedimentary log at La Rochette (St Antonin Syncline) showing the transition from the outer-ramp mudstone facies association (P5) to the overlying Globigerina Marl. The outer-ramp is represented by mudstone and wackestone interbeds. The fauna is of a low diversity and is dominated by large, flat Discocyclina and Operculina with abundant bioturbation and bivalve horizons. Intervals enriched in organics and with no bioturbation occur, which may indicate periods of stagnation as the water depths increased.

mudstones and siltstones and the proportion of bioclasts decreases as the water depths increase. As the water continues to deepen anoxic conditions may occur indicated by an abundance of organic debris and a complete lack of body fossils and bioturbation. The facies association passes up into the pelagic Globigerina Marl as the carbonate ramp is flooded.

Fig. 5.26: Interbedded marls and wackestones of the outer ramp facies association at La Rochette deposited during the final drowning of the carbonate ramp.

5.5. Depositional Model

The Nummulitic Limestone in Haute Provence again represents deposition on a carbonate ramp dominated by larger benthonic foraminifera (Fig. 5.27). Unlike Haute Savoie, however, coralline red algae are very rare leading to a difference in the facies encountered. The ramp can be divided into inner-, middle- and outer-ramp settings based on the sediment textures and benthonic foraminiferal palaeoecology (Chapter 2).

The inner ramp is dominated by relatively high-energy deposition occurring above or around FWWB and is represented by the development of bioclast shoals, which are thought to have formed low relief, discontinuous features, that proliferated over structural highs in the basin. The facies are dominated by pack- and grainstones with rare mud- and wackestones deposited in the sheltered inter-shoal areas. Three distinct bioclast associations are encountered, representing different relative water

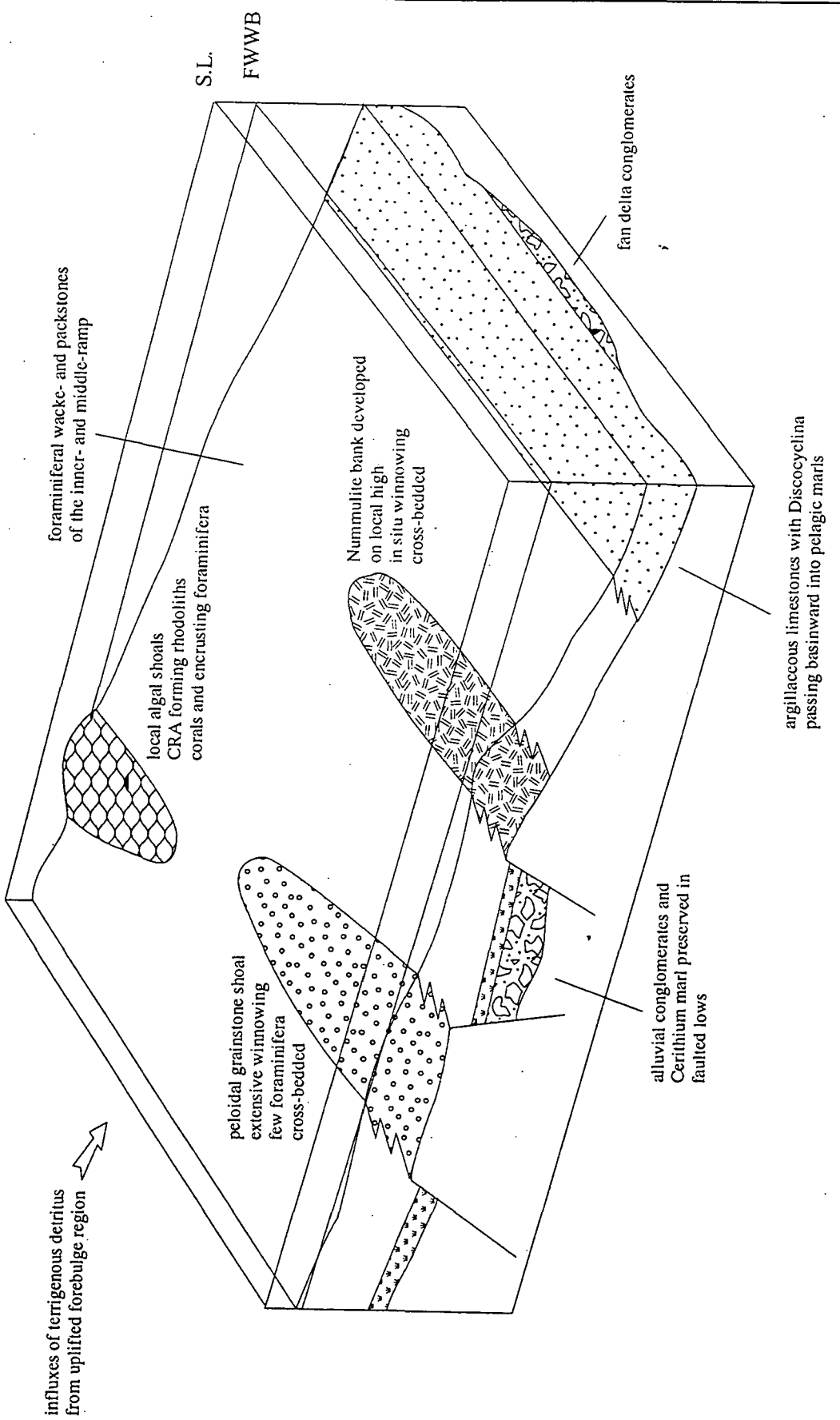

Fig. 5.27: Depositional model of the Nummulitic Limestone in Haute Provence based on measured sections, showing the bioclast shoals dominating the inner-ramp and depositional highs, passing into the packstones and wackestones of the middle-ramp and the mudstones and marls of the outer-ramp and basin.

depths. Grainstones dominated by peloids and skeletal debris with rare foraminifera (facies association P1) are deposited in the shallowest waters, with the total removal of micrite by wave action producing a grainstone texture. Deeper waters are dominated by the development of monospecific accumulations of *Nummulites* (P2) or coralline red algae, corals and encrusting foraminifera (P3) which were deposited around FWWB, with some micrite being preserved. The latter, algal facies association is rare, only occurring at one locality in the study area (Pont Noir).

The middle-ramp (facies association P4) is dominated by wackestones and was deposited below FWWB. There was an active benthos producing abundant bioturbation and the dominant bioclasts preserved are benthonic foraminifera. The shape and nature of the foraminifera vary with relative water depth, with the upper middle-ramp dominated by robust *Nummulites* with *Amphistegina* and Orbitolinids, passing into the lower middle-ramp wackestones containing flat *Discocyclina* and *Operculina*. Local packstones are thought to be the result of storm reworking, but Discocyclinid accumulations as seen in Haute Savoie (Section 4.5.3.a) are not developed.

The outer-ramp is represented by facies association P5, which is dominated by laminated, argillaceous, silty mudstones and marl. The low proportion of bioclasts is dominated by *Discocyclina* and *Operculina* with local wackestones developed, and the sediments are commonly bioturbated. Local anoxic conditions developed, represented by organic-rich silts and marls, devoid of bioclasts and bioturbation. The sediments grade into the marl, which represents the final flooding of the carbonate ramp due to accelerating flexural subsidence (Chapter 7).

Chapter 6

Basal Unconformity

6.1. Introduction

The basal unconformity of the Nummulitique Formation separates the Mesozoic passive margin succession from the foreland basin fill and marks a major phase of uplift and erosion prior to the development of the foreland basin. This chapter deals with the nature of the unconformity as observed in the field in Haute Savoie and Haute Provence, and proposes possible mechanisms for its formation.

6.2. Nature of the Unconformity

The basal unconformity is an irregular surface with local relief that developed prior to the deposition of the Nummulitique. This section describes its characteristics and the processes involved in its generation.

6.2.1. Haute Savoie

In Haute Savoie the unconformity generally occurs above Senonian micrites, though locally greensand (La Communaille), black mudrocks (Mont Durand, north side) or even the Urgonian (Mont Durand, south side; Charollais et al., 1977) may be exposed as the substratum. Thus a varying depth of erosion is represented by the unconformity.

In the Thônes Syncline, the unconformity is directly overlain by the marine Nummulitic Limestone (Chapter 4). The unconformity is generally a planar erosion surface with an overlying breccio-conglomerate lag up to 20 cm thick which contains clasts of the substratum and was described in more detail in Section 4.3.1.

The unconformity is commonly identified by the stark contrast between the thinly bedded, pale Senonian micrites and the darker, massive, overlying Nummulitic Limestones, which is particularly evident at La Place, near Le Chinaillon (Fig. 6.1). This outcrop clearly shows the planar nature of the erosion surface and also the very low angle of discordance. Immediately below the erosion surface, there appears to be a thin zone of leaching extending for about 50cm into the Senonian. This was impossible to sample due to the steep quarry face, but is thought to have been generated during the development of the unconformity.

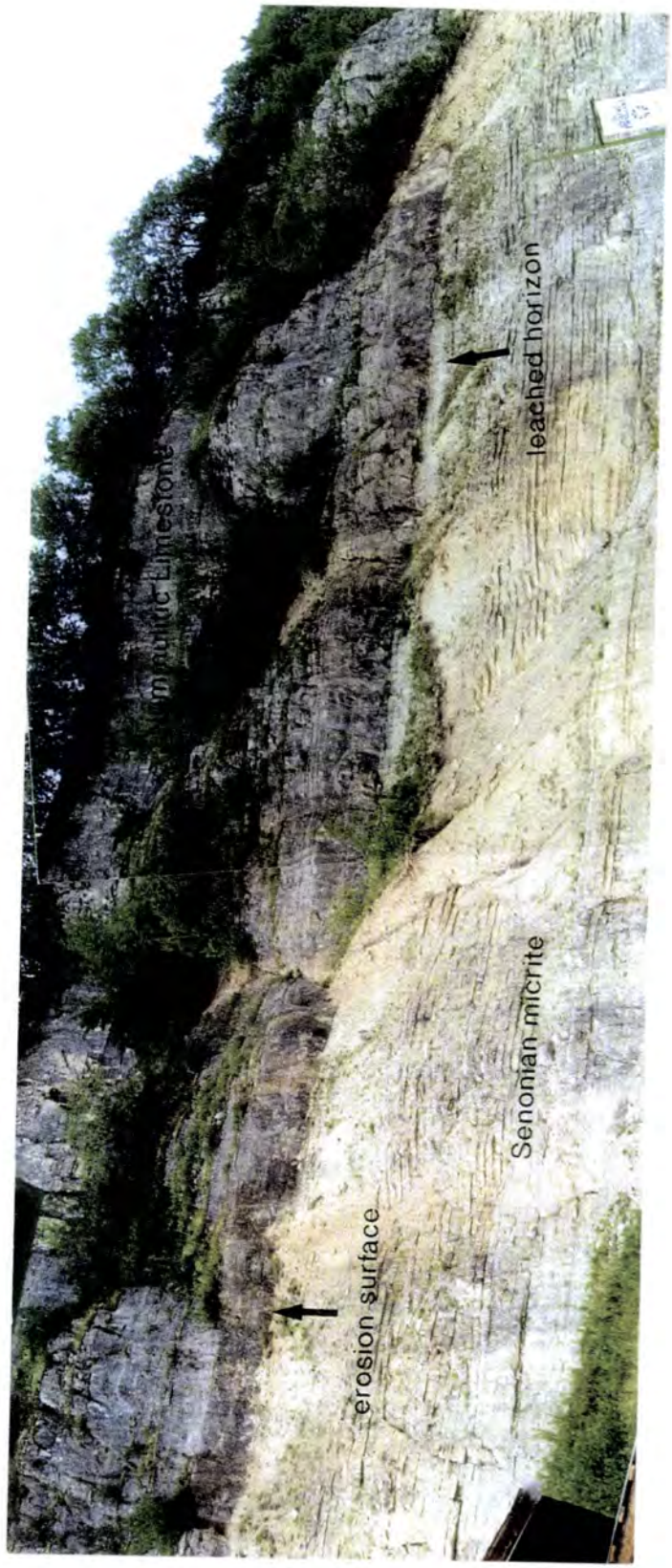

Fig. 6.1: The basal unconformity exposed at La Place, between thinly-bedded Senonian micrites and the more massive Nummulitic Limestone. The unconformity here is planar and there is no marked angular discordance. Note the thin leaching zone directly beneath the contact. Quarry 15m high.

Elsewhere a palaeokarst may be preserved (Le Chinaillon, Col de la Colombière) with dissolution fissures extending into the substratum to a maximum depth of 20cm. These are infilled with a lithic quartzitic wackestone containing a marine fauna (microfacies SWq). The karst surface is irregular (Fig. 6.2), and the relief is infilled with a breccio-conglomerate (microfacies SCG) which contains reddened clasts of the substratum.

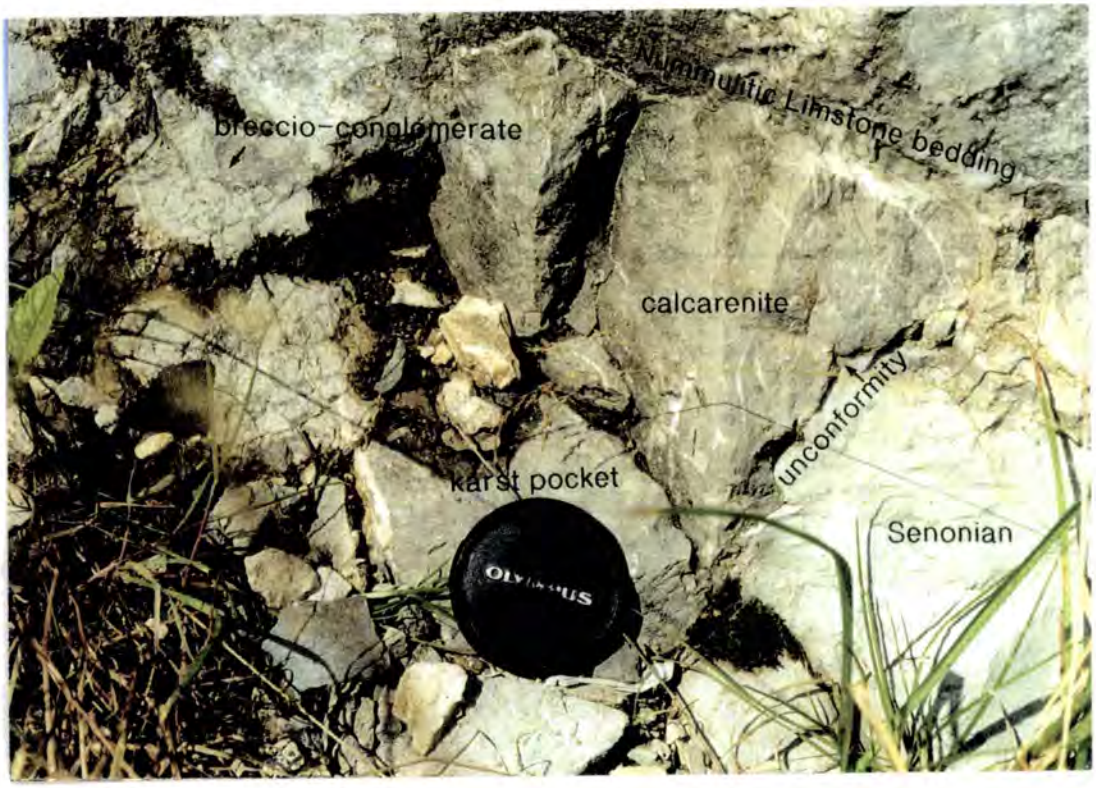

Fig. 6.2: Palaeokarst developed at the unconformity exposed at Le Chinaillon. The surface of the Senonian is irregular and infilled by breccio-conglomerate and marine calcarenites. Scale=5cm.

Borings occur on the erosion surface and bored clasts are present in the overlying breccio-conglomerate (Fig. 6.3).

On the Massif de Platé, the unconformity may be overlain by either the Nummulitic Limestone or the terrestrial and marginal marine sediments of the Infranummulitique (Chapter 3). On the Desert de Platé, near Les Grandes Platières, the Infranummulitique can be seen to pinch out against topography developed on the unconformity, and locally appears to cut into the underlying Senonian (Fig. 6.4). The top of the Senonian has been locally reworked by *Microcodium* (Pairis and Pairis, 1975), which is also present in the lower beds of the overlying facies, indicating subaerial conditions (Esteban and Klappa, 1983).

The unconformity has a low degree of angular discordance, with the Senonian and Nummulitique bedding surfaces subparallel, though locally a distinct angular

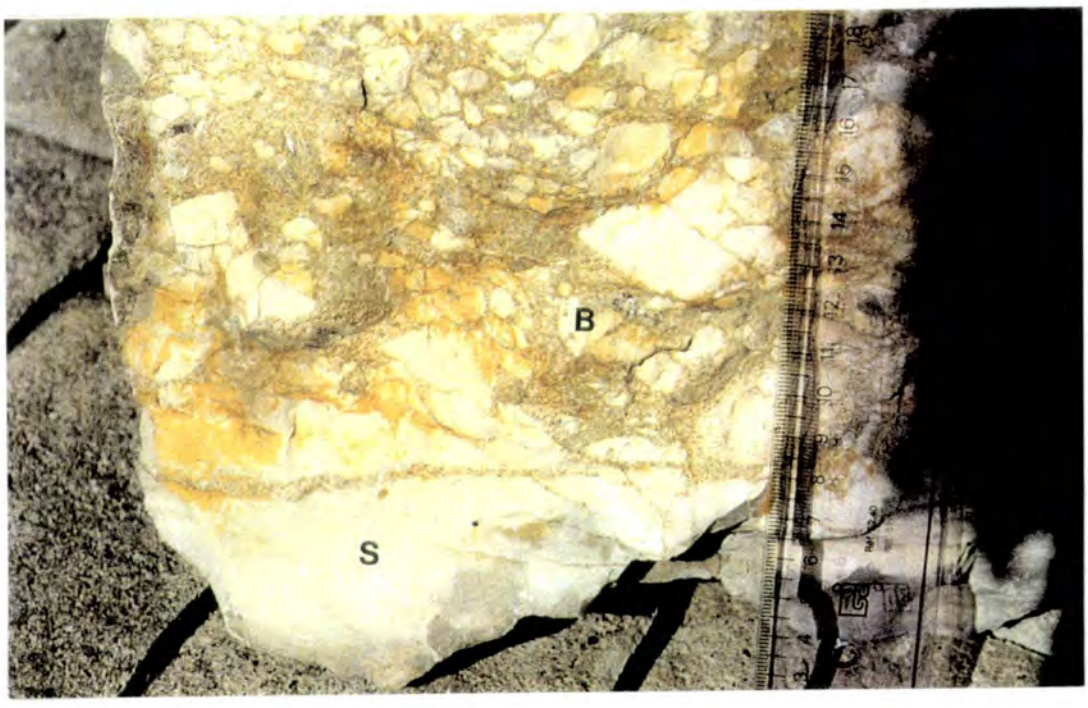

Fig. 6.3: Boulder from the unconformity showing the dissolution and infill of karst fissures in the Senonian with the overlying breccio-conglomerate. Reddened clasts and karst development indicate subaerial exposure, while borings on the clasts indicate a period of marine reworking prior to the onset of sedimentation.

Fig. 6.4: Contact between the Senonian micrites and the Infranummulitique conglomerates on the Desert de Platé showing the irregularity of the erosion surface beneath the conglomeratic channels.

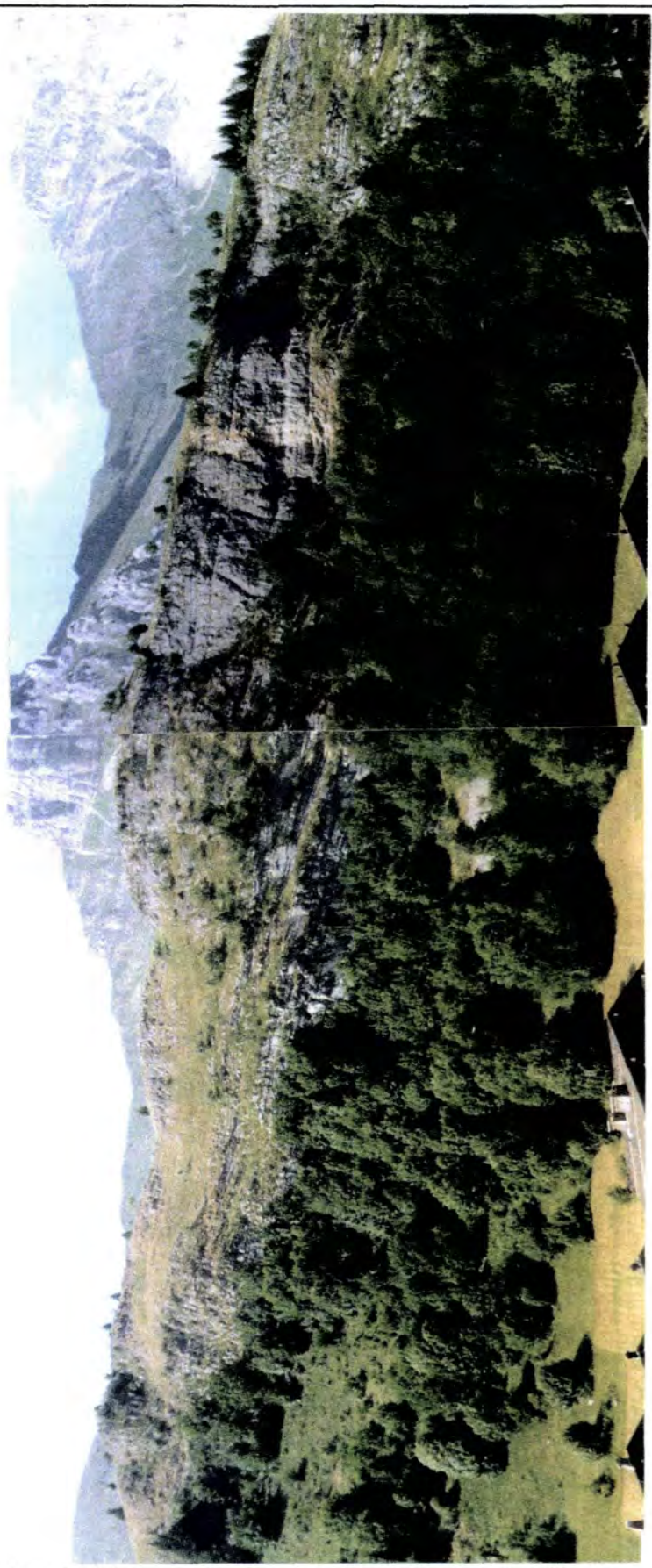

Fig. 6.5: Photograph of the unconformity exposed in cliffs above Le Chinaillon, showing the varying angular discordance produced by local folding of the Senonian micrites. Nummulitic Limestone=60m thick.

discordance may occur due to local folding of the substratum (Fig. 6.5) prior to the Tertiary transgression (Le Chinaillon, Flaine).

The degree of erosion of the substratum and existence of local palaeokarst features and reddened clasts indicates that the development of the unconformity was dominantly due to subaerial exposure. The relief of a karst surface is dependent on the elevation of the erosion surface above base-level (here sea-level) and the time of exposure of the substratum to dissolution processes (Choquette and James, 1988). The low relief present on the unconformity reflects a low elevation and short exposure time providing all the karst features are preserved. However, the removal of a significant amount of the Mesozoic succession indicates that exposure was fairly prolonged which suggests that some of the karst profile has been removed, possibly during a subsequent period of marine erosion (Crampton, 1992), during which the erosion surface was bored. The removal of karst appears to have gone to completion on depositional highs where no karst is present (Tête de la Sallaz) as it is unlikely, given the uniform nature of the substratum, that none was developed.

On the Massif de Platé, the erosion of the substratum beneath the Infranummulitique is interpreted to have been modified by channels cutting into the substratum during the deposition of the sheet conglomerate and *Microcodium* wackestone facies. Again, no karst is evident, and may have been planed off by the abrasive action of the conglomeratic bedload of the channels.

6.2.2. Haute Provence

The unconformity in Provence exhibits a greater topographic relief and a more variable degree of angularity due to the local development of kink folds (Hamiti, 1994; Apps, 1987). The unconformity is overlain by either the Infranummulitique or the Nummulitic Limestone. Where the Infranummulitique is present, relief can be seen on the basal erosion surface which appears to control the distribution of the Infranummulitique (Fig. 6.6). This can be seen at Peyresq, where the massive conglomerates thin and terminate against an inherent topography which does not affect the overlying limestones. Previous workers (Apps, 1987; Hamiti, 1994) have attributed this topography to be partly due to the effects of folding and/or faulting developed prior to the onset of sedimentation. The erosion surface beneath the conglomerates is locally planar (Fig. 6.7) and is thought to have undergone scouring during the transport and deposition of the conglomerates, reworking *Microcodium* fragments.

Where the unconformity is overlain by the Nummulitic Limestone, a thin conglomeratic lag is present and there is a low-angle discordance between the Senonian substratum and the Tertiary sediments. A gentle topography may be

Fig. 6.6: Conglomerate cliffs of the Infranummulitique exposed near Peyresq. The distribution of the conglomerates is controlled by topography on the unconformity surface, filling depositional lows and thinning over the corresponding highs. Cliffs=40m high.

Fig. 6.7: Basal contact of the conglomerates at Peyresq showing the planar surface of the unconformity. Scale=1m.

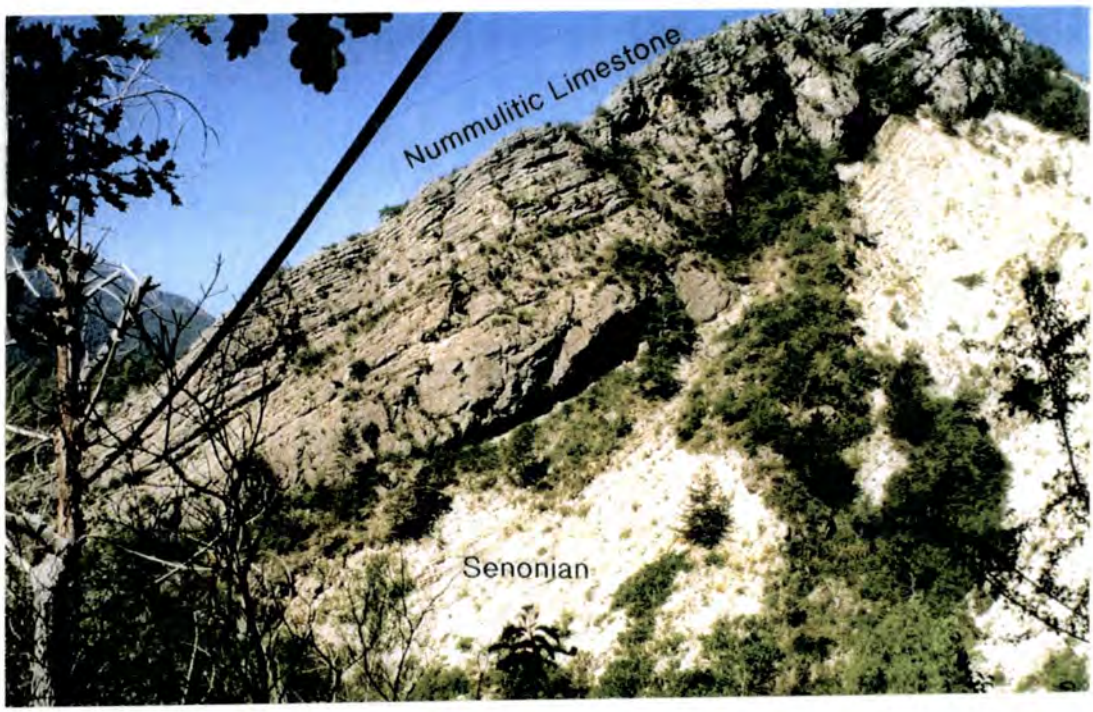

Fig. 6.8: Unconformity at Puget-Theniers between Senonian marls and the Nummulitic Limestone showing the gentle topography due to folding infilled with the overlying marine beds. Nummulitic Limestone approximately 20m thick.

developed, infilled by the basal Nummulitic Limestone (Fig. 6.8).

Due to the degree of erosion of the substratum and the development of a pronounced topography on the erosion surface, the unconformity is thought to have developed dominantly under subaerial conditions though direct evidence for this is sparse. Karst development is uncommon and equivocal; local sharp relief is present on the erosion surface (Fig. 6.9) which may represent a preserved karst surface, though this is not certain.

Fig. 6.9: Erosional relief on the unconformity between fissile Senonian marls and the Nummulitic Limestone. This unusual sharp relief may be the remnants of a palaeokarst. Depressions are infilled with a breccio-conglomerate. Scale=40m.

However, the overlying Infranummulitique contains reddened clasts and matrix, *Microcodium* crusts and reworked *Microcodium* occurs in the basal beds of marginal marine facies (Chapter 3) indicating deposition under terrestrial conditions. This

suggests that the unconformity was also likely to have developed due to subaerial erosion, producing coarse detritus redeposited as the conglomeratic facies. The lack of karst in the area is thought to be due to the fissile nature of the Senonian marls in the area, which would tend to erode friably rather than developing karst fissures through dissolution.

Evidence of marine reworking is more common, with boring of the erosion surface (Fig. 6.10) and of clasts in the overlying conglomerate, and further erosion may have occurred in the swash zone during transgression, as the first marine deposits present are offshore shoals.

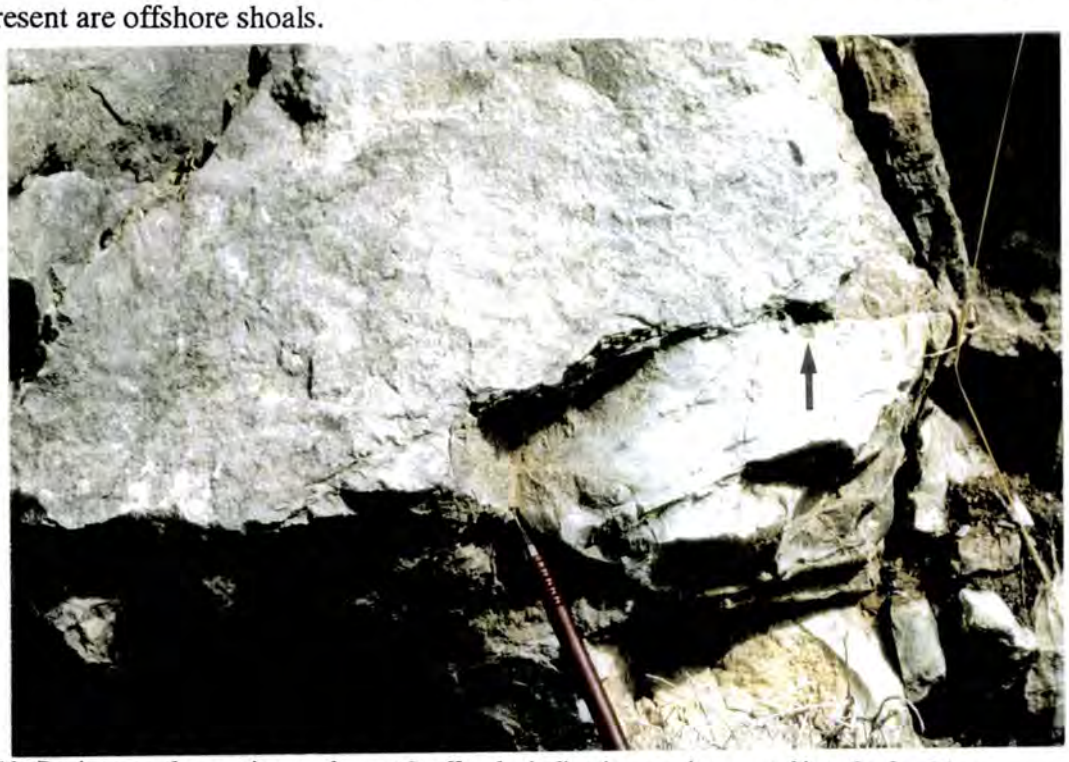

6.10: Borings on the erosion surface at Scaffarels, indicating marine reworking. Scale=14cm.

6.3. Depth of Erosion and the Effects of Pre-existing Structures

In the Alpine foreland basin as a whole, the depth of erosion of the substratum increases from east to west (south-east to north-west in Switzerland) producing an increasing stratigraphic gap towards the foreland, with progressively younger Tertiary formations overlying progressively older Mesozoic passive margin sediments (Herb, 1988; Bodelle, 1971) as the focus of erosion and sedimentation migrates over the foreland (Fig. 6.11).

The youngest Mesozoic sediments, of Upper Maastrichtian age, occur in eastern Switzerland and are overlain by Lower Eocene (Ypresian) sediments, representing a stratigraphic gap of only 15 Ma (Lihou, 1995). In the Franco-Italian

Alps, the Tertiary (Lower to Middle Eocene) overlies Campanian sediments (25-40 Ma gap; Campredon, 1977), whereas further west, in the study area around Annot and Entrevaux, Middle to Upper Eocene sediments overlie the Lower Santonian (41-48 Ma gap; Campredon, 1977; Bodelle, 1971). Still further west, around Barrême, the substratum is eroded down to the Apto-Albian to Neocomian, with the unconformity representing an increased stratigraphic gap of 60-100 Ma (Bodelle, 1971). In Haute Savoie, the stratigraphic gap is more constant, with a Priabonian succession overlying a Lower Senonian substratum (35-43 Ma gap; Chaplet, 1989).

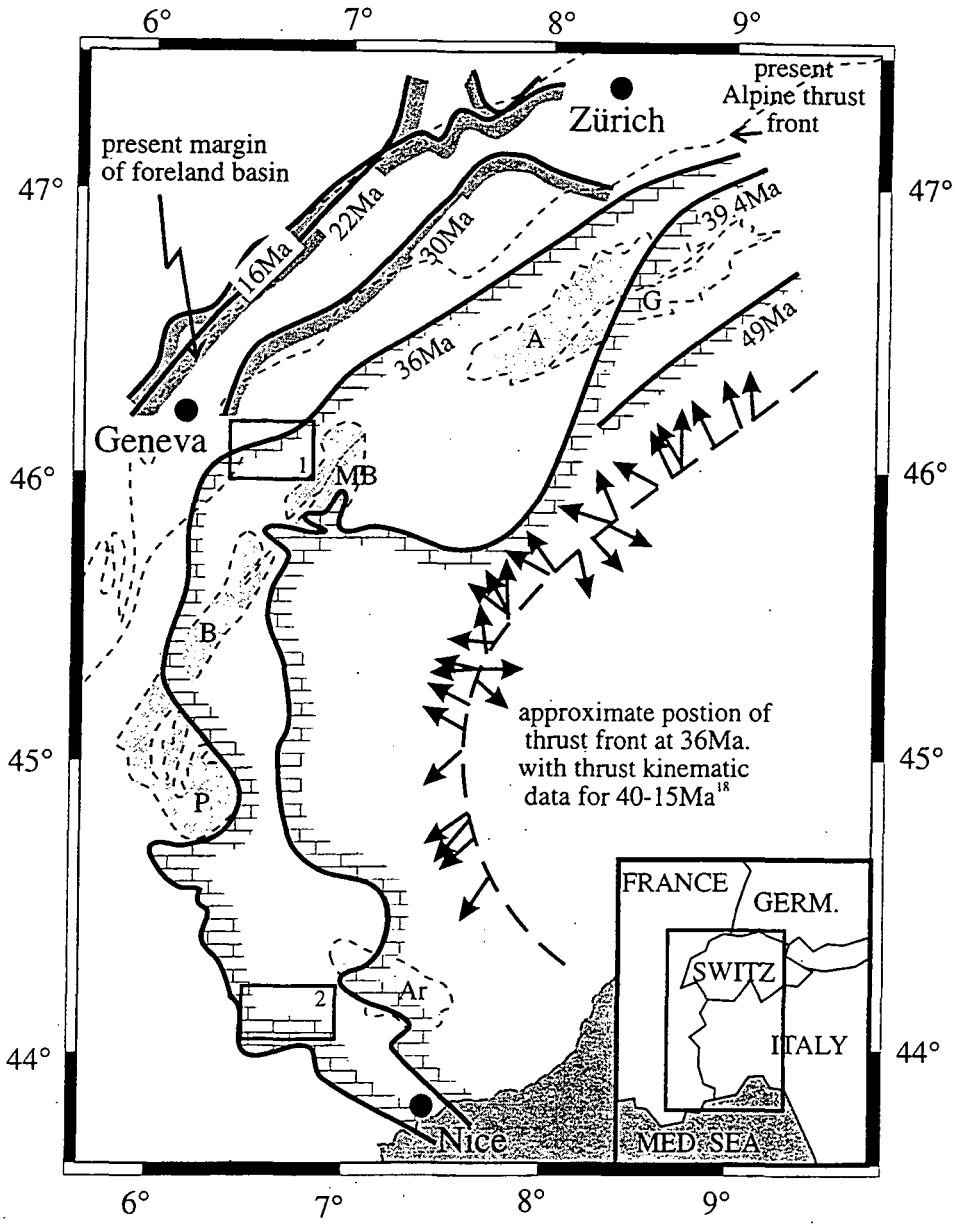

Fig. 6.11: Reconstruction of the position of the Nummulitique which marks the migration of the cratonic margin of the basin over the foreland as the Alpine orogenic wedge advanced. The two field areas are shown: 1) Haute Savoie, 2) Haute Provence. Adapted from Sinclair (in press).

The increasing stratigraphic gap towards the foreland is a common feature seen around the whole of the Alpine Foreland Basin. In Western Switzerland, this phenomenon may be explained by a thinning of the Mesozoic passive margin succession towards the north (Crampton, 1992), with a constant level of erosion producing a larger gap in the stratigraphy, though an increasing depth of erosion towards the foreland prior to the Eocene transgression cannot be discounted (Crampton and Allen, 1995; Herb, 1988). In eastern Switzerland, however, the increasing depth of erosion over a short distance cannot be accounted for by a thinning of the Mesozoic formations (Crampton and Allen, 1995). In France the story appears to have been complicated by tectonic events during the Lower Cretaceous and the onset of Pyrenean compression during the Upper Cretaceous producing a more complex Cretaceous stratigraphy, and also due to the pronounced effects of pre-nummulitic tectonism during the Upper Cretaceous/Palaeocene (Section 1.4). This produces local variations in the substratum, seen in the Thônes Syncline at La Communaille and Mont Durand, where it consists of Apto-Albian greensand and black muds and Barremian-Aptian Urgonian limestone (Charollais et al., 1977). This anomaly can be attributed to the effects of post-Upper Cretaceous faulting (Chaplet, 1989) producing local highs with a greater level of erosion, which persisted during the deposition of the Nummulitique producing sites for preferential shoal development (Lateltin and Müller, 1987) with the corresponding lows acting as depocentres for the Infranummulitique (Pairis and Pairis, 1975). Similarly, in Haute Provence, the Nummulitique locally overlies Middle Cretaceous sediments commonly occurring in the hinge area of anticlinal structures or on the limbs of synclines formed during the interaction of Pyrenean and Alpine deformations prior to the Nummulitic transgression and can again be explained by greater levels of erosion occurring over local highs in the substratum as the topography was planed off prior to the Tertiary transgression (Apps, 1987).

6.4. Causes of Erosion

The unconformity was formed during a period of subaerial exposure (karst development, *Microcodium*, palaeosols, terrestrial sediments) that occurred after the deposition of the Senonian formations and prior to the Tertiary transgression, with the corresponding removal of 150->350m of the Cretaceous strata (thickness data from Chaplet, 1989; Trümpy 1980).

6.4.1. Eustatic sea-level fall

A possible mechanism for the development of the basal unconformity is that of eustatic sea-level fall which was postulated by Herb (1988). The substratum over much of the study areas consists of the Mesozoic Seewen Formation and locally the Wang Formation, which represent pelagic deposition in estimated water depths of 100-300m and 100-800m respectively (Wildi et al., 1989; Crampton, 1992). Thus, for subaerial erosion, a eustatic sea-level fall of at least 100m is necessary for even the shallowest sediments to be exposed. The global sea-level curve for the Cenozoic by Haq et al. (1988) documents a fall of 150m during the Palaeocene/Eocene, which would account for this minimum base-level fall. However, the dominance of conglomerates in the terrestrial deposits of Haute Provence indicates the development of a significant relief between the source area and the depocentre, estimated as up to 300m by Apps (1987), though this amount seems somewhat excessive. The eustatic sea-level fall alone, is unlikely to be sufficient to produce this relief. Similarly, a eustatic control does not explain the diachroneity of the transgression, which differs by at least 18Ma between eastern Switzerland and south-eastern France (Lihou, 1995; Weidmann et al., 1991; Bodelle, 1971) and its obliquity with respect to the underlying passive margin in Switzerland.

6.4.2. Forebulge uplift

Another possible explanation for the erosion of the unconformity is the development of an uplifted forebulge region prior to the subsidence of the foreland basin. The development of forebulges (or peripheral bulges) has been described in detail and modelled by a number of workers and has been documented from many foreland basins (Crampton and Allen, 1995; Sinclair et al., 1993; Pigram et al., 1989; Quinlan and Beaumont, 1984; Bradley and Kusky, 1986; Plint et al., 1993; Beaumont, 1981).

The basal unconformity of the Swiss Alpine Foreland Basin has been proposed as being due to forebulge uplift due to two main criteria (Crampton and Allen, 1995): i) the marine onlap of the Tertiary succession is oblique to the trend of the Mesozoic passive margin, and ii) the marine onlap occurs at a much slower rate than would be expected from the third order cycles; 10 - 20 Myr duration as opposed to the order of 10^6 years for third order eustatic variations.

The unconformity in France shows a similar slow onlap rate (Lutetian to Upper Priabonian) though the onlap of the Cretaceous and Tertiary formations are subparallel. In addition, the depth of erosion increases towards the foreland. However, there is no definite evidence that this phase of uplift and erosion was

produced by the development of a forebulge, as there was significant tectonism in France prior to the deposition of the Tertiary succession.

6.4.3. Deformation of the foreland plate

In France, the pre-nummulitic phase of uplift and erosion may have been complicated by the existence of tectonic regimes other than that of the advancing Alpine deformation front. In Haute Savoie, the proximity to the developing Rhine and Bresse grabens must be taken into account in the structural development of the area, and in Haute Provence, the effects of both Pyrenean and Alpine compressions must be considered.

6.4.3.1. Doming of the Rhine and Bresse Grabens

The north-west European rift system including the Rhine and Bresse Grabens started to develop in Late Cretaceous times with associated volcanic activity in the Rhine Graben (Illies, 1977). Mantle upwelling occurred associated with the volcanism, but the timing of this is disputed. Illies (1977) cites gravity sliding from an uplifted dome as being the propagating mechanism for extension that accelerated during the Late Eocene, i.e. doming in the southern Rhine Graben would have been present during the development of the erosional unconformity in the Alpine Foreland Basin. However, Laubscher (1992) only mentions doming from post-Eocene times, associated with the development of a mantle diapir producing the flank uplift in the Schwarzwald and Vosges, which he suggests was enhanced by the Miocene forebulge of the Alpine Foreland Basin.

North-south oriented compressional structures are also evident in the Bresse Graben, though no associated volcanism is described (Debrand-Passard, 1984). This folding has been attributed to the Pyrenean compression which produced post-Cretaceous uplift and deformation in the Bresse area (Rat, 1978).

Crampton and Allen (1995) also suggest doming in the Rhine Graben as a candidate for producing the erosional unconformity, but they have discounted it for the Swiss foreland basin as it does not explain the NE-SW trend of the uplift in Switzerland.

6.4.3.2. Pyrenean and Alpine compression

As has already been mentioned (Chapter 1), France experienced the effects of both the Pyrenean and Alpine compressions from Late Cretaceous times (Debrand-Passard, 1984). This interference of compressive stresses particularly affected southern France, with both forces active during Middle Eocene times in Provence (Apps, 1987). The Middle Eocene saw the major compressive phase in the area, though older Upper

Cretaceous and Palaeocene phases were important in producing discontinuities (Tempier, 1987).

Thus, south-east France experienced a more complex evolution of tectonic events and the resultant stress fields prior to Alpine induced subsidence compared to Switzerland, where complications only affected the western end of the foreland basin.

6.5. The Basal Unconformity - Evidence of Forebulge Uplift?

The diachroneity and coastal onlap pattern of the foreland basin fill reflects the progressive migration of the basin over the foreland as the orogeny advanced, with the youngest Tertiary successions overlying more deeply eroded Mesozoic passive margin sediments towards the west/north-west. This effect could conceivably be caused by the migration of an uplifted region ahead of the basin subsidence, with more prolonged exposure in the west producing a greater depth of erosion. However, isopach maps for the Mesozoic (Debrand-Passard, 1984) show that the Cretaceous sediments thin and pinchout towards the NW in Haute Savoie and the S/SE in Haute Provence, indicating that the increasing depth of erosion may be produced by the removal of the same amount of material from a thinner succession. The direction of thinning of the Mesozoic is also in the same direction as the onlap of the Tertiary basin fill. One of the criteria for the existence of a forebulge to the Swiss foreland basin is the oblique relationship between the passive margin succession and the sediments overlying the unconformity (Crampton and Allen, 1995). This shows that the erosion could not have developed due to eustatic variations, as the trends of the two successions would be expected to be the same, and that the increasing depth of erosion towards the foreland is probably not simply due to the effects of the thinning of the Mesozoic as again this would show a parallel trend to the strike of the Mesozoic formations. Additional evidence for the existence of a forebulge is the more developed karst profile in western Switzerland compared with the east (Herb, 1988) which is interpreted to represent a more prolonged period of exposure, which, coupled with the obliquity of the transgression, suggests the migration of a forebulge ahead of the basin.

In France the relationship between the trend of the passive margin succession and that of the basin fill does not provide evidence of an obliquity of transgression and could conceivably be caused by a drop in sea-level. The degree of erosion estimated is greater than that expected from a eustatic drop in sea-level, but this could be due to the effects of the various tectonic events affecting south-east France from Late Cretaceous times. There is also no evidence of prolonged exposure in the form of more mature karst profiles developing further west.

Thus, the lack of unequivocal evidence for the development of a forebulge in France makes it difficult to say whether this was the dominant process in the development of the basal unconformity of the foreland basin succession. By comparison of the stratigraphy and development of the basin with that of the Swiss basin, it is possible to say that it is likely an uplifted forebulge region migrated ahead of the subsiding basin, but without further detailed study of the basal unconformity, it is difficult to say conclusively whether it developed due to the existence of a migrating forebulge.

Chapter 7

Sequence Stratigraphy, Relative Sea-Level and Correlation of the Nummulitique: Implications for Basin Development

7.1. Introduction

The Nummulitique represents the development of a carbonate ramp during the early stages of foreland basin subsidence. Due to the sensitivity of carbonate systems to external controls such as relative sea-level, clastic influx and nutrient influx, the changing carbonate system can be used to interpret the variations in relative sea-level and environmental factors during the early development of the basin.

This chapter briefly outlines the controls on carbonate deposition and carbonate sequence stratigraphy and discusses the sequence stratigraphic development of the Nummulitique and the cyclicity within the formation which can be used for correlation in each field area. Finally, the implications for the early foreland basin development and possible reasons for variations between the two field areas will be discussed.

7.2. Controls on Carbonate Deposition

The response of a carbonate platform to variations in relative sea-level (rsl) is governed by its growth potential and hence by the productivity of the carbonate producing organisms in the shallow euphotic zone. This has been discussed by many workers (Schlager, 1981; Kendall and Schlager, 1981; James and Kendall, 1992; Bosscher and Schlager, 1992; Bosscher, 1992) and will only be mentioned briefly in this thesis.

Most carbonate is produced in less than 10-20 m water depth (Schlager, 1981), below which there is an abrupt reduction in productivity which gradually continues to decrease towards the photic limit in 50-100 m water depth (Fig. 7.1). The growth potential of a carbonate platform is its ability to produce sediment and grow upwards (Bosscher and Schlager, 1992) and is therefore controlled by the productivity of the system. Growth potential has been studied by observing the response of modern carbonate platforms to the Holocene glacio-eustatic transgression, during which the

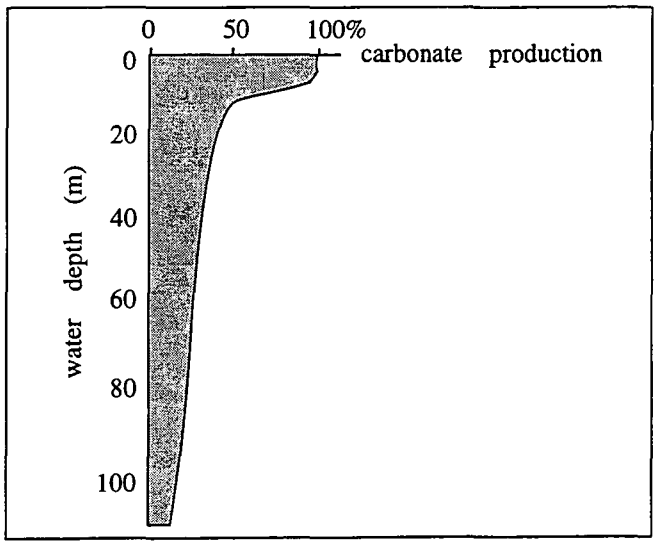

Fig. 7.1: Variation in carbonate productivity with increasing depth. After Schlager (1991)

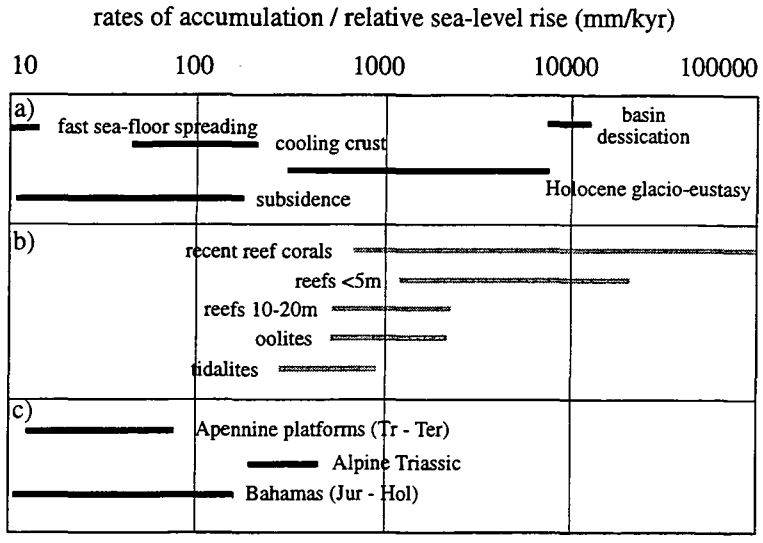

Fig. 7.2: Comparison of rates of relative sea-level rise versus the accumulation rates of modern and ancient carbonate platforms. Carbonate production potential outpaces all but the most rapid sea-level rises. After Schlager (1981).

maximum growth rate was 1200 mm/kyr (Bosscher and Schlager, 1992). Comparison with ancient platforms in the literature showed that during most of geological time, platforms could grow at rates of up to 1000 m/Ma (Bosscher and Schlager, 1992), and should therefore have been able to outpace all but the most rapid rises in sea-level (Schlager, 1981) which are generally of the order of tens to a few hundreds of m/Ma (Fig. 7.2). The accumulation potential of a platform is limited by the position of sea-level and is not constant across a platform, being greater at the fast growing reefs and shoals of the platform margins. This growth differential produces platform growth

conforming to the "bucket principle" of Kendall and Schlager (1981), where the lower productivity platform interior lags behind the rapidly growing reefs of the rim. Ramp carbonates do not show the same marked growth differential, but exhibit a decrease in productivity along the ramp profile as water depths increase towards the basin.

Thus, the geometry of a developing carbonate platform is controlled not only by relative sea-level variations, but also by controls on the productivity of the carbonate system which govern the ability of the platform to keep-up, overtake, drown or be exposed by relative sea-level change. The productivity of the system is controlled by the carbonate producing organisms, many of which rely on photosynthesis or photosynthetic symbiotic algae to fix nutrients and which are highly adapted to nutrient-poor, clear, warm waters (Hallock and Schlager, 1986). The main controlling factors on carbonate productivity are those that affect these organisms, i.e. light, temperature, nutrient supply, oxygenation and clastic influx, which are discussed below.

7.2.1. Carbonates and changes in relative sea-level

Due to the fact that most carbonate is produced *in situ* by organisms, the response of a carbonate system to variations in relative sea-level differs from that of a siliciclastic system which is dependent on external sediment supply into the depositional environment and which can be cut off and restarted in any water depth (Schlager, 1991). The response of the carbonate system to changes in relative sea-level has been studied in detail by Schlager (1981, 1989, 1991), Kendall and Schlager (1981), Burchette and Wright (1992), Hunt and Tucker (1993), Tucker et al. (1993) and Handford and Loucks (1994).

7.2.1.1. Relative sea-level fall

As carbonates have a tendency to build up to sea-level, a drop in relative sea-level will expose a widespread area of the inner platform (Kendall and Schlager, 1981), the amount of carbonate exposed depending on the geometry of the platform and the magnitude of the sea-level fall (Burchette and Wright, 1992). With rimmed shelves, a small relative sea-level fall will expose a large area of the inner platform, and the steep flanks tend to preclude the basinward migration of the locus of carbonate deposition. Carbonate ramps, with very low-angle basinward slopes, respond to relative sea-level fall with a basinward migration of facies, with the previous shallow, inner ramp becoming exposed (Fig. 7.3). The exposed part of the platform becomes susceptible to karstification and cliff erosion (Kendall and Schlager, 1981), freshwater cementation and, if a warm climate, palaeosol development (Tucker et al., 1993). If the basin is confined, a fall in relative sea-level can lead to basin

restriction and basinal evaporites may be deposited. Large relative sea-level falls such as those associated with glacio-eustasy with a magnitude of 100m or more may cause exposure of the entire platform, shutting down carbonate sedimentation (Burchette and Wright, 1992).

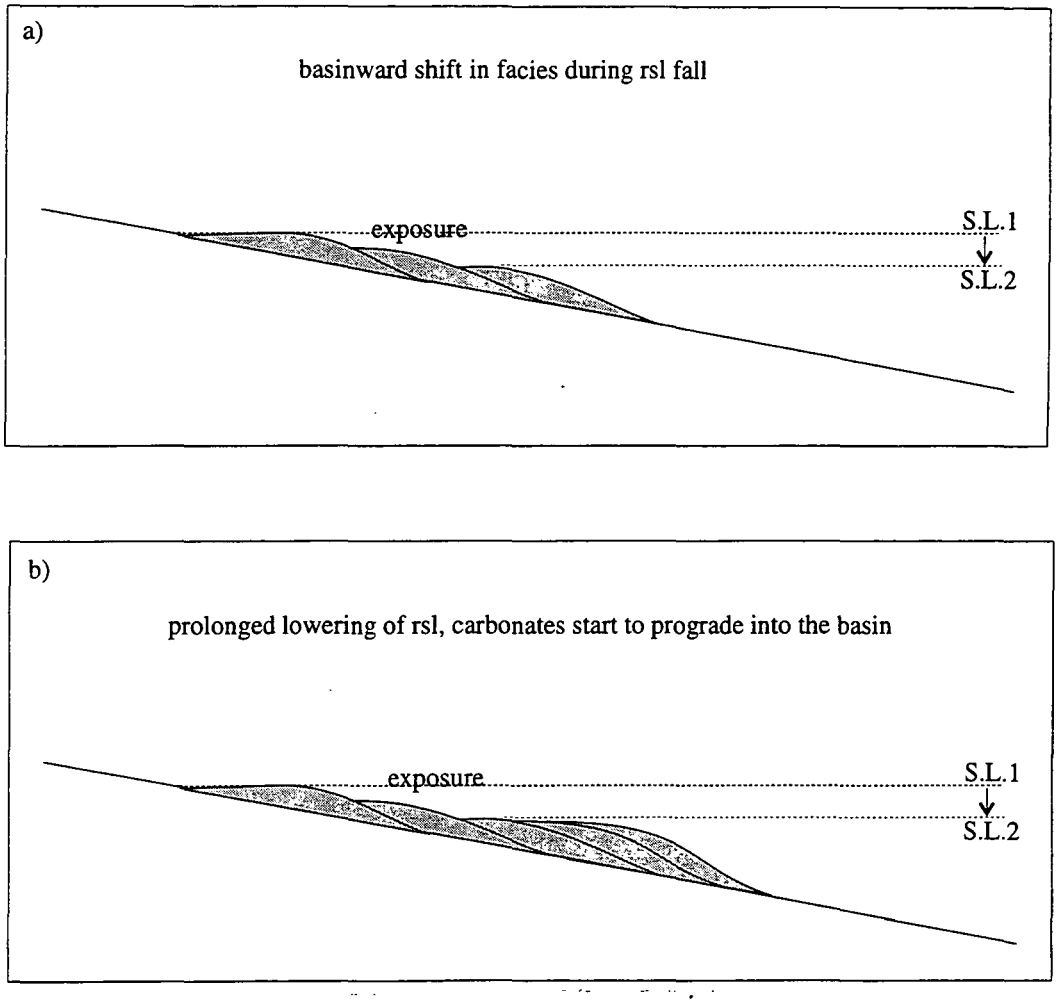

Fig. 7.3: Response of a carbonate ramp system to relative sea-level fall and the geometries developed. After Tucker et al. (1993).

7.2.1.2. Relative sea-level rise

As carbonates have accumulation rates of up to 1000 m/Ma (Bosscher and Schlager, 1992) most healthy carbonate systems should be able to keep pace with all but the most rapid eustatic sea-level rises and rises associated with regional tectonism. There are three main responses of carbonate systems to relative sea-level rise: keep-up, catch-up and platform drowning (Sarg, 1988; Kendall and Schlager, 1981). Immediately after transgression, the increase in water depth causes a reduction, usually temporary, in the productivity of the system. Thus there is a "lag time" before productivity again reaches its full potential, and this may be represented by slow,

pelagic sedimentation or the development of hardgrounds (Kendall and Schlager, 1981; Read et al., 1986). This lag time typically lasts for 2000 - 5000 years (Schlager, 1991) and is especially common during the flooding of previously exposed platforms. In a keep-up carbonate system, the carbonate productivity rate is greater than or equal to the rate of creation of accommodation space caused by the relative sea-level rise, and the platform can aggrade, keeping up with sea-level and it may prograde out into the basin (Fig. 7.4). In catch-up carbonate systems, the productivity rate is less than the initial rate of sea-level rise and incipient drowning may occur. A later slowing of the rate of sea-level rise allows the carbonate system to recover and build up to sea-level.

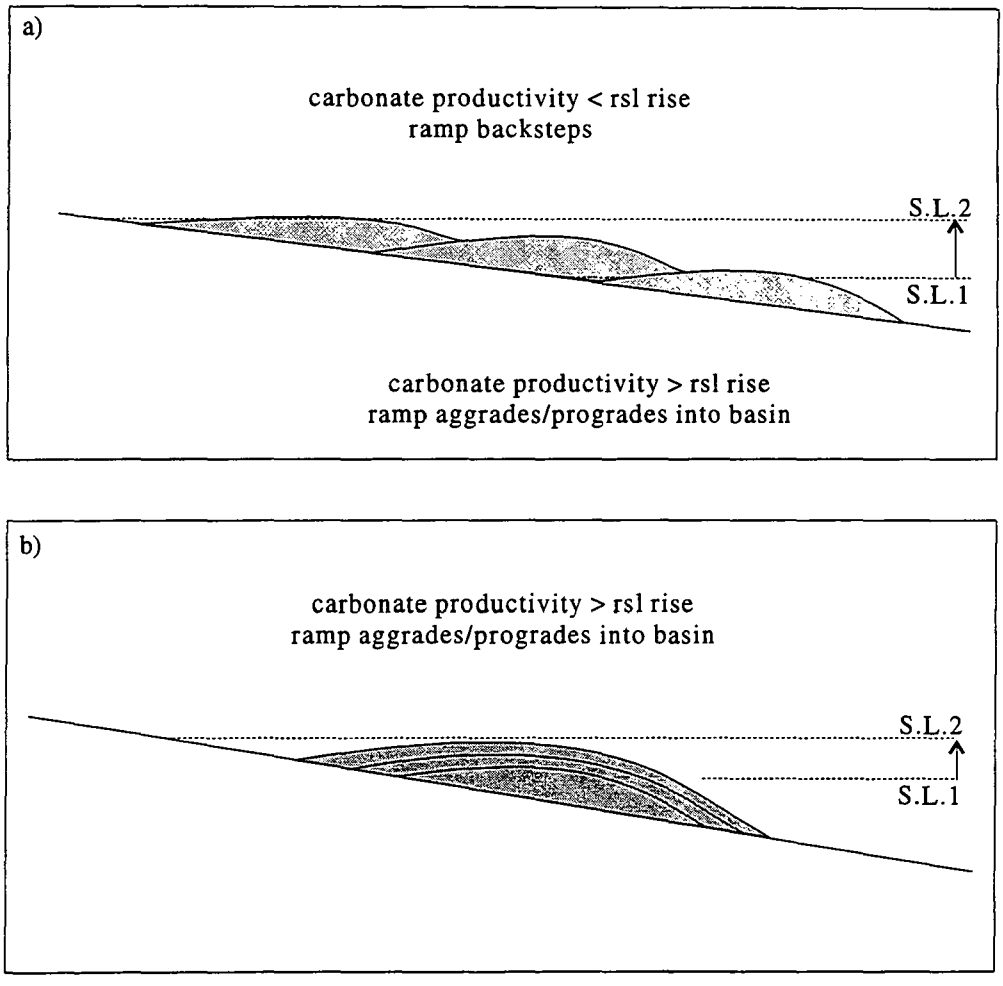

Fig. 7.4: Response of a carbonate ramp system to relative sea-level rise showing the geometries developed with a) low productivity and b) high productivity. After Tucker et al. (1993).

When a platform is permanently drowned, the rate of sea-level rise is greater than the carbonate productivity rate such that the system is unable to recover and a "drowning unconformity" (Schlager, 1989) is produced which may be marked by phosphate,

glauconite, ferromanganese oxide crust or hardground development (Hallock and Schlager, 1986) and which is overlain by pelagic or hemipelagic carbonates and/or siliciclastics (Schlager, 1989). Carbonate ramps may simply show a backstepping of facies shorewards during slower relative sea-level rises due to their constant basinward slope (Burchette and Wright, 1992). With more rapid rises, drowning occurs, though the unconformity produced is generally less pronounced than that developed on flat-topped platforms (Schlager, 1981).

As has already been discussed, estimated carbonate accumulation rates should be able to keep pace with all but the most rapid sea-level rises (Bosscher and Schlager, 1992). In order to drown a platform it must be submerged below the euphotic zone requiring a rapid sea-level rise of 50-100 m, such as those produced by glacio-eustasy. Other causes of relative sea-level rise, such as regional tectonic subsidence of passive margins and foreland basins are generally too slow to cause drowning, as the subsidence rates only outpace carbonate production rates during the initial lag phase (Schlager, 1981). Platform drowning has occurred throughout geological time, during much of which glacio-eustasy was not a contributing factor to relative sea-level rises (Schlager, 1981). Therefore, in order for relative sea-level rise to outpace productivity a mechanism must be found capable of either producing rapid pulses of relative sea-level rise or of reducing the productivity and growth potential of the carbonate system.

Pulses of relative sea-level rise can be produced by local tectonics such as episodic movement along transtensional fault systems or segmented passive margin (Schlager, 1981), which are common sites of platform drowning.

As productivity is controlled by carbonate secreting organisms, a sensitivity to environmental controls has been proposed. Detailed accounts may be found in Schlager (1981, 1991), Hallock and Schlager (1986), Hallock et al. (1988) Bosscher (1992) and Genin et al. (1995). The dominant factors in reducing the carbonate productivity of a system are climate, light intensity, siliciclastic influx and nutrient supply.

An increase of nutrient supply into a carbonate system can have a dramatic effect on the carbonate producing organisms, the majority of which are adapted to nutrient-poor conditions and rely on photosynthesis, and therefore light intensity, to fix nutrients (Hallock and Schlager, 1986). Increasing the supply of nutrients, by terrigenous influx, oceanic upwelling or oceanic overturn increases the abundance of plankton and suspension feeding animals, fleshy green algae and bacteria which grow on hard substrates such as reefs. These reduce the light intensity and increase bioerosion of the carbonate system. Both these factors reduce the overall productivity of the system and thereby promote platform drowning. Though studies have mainly been carried out on coral systems (Hallock and Schlager, 1986; Hallock et al., 1988;

Genin et al., 1995) the necessity of photosynthesis for other carbonate producers such as large benthonic foraminifera and calcareous algae suggests that the effects of increased nutrient supply into these systems would produce a similar reduction of productivity (Hallock and Schlager, 1986; Bosscher, 1992; Brasier and Green, 1993).

A change in climate may also induce environmental stress on the carbonate producing benthos (Schlager, 1981) as climate controls temperature, water circulation and the influx of terrigenous clastics (Tucker and Wright, 1990; Genin et al., 1995) which can reduce productivity by cooling oceanic waters, upwelling of nutrients and reduction of light intensity, nutrient influx and clastic poisoning respectively.

Thus, the response of a carbonate system to variations in relative sea-level is more complicated than that of a siliciclastic system and environmental factors should also be considered when studying the evolution of a carbonate platform.

7.3. Carbonate Sequence Stratigraphy - a Brief Overview

As carbonates and siliciclastics differ in their response to relative sea-level change, the sequence development in the two systems would also be expected to differ. It is assumed that the reader has a basic knowledge of the principles of sequence stratigraphy, details of which can be found in Vail et al. (1977), Van Wagoner et al. (1989) and Van Wagoner et al. (1990). This section deals briefly with the main characteristics of carbonate sequence stratigraphy and in particular its application to carbonate ramp systems. In this section, the term "ramp" refers to a homoclinal ramp; distally-steepened ramps shall be referred to as such. For a full discussion the reader should refer to Kendall and Schlager (1981), Sarg (1988), Schlager (1991, 1992) and Handford and Loucks (1994), and for specific reference to carbonate ramp systems to Burchette and Wright (1992), Hunt and Tucker (1993) and Tucker et al. (1993).

7.3.1. Sequence boundary (SB)

a) Type 1 sequence boundary

A type 1 sequence boundary occurs when rsl drops below the platform margin and this is characterised on rimmed platforms by foreslope erosion and the basinward migration of the fresh-water lens (Sarg, 1988). This leads to subaerial exposure of the inner platform and subsequent karstification, meteoric diagenesis, calcrete development and valley incision (Sarg, 1988; Schlager, 1992; Tucker et al., 1993).

b) Type 2 sequence boundary

A type 2 sequence boundary represents a lesser drop in rsl to the level of or just below the platform margin (Sarg, 1988), again leading to exposure of the inner platform, producing similar characteristics to the type 1 SB. However, no significant foreslope erosion occurs and rsl begins to rise once again after a relatively short time period.

On carbonate ramps, both types of rsl change will produce a basinward migration of facies, which will be more significant for a type 1 SB producing a more conspicuous unconformity than a type 2 SB, and there will be a greater contrast in the facies below and above a type 1 SB compared with a type 2 SB (Tucker et al., 1993). Due to the continual slope of a homoclinal ramp, the SB is likely to be heterogeneous and diachronous (Burchette and Wright, 1992).

7.3.2. Lowstand systems tract (LST)

On a rimmed platforms the LST is represented by either carbonate lowstand deposits, a platform margin wedge or an onlapping evaporite wedge (Sarg, 1988), though the steepness of the platform margin may hinder wedge development. The wedges may be composed of either allochthonous carbonate sediment redeposited after slope-front erosion during the development of a type 1 SB (turbidite fans, megabreccias; Hunt and Tucker, 1993) or autochthonous carbonate or evaporite wedges deposited on the slope of the underlying highstand. Lowstand shedding is not significant in carbonate systems as no sediment is produced on the exposed platform (Schlager, 1991) and exposure generally results in chemical rather than mechanical reworking of the platform, unless steep slopes are developed (Hunt and Tucker, 1993).

On carbonate ramps, the lowstand deposits and those of the previous highstand are often difficult to differentiate unless there is clear evidence of exposure, as there are no definitive carbonate lowstand deposits (Tucker et al., 1993; Burchette and Wright, 1992) though clastic or evaporite deposition may occur (Calvet et al., 1990). The lack of a significant slope precludes the development of slumps or debris flows. If there is a still-stand during the LST, prograding inner-ramp sands may produce a sand body analogous to the siliciclastic Shelf Margin Wedge (Tucker et al., 1993). If erosion of the previous platform was extensive during the rsl fall, it is possible to see local siliciclastic deposition after incision.

7.3.3. Transgressive systems tract (TST)

When rsl begins to rise more rapidly, the sediments of the LST are flooded producing the transgressive surface (ts). This is overlain by a retrogradational early

TST, with hardgrounds typically developing basinward of the new locus of carbonate deposition (Sarg, 1988). The development of the TST carbonates may show catch-up or keep-up characteristics, with a variety of resultant geometries possible (see Tucker et al., 1993 for discussion).

In ramp settings, the energy of the ramp determines the sediment type deposited during the TST, with high-energy ramps characterised by grainstones and low-energy ramps by wackestones and packstones with only local grainstone development (Burchette and Wright, 1992). The rate of subsequent rsl rise determines the geometries produced; a rapid rate of rsl rise results in backstepping of the inner-ramp facies with corresponding condensed mid- and outer-ramp sediments, whereas a slow rate of rsl rise will result in aggradation or even progradation of the system (Fig. 7.4) as carbonate productivity equals or outpaces the creation of accommodation space (Tucker et al., 1993). Changes in stacking geometries can occur within the TST, though this does not necessarily indicate a variation in the rate of rsl rise but could be due to environmental factors. Isolated offshore buildups typically develop during the TST (Burchette and Wright, 1992; Tucker et al., 1993).

7.3.4. Highstand systems tract (HST)

The HST represents the phase of maximum sedimentation and is commonly represented by an aggradational system developing to progradational as the rate of rsl rise slows (Sarg, 1988). Due to the high productivity during sea-level highstands, platform shedding may occur, producing basin floor aprons of shallow-water debris (Hunt and Tucker, 1993). This is most evident on platforms with steep flanks (Schlager, 1991, 1992).

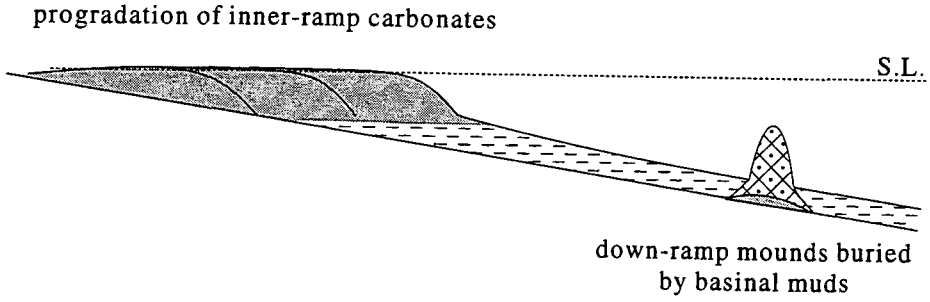

Fig 7.5: Progradation of a ramp system during the HST. After Tucker et al. (1993).

Parasequences on carbonate ramps tend to be dominated by grainy facies and show a systematic shallowing-upwards trend and karstic surfaces may cap the uppermost parasequences in the HST (Burchette and Wright, 1992; Tucker et al., 1993). The HST is the most likely time for the ramp to evolve to a distally steepened ramp due to the development of clinoforms filling up the accommodation space (Fig. 7.5).

7.4. Sequence Stratigraphy of the Nummulitique

The Nummulitique was deposited during the development of a single sequence during early basin subsidence. This section deals with the large-scale (3rd order) sequence development. The cyclicity and stacking patterns within the formation developed in each field area are described in Section 7.5.

7.4.1. Basal unconformity - sequence boundary

The onset of development of the Nummulitique is marked by a major regional fall in rsl causing erosion of the Mesozoic (mostly Senonian) substratum and the development of topography on the erosion surface. The unconformity shows clear evidence of subaerial exposure, with *Microcodium* encrustation of the substratum, karst dissolution of competent limestones (Haute Savoie) and palaeosol development where the substratum is more fissile (Haute Provence).

This major rsl fall which caused subaerial exposure of pelagic Cretaceous sediments shows the characteristics of a type 1 sequence boundary *sensu* Vail et al. (1977). It also shows evidence of tectonism, suggesting that the rsl fall may not have been due entirely due to eustatic sea-level fall, which was discussed in more detail in Chapter 6. The basal unconformity is also a megasequence boundary separating two different phases of basin development around the Alps; the Mesozoic passive margin and the Tertiary foreland basin. Subaerial exposure of the Senonian indicates a relative sea-level fall of at least 100m (Chapter 6), with subsequent erosion of at least 150m of the substratum (complete removal of the Wang Formation; Chaplet, 1989) leading to a total rsl fall of at least 250m.

7.4.2. The Infranummulitique and basal clastics - late lowstand and transgressive systems tracts

The first sediments deposited above the unconformity are the terrigenous clastics of the Infranummulitique (described in Chapter 3) which were deposited in morphological lows on the unconformity (Fig. 7.6). The coarse nature of the lower Infranummulitique sediments (pebble conglomerates) indicate that there was

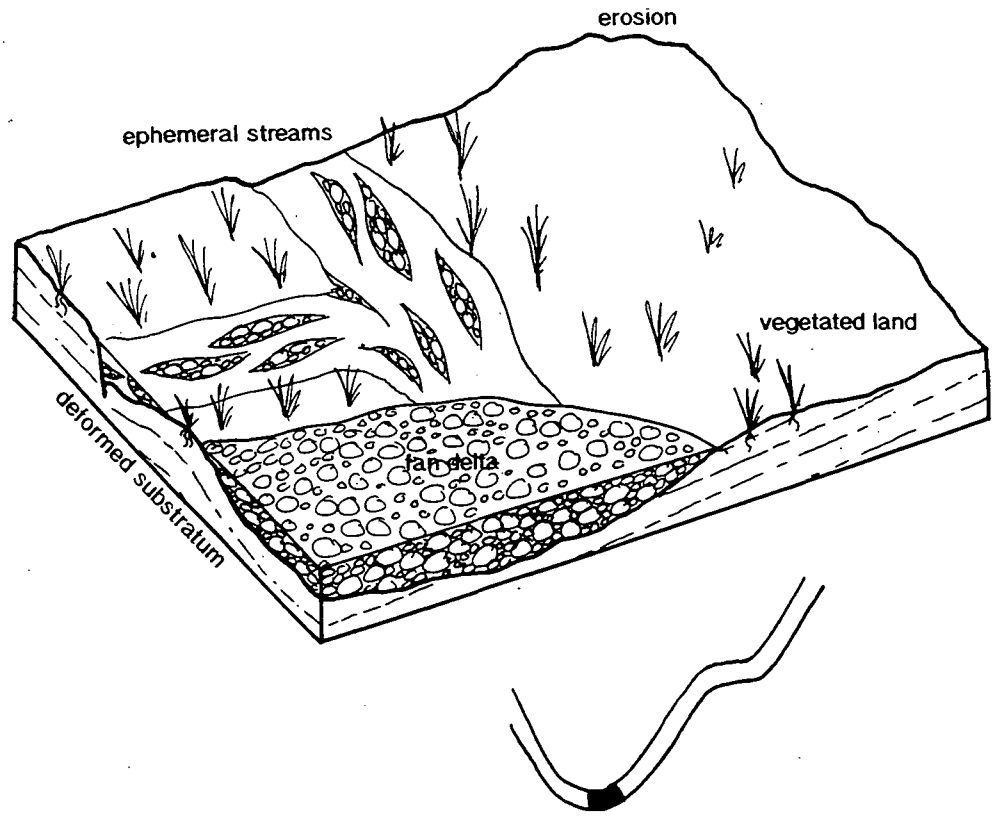

Fig. 7.6: Block diagram of the late LST of the Nummulitique Formation. Coarse terrigenous carbonate is being deposited in structural lows on the deformed substratum in ephemeral stream and fan delta settings. Deposition occurs close to vegetated land with eroding high ground acting as source areas for the coarse carbonate detritus.

significant relief between the source and depocentre, and the evidence of marine influence in the fan delta conglomerates suggests that deposition occurred during the onset of rsl rise, i.e. late LST. Though the base of the succession is erosive, there is no direct evidence in the study areas for valley incision, with the sediments appearing to infill pre-existing lows rather than cutting new topography. The ephemeral stream system could represent the early lowstand, but palaeoslope measurements (Thome, 1987) and the lack of evidence for its development below the fan delta succession suggests that it acted as a feeder system for the fan delta conglomerates and the lenticular conglomerates are interpreted as representing a landward expression of the late LST.

A change in sediment type and an increase in marine influence marks the transgressive surface, with an almost complete shutting down of coarse clastic supply into the system, indicating that relief was less significant (Fig. 7.7). Marine erosion occurred where the lower beds of the Infranummulitique were absent. The early TST is represented by the *Microcodium* wackestone and *Cerithium* marls (coastal deposits

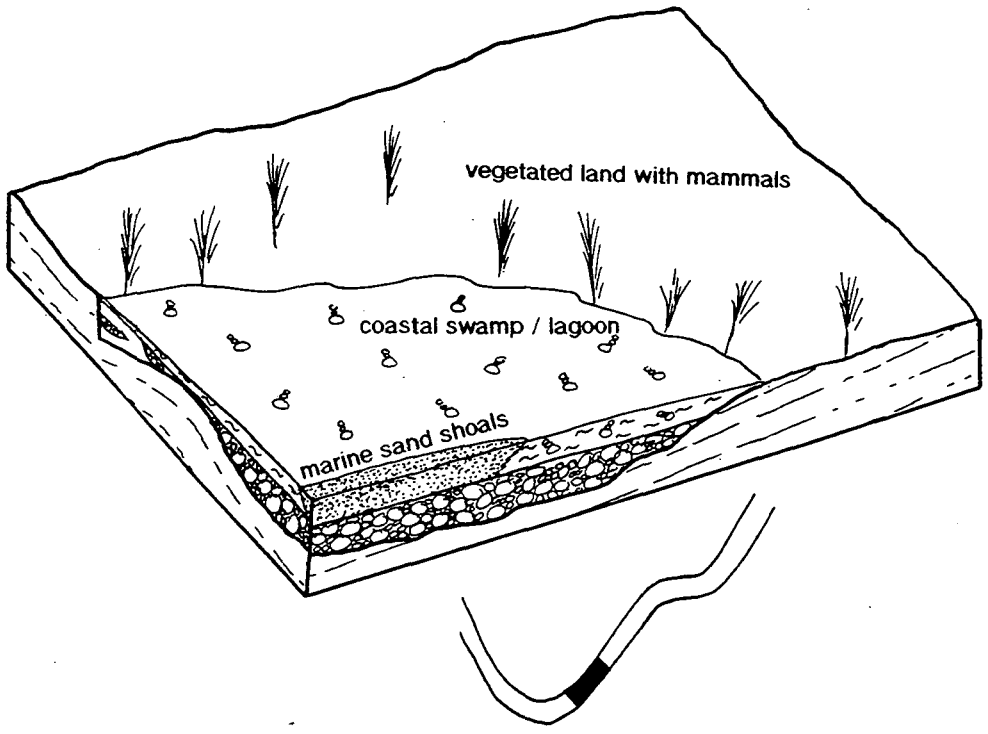

Fig. 7.7: Block diagram of the TST of the Nummulitique. Coarse terrigenous supply has ceased and deposition occurs in a coastal swamp / lagoon setting with the development of the Cerithium *marl. Continued transgression causes the development of offshore quartz-sandstone shoals, which may eventually form a transgressive sheet sandstone.*

and brackish lagoon) which still contain significant detrital quartz and small, sand-grade lithoclasts. In Haute Savoie, the late TST is represented by quartz-rich shoals containing a fauna indicative of fully marine conditions, with evidence of reworking above FWWB. These are thought to have acted as barriers protecting the *Cerithium* marls. In Haute Provence, the late TST is represented by the appearance of small corals in the *Cerithium* marl and the development of local coral patch reefs (Apps, 1987), indicating fully marine conditions. The increase in marine influence up-section and a cessation of coarse clastic supply is consistent with shoreline regression during a rsl rise with accompanying slow sedimentation rates.

7.4.3 The Nummulitic Limestone - highstand systems tract and ramp progradation

The maximum flooding surface separating the TST and the succeeding HST is taken to be the end of detrital influx into the system and the onset of carbonate production, with an accompanying proliferation of the marine fauna. This corresponds to a ravinement surface between the Infranummulitique or the basal clastics and the offshore Nummulitic Limestone, or, where the Infranummulitique is absent, to a

marine erosion surface at the top of the Mesozoic substratum with *Lithophaga* borings. Where the Infranummulitique is absent, the base of the HST is commonly marked by a conglomeratic lag, indicating that at these localities the sequence boundary and transgressive surface are coincident.

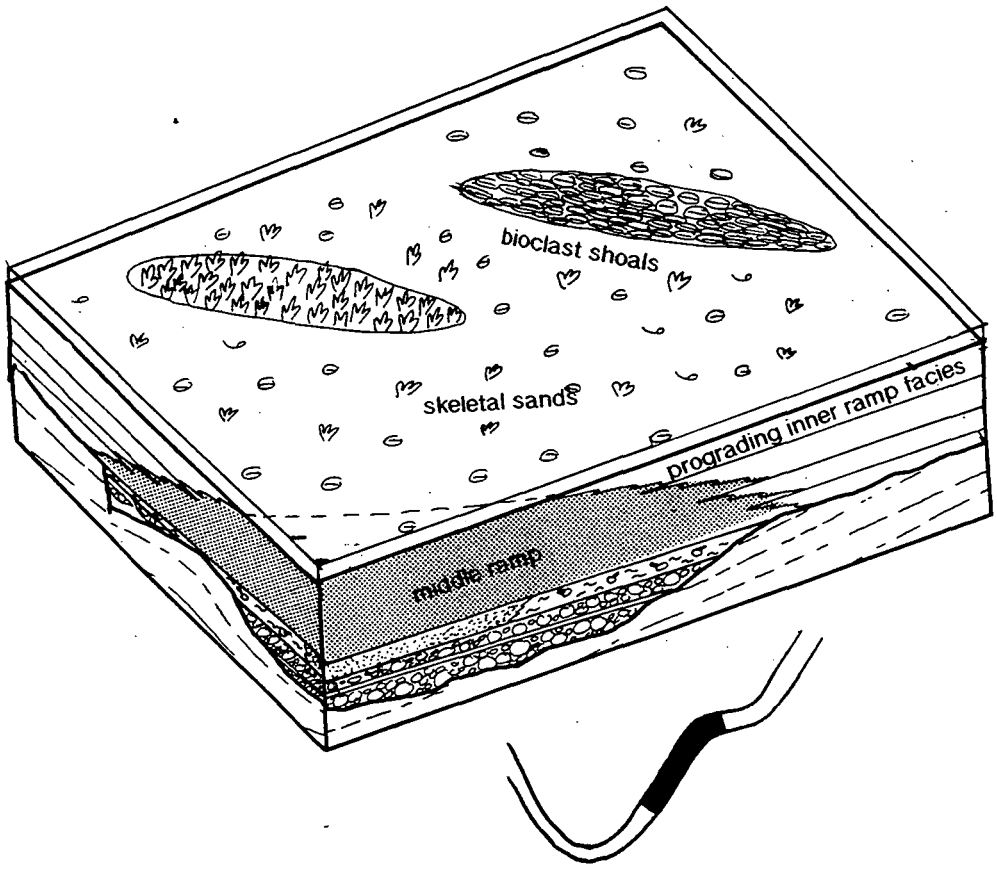

Fig. 7.8: Block diagram of the HST leading to the deposition of the Nummulitic Limestone. Flooding shuts down the supply of all clastic detritus into the basin providing suitable conditions for the setting up of carbonate production. As sea-level continues to rise, productivity is able to keep pace with the creation of accommodation space and the ramp system progrades out into the basin leading to the widespread development of bioclast shoals.

The HST is represented by the aggradation and progradation of the nummulitic ramp (Fig. 7.8), with the stacking geometries dependent on location (see Section 7.5). The Nummulitic Limestone contains a prolific marine fauna of larger benthonic foraminifera and calcareous red algae which may be winnowed forming bioclastic shoals. The succession shows an upwards increase in the proportion of inner-ramp shoal facies, dominated by grain-supported textures (packstones, grainstones and boundstones). The topography on the unconformity is still evident during the early HST, with some emergent highs persisting while the early progradational cycles were

developing in the intervening lows; however these became blanketed by the ramp sediments and acted as preferential sites for shoal and, rarely, reef development. In more basinal sections, the HST is represented by a single, coarsening upwards cycle, indicative of a condensed succession developing in areas of low sedimentation.

The end of the HST is marked by extensive inner-ramp facies in all but the most basinal sections, representing the time of maximum regression in the basin and a slowing, or possibly even stillstand, in the rate of rsl rise.

7.4.4. Transition to marls - candidate sequence boundary and TST in a subsiding basin

The transition to the *Globigerina* marls is marked by a change from aggradation and progradation to retrogradation and transgression (Fig. 7.9).

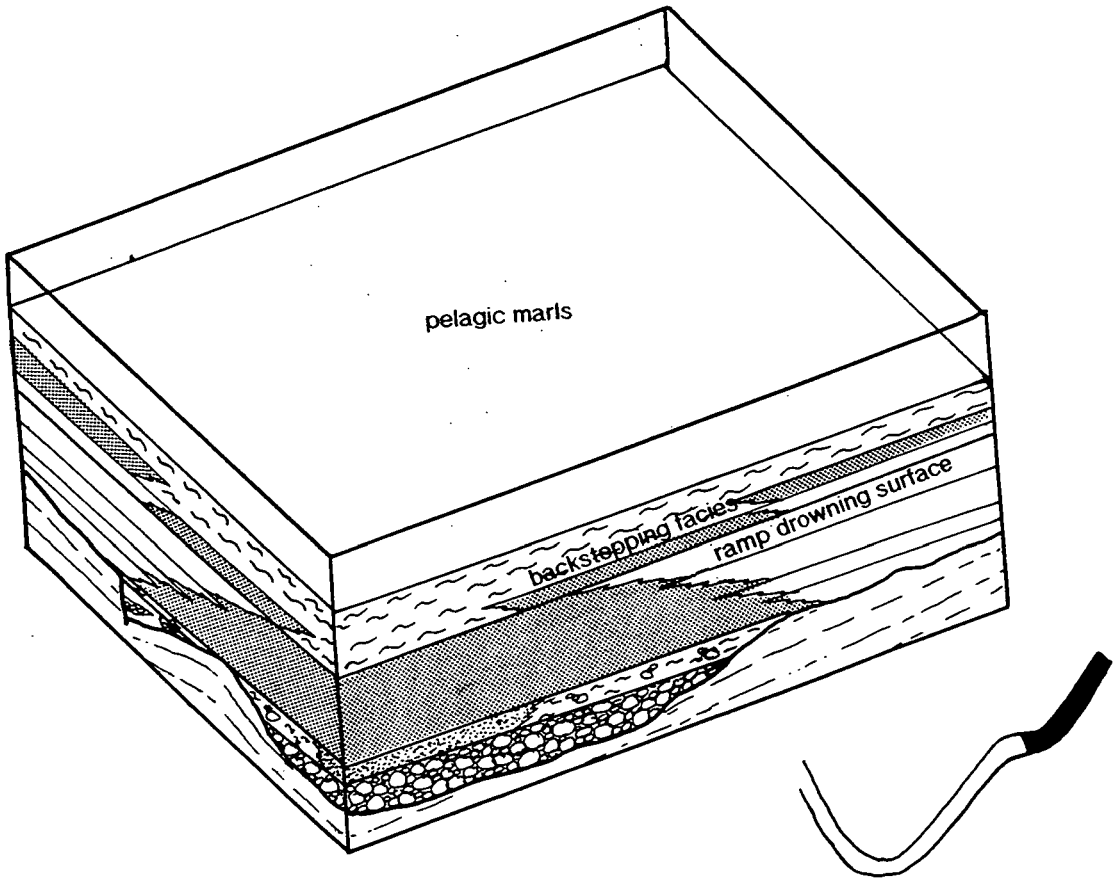

Fig. 7.9: Block diagram of the drowning of the carbonate ramp and the TST in the marls. Increasing subsidence rates and the reduction of carbonate productivity lead to rapid drowning of the ramp system and the onset of pelagic deposition. There are no evident rsl falls due to the increasing effects of subsidence dominating the rsl curve.

The boundary between these two geometries represents the transition from the HST of the underlying Nummulitic Limestone to the overlying TST marked by the transition to the Globigerina Marls. As the HST is bounded above by the presence of a sequence

boundary (Van Wagoner et al., 1988), the end of progradation/aggradation of the carbonate ramp is therefore a candidate sequence boundary, though the succession shows an overall deepening upwards trend. For this surface to be confirmed as a sequence boundary, it is necessary to find evidence of a relative sea-level fall within the basin, which does not seem to be present in the facies encountered. However, due to the migration of the developing basin over the exposed foreland plate, it is conceivable that a correlatable unconformity exists landward of the transition to the marls which may show evidence of a relative sea-level fall. If this were the case, the drowning surface separating the HST and subsequent TST could be a candidate sequence boundary. If this change in geometry of the succession does represent a sequence boundary, the facies record a slowing or stillstand in rsl rise rather than a rsl fall. This is thought to be due to the interaction of eustatic variations and accelerating subsidence producing a "sea-level staircase" pattern of rsl rise (Morrow, 1986). No overlying lowstand is developed and the Nummulitic Limestone highstand is overlain by the second transgressive systems tract (TST2) with a retrogradational geometry associated with a deepening into the pelagic marls. This transition is equivalent to the drowning unconformity (Schlager, 1989) representing the demise of the carbonate ramp system. Unlike rimmed platforms where such unconformities are marked by an abrupt hiatus with mineralisation, on ramps the transition from shallow-marine to pelagic deposits tends to be more gradual (Schlager, 1989). The end of TST2 is a maximum flooding surface within the marls, marked by the maximum diversity of planktonic foraminifera and the corresponding minimum diversity of benthonic foraminifera (Thome, 1987).

7.4.5. Foreland basin migration - diachronous sequence development?

Due to the migration of the foreland basin with time over the foreland plate, similar variations in relative sea-level will occur at different time-slices due to the varying effects of subsidence as the basin develops. Assuming the migration of the basin can be taken as a continuum process (Sinclair et al., 1991), at any given time the various stages of development of the stratigraphy will be occurring at different points in the basin along a transect perpendicular to the basin strike (Fig. 7.10). It is the lateral migration of the basin which produces the vertical superposition of facies seen within the stratigraphy, and as these facies are produced by the rsl variations, dominated by the subsidence of the basin, then the basin migration would appear to control the rsl change seen at any given point within the basin. This implies that at a given time, erosion is occurring in the foreland prior to basin subsidence, terrestrial deposition is occurring near the coastline, marine carbonates are prograding into the

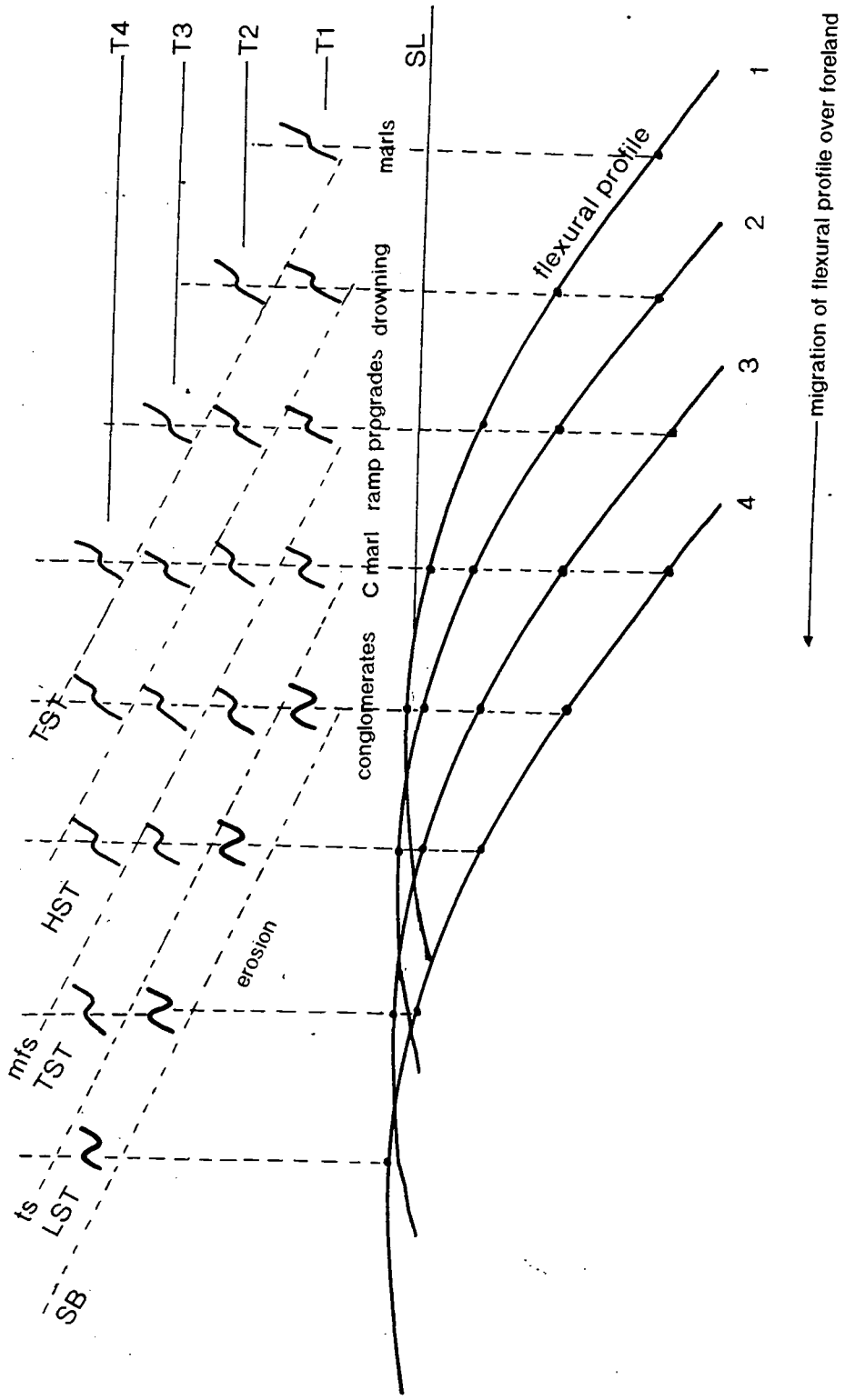

Fig. 7.10: Diachroneity of sequence development in a foreland basin setting. The upper part of the diagram illustrates the changing rsl curve as subsidence is superimposed on a sinusoidal eustatic signature at four time slices, showing the decreasing effects basinwards of eustatic falls as the Nummulitique succession develops. It is possible for a particular rsl signature to occur somewhere within the migrating foreland basin at any given time. This leads to a backstepping of both the facies and the sequence development over the foreland with time, necessitating extra care when attempting a correlation between different areas of the basin.

shallow slowly subsiding basin and these are being flooded by pelagic marls further out into the basin where subsidence is accelerating. Thus, at any given level in the stratigraphy, there is a correlatable unconformity being developed on the exposed foreland plate. This makes sequence stratigraphic interpretation within the underfilled foreland basin stratigraphy somewhat dubious as the key surfaces are diachronous perpendicular to the strike of the basin, whereas the principles of sequence stratigraphy state that these bounding surfaces contain time-significant packets of strata. This indicates that the sequence development along a transect perpendicular to the strike of the basin is necessarily diachronous and therefore cannot be used in correlating time-lines within the stratigraphy. This effect is particularly well developed in the Alpine Foreland Basin, where similar stratigraphic successions are developed at different times in different parts of the basin, with the key surfaces of sequence boundary, transgressive surface and mfs developing at different times depending on the stage of location of the stratigraphic succession within the migrating foreland basin. Though the formation may be divided into the various systems tracts according to the rsl variations, it is particularly important to recognise the diachroneity of the basin development, and hence sequence development, before attempting any correlations based on the sequence stratigraphy. Viable correlations of the basin stratigraphy may be carried out in conjunction with additional evidence of time-equivalence of the succession, which includes biostratigraphical dating of the succession, the recognition of specific eustatic signatures in the stratigraphy, or the correlation of along-strike successions.

7.5. Cyclicity within the Nummulitique

7.5.1. The Infranummulitique

7.5.1.1. Conglomerates

The lenticular conglomerate succession is only seen at one locality (Log P1), but shows a clear cyclicity with beds of conglomerate separated by thick nodular marls. Apps (1987) studied the soil profiles developed in the marls and observed a change in the soil type up-section. She interpreted this to be the result of a rise in the level of phreatic ground-waters associated with increasingly marine porewaters related to a rise in rsl. As the succession represents an ephemeral stream system, autocyclicity may have contributed to the cyclicity seen in the succession, but due to the lack of lateral exposure it is impossible to determine the lateral continuity of the sediments.

However, a similar cyclicity is developed in the massive conglomerate seen at Peyresq (Logs P2, P3, P4), where lateral continuity of the facies may be observed.

These conglomerates are closer to the palaeoshoreline, deposited in a fan delta setting, with clear evidence of marine reworking (borings, local marine fauna) and they therefore may show a better indication of rsl variations.

The succession can be divided into three high frequency cycles (10m thick), each with an erosive base cutting down into the top of the underlying sediments. This is overlain by massive conglomerate, with evidence of marine conditions, passing up into bedded conglomerate. The conglomerate is overlain by nodular marls, the top of which is cut by the base of the cycle above.

The erosion evident at the base of each cycle is associated with a rsl fall, during which increased erosion in the source area and reactivation of the fluvial system produced a renewed influx of coarse clastic detritus into the system. The subsequent stillstand allowed reworking of the erosion surface, evident in the presence of burrows on the basal unconformity surface prior to the deposition of the conglomerates. Relative sea-level rise promoted the deposition of the conglomerates and the transgression of the sea over the previous exposure surface. The massive nature of the basal part of the conglomerates indicates rapid sedimentation rates and the appearance of bedding higher up in the cycle suggests a slowing of clastic influx, allowing the reworking of the gravels and the development of low bars. This change within the conglomerates is thought to be associated with an increasing rate of rsl rise. The conglomeratic influx is shut down and the reworked top of the conglomerate is interpreted to represent the maximum flooding surface of the individual cycle. Sedimentation rates are now much slower, leading to the deposition of fine-grained, shallow marine marls. The marls are thought to build up to sea-level as the rate of rsl rise slows and the subsequent still-stand and onset of rsl fall promotes the pedogenic reworking of the sediments. However, no distinct soil profiles are developed (Apps, 1987) suggesting that the period of exposure was relatively short. Relative sea-level fall causes the erosion of the top of the cycle. Similar processes are also thought to control the cyclicity seen in the thinner massive conglomerates on the Desert de Platé, Haute Savoie (Log S11), with bioturbated marine sandstone deposited during the highstands in lieu of the marls seen at Peyresq.

The lateral continuity of the fine-grained marls, visible for over 1km, suggests that autocyclicity can be ruled out as the cause of the cyclicity within the succession, though it is likely to govern the migration of the channels across the area. The cyclicity produced can therefore be related to changes in rsl.

At Argens, thought to be a landward equivalent of the Peyresq system, the same number of cycles is developed (10-12m thick), though the conglomerates are thinner and not laterally continuous. The similarity of the cycles and probable source areas of the two systems suggests that the cyclicity developed in the lenticular

conglomerate/nodular marls is also due to rsl variations rather than autocyclicity, with the influx and deposition of the conglomerates from ephemeral streams during rsl fall and subsequent rise, and the cut-off of clastic supply and deposition and pedogenic reworking of the continental nodular marls occurring above the maximum flooding surface of each cycle. Marine influences do not affect the Argens succession.

The marine influence on the succession increases up-section (higher density of borings, influence of brackish waters), indicating that the cyclicity developed on the transgressive part of the lower order relative sea-level curve.

7.5.1.2. Cerithium *marl and* Microcodium *wackestone*

Cyclicity is well developed in the Cerithium marl at Col du Colonney (Log S11) where small-scale (2-4m) coarsening-upward cycles are evident. Nine cycles are developed over a 20m thick succession. The base of each cycle is represented by an erosively based lag consisting of bored Cretaceous clasts, abundant bivalve shells, gastropods and common oyster encrustations. This basal lag is overlain by carbonate mud with small *Cerithium* genus gastropods and coarsens up into bioturbated mudstone with large *Cerithium*, ribbed and smooth-shelled bivalves and oysters.

The environment of deposition of the marls is a low-energy, brackish coastal plain or lagoon. The presence of borings on clast surfaces indicates periodic marine incursions and the encrusting oysters indicate relatively hard, flooded sediment surfaces (Clarkson, 1986). This indicates that the clast-rich, shelly lags represent marine reworking of the sediment, with higher-energy waters winnowing out the fines and with oyster encrustations and borings developing during a concurrent pause in sedimentation.

The introduction of clasts into the system and erosion of the top of the underlying cycle occurs during a fall in rsl. The reworking of clasts and eroded debris in a marine environment indicates a transgression produced by the subsequent rise in rsl. The base of the shelly lag and concentration of clasts and shells thus represents the transgressive surface of the cycle. The shelly lag is reworked in the marine environment, which winnows out the fine sediment. The occurrence of borings and the concurrent colonisation of the sediment surface by oysters indicates a pause in sedimentation produced by flooding within the marine environment; this reworking is thought to indicate the maximum flooding surface of the cycle. The subsequent slowing of the rate of rsl rise allows the sediment to infill the available accommodation space promoting a return to brackish water conditions and the development of the coarsening-upward trend from mudstones to mollusc wackestones. Subsequent rsl fall causes erosion of the top of the cycle and further clast influx, overlain by the transgressive lag.

The presence of a 2m thick cross-bedded sandstone towards the top of the *Cerithium* marl (Log S11, 20.5m) is interpreted to be the result of a more prolonged marine incursion with the development of a sandy shoal in relatively high-energy offshore conditions.

At L'Epine and Ivoire (Logs S14 and P5) the cyclicity is less well developed, showing only an overall coarsening and deepening upwards from brackish water organic-rich mudstones to *Cerithium* marls with a wackestone texture, which pass up into the marine beds of the Nummulitic Limestone. At L'Epine, the base of the succession consists of the marine *Microcodium* wackestone before the development of brackish water conditions. This may coincide with the prolonged marine transgression producing the sand shoal at Col du Colonney. The succession is capped by a coal horizon indicating local restriction and the development of reducing conditions prior to marine flooding at the top of the succession.

7.5.2. Basal Clastics

The basal clastics (facies association S0) represent the waning of clastic supply into the basin after marine transgression. The transgression associated with the base of the sandstones is commonly marked by a lag deposit, with reworked lithoclasts and shell debris. Thicker sections (Col du Colonney, Flaine, Paccaly) may show a crude cyclicity with muddy sandstones passing up into clean winnowed sandstones which show evidence of reworking above FWWB (cross-bedding).

Internal erosion surfaces are no longer apparent, implying that the rate of rise of rsl has increased such that the corresponding falls no longer lead to exposure of the top of the cycle, instead producing reworking by wave action. Subsequent rsl rises produced an increased proportion of carbonate mud in the sediment and an absence of sedimentary structures.

The lenticular nature of the sandstones indicates that autocyclic shoal migration may play a part in developing the observed cyclicity, especially in view of the wide variation in the number and characteristics of the cycles produced at different localities. The variation in the number of cycles may in part reflect the continuing effects of the pre-existing topography on the Mesozoic erosion surface, with the thicker sandstones developed above or in close proximity to the depocentres for the Infranummulitique.

7.5.3. The Nummulitic Limestone

The Nummulitic Limestone can be divided up into a series of shallowing-upward cycles based on the microfacies interpretation outlined in Chapters 5 and 6.

The cyclicity in the measured sections is illustrated in the correlations shown in Section 7.6.

7.5.3.1. Haute Savoie

For the carbonate ramp succession, the Haute Savoie field area can be divided into three distinct sections: west and central Thônes Syncline, east Thônes Syncline and the Massif de Platé.

West and Central Thônes Syncline

This area shows the best development of cyclicity within the Nummulitic Limestone in the field area. The succession can be divided into a series of shallowing-upward cycles within an overall progradational trend, with the number of cycles developed depending on whether the locality studied represented deposition on a structural high or corresponding low. The maximum number of cycles developed occurs at Le Chinaillon (Log S1) where the succession can be divided into 7 shallowing-upward cycles prior to the drowning of the carbonate ramp.

The base of the Nummulitic Limestone, directly overlying the basal clastics, is dominated by mud-rich microfacies, with evidence of storm reworking producing local Discocyclinid packstones. The fauna dominating these lower cycles is indicative of the middle- to outer-ramp indicating a significant raising of rsl between the deposition of the shallow marine sand shoals and the onset of carbonate ramp development. The basal surface, representing the onset of carbonate production, is interpreted to represent the maximum flooding surface within the formation. Moving up section, the cycles thin and contain progressively more inner-ramp facies (algal packstones and boundstones) due to the development of algal shoals, which indicates an overall filling of the accommodation space and the progradation of the ramp out into the basin. The mudstones deposited at the base of each section represent the initial "lag time" after flooding while the carbonate factory was below its full production potential.

The cycle tops generally indicate deposition above FWWB and there is no evidence of subaerial exposure. This indicates that either rsl falls were not sufficient to expose the tops of the cycles, or that rsl rise slowed or reached a stillstand allowing the sediments to build up above FWWB. These inner-ramp sediments were flooded during the subsequent increase in the rate of rsl rise and the base of the successive cycle was deposited below FWWB on the middle-ramp.

These cycle characteristics are evident at all localities studied on the western limb of the Thônes syncline, though the number of cycles developed varies. Tête de la Sallaz, Meubles Montagnardes and La Communaille sections (Logs S6, S5 and S4

respectively) have fewer cycles and lack the basal clastic facies. This indicates that they were deposited on structural highs (also evident in the level of erosion of the substratum) and would therefore be flooded later in the rising relative sea-level curve than the corresponding lows. These localities also act as preferential sites for shoal development, with early development of grain-dominated inner-ramp facies. By the time of development of the last three cycles prior to ramp drowning, the underlying topography had been smoothed by the accumulating carbonate sediments and inner-ramp facies were deposited over the whole area.

The uppermost shoaling-up cycle, generally the thinnest in each section, represents the time of maximum regression and progradation into the basin, after which carbonate productivity was outpaced by rsl rise and the ramp was flooded, with a single fining and deepening upwards trend representing the transition to the overlying marls.

Eastern Thônes Syncline

This area appears to have been more basinal, with thicker basal clastics accumulated than seen in the west, and a very thin Nummulitic Limestone deposited, with no inner-ramp facies. Due to the basinal nature of the sediments, cyclicity is very poorly developed, with the succession above the basal clastics represented by a single shallowing-upward unit. As platform drowning can be taken as synchronous across a ramp for correlative purposes (Schlager, 1981), the thinner succession is thought to represent the same time period as the sections studied on the western limb of the syncline and is thus interpreted as being a condensed section due to the lower productivity rates in more basinal settings. The shallowing-upward trend represents the overall progradation of the ramp into the basin during the HST of the formation. Platform drowning is indicated in these sections by an increased fissility of the sediments produced by the onset of argillaceous and detrital influx.

Massif de Platé

This area represented another topographic high with the proliferation of algal shoals. The effects of the pre-existing topography, already seen to have influenced the distribution of the Infranummulitique, led to a more variable cyclicity than that in the Thônes Syncline, with between two and four cycles developed. There is no clear trend in the cycle thicknesses developed, which suggests accommodation space variations across the area. The succession shows progradation from middle-ramp mudstone and wackestone dominated cycles to more dominant algal shoal facies immediately prior to platform drowning. Shoal development is not as closely related to pre-Nummulitic topography due to the infill of the Infranummulitique, with shoal facies dominating

the sediments at Col du Colonney (pre-Nummulitic low; Log S11) and Flaine (high; Log S13), whereas the intermittent high at East Flaine (Log S12) has a thin succession dominated by middle-ramp sediments (i.e. deeper water) and is thought to indicate local condensation due to slower sedimentation rates.

Platform drowning is interpreted to be synchronous across the Haute Savoie field area, producing the correlations shown in Section 7.6.

7.5.2.2. Haute Provence

The Nummulitic Limestone in Haute Provence shows an initial aggradational geometry rather than progradation. The maximum flooding surface at the base of the succession represents a lower rise in rsl compared with Haute Savoie, with a transition from coastal deposits (*Cerithium* marl, fan delta) to inner-ramp bioclastic shoals dominated by either *Nummulites* or peloids.

The Haute Provence field area can be divided into two main areas, with distinct cycle development: the northern synclines, with five shallowing-upward cycles developed prior to ramp drowning, and the St Antonin Syncline, with eight cycles.

In the St Antonin Syncline, the basal five cycles show an aggradational geometry, with the cycles dominated by inner-ramp facies representing widespread bioclast shoal development. The flooding surfaces separating each cycle only represent a minor landward facies shift, and inner-ramp sedimentation was soon restored. Cycle tops show no evidence of exposure, but the rsl fall was sufficient to promote reworking of the bioclastic sands above FWWB. Above the maximum regression a retrogradational trend was established, with each successive cycle containing more middle- or outer-ramp facies and each flooding surface representing an increased landward shift in facies which could not be compensated for by the carbonate productivity. The cycles developed show a crude thickening upwards trend, representing the increasing accommodation space, but this may not be seen over the whole area due to the local facies variations. This represents the backstepping of the carbonate ramp prior to platform drowning.

In the northern synclines, which encompass the Allons, Annot and Agnère Synclines, the base of the succession is again aggradational (basal 3 cycles) with the flooding surfaces representing a transition to middle-ramp sedimentation shallowing up to inner-ramp shoal facies with wave reworking. The final shallowing upwards cycle prior to ramp drowning represents a minor phase of retrogradation across most of the area showing a deepening of the facies developed, though in shoal dominated successions (Pont Noir, Log P10; Col du Fa, Log P8) the higher carbonate

productivity is able to maintain the aggradational trend. This indicates shallower waters probably due to the inherent topography on the Mesozoic substratum.

Platform drowning in all sections is more prolonged than that in Haute Savoie, showing a deepening-upwards from inner/middle-ramp facies through middle-ramp facies, with storm generated Discocyclinid packstones, to the fissile, argillaceous, organic-rich outer-ramp/basinal marls.

The pre-existing topography shows a less marked effect on the development of the Nummulitic Limestone in Haute Provence, indicating that relief was probably less than that in Haute Savoie, with no discrepancy in the number of cycles developed between sections measured within each area. The relief is only evident in the variation in facies constituting the cycles. This is demonstrated in a comparison of the sections measured at Col du Fa (Log P8) and Castellet les Sausses (Log P9), which lie either side of the Rouaine Fault. Col du Fa, on the footwall of the fault, shows extensive nummulite shoal deposition and is dominated by cross-bedded inner-ramp facies. Castellet les Sausses, on the downthrown side, represents a more basinal succession, dominated by argillaceous middle-ramp facies. This indicates that there was relief across the fault, producing deeper waters on the downthrown side. However, the similarity in the number and thickness of the cycles developed and the geometries on either side of the fault indicates that this fault was not active during the deposition of the Nummulitic Limestone. La Rochette (Log P11) also represents a more basinal succession compared to Collongues (Log P12) and Pont au Miolans (Log P13), with thinner cycles indicating lower productivity rates.

The age of the transition to the marls (top planktonic foraminifera zone P15) is the same across the whole of the Haute Provence field area, so the extra cycles developed in the St Antonin Syncline indicate that this area underwent an earlier transgression than the northern synclines. This is also indicated by the presence of a thicker succession dated as Upper Lutetian to Priabonian (Zone B of Bodelle, 1971) compared to the northern synclines. These earlier cycles may have been developed at the same time as the deposition of the Infranummulitique further north.

7.6. Relative Sea-level Variations in the Eocene French Alpine Foreland Basin

7.6.1. Magnitude and duration of relative sea-level cycles as deduced from the Nummulitique

An estimation of the magnitude of relative sea-level change during the deposition of the Nummulitique can be obtained from the microfacies of the carbonate

ramp and the approximate water depths as indicated by the ramp fauna (Fig. 7.11) based on Omani nummulitic limestones described by Racey (1990; his fig. 7.4).

In Haute Savoie, the initial marine transgression represents a transition from exposed land or offshore, shallow-marine sand shoals, deposited above FWWB in around 10m water depth, to lower middle-ramp facies, the presence of *Discocyclina* suggesting waters of >20m (Hallock, pers. comm.) and estimated at >50m (Racey, 1990). This indicates a rsl rise of at least 20m, and probably up to 50m, at the onset of marine transgression. Subsequent cycles during the progradational part of the formation, are capped by flooding surfaces between shallow inner-ramp algal shoals (10-50m water depth) and lower inner-ramp to upper middle-ramp packstones and wackestones (50m) indicating a rsl rise of up to 40m. Towards the top of the formation, flooding becomes more pronounced, marking a transition to deeper water facies representing a submergence of the top of the final regressive cycle to >50m based on the presence of abundant flat *Discocyclina* and *Operculina*. Continued, increasing flooding, outpacing carbonate accumulation rates leads to the transition to pelagic marls in waters of >130m (below photic zone).

In Haute Provence, the initial transgression is marked by a transition from coastal lagoon/swamp (0m) to offshore, peloidal shoals or nummulite banks in 10-50m water depth. Peloidal muds from the Bahamas are being deposited in waters of 2-6m at present (Flügel, 1982), though the effect of wave action on the sediments of the Nummulitic Limestone indicates that the peloids have been washed offshore into higher energy waters, probably of similar depths to the upper parts of the nummulite banks, based on the close relationship of the facies of both shoal types observed in the field. Therefore, the initial flooding in Provence represents a rsl rise of 10-50m, i.e. less than that in Haute Savoie. The cycles produced during the aggradational phase of ramp development are capped by flooding surfaces representing a transition from inner-ramp shoals to lower inner-ramp and rarely upper middle-ramp (around 50m; no flat Discocyclinids) i.e. a rsl rise of up to 40m. The top of the formation shows the same characteristics as that in Haute Savoie, though the more prolonged nature of the drowning of the ramp indicates that productivity was not as drastically outpaced by rsl rise during the early stages of ramp drowning. This effect may also be due to local variations in the subsidence rates around the Alpine Arc. Crampton (1992) showed that subsidence rates during the deposition of the Nummulitic Limestone were more rapid in the Champsaur ($40mMa^{-1}$) than in Switzerland ($20mMa^{-1}$), so it is conceivable that variations in subsidence rate could occur between Haute Savoie and Haute Provence.

The average duration of the development of the Nummulitique cycles can be estimated from the total time of deposition of the formation divided by the number of

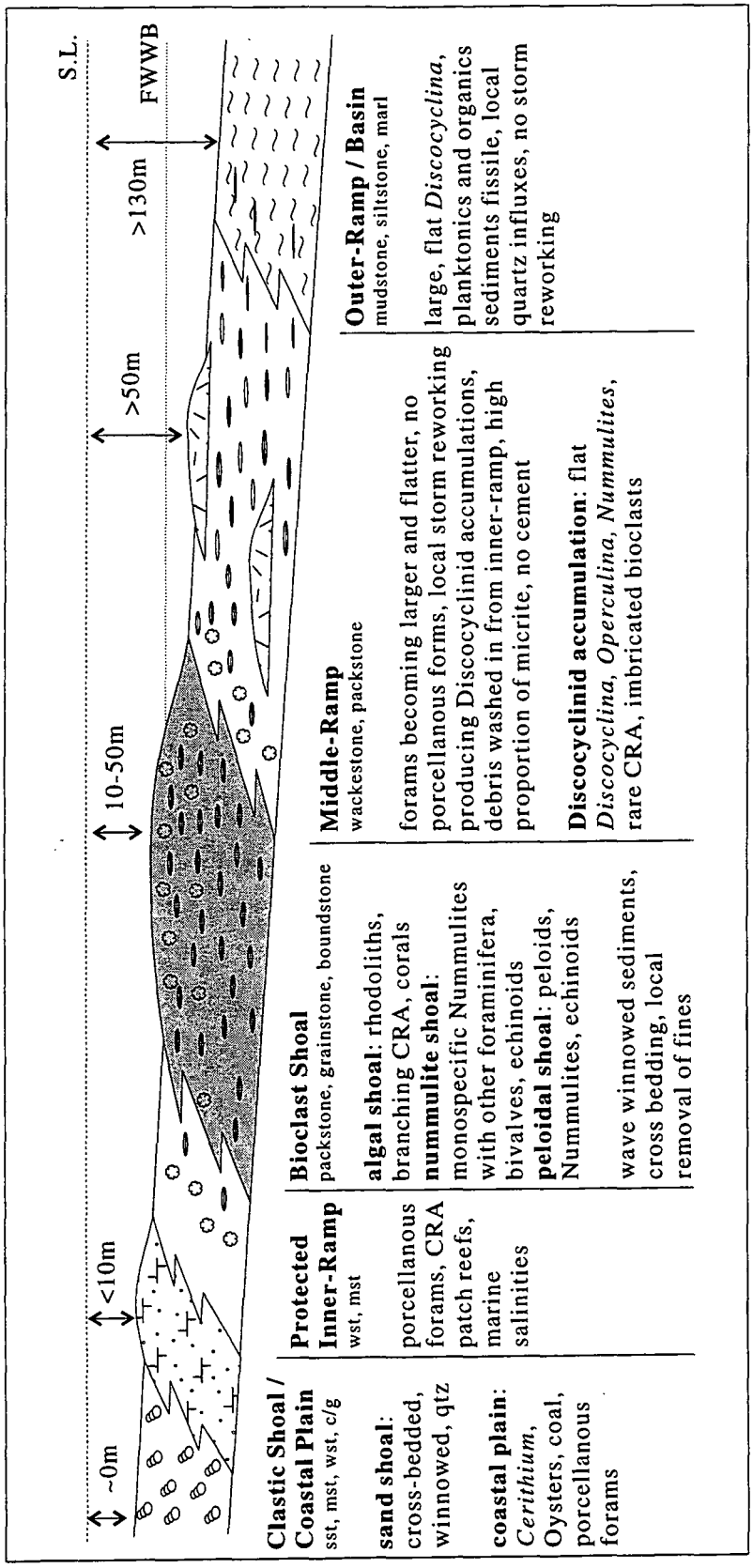

Fig. 7.11: Characteristic facies of the nummulitic carbonate ramp showing the distribution of foraminifera, algae and the main facies of the succession. Water depths are based on Racey (1990, fig. 7.4).

cycles developed. Due to the poor constraint of dating within the Infranummulitique, the cycle duration has been calculated only for the Nummulitic Limestone, with the estimate based on the thickest sections measured as these represent the maximum development of the limestone. In Haute Savoie the thickest sections contain eight cycles developed between mid-P16 and the Eocene Oligocene boundary (Pairis, 1988; Weidmann at el., 1991; Gorin et al., 1989) representing 1-1.5 Myr. In Haute Provence, eight cycles were developed between upper-P14 and upper-P15 (1.5-2 Myr). The duration of the cycles varies from 125-180 kyr in Haute Savoie and 180-200 kyr in Haute Provence.

Thus, the possible rates of rsl change during the development of the high frequency cycles were approximately 50m per 100 kyr, i.e. 5mm/yr, a rate which is comparable to that of glacio-eustatic sea-level variations.

7.6.2. Causes of relative sea-level variations

7.6.2.1. Eocene eustatic sea-level curve

The Eocene eustatic sea-level curve of Haq et al. (1988) is reproduced in Fig. 7.12. This shows sea-level falls at the base of the Lutetian (100m), Bartonian (40m) and Priabonian (75m) with subsequent rises of the same order of magnitude as the fall. Such sea-level changes would produce erosion and subsequent transgression as seen in Arâches (large nummulite limestone), Haute Provence and Haute Savoie respectively. However, the magnitude of the fall does not account for the amount of erosion produced at the basal unconformity, and the long-term sea-level curve depicts an overall lowering of eustatic sea-level from mid-Ypresian to the end Priabonian with a subsequent rise in the Oligocene. The sediments in each field area demonstrate an overall deepening trend from the basal unconformity, through the Nummulitique and into the *Globigerina* Marls, with the drowning of the carbonate platform in both areas corresponding to a sea-level fall on the eustatic curve; however, it must be emphasised that the inaccuracy of dating the formation means that the correlation of an event in the stratigraphic record is difficult to tie-in with the Haq et al. (1988) eustatic sea-level curve. The overall discrepancy in rsl variations between the French Alpine Foreland Basin and the Haq et al. (1988) eustatic sea-level curve indicates that eustasy was unlikely to be the dominant control on the development of the sedimentary succession being discussed here, though it is probable that short term, small-scale eustatic variations were responsible for the cyclicity produced within the formation, the duration of which is the same order of magnitude as the 4th order sea-level variations of Vail et al. (1977).

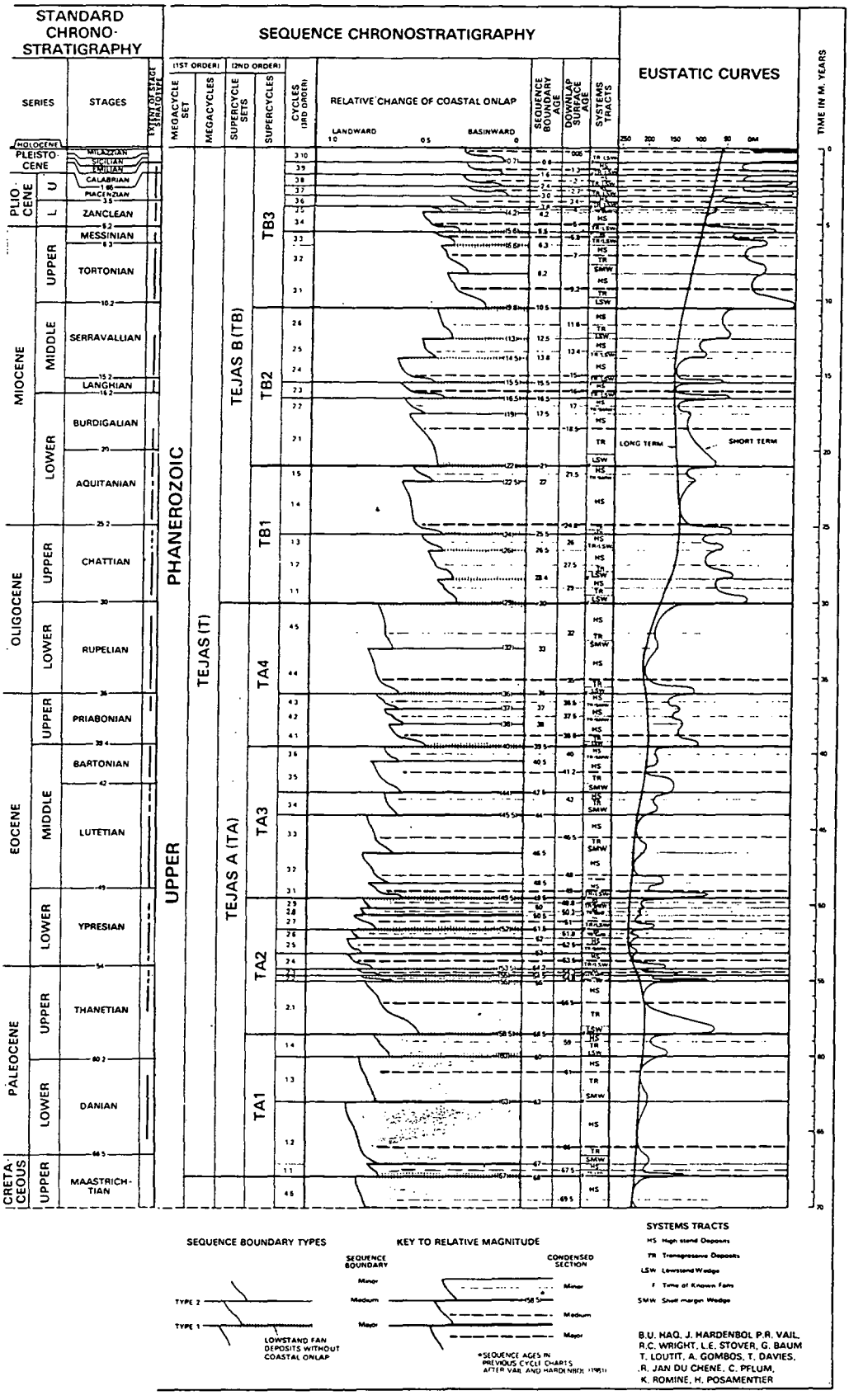

Fig. 7.12: Extract of the Cenozoic eustatic sea-level curve from Haq et al. (1988).

7.6.2.2. Tectonism

As eustasy is unlikely to be wholly responsible for the stratigraphic succession produced in the Nummulitique, it is necessary to invoke another control on the relative sea-level variations, the most obvious of which is the development of the Alpine Foreland Basin.

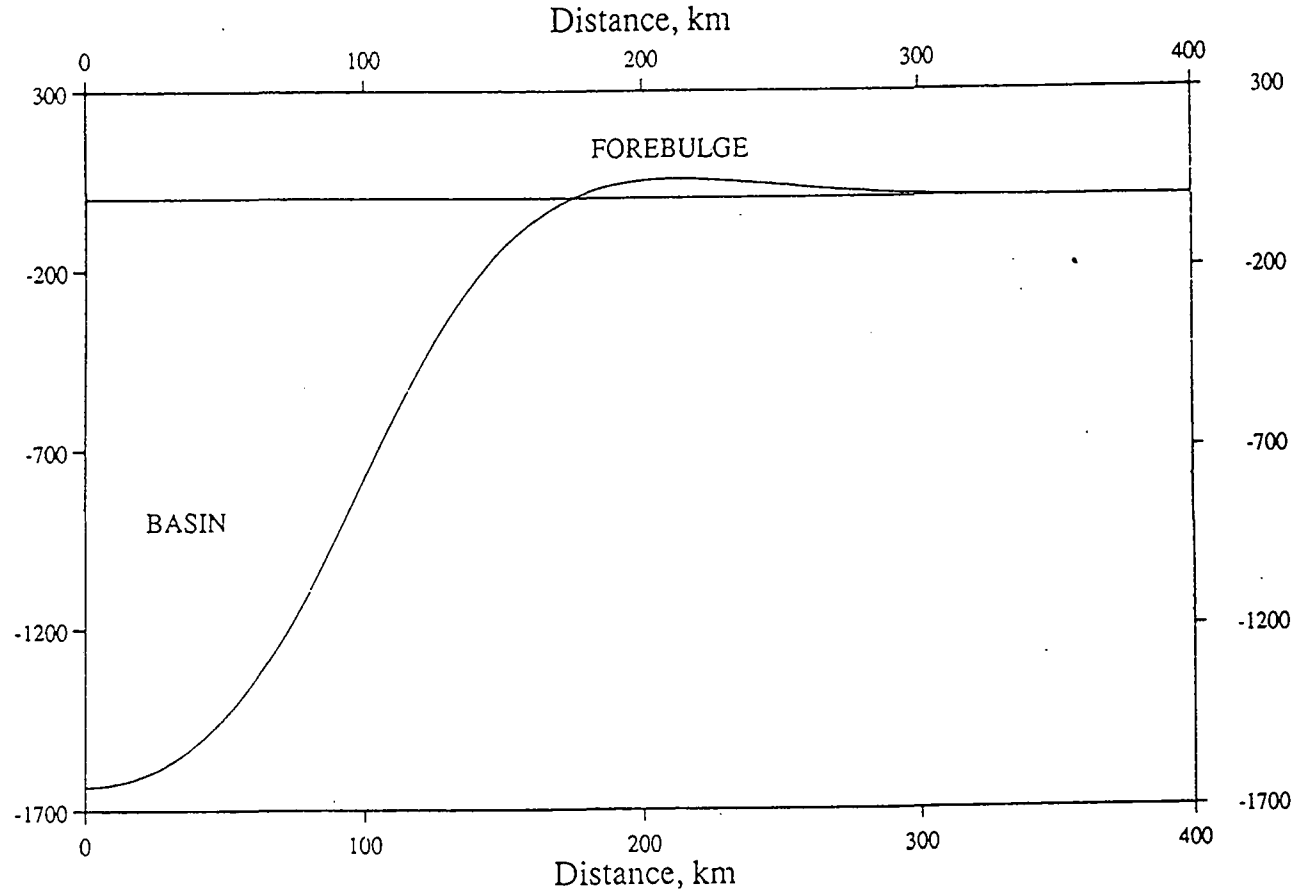

Fig. 7.13: The flexural response of a plate (Te = 15km) to loading by an orogenic wedge. From Crampton (1992, fig. 2.1).

Foreland basins have a convex-up subsidence curve with an initial phase of forebulge uplift followed by accelerating subsidence of a fixed point on the foreland plate as the orogenic load approaches (Fig. 7.13), producing an asymmetric basin which deepens towards the mountain belt. Forebulge uplift, which produces prolonged exposure of a foreland plate with up to 200m of erosion (Plint et al., 1993; Crampton and Allen, 1995), may contribute to the development of the basal unconformity in conjunction with other tectonic events (see Chapter 6). Rates of subsidence for the underfilled stage of the Alpine Foreland Basin in the Champsaur were estimated by Crampton (1992) as having values of 40 mMa^{-1} for the Nummulitic Limestone, 80 mMa^{-1} for the Globigerina Marls and 250 mMa^{-1} for the Taveyannaz Sandstone.

Continual subsidence in a basin enhances the rises on the resultant rsl curve (Fig. 7.14), producing a sea-level staircase (Morrow, 1986). The increasing subsidence rate

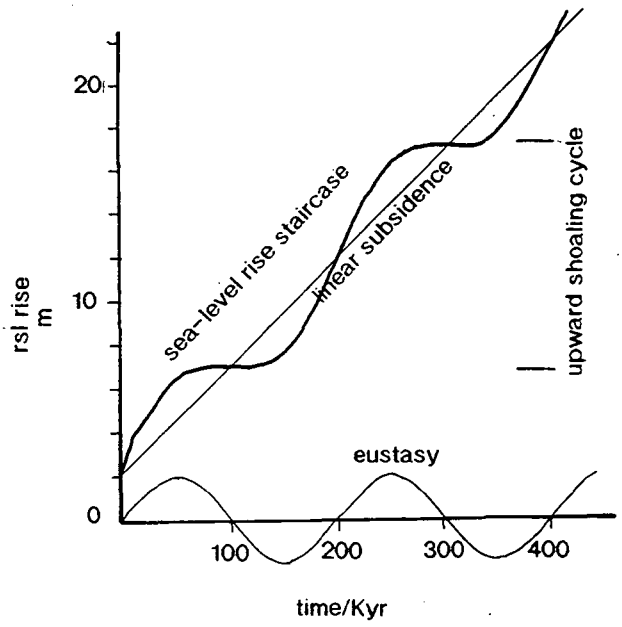

Fig. 7.14: Sea-level staircase produced by the superposition of a sinusoidal eustatic sea-level curve and linear subsidence, showing the enhancement of rises on the rsl curve. This effect is thought to have occurred in the underfilled Alpine foreland basin, though the effects of increasing subsidence rates with time produce progressively greater amplification of sea-level rises as the basin develops. After Morrow (1986, fig. 2).

in a foreland basin will significantly affect the relative sea-level curve for the basin, as the magnitudes of rate of subsidence become significantly greater than those of eustatic sea-level change, estimated as 10-90 mMa^{-1}, though glacio-eustatic rates may exceed this value (Schlager, 1991; Bosscher, 1992; Blanchon and Shaw, 1995). This indicates that as the basin develops eustatic variations should produce a less marked effect on the stratigraphy of the basin fill (Fig. 7.15). This is observed in the Nummulitique, with rsl falls producing exposure clearly evident during the deposition of the Infranummulitique during the earliest stages of subsidence, when subsidence rates were not sufficient to counteract the effects of eustatic sea-level falls; subaerial exposure is evident in the sedimentary succession in palaeosol development and increased clastic influxes. By the time of the marine transgression producing the Nummulitic Limestone, the increase in water depth due to subsidence accentuates the rising portion of the rsl curve, such that the subsequent eustatic sea-level falls cannot counteract the effects of increasing subsidence and therefore do not lead to subaerial exposure, but allow the carbonate system to build up above FWWB developing the bioclast shoals. As subsidence rates continue to increase, the rises in rsl can no longer be compensated for by the productivity of the carbonate system and the platform

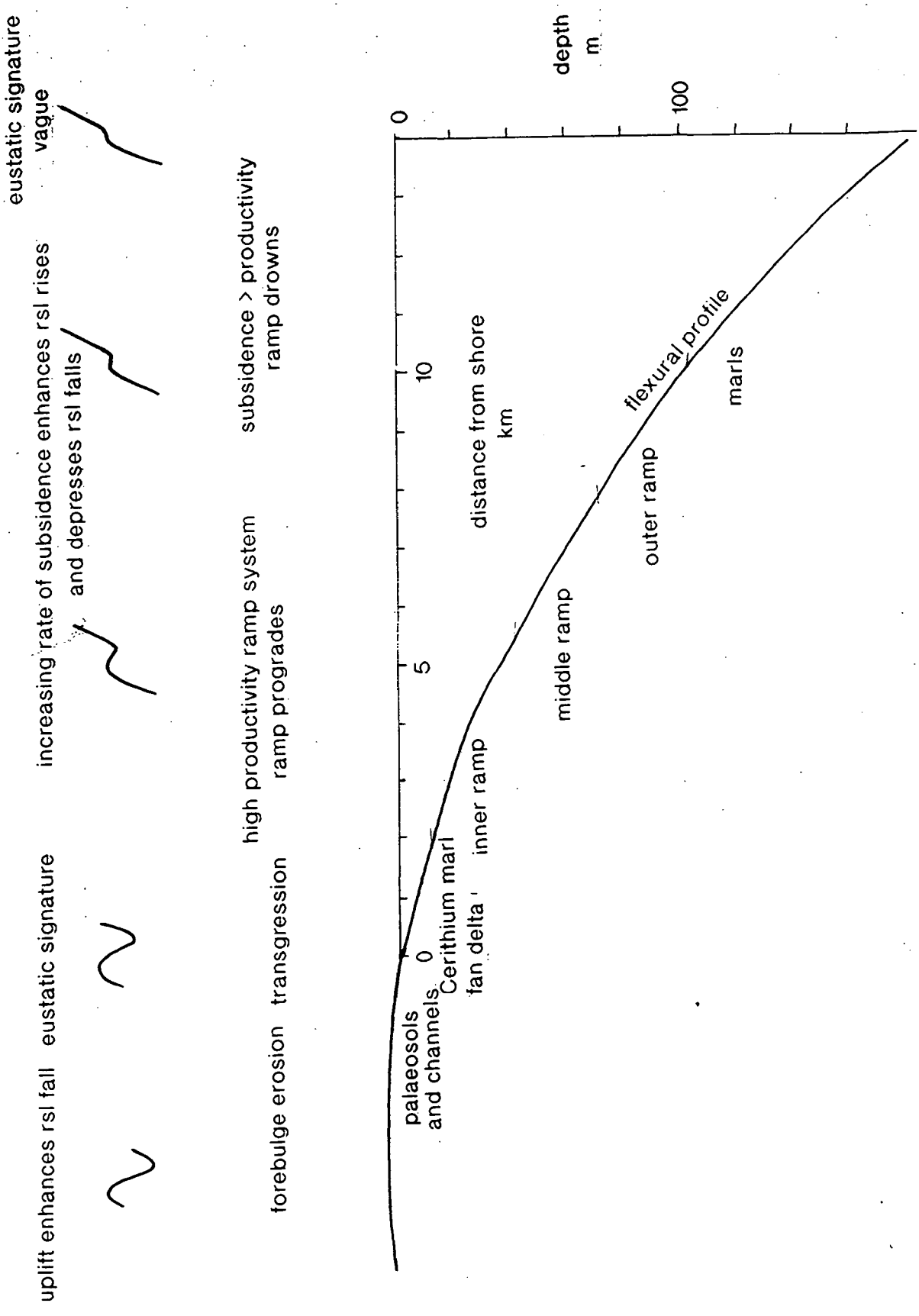

Fig. 7.15: Relative sea-level variations in the Alpine foreland basin. Flexural profile based on Crampton (1992, fig. 2.6): Te = 10km, thrust advance rate = 5mm/yr leading to a migration of 10km in 1Ma. The upper part of the diagram shows the varying rsl curve as subsidence rates increase and the relationship to the stratigraphy in the Nummulitique.

drowns. However, the combination of eustasy and tectonic subsidence is still less than the growth potential of a healthy carbonate platform, indicating that the productivity of the platform has been reduced by some other factors, which will be discussed below.

The above discussion suggests that tectonics are the controlling factor in the creation of accommodation space within the basin, producing the deepening-upwards stratigraphy characteristic of the Alpine Foreland Basin. Tectonic processes may also contribute to the cyclicity observed within the formation, by way of the effects of intra-plate stresses or episodic convergence.

Fluctuations in intra-plate stresses have been invoked as a cause for third-order sea-level changes, the effects of which can produce sea-level fluctuations of 10-100m (Cloetingh, 1988). The effects of intra-plate stresses in a foreland basin are particularly evident in the forebulge region, where compressive or tensional stresses may increase or decrease the height of the forebulge respectively, modifying the onlap pattern produced in the basin stratigraphy, and reactivating basement structures. However, the fluctuations of intra-plate stresses described from passive margins are in the order of a few tens of millions of years which is an order of magnitude larger than the duration of deposition of the Nummulitique. Thus, intra-plate stresses may modify the development of the foreland basin, but are of too long a duration to influence the cyclicity within the Nummulitique.

Variations in subsidence and hence accommodation space may also be produced by episodic loading of the foreland plate. Varying nappe migration rates within the orogenic wedge have been cited as affecting the development of foreland basin stratigraphy from basins around the world. Sinclair et al. (1991) explained the existence of the base Burdigalian unconformity in the Molasse fill of the North Alpine Foreland Basin as being due to a slowing of the thrust advance rate associated with the underplating of the external massifs, and Jordan (1981) modelled the variations in foreland basin topography by the emplacement of individual thrust nappes. Cyclicity associated with thrust emplacement in the Pyrenees has been described by Puidefabregas et al. (1986), and Quinlan and Beaumont (1984) showed that episodic advance of the orogenic wedge would produce a relaxation of the flexed lithosphere during pauses in orogenic advance producing a migration of the forebulge towards the deformation front and erosion of the basin fill. This is not seen to occur in the underfilled Alpine Foreland Basin. The emplacement of individual thrust nappes as the cause of cyclicity within the Nummulitique was discounted by Crampton (1992) in modelling the Swiss Alpine Foreland Basin. She noted that within the time-scale of the cyclicity of the formation (100kyr), thrust emplacement, which is thought to occur at 10-20mmyr^{-1}, would not be sufficient to produce a significant sea-level change

within the overall basin subsidence to produce the observed cyclicity, but that thrust emplacement may control longer-term transgressions, though dating of fault movements is not accurate enough to constrain this.

7.6.3. Relative sea-level during the deposition of the Nummulitique

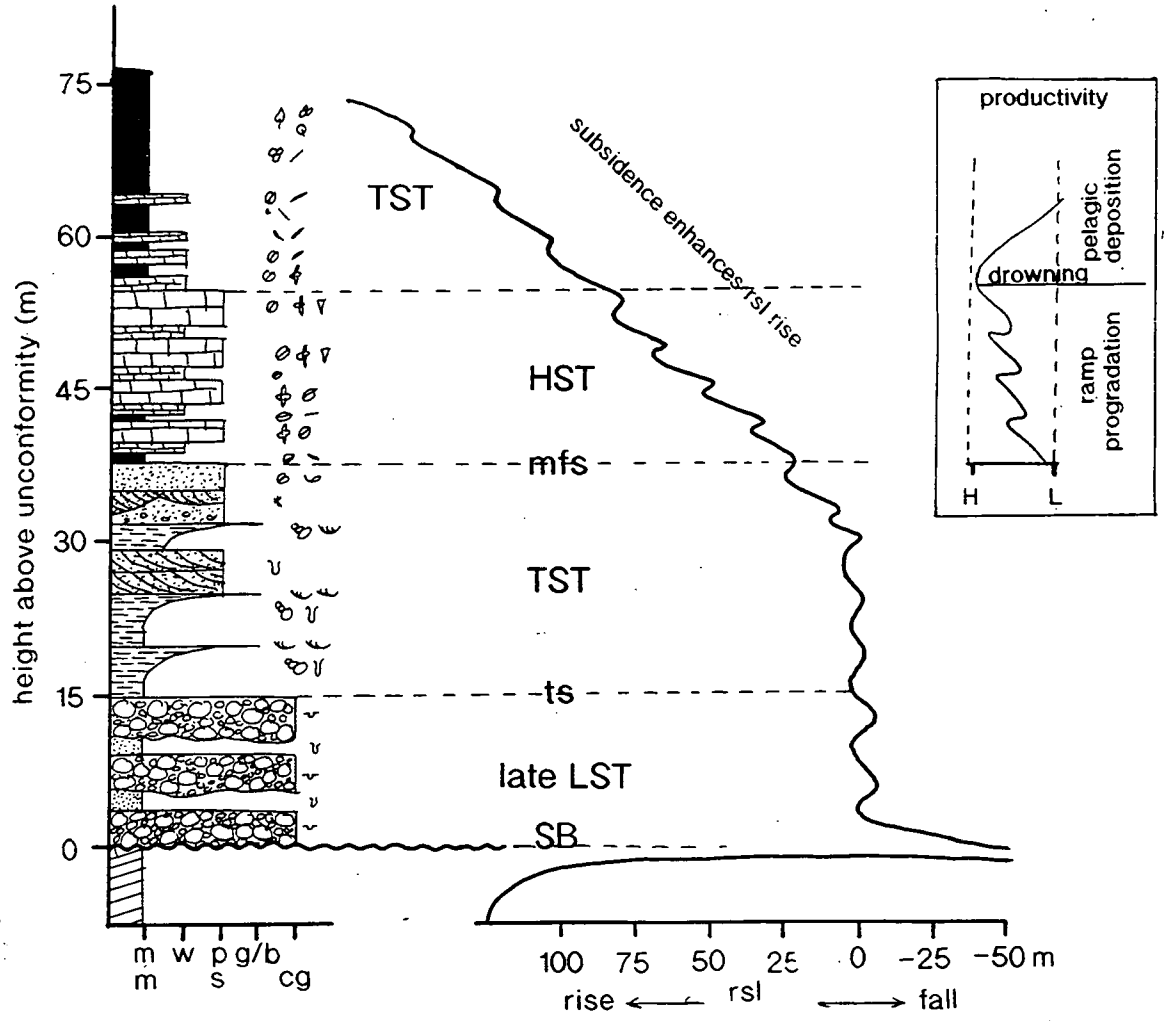

Fig. 7.16: Simplified vertical section through the Nummulitique Formation showing the relative sea-level variations producing the deepening upwards succession and the small-scale cyclicity. The sequence stratigraphic interpretation is shown to the right of the log. Magnitudes of rsl variations are approximate and based on the benthos distribution shown in Fig. 7.11. The insert shows the varying productivity during the development of the carbonate ramp system. Flooding events temporarily reduced productivity but the system was able to catch up until external factors (nutrients, climate, clastics) caused a drastic reduction in productivity and the ramp drowned.

The relative sea-level curve responsible for the deposition and drowning of the Nummulitique (Fig. 7.16) is interpreted to be dominated by the effects of foreland basin subsidence, with the 3rd order eustatic sea-level variations, possibly enhanced by tectonics, producing the sequence development within the overall sea-level rise and

4th order eustatic sea-level variations producing the cyclicity within the formation (sea-level staircase effect of Morrow, 1986). The existence of a eustatic signature on a tectonically controlled relative sea-level curve has also been suggested by workers from the Alberta Foreland Basin (Plint et al., 1993) and the Pyrenees (Pujalte et al., 1993).

7.6.4. Platform drowning

Though the relative sea-level curve demonstrates a progressive increase in the creation of accommodation space, the productivity of a healthy carbonate system should be able to keep pace with this. The rapid demise of the carbonate system in the Alpine Foreland Basin therefore indicates a reduction in the productivity of the carbonate system promoting platform drowning, and this could be due to a number of factors.

7.6.4.1. Nutrient excess

As has already been discussed in Section 7.1, an increase in the amount of nutrients supplied into a system can significantly reduce the productivity of a carbonate platform. Towards the top of the Nummulitique, the proportion of detrital quartz and organic particles increases indicating a renewal of terrigenous input into the distal part of the foreland basin as the proximal siliciclastics advanced ahead of the deformation front. The terrigenous run-off from the advancing orogeny will produce an influx of nutrients into the basin due to high weathering rates in the orogenic wedge feeding nutrients into rivers. Hallock and Schlager (1986) proposed that this nutrient influx will affect the carbonate system before burial of the succession beneath the advancing siliciclastic wedge due to the effects of a "nutrient halo" advancing ahead of the siliciclastics. The effects of these nutrient-rich waters reaching the distal side of the basin ahead of the siliciclastic flysch (Taveyannaz and Annot Sandstones) may be sufficient to have reduced the productivity and hence growth rate of the carbonate ramp such that it could no longer keep up with the creation of accommodation space as subsidence rates increased. Hallock and Schlager (1986) proposed this effect as being the cause of reduced productivity and hence platform drowning and transition to starved basin deposition during the development of the Ordovician Appalachian Foreland Basin. Thus, the effect on carbonate productivity of nutrient-rich waters derived from terrigenous input from the orogenic wedge may be a contributory, though neglected, factor in the carbonate-to-starved-basin transition in other foreland basins.

7.6.4.2. Siliciclastic influx

Walker et al. (1983) proposed that the influx of siliciclastics was the dominant factor in reducing the productivity of the carbonate platform of the Appalachian foreland basin. This productivity reduction occurs due to increased turbidity of the basin waters reducing light intensities and increased nutrients affecting suspension feeders in distal regions of terrigenous influx. However, this is very closely liked to the effects of the "nutrient halo" described above. Schlager (1981) stated that poisoning of a carbonate system by siliciclastics generally occurs during a sea-level highstand. The drowning of the nummulitic carbonate ramp occurred prior to the maximum flooding surface of the underfilled foreland basin during the transgressive systems tract. The maximum flooding surface occurs some 30m into the Globigerina Marls (Thome, 1987) and significantly before the onset of clastic sedimentation. Though an increase in detrital, silt-grade quartz is seen during the transition to the marls, this is generally only of the order of 5-20%, with some localities experiencing no quartzitic influx during platform drowning. This proportion of quartz is significantly less than that deposited at the base of the formation after which the carbonate system proliferated. This indicates that poisoning of the system by siliciclastic influx is not a significant factor in causing the demise of the carbonate ramp, though it may have enhanced the effects of other factors.

7.6.4.3. Climatic cooling

A pulse of global cooling occurred around the Eocene/Oligocene boundary following a general climatic cooling trend from Middle Eocene times (Keller, 1983; Shackleton and Kennet, 1975), determined from stable isotope studies on foraminifera and deep-sea drilling in low latitudes of the northern hemisphere and high latitudes of the southern hemisphere. These studies indicate that cooling occurred episodically, with the peak occurring at the Eocene/Oligocene boundary. The effect of this cooling event has been described from the north-eastern Australia platforms of the Great Barrier Reef system (Davies et al., 1989, fig. 16), where cooling produced a transition from tropical, chlorozoan faunal assemblages to temperate, foramol assemblages (Fig. 7.17). The coolest temperatures were around the Eocene/Oligocene boundary and during the early Oligocene, after which climatic warming produced a return to tropical conditions during the Miocene.

As discussed before climatic cooling can increase the influx of terrigenous clastics and hence nutrients into a system as well as the temperature affecting the faunal assemblages (Tucker and Wright, 1990; Schlager, 1981). The assemblage of the Nummulitique is foramol to rhodalgal (Carannante et al., 1988), being dominated

by benthonic foraminifera and CRA with rare corals, and is indicative of cooler, sub-tropical to temperate waters. Thus climatic cooling may not have significantly affected

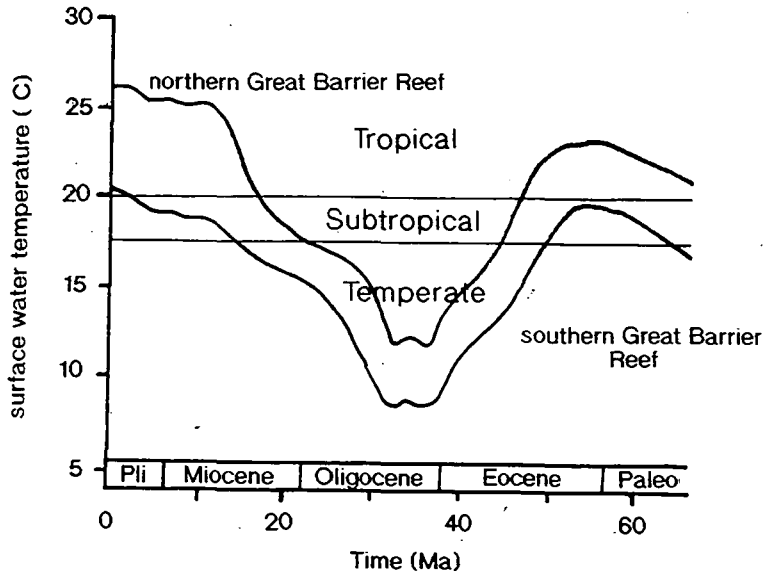

Fig. 7.17: Climatic variations and their effects on the carbonate platforms of north-east Australia. Note the low occurring around the Eocene/Oligocene boundary. After Davies et al. (1989).

the benthos, as the genera are tolerant of cooler waters, but it may have contributed to the demise of the carbonate system by a reduction in the productivity of those organisms through a lowering of water temperatures and an increase in the terrigenous input into the system.

The drowning of the nummulitic carbonate ramp is interpreted to be the result of a number of closely related factors dominated by the accelerating subsidence of the basin and the increase in nutrients due to the progradation of the siliciclastic flysch across the basin. The increase in nutrients, possibly aided by the onset of siliciclastic input, is thought to have contributed to the reduction in carbonate productivity and growth potential of the ramp system, such that it was no longer able to keep up with the increasing rates of subsidence and the creation of accommodation space. This led to the backstepping and eventual drowning of the platform and the transition to pelagic marl deposition. The more abrupt drowning that occurs in Haute Savoie compared to Haute Provence is interpreted to be due to the additional effect of the pulse of global cooling at the Eocene/Oligocene boundary, reducing productivity and coincident with the drowning in this area, but occurring during deposition of the marls elsewhere in the basin.

7.7. Correlation

The cyclicity described in Section 7.4. has been used to attempt a sequence stratigraphic correlation of the sedimentary sections measured in each field area, taking into account the diachroneity of the basin development. Correlations have been carried out within each field area (the palaeogeographic relationships of the measured sections are shown in Fig. 7.18), but no attempt has been made to correlate between the two areas due to the different ages of the formation. Due to the poor resolution of the biostratigraphic dating, it is virtually impossible to tie a particular rsl variation with an event on the eustatic sea-level curve of Haq et al. (1988) and it is therefore impossible to tie the cycles of similar age in the two areas.

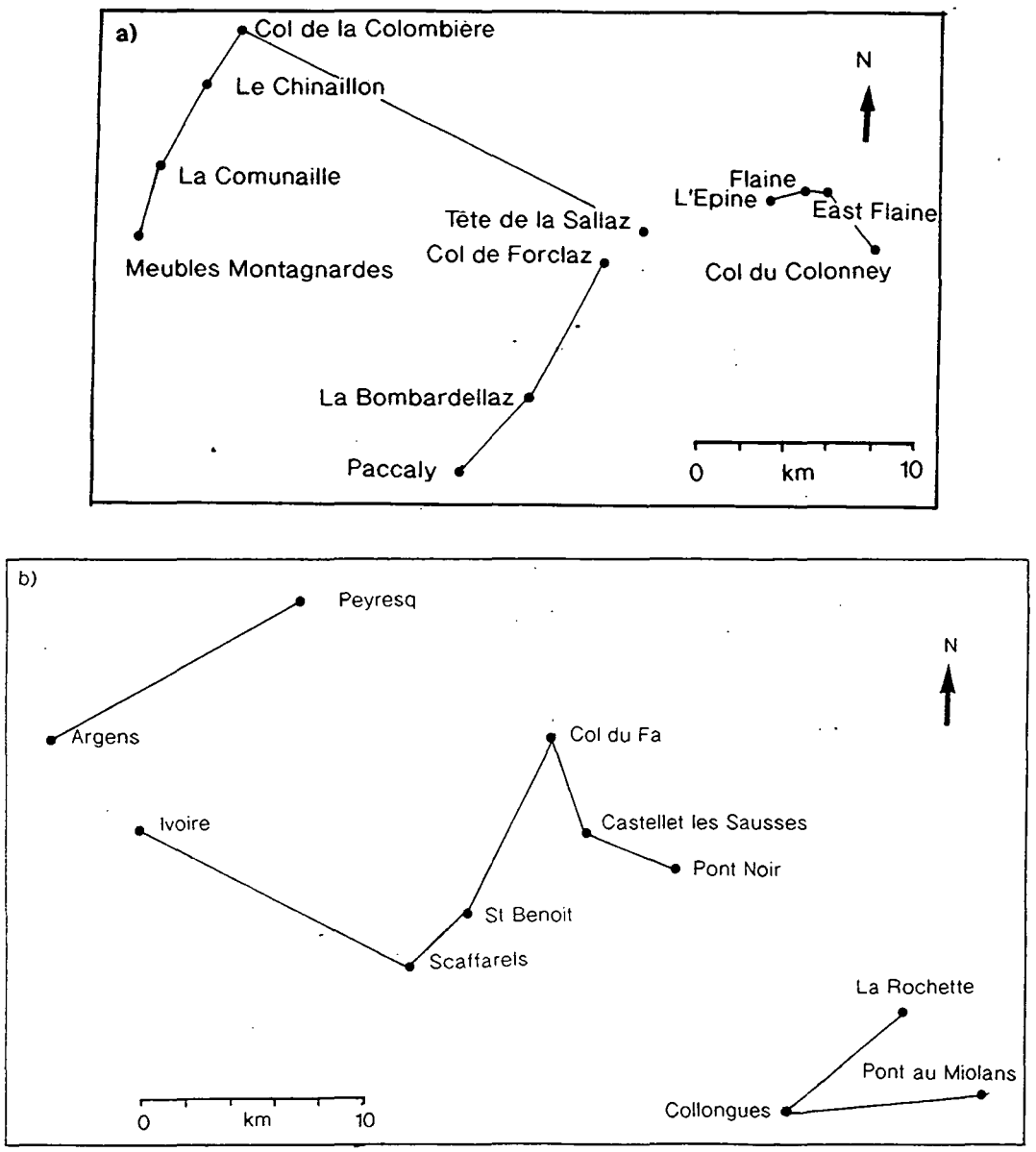

Fig. 7.18: Palaeogeographic relationships of measured sections in a) Haute Savoie and b) Haute Provence. Line length restorations based on sections in Guellec et al. (1990; Haute Savoie) and Sinclair (in press; Haute Provence).

Fig. 7.19: Correlation of the sections measured in the west and central Thônes Syncline, Haute Savoie showing the restored distances between localities.

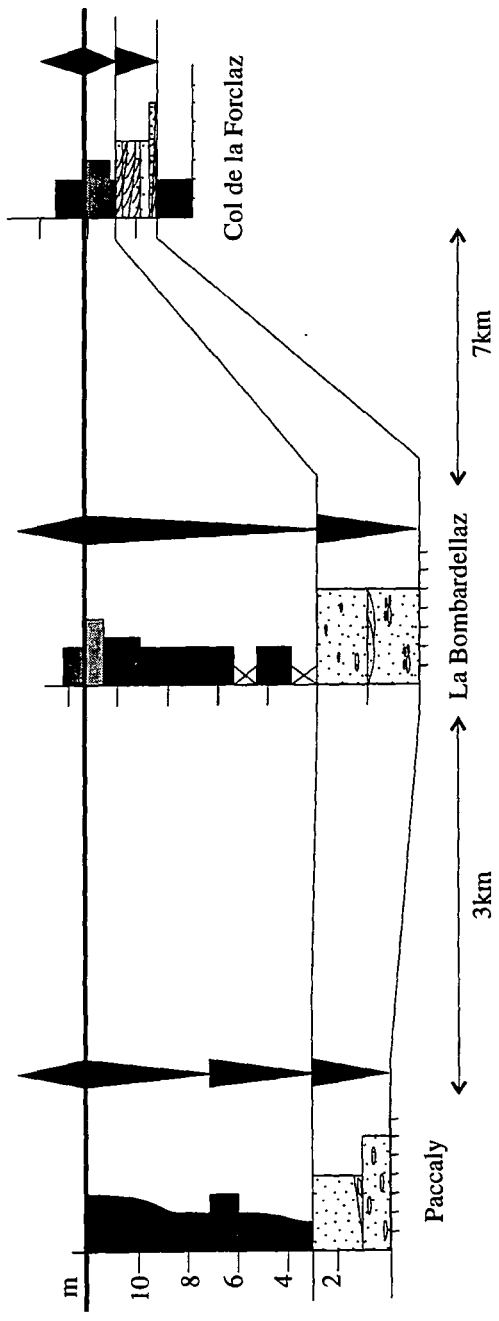

Fig. 7.20: Correlation of sections measured in the east Thônes Syncline, Haute Savoie, showing the restored distances between localities.

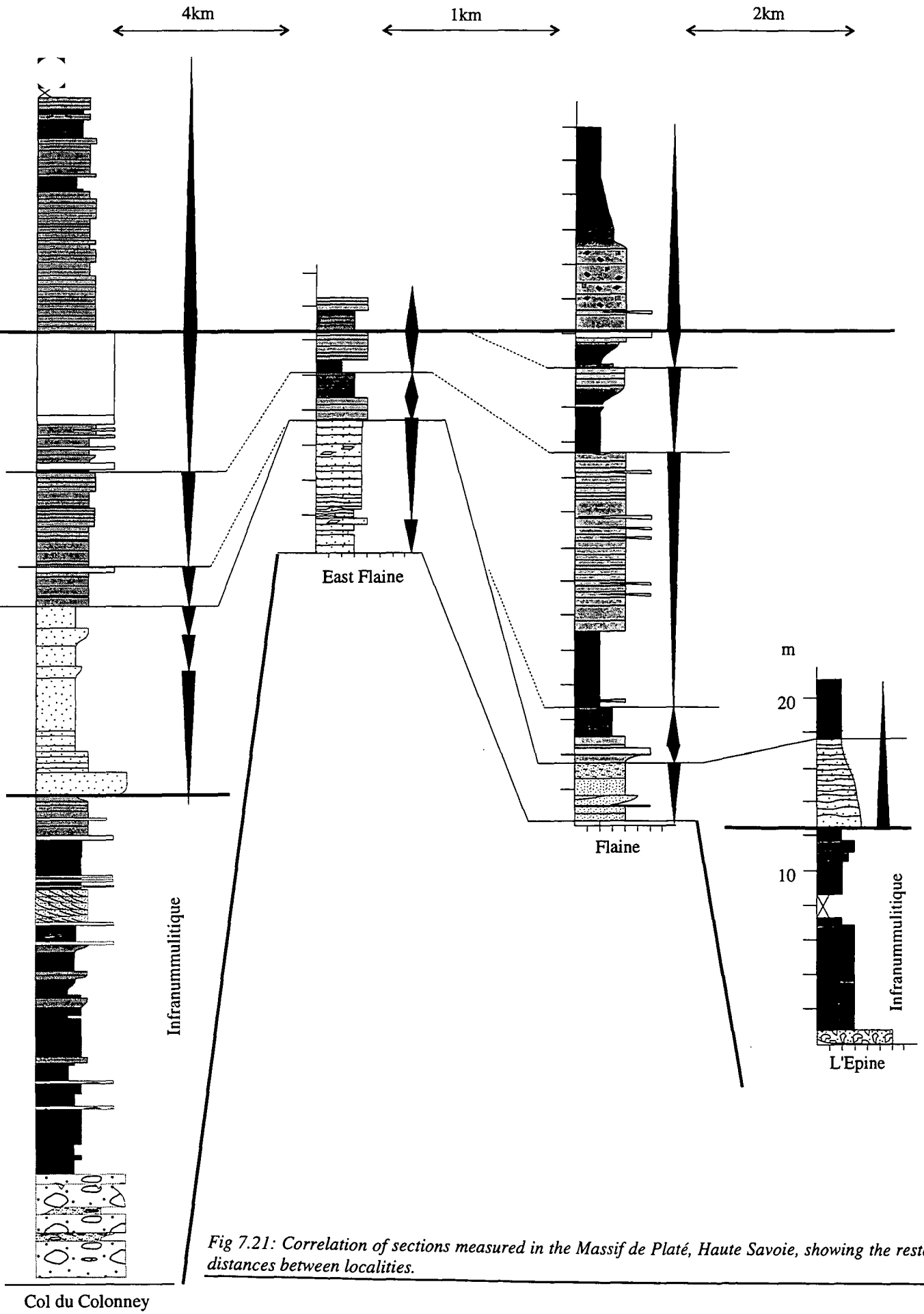

Fig 7.21: Correlation of sections measured in the Massif de Platé, Haute Savoie, showing the restored distances between localities.

The correlation lines have been hung from the ramp drowning surface, above which carbonate production rapidly decreased and which can be taken as synchronous within each area for stratigraphic purposes (Schlager, 1981). The flooding surfaces bounding the cycles are taken as time-lines as they are thought to represent the eustatic signature on the relative sea-level curve for the basin and have been used to correlate within the formation and show the lateral variation in facies in a given time period. The Nummulitic Limestone in Haute Savoie was initially considered in three distinct areas based on the facies present; west-central Thônes Syncline, east Thônes Syncline and the Massif de Platé, the correlations of which are shown in Figs. 7.19, 7.20 and 7.21. These were then linked to produce the fence diagram shown in Fig. 7.25, which demonstrates the lateral variability in the facies distribution. Haute Provence was divided by syncline, producing the correlations shown in Figs. 7.22 and 7.23, which were linked to produce the fence diagram shown in Fig. 7.26.

Problems occurred when attempting to correlate the Infranummulitique due to the limited distribution of the sediments and a lack of reliable age data. In Haute Savoie no attempt has been made to correlate between outcrops, as deposition was thought to have occurred within a compartmentalised developing basin. In Haute Provence good lateral exposure at Peyresq enabled the correlation of the logs measured around the village and an attempt has been made to tie the cycles developed at Peyresq with those in the lenticular conglomerates seen at Argens (Fig. 7.24). However, due to the lack of dating of the sediments it is by no means certain that the cycles developed at the two localities represent the same rsl variations.

7.8. Development of the Nummulitique

The development of the Nummulitique has been based on the fence diagrams shown in Figs 7.25 and 7.26. The locations of the measured sections were restored to pre-Alpine compression using the balanced cross-sections in Guellec et al. (1990) for Haute Savoie, and Sinclair (in press) for Haute Provence, and are illustrated on the maps in Fig. 7.18. The palaegeographic maps were constructed by projecting the localities along strike onto a restored cross-section. As the restored cross-sections were produced using line-length restoration, they will represent minimum values of shortening across the areas. The fence diagrams only show approximate palaeogeographic locations due to the problems of scaling and for clarity of illustration.

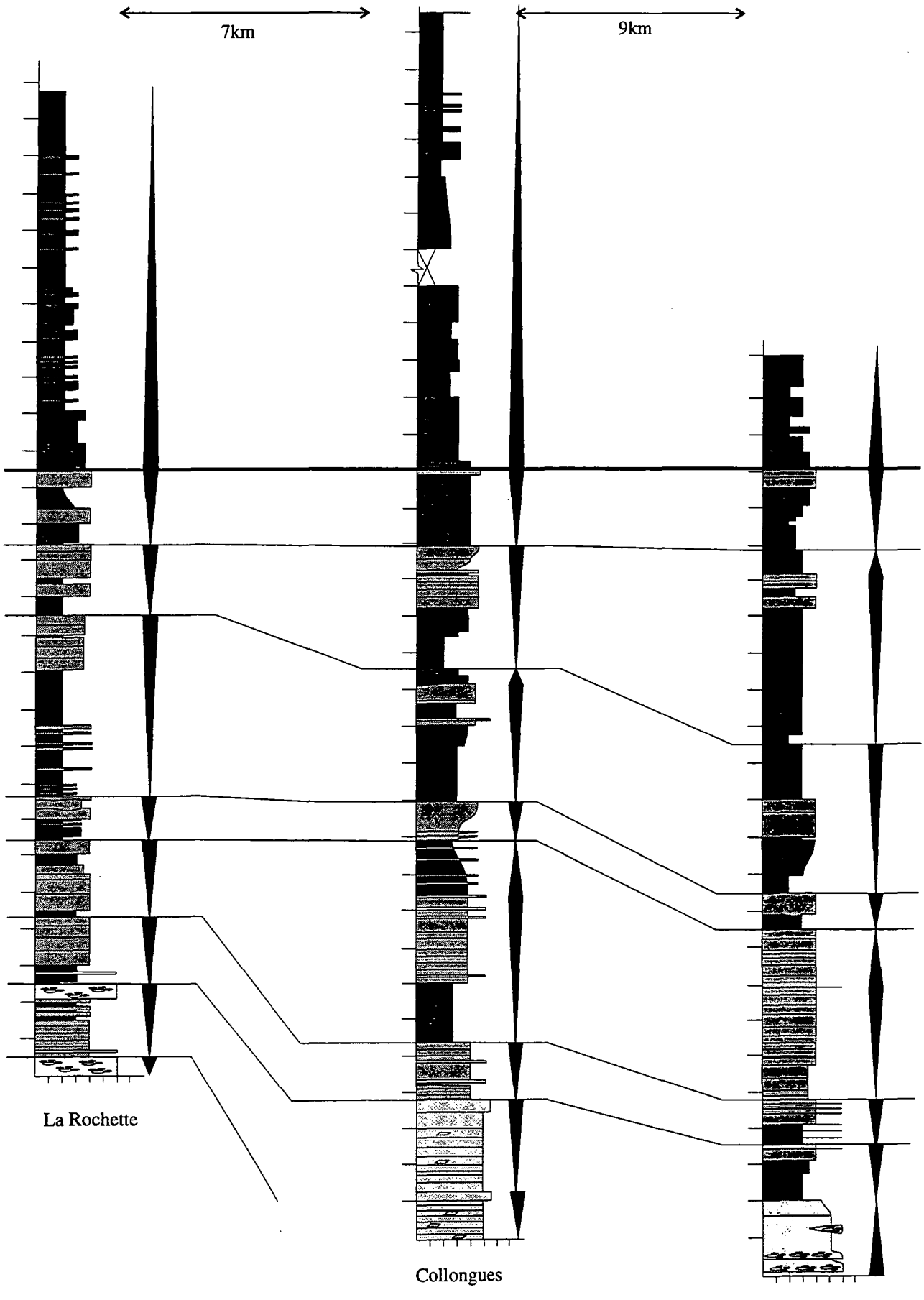

Fig. 7.22: Correlation of sections measured in the St Antonin Syncline, Haute Provence, showing the restored distances between localities.

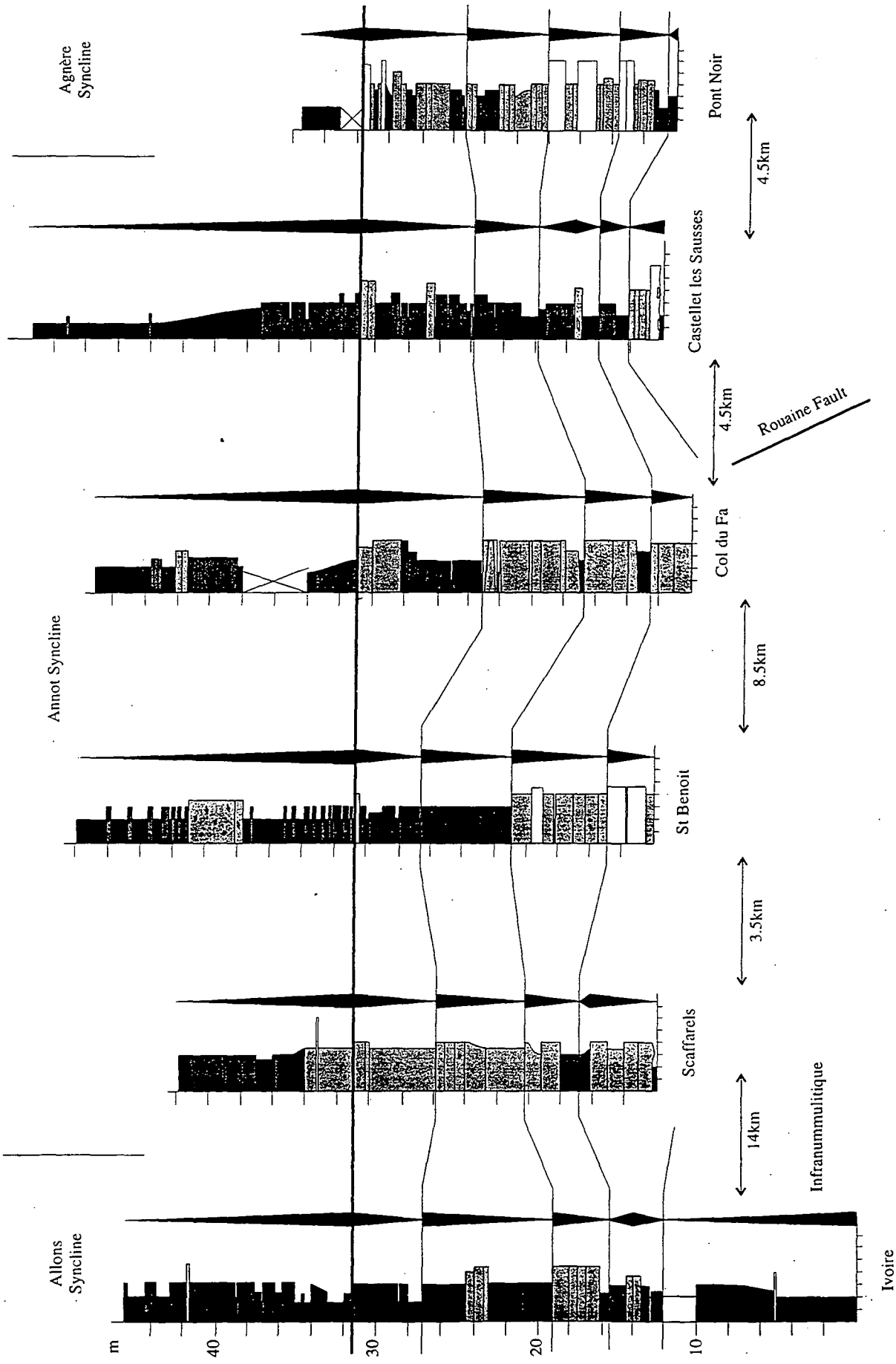

Fig. 7.23: Correlation of sections measured in the Allons, Annot and Agnère Synclines, Haute Provence, showing the restored distances between localities.

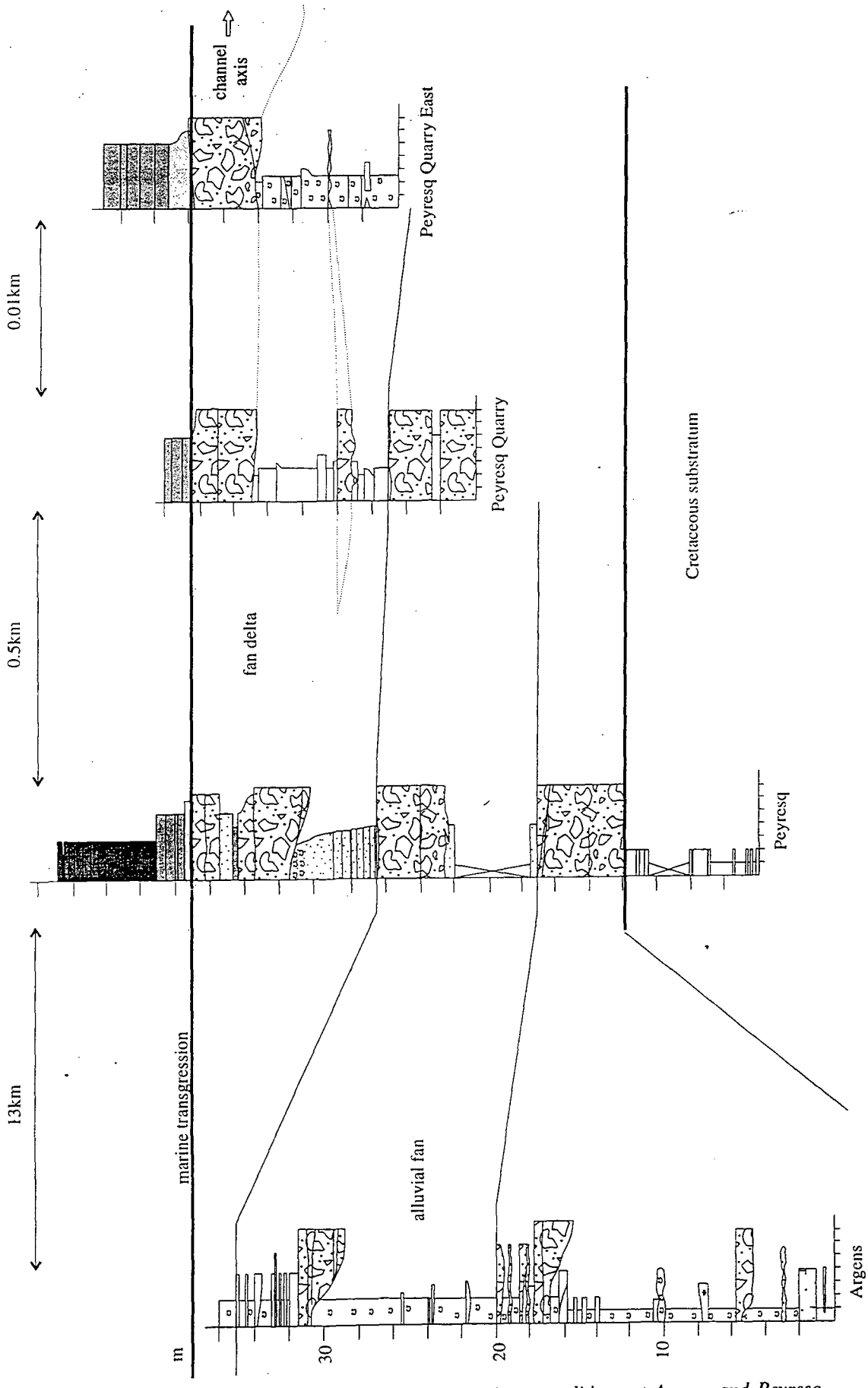

Fig. 7.24: Correlation of sections measured through the Infranummulitique at Argens and Peyresq, Haute Provence, showing the restored distances between localities.

7.8.1. Haute Savoie

Deposition of the Infranummulitique was localised to the Massif de Platé, where the various facies developed within pre-Nummulitic structural lows (Pairis and Pairis, 1975). It is probable that these lows (Desert de Platé, L'Epine, Arâches) were not connected during the deposition of the earliest deposits as the facies are not equivalent at each locality. Arâches saw the development of an early phase of nummulitic limestone prior to the deposition of the Infranummulitique elsewhere in the area. This may be an erosional remnant as reworked clasts of a limestone containing large *Nummulites*, similar to that in situ at Arâches are present in the conglomerates on the Desert de Platé. This limestone is interpreted to represent an early phase of marine transgression which was subsequently eroded and has only been preserved within a depositional low in the substratum. This was subsequently infilled with lacustrine sediments (Pairis and Pairis, 1975) which are not seen elsewhere in the field area, indicating that this locality was not affected by the earliest stages of the main transgression over the area. The Desert de Platé has the most developed Infranummulitique, with the onset of rsl rise indicated by the deposition of coarse terrigenous carbonates derived from local highs and deposited in a fan delta setting. Continuing rsl rise led to the shut down of coarse clastic supply into the basin and a coastal swamp/ lagoon developed extending as far as L'Epine, but was absent over the exposed highs around Flaine.

The first evidence of a widespread marine transgression affecting the area is a transgressive sandstone present at the base of the Nummulitic Limestone (basal clastic facies association). This sandstone is present in all sections except La Communaille, Meubles Montagnardes and Tête de la Sallaz. Reworked clasts of greensand, the substratum at La Communaille, are found in the transgressive sand at Le Chinaillon indicating that the three localities mentioned above were still eroding highs.

Continuing rsl rise shut down the supply of quartz and the carbonate factory was set up leading to the development of the nummulitic carbonate ramp. The lack of evidence for steep slopes during the deposition of the Nummulitic Limestone indicates that the topography had been smoothed by a combination of continuing erosion on the emergent highs and the early clastic sediments infilling the intermittent lows. Sedimentation in the area initiated in a middle-ramp setting, indicating water depths of >50m, but carbonate productivity was able to outpace the creation of accommodation space and the facies were able to build up to sea-level across most of the area. The NW limb of the Thônes syncline was an area of prolific algal development, with shoals and rarely patch reefs developing at Col de la Colombière, Tête de la Sallaz and Meubles Montagnardes; the previously exposed highs had now become sites for preferential shoal development. A basinal area developed to the SE,

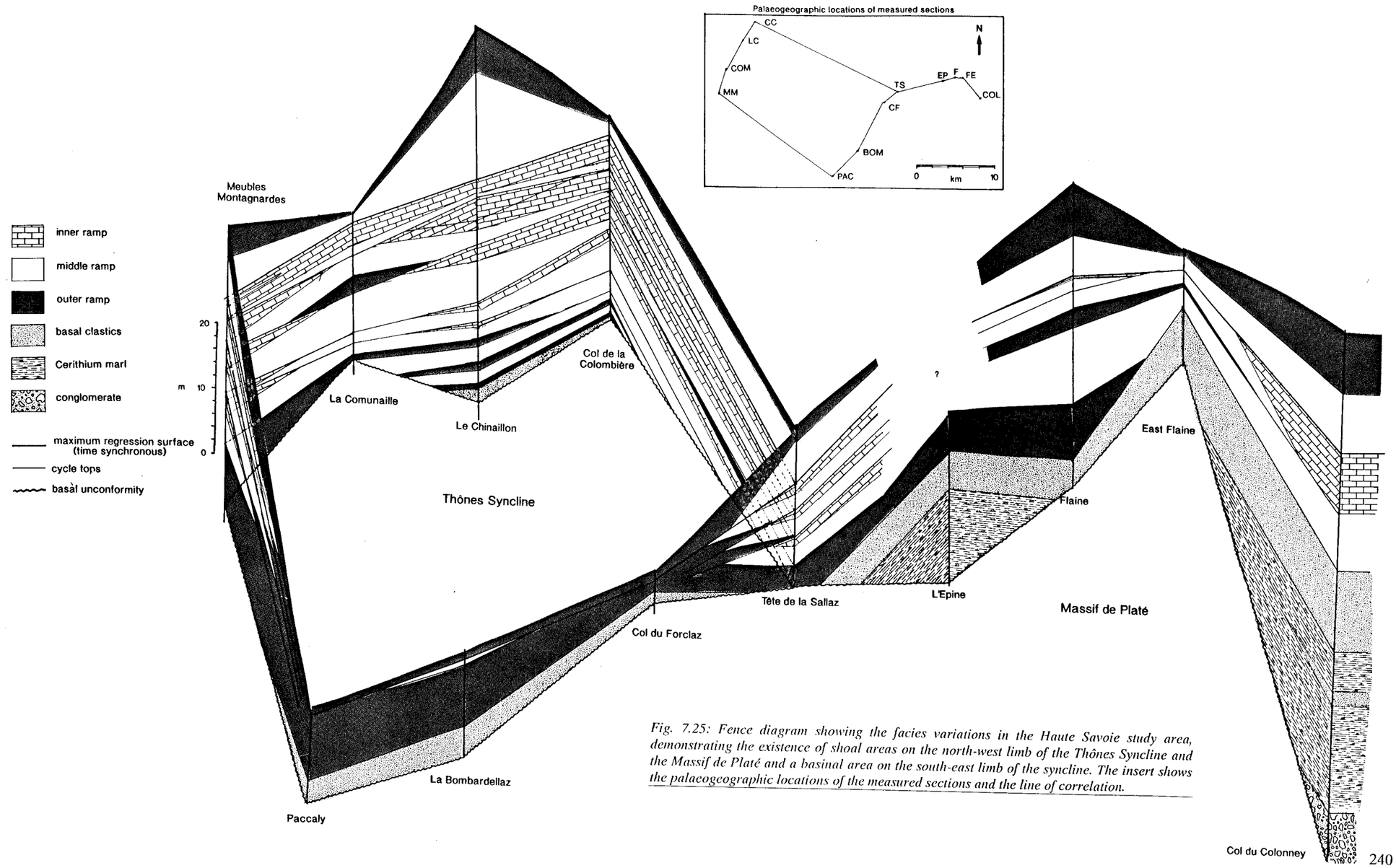

Fig. 7.25: Fence diagram showing the facies variations in the Haute Savoie study area, demonstrating the existence of shoal areas on the north-west limb of the Thônes Syncline and the Massif de Platé and a basinal area on the south-east limb of the syncline. The insert shows the palaeogeographic locations of the measured sections and the line of correlation.

with Paccaly, La Bombardellaz and Col de Forclaz developing a very thin succession dominated by middle and outer-ramp facies. The relationship between the Thônes Syncline and the Massif de Platé is unclear due to the erosion of the Arve Valley. The basinal area developed around Paccaly is thought to be a sub-basin developed due to topographic effects, though why no Infranummulitique was deposited here is unclear. It is not thought to represent a more distal setting within the foreland basin as the ages of the limestone in the Massif de Platé (shoal area) and the Thônes Syncline (basin and shoal areas) are equivalent. If Paccaly represented a distal foreland basin setting, then the shoal development on the Massif de Platé would represent an earlier phase of foreland transgression and the succession would be expected to be older than that in the Thônes Syncline.

The nummulitic ramp continued to prograde into the basin until the Eocene/Oligocene boundary, when a combination of increasing subsidence rates and a reduction in carbonate productivity caused the system to drown and be succeeded by hemipelagic deposition. The carbonate ramp is thought to have backstepped further onto the foreland as was the case in Switzerland and the Champsaur (Crampton, 1992) so that younger limestones are expected to have been deposited further west of the study area.

7.8.2. Haute Provence

The distribution of the Infranummulitique is again restricted to local depositional lows around Collongues, La Rochette and Amirat in the south of the area (Bodelle, 1971) and at Peyresq and Argens in the north. Due to poor exposure it is uncertain whether any Infranummulitique sediments were deposited in the Entrevaux and Puget-Theniers Synclines.

The Tertiary transgression appears to have commenced earlier in the SE of the area, with a thicker succession dated as Upper Bartonian to Lower Priabonian (Zone B, Bodelle, 1971) in the St Antonin Syncline compared with the northern synclines. As the Infranummulitique is thought to have been deposited directly before the marine transgression, this implies that the Infranummulitique in the south of the area is older than that in the north, due to a backstepping of facies to the NW as rsl continued to rise. The equivalent age of the transition to the marls in both the south and the north of the area suggests that carbonate ramp deposition was more prolonged in the south, which is indicated by a greater number of cycles developed in the St Antonin sections and a phase of retrogradation leading to middle-ramp deposition as the focus of inner-ramp sedimentation migrated to the north-west. The effects of pre-depositional topography are evident in the facies developed, with some sections (La Rochette, Castellet les Sausses, St Benoit) dominated by deeper water middle and outer-ramp

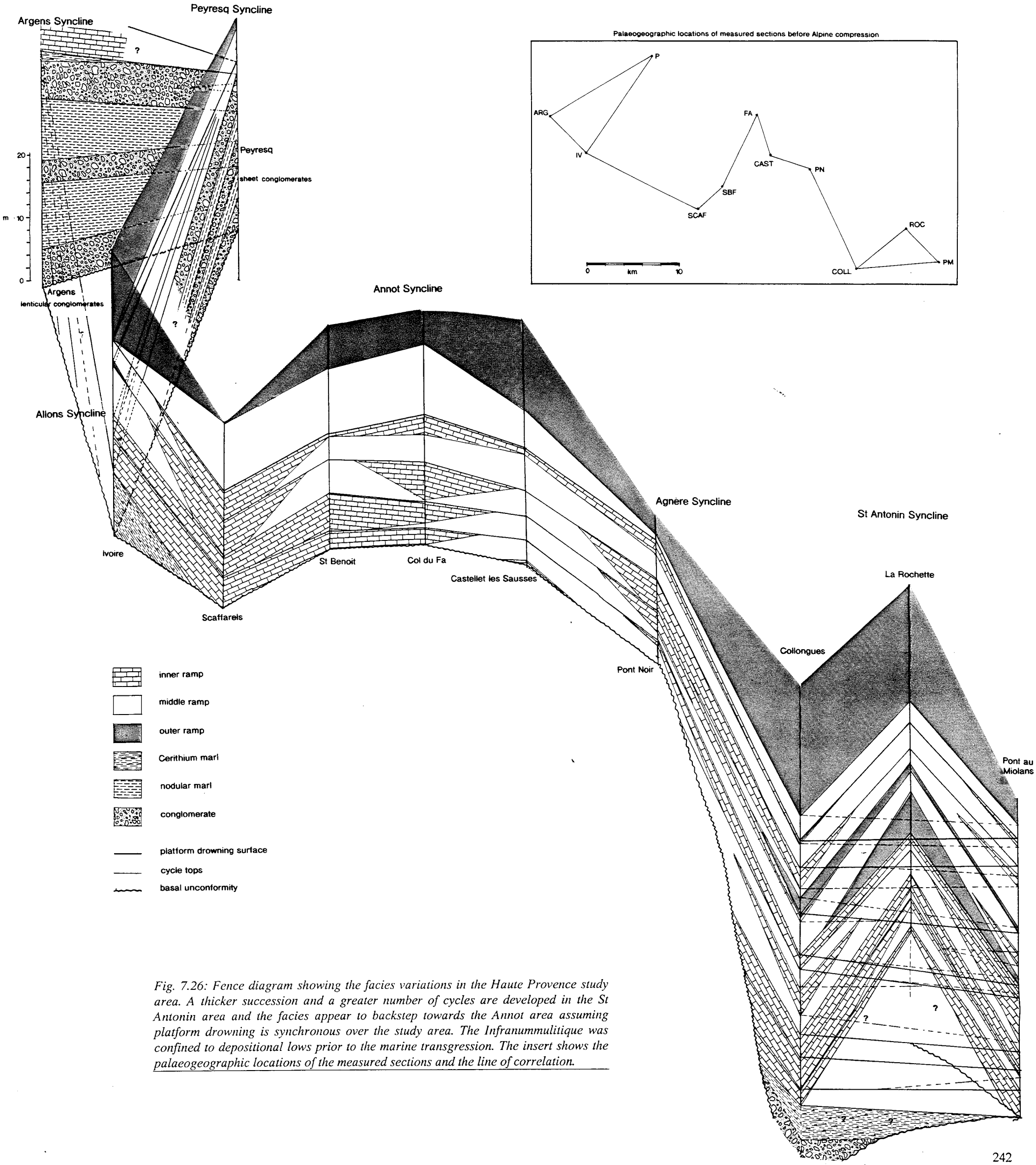

Fig. 7.26: Fence diagram showing the facies variations in the Haute Provence study area. A thicker succession and a greater number of cycles are developed in the St Antonin area and the facies appear to backstep towards the Annot area assuming platform drowning is synchronous over the study area. The Infranummulitique was confined to depositional lows prior to the marine transgression. The insert shows the palaeogeographic locations of the measured sections and the line of correlation.

facies and thought to have been deposited in morphological lows on the unconformity surface. The succession at Castellet les Sausses is presently located on the downthrown side of the Rouaine fault, which experienced major movement during the deposition of the Globigerina marls. The development of deeper water facies at this locality during the limestone deposition indicates that there may have been some activity on this fault prior to the marine transgression. The Annot area was dominated by shallow-water shoal development, which may have occurred contemporaneously to the deposition of the Infranummulitique around Peyresq, due to the very thin Nummulitic Limestone developed, but field relationships are unclear and biostratigraphic dating is not accurate enough to confirm this.

The drowning of the ramp system and the transition to hemipelagic marl deposition occurred during the Middle Priabonian and appears to have been more rapid in the more distal, St Antonin area. This drowning caused a backstepping of facies, with carbonate ramp deposition sited around Barrême during the Upper Priabonian (Bodelle, 1971; Evans and Mange-Rajetsky, 1991).

7.9. Implications for basin development

The basal unconformity between the Mesozoic passive margin succession and the overlying Tertiary sediments indicates that the Tertiary basin developed following a period of significant subaerial exposure, with associated deformation and erosion of the substratum. The existence of pre-nummulitic deformation suggests that the subaerial exposure did not simply occur due to eustatic sea-level fall, but that tectonic processes are likely to have been responsible for the uplift of the Mesozoic. This could be associated with forebulge uplift ahead of the subsiding Alpine foreland basin as proposed for the unconformity in Switzerland by Crampton and Allen (1995), but the two areas studied in France show evidence of tectonism not seen in Switzerland, indicating that the deformation is not as straightforward as simply the upwards-flexing of the foreland plate. In Savoie, normal faulting prior to the Tertiary transgression, described by Pairis and Pairis (1975) and Lateltin and Müller (1987), is thought to be associated with the development of extensional graben systems in the European plate and any associated uplift could be due to doming associated with extensional magmatism. In Haute Provence, the effects of the Pyrenean orogeny are evident in E-W trending fold structures (Apps, 1987) and interference with Alpine compressive events is thought to have further enhanced the uplift and provided localised depocentres for subsequent sedimentation. The similarity of the trends of the Mesozoic and Tertiary platform facies means that there is no decisive evidence for

forebulge uplift, but given the evidence from the Swiss foreland it is possible that it did have some part to play in the development of the basal erosion surface.

The diverse tectonics affecting the study areas produced a relatively complex topography with the lows produced by folding and/or faulting acting as local depocentres for the material eroded from the uplifted foreland plate. These sediments, the Infranummulitique, mark the beginning of relative sea-level rise thought to indicate the onset of basin subsidence, with marine transgression (Nummulitic Limestone deposition) occurring relatively soon afterwards. The sediments in the two areas studied show a similar stratigraphic development but are of different ages which implies that the rising sea-level did not occur solely due to eustatic variations. The succession seen is thought to have formed due to the migration of the basin over the foreland plate, causing backstepping facies over time and producing a diachroneity in the sedimentary succession between areas. Thus, the age of the first sediments deposited over the unconformity can be used to locate the position of the distal edge of the basin at a given time, which shows a general migration from east to west / southeast to northwest.

The cyclicity within the early basin stratigraphy records the effects of increasing basin subsidence on the rsl curve. The earliest sedimentation, represented by coastal deposits laid down during the early phases of subsidence, shows clear evidence of relative sea-level falls producing subaerial exposure and marine transgression, interpreted to be the effects of short-term eustatic sea-level variations on the foreland plate. These eustatic sea-level falls became less significant as the transgression continued, with the cyclicity in the Nummulitic Limestone showing a progressive enhancement of the rising part of the rsl curve up-section, with no subaerial exposure produced during the falls, even though the sediments were deposited in relatively shallow-water settings. This is thought to be due to the effects of increasing rates of subsidence as the basin developed, a characteristic typical of foreland basins (Homewood et al., 1986). Further evidence for the cyclicity being dominated by basin subsidence rather than eustatic variations is the similarity in the cyclicity and rsl curve produced in the two study areas in successions of different ages. This shows that the succession was not produced by eustatic variations alone, but that the control of flexural subsidence on the sedimentary succession produced backstepping facies as the basin migrated over the foreland. Continuing increasing rates of subsidence lead to the virtual obliteration of eustatic signatures in the upper part of the formation, and coupled with a reduction in the productivity, thought to be due to nutrients associated with the advance of the detrital flysch, led to the development of a basin starved of sediment input and the deposition of hemipelagic marls.

The difference in the sedimentary development of the two study areas emphasises the fact that although the stratigraphic development is similar around the Alpine Foreland Basin, the sediments are affected by local topography, substratum and also the flora and fauna present during the onset basin development at different times. The presence of abundant quartz at the base of the formation in Savoie is thought to be due to erosion locally reaching down to the Albian greensands, seen in the study area at La Communaille. The abundance of coralline red algae is thought to be evolutionary; most of the Upper Priabonian limestones around the Alps seen in Dévoluy (Meckel et al., submitted), Champsaur (Crampton, 1992), Barrême (Meckel, pers. comm.) and Haute Savoie are characterised by abundant algal development. Older limestones, from the Ypresian in eastern Switzerland (Lihou, 1995) to the Lutetian at Arâches and Bartonian in Provence are dominated by large foraminifera dominated by *Nummulites*, *Discocyclina* and *Assilina* which acted as bank builders. This indicates that the age of the formation is significant in determining the palaeoecology of the carbonate ramp. It could be a climatic effect, due to the cooling of global climate during the Eocene leading to a dominance of CRA, tolerant of cooler waters. However, corals, which require warm waters, are commonly associated with the algal facies and foraminifera are abundant, though no longer the dominant bank builders, indicating that climate is probably not the dominant control, but rather the diversification of reef builders following the late Cretaceous extinctions, leading up to the establishment of the modern coral reef provinces during the Miocene (Bryan, 1991).

7.10. Summary

The relative sea-level variations controlling the development of the Nummulitique are interpreted to be the interplay of 4th order eustatic sea-level variations and the increasing rates of basin subsidence as the orogenic wedge advanced towards the foreland.

The Infranummulitique represents the onset of subsidence, with marine transgression shutting down the supply of terrigenous carbonate and siliciclastic detritus into the basin providing optimum conditions for carbonate ramp development. Initially, the productivity of the system was able to keep pace with the creation of accommodation space within the basin producing an aggradational or progradational geometry as the carbonate ramp developed. As flexural subsidence rates continued to increase, a contemporaneous reduction in the productivity of the carbonate system, thought to be due to nutrient-rich waters advancing ahead of the turbiditic flysch, reduced carbonate growth rates such that the sediments could no longer keep up with the creation of accommodation space and the ramp was drowned

producing an abrupt transition to hemipelagic marl deposition. The long-term sea-level rise is not thought to be eustatic due to the development of similar stratigraphic successions at different times in the two study areas. This diachroneity of the succession around the Alps indicates that the dominant control on the early basin stratigraphy is the flexural subsidence of the foreland plate.

The cyclicity within the formation can be used to correlate between measured sections in a field area. However, care must be taken as sequence development within a foreland basin is markedly diachronous and so correlations must be carried out in conjunction with the available biostratigraphy. These correlations show the effects of pre-nummulitic topography on the unconformity, localising the Infranummulitique and producing distal ramp successions in depositional lows, as well as demonstrating the backstepping of the facies over the foreland as the basin develops.

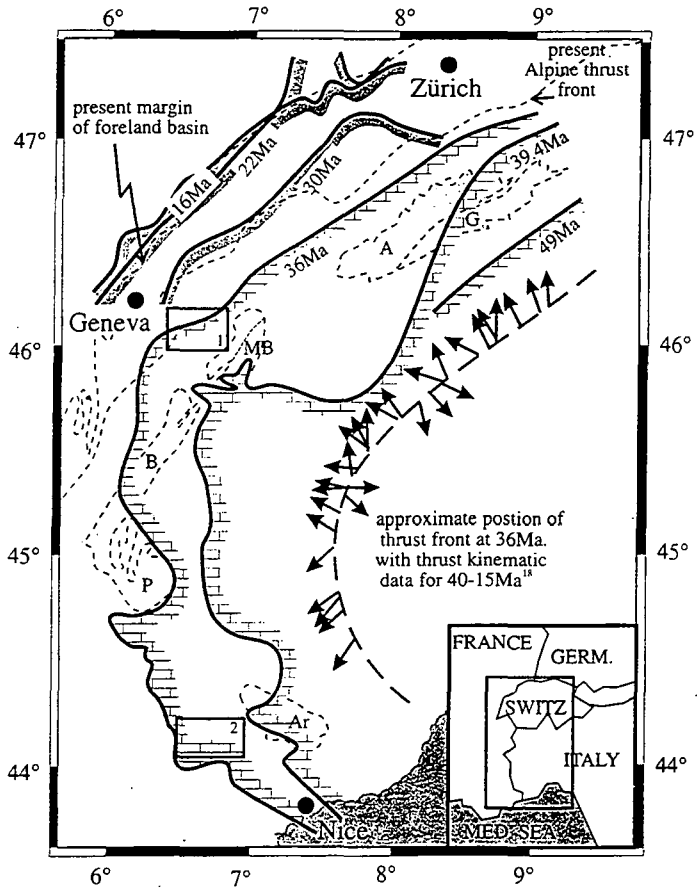

Fig. 7.27: Palaeogeographic reconstruction of the position of the Nummulitique which backsteps over the foreland and demonstrates the westerly migration of the foreland basin. From Sinclair (in press).

The backstepping facies can be used to constrain the position of the distal margin of the foreland basin at a given time (Sinclair, in press), which demonstrates the migration of the basin from east to west / southeast to northwest during the Eocene (Fig. 7.27).

Chapter 8

Conclusions and Discussion: The Alpine Nummulitique; Diachronous Sedimentation in a Developing Foreland Basin

8.1. Tertiary Sedimentation around the Alpine Arc

This section aims to put the Nummulitique of the two study areas in the context of the Alpine Foreland Basin as a whole, and highlights the variation in time and space of similar Tertiary successions around the Alpine Arc, and the problems this may produce in attempting stratigraphic correlations between areas. The distribution of the Tertiary sediments in Switzerland is shown in Fig. 8.1 (from Herb, 1988) and in France in Fig. 8.2 (from Debrand Passard, 1984). The main events are summarised in Table 8.1.

8.1.1. Palaeocene

Palaeocene deposits around the Alps are limited to eastern Switzerland as relict evidence in the Blattengrat Unit of an early phase of transgression over the eroded Upper Cretaceous substratum (Herb, 1988) and as a record of continuous sedimentation in the internal southerly derived Sardona Unit (Sinclair et al., 1991).

In the Blattengrat unit, the Palaeocene is represented by the erosional remnants of the Fliegenspitz Formation; brown to black marls with limestone interbeds, deposited in a neritic setting (100m; Herb, 1988) with detrital influences (Lihou, 1995). The formation has been dated as Thanetian (planktonic foraminiferal zones P3-6) based on planktonic foraminifera, though reworked Cretaceous foraminifera of Maastrichtian age are also present, showing that the stratigraphic gap produced by erosion represents a relatively short time period (Upper Maastrichtian - Lower Thanetian; Lihou, 1995). The erosion prior to the deposition of the Fliegenspitz Formation is thought to be submarine, thus indicating that this region was not subaerially exposed prior to the Tertiary transgression. Subsequent erosion removed most of the formation, with local remnants the only evidence of this early transgression and sedimentation in the embryonic foreland basin to the Alps.

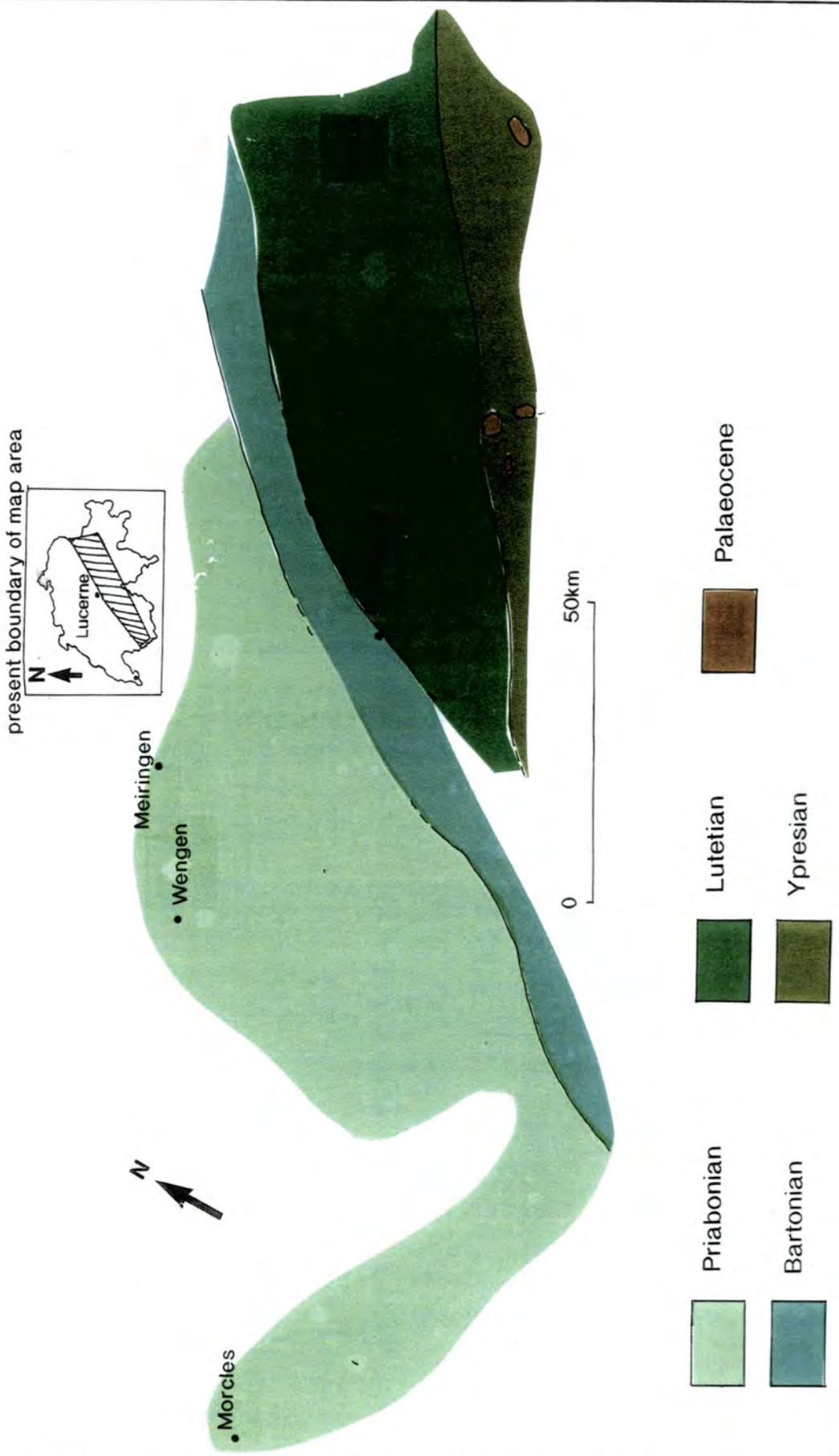

Fig. 8.1: Palinspastic restoration of the Tertiary transgression in Switzerland showing the younging of the sediments from east to west as the basin migrated over the foreland. From Herb (1988, fig. 9).

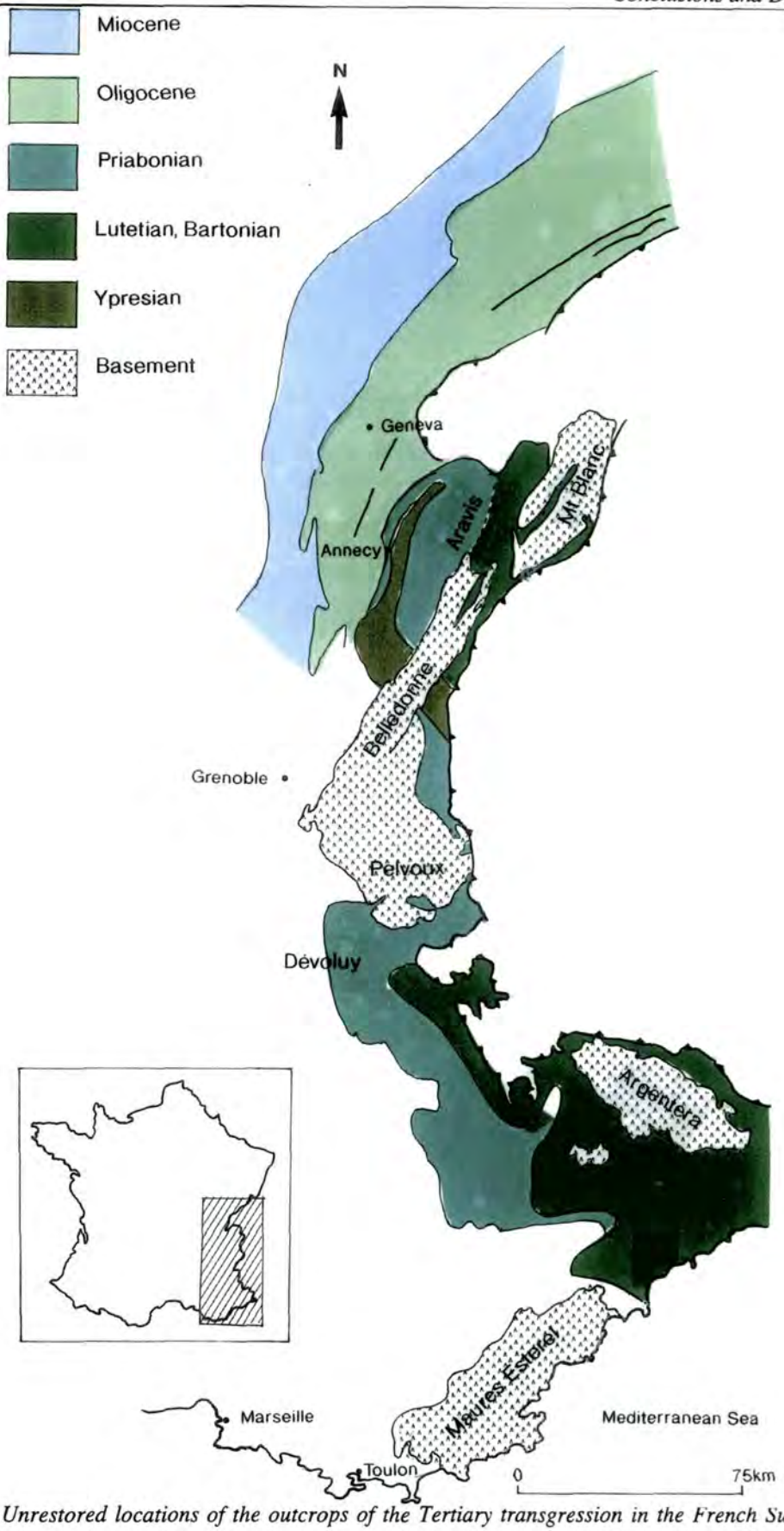

Fig. 8.2: Unrestored locations of the outcrops of the Tertiary transgression in the French Subalpine Chains, showing the younging from east to west of the sediments as the basin migrated across the foreland. From Debrand Passard (1984, map G1).

8.1.2. Eocene

8.1.2.1. Ypresian

The Ypresian saw the second marine transgression in eastern Switzerland, represented in the Blattengrat Unit by the clastic Batöni Sandstone Member and in the Einsiedelner Nummulitenkalk by a basal greensand (Herb, 1988; Lihou, 1995). Both sandstones contain glauconite and are relatively coarse-grained, representing offshore shelf deposition. The more widespread distribution of the sediments shows the increasing extent of the transgression through time, with the transgression progressing from south-east to north-west. The sandstones are dated as lowermost Ypresian, but may extend into the Upper Palaeocene (Herb, 1988). This transgression again shows the first sediments overlying the erosional unconformity to have been deposited in relatively deep water, with abundant glauconite indicating very low sedimentation rates.

Following the end of clastic sedimentation, limestone deposition commenced in the developing basin with the proliferation of the Nummulitic Limestones of the Blattengrat Unit and Einsiedelner Nummulitenkalk. The Nummulitic Limestone in eastern Switzerland represents continual sedimentation during the Upper Ypresian, with the progradation of shallow-marine limestones out into the basin which contained a fauna dominated by bank-forming *Nummulites* and *Assilina* with local *Lithothamnium* development (Herb, 1988; Lihou, 1995). Variations in eustatic sea-level are evident as correlatable greensands and condensation horizons, within an overall deepening-upwards trend, with a phase of progradation marking a major rsl fall at the end of the Ypresian in the Blattengrat Unit (Lihou, 1995). The overall deepening upwards trend is thought to be due to the effects of tectonic subsidence in the area through comparison with the eustatic sea-level curves of Haq et al. (1988).

During this time, SE France was emergent (Debrand-Passard, 1984), though a marine gulf is thought to have existed in western Switzerland and the Bauges, Haute Savoie (Herb, 1988; Pairis, 1988).

8.1.2.2. Lutetian

The Lutetian saw a rapid deepening in eastern Switzerland with the drowning of the nummulitic ramp occurring after the regression at the end of the Ypresian. This produced the transition into the pelagic Flecken and Globigerina Marls in the Blattengrat and Einsiedelner Units respectively (Lihou, 1995; Herb, 1988) as the rates of tectonic subsidence increased producing the initial deepening upwards succession characteristic of underfilled foreland basins. Contemporaneous with this deepening, the marine transgression progressed further NW over the exposed foreland in

Switzerland (Herb, 1988), depositing the glauconitic sandstones and Nummulitic Limestones of the Bürgen Formation, which was also characterised by monospecific *Nummulites* and *Assilina* banks (Crampton, 1992).

Subsidence commenced in the Franco-Italian Alpes Maritimes, with the deposition of the terrestrial and marginal-marine Infranummulitique (Campredon, 1966, 1977). This was subsequently transgressed by marine Nummulitic Limestone during the Upper Lutetian while further west, in the Annot area of Haute Provence, terrigenous Infranummulitique deposition had commenced in the St Antonin Syncline localised within topographic lows on the substratum (Bodelle, 1971), thought to be due to the combined effects of the Pyrenean and Alpine orogenies (Apps, 1987). The migration of facies demonstrates a basinwide trend of westerly backstepping facies over the foreland as the basin developed.

Relict evidence of an Upper Lutetian transgression is preserved within fault blocks in the Massif de Platé, Haute Savoie (Pairis and Pairis, 1975), indicating the presence of a faulted topography by this time, thought to be associated with the onset of extension in the Rhine and Bresse Graben systems.

Lutetian Nummulitic Limestones are characterised by large *Nummulites* and *Assilina* which had a tendency to build banks in shallow waters (e.g. Crampton 1992). Sandstones are common at the base of the formation in Switzerland, but are absent in France, probably reflecting differences in the substratum around the Alps.

8.1.2.3. Bartonian

Marl deposition continued during the Bartonian in the pelagic starved basin in eastern Switzerland, with the transition from shallow-water limestones to pelagic marls occurring in central Switzerland and the eastern Alpes Maritimes (Herb, 1988; Crampton, 1992; Campredon, 1977). The onset of flysch sedimentation in these internal areas commenced during the Upper Bartonian. In the external Swiss autochthon, the shallow-marine Hohgant Formation was deposited (Herb, 1988).

Haute Savoie saw a phase of regression, thought to be unrelated to foreland basin subsidence, following the Upper Lutetian transgression, leading to erosion of the Lutetian Nummulitic Limestone and an upwards transition to lacustrine facies within the faulted low (Pairis and Pairis, 1975). Elsewhere on the Massif de Platé, deposition of the Infranummulitique commenced with conglomeratic sedimentation in fluvial and fan delta settings, the clasts of which include cannibalised remnants of the earlier Nummulitic Limestone. This deposition was localised to faulted lows (Pairis and Pairis, 1975), with the terrigenous sediments derived from local highs and reflecting the lithologies exposed and undergoing erosion at that time. The rest of the area was emergent and undergoing erosion and karstification.

Fully marine conditions had now been established in the St Antonin area, with the deposition of shallow-marine Nummulitic Limestone, overlying the Infranummulitique and blanketing the earlier topography on the unconformity. The transgression progressed westward during the Bartonian, with the base of the succession younger in the Annot Syncline to the NW (Bodelle, 1971; Campredon, 1977). The Nummulitic Limestone represents the development of bioclastic shoals dominated by *Nummulites*, though the large bank-building forms prevalent in the Lutetian had now become extinct. The focus of shallow-water shoal deposition during the late Bartonian had extended NW to the Annot Syncline, with local facies variations reflecting the inherent topography on the erosion surface. The deposition of the Infranummulitique had also backstepped further onto the foreland, now located around Argens, where an ephemeral stream system is thought to have fed the marginal marine fan delta system exposed at Peyresq. Deposition was localised in synclinal lows. Sedimentation had also commenced further north in Dévoluy, with the deposition of the continental Pierroux Conglomerate (Meckel et al., submitted).

The widespread transgression occurring during the Priabonian has been attributed by Pairis (1988) to the incorporation of the Briançonnais and Subbriançonnais into the thrust pile (Crampton, 1992).

8.1.2.4. Priabonian

The Priabonian saw the furthest west extent of deposition of the Nummulitic Limestone and associated sediments, with the onset of marine deposition in Haute Savoie, Dévoluy (Meckel et al., submitted), the Champsaur (Crampton, 1992), Barrême (Evans and Mange-Rajetsky, 1991) and Peyresq.

In the internal zones in eastern Switzerland, turbiditic flysch deposition of the Taveyannaz Sandstones continued, with the development of olistoliths indicating synsedimentary tectonic activity (Crampton, 1992). In the Alpes Maritimes, the Annot Sandstones advanced westwards from the Menton area.

Haute Provence recorded the onset of increasing rates of subsidence by a backstepping of the nummulitic bank facies from St Antonin to Annot, with a corresponding onset of deepening evident in the sedimentary succession around St Antonin. This is thought to coincide with the onset of shallow marine sedimentation around Argens. The Nummulitic Limestone in Haute Provence is dominated by small *Nummulites* which formed bioclastic shoals on a homoclinal carbonate ramp. Accelerating basin subsidence rates led to the final drowning of the carbonate ramp during the Middle Priabonian.

In Dévoluy, marine transgression led to the deposition of Nummulitic Limestone with foraminifera and abundant CRA occurring as rhodoliths and as

"pseudo-reefal" facies developed on large redeposited blocks of the Senonian (Meckel et al., submitted). The succession shows an overall deepening upwards, with the transition to the marls occurring during the Late Priabonian.

Champsaur saw the onset of sedimentation following a phase of tectonism associated with thrusting locally exposing crystalline basement (Crampton, 1992). The facies developed reflect the nature of the substratum; basal terrigenous clastics contain basement clasts; the crystalline basement promoted the development of immature coral-algal reefs, favouring hard substrates, whereas in the south of the area, a softer substratum of Jurassic marls promoted the deposition of foraminiferal limestones, representing a soft, muddy substrate (Crampton, 1992). The ramp was flooded during the Upper Priabonian and turbiditic flysch sedimentation commenced before the Oligocene.

In Haute Savoie, widespread marine sedimentation did not commence until the Upper Priabonian (Pairis, 1988; Weidmann et al., 1991) with lagoon/coastal plain sedimentation persisting in the depositional lows. The lower marine deposits of the Nummulitic Limestone are quartzitic limestones reflecting the waning of clastic supply into the basin, which are overlain by algal-nummulitic limestones with abundant CRA occurring as rhodoliths and forming gravels and shoals. The facies again reflect the pre-depositional topography in the area, with prolific algal shoal and rarely coral-algal reef development occurring over depositional highs. Nummulitic Limestone deposition persisted until the Eocene/Oligocene boundary (Pairis, 1988; Lateltin and Müller, 1987).

The end of the Priabonian saw the onset of turbiditic flysch deposition over most of the basin, including Switzerland, Champsaur and the Alpes Maritimes, and shallowing-upwards siliciclastic deposition in Dévoluy associated with tectonism (Meckel et al., submitted).

8.1.3. Oligocene

The drowning of the carbonate ramp and transition to pelagic marl deposition occurred during the lowermost Oligocene in Haute Savoie with the transition to turbiditic flysch sedimentation occurring soon afterwards, ending the shallow marine deposition represented by the present day outcrops. In the Alpes Maritimes, Dévoluy and the Champsaur flysch sedimentation continued, commencing in the Annot area during the lowermost Oligocene.

Folding and thrusting in the internal zones produced olistostromes, and nappe emplacement occurred soon after the deposition of the Annot Sandstone in Haute Provence (Hamiti, 1994). Sedimentation continued with the transition to the overfilled basin and molasse deposition.

Age	Area	Stratigraphy	Sediments	Relative Sea-Level and Depositional Setting	Basin Evolution
Palaeocene **Thanetian**	Eastern Switzerland	Blattengrat Unit: Fliegenspitz Formation	black, neritic marls	submarine erosion followed by transgression subsequent erosion removes most of sediments	initiation of foreland basin first transgression
Eocene **Ypresian**	Eastern Switzerland	Blattengrat Unit: Batöni Sandstone Einsiedelner Formation: basal greensand	glauconitic offshore clastic deposition	transgression over erosional unconformity, low sedimentation rates	second transgression, migration of transgression from SE-NW
Upper Ypresian	Eastern Switzerland	Blattengrat Unit Einsiedelner Nummulitenkalk	shallow-marine Nummulitic Limestones with correlatable greensands	continual sedimentation progradation of shallow-marine limestones into the basin bank forming foraminifera	eustatic variations evident on overall deepening upwards rsl curve
	France		erosion	emergent local marine gulf in Savoie	area not yet affected by foreland basin subsidence, possible development of forebulge
Lutetian	Eastern Switzerland	Flecken and Globigerina Marls	fissile pelagic marls	deepening to starved basin deposition	accelerating rates of subsidence outpace sedimentation rates
	Central Switzerland	Bürgen Formation	Nummulitic Limestones and glauconitic sandstone	bank building foraminifera	onset of subsidence and first transgression in Central Switzerland facies migrating NW

Table 8.1: Tertiary sedimentation in the Alps, showing the age, location and formation names of the main sedimentary units and their relationship to the developing foreland basin.

Age	Area	Stratigraphy	Sediments	Relative Sea-Level and Depositional Setting	Basin Evolution
	France - Alpes Maritimes	Infranummulitique	localised terrigenous carbonate deposition	terrestrial and marginal marine sedimentation recording early transgression	onset of subsidence in France, early depocentres controlled by pre-existing topography on subaerial unconformity area affected by Pyrenean tectonics
		Nummulitic Limestone	carbonate ramp sediments	progradation of ramp into basin, transgression affects previously exposed highs	first marine transgression, basin subsidence more evident
	France - Haute Provence	Infranummulitique	terrigenous carbonates and palaeosols	terrestrial and marginal marine sedimentation in local depocentres	onset of subsidence continued emergence of most of area
	France - Haute Savoie	Nummulitic Limestone with large *Nummulites* erosion	shallow marine carbonates, only preserved locally in faulted graben	early transgression prior to foreland subsidence, possibly eustatic subsequent erosion removes sediments from rest of area	early eustatic signature during emergent period forebulge uplift? faulting
Bartonian	Eastern Switzerland	Flecken and Globigerina Marls Taveyannaz Sandstone	continued pelagic sediments turbiditic flysch	starved basin onset of influx of orogen derived siliciclastics	approaching orogen, increasing subsidence rates, increasing sedimentation rates
	Central Switzerland	Bürgen Formation	flooding of carbonate ramp, onset of pelagic sedimentation	transition to starved basin	accelerating subsidence

Table 8.1 (cont'd): Tertiary sedimentation in the Alps, showing the age, location and formation names of the main sedimentary units and their relationship to the developing foreland basin.

Age	Area	Stratigraphy	Sediments	Relative Sea-Level and Depositional Setting	Basin Evolution
	France - Alpes Maritimes	Marnes Bleues	flooding of carbonate ramp, onset of pelagic sedimentation	transition to starved basin	accelerating subsidence
	Haute Provence	Nummulitic Limestone in St Antonin Annot areas Infranummulitique around Peyresq	carbonate ramp progradation local terrigenous carbonates	onset of marine transgression	continued subsidence facies migrating W/NW effects of earlier structures evident in terrigenous depocentres
	Dévoluy	Pierroux Conglomerate	terrigenous carbonates		onset of subsidence
	Haute Savoie	Infranummulitique	regression, erosion, terrigenous carbonates	marginal marine sediments localised in faulted grabens	onset of subsidence
Priabonian	Switzerland	Taveyannaz Sandstones	turbiditic flysch olistostromes	continued influx from mountain belt	facies migrating W/NW
	France - Alpes Maritimes	Annot Sandstone	turbiditic flysch	onset of influx from mountain belt	orogenic wedge approaching SE France
	Haute Provence	Nummulitic Limestones Marnes Bleues	deepening of facies in SE, focus of shoal deposition now around Annot transition to pelagic marls	onset of ramp backstepping and drowning ramp drowning across area	increasing subsidence rates
	Dévoluy	Nummulitic Limestone Queyras Marlstone	shallow marine carbonates pelagic marl turbiditic flysch	marine transgression and deepening	onset of basin subsidence and subsequent accelerating subsidence rates

Table 8.1(cont'd): Tertiary sedimentation in the Alps, showing the age, location and formation names of the main sedimentary units and their relationship to the developing foreland basin.

Age	Area	Stratigraphy	Sediments	Relative Sea-Level and Depositional Setting	Basin Evolution
	Champsaur	Nummulitique Champsaur Sandstone	terrigenous clastics Nummulitic Limestone pelagic marls turbiditic flysch	rapid transgression, deepening and influx of siliciclastics	deposition over basement thrust slice increasing subsidence producing deepening-upwards succession
	Haute Savoie	Nummulitic Limestone	carbonate ramp progradation sediments blanket previous topography	main marine transgression due to basin subsidence	restored western limit of Nummulitic Limestones
Oligocene	Alpes Maritimes Dévoluy Champsaur	Annot Sandstone St Disdier Sandstone	continued flysch sedimentation	continued influx from mountain belt	orogenic front advancing W
	Haute Provence	Annot Sandstone	turbiditic flysch olistostromes	influx from mountain belt	orogenic front advancing W nappe emplacement
	Haute Savoie	Globigerina Marl Taveyannaz Sandstone	pelagic marl turbiditic flysch, slumps	flooding of carbonate ramp, starved basin and onset of influx from mountain belt	accelerating subsidence, synsedimentary faulting orogenic wedge advancing W

Table 8.1 (cont'd): Tertiary sedimentation in the Alps, showing the age, location and formation names of the main sedimentary units and their relationship to the developing foreland basin.

8.2. Discussion

8.2.1. Why does the stratigraphy represent foreland basin development?

A number of factors indicate that this stratigraphy is the result of the migration of a developing foreland basin rather than the effects of eustatic sea-level variations or other tectonic causes. The most noticeable feature from maps is the arcuate nature of the distribution of the present-day outcrops of the Tertiary stratigraphy, which closely mirrors the arcuate nature of the Alpine fold- and thrust-belt. Though this could feasibly be the result of more recent Alpine deformations, a similar trend is observed in the relatively undeformed Alpine Molasse, indicating that the main depocentres mimicked the trend of the developing orogeny. The stratigraphy developed reflects increasing relative sea-level, irrespective of the age of the sediments, indicating a tectonic rather than eustatic control on relative sea-level rise. The erosion surface at the base of the Tertiary succession is thought to reflect the development of an uplifted forebulge region ahead of the foreland basin, though the only direct evidence for this occurs in Switzerland, where the 20° variation in strike between the Mesozoic passive margin succession and the overlying Tertiary precludes simple eustatic sea-level fall. In France, the picture has been complicated (Chapter 6) by other tectonism at the time of predicted forebulge uplift.

The Tertiary sedimentary succession records an increase in the rates of subsidence in both France and Switzerland (Crampton, 1992), a characteristic of developing foreland basins as the orogenic wedge advances and producing the typical asymmetric profile. The transition up-section to orogenically derived flysch, suggests the sedimentary succession developed due to a migrating foreland basin rather than other tectonic processes as it indicates the approach of the orogenic deformation front as collision continued. This migration produced the similar sedimentary succession encountered from eastern Switzerland to SE France, with the diachroneity marking the migration of the basin with time. The time interval between the deposition of the earliest nummulitic limestones in Switzerland (Thanetian) and the latest limestones in SE France (Upper Priabonian) is too great to be attributable to continual eustatic sea-level rise.

8.2.2. Development of the Alpine Foreland Basin

The stratigraphy described in Section 8.1 suggests that the onset of sedimentation in the Alpine Foreland Basin occurred in eastern Switzerland during the Palaeocene (Lihou, 1995; Herb, 1988). The existence of a continuous stratigraphy (Sardona Unit) and a small stratigraphic gap produced by submarine erosion

(Blattengrat Unit) indicates that sedimentation occurred close to the deformation front during the initiation of basin subsidence. As time progressed, the increased loading of the orogenic wedge produced a subaerial forebulge ahead of the subsiding basin, which was subsequently incorporated into the basin development. The ages of the first marine sediments overlying the resultant unconformity demonstrate that the marine transgression due to the effects of migrating basin subsidence progressed from SE to NW across Switzerland during the Ypresian and Lutetian (Lihou, 1995; Herb, 1988; Crampton, 1992), and subsidence due to orogenic loading was also occurring around the present French-Italian border (Campredon, 1966, 1977), with the foreland basin mirroring the arcuate nature of the Alpine orogenic front. With further compression, this westerly migration continued, shown by the backstepping of the facies over the foreland during the Bartonian, while the more internal zones underwent the transition to deep water marl and flysch deposition. The two study areas represent positions on the furthest west restored distal margin of the basin, with deposition occurring during the Priabonian.

The Swiss foreland basin has been modelled by a number of workers (Sinclair et al., 1991; Crampton, 1992) and the stratigraphy can be produced by the flexure of a continuous plate due to continuous loading by an orogenic wedge. In France, however, the early sedimentation and tectonism have been complicated by the effects of tectonism within the foreland plate, noted by Crampton (1992) in the Champsaur, Meckel et al. (submitted) in Dévoluy and clearly evident in the distribution of the earliest sediments in the two study areas. A simple flexural model is not sufficient to explain the structures and stratigraphic distribution observed.

8.2.3. The Nummulitique as an indicator of marine transgression

The Nummulitique represents the earliest sedimentation during the onset of subsidence around the Alpine Arc, with the resultant succession thought to reflect the effects of both tectonics and eustasy.

Sedimentation started in the study areas with the continental and marginal marine Infranummulitique, which is laterally discontinuous, reflecting the positions of local depocentres produced due to the inherent topography on the uplifted land surface. This topography is thought to be the result of the effects of extension in the NW European plate responsible for the Rhine and Bresse graben systems, and, further south, the interference of the Alpine and Pyrenean orogenies. The Infranummulitique can be divided into four main facies associations. The lenticular conglomerate/nodular marl association was deposited by ephemeral streams in an alluvial plain. The discrete conglomerates represent deposition by bedload traction from channelised flows during high-energy events. Channel abandonment and/or migration resulted in the deposition

of fine-grained carbonate in a floodplain or palustrine environment which was subsequently reworked by pedogenesis. The sheet conglomerate facies association represents deposition in a marginal marine fan delta, thought to be fed by the alluvial system. Deposition was from high-energy channelised flow, with channel amalgamation and migration producing laterally continuous conglomerates. Borings and foraminifera indicate marine conditions. Pauses in coarse detrital influx led to the deposition of fine-grained carbonate under marine conditions, which was subsequently exposed. The *Microcodium* wackestone was again deposited in channels, in a marine environment proximal to the vegetated land surface. The *Cerithium* marl represents deposition in a low-energy, brackish coastal plain/lagoon developed after the cessation of coarse carbonate detritus into the basin. The onset of subsidence and the marine transgression is marked by the increasing of marine influences up-section The cyclicity produced in the sedimentary succession during this period of slow subsidence is interpreted to be the results of eustatic sea-level variations, producing periodic marine incursions and subaerial exposure in the more coastal areas.

True marine conditions are marked by the transition up into the Nummulitic Limestone, with the flooding of the land surfaces marked by the development of quartzitic limestone shoals deposited in shallow waters (above FWWB). True carbonate deposition commenced at the end of clastic supply into the basin and the carbonate ramp developed, dominated by large benthonic foraminifera and calcareous red algae. The dominance of mud-rich facies indicates a low-energy ramp, with storm reworking producing middle-ramp foraminiferal accumulations. The shallowest waters of the inner-ramp are represented by the deposition of winnowed bioclastic shoals above FWWB dominated by CRA with local coralgal patch reefs (Haute Savoie), or *Nummulites* and peloids (Haute Provence). Inherent topography may still be evident at the onset of the marine transgression, with the basal cycles absent over depositional highs, though the development of a carbonate ramp system indicates that topographic slopes were low. The Nummulitic Limestone shows an overall deepening from base to top, controlled by tectonism as subsidence rates increase. However, the cyclicity within the succession represents progradation of the carbonate ramp out into the basin, indicating that the productivity of the carbonate system was able to match or even outpace the creation of accommodation space during the early stages of transgression. The cyclicity produced within the succession no longer shows evidence of subaerial exposure, with the top of the cycles represented by shallow marine deposition. This indicates that the effects of the basin subsidence were starting to enhance the relative sea-level rises. As the basin continued to develop, this effect became more marked, until the carbonate productivity could no longer keep pace with the rising relative sea-level and the ramp backstepped and was eventually drowned.

The effects of increasing subsidence rates are thought to be enhanced by environmental factors due to the approaching siliciclastic flysch and the global cooling experienced during the Eocene. The backstepping upper part of the Nummulitic Limestone shows a less marked cyclicity, being dominated by a simple deepening upwards facies profile. The less marked cyclicity is thought to be due to the increased effects of subsidence on the rsl curve producing the transition to the Globigerina Marls. The marls represent the deepest water sediments in the succession, starved of both siliciclastic and carbonate sedimentation prior to the arrival of the orogenically derived turbiditic flysch.

Thus, the controls on relative sea-level variations represented by the Nummulitique Formation are dominated by the tectonism of the developing foreland basin, which produces a similar deepening upwards stratigraphy around the Alpine Arc during the underfilled stage of basin development, with superimposed, small-scale eustatic variations producing the cyclicity within the formation. The succession shows the decreasing influence of eustatic variations as the subsidence of the basin continues, and the tectonic influence on rsl becomes dominant.

8.2.4. Diachronous sedimentation - problems with correlation

The tectonic control on relative sea-level has led to the development of a diachronous stratigraphic succession around the Alps, containing very similar facies, but younging from SE to NW from Thanetian to Upper Priabonian as the facies backstepped across the foreland as the basin developed. This leads to problems in correlating between different parts of the basin. The faunal content of the formation makes accurate dating difficult due to the longevity of species of large benthonic foraminifera and a paucity of planktonic foraminifera. Thus it is almost impossible to determine with certainty beds or cycles of the same age in different areas.

Problems also arise with the use of sequence stratigraphy as a correlative tool in a foreland basin setting as the relative sea-level responsible for the sequence development in the underfilled basin sediments is dominated by the tectonic subsidence of the basin, which occurred at different times around the basin. This leads to a diachroneity of the sequences produced, with the SB and LST developed on the uplifted forebulge region, the TST during the onset of transgression and the HST during carbonate ramp deposition. Eustatic signatures in the early cyclicity would be viable for correlation, but due to the poor constraints on dating the sediments it is impossible to tie individual events with the global sea-level curve (Haq et al., 1988).

It is possible to attempt correlations within a small area of the basin such as the two study areas, or between successions deposited along basin strike, as flooding surfaces, such as the demise of the carbonate ramp succession, may be taken as

contemporaneous. It must also be noted that even within a relatively small area, it is possible to see the onset of facies backstepping (e.g. in the Annot area), which may indicate a diachroneity of the ramp flooding surface. It is also difficult to tie the cyclicity in the Infranummulitique with that of the Nummulitic Limestone due to the lack of fossils in the lower conglomeratic units.

8.3. Conclusions

1) The Nummulitique of the French Alps can be divided into two informal members based on their characteristic sedimentology:

i)The lower Infranummulitique (terrigenous derived allochthonous carbonates)

ii)The Nummulitic Limestone (autochthonous carbonate ramp sediments)

2) The base of the succession is marked by an erosional unconformity, locally angular, separating the Mesozoic passive margin substratum from the Tertiary foreland basin fill. The unconformity shows evidence of subaerial exposure (karst, *Microcodium*) with significant erosion and tectonism prior to the subsidence of the foreland basin and deposition of the basin fill.

3) The Infranummulitique was deposited in topographic lows on the unconformity produced by tectonism and erosion. It can be divided into four main facies associations: lenticular conglomerate/nodular marl, sheet conglomerate, *Microcodium* wackestone and *Cerithium* marl. The lenticular conglomerate is interbedded with nodular marls and represents deposition of coarse carbonate detritus from bed-load traction in ephemeral streams cutting across a vegetated alluvial plain. The sheet conglomerates were deposited in a marginal marine fan delta setting, with marine reworking producing bored clast surfaces and marine fauna in the matrix and interbedded fine sediments. The *Microcodium* wackestone was deposited in a nearshore marine environment from channelised flows. The *Cerithium* marl represents deposition in a brackish water coastal plain / lagoon, with vegetation leading to local coal horizons and marine incursions producing local sand bodies.

4) The Nummulitic Limestone represents deposition on a low-energy carbonate ramp dominated by larger benthonic foraminifera and calcareous red algae. It can be divided into a number of characteristic microfacies based on the depositional texture and faunal content of the sediment. Foraminiferal palaeoecology has been used to assign these microfacies to relative water-depths and positions on the carbonate ramp. The inner-ramp is represented by grain supported packstones and grainstones deposited as

bioclast shoals above FWWB (CRA, robust *Nummulites, Amphistegina*, Miliolids, peloids), passing down-ramp into more mud-rich bioclastic wackestones of the middle-ramp (intermediate to flat *Nummulites*, *Discocyclina*, *Operculina*), with local packstones the result of storm reworking. The deep, outer-ramp is represented by mudstones with a sparse fauna of large flat *Discocyclina* and planktonic foraminifera. Lateral facies variations mark the continued effects of the inherent topography on the unconformity, with highs acting as sites for preferential shoal development.

5) Detailed sedimentological study has highlighted the cyclicity within the formation which has been used to assign a sequence stratigraphic framework to the formation and to attempt correlations between measured sections. The basal unconformity represents a megasequence boundary separating the Mesozoic passive margin succession from the overlying Tertiary foreland basin fill, marking a significant change in the tectonic evolution of the region. The Infranummulitique was deposited during the late lowstand systems tract (conglomerates) and transgressive systems tract (*Cerithium* marl, basal clastics). The maximum flooding surface marks the end of clastic supply into the basin and the onset of carbonate sedimentation. The Nummulitic Limestone prograded out into the basin during the highstand systems tract and backstepped during the deepening to the subsequent transgressive systems tract. Accelerating relative sea-level rise associated with environmental stress on the carbonate system during the transgression led to the flooding of the carbonate ramp and the transition to pelagic marls.

6) The cyclicity can be used to correlate between sections measured within each field area taking the ramp flooding surface as synchronous. The correlations illustrate the localised distribution of the Infranummulitique and the effects of inherent topography on the early deposition of the Nummulitic Limestone, identifying cycles missing at the base of the formation over depositional highs, facies variations across the areas, condensed sections developed within depositional lows and the backstepping of depocentres across the foreland.

7) The Nummulitique Formation was deposited during the early subsidence of the Alpine Foreland Basin which formed due to the lithospheric flexure of the European plate during loading by the Alpine orogenic wedge.

8) The French Nummulitique cannot be modelled by simple lithospheric flexure, which reproduced the Swiss stratigraphy, due to the complexities in tectonics during the development of the unconformity. There is no direct evidence for forebulge uplift

in France, though by comparison with Switzerland it is likely to have contributed to the uplift of the Mesozoic. Additional tectonic events which must be considered are the extension and volcanic doming associated with the Rhine and Bresse graben system and the additional effects of the Pyrenean compression to the south.

9) The study areas represent the restored westerly limit of development of the underfilled foreland basin, with the youngest Nummulitique outcropping in the Alps at present. Similar sedimentary successions were deposited throughout the development of the foreland basin, which initiated in eastern Switzerland during the Palaeocene and migrated NW across the foreland producing a diachronous stratigraphy younging NW.

10) The migration of the foreland basin produces problems in correlating between different areas in the basin, due to the diachroneity of both the sedimentary succession and the sequence development in the basin. The relative sea-level variations controlling the sequence development are dominated by the tectonic subsidence of the basin and therefore the systems tracts and key surfaces developed young from SE to NW, making correlation by this method potentially problematic. In order to carry out a reliable correlation it is necessary to constrain biostratigraphical dating, identify individual cycles on the global sea-level curve and/or ensure that the areas considered lie around the strike of the basin.

References

Adey, W.H. and MacIntyre, I.G., (1973). Crustose Coralline Algae: A re-evaluation in the Geological Sciences. Bull. Geol. Soc. America, 84, 883-904.

Aigner, T., (1982). Event stratification in Nummulite accumulation and in shell beds from the Eocene of Egypt. In: Einsele, G. and Seilacher, A. (eds). Cyclical and Event Stratification. Springer Verlag. 248-261.

Aigner, T., (1983). Facies and origin of Nummulitic buildups: an example from the Gisa Pyramids Plateau (Middle Eocene, Egypt). Neues Jahrbuch Palaontologisches Abhandlung, 166/3, 347-368.

Aigner, T., (1985). Biofabrics as dynamic indicators in nummulite accumulations. J. Sed. Petrology, 55/1, 131-134.

Allen, P.A., Homewood, P. and Williams, G.D., (1986). Foreland basins: an introduction. In: Allen, P.A. and Homewood, P., (eds). Foreland Basins. I.A.S. Spec Pub. 8, 3-14.

Allen P.A., Crampton, S.L. and Sinclair, H.D., (1991). The inception and early evolution of the North Alpine Foreland Basin, Switzerland. Basin Research, 3, 143-163.

Apps, G.M., (1987). Evolution of the Grès d'Annot Basin, SW Alps. Unpubl. PhD thesis, Univ. Liverpool.

Beaumont, C., (1981). Foreland Basins. Geophysics J. Royal Astr. Soc., 65, 291-239.

Blanchon, P. and Shaw, J., (1995). Reef drowning during the last glaciation: Evidence for catastrophic sea-level rise and ice-sheet collapse. Geology, 23/1, 4-8.

Blondeau, A., (1972). Les Nummulites. De l'enseignement à la recherche. Sciences de la Terre. Vuibert, 254pp.

Bodelle, J., (1971). Les Formations Nummulitique de l'Arc de Castellane. Unpubl. PhD thesis, Univ. Nice.

Bodelle, J. and Campredon, R., (1968). Les Formations à *Microcodium* dans les Alpes-Maritimes Franco-Italiennes et les Basses-Alpes leur importance paléogéographique. Mém. B.R.G.M. 69, 409-415.

Bosellini, A. and Ginsburg, R.N., (1971). Form and internal structure of Recent algal nodules (rhodolites) from Bermuda. J. Geology, 79, 669-682.

Bosence, D.W.J., (1983). The occurrence and ecology of recent rhodoliths - a review. In: Peryt, T.M. (ed.). Coated Grains , Springer Verlag, Berlin. 225-242.

Bosence, D.W.J., (1985). The 'Coralligène' of the Mediterranean - a Recent analog for the Tertiary coralline algal limestones. In Toomey, D.F. and Nitecki, M.H. (eds). Palaeoalgology: Contemporary Research and Applications. Springer Verlag, Berlin. 216-225

Bosence, D.W.J. and Pedley, H.M., (1982). Sedimentology and palaeoecology of a Miocene coralline algal biostrome from the Maltese Islands. Palaeogeog., Palaeoclim., Palaeoecol., 38, 9-43.

Bosscher, H., (1992). Growth potential of coral reefs and carbonate platforms. PhD thesis, Vrije Universiteit, Amsterdam.

Bosscher, H. and Schlager, W., (1992). Accumulation rates of carbonate platforms. J. Geology, 101, 345-355.

Boussac, J., (1912). Etudes stratigraphiques sur le Nummulitique Alpin. Mém. Serv. Carte. Géol. France, 662pp.

Bradley, D.C. and Kidd, W.S.F., (1991). Flexural extension of the upper continental crust in collisional foredeeps. Bull. Geol. Soc. America, 103, 1416-1438.

Bradley, D.C. and Kusky, T.M., (1986). Geologic evidence for the rate of plate convergence during the Taconic arc-continent collision. J. Geology, 94, 667-681.

Brasier, M.D. and Green, O.R., (1993). Winners and losers: stable isotopes and microhabitats of living Archaiadae and Eocene *Nummulites* (larger foraminifera). Marine Micropalaeo., 20, 267-276.

Bryan, J.R., (1991). A Paleocene coral-algal-sponge reef from southwestern Alabama and the ecology of Early Tertiary reefs. Lethaia, 24, 423-438.

Burbank, D.W., Puídefabregas, C. and Muñoz, J.A., (1992). The chronology of Eocene tectonic and stratigraphic development of the eastern Pyrenean foreland basin, Northeast Spain. Bull. Geol. Soc. America, 104, 1101-1120.

Burchette, T.P. and Wright, V.P., (1992). Carbonate ramp depositional systems. Sed. Geol., 79, 3-57.

Buxton, M.W.N. and Pedley, H.M., (1989). A standardised model for Tethyan Tertiary carbonate ramps. J. Geol. Soc. London, 146, 746-8

Calvet, F., Tucker, M.E. and Henton, J.M., (1990). Middle Triassic carbonate ramp systems in the Catalan Basin, northeast Spain: facies, systems tracts, sequences and controls. In: Tucker, M.E., Wilson, J.L., Crevello, P.D., Sarg, J.F. and Read, J.F., (eds). Carbonate Platforms: facies sequences and evolution. I.A.S. Spec. Pub. 9, 79-108.

Campredon, R., (1966). Les Couches à *Microcodium* et à *Cérithium diaboli* des environs de Trucco (Alpes Maritimes Italiennes). C. R. Acad. Sci. Paris, t 262, Série D, 1195-1197.

Campredon, R., (1977). Les formations paléogènes des Alpes Maritimes Franco-Italiennes. Mém. Soc. Géol. France, 9, 199pp.

Carannante, G., Esteban, M., Milliman, J. and Simone, L., (1988). Carbonate lithofacies as paleolatitude indicators: problems and limitations. Sed. Geol., 60, 333-346.

Chaplet, M., (1989). Etude géologique du Massif Subalpin des Bornes (Haute Savoie). Unpubl. PhD thesis, Univ. Chambéry.

Chaplet, M., (1992). Relations stratigraphiques et tectoniques entre nappe des Aravis et Bornes externes dans le synclinal de nappes de Thônes. (Massif subalpin des Bornes - Haute Savoie - France). Eclog. Geol. Helv., 85/1, 23-61.

Charollais, J., Pairis, J-L. and Rosset, J., (1977). Comte rendu de l'excursion de la Société Géologique Suisse en Haute Savoie (France) du 10 au 12 octobre 1976. Eclog. Geol. Helv., 70/1, 253-285.

Charollais, P., Hochuli, P.A., Oertli, H.J., Perch Nielsen, K., Tourmarkine, M., Rögl, F. and Pairis, J-L., (1980). Les Marnes à Foraminifères et les Schistes à Meletta des chaînes subalpines septentrionales (Haute Savoie, France). Eclog. Geol. Helv., 73/1, 9-69.

Choquette, P.W. and James, N.P., (1988). Introduction. In: James, N.P. and Choquette, P.W. (eds). Paleokarst. Springer Verlag, 1-25.

Clarkson, E.N.K., (1986). Invertebrate palaeontology and evolution. 2nd Edition. Unwin Hyman Inc. 382pp.

Cloetingh, S., (1988) Intraplate stresses: a tectonic cause for third-order cycles in apparent sea-level? In: Wilgus et al., (eds). Sea-level changes: an integrated approach. S.E.P.M. Spec. Pub., 42, 19-31.

Collet, L.W. and Lillie, A., (1938). Le Nummulitique de la Nappe de Morcles entre Arve et Rhône. Eclog. Geol. Helv., 31/1, 105-123.

Crampton, S.L., (1992). Inception of the Alpine Foreland Basin: Basal unconformity and Nummulitic limestone. 2 vols. Unpubl. PhD Thesis, Univ. Oxford.

Crampton, S.L. and Allen, P.A., (1995). Recognition of forebulge unconformities associated with early stage foreland basin development: example from the North Alpine Foreland Basin. Bull A.A.P.G., 79/10, 1495-1514.

Davies, P.J., Symonds, P.A., Feary, D.A. and Pigram, C.J., (1989). The evolution of the carbonate platforms of north-eastern Australia. In: Crevello, P.D., Wilson, J.L.,

Sarg, J.F. and Read, J.F., (eds). Controls on carbonate platform and basin development. S.E.P.M. Spec. Pub. 44, 233-258.

Davis, D., Suppe, J. and Dahlen, F.A., (1983). Mechanics of fold-and-thrust belts and accretionary wedges. J. Geophys. Research, 88/B2, 1153-1172.

Debrand-Passard, S., (1984). Synthèse géologique du sud-est de la France. Volume 1: Stratigraphie et paléogéographie. Mém. B.R.G.M. 125, 615pp.

Delamette, M., (1993). Le Pays de Mont-Blanc. Editions Gap, 239pp.

Detraz, H., Müller, A., Müller, D. and Villars, F., (1986). Etude préliminaire de la stratigraphie et de la sédimentologie de la Châine des Aravis. Arch. Sci. Genève, 39/3, 365-376.

Dewey, J.F., Helman, M.L., Turo, E., Hutton, D.W.H. and Knott, S.D., (1989). Kinematics of the Western Mediterranean. In: Coward, M.P., Dietrich, D. and Park, R.G., (eds). Alpine Tectonics. Geol. Soc. Spec. Pub. 45, 265-283.

Dickinson, W.R., (1974). Plate tectonics and sedimentation. In: Dickinson, W.R. (ed). Tectonics and sedimentation. S.E.P.M. Spec. Pub. 22, 1-22.

Dorobek, S.L., (1995). Synorogenic carbonate platforms and reefs in foreland basins: controls on stratigraphic evolution and platform/reef morphology. In: Dorobek, S.L. and Ross, G.M. (eds). Stratigraphic evolution of foreland basins. S.E.P.M. Spec. Pub. 52, 127-147.

Dunham, R.J., (1962). Classification of carbonate rocks according to depositional texture. In: Ham, W.E. (ed.). Classification of carbonate rocks. A.A.P.G. Memoir 1, 108-121.

Ekes, C., (1993). Bedload-transported pedogenic mud aggregates in the Lower Old Red Sandstone in southwest Wales. J. Geol. Soc. London, 150, 469-471.

Esteban, M. and Klappa C.F., (1983). Subaerial exposure environment. In: Scholle, P.A., Bebout, D.G., Moor C.H. (eds). Carbonate Depositional Environments. A.A.P.G. Memoir 33, 2-53.

Evans, M.J. and Mange-Rajetsky, M.A., (1991). The provenance of sediments of the Barrême thrust top basin, Haute Provence, France. In: Morton, A.C., Todd, S.P. and Haughton, P.D.W. (eds). Developments in sedimentary provenance studies. Spec. Publ. Geol. Soc., 57, 323-342.

Flügel, E., (1982) Microfacies analysis of limestones. Springer Verlag. 633pp.

Fujiwara, H. and Pairis, J-L., (1969). Aperçu sur le Nummulitique de la région de Saint-Auban (Alpes Maritimes). Géologie Alpine, t 45, 213-226.

Genin, A., Lazar, B, and Brenner, S., (1995). Vertical mixing and coral death in the Red sea following the eruption of Mount Pinatubo. Nature, 377, 507-510.

Ghose, B.K., (1976). Paleoecology of the Cenozoic reefal foraminifers and algae - a brief review. Palaeogeog., Palaeoclim., Palaeoecol., 22, 231-156.

Gorin, G., Gülaçar, F. and Cornioley, Y., (1989). Organic geochemistry, maturity, palynofacies and palaeoenvironment of Upper Kimmeridgian and Lower Tertiary organic-rich samples in the southern Jura (Ain, France) and subalpine massifs (Haute Savoie, France). Eclog. Geol. Helv., 82/2, 491-515.

Guellec, S., Mugnier, J-L., Tardy, M. and Roure, F., (1990). Neogene evolution of the western Alpine Foreland in the light of ECORS data and balanced cross-section. In: Roure, F., Heitzmann, P. and Polino, R. (eds). Deep structure of the Alps. Mém. Soc. Géol. France, Paris, 156, 165-184.

Hallock, P., (1979). Trends in test shape with increasing depth in large symbiont-bearing foraminifera. J. Foram. Research, 9/1, 61-19.

Hallock, P. and Glenn, C.E., (1985). Numerical analysis of foraminiferal assemblages: a tool for recognising depositional facies in Lower Miocene reef complexes. J. Paleontology, 59/6, 1382-1394.

Hallock, P. and Glenn, C.E., (1986). Larger foraminifera: a tool for palaeoenvironmental analysis of Cenozoic carbonate depositional facies. Palaios, 1, 55-64.

Hallock, P., Hine, A.C., Vargo, G.A., Elrod, J.A. and Jaap, W.C., (1988). Platforms of the Nicaraguan Rise: Examples of the sensitivity of carbonate sedimentation to excess trophic resources. Geology, 16, 1104-1107.

Hallock, P. and Schlager, W., (1986). Nutrient excess and the demise of coral reefs and carbonate platforms. Palaios, 1, 389-398.

Hamiti, M., (1994). Géometrie, cinématique et méchanisms des chevauchements synschisteux dans une région prealablement déformée. Example de la couveture sédimentaire à l'ouest du massif de l'Argentera (Alpes Occidentales Français). Unpubl. PhD thesis, Université de Droit, d'Economie et des Sciences d'Aix-Marseille.

Hancock, P.L. and Bevan, T.G., (1987). Brittle modes of foreland extension. In: Coward, M.P., Dewey, J.F. and Hancock, P.L. (eds). Continental extension tectonics. Geol. Soc. Spec. Pub. 28, 127-137.

Handford, R.C. and Loucks, R.G., (1994). Carbonate depositional sequences and systems tracts - responses of carbonate platforms to relative sea-level changes. In: Loucks, R.G. and Sarg, J.F., (eds). Carbonate sequence stratigraphy: recent developments and applications. A.A.P.G. Memoir 57, 3-42.

Haq, B.U., Hardenbol, J. and Vail, P.R., (1988). Mesozoic and Cenozoic chronostratigraphy and cycles of sea-level change. In: Wilgus, C.K., Hastings, B.S., Kendall, C.G.St.C., Posamentier, H.W., Ross, C.A. and Van Wagoner, J.C. (eds), Sea level changes: an integrated approach. S.E.P.M. Spec. Pub. 42, 71-108.

Hart, B.S. and Plint, A.G., (1993). Tectonic influence on deposition and erosion in a ramp setting: Upper Cretaceous Cardium Formation, Alberta Foreland Basin. Bull. A.A.P.G., 77/12, 2092-2107.

Herb, R., (1988). Eocaene Paläogeographie und Paläotektonic des Helvetikums. Eclog. Geol. Helv., 81/3, 611-657.

Hirst, J.P.P. and Nichols, G.J., (1986). Thrust tectonic controls on Miocene alluvial distribution patterns, southern Pyrenees. In: Allen, P.A. and Homewood, P., (eds). Foreland Basins. I.A.S. Spec. Pub. 8, 247-258.

Homewood, P., Allen, P.A. and Williams, D.G., (1986). Dynamics of the Molasse Basin of western Switzerland. In: Allen, P.A. and Homewood, P., (eds). Foreland Basins. I.A.S. Spec. Pub 8, 199-218.

Hottinger, L., (1983). Processes determining the distribution of larger foraminifera in space and time. In: Meulenkamp, J.E., (ed.). Reconstruction of Marine Palaeoenviroments. Bull. Utrecht Micropal., 30, 239-253.

Huggenberger, P. and Wildi, W., (1991). La tectonique du massif des Bornes (Chaines Subalpines, Haute Savoie, France). Eclog. Geol. Helv., 84/1, 125-149.

Hunt, D. and Tucker, M.E., (1993). Sequence stratigraphy of carbonate shelves with an example from the mid-Cretaceous (Urgonian) of southeast France. In: Posamentier, H.W., Summerhayes, C.P., Haq, B.U. and Allen, G.P., (eds). Sequence stratigraphy and facies associations. I.A.S. Spec. Pub. 18, 307-342.

Illies, J.H., (1977). Ancient and recent rifting in the Rhinegraben. Geologie en Mijnbouw, 56/4, 329-350.

James, N.P. and Kendall, A.C., (1992). Introduction to carbonate and evaporite facies models. In: Walker, R.G. and James, N.P. (eds). Facies Models - response to sea-level change. Geol. Ass. Canada Publ., 265-275.

Johnson, J.H., (1961). Limestone building algae and algal limestones. Johnson Publ. Co., Colorado. 297pp.

Jordan, T.E., (1981). Thrust loads and foreland basin evolution, Cretaceous, western United States. Bull. A.A.P.G., 65/2, 2506-2520.

Keller, G., (1983) Paleoclimatic analyses of Middle Eocene through Oligocene planktic foraminiferal faunas. Palaeogeog., Palaeoclim., Palaeoecol., 43, 73-94.

Kendall, C.G.St.C. and Schlager, W., (1981). Carbonates and relative changes in sea level. Marine Geology, 44, 181-212.

Kerkhove, C., (1979). Notice explicative de la feuille Gap à 1/250 000. Bureau Rech. Géol et Minières, 35, 46pp.

Klappa, C.F., (1978). Biolithogenesis of *Microcodium*: elucidation. Sedimentology, 25, 489-522.

Lateltin, O. and Müller, D., (1987). Evolution paléogéographique du Bassin des Grès de Taveyannaz dans les Aravis (Haute Savoie) à la fin du Paléogène. Eclog. Geol. Helv., 80/1, 127-140.

Laubscher, H., (1992). Jura kinematics and the Molasse Basin. Eclog. Geol. Helv., 85/3, 653-675.

Lemoine, M and Grasziansky, P.C., (1988). Histoire d'une marge continentale passive: les Alpes occidentales au Mésozoïque. Introduction. Bull. Soc. Géol. France, 8, t.IV,/4, 597-600.

Lihou, J.C., (1994). Reconstructing the geometry of the embryonic North Alpine Foreland Basin, Eastern Switzerland. Pub. Abstract, Géol. Alpine. Série Spéciale "Colloques et Excursions", 4, 68-69.

Lihou, J.C., (1995). A new look at the Blattengrat unit of eastern Switzerland: Early Tertiary foreland basin sediments from the south Helvetic Realm. Eclog. Geol. Helv., 88/1, 91-114.

Loeblich, A.R. and Tappan, H., (1964). Treatise on invertebrate paleontology. Part C, Protista 2, Sarcodina, chiefly "Thecamoebians" and Foraminiferida. Geol. Soc. America. 2 vols, 900pp.

Mack, G.H. and James, W.C., (1994). Paleoclimate and the global distribution of paleosols. Journal of Geology, 102, 360-366.

May, M.T., Furer, L.C., Kvale, E.P., Suttner, L.J., Johnson, G.D. and Meyers, J.H., (1995). Chronostratigraphy and tectonic significance of Lower Cretaceous conglomerates in the foreland of central Wyoming. In: Dorobek, S.L. and Ross, G.M. (eds). Stratigraphic evolution of foreland basins. S.E.P.M. Spec. Pub. 52, 97-110.

Meckel III, L.D., Ford, M. and Bernoulli, D., (submitted). Tectonic and sedimentary evolution of a foreland basin in the corner of an orogenic arc: The Tertiary Dévoluy Basin, External Western Alps, SE France. J. Geol. Soc. London.

Miall, A.D., (1977). A review of the braided river depositional environment. Earth Sci. Reviews, 13, 1-62.

Morrow, D.W., (1986). The sea-level rise staircase on continental margins and the origin of upwards-shoaling carbonate sequences. Bull. Can. Pet. Geol., 34/2, 284-285.

Mougin-Grosso, F. and Pairis, J-L., (1973). Remarques sur la sédimentation tertiaire dans la partie est de la structure d'Annot. (Alpes de Haute-Provence). Annales du Centre Univ. de Savoie, t 1, 99-118.

Murray, J.W., (1991). Ecology and Palaeoecology of benthic foraminifera. Longman Group, 397pp.

Pairis, B. and Pairis, J-L., (1975). Précisions nouvelles sur le Tertiaire du Massif de Platé (Haute Savoie). Géol. Alpine, 51, 83-127.

Pairis, B. and Pairis, J-L., (1978). Mécanisms de deformation dans le massif de Platé (Haute Savoie). Annales du Centre Univ. Savoie, III, Sciences Naturelles, 37-52.

Pairis, J-L., (1988). Paléogène marin et structuration des Alpes Occidentales Françaises (domaine externe et confins sub-occidentaux de subbriançonnais). Unpubl. PhD thesis, l'Univ. Joseph Fourier, Grenoble 1.

Pairis, J-L., Bellière, J. and Rosset, J., (1992). Cluses - Notice explicative de la feuille Cluses à 1:50 000. Edit. B.R.G.M., 89pp.

Pedley, A., (1994). Eocene foreland basin carbonate facies, the external Sierras, Spanish Pyrenees. Unpubl. PhD Thesis, Univ. London.

Pfiffner, O.A., (1986). Evolution of the North Alpine Foreland Basin in the central Alps. In: Allen, P.A. and Homewood, P. (eds). Foreland Basins. I.A.S. Spec. Pub. 8, 219-228.

Pigram, C.J.. Davies, P.K., Feary, D.A. and Symonds, P.A., (1989). Tectonic controls on carbonate platform evolution in southern Papua New Guinea: passive margin to foreland basin. Geology, 17, 199-202.

Plint A.G., Hart, B.S. and Donaldson, W.S., (1993). Lithospheric flexure as a control on stratal geometry and facies distribution in Upper Cretaceous rocks of the Alberta Foreland Basin. Basin Research, 5, 69-77.

Puídefabregas, C., Muñoz, J.A. and Marzo, M., (1986). Thrust belt development in the eastern Pyrenees and related depositional sequences in the southern foreland basin. In: Allen, P.A. and Homewood, P. (eds). Foreland Basins. I.A.S. Spec. Pub 8, 229-246.

Pujalte, V., Robles, S., Robador, A. Baceta, J.I., and Orme-Etxebarria, X., (1993). Shelf-to-basin palaeogeography and depositional sequences, western Pyrenees, north Spain. In: Posamentier, H.W., Summerhayes, C.P., Haq, B.U. and Allen, G.P., (eds). Sequence stratigraphy and facies associations. I.A.S. Spec. Pub. 18, 369-395.

Quinlan, G.M. and Beaumont, C., (1984). Appalachian thrusting, lithospheric flexure and the Paleozoic stratigraphy of the Eastern Interior of North America. Can. J. Earth Sci., 21, 973-996.

Racey, A., (1990). Nummulitid biostratigraphy and Paleogene palaoenvironments of the Sultanate of Oman. Unpubl. PhD thesis, Univ. London, 510pp.

Rat, P., (1978). Les phases tectoniques au Tertiare dans le nord du Fossé Bressan et ses marges bourgingnonnes en regard des systèmes d'érosion et de la sédimentation. Comtes Rendus Soc. Géol. France, 5, 231-234.

Read, J.F., (1980). Carbonate ramp-to-basin transitions and foreland basin evolution, Middle Ordovician, Virginia Appalachians. Bull. A.A.P.G., 64/10, 1575-1612.

Read, J.F., Grotzinger, J.P., Bova, J.A. and Koerschner, W.F., (1986). Models for generation of carbonate cycles. Geology, 14, 107-110.

Ricci Luchi, F., (1986). The Oligocene to Recent foreland basins if the northern Apennines. In: Allen, P.A. and Homewood, P. (eds), Foreland Basins. I. A. S. Spec. Pub. 8, 105-139.

Robertson, A.H.F., (1988). Late Cretaceous chemical sediments related to a carbonate platform - foreland basin transition in the Oman Mountains. Sed. Geol. 57, 1-15.

Roure, J., (1980). Notice explicative de la feuille Nice à 1/250 000. Bur. Rech. Geol. Min., 40, 94pp.

Roure, F., Brun, J.P., Colletta, B. and Vandendriessche, J., (1992). Geometry and kinematics of extensional structures in the Alpine Foreland Basin of SE France. J. Struct. Geol., 14/5, 503-519.

Sami, T.T. and James, N.P., (1993). Evolution of an early Proterozoic foreland basin carbonate platform, lower Perthei Group, Great Slave Lake, Northwest Canada. Sedimentology, 40, 403-430.

Sarg, J.F., (1988). Carbonate Sequence Stratigraphy. In: Wilgus, C.K., Hastings, B.S., Kendall, C.G.St.C., Posamentier, H.W., Ross, C.A. and Van Wagoner, J.C. (eds). Sea level changes: an integrated approach. S.E.P.M. Spec. Pub. 42,155-181.

Sartorio, D. and Venturini, S., (1988). Southern Tethys biofacies. Agip S.p.A., S. Donato Milanese. 235pp.

Schaub, H., (1981). Nummulites et Assilines de la Téthys paléogène. Taxinomie, phylogenèse et biostratigraphie. Schweizerisches Paläontologisches Abhandlungen, 104, 236pp.

Schlager, W., (1981). The paradox of drowned reefs and carbonate platforms. Bull. Geol. Soc. America, 92/1, 197-211.

Schlager, W., (1989). Drowning unconformities on carbonate platforms. In: Crevello, P.D., Wilson, J.L., Sarg, J.F. and Read, J.F., (eds), Controls on carbonate platform and basin development. S.E.P.M. Spec. Pub. 44, 15-25.

Schlager, W., (1991). Depositional bias and environmental change - important factors in sequence stratigraphy. Sed. Geol., 70, 101-130.

Schlager, W., (1992). Sedimentology and sequence stratigraphy of reefs and carbonate platforms. A.A.P.G. Cont. Education Course Notes, 34, 71pp.

Shackleton, N.J. and Kennet, J.P., (1975). Palaeotemperature history of the Cenozoic and the initiation of Antarctic glaciation: oxygen and carbon isotope analysis in D.S.D.P. sites 277, 279 and 281. D.S.D.P. Initial Report 29, 723-755.

Siddans, A.W.B., (1979). Arcuate fold and thrust patterns in the subalpine chains of SE France. J. Struct. Geol., 1/2, 117-126.

Sinclair, H.D., (in press). Plan-view curvature of foreland basins and its implications for the palaeostrength of the lithosphere underlying the western Alps. Basin Research.

Sinclair, H.D. and Allen, P.A., (1992). Vertical versus horizontal motions in the Alpine orogenic wedge: stratigraphic response in the foreland basin. Basin Research, 4/3, 215-232.

Sinclair, H.D., Coakley, B.J., Allen, P.A. and Watts, A.B., (1991). Simulation of foreland basin stratigraphy using a diffusion model of mountain belt uplift and erosion: and example from the central Alps, Switzerland. Tectonics, 10/3, 599-620.

Tankard, A.J., (1986). On the depositional response to thrusting and lithospheric flexure: examples from the Appalachian and Rocky Mountain basins. In: Allen, P.A. and Homewood, P. (eds). Foreland Basins, I.A.S. Spec. Pub. 8, 369-394.

Tempier, C., (1987). Modèle nouveau de mise en place des structures provençales. Bull. Soc. Géol. France, 8, tIII/3, 533-540.

Thome, M., (1987). Le paléogène marin dans les synclinaux de la moyenne vallée du Verdon. (Stratigraphie et tectonique synsédimentaire). Thése dipl. de geologue, Univ. Grenoble, 112pp.

Tricart, P., (1984). From passive margin to continental collision: a tectonic scenario for the western Alps. Am. J. Sci., 284, 97-120.

Trümpy, R., (1980). Geology of Switzerland: a guide book. Part A: An outline of the geology of Switzerland. Schweizerische Geologische Komission, 104pp.

Tucker, M.E., (1991). Sedimentary petrology. 2nd edition. Blackwell Scientific Pubs 260pp.

Tucker. M.E., Calvet, F. and Hunt, D.W., (1993). Sequence stratigraphy of carbonate ramps: systems tracts, models and application to the Muschelkalk carbonate platforms of eastern Spain. In: Posamentier, H.W., Summerhayes, C.P., Haq, B.U. and Allen, G.P., (eds). Sequence stratigraphy and facies associations. Spec. Pub. I.A.S., 18, 397-415.

Tucker. M.E. and Wright, V.P., (1990). Carbonate sedimentology. Blackwell Scientific Pubs, 482pp.

Vail, P.R., Mitchum, R.M., Todd, R.G., Widmier, J.M., Thompson III, S., Sangree, J.B., Bubb, J.N. and Hatlelid, W.G., (1977). Seismic stratigraphy and global changes of sea-level. In: Payton, C., (ed.). Seismic stratigraphy - applications to hydrocarbon exploration. A.A.P.G. Memoir, 26, 49-212.

Van Wagoner, J.C., Posamentier, H.W., Mitchum, R.M., Vail, P.R., Sarg, J.F., Loutit, T.S. and Hardenbol, J., (1988). An overview of the fundamentals of sequence stratigraphy and key definitions. In: Wilgus, C.K., Hastings, B.S., Kendall, C.G.St.C., Posamentier, H.W., Ross, C.A. and Van Wagoner, J.C. (eds). Sea level changes: an integrated approach. S.E.P.M. Spec. Pub. 42, 39-45.

Van Wagoner, J.C., Mitchum, R.M., Campion, K.M. and Rahmanian, V.D., (1990). Siliciclastic sequence stratigraphy in well logs, cores and outcrops: concepts for high-resolution correlation of time and facies. A.A.P.G. Meth. Expl. Series, 7, 55pp.

Veevers, J.J, Falvey, D.A. and Robins S., (1978). Timor trough and Australia: facies show topographic wave migrated 80km during the past 3Ma. Tectonophysics, 45, 217-227.

Walker, K.R., Shanmugam, G. and Ruppel, S.C., (1983). A model for carbonate to terrigenous clastic sequences. Bull. Geol. Soc. America, 94, 700-712.

Watts, A.B., (1992). The effective elastic thickness of the lithosphere and the evolution of foreland basins. Basin Research, 4/3, 169-178.

Weidmann, M., Franzen, J. and Berger, J-P., (1991). Sur l'âge des Couches à Cérithes ou Couches des Diablerets de l'Eocène alpin. Eclog. Geol. Helv., 84/3, 893-919.

Wildi, W., Funk, H. Loup, B., Amato, E. and Huggenberger, P., (1989). Mesozoic subsidence history of the European marginal shelves of the Alpine Tethys (Helvetic Realm, Swiss Plateau and Jura). Eclog. Geol. Helv., 82/3, 817-840.

Wooler, D.A., Smith, A.G. and White, N., (1992). Measuring lithospheric stretching on Tethyan passive margins. J. Geol. Soc. London, 149, 517-532.

Wray, J.L., (1977). Calcareous Algae. Elsevier, 185pp.

Wright, V.P. and Tucker, M.E., (1991). Calcretes. I.A.S. reprints volume 2, 1-22.

Yang, K-M. and Dorobek, S.L., (1995). The Permian Basin of West Texas and New Mexico: tectonic history of a "composite" foreland basin and its effects on stratigraphic development. In: Dorobek, S.L. and Ross, G.M. (eds). Stratigraphic evolution of foreland basins. Spec. Pub. S.E.P.M. 52, 149-174.

Ziegler, P.A., (1988). Evolution of the Arctic-North Atlantic and the Western Tethys. A.A.P.G. Memoir 43, 198pp.

Appendix 1

Measured Sedimentary Sections

Key to Sedimentary Logs

Foraminifera:

- *Nummulites*
- *Amphistegina*
- *Operculina*
- *Discocyclina*
- Orbitolinids
- Miliolids
- Textulariids
- Planktonics

Other bioclasts:

- calcareous red algae
- rhodolith
- bivalve
- oyster
- solitary coral
- colonial coral
- echinoid
- bryozoan
- serpulid worm tubes
- gastropod
- plant debris
- skeletal debris
- peloids
- lithic clasts

Sedimentary structures:

- bioturbation
- cross-bedding (planar)
- cross-bedding (trough)
- ripple lamination
- undulose lamination
- flat lamination
- karst
- borings

Diagenetic features:

- calcite cement
- * glauconite
- P pyrite
- Microcodium
- nodules

Lithological symbols:

Clastic:

- mudrock
- siltstone
- sandstone
- conglomerate

Carbonates (Dunham classification):

- mudstone
- wackestone
- packstone
- grainstone
- boundstone

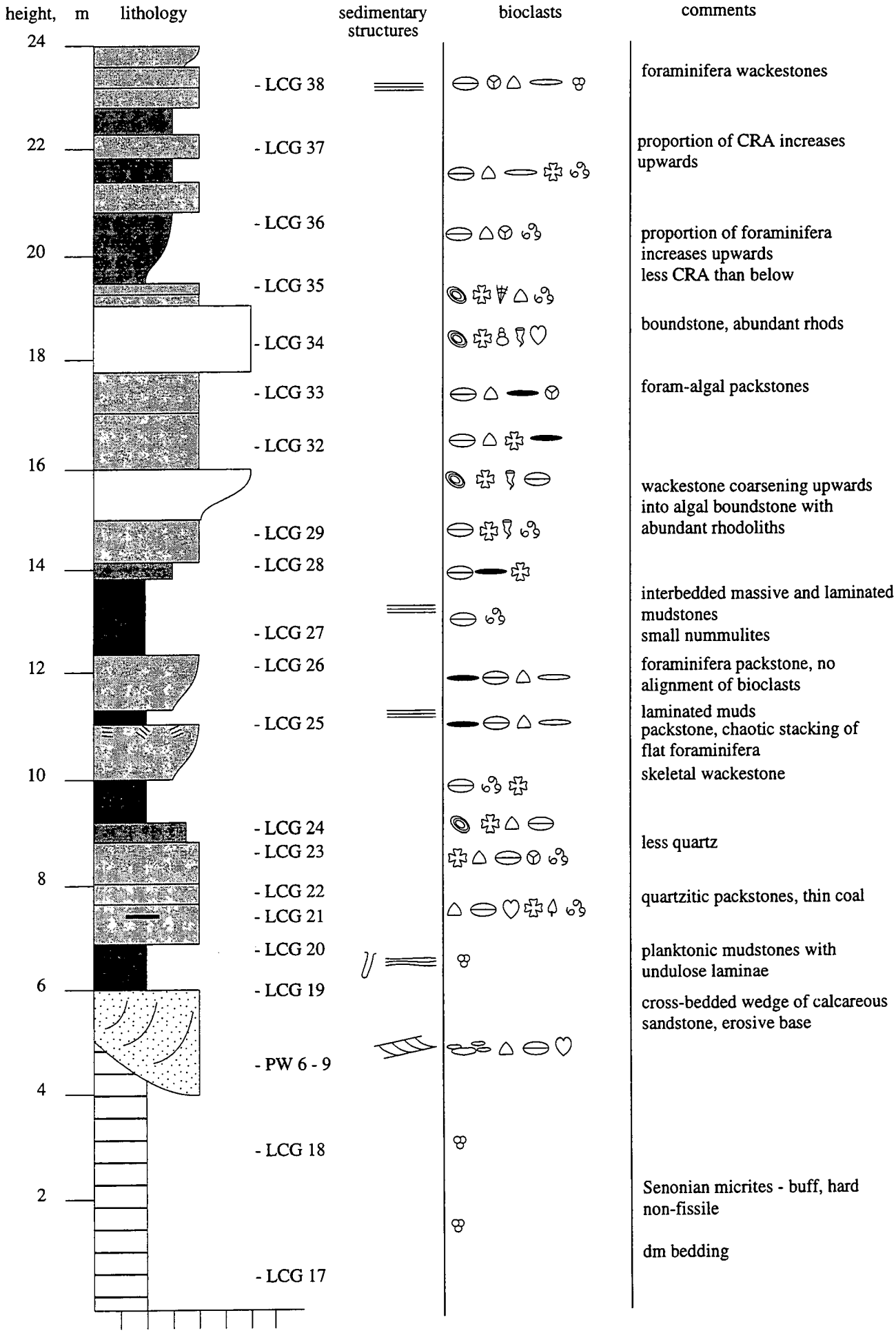

Log S1: Le Chinaillon - Gulley

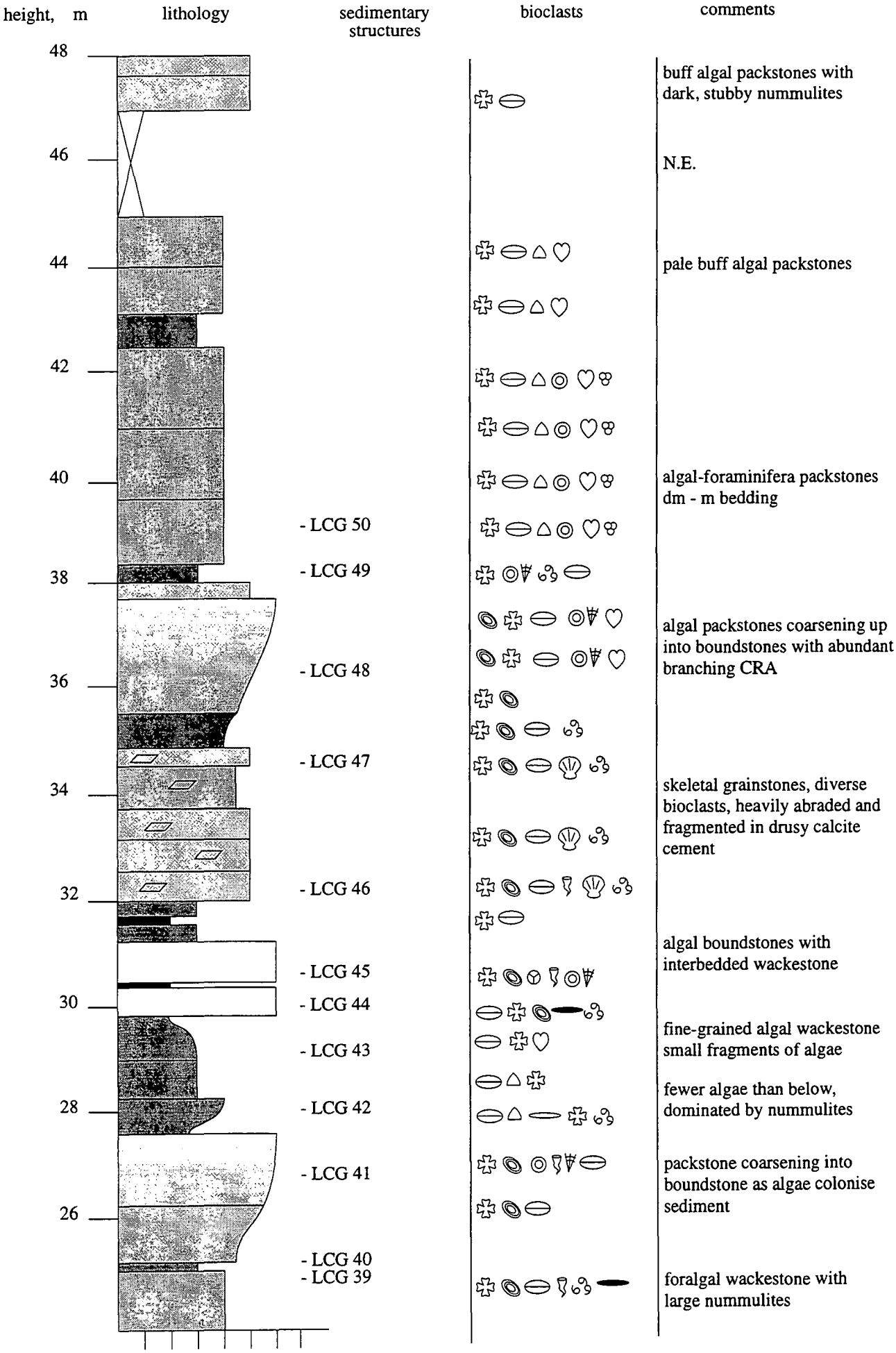

Log S1: Le Chinaillon - Gulley

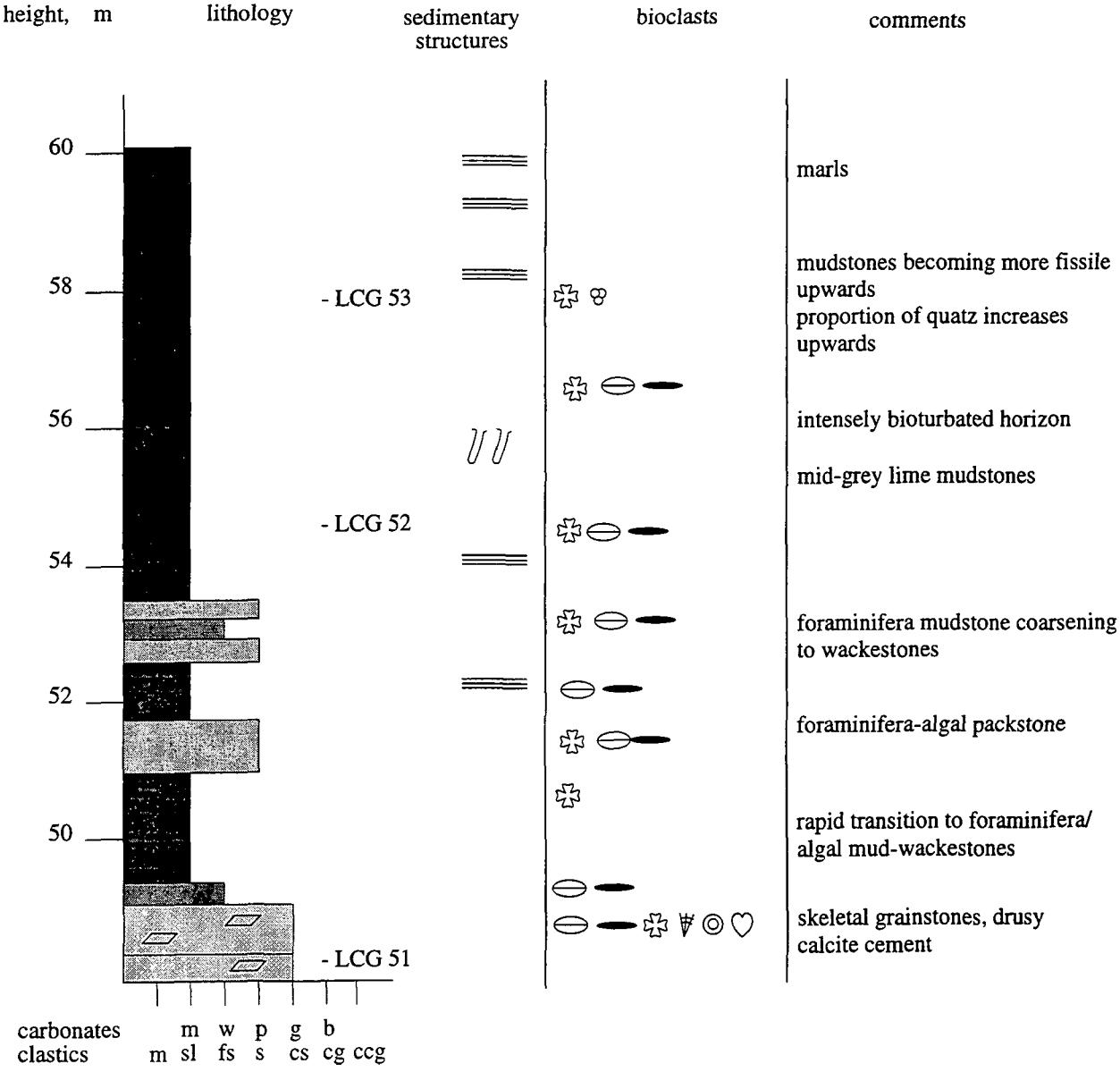

Log S1: Le Chinaillon - Gulley

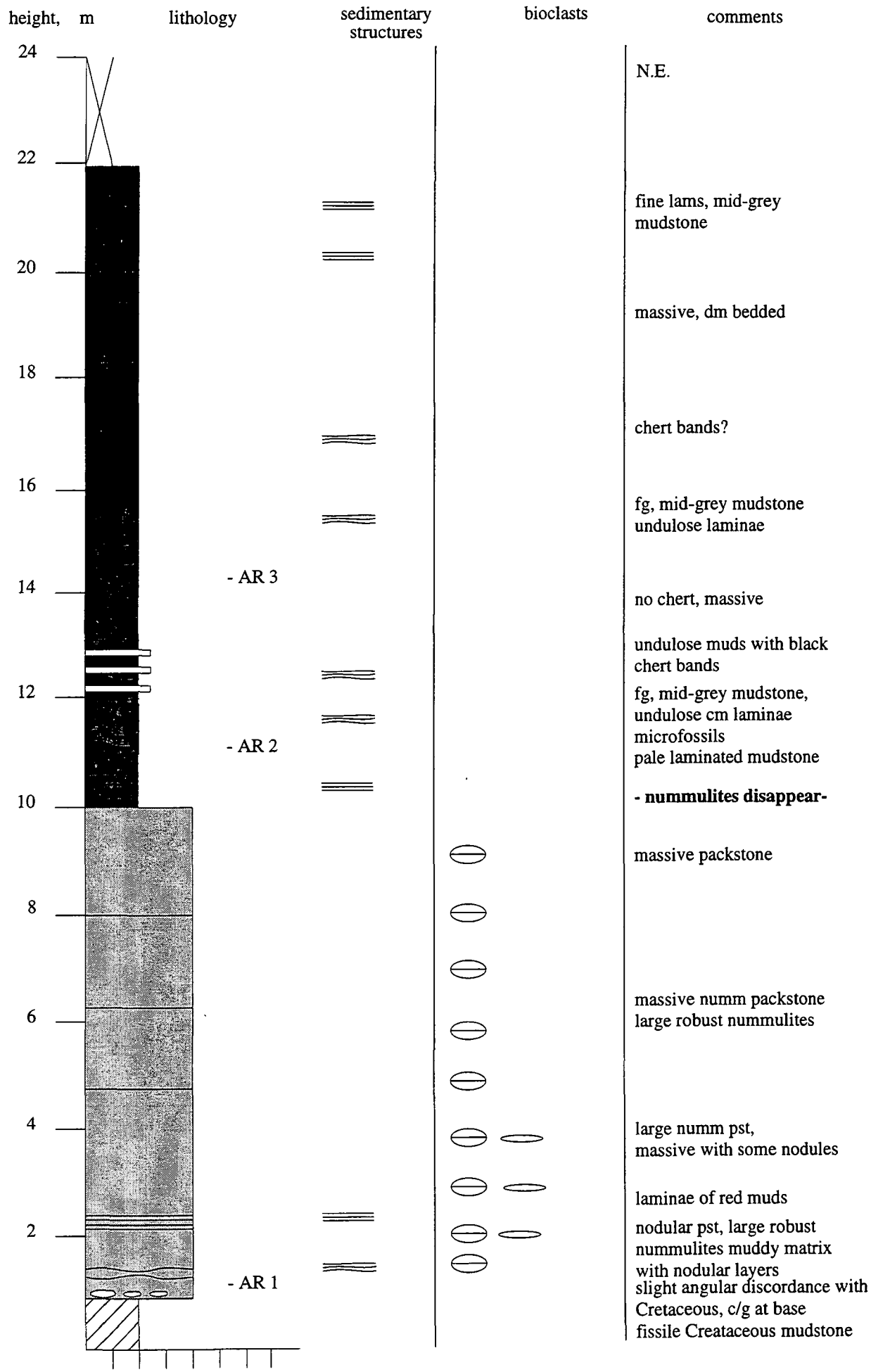

Log S15: Araches

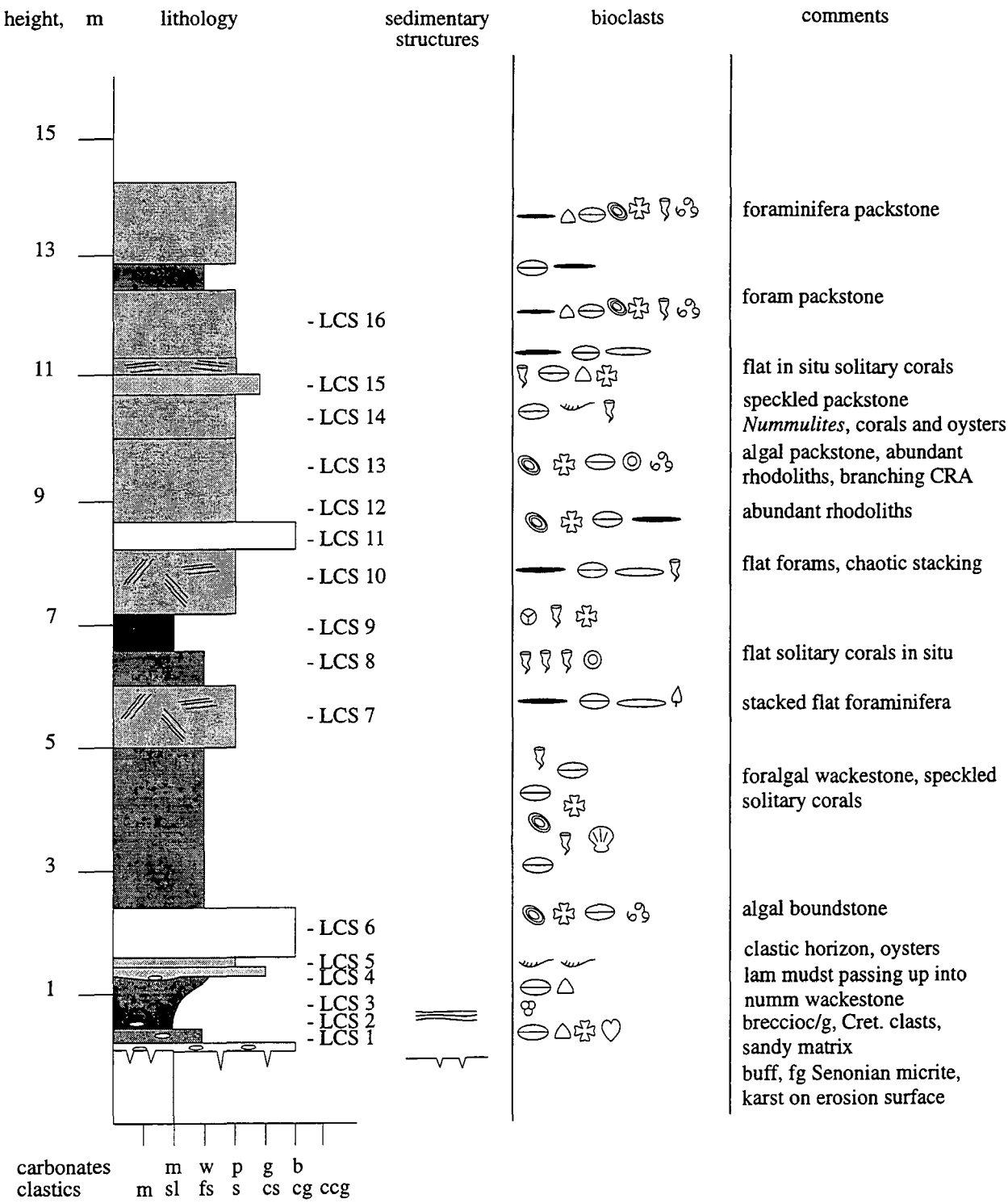

Log S2: Le Chinaillon - Superette

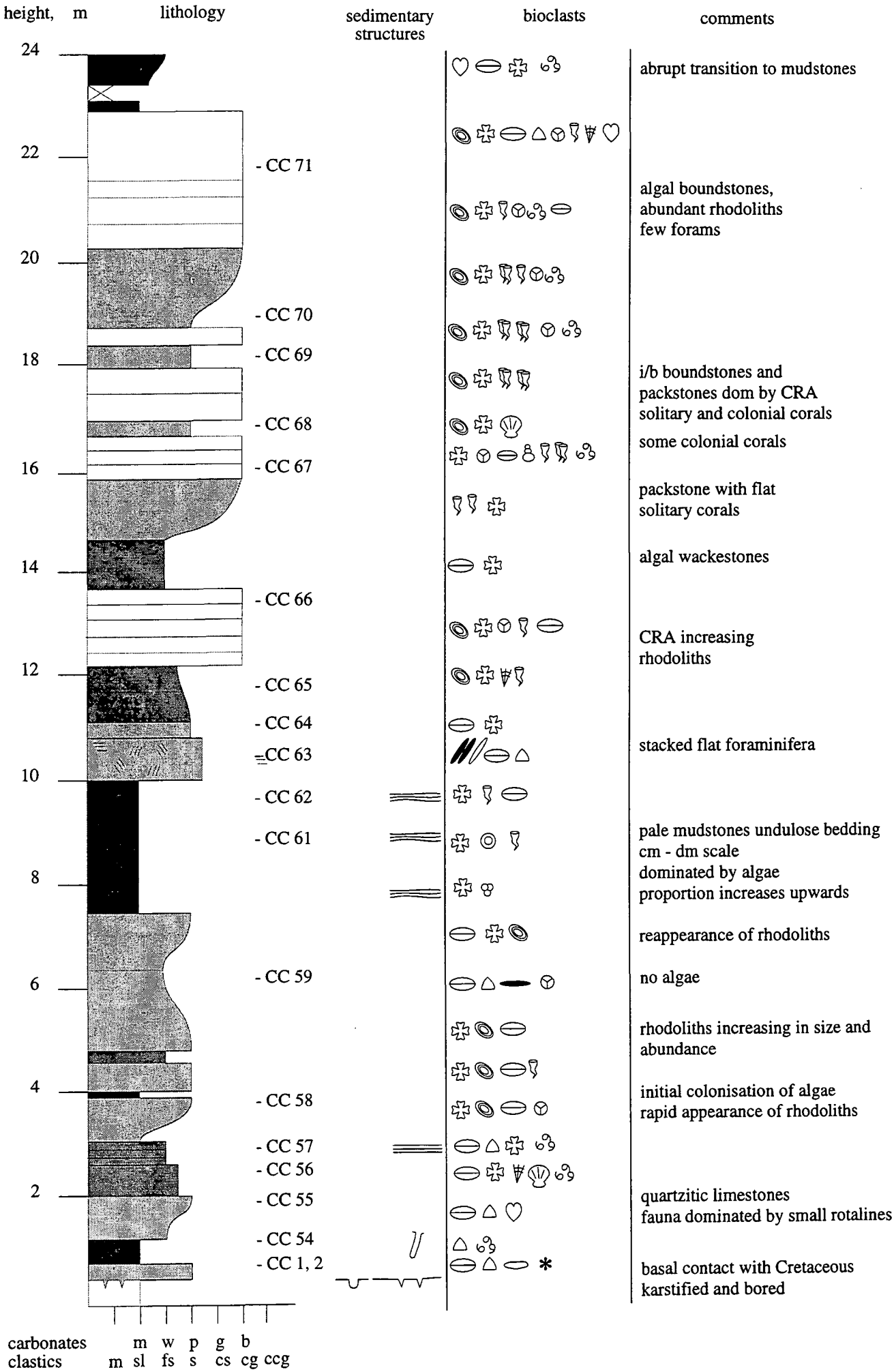

Log S3: Col de la Colombière

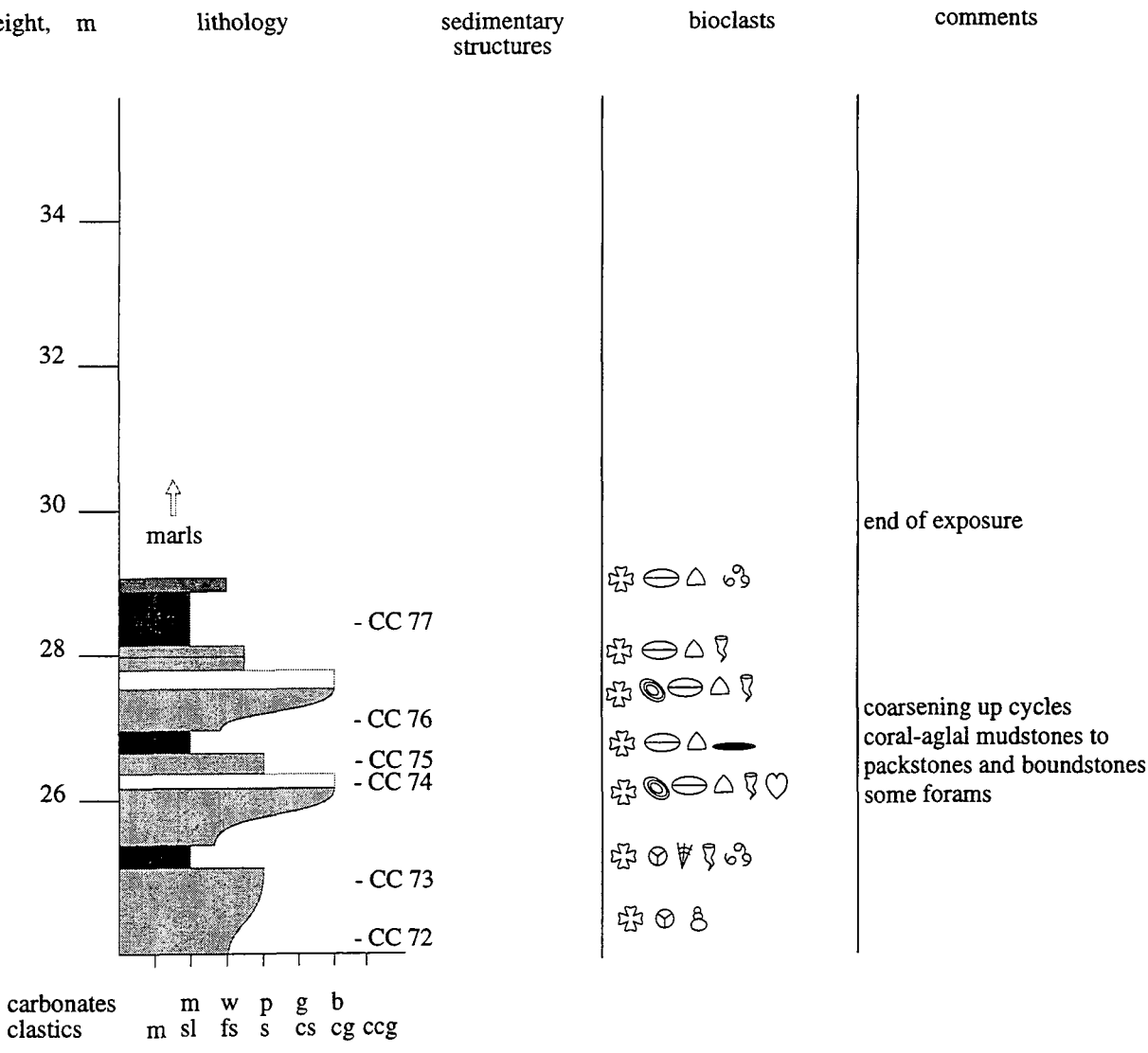

Log S2: Col de la Colombière

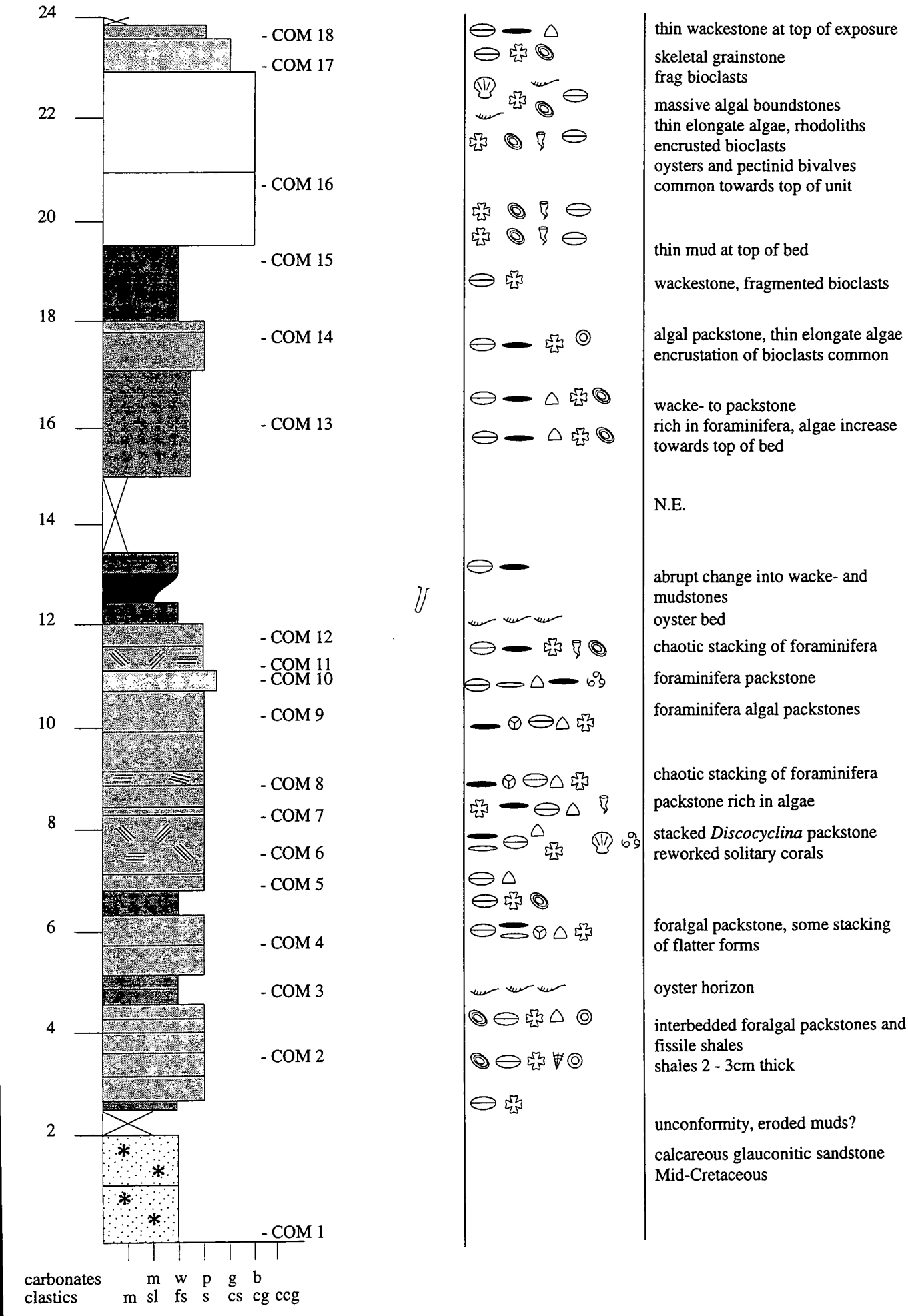

Log S4: La Communaille

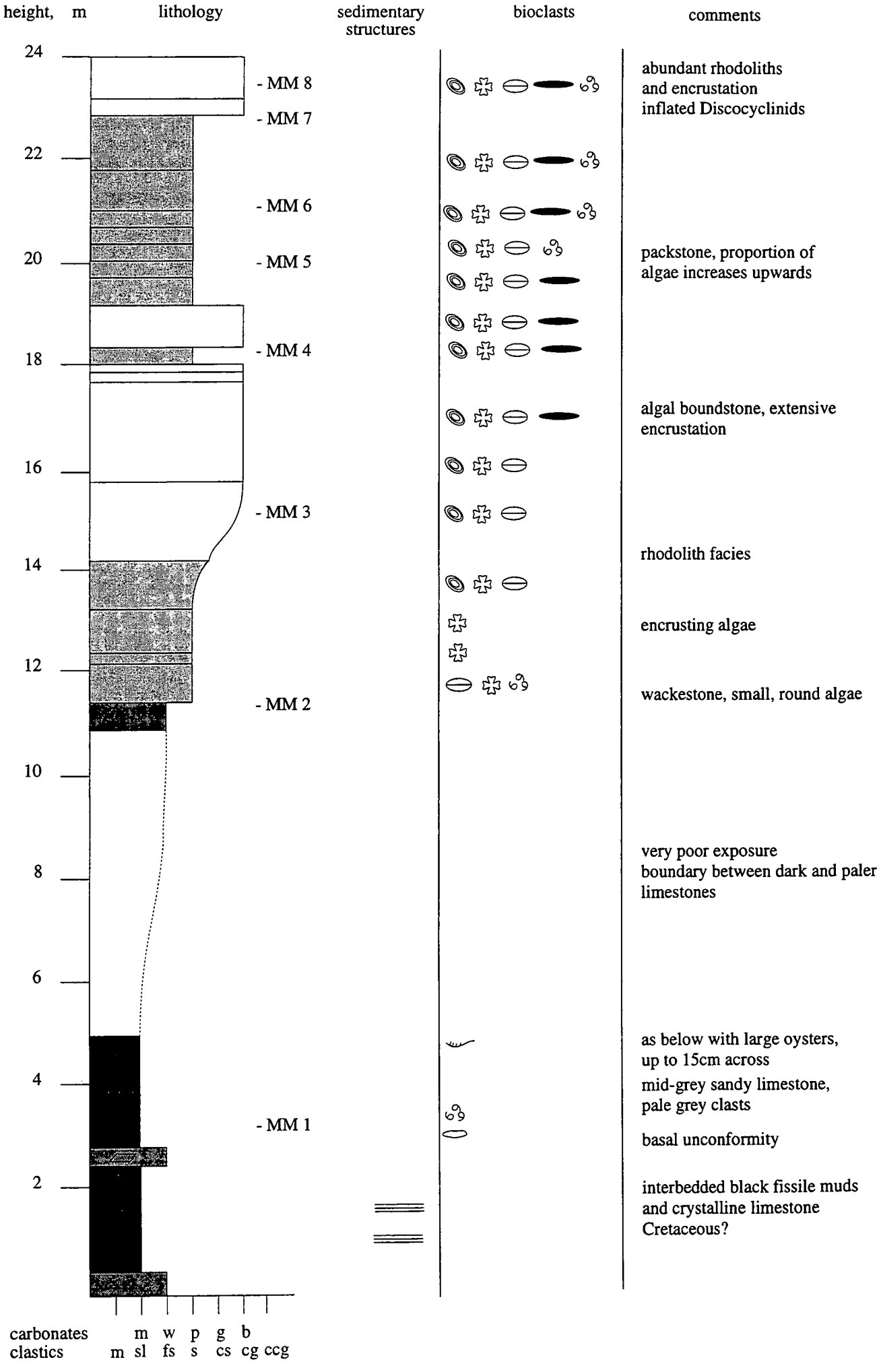

Log S5: Meubles Montagnardes

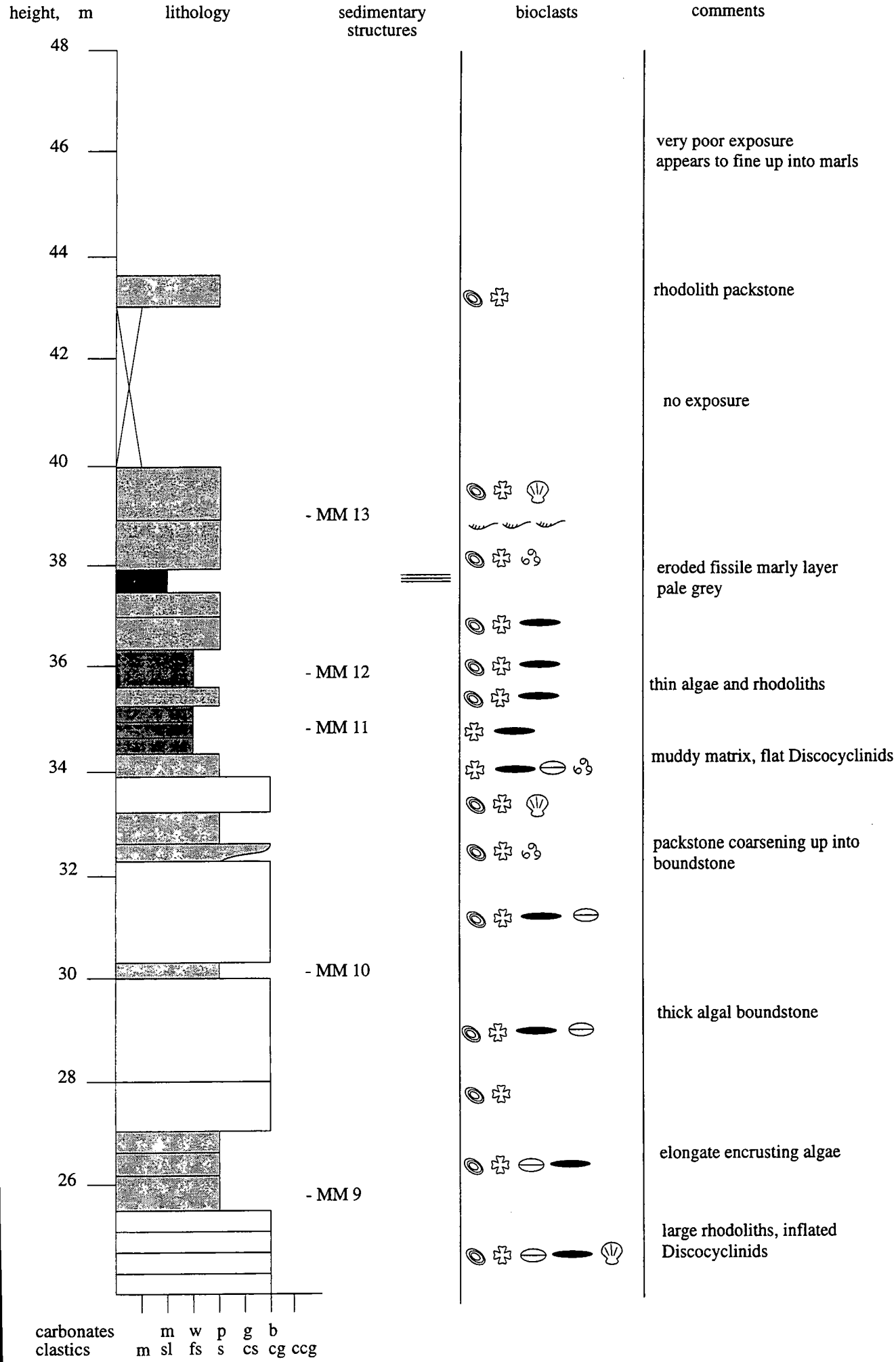

Log S5: Meubles Montagnardes

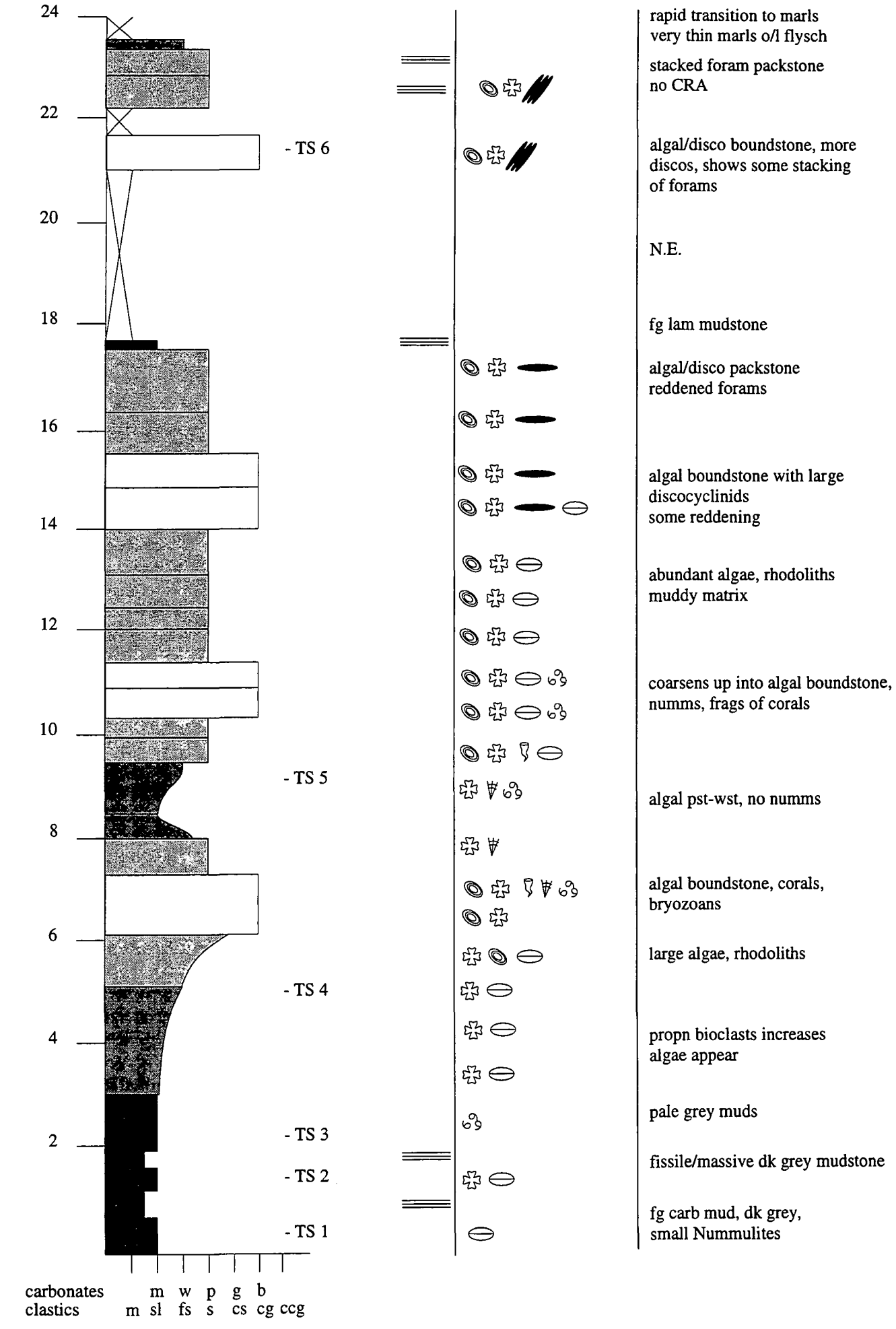

Log S6: Tete de la Sallaz

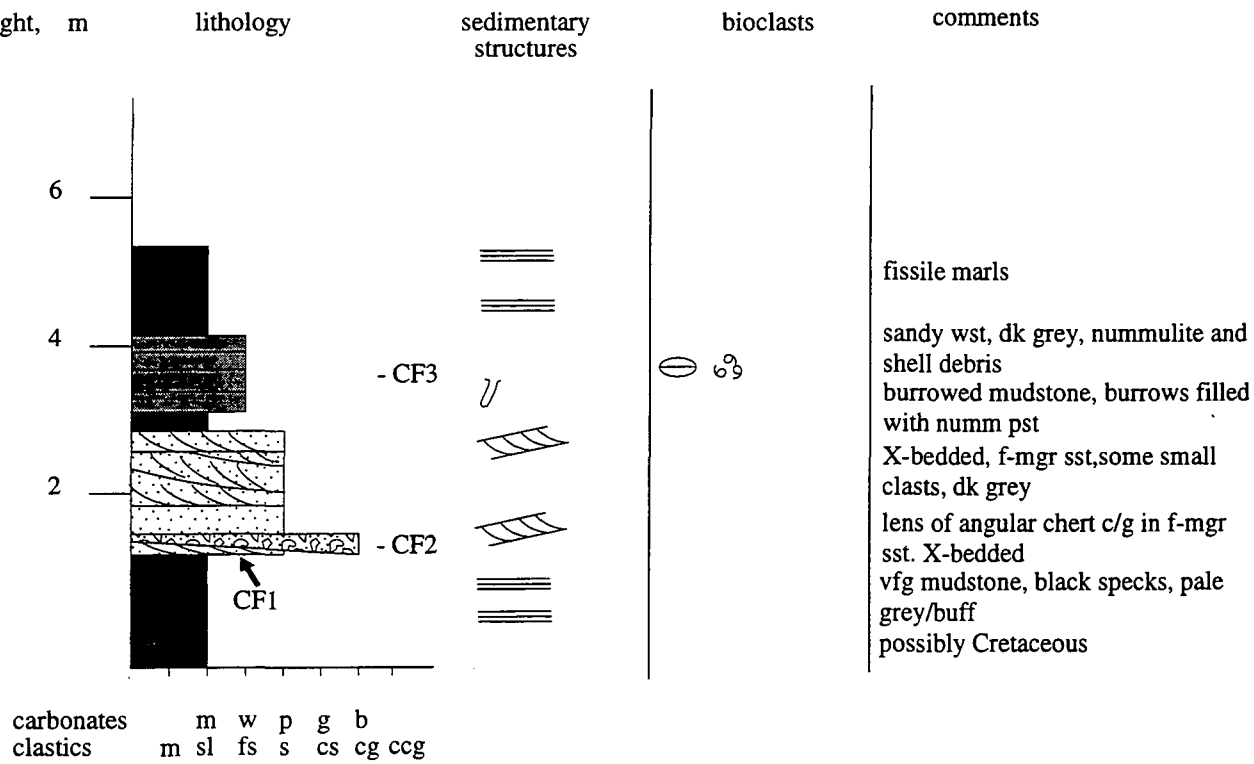

Log S7: Col du Forclaz

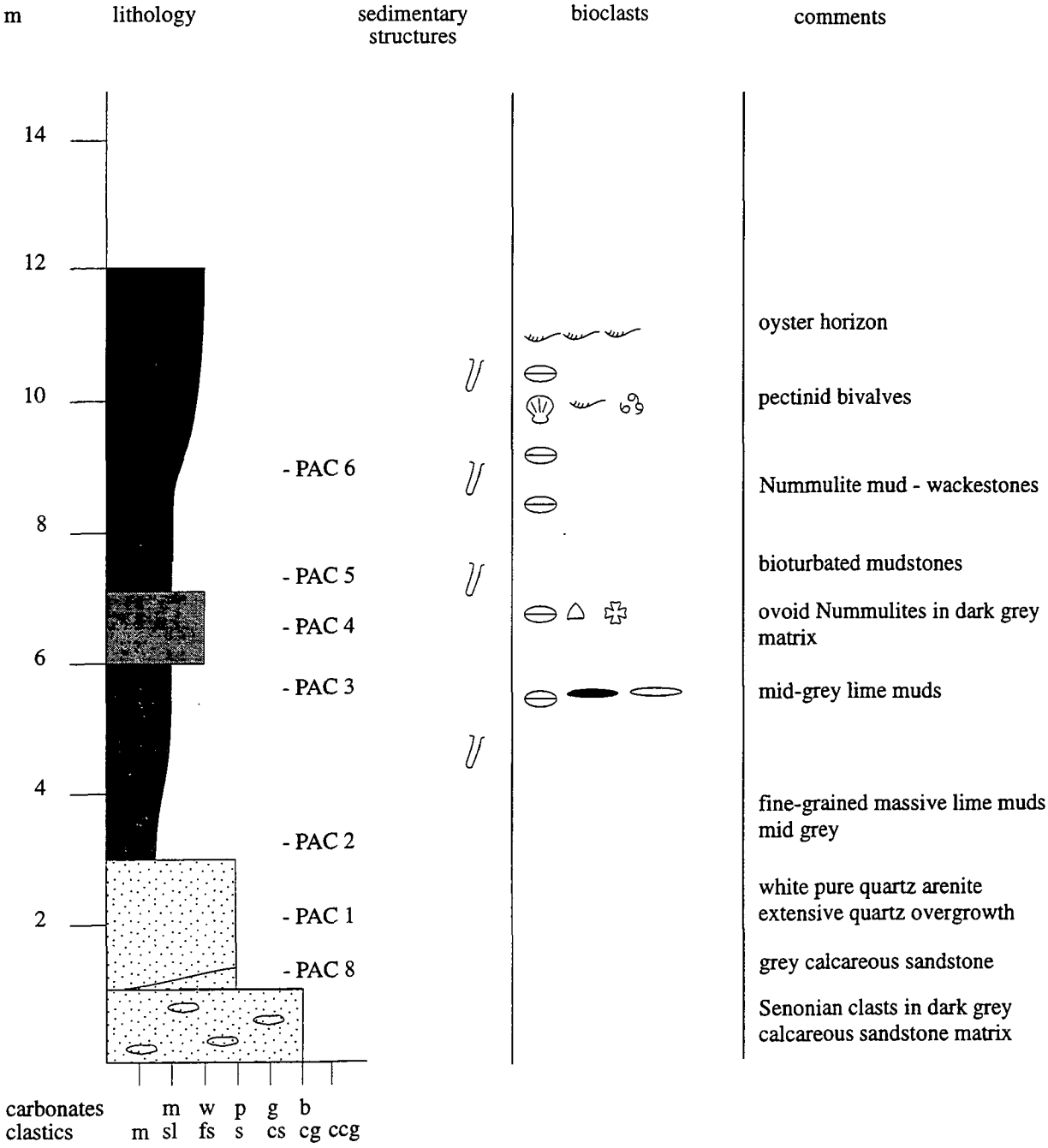

Log S8: Paccaly

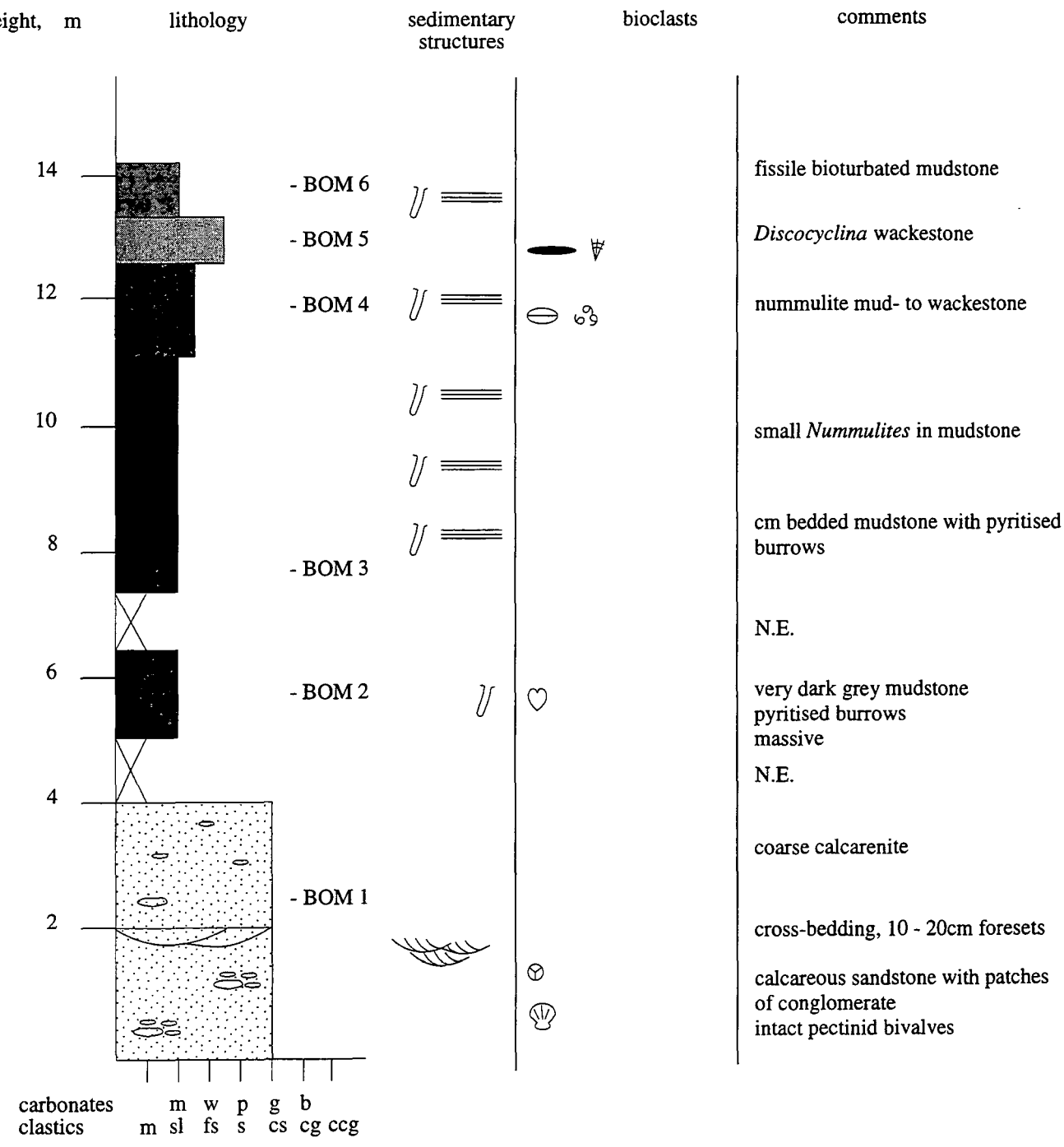

Log S9: La Bombarbellaz

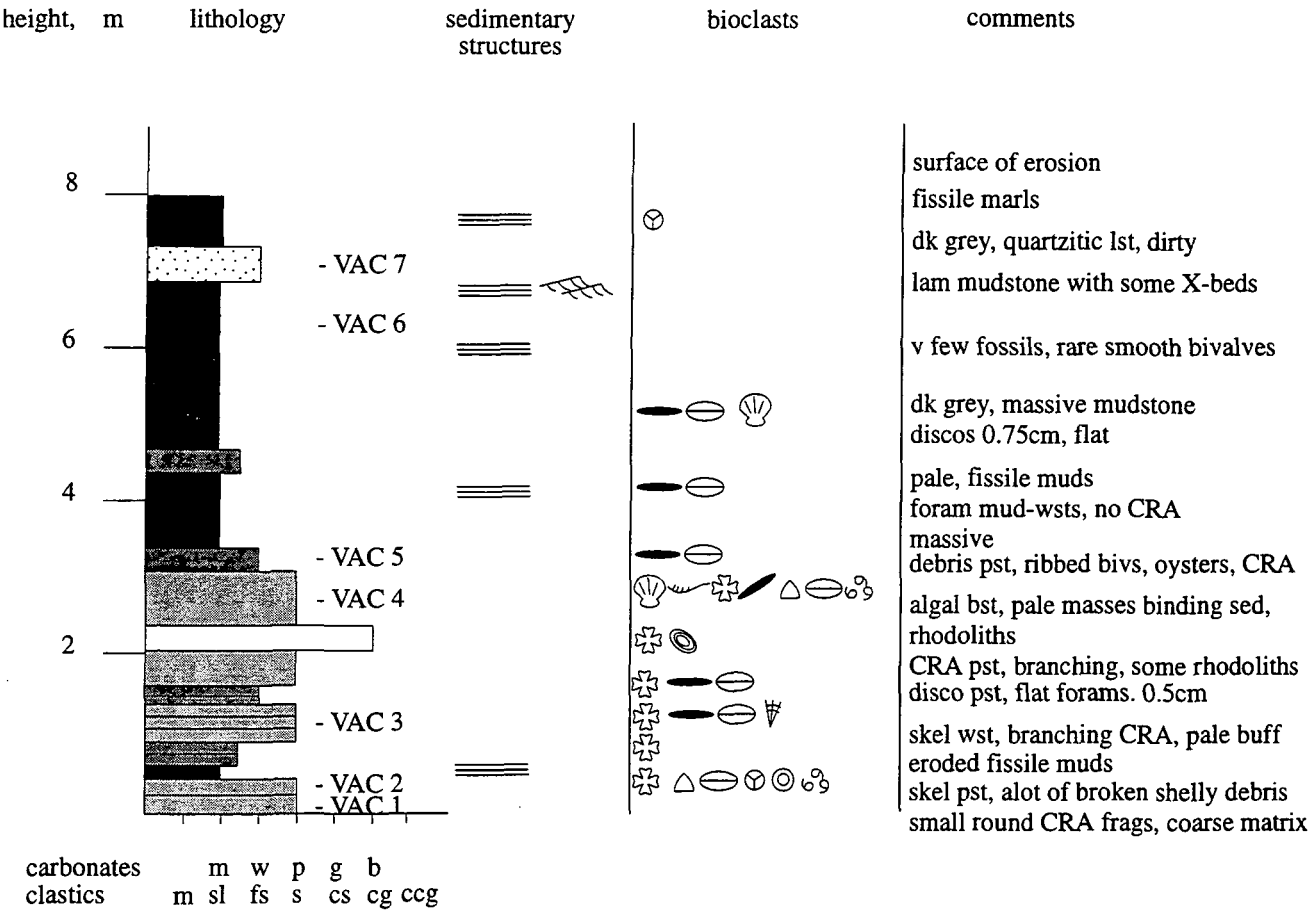

Log S10: La Vacherie

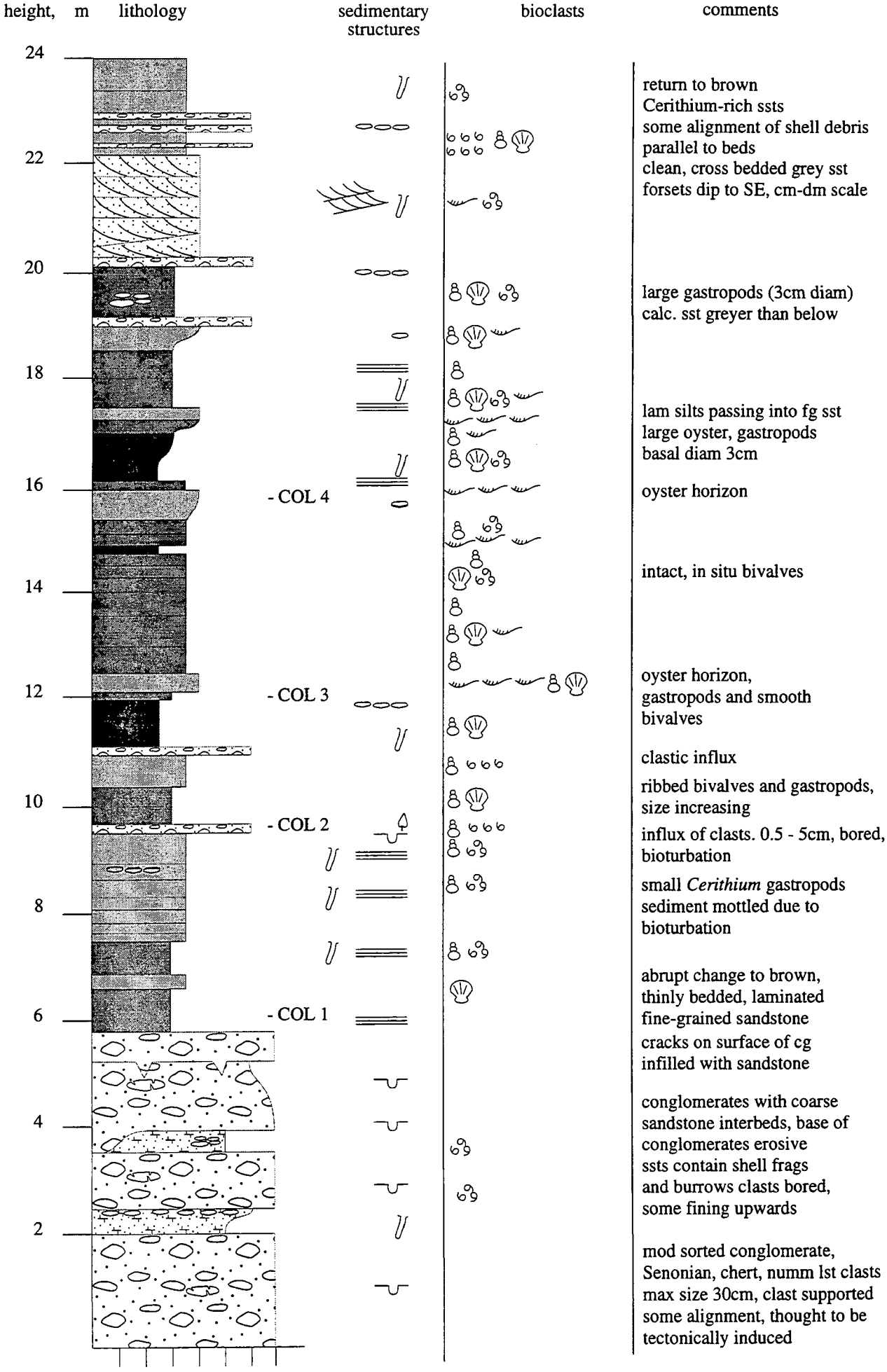

Log S11: Col du Colonney

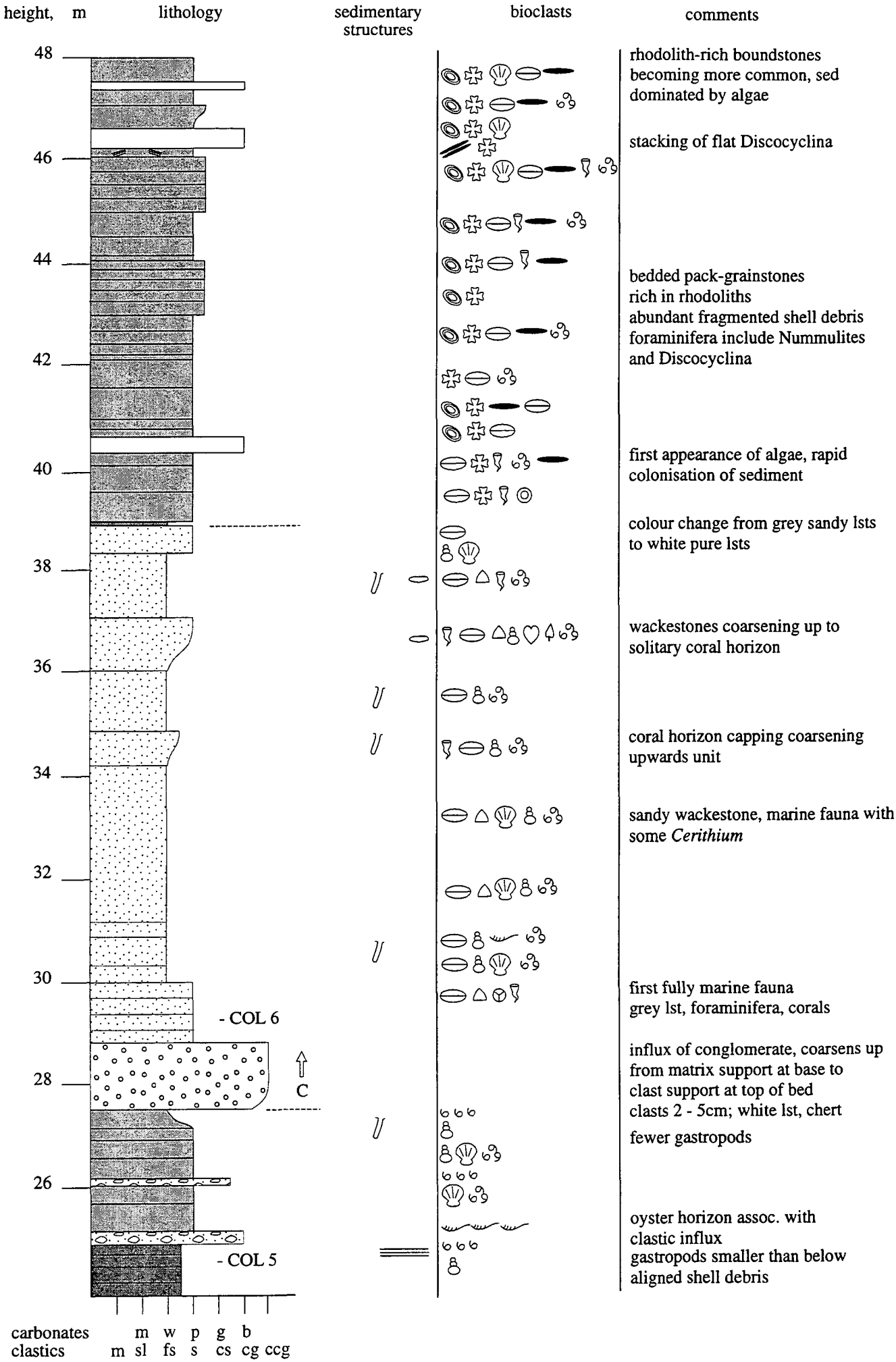

Log S11: Col du Colonney

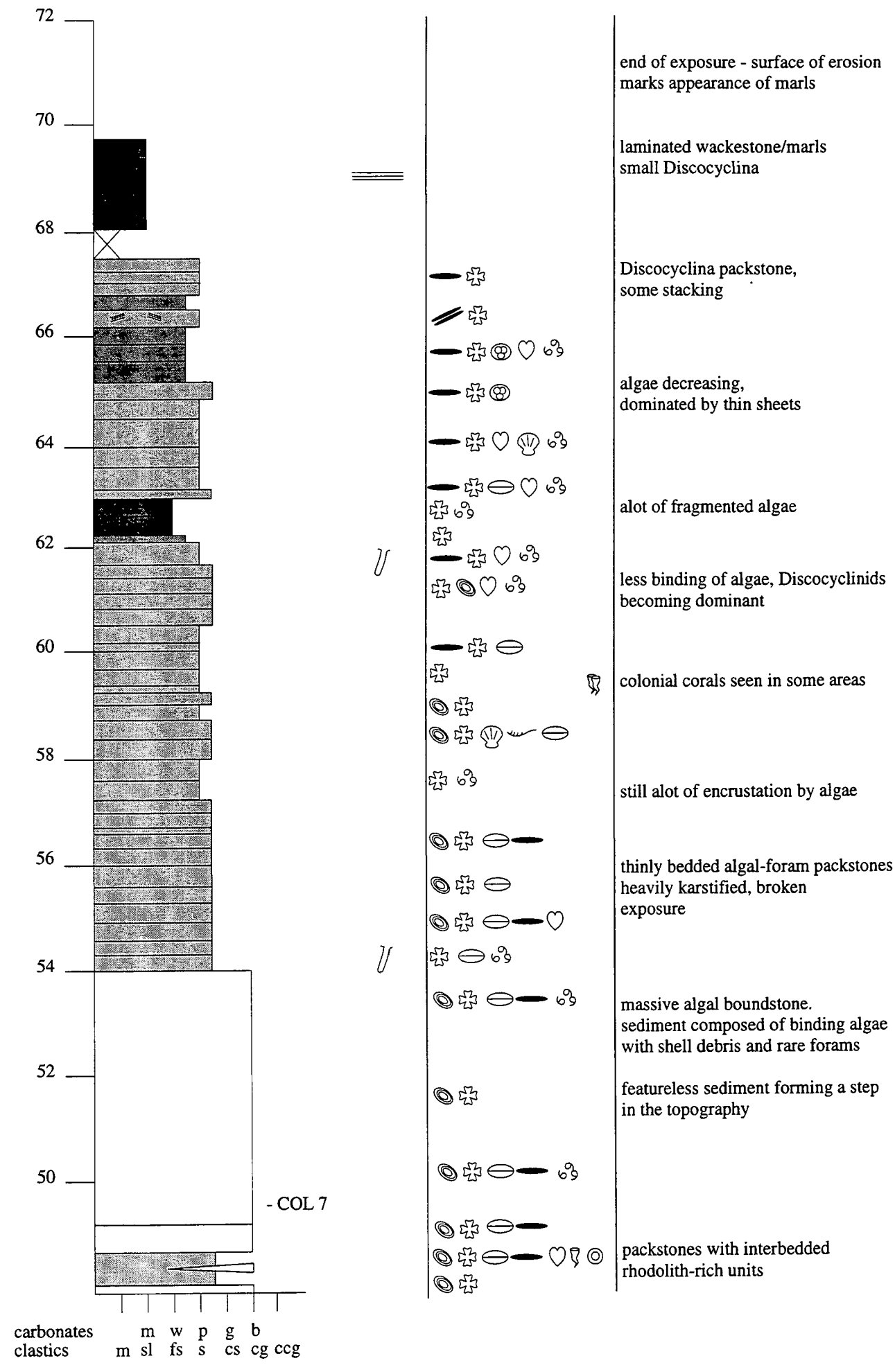

Log S11: Col du Colonney

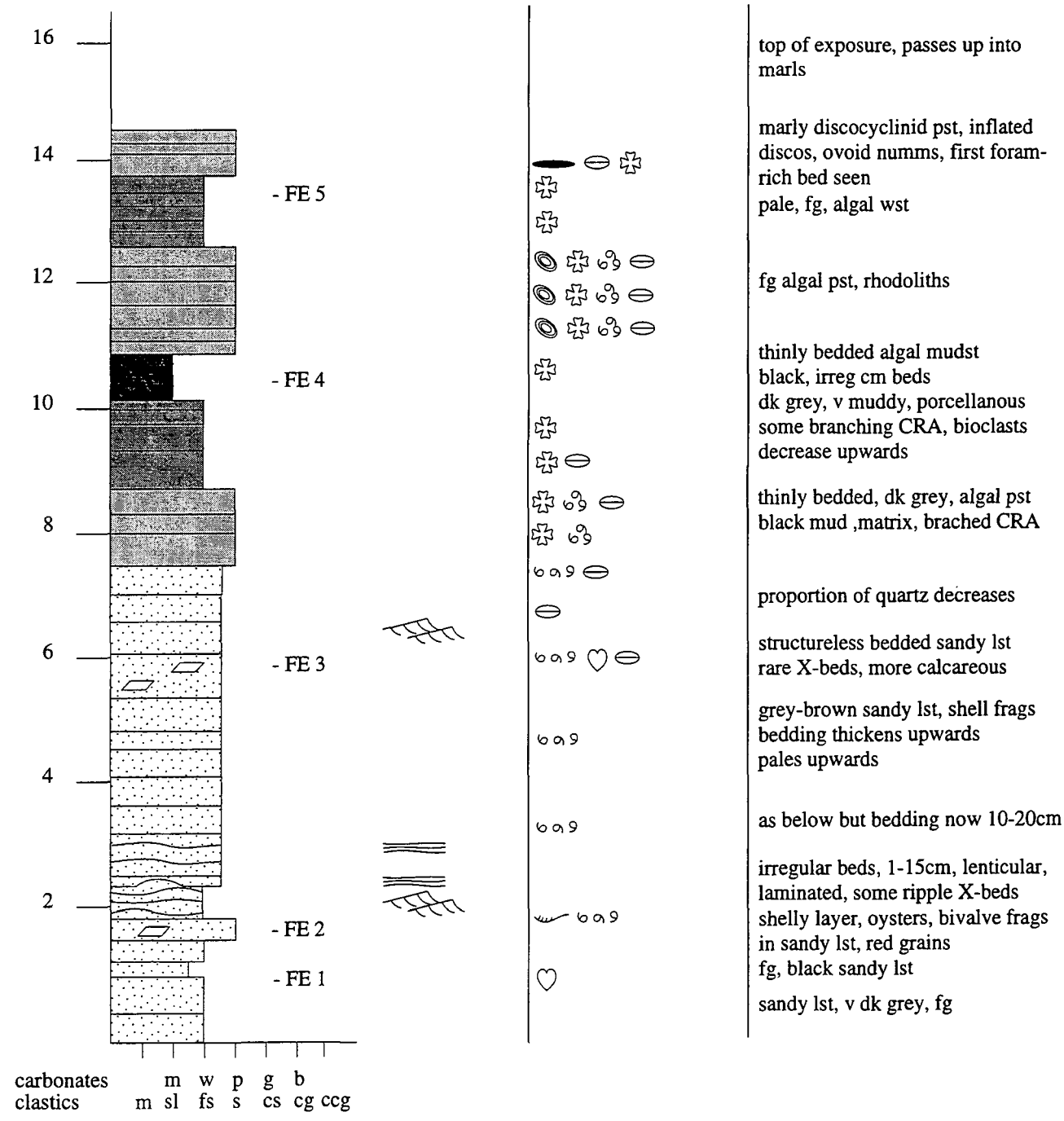

Log S12: Flaine East

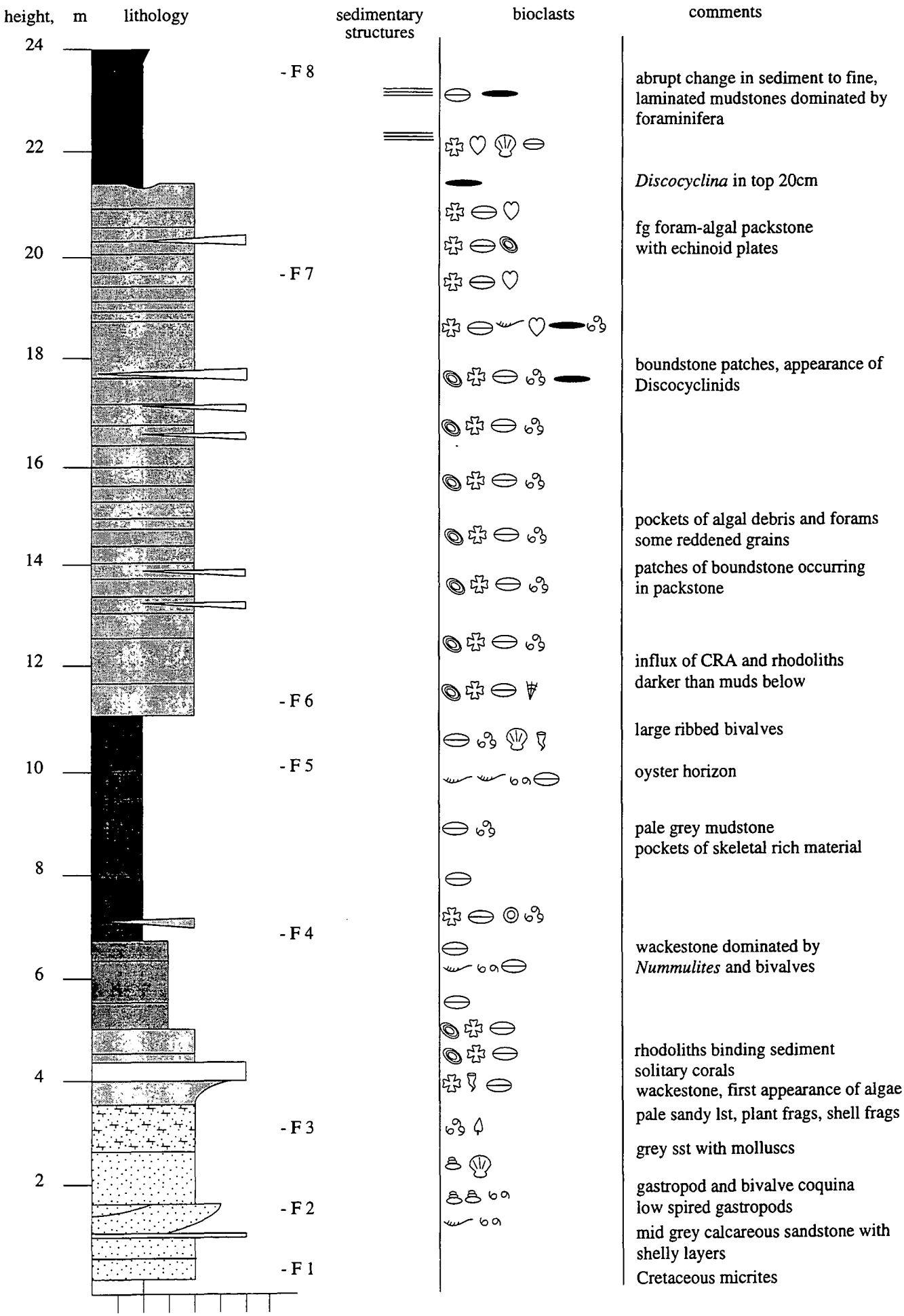

Log S13: Flaine

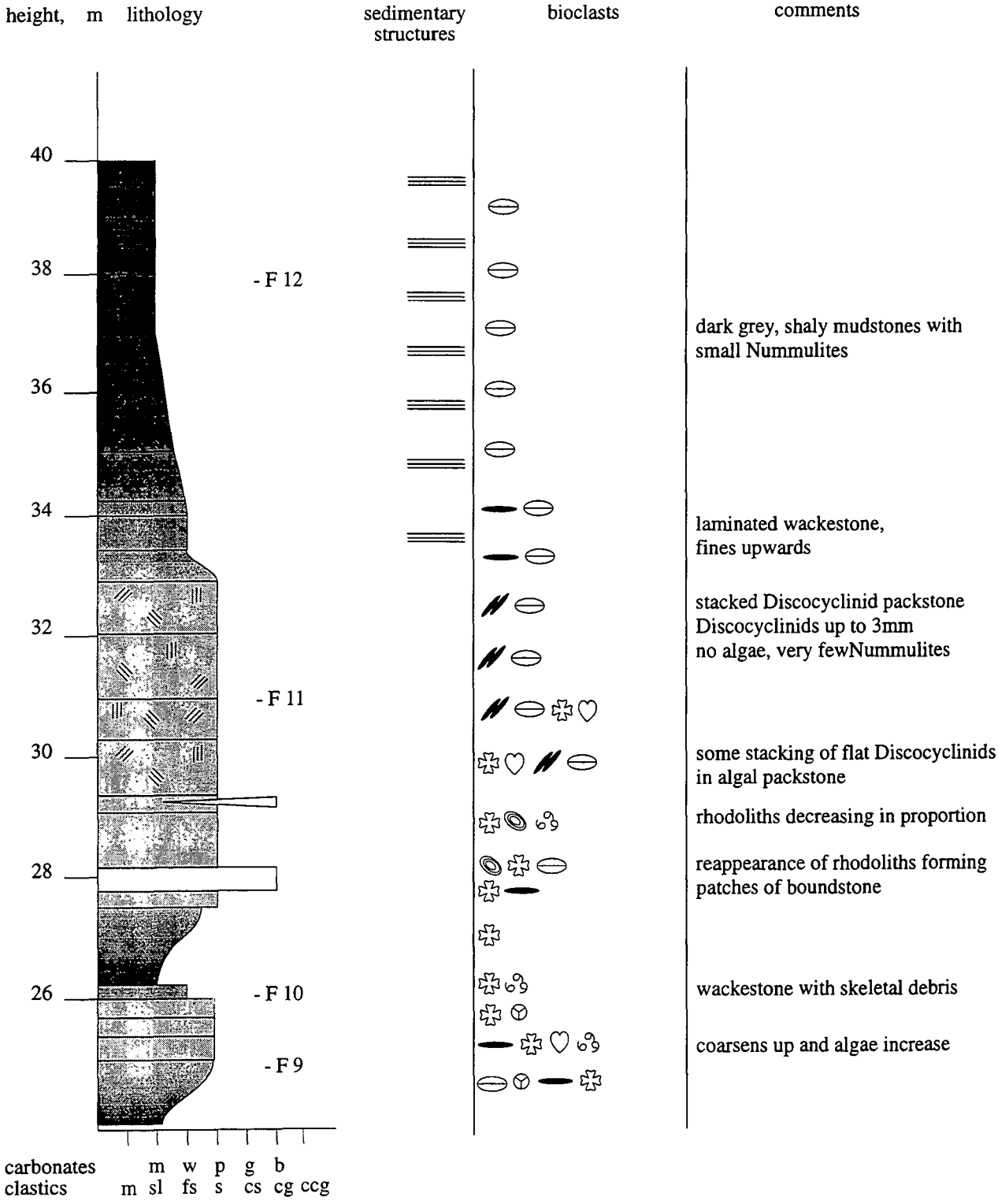

Log S13: Flaine

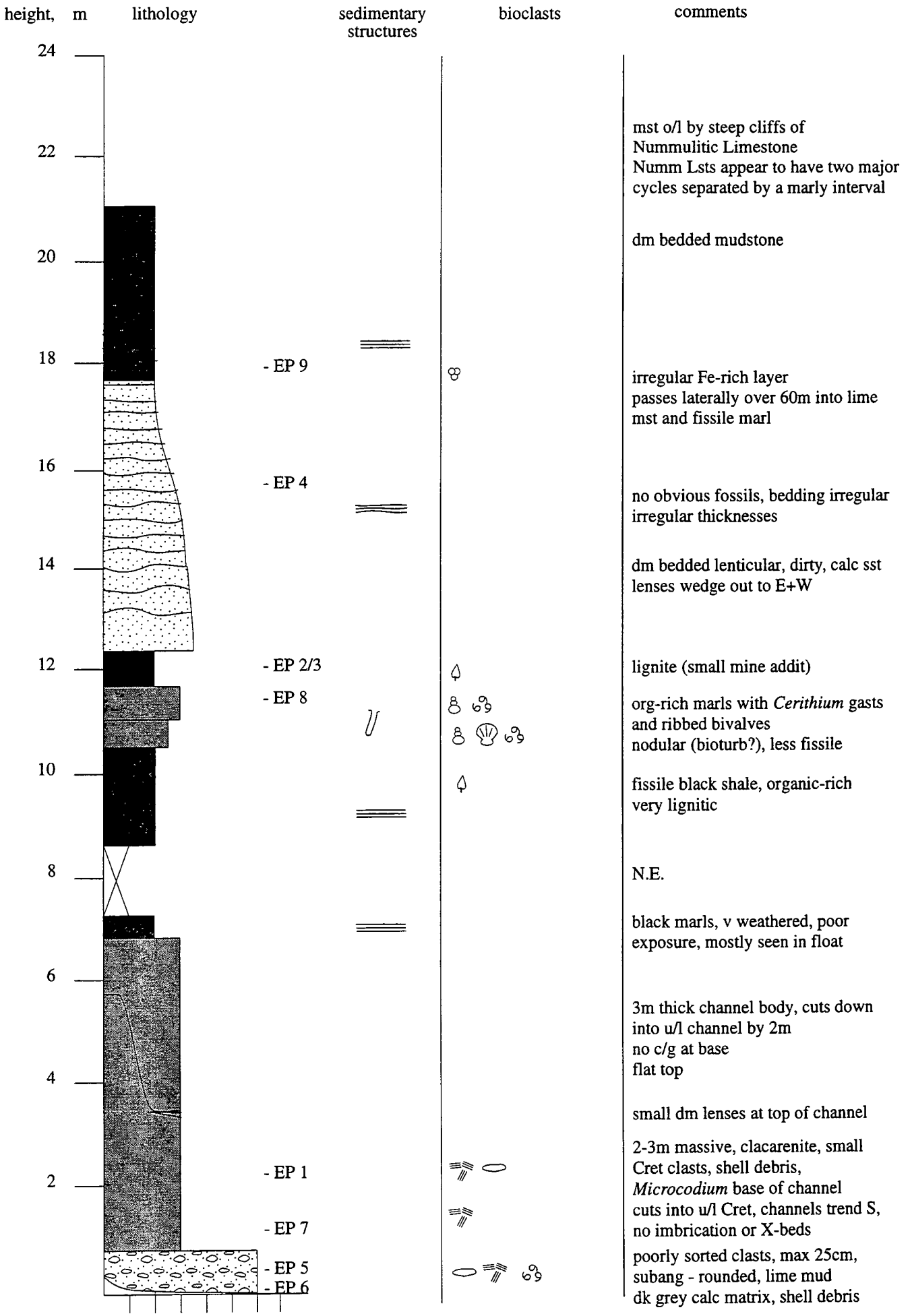

Log S14: L'Epine (base)

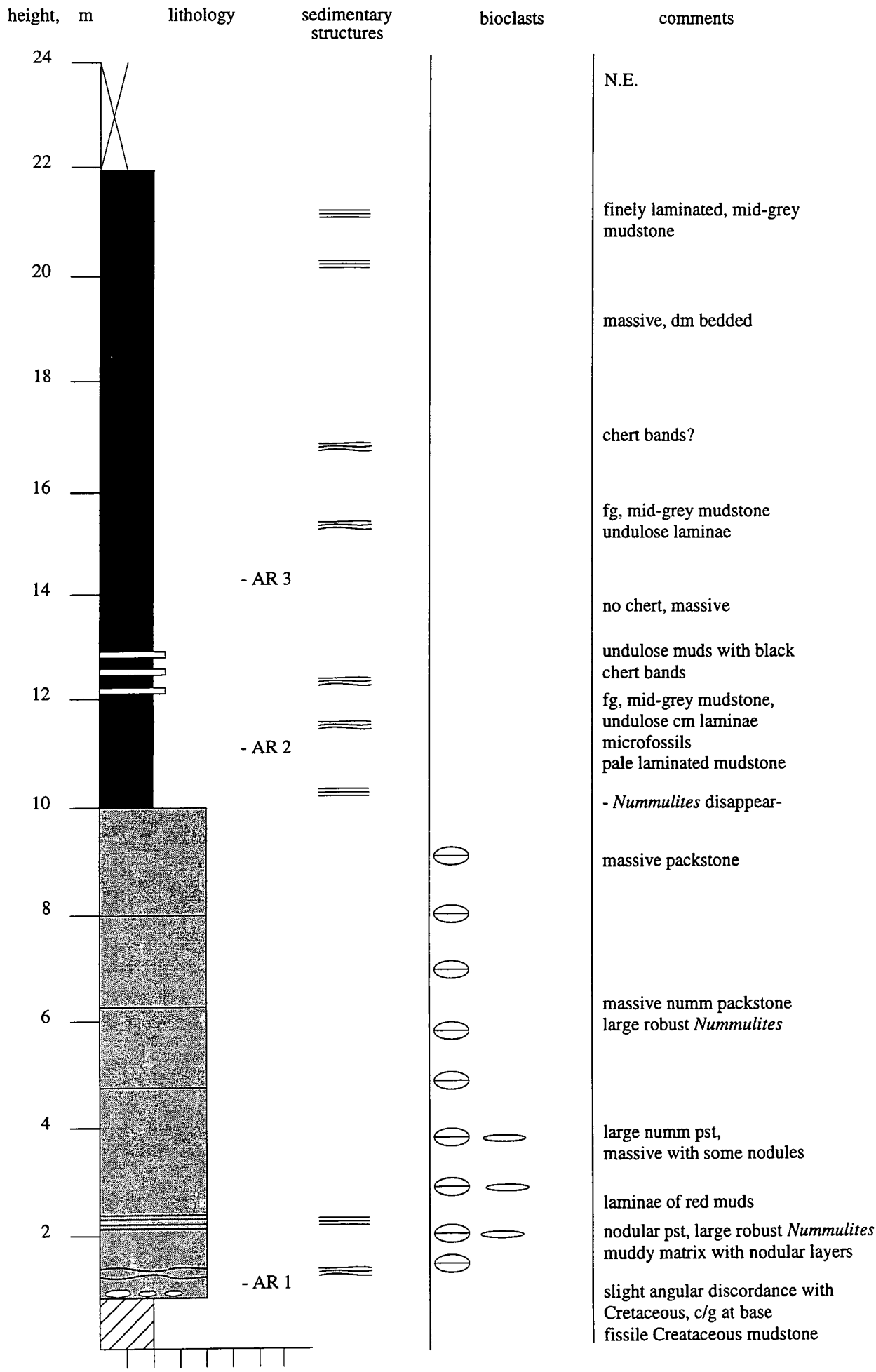

Log S15: Araches

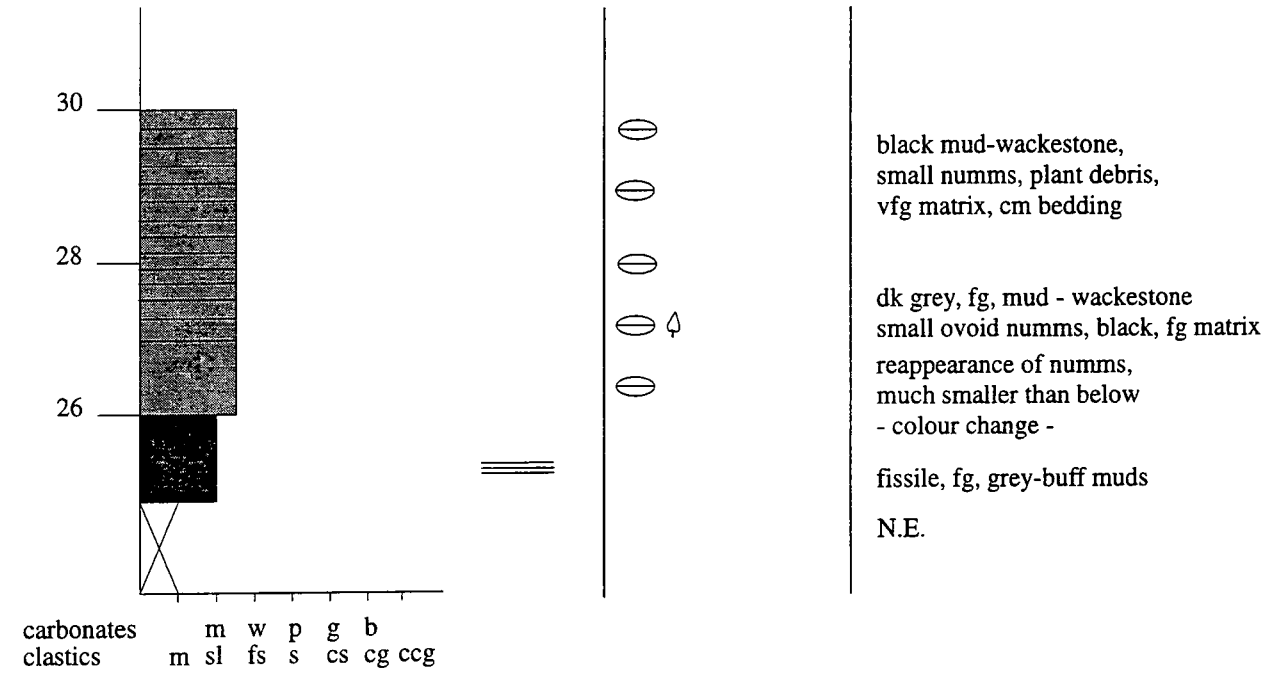

Log S15: Araches

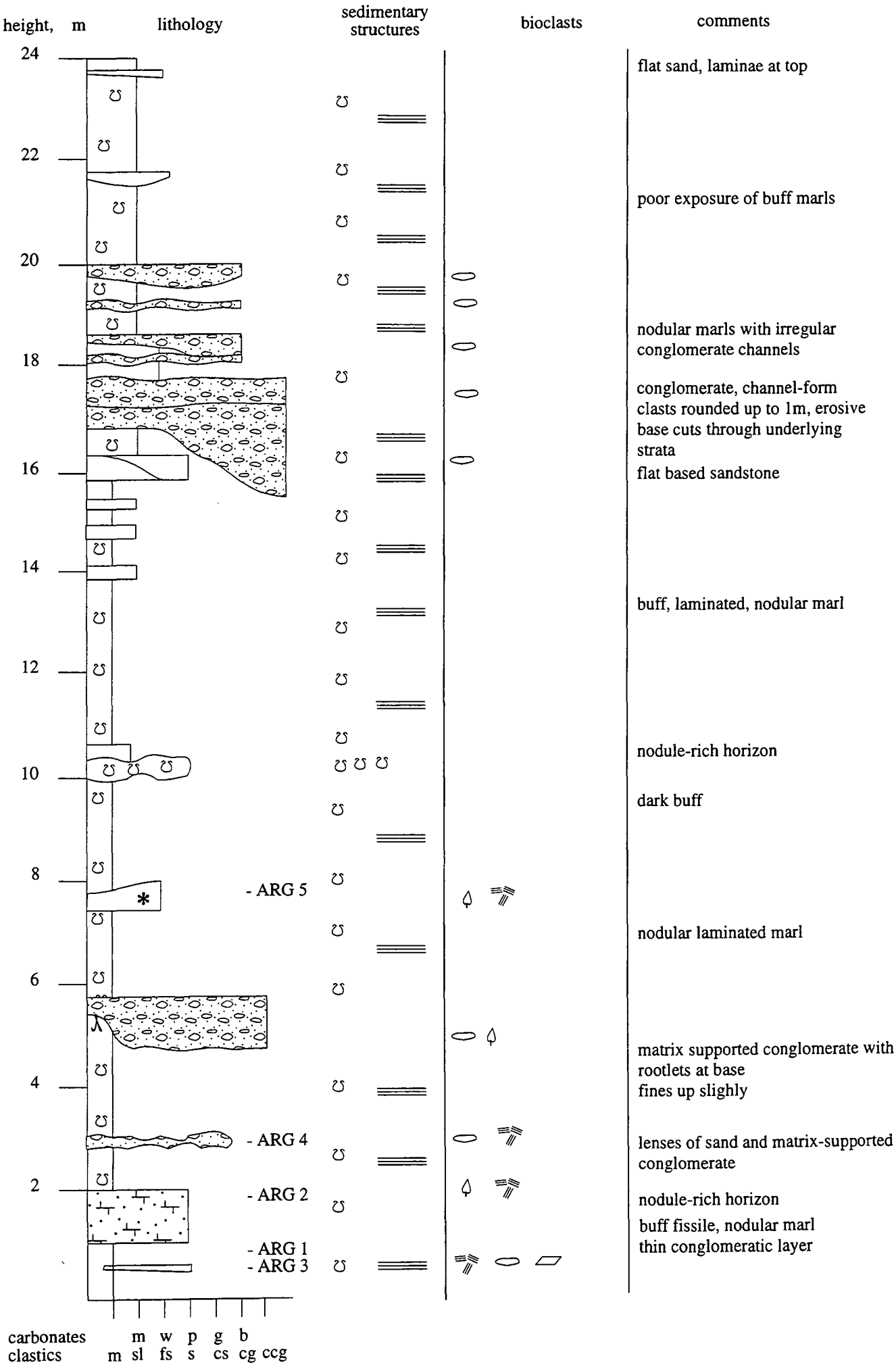

Log P1: Argens

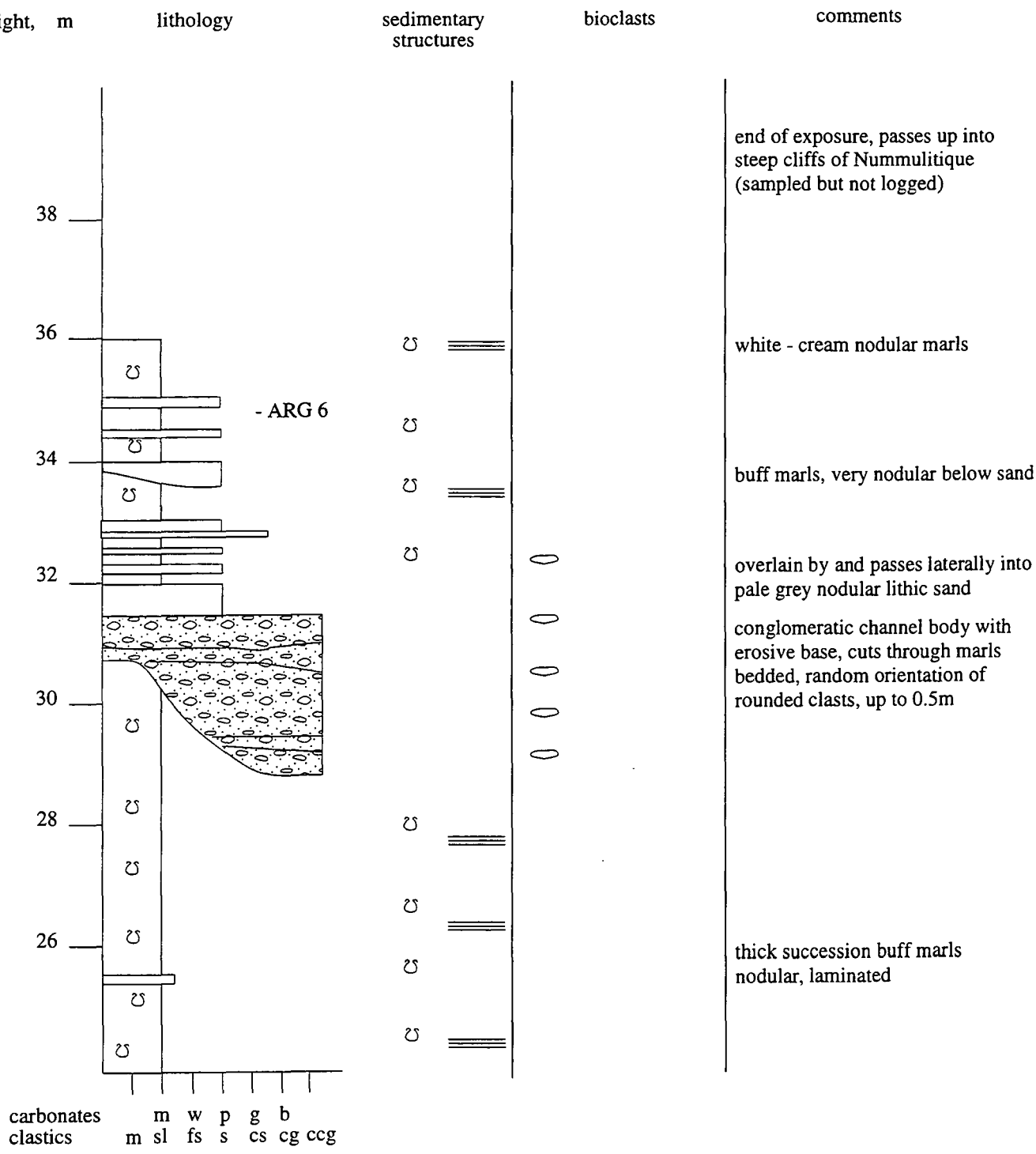

Log P1: Argens

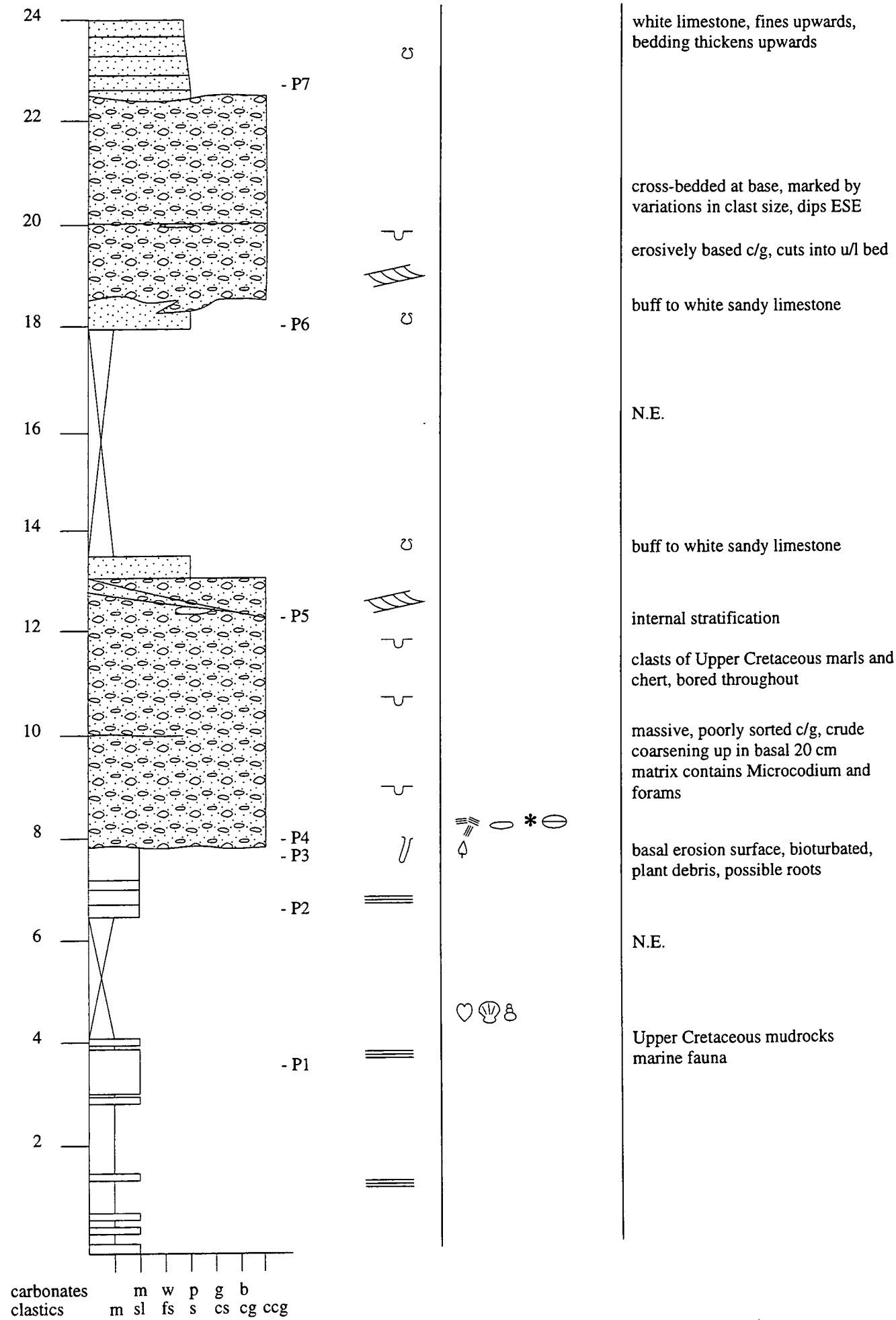

Log P2: Peyresq

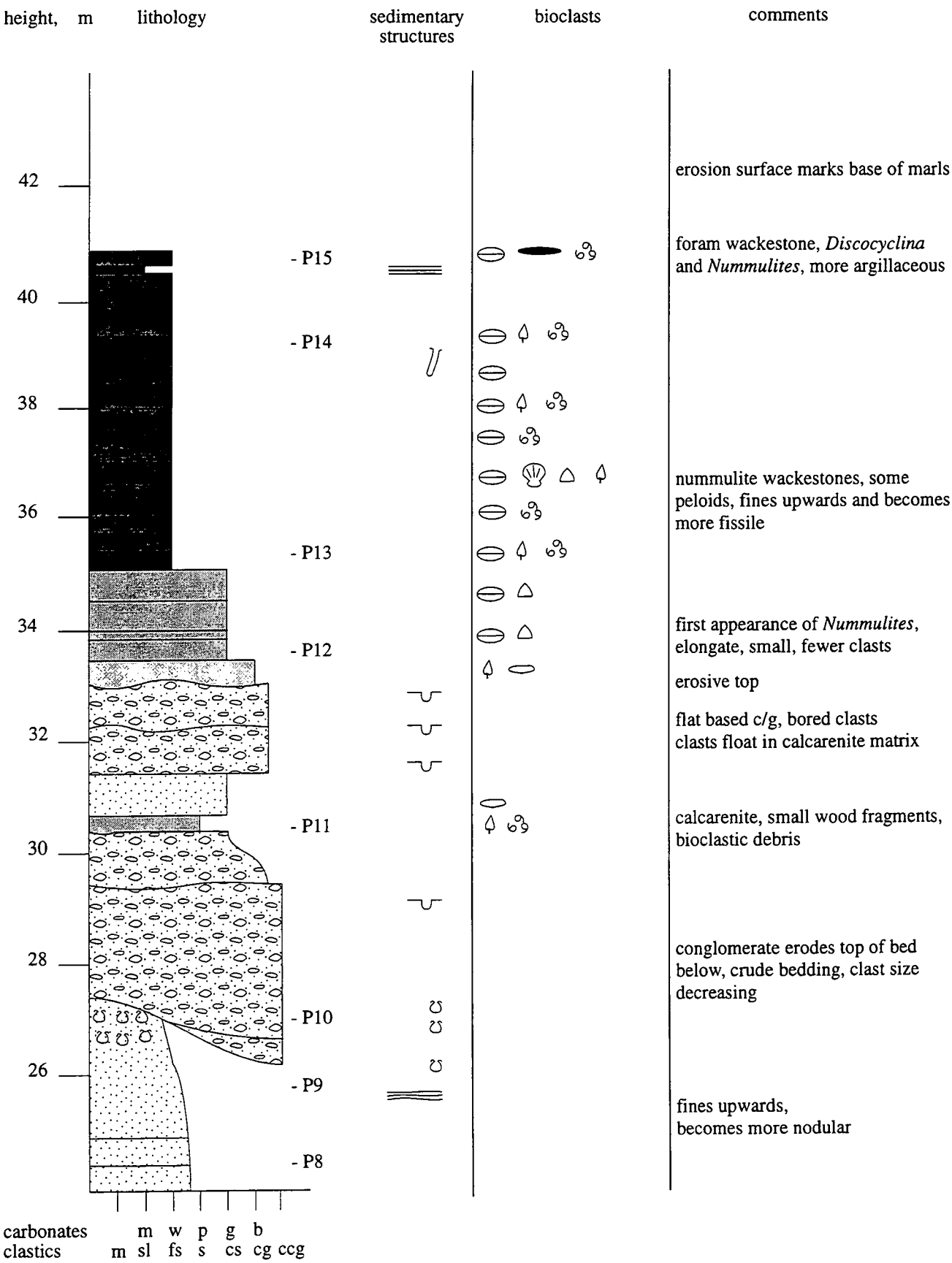

Log P2: Peyresq

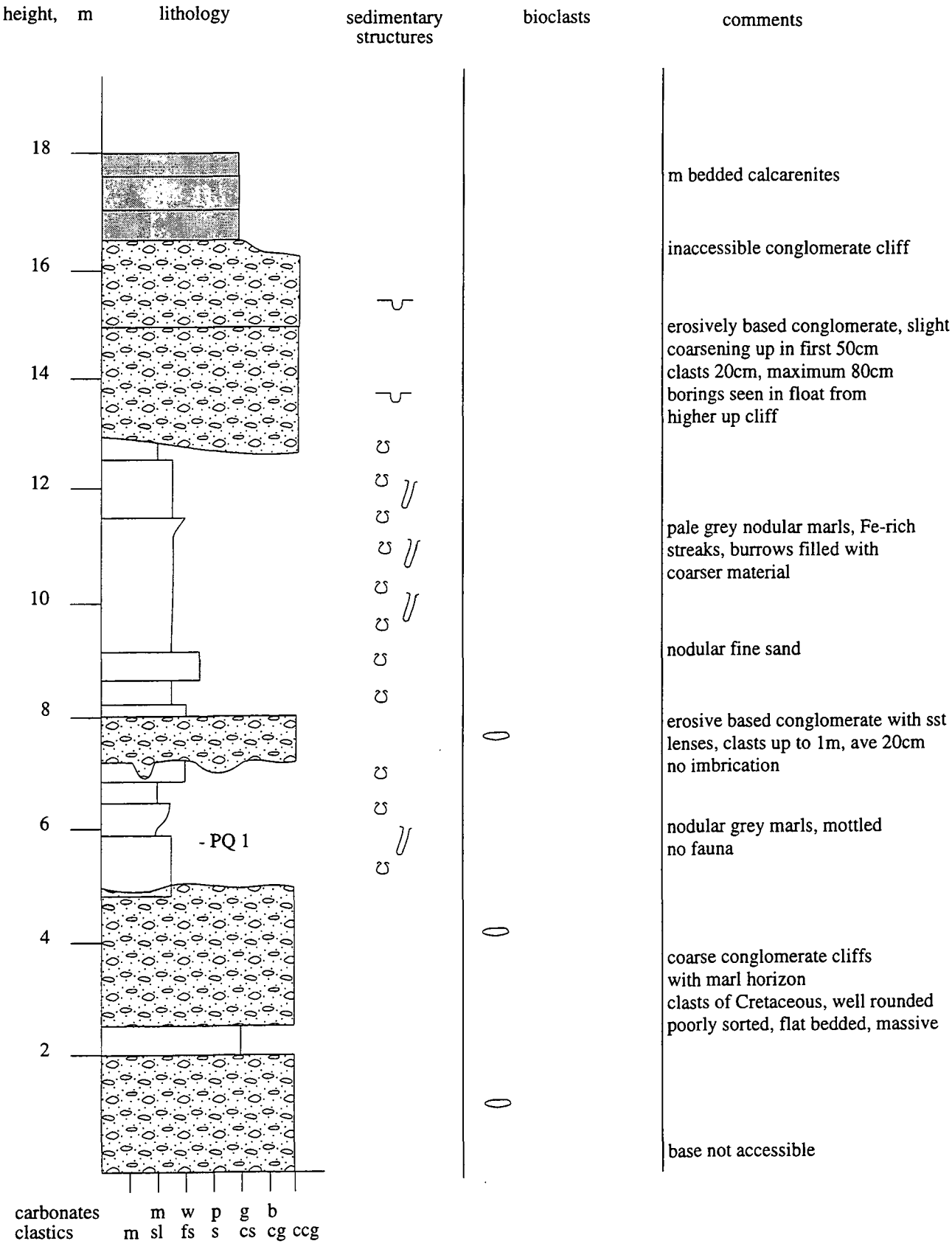

Log P3: Peyresq Quarry

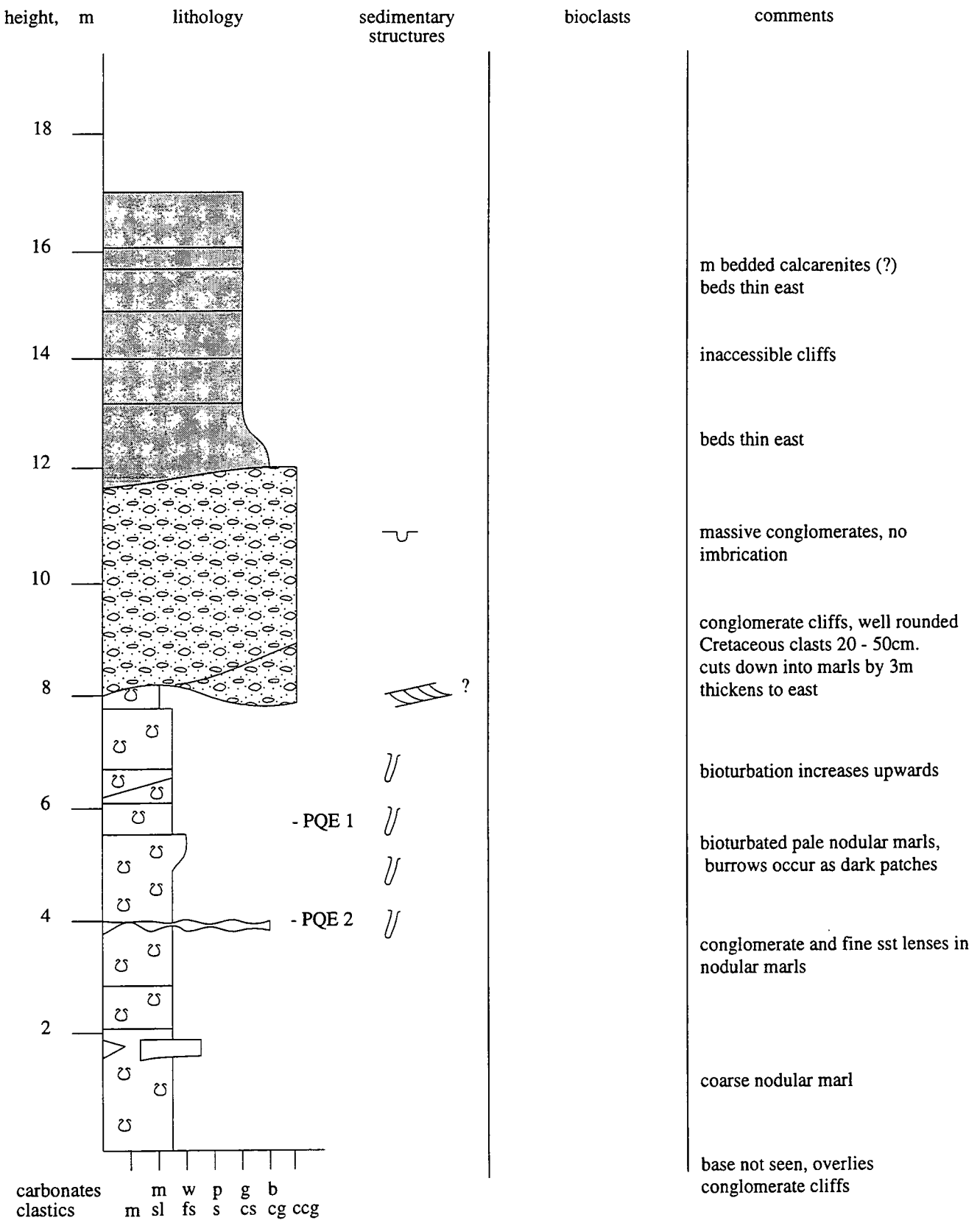

Log P4: Peyresq Quarry East

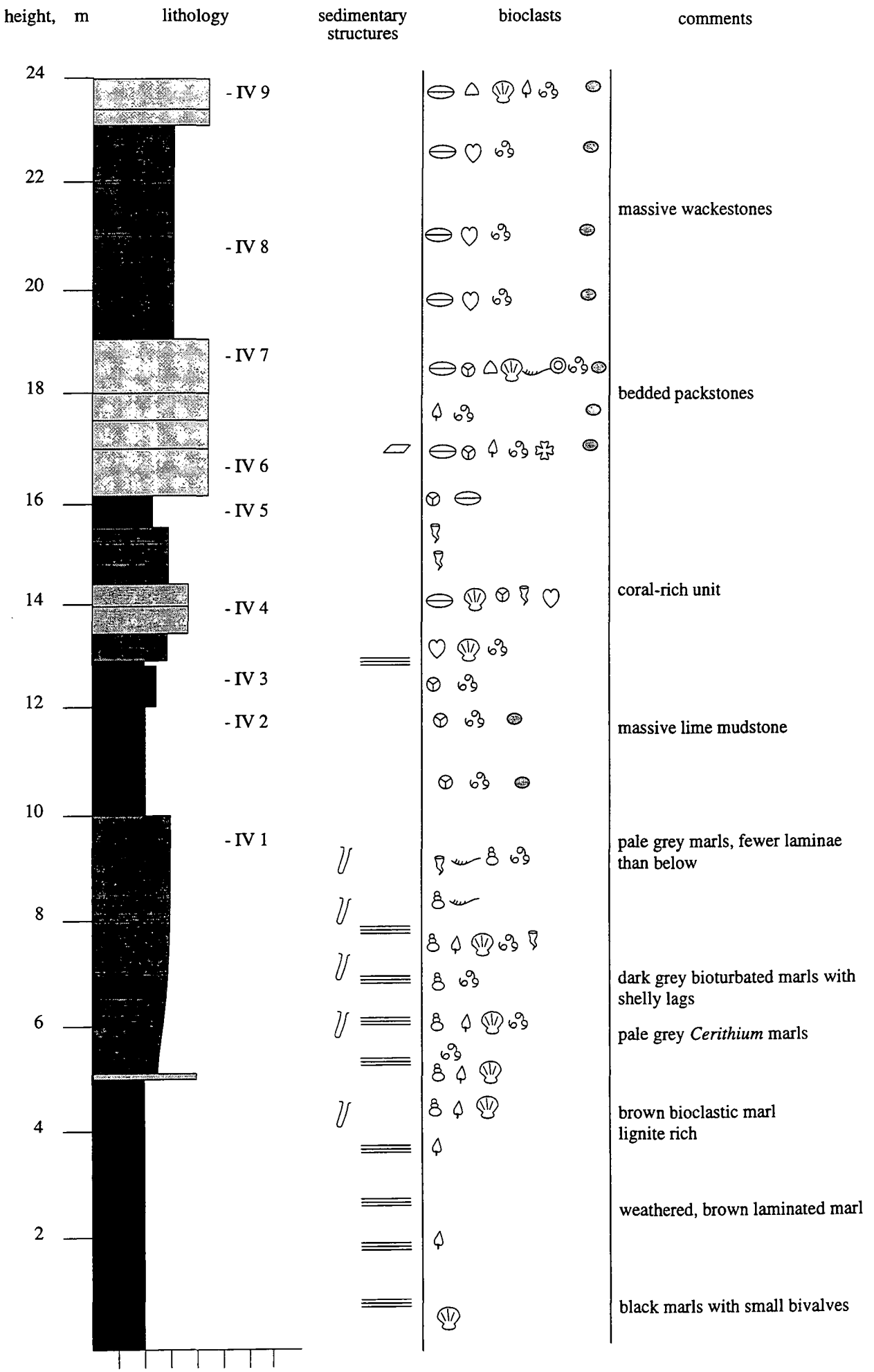

Log P5: Ivoire

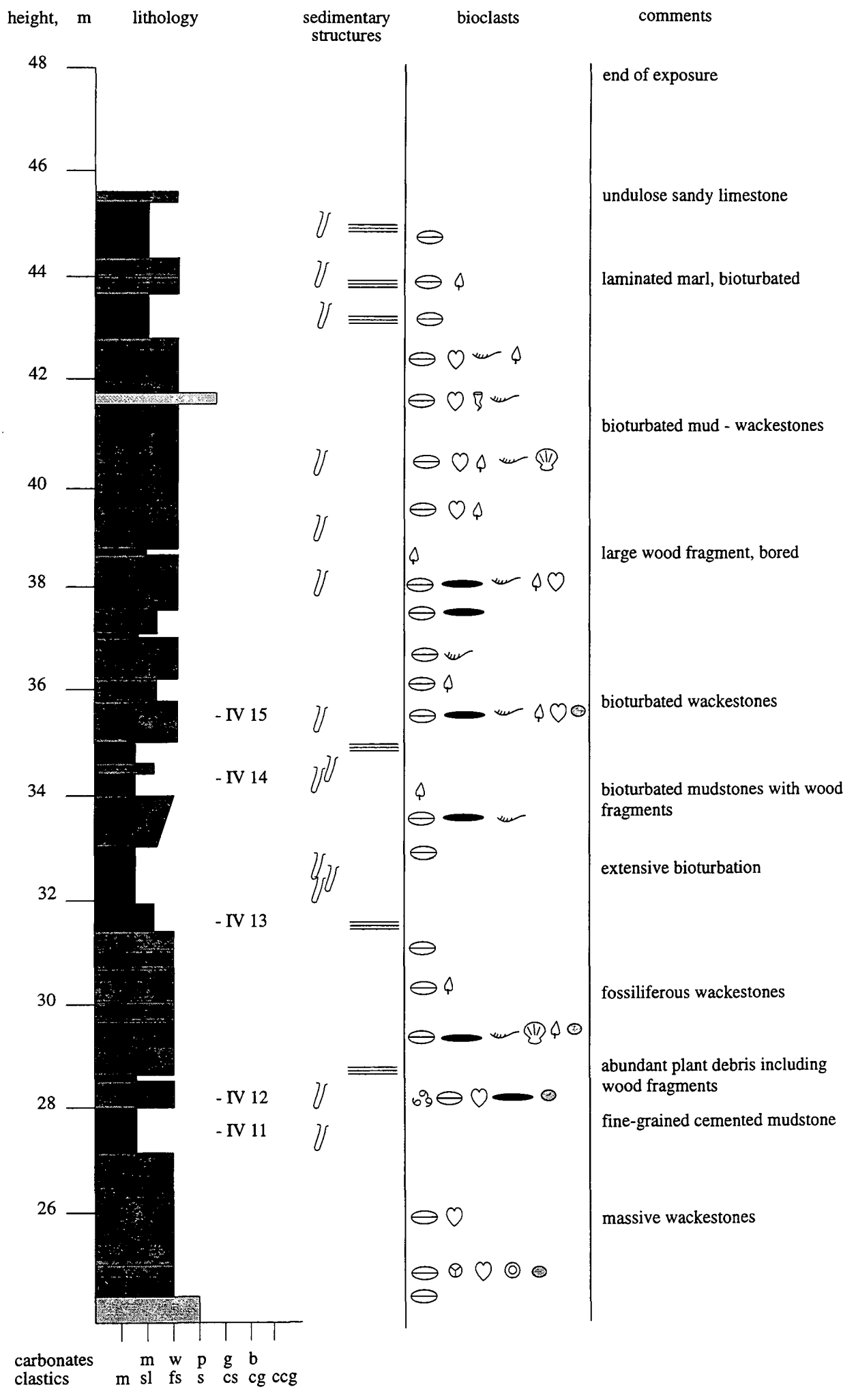

Log P5: Ivoire

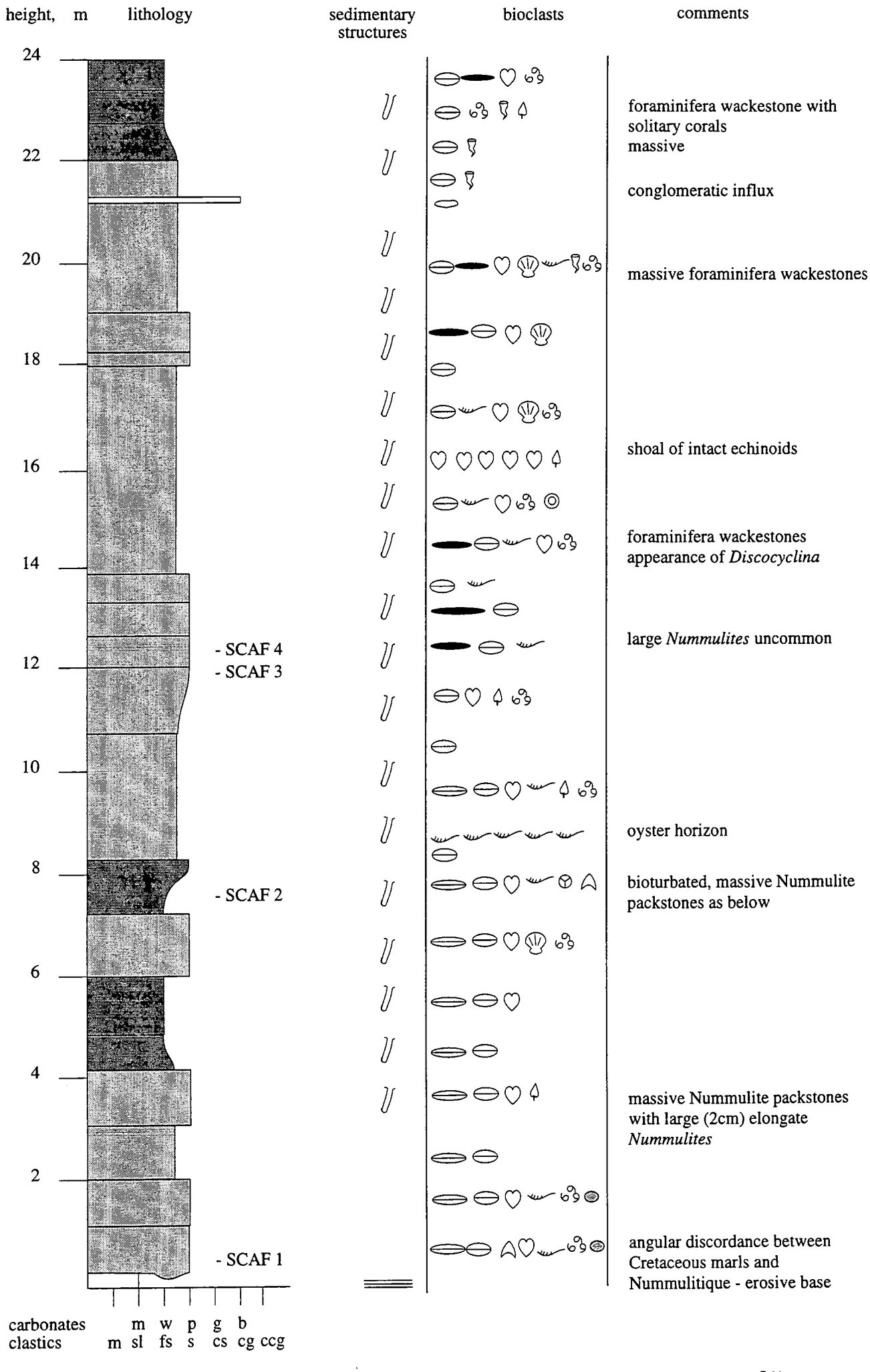

Log P6: Scaffarels

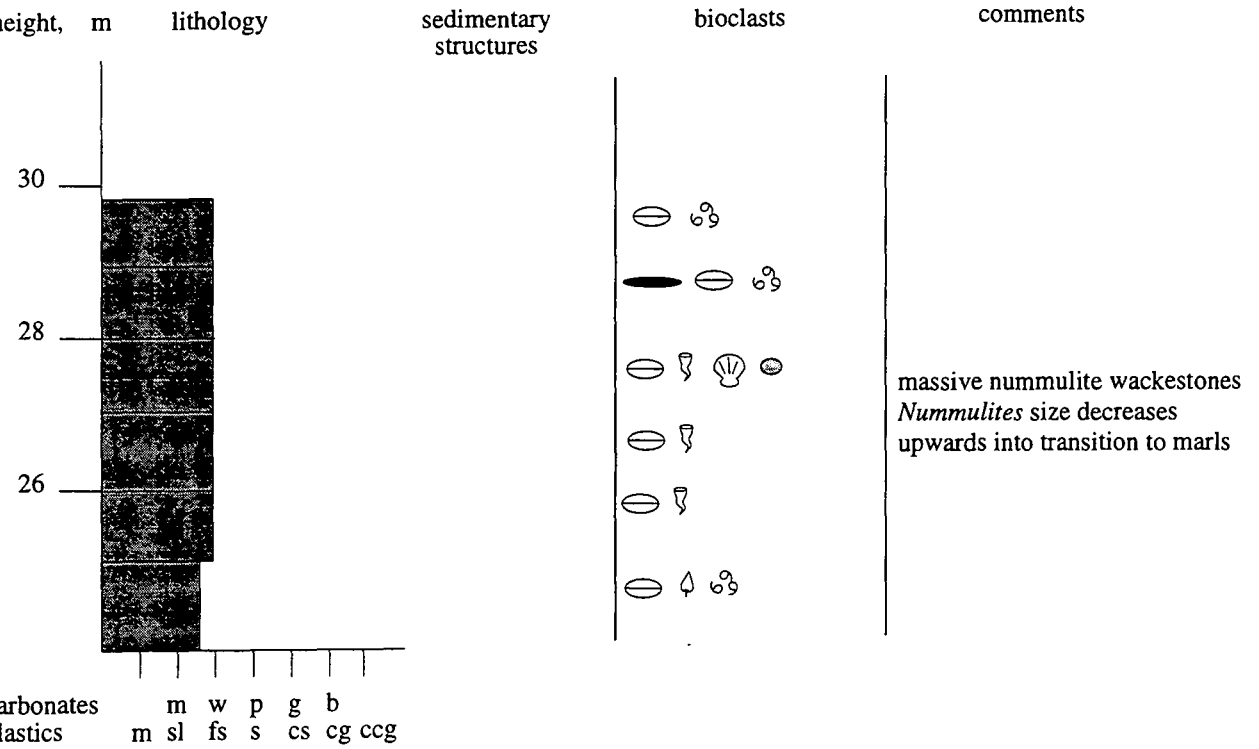

Log P6: Scaffarels

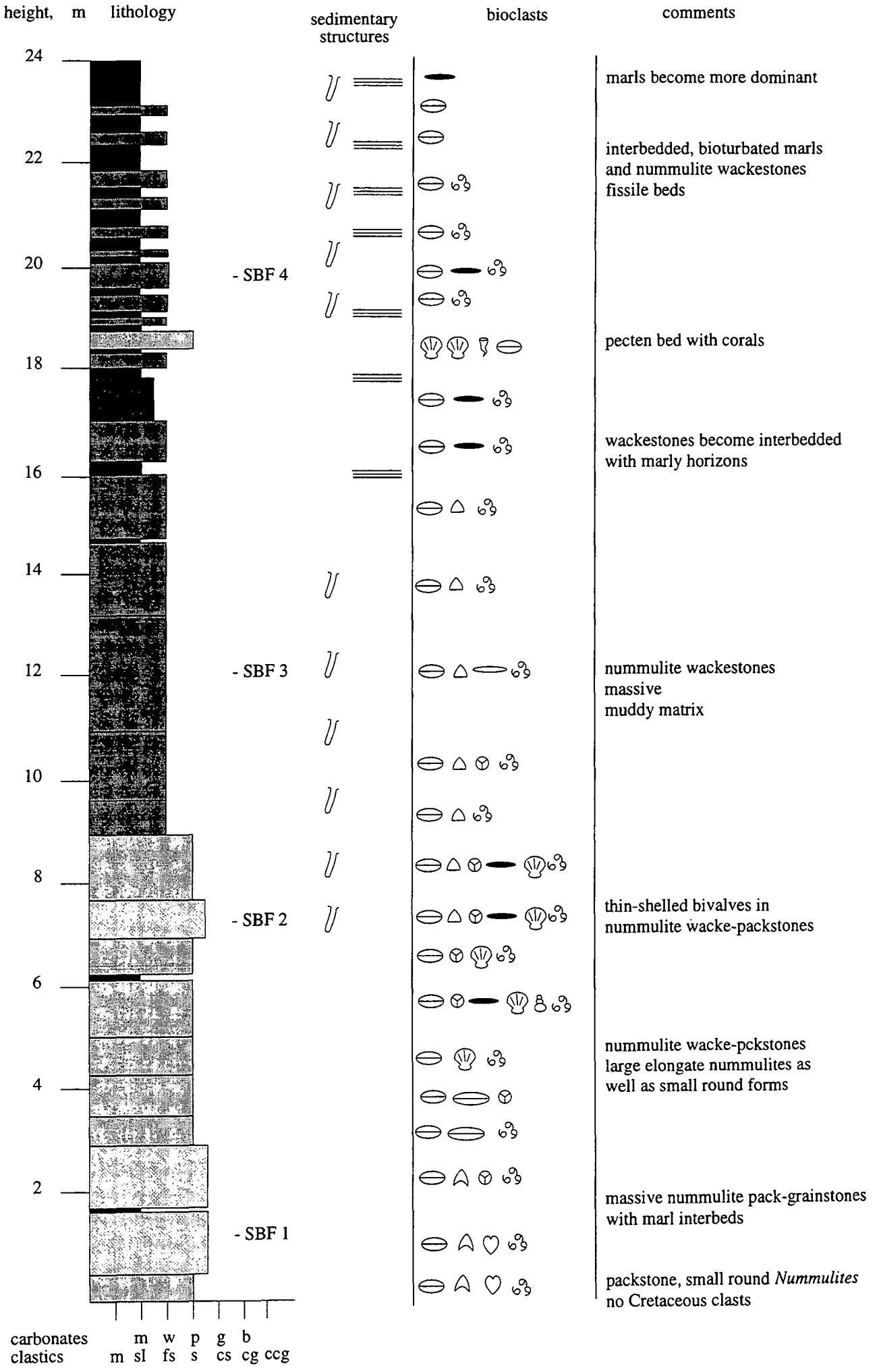

Log P7: St Benoit

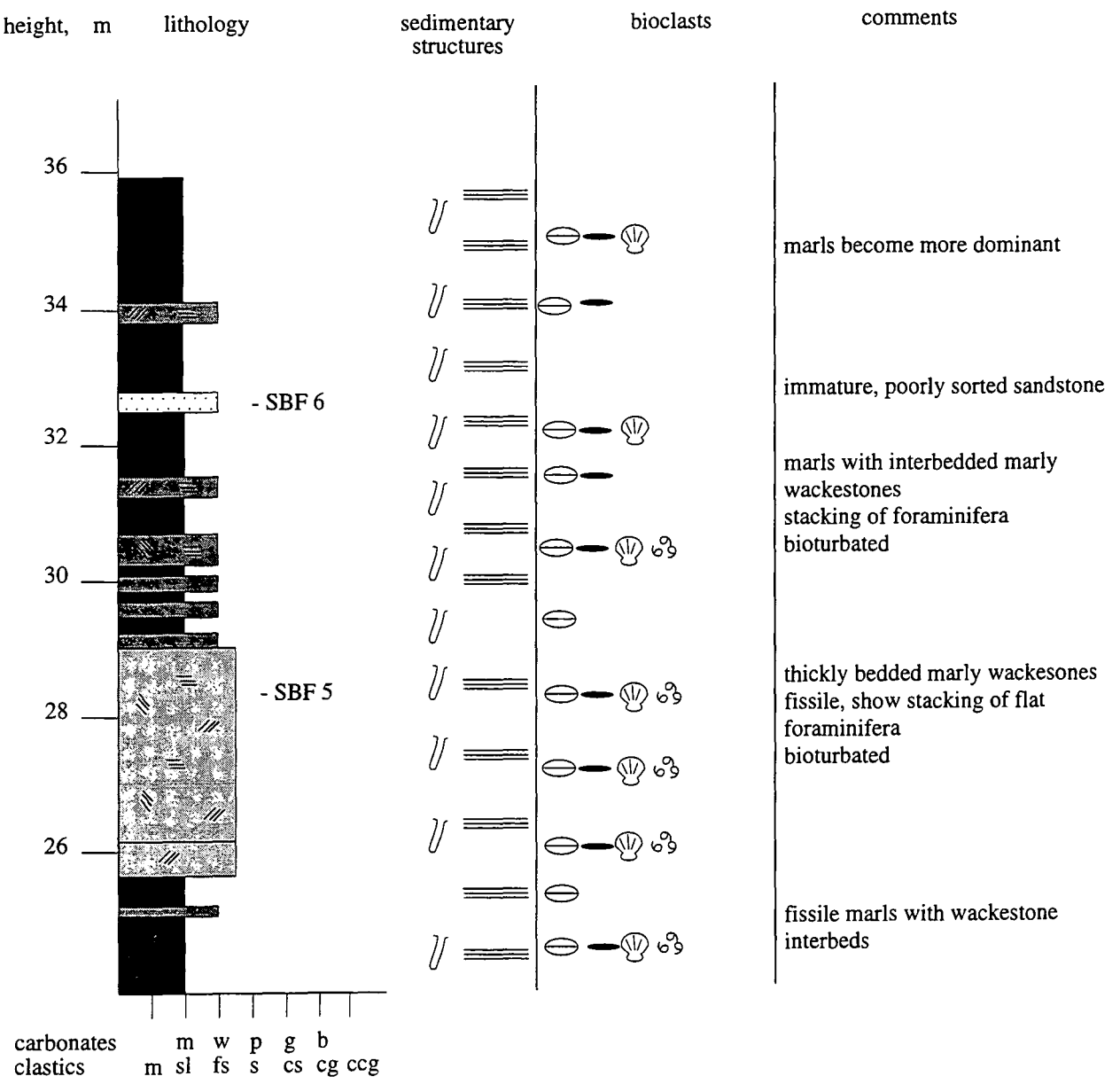

Log P7: St Benoit

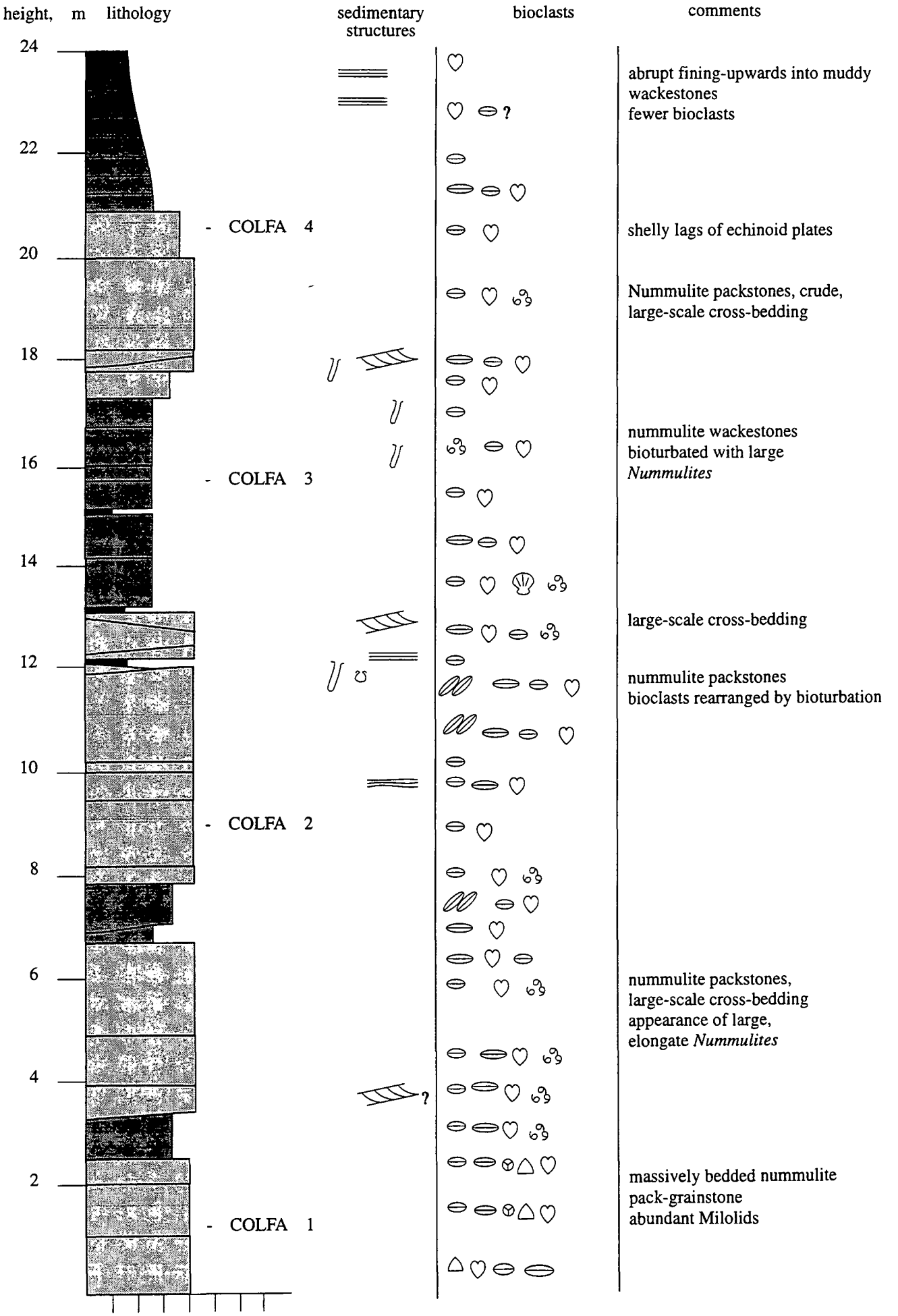

Log P8: La Col du Fa

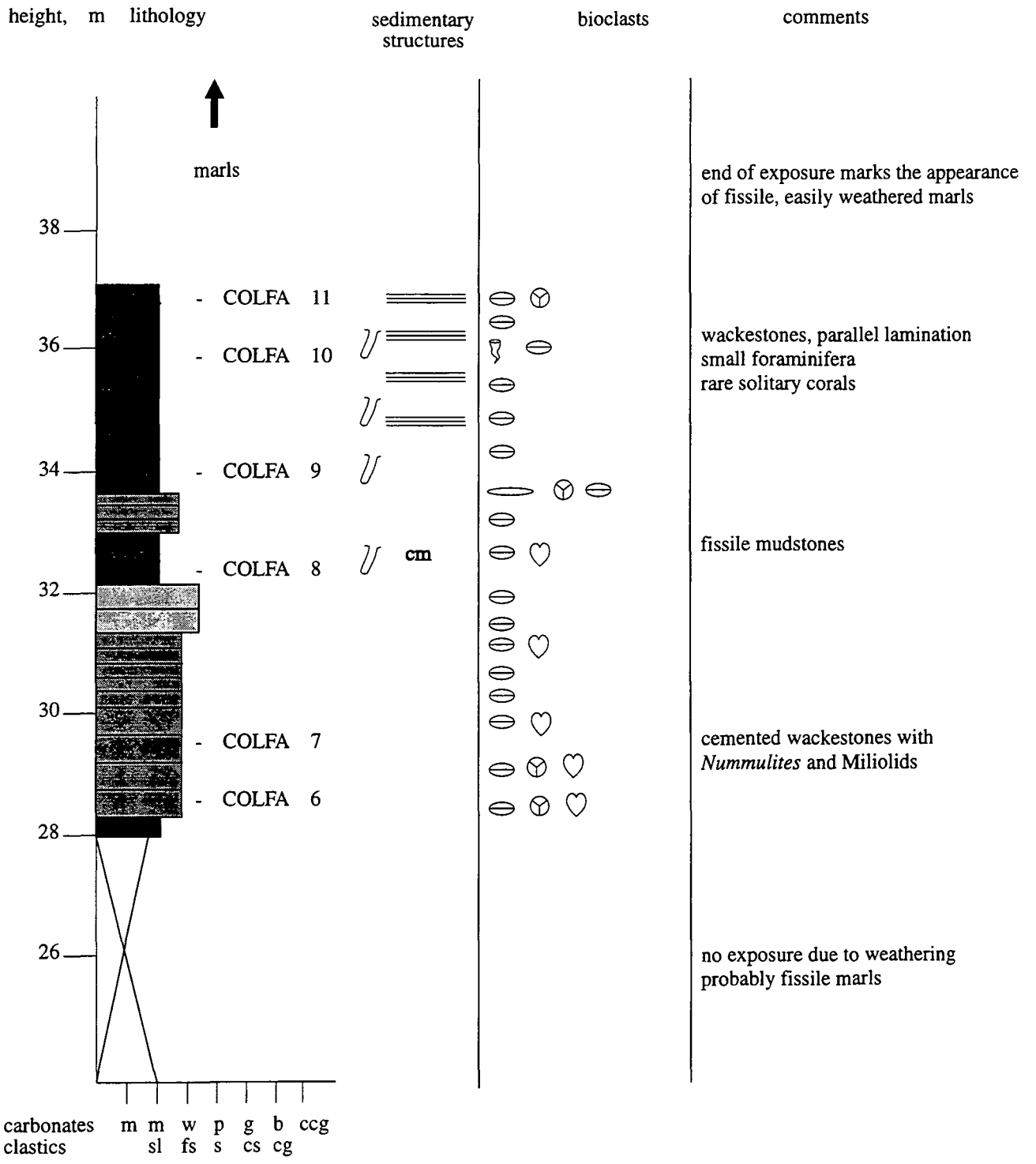

Log P8: La Col du Fa

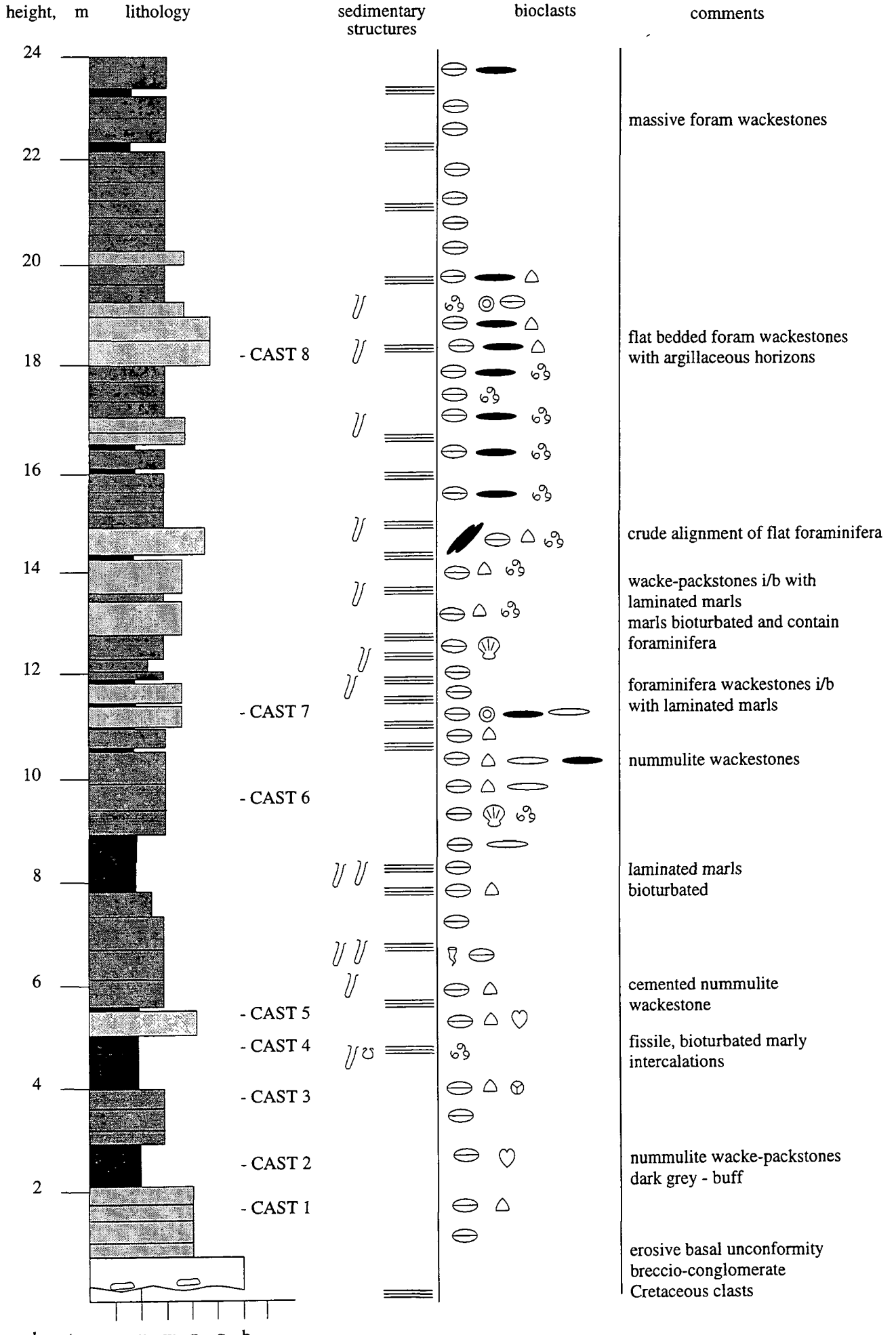

Log P9: Castellet les Sausses

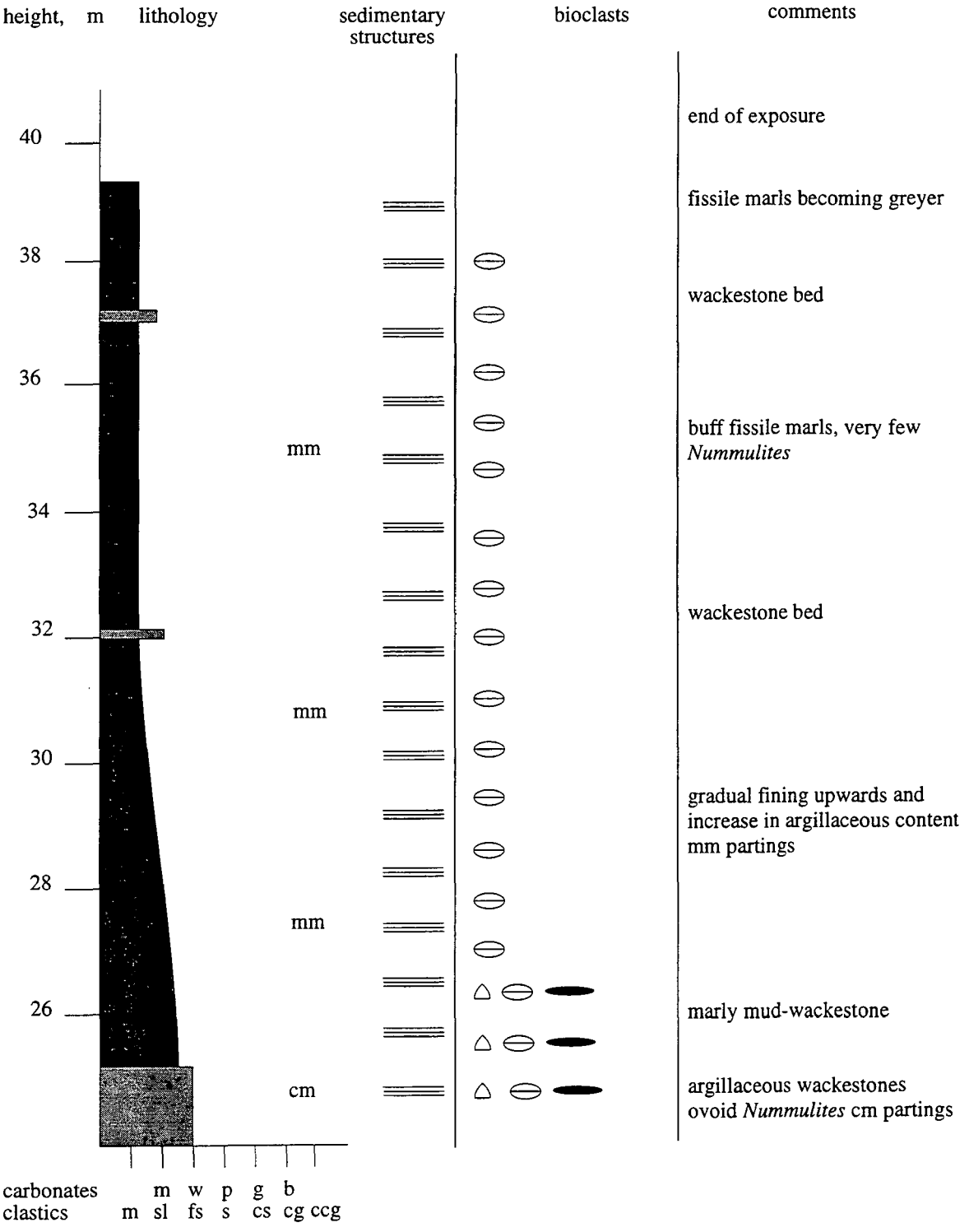

Log P9: Castellet les Sausses

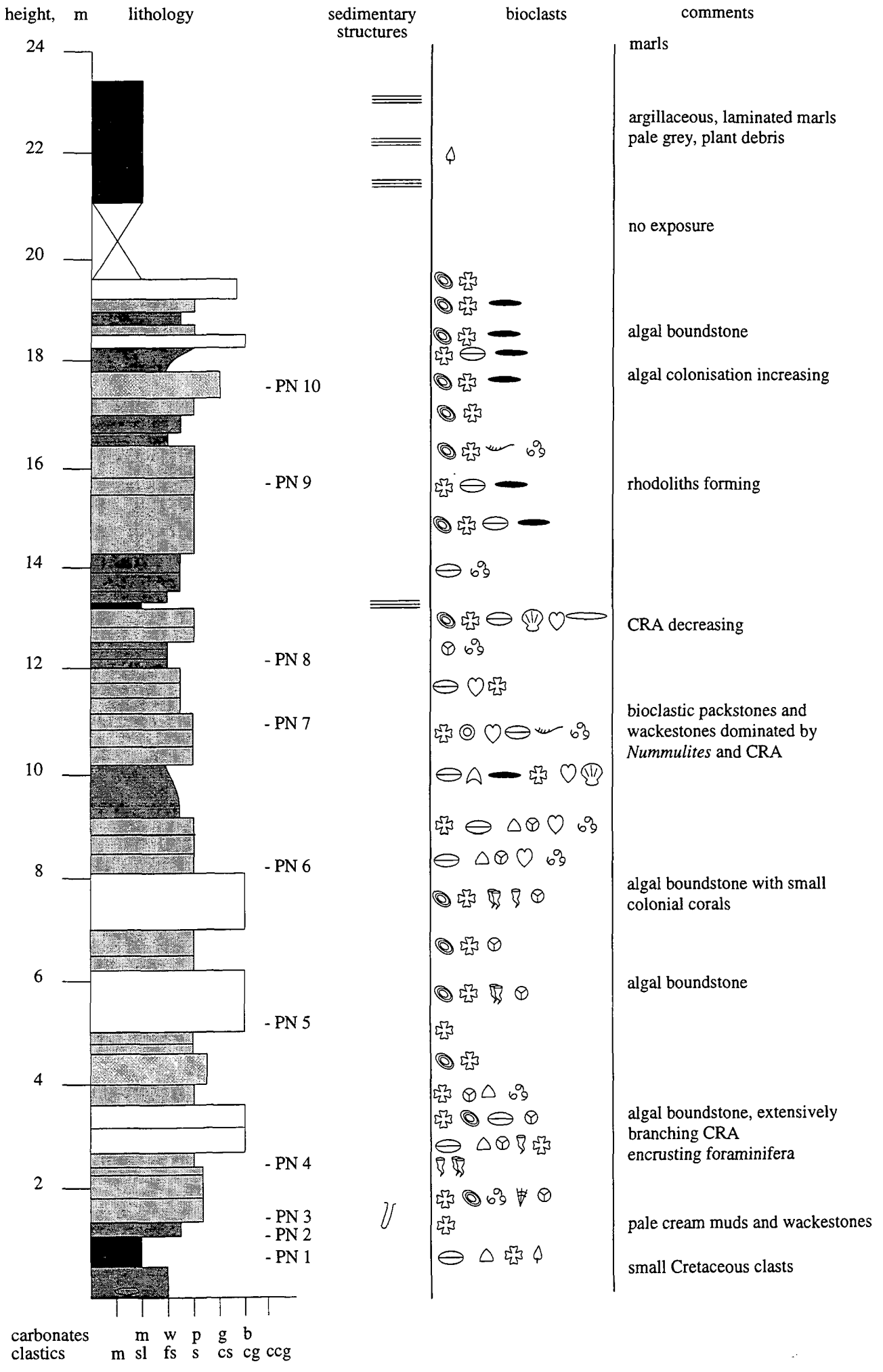

Log P10: Pont Noir

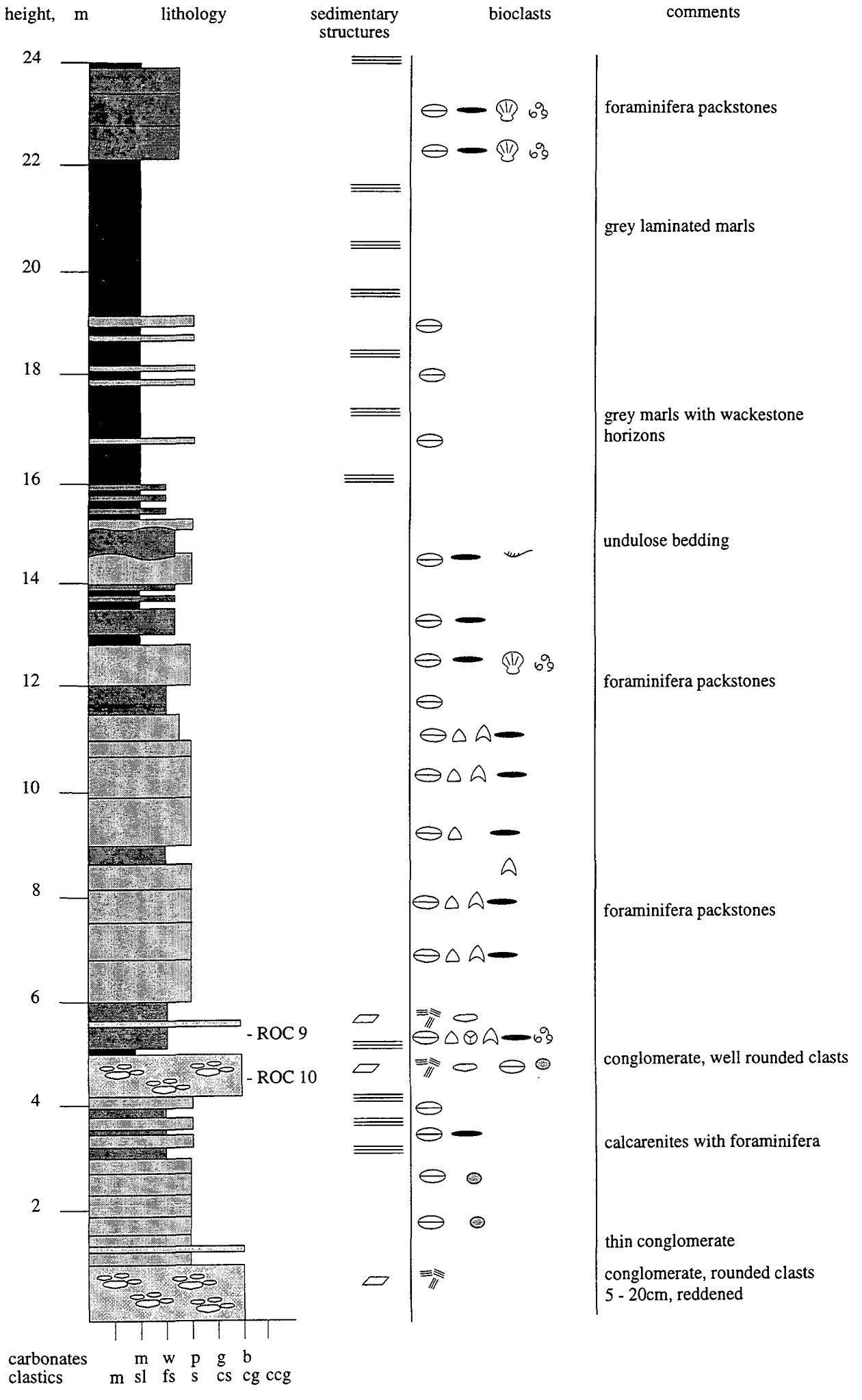

Log P11: La Rochette

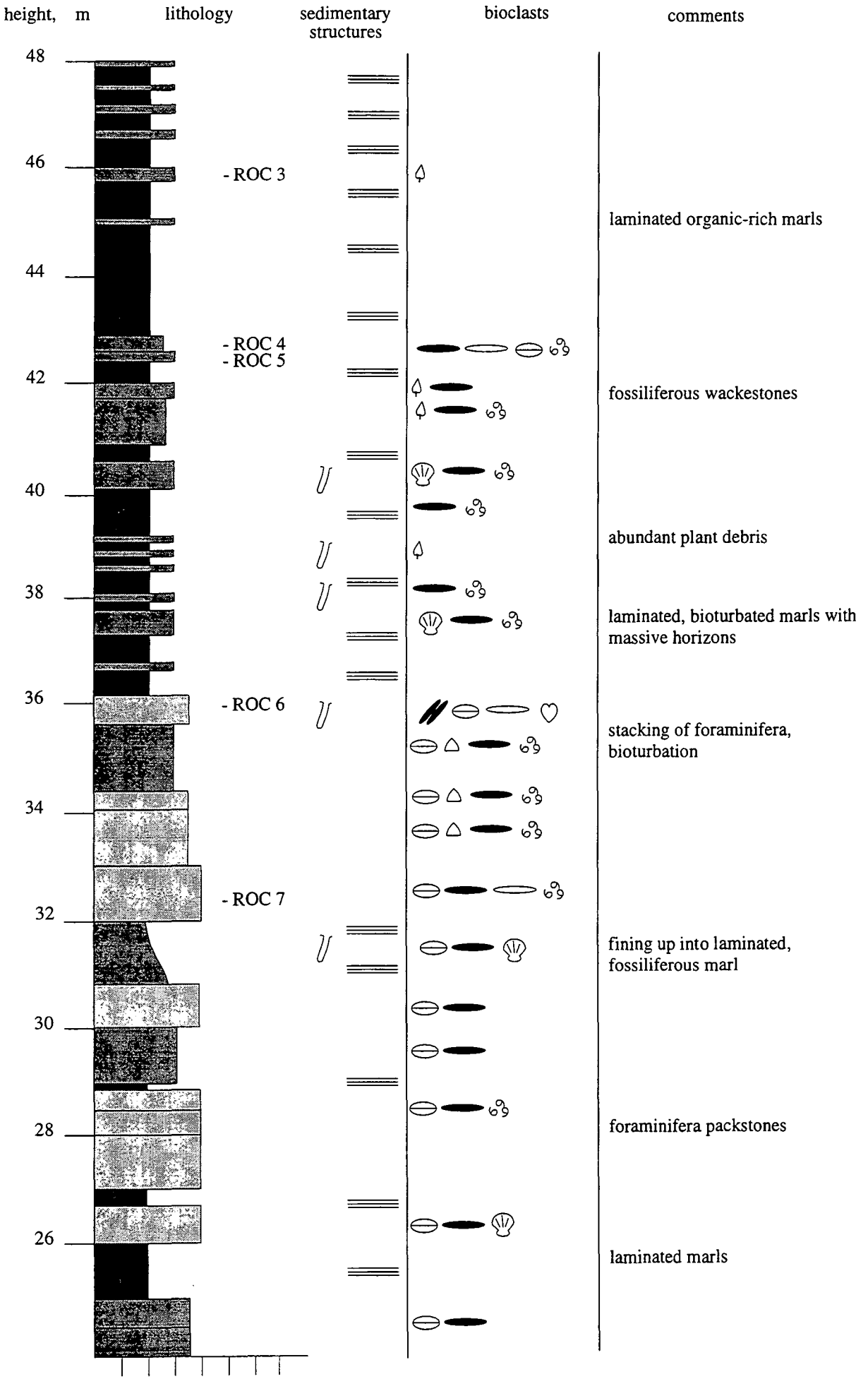

Log P11: La Rochette

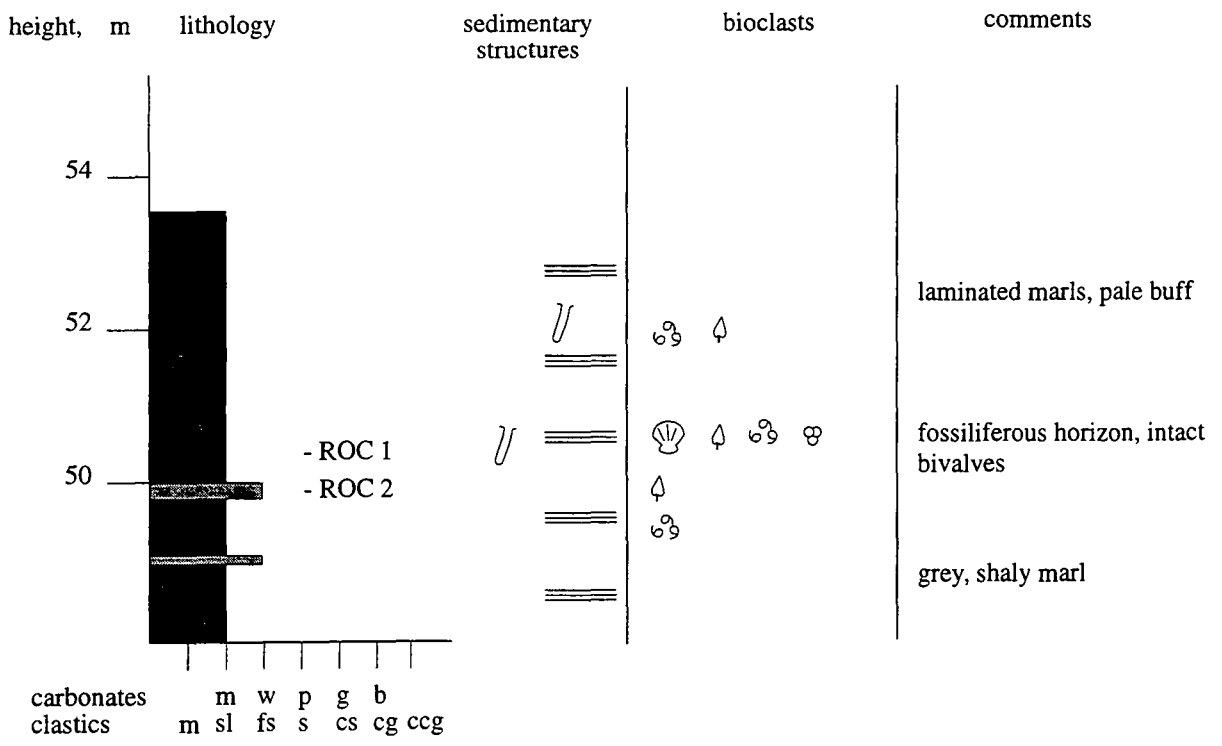

Log P11: La Rochette

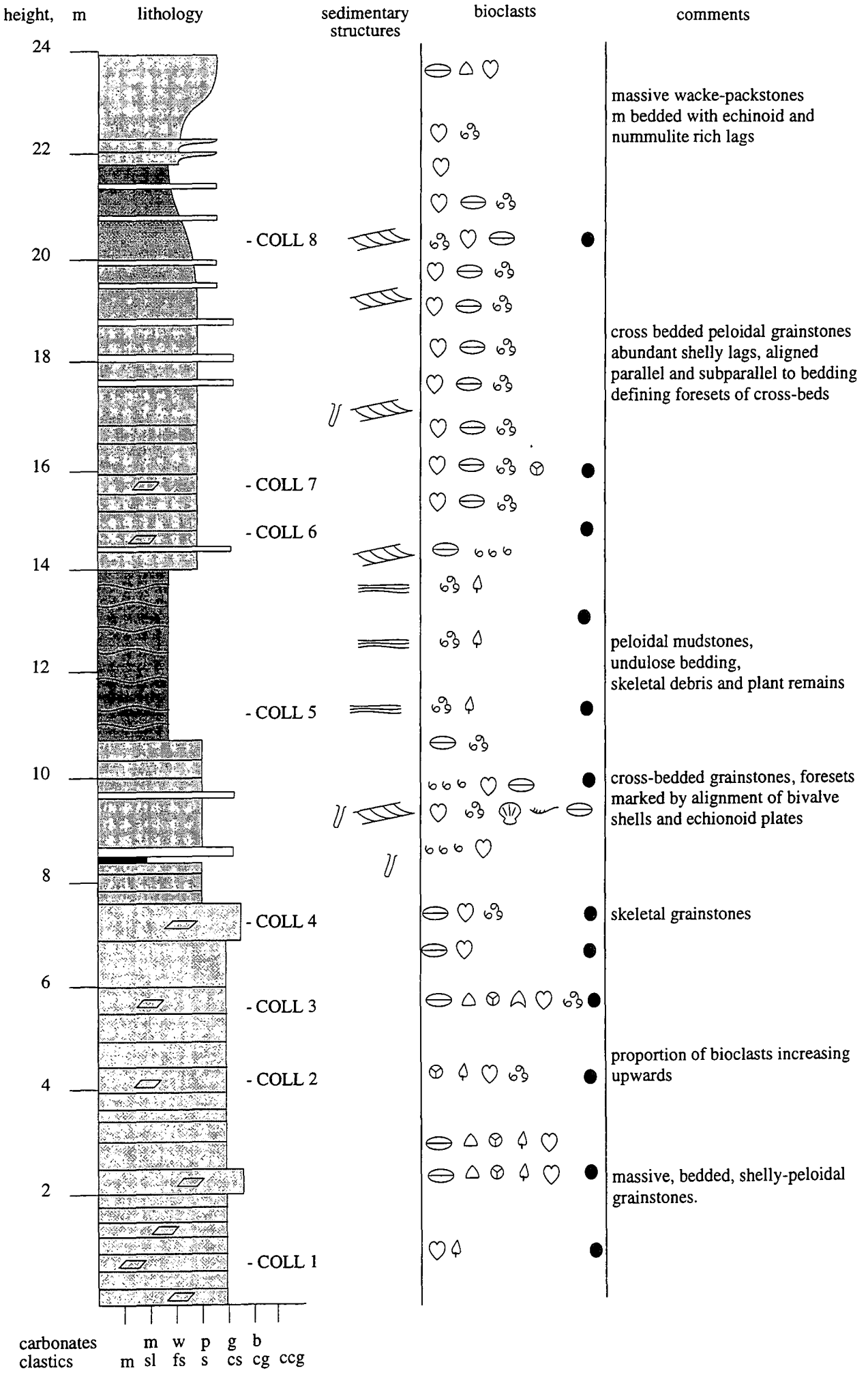

Log P12: Collongues

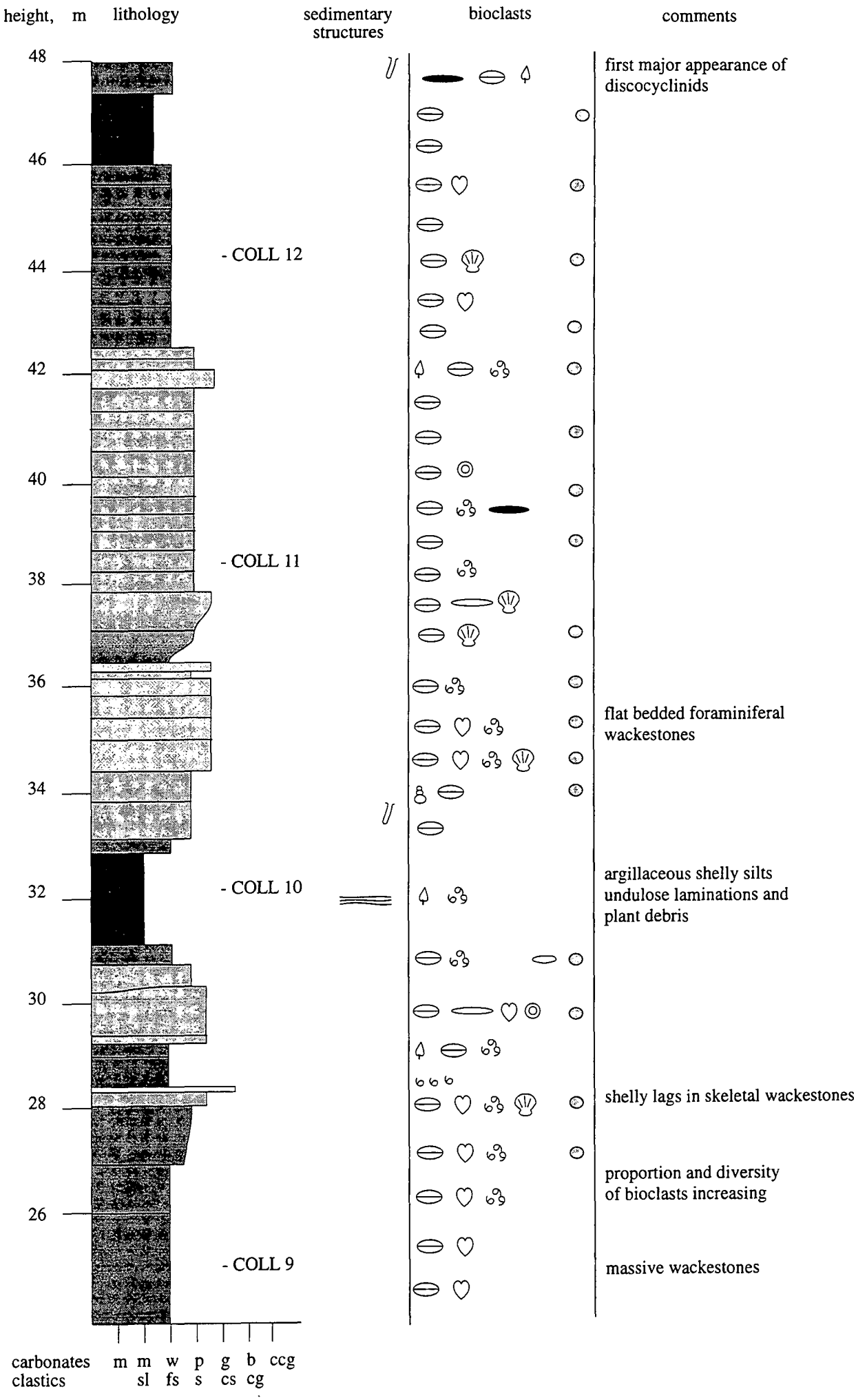

Log P12: Collongues

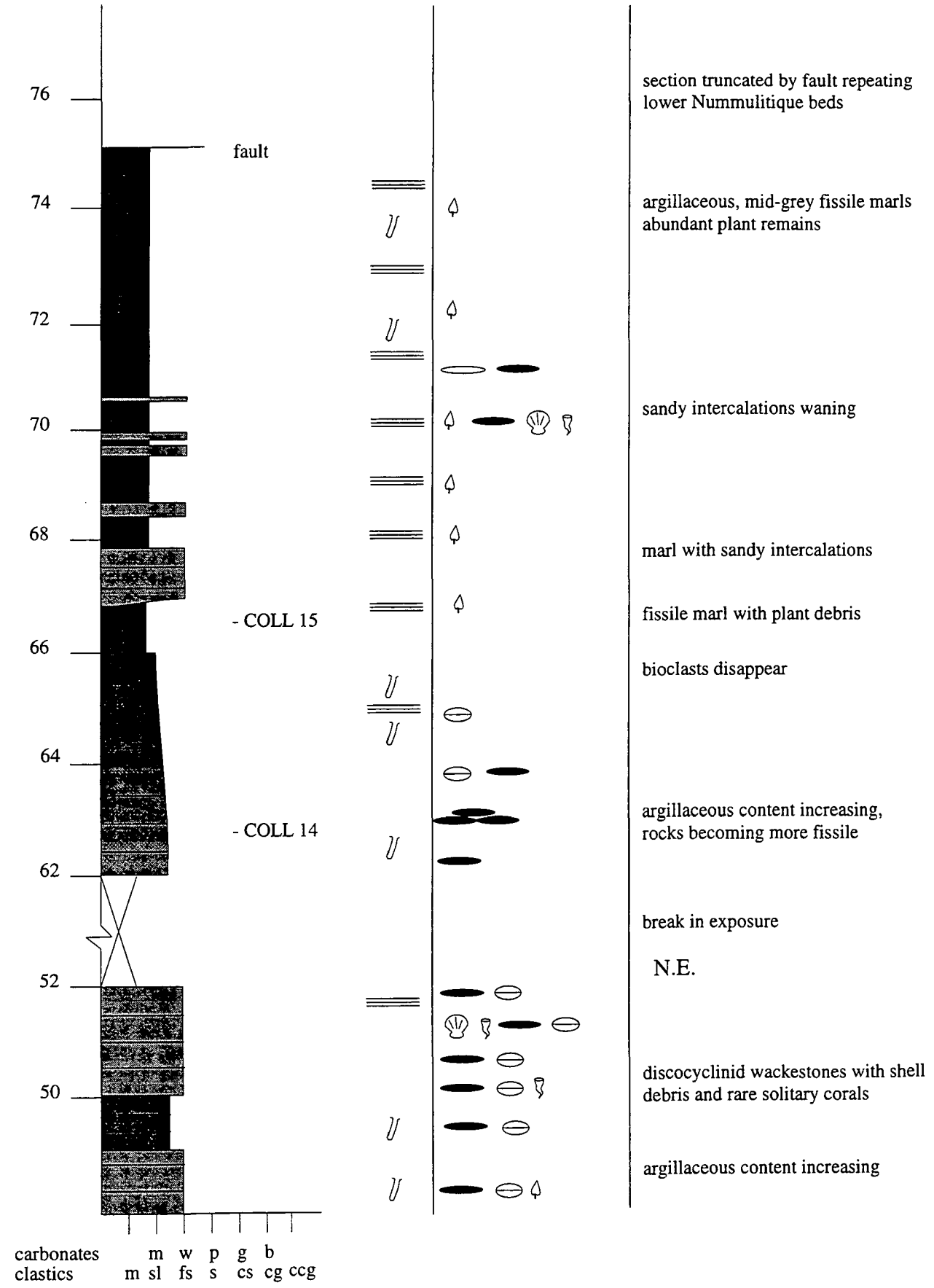

Log P12: Collongues

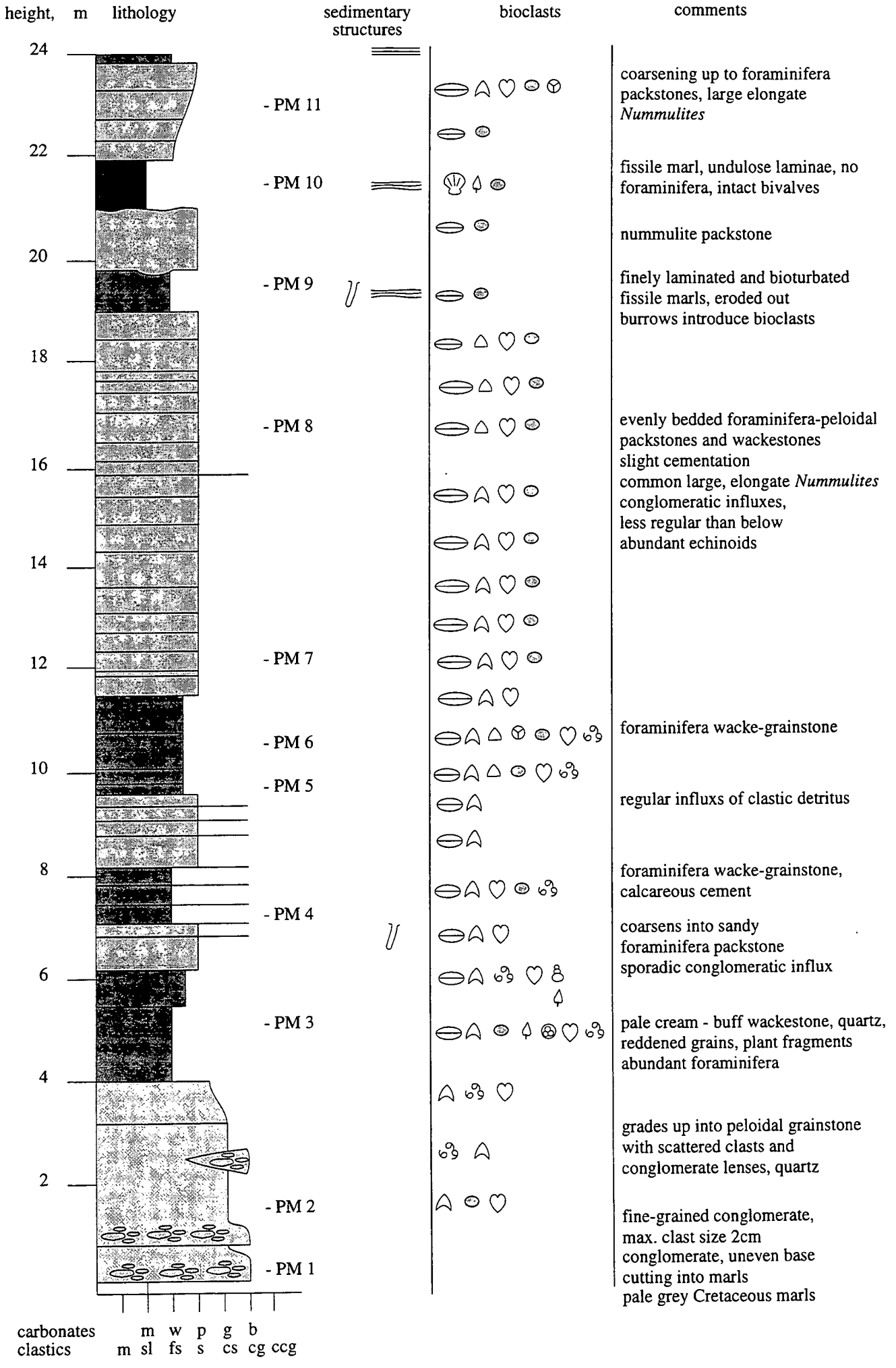

Log P13: Pont au Miolans

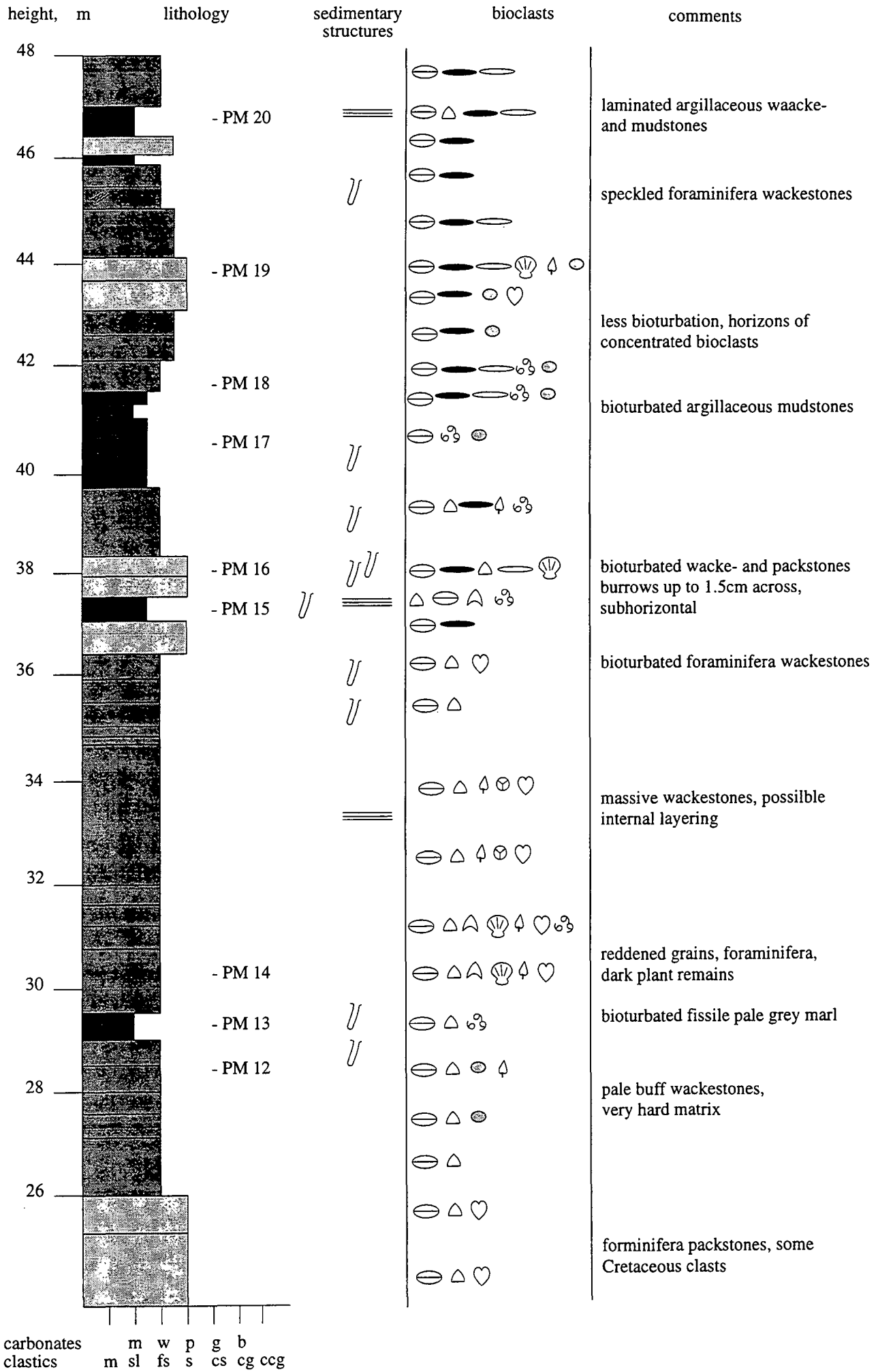

Log P13: Pont au Miolans

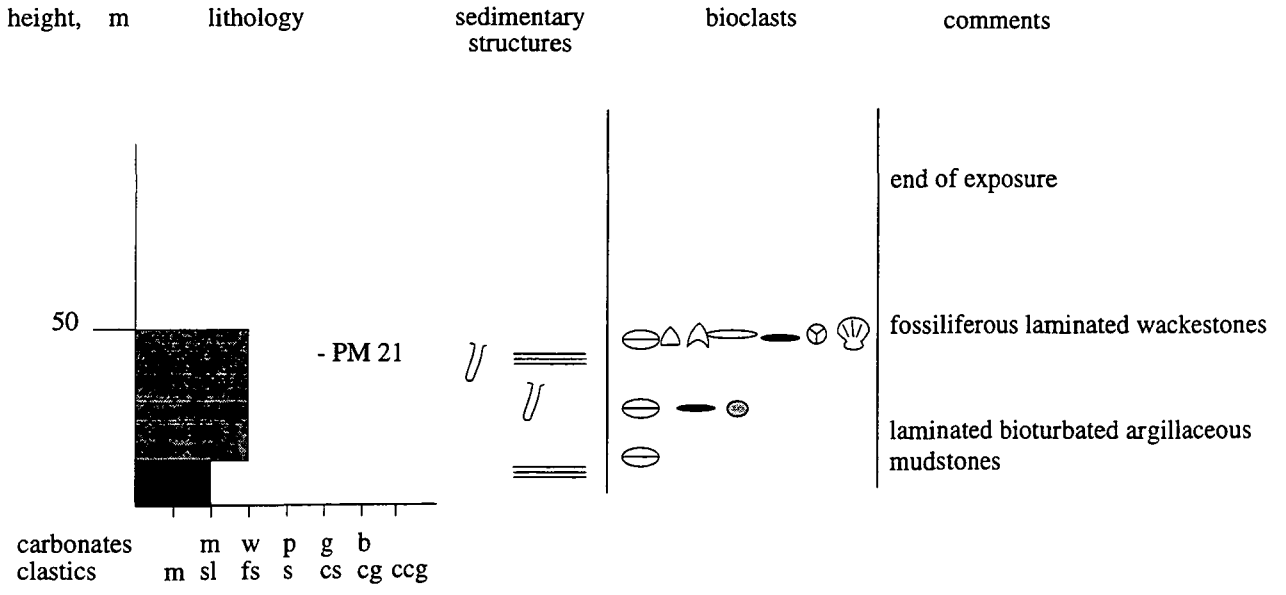

Log P13: Pont au Miolans

Appendix 2

Nummulitique Microfacies

sample	facies	micrite	quartz	glauconite	cte patches	cte grains	chert	pyrite	lithics	clays	organics
P4	conglomerate matrix	10	20	1	0	0	0	0	60		0
P5	nodular marl	60	0	2	10	2	2	0	10		0
P6	nodular marl	55	1	1	20	10	2	0	0		0
P7	nodular marl	60	2	2	10	10	2	2	0		2
P8	nodular marl	80	2	2	10	0	2	2	2		0
P9	nodular marl	70	1	2	10	5	2	1	0		0
P10	nodular marl	75	5	0	5	5	2	2	0		2
P11	nodular marl	45	5	1	20	25	2	1	0		0
PQ1	nodular marl	40	5	1	40	5	0	1	2		5
PQE1	nodular marl	80	2	0	5	0	0	2	5		0
PQE2	nodular marl	90	2	0	1	2	0	2	0		2
ARG1	nodular marl	35	1	1	15	2	5	1	35		1
ARG2	nodular marl	35	2	1	12	2	5	0	40		2
ARG3	clast										
ARG4	conglomerate	0	0	0	0	0	0	0	30		0
ARG5	nodular marl	60	2	1	20	2	0	2	5		5
ARG6	nodular marl	60	2	2	5	5	5	5	10		0
RC2	nodular marl	30	0	1	5	0	10	0	50		2
I2	Cerithium marl	55	2	1	0	0	2	5	0		5
EP1	Microcodium wackestone	45	5	0	5	0	0	1	5		0
EP2	coal	0	0	0	0	30	2	0	0		60
EP3	coal	0	0	0	0	40	0	0	0		55
EP6	Microcodium wackestone	30	5	0	0	0	2	5	35		0
EP7	Microcodium wackestone	55	5	0	2	0	5	2	10		0
EP8	Cerithium marl	70	2	0	0	0	2	2	0		0
ChP1	calcareous sandstone	0	45	0	0	0	1	0	1	2	5
ChP2	organic mudstone	50	5	0	0	0	0	5	0	0	20
ChP3	Cerithium marl	50	5	0	0	0	0	5	0	0	5
COL1	calcareous sandstone	35	30	1	0	5	1	5	0	0	10
COL2	Cerithium marl	10	10	0	0	0	0	5	10	0	10
COL3	Cerithium marl	45	20	0	0	0	0	5	0	0	2
COL4	calcareous sandstone	35	35	1	0	0	0	2	15	0	0
COL5	calcareous sandstone	40	35	1	0	0	0	2	0	0	5

sample	microcod	bivalves	gastropod	echinoid	coral	miliolid	textulariid	numm	rotaliid	charophy?	shell hash	peloids	calcisph
P4	5	0	0	0		0	0	1	0		0		0
P5	1	0	0	1		0	1	0	0		0		5
P6	5	0	0	1		0	1	0	0		0		2
P7	5	0	0	0		0	2	0	0		0		0
P8	2	0	0	0		0	2	0	0		0		0
P9	2	0	0	1		0	2	0	0		0		0
P10	2	0	0	0		0	2	0	0		0		0
P11	0	0	0	0		0	0	0	0		0		0
PQ1	0	0	0	0		0	0	0	0		0		0
PQE1	2	0	0	0		0	0	0	0		0		2
PQE2	0	0	0	0		0	0	0	0		0		2
ARG1	5	0	0	0		0	1	0	0		0		0
ARG2	5	0	0	1		0	1	0	0		0		0
ARG3													
ARG4	5	0	0	0		0	0	0	0		0		0
ARG5	5	0	0	0		0	0	0	0		0		0
ARG6	0	0	0	1		0	0	0	0		0		5
RC2	2	0	0	2		0	0	0	0		0		0
I2	0	2	20	0		0	0	0	0		2	10	1
EP1	20	0	0	5	0	0	5	0	2	0	0	0	0
EP2	0	5	0	0	0	0	0	0	0	5	0	0	0
EP3	0	0	0	0	0	0	0	0	0	5	0	0	0
EP6	25	1	0	1	0	0	2	2	0	0	0	0	0
EP7	20	0	0	2	0	0	5	1	0	0	0	0	0
EP8	0	0	10	5	0	1	0	0	0	0	15	0	0
ChP1	0	0	0	0	0	0	0	1	0	0	0	0	0
ChP2	0	10	0	2	0	5	0	2	0	0	0	0	0
ChP3	0	5	30	0	0	0	0	2	0	0	0	0	0
COL1	0	0	0	2	0	0	0	0	0	0	10	0	1
COL2	2	5	50	0	0	0	0	0	0	0	0	0	0
COL3	0	5	10	1	0	1	0	0	0	0	10	0	0
COL4	0	0	0	2	0	1	0	0	0	0	10	0	0
COL5	0	5	5	5	0	1	0	1	2	0	0	0	0

sample	plankton	spicules	cement 1	cement 2	cement 3	reddening	nodular	bioturb	fractures	pyrite form
P4		0	0 cte	n/a	n/a	microcod	no	no	no	n/a
P5		2	2 fg cte	chert	n/a	microcod	slight	no	thin	n/a
P6		0	2 fg cte	cg cte	chert	no	no	no	no	n/a
P7		5	0 fg cte	cg cte	chert	no	slight	no	extensive	framboidal in micrite
P8		1	1 fg cte	cg cte	chert	no	yes	no	cut sediment	framboidal in matrix
P9		2	2 cg cte	cg cte	chert	no	less	no	yes	framboidal
P10		0	0 fg cte	cg cte	chert	seams	yes	no	thin, extensive	round patches in matrix
P11		0	0 fg cte	cg cte	chert	no	yes	no	no	framboidal
PQ1		0	0 fg cte	n/a	n/a	no	yes	no	around nodules	dunno
PQE1		0	0 fg cte	n/a	n/a	no	less	no	little	framboidal clusters
PQE2		0	0 fg cte	cg cte	n/a	no	yes	no	thin	framboidal clusters
ARG1		0	0 fg cte	cg cte	chert	microcod	yes	no	around nodules	framboidal clusters
ARG2		0	0 fg cte	cg cte	chert	microcod, lithics	yes	no	irregular + chert	n/a
ARG3										
ARG4		0	0 vcg cte	n/a	n/a	poss	no	no	no	n/a
ARG5		0	0 fg cte	cg cte	n/a	matrix around nodules	yes	no	few, org. seams	cubic
ARG6		0	0 fg cte	rad cte	chert	matrix patches	slight	no	v broken up	framboidal
RC2		0	0 fg cte	chert	n/a	no	slight	no	anastomosing	n/a
I2		0	0 cte mosaic	n/a	n/a	no	no	poss	no	framboidal clusters
EP1		0	0 cte mos	chert	n/a	no	no	yes	no	framboidal
EP2		0	0 cte	chert	n/a	no	no	no	org rich	n/a
EP3		0	0 cte	n/a	n/a	no	no	no	veins	n/a
EP6		0	0 cte	chert	n/a	no	no	no	no	cubic, around clasts
EP7		0	0 fg cte	chert	n/a	no	slight	no	org seam	cubic, framboidal
EP8		0	0 chert	n/a	n/a	no	no	no	org seams	cubic
ChP1		0	0 cte mosaic	n/a	n/a	no	no	no	no	n/a
ChP2		0	0 cte mos	n/a	n/a	no	no	no	no	cubic, framboidal
ChP3		0	0 cte mos	n/a	n/a	no	no	no	no	framboidal in forams
COL1		1	0 n/a	n/a	n/a	no	no	yes	no	framboidal
COL2		0	0 cte mos	n/a	n/a	no	no	no	no	framboidal
COL3		0	0 cte mos	n/a	n/a	no	no	no	no	framb, in shells + matrix
COL4		0	0 n/a	n/a	n/a	no	no	no	no	framboidal
COL5		0	0 n/a	n/a	n/a	no	no	yes	no	framboidal

sample	facies	numm	amphi	operc	disco	textul	miliolids	algae	serpulid	corals	bryozoa	bivalves	echinoid	gastro	plankt	calci	sh hash	matrix	quartz	glauc	lithics	cement	
AR1	nummulite wackestone	20	0	0	0	0	0	0	0	0	0	0	5	0	0	0	7	75	7	0	0	0	
BOM1	quartzitic grainstone	0	0	0	0	2	2	0	0	0	0	0	5	0	0	0	0	0	25	0	25	40	
BOM2	mudstone	0	2	2	0	2	0	0	0	0	0	0	0	0	5	0	10	80	3	0	0	0	
BOM3	mudstone	0	0	0	0	2	0	0	0	0	0	0	0	0	2	0	2	93	1	0	0	0	
BOM4	mudstone	0	0	0	0	2	0	0	0	0	0	0	0	0	2	2	5	89	0	0	0	0	
BOM5	mudstone	0	0	0	0	0	0	0	0	0	0	0	0	0	2	2	0	88	2	2	0	0	
BOM6	mudstone	0	1	0	2	1	0	0	0	0	0	0	0	1	1	0	6	84	2	0	1	0	
CC1	quartzitic wackestone	10	2	0	0	1	2	5	0	0	0	5	10	0	0	0	10	10	30	1	0	10	
CC2	nummulite packstone	30	10	0	0	0	2	2	0	0	0	5	7	0	0	0	10	15	10	1	10	0	
CC54	quartzitic wackestone	0	2	0	0	0	0	0	0	0	0	0	0	0	0	0	20	50	20	15	0	0	
CC55	quartzitic wackestone	10	10	0	0	0	0	1	0	0	1	2	10	0	5	0	10	40	15	5	10	0	
CC56	quartzitic wackestone	15	1	0	0	0	0	1	0	0	10	10	5	0	0	0	10	60	25	3	10	0	
CC57	nummulite wackestone	10	10	0	0	0	1	5	0	0	2	0	2	2	0	0	10	60	10	2	2	5	
CC58	nummulite wackestone	15	10	0	0	0	10	15	0	2	1	0	5	0	0	0	7.5	42	7.5	1	0	0	
CC59	nummulite wackestone	15	15	0	5	0	5		0	1	0	0	5	0	5	0	2	55	15	1	0	0	
CC61	algal mudstone	0	0	0	0	1	0	10	2	1	5	0	2	0	10	0	0	70	1	0	0	0	
CC63	discocyclinid packstone	10	5	5	20	0	0	0	0	0	0	2	0	0	0	0	0	55	5	1	0	0	
CC65	algal boundstone	0	0	0	2	2	2	40	5	10	10	0	0	2	0	0	5	30	1	0	0	0	
CC66	algal boundstone	2	0	2	2	0	10	40	2	10	5	0	2	5	0	0	5	22	1	0	0	0	
CC67	coralgal pack-boundstone	2	0	0	0	0	5	15	0	50	0	0	1	0	0	0	10	28	0	0	0	0	
CC68	algal packstone	5	2	0	0	0	2	25	5	0	2	10	5	1	0	0	15	35	0	0	0	7	
CC69	coralgal pack-boundstone	2	2	0	1	1	10	20		50	10		2	1	0	0	0	10	0	0	0	0	
CC70	algal boundstone	2	2	0	0	2	5	65	0	5	2	0	2	0	0	0	2	15	0	0	0	0	
CC71	numm-algal packstone	7.5	7.5	0	0	2	5	20	0	10	5	5	5	0	0	0	10	45	1	0	0	0	
CC72	mudstone	0	0	0	0	0	0	5	0	0	10	5	3	0	0	0	10	65	1	0	0	0	
CC73	algal packstone	0	0	0	0	5	2	20	0	5	5	2	2	1	0	0	0	60	0	0	0	8	
CC74	algal boundstone	5	10	0	0	0	0	50	0	0	2	2	2	0	0	0	2	20	0	0	0	10	
CC75	algal packstone	5	5	1	2	5	2	10	0	0	1	1	5	0	0	0	5	61	1	0	0	0	
CC76	skeletalmudstone	0	0	0	2	5	0	5	0	5	5	0	3	0	0	0	5	75	0	0	0	0	
CC77	skeletal wackestone	0	0	0	0	2	0	7.5	0	1	2	5	2	0	0	0	7.5	80	0	0	0	0	
COL6	nummulite wackestone	5	5	0	0	0	5	0	2	0	0	0	0	5	0	0	10	68	10	0	5	0	
COL7	coralgal pack-boundstone	1	0	0	0	0	2	5	0	40	5	0	5	0	0	0	15	27	0	0	0	15	
COM2	skeletal wackestone	1	1	0	1		5	10	5	10	10	1	2	2	0		5	50	2	1	0		
COM3	skeletal wackestone	5	5	0	2		1	5	5	0	3	1	2	2	0		10	68	5	1	0		
COM4	foram packstone	20	5	5	10		10	1	0	0	1	0	1	1	0		5	50	2	1	0		
COM5	nummulite wackestone	7.5	7.5	0	1		0	5	1	0	2	0	3	2	1		15	70	2	1	0		
COM6	discocyclinid packstone	15	5	10	40		0	0	0	0	0	0	0	0	0		3	29	1	0	0		
COM7	skeletal wackestone	5	5	0	5	0	5	15	5	0	5	0	5	2	0		15	47	1	0	0		
COM8	skeletal wackest	0	0	0	0		10	15	5	1	5	0	5	2	0		5	42	1	0	0		
COM9	algal packstone	5	0	0	0		5	25	5	2	5	0	2	0	0		5	49	1	0	0		
COM10	disco-operc wackestone	10	5	10	5		0	2	0	0	2	0	2	0	0		15	64	2	0	0		
COM11	coralgal pack-boundstone	2	0	0	2		5	10	5	30	2	0	2	5	0		20	46	1	0	0		
COM12	algal grainstone	5	0	0	2		5	45	0	10	0	5	0	2	0		10	26	1	0	0		
COM13	nummulite packstone	15	5	10	5		5	0	0	0	0	1	0	0	0		15	59	1	1	0		
COM14	algal packstone	1	0	1	2		5	50	1	2	2	0	5	1	0		2	30	0	0	0		
COM15	nummulite wackestone	10	5	0	5		2	5	0	0	0	0	2	2	0		20	69	1	0	0		
COM16	skeletal wackestone	0	0	0	2		2	15	2	3	5	0	2	2	0		15	71	0	0	0		
COM17	nummulite wackestone	10	0	0	5		0	10	0	0	0	2	20	2	0		15	51	0	0	0		
COM18	nummulite wackestone	10	2	0	5		2	3	0	0	2	0	20	2	0		15	54	2	0	0		
EP4	quartzitic grainstone	0	0	0	0	0	0	0	0	0	0	0	0	0	0	0	0	0	50	0	0	50	
EP9	mudstone	0	0	0	0	0	0	0	0	0	0	0	0	0	5	0	2	93	0	0	0	0	
F1	quartzitic wackestone	1	0	0	0	0	0	0	0	0	0	0	5	0	0		40	24	15	0	5	1	
F2	mollusc packstone	0	0	0	0	5	5	0	0	0	0	20	0	15	0		15	22	15	0	0	2	

sample	facies	numm	amphi	operc	disco	textul	miliolids	algae	serpulid	corals	bryozoa	bivalves	echinoid	gastro	plankt	calci	sh hash	matrix	quartz	glauc	lithics	cement
F3	quartzitic grainstone	0	0	0	0	0	5	0	0	0	0	0	0	0	0		10	0	25	1	5	55
F4	skeletal mudstone	0	0	0	0	0	1	0	0	0	0	3	2	3	2		0	89	0	0	0	0
F5	coral wackestone	0	0	0	0	2	0	20	0	15	2	0	0	0	0		0	60	0	0	0	0
F6	skeletal wackestone	1	0	0	0	0	1	15	0	0	5	0	20	1	0		20	57	0	0	0	0
F7	skeletal grainstone	5	0	0	0	0	5	25	0	0	0	0	20	5	0		0	0	0	0	0	40
F8	skeletal wackestone	1	0	0	0	0	2	15	2	2	10	0	5	2	0		10	61	0	0	0	0
F9	algal boundstone	0	0	0	1	5	1	30	0	0	10	2	5	1	0		0	30	0	0	0	5
F10	skeletal wackestone	0	0	0	0	5	2	15	0	5	5	0	5	0	0		1	64	0	0	0	0
F11	foralgal packstone	5	0	5	15	0	0	25	0	0	5	0	5	2	0		5	36	0	0	0	0
F12	mudstone	0	0	0	0	0	0	0	0	0	0	0	2	5	5		0	83	5	0	0	0
FE1	quartzitic wackestone	0	0	0	0	0	0	0	0	0	0	0	10	0	0		70	0	20	0	0	0
FE2	quartzitic grainstone	0	0	0	0	0	0	0	0	0	0	5	1	1	0		5	0	30	0	0	68
FE3	quartzitic grainstone	0	0	0	0	0	1	0	0	0	0	2	5	0	0		5	0	35	0	10	65
FE4	skeletal mudstone	0	0	0	0	0	0	5	0	0	0	0	2	1	0		10	82	0	0	0	5
FE5	algal mudstone	0	0	0	0	0	0	10	2	0	5	0	0	0	0		2	87	0	0	0	0
PW6	quartzitic wackestone	0	2	0	0	0	2	2	0	0	0	0	10	0	0	2	25	10	15	2	15	15
PW7 burr	nummulite wackestone	0	25	0	0	0	0	0	0	0	0	0	5	0	0	0	0	28	7	5	30	0
PW9	nummulite packstone	15	15	0	1	2	2	5	0	0	0	5	5	0	0	0	10	20	7	0	15	0
LCG19	quartzitic grainstone	1			0		0	10	0	0	0	0	15	0	0		5	0	15	1	10	35
LCG20	planktonic mudstone	0			0		0	0	0	0	0	0	3	0	25		0	70	5	1	0	0
LCG21	nummulite packstone	10	25		0		0	5	0	0	1	0	10	0	0		0	20	10	1	20	0
LCG22	numm-algal packstone	10	5		2		2	10	0	0	0	0	5	0	0		10	55	10	1	5	5
LCG23	algal packstone	7	7		0		5	25	0	5	5	0	5	0	0		0	20	1	1	10	15
LCG24	discocyclinid packstone	5	5	2	20		1	0	0	0	0	0	0	0	0		0	70	2	1	1	0
LCG25	disco-operc wackestone	10	5	2	10		0	0	1	0	2	1	1	0	5		20	55	2	1	0	0
LCG27	skeletal mudstone	2			0		2	0	0	0	0	0	2	0	5		30	90	5	1	0	0
LCG28	foram packstone	15	5	2	10		1	1	0	0	1	0	5	0	2		5	50	5	1	0	0
LCG29	numm-algal packstone	10	5		5	0	2	15	0	5	1	0	1	0	2		30	35	1	0	0	0
LCG32	foralgal packstone	10	5	5	7		5	10	0	5	5	0	1	0	0		25	45	1	1	0	0
LCG33	nummulite packstone	15	5	5	5		0	0	0	0	2	0	1	0	10		10	58	1	0	0	0
LCG34	algal boundstone	3	3	0	2	2	5	50	1	15	0	1	5	5	0		5	15	2	0	0	0
LCG35	algal boundstone	0	10		5	1	0	40	1	1	5	0	5	0	1		15	35	1	0	0	0
LCG36	nummulite wackestone	10	10		2	5	5	0	0	0	0	5	2	0	5		20	60	1	0	0	0
LCG37	nummulite wackestone	25	5	5	0	0	5	1	5	0	1	2	10	0	0		20	35	1	1	0	0
LCG38	nummulite wackestone	20	5	5	1	5	10	1	1	0	0	1	5	0	10		20	45	5	0	0	0
LCG39	algal boundstone	5			5	2	2	30	1	10	1	0	1	0	0		15	45	1	0	0	0
LCG41	algal boundstone	2		1	1	2	1	50	2	2	2	0	5	2	0		1	20	1	0	0	0
LCG42	nummulite wackestone	30					5	5	2			2	5	0			20	60	1		0	
LCG43	algal packstone	15	0	5	0	5	0	30	1	0	2	0	25	0	5		0	10	1	0	0	15
LCG43	algal packstone	15	0	5	0	5	0	20	0	0	2	0	25	0	0	0	0	10	1	0	0	15
LCG44	numm-algal packstone	25			5	2	2	20	0	0	0	0	5	0	1		20	40	0	0	0	5
LCG45	algal packstone	0	0	0	0	0	5	40	5	15	10	0	1	0	0		5	25	0	0	0	0
LCG46	skeletal grainstone	5	0	0	0	0	1	20	1	5	0	10	5	0	5		10	10	1	0	0	30
LCG47	algal grainstone	5			0		1	40	1	0	1	10	2	0	5		0	20	0	0	0	15
LCG48	algal packstone	5			0		0	25	5	0	10	10	5	0	0		10	40	0	0	0	0
LCG49	skeletal wackestone	0			0		1	15	5	1	10	1	1	0	1		10	60	1	0	0	0
LCG50	algal packstone	10	5	0	0	1	1	35	5	0	5	5	10	1	10		0	15	1	0	0	0
LCG51	skeletal grainstone	10	0	0	10	0	0	10	5	0	5	0	7	0	5		10	28	5	1	0	20
LCG53	algal mudstone	0			0		1	10	0	0	5	0	1	0	5		10	45	15	5	0	0
LCS1	quartzitic wackestone	1	5	0	0	0	0	25	0	0	0	1	25	0	0	0	0	15	20	1	5	0
LCS2	planktonic mudstone	0	0	0	0	0	0	0	0	0	0	0	0	0	20	0	0	80	1	0	0	0
LCS3	nummulite wackestone	5	5	0	0	0	1	0	1	0	0	7	5	0	10	0	0	30	5	1	1	0
LCS5	nummulite wackestone	15	10	0	0	0	1	10	0	0	0	5	5	0	2	0		25	15	1	5	0
LCS6	numm-algal packstone	10	5	0	0	1	5	10	0	0	0	1	5	0	0	0	5	30	2	1	0	0

sample	facies	numm	amphi	operc	disco	textul	miliolids	algae	serpulid	corals	bryozoa	bivalves	echinoid	gastro	plankt	calci	sh hash	matrix	quartz	glauc	lithics	cement	
LCS8	coral wackestone	5	0	0	0	0	2	3	5	30	1	1	5	0	1	0	0	50	1	1	0	0	
LCS9	skeletal wackestone	1	0	0	0	1	4	5	1	0	1	0	5	0	5	0		60	0	0	0	10	
LCS10	discocyclinid packstone	20	0	0	30	0	0	0	0	0	0	0	1	0	0	0	7	30	7	1	0	0	
LCS11	algal boundstone	5	2	0	3	0	5	40	1	1	1	1	0	0	0	0	0	40	0	2	1	0	
LCS13	algal packstone	5	0	0	1	2	3	30	5	0	5	0	5	0	0	0	5	40	2	0	0	0	
LCS14	foram packstone																						
LCS15	numm-algal packstone	10	15	0	0	0	5	15	1	5	1	0	5	0	0	0	20	35	2	0	0	0	
LCS16	numm-algal packstone	5	5	0	10	0	0	20	2	0	0	5	3	0	0	0	0	45	5	0	0	0	
MM1	quartzitic grainstone	0	0	0	0	0	0	0	0	0	2	0	1	0	0		1	5	15	7.5	30	38	
MM2	algal packstone	0	0	0	0	5	5	20	2	0	10	0	5	5	0		10	48	1	0	0	5	
MM3	foralgal packstone	20	5	5	25	0	0	10	0	0	0	0	10	0	0		0	25	1	0	0	0	
MM4	foralgal packstone	7	5	0	10	2	0	20	2	0	0	0	15	0	0		0	39	1	0	0	0	
MM5	algal debris packstone	5	5	0	10	2	5	30	0	0	1	0	5	5	0		5	27	0	0	0	5	
MM6	numm-algal packstone	15	7.5	0	5	2	2	20	0	0	5	0	7.5	5	0		25	36	0	0	0	5	
MM7	algal debris packstone	5	5	0	0	2	2	30	2	0	2	0	7	2	0		0	38	0	0	0	5	
MM8	algal packstone	2	0	0	2	0	0	20	2	0	10	2	10	5	0		5	47	0	0	0	0	
MM9	skeletal wackestone	2	0	0	2	0	2	15	2	5	10	2	5	5	0		0	50	0	0	0	0	
MM10	skeletal wackestone	0	0	0	1	5	5	10	0	0	10	2	7	5	0		2	55	0	0	0	0	
MM11	skeletal wackestone	0	0	0	2	2	2	10	2	0	5	2	5	2	0		5	67	0	0	0	0	
MM12	skeletal mudstone	0	0	1	0	1	0	5	2	1	5	0	2	0	0		5	83	0	0	0	0	
MM13	algal grainstone	5	2	0	2	2	2	25	0	0	5	0	5	0	0		0	5	0	0	0	37	
PAC1	quartz arenite	0	0	0	0	0	0	0	0	0	0	0	0	0	0	0	0	0	100	0	0	0	
PAC2	mudstone	0	1	0	0	0	0	0	0	0	0	0	0	0	0	0	2	92	2	0	0	2	
PAC3	foram mudstone	2	1	1	0	0	0	0	0	0	0	0	0	0	0	0	0	96	5	0	0	5	
PAC4	nummulite wackestone	10	10	0	0	0	0	0	0	0	0	2	2	0	0	2	0	76	2	0	0	0	
PAC5	foram mudstone	2	0	0	0	1	0	0	0	0	0	1	1	0	0	0	5	95	2	0	0	0	
PAC6	nummulite wackestone	25	5	0	2	0	0	0	1	5	0	0	5	0	0	0	10	53	2	0	0	0	
PAC7	disco-operc wackestone	5	5	5	0	5	0	0	1	1	0	0	2	0	0	0	5	81	2	0	0	0	
PAC8	quartzitic grainstone	0	1	0	0	0	0	0	0	0	0	0	1	0	0	0	0	0	60	0	5	43	
TS2	skeletal wackestone	5	0	0	0	1	1	5	0	10	2	2	5	1	0	0	15	68	0	0	0	0	
TS4	skeletalmudstone	0	0	0	0	1	2	2	0	0	2	1	2	1	0	0	0	89	0	0	0	0	
TS5	skeletal mudstone	0	0	0	0	0	2	5	0	5	2	0	5	0	0	0	10	81	0	0	0	0	
TS6	discocyclinid packstone	5	0	0	20	0	0	50	0	0	2	2	5	2	0	0	5	14	0	0	0	0	
TS7	foram packstone	10	5	0	25	0	0	0	0	0	5	0	5	0	0	0	20	40	0	0	0	0	
VAC2	algal packstone	2	5	0	2	4	5	10	1	0	2	0	0	5	0	0	0	35	0	0	0	5	
VAC3	algal packstone	0	1	0	0	2	2	30	1	0	10	0	5	2	0	0	3	44	0	0	0	0	
VAC4	algal packstone	3	3	0	5	0	2	10	0	0	0	0	2	0	0	0	60	8	3	1	0	5	
VAC5	skeletal wackestone	0	0	0	5	2	0	0	0	0	2	0	2	0	0	0	20	60	7	2	0	0	
VAC6	mudstone	0	0	0	0	0	0	0	0	0	0	0	0	5	2	0	10	75	5	3	0	0	
VAC7	quartzitic wackestone	0	0	0	0	0	5	0	0	0	0	0	0	0	0	0	30	35	20	5	0	0	

sample	facies	numm	amphi	opere	disco	text	miliolids	alveo	orbit	CRA	serpul	corals	bryozoa	bivalves	echin	gastro	plankt	calci	sh hash	peloids	matrix	quartz	glauc	organics	lithics	cement	micro	
A1	peloidal grainstone	0	0	0	0	0	7.5	0	1	0	0	0	0	0	5	2	5	0	5	5	15	20	5	0	2	5	20	2
A2	peloidal grainstone	5	2	0	0	0	0	0	0	0	0	5	0	0	3	5	0	0	0	0	40	0	5	1	0	0	30	0
A3	peloidal grainstone	2	2	0	0	0	5	0	1	0	2	0	0	0	2	0	0	0	0	40	10	5	2	0	0	25	0	
A4a	peloidal grainstone	5	0	0	0	0	2	0	0	0	5	0	0	0	0	0	0	0	2	35	20	7.5	1	5	0	20	0	
A4b	nummulite packstone	35	5	0	0	0	5	0	0	0	10	2	0	7.5	0	0	0	0	5	7.5	5	2	1	2	2	10	0	
RC3	peloidal foram grainstone	20	0	0	0	0	5	0	0	0	20	0	0	5	5	0	0	0	0	20	2	1	0	0	10	15	0	
RC4	peloidal grainstone	2	0	0	0	0	2	0	2	0	0	0	0	0	0	0	0	0	0	40	0	0	0	0	0	54	0	
AL1	peloidal grainstone	2	0	0	0	0	0	0	0	0	2	0	0	0	5	0	0	5	5	35	20	5	0	2	5	15	0	
CAST1	nummulite packstone	30	5	0	0	1	1	0	0	0	0	0	0	3	5	0	0	0	10	10	20	1	1	1	10	0	2	
CAST2	skeletal mudstone	7	5	1	0	0	0	0	0	0	0	0	0	0	1	0	0	0	10	0	74	5	0	0	0	0	0	
CAST3	numm-miliolid pack-grainstone	15	2	2	0	0	10	0	0	0	5	0	0	2	5	0	0	0	15	5	15	1	0	1	0	20	0	
CAST4	skeletal mudstone	1	0	0	0	0	0	0	0	0	0	0	0	0	0	0	0	0	5	0	85	5	1	1	0	0	0	
CAST5	numm-miliolid pack-grainstone	15	5	2	0	2	15	0	0	0	0	2	0	2	2	0	0	0	5	5	14	1	0	0	0	30	0	
CAST6	foram wacke-packstone	10	1	5	2	0	2	0	0	0	0	0	0	2	1	1	0	0	2	0	70	1	1	0	0	5	0	
CAST7	nummulite packstone	20	5	5	0	2	5	0	0	0	2	0	0	5	0	0	0	0	10	5	30	1	1	0	0	10	0	
CAST8	disco/opere wackestone	15	0	10	10	0	1	0	0	0	0	0	0	0	0	0	0	0	10	0	50	1	0	0	0	0	0	
FA1	nummulite packstone	35	2	0	0	0	1	0	5	0	2	0	0	0	10	0	0	0	10	5	7	2	0	0	0	15	0	
FA2	nummulite packestone	40	0	0	0	0	0	0	5	0	0	0	0	2	5	0	0	0	2	10	23	1	0	0	0	5	0	
COLFA1	foram wacke-grainstone	20	5	0	0	0	5	0	7.5	0	0	0	0	0	7.5	0	0	0	10	15	0	0	0	3	0	27	0	
COLFA2	nummulite packestone	30	5	0	0	1	2	0	2	0	1	0	0	0	5	0	0	0	0	0	30	4	0	0	10	10	0	
COLFA3	foram wacke-packstone	15	5	0	0	1	0	0	2	0	0	0	0	0	5	0	0	2	15	0	43	2	1	0	10	0	0	
COLFA4	foram wacke-packstone	10	1	0	0	1	7	2	0	0	1	0	0	5	2	0	0	0	10	0	50	1	0	0	5	2	0	
COLFA5	foram wacke-grainstone	15	10	0	0	0	2	0	2	0	1	0	0	0	5	0	0	4	5	15	30	2	0	5	2	10	0	
COLFA6	numm-miliolid pack-grainstone	10	3	2	0	7	10	0	2	0	2	0	0	0	0	0	0	0	10	10	20	1	1	0	0	20	0	
COLFA7	numm-miliolid pack-grainstone	20	5	0	0	0	7	2	2	0	0	2	0	5	0	0	0	0	5	5	35	1	0	0	5	15	0	
COLFA8	foram wacke-grainstone	5	2	0	0	1	1	0	0	0	1	0	0	0	0	0	0	0	10	10	50	3	1	2	0	15	0	
COLFA9	foram wacke-grainstone	10	1	5	1	1	2	0	0	0	2	0	0	5	2	0	0	0	10	12	25	3	0	2	0	20	0	
COLFA10	foram wacke-grainstone	5	3	5	0	0	0	0	0	0	1	0	0	5	0	0	0	2	10	12	30	4	0	0	2	20	0	
COLFA11	foram wacke-packstone	15	5	5	5	0	2	0	0	0	2	0	0	0	2	0	0	5	5	5	43	5	0	1	0	0	0	
COLL1	peloidal grainstone	0	0	0	0	2	2	0	0	0	0	0	0	0	0	1	0	0	2	20	0	2	1	0	0	70	0	
COLL2	peloidal grainstone	0	0	0	0	2	3	0	0	0	0	0	0	0	0	0	0	0	5	30	0	1	1	0	0	53	0	
COLL3	peloidal grainstone	0	2	0	0	0	7	0	3	0	0	0	0	0	2	0	0	0	5	10	0	0	1	0	0	70	0	
COLL4	peloidal grainstone	2	1	0	0	0	1	0	0	2	0	0	0	0	2	0	0	0	25	50	5	1	0	0	2	10	0	
COLL5	peloidal mudstone	0	0	0	0	0	0	0	0	0	0	0	0	0	0	0	0	0	35	7	30	15	2	0	0	11	0	
COLL6	peloidal grainstone	0	0	0	0	0	0	0	0	0	0	0	0	0	0	0	0	0	20	40	0	0	0	0	0	40	0	
COLL7	peloidal grainstone	10	0	0	0	0	5	0	2	0	2	0	2	2	20	0	0	0	0	35	0	0	0	0	0	22	0	
COLL8	peloidal mudstone	0	0	0	0	0	0	0	0	0	0	0	0	0	2	0	0	0	10	10	60	10	0	0	0	0	0	
COLL9	foram wacke-packstone	5	1	0	0	0	0	0	2	0	0	0	0	0	0	0	0	0	20	0	50	20	2	0	0	0	0	
COLL10	peloidal mudstone	2	1	0	0	1	0	0	0	0	0	0	0	0	0	0	0	0	15	10	71	7	3	0	0	0	0	
COLL11	peloidal mudstone	5	0	0	0	0	0	0	2	0	0	0	0	0	0	0	0	0	15	7	74	7	0	0	0	0	0	
COLL12	skeletal mudstone	10	2	1	0	0	1	0	0	0	0	0	0	0	0	0	0	0	20	0	52	10	0	0	0	0	0	
COLL13	foram wacke-packstone	10	2	2	2	0	0	0	0	0	1	0	0	1	2	0	0	0	5	0	60	5	0	0	0	0	0	
COLL14	disco/opere wackestone	5	0	10	5	0	0	0	0	0	0	2	0	0	0	0	0	0	10	0	66	2	0	0	0	0	0	
COLL15	peloidal mudstone	0	0	0	0	0	0	0	0	0	0	0	0	0	0	0	0	0	0	0	90	10	0	0	0	0	0	
I4	coral wackestone	0	0	0	0	1	7.5	0	0	0	0	30	0	5	0	2	0	0	10	7.5	25	2	1	2	0	0	0	
IV1	coral wackestone	0	0	0	0	0	5	0	0	0	0	30	0	5	0	5	0	0	10	0	40	5	0	0	0	0	0	
IV2	peloidal grainstone	2	0	0	0	2	2	0	0	1	0	0	0	0	1	0	0	0	10	35	0	1	0	0	0	45	0	
IV3	skeletal mudstone	0	0	0	0	2	5	0	0	0	0	2	0	2	0	0	0	0	25	0	62	2	0	0	0	0	0	
IV4	coral wackestone	2	0	0	0	2	10	3	0	0	0	20	0	0	0	0	0	0	2	0	30	1	0	0	0	30	0	
IV5	skeletal mudstone	2	0	0	0	2	5	0	0	0	0	5	0	2	2	0	0	0	10	7	40	2	1	0	0	20	0	
IV6	peloidal grainstone	2	0	0	0	2	5	0	0	1	0	2	0	1	5	5	0	0	10	25	25	3	0	0	1	15	0	
IV7	foram grainstone	10	5	0	0	0	0	0	0	0	10	0	0	0	2	0	0	0	10	30	0	2	1	0	0	30	0	
IV8	peloidal grainstone	2	0	0	0	0	1	0	0	0	0	0	0	0	2	0	2	0	10	30	0	3	0	0	0	50	0	
IV9	peloidal foram wackestone	20	2	0	0	0	0	0	0	0	1	0	0	0	0	0	0	0	5	15	40	7	1	5	0	0	0	
IV10	peloidal foram wackestone	5	2	0	0	0	0	0	0	0	2	0	0	0	5	0	0	0	7	15	55	7	1	1	0	0	0	
IV11	peloidal grainstone	2	0	1	0	0	2	0	0	0	0	0	0	0	5	0	0	0	5	35	20	3	0	0	0	25	0	
IV12	peloidal foram wackestone	20	0	0	0	2	2	0	0	0	0	0	0	5	5	0	2	5	0	15	40	5	0	2	0	0	0	
IV13	peloidal wackestone	1	0	0	0	0	0	0	0	0	0	0	0	0	2	0	0	5	10	40	40	2	1	0	0	0	0	
IV14(burr)	peloidal wackestone	0	0	0	0	0	0	0	0	0	0	0	0	0	0	0	0	5	10	25	58	2	0	0	0	0	0	
IV15	nummulite packstone	30	5	0	0	0	0	0	0	0	0	0	0	5	5	0	0	2	0	20	25	2	1	5	0	0	0	
IV16	nummulite packstone	30	5	0	0	0	0	0	0	0	0	0	0	5	5	0	0	2	0	20	25	2	1	5	0	0	0	
P12	foram wacke-packstone	5	2	1	0	0	0	0	0	0	0	0	5	0	5	0	0	2	5		40	5	0	0	10	30		
P13	foram wacke-packstone	5	5	0	0	0	0	0	0	0	0	0	0	0	5	0	0	0	5		55	2	0	0	5	25		
PM2	peloidal grainstone	2	0	0	0	1	1	0	15	0	0	0	1	0	5	0	0	0	7	15	0	3	0	0	5	45	0	

sample	facies	numm	amphi	opere	disco	text	miliolids	alveo	orbit	CRA	serpul	corals	bryozoa	bivalves	echin	gastro	plankt	calci	sh hash	peloids	matrix	quartz	glauc	organics	lithics	cement	micro	
PM3	peloidal grainstone	2	1	0	0	0	0	0	7	0	0	0	0	0	0	0	0	0	15	20	30	2	1	0	2	20	0
PM4	peloidal grainstone	10	0	0	0	1	0	0	5	0	0	0	0	0	0	0	0	0	10	30	0	1	1	0	5	37	0
PM5	peloidal foram grainstone	15	5	0	0	2	3	0	15	0	0	0	0	0	5	0	0	0	5	25	0	0	0	0	10	20	0
PM6	nummulite packstone	30	5	0	0	0	0	0	10	0	0	0	0	1	5	0	0	0	5	25	5	1	1	0	0	15	0
PM7	peloidal foram grainstone	10	2	0	0	0	0	0	7	0	0	0	0	0	5	0	0	0	5	20	15	5	2	0	0	22	0
PM8	nummulite packstone	50	5	0	0	0	0	0	5	0	0	0	0	0	10	0	0	0	0	20	10	1	1	0	0	10	0
PM9 (sed)	peloidal mudstone	0	0	0	0	0	0	0	0	0	0	0	0	0	0	0	2	0	5	10	60	15	1	0	0	0	0
PM10	peloidal mudstone	0	0	0	0	0	0	0	0	0	0	0	0	0	0	0	0	0	7	10	73	10	0	0	0	0	0
PM11	peloidal foram wackestone	10	2	0	0	0	5	0	5	0	0	0	0	0	2	0	0	0	0	25	50	20	1	0	0	0	0
PM12	foram wacke-grainstone	10	5	0	0	0	3	0	2	0	0	0	0	1	2	0	0	1	0	40	15	2	1	0	1	15	0
PM13	skeletal mudstone	5	5	0	0	0	2	0	0	0	0	0	0	0	0	0	0	0	30	0	37	15	1	0	5	0	0
PM14	skeletal mudstone	0	3	1	0	0	0	0	5	0	0	0	0	0	2	0	1	0	0	0	40	10	0	0	5	30	0
PM15	foram wacke-packstone	5	10	0	0	0	1	0	5	0	0	0	0	0	2	0	0	0	10	0	27	15	0	0	5	20	0
PM16	foram wacke-packstone	5	5	5	0	0	0	0	2	0	0	0	0	0	2	0	0	0	20	0	30	15	0	0	5	10	0
PM17	peloidal mudstone	2	0	1	0	0	2	0	2	0	0	0	0	0	0	0	0	0	5	25	30	5	0	0	0	30	0
PM18	peloidal grainstone	2	2	1	1	0	4	0	5	0	0	0	0	0	0	0	0	0	30	30	0	5	1	0	0	24	0
PM19	peloidal foram wackestone	20	5	5	2	0	0	0	0	0	0	0	0	2	5	0	0	0	0	10	35	8	0	0	7	0	0
PM20	disco/opere wackestone	10	3	10	5	0	2	0	0	0	0	0	0	0	1	0	0	0	10	10	35	15	0	0	0	0	0
PM21	foram wacke-packstone	10	5	5	5	0	3	0	0	0	0	0	0	0	0	0	0	0	0	5	60	7	0	0	0	0	0
PN6	peloidal foram grainstone	5	0	0	0	1	5	0	5	5	0	3	5	0	0	0	0	0	0	30	0	0	1	0	2	40	0
PN7	foralgal pack-grainstone	2	0	0	0	5	5	0	2	10	0	0	5	5	2	0	0	0	0	15	0	0	0	0	5	45	0
PN8	foralgal pack-grainstone	10	0	0	0	0	2	0	10	20	0	0	0	0	5	0	0	0	0	5	30	0	0	0	0	15	0
PN9	foralgal wacke-packstone	5	2	5	5	0	0	0	0	10	0	5	0	0	5	0	0	0	10	0	50	1	0	0	0	0	0
PN10	foralgal wacke-packstone	5	2	0	10	2	0	0	0	20	0	0	0	0	5	0	0	0	15	0	40	0	0	0	0	0	0
ROC1	disco/opere wackestone	5	2	0	10	0	0	0	0	0	0	0	0	2	5	0	2	0	5	0	50	5	1	0	0	0	0
ROC2	organic siltstone	0	0	0	0	0	0	0	0	0	0	0	0	0	0	0	0	0	0	0	35	20	0	15	0	30	0
ROC3	organic siltstone	0	0	0	0	0	0	0	0	0	0	0	0	0	0	0	0	0	0	0	35	20	1	10	0	35	0
ROC4	disco/opere wackestone	3	0	0	10	0	1	0	0	0	0	0	0	2	2	0	0	2	10	0	50	7.5	2	0	0	10	0
ROC5	disco/opere wackestone	5	2	10	10	0	2	0	0	0	0	0	0	0	2	0	2	0	10	5	40	2	0	0	0	10	0
ROC6	disco/opere wackestone	10	0	2	10	0	0	0	0	0	0	0	0	2	5	0	0	0	15	0	50	2	1	0	0	0	0
ROC7	disco/opere wackestone	10	0	10	10	0	1	0	0	0	1	2	0	0	5	0	0	0	15	0	50	2	1	0	0	0	0
ROC9	nummulite-miliolid pack-grainston	20	5	0	5	0	10	0	5	0	0	0	0	0	5	0	0	0	20	5	20	2	1	0	5	10	0
ROC10	peloidal grainstone	10	0	0	0	0	0	0	5	0	0	0	0	0	0	0	0	0	5	20	0	5	0	0	50	15	0
SBF1	foram wacke-packstone	20	5	0	0	2	2	0	15	0	0	0	0	1	5	0	0	0	7.5	7.5	30	1	0	0	5	5	1
SBF2	peloidal foram wackestone	10	10	2	0	0	5	0	2	0	0	0	0	0	5	0	0	0	0	10	10	45	1	0	0	0	0
SBF3	peloidal foram wackestone	15	5	5	2	1	0	0	2	0	2	0	0	0	5	0	0	0	10	10	40	5	0	0	0	0	0
SBF4	disco/opere wackestone	10	0	5	15	1	0	0	0	0	2	0	0	0	0	0	0	0	20	0	50	0	0	0	0	0	0
SBF6	immature sandstone	0	0	0	0	0	0	0	0	0	0	0	0	0	0	0	0	0	0	0			0	0			0
SCAF1	foralgal pack-grainstone	20	2	0	2	2	2	0	10	10	0	0	0	0	7.5	0	0	0	0	15	5	2	1	0	10	15	0
SCAF2	foram pack-grainstone	7.5	0	0	0	3	7	0	10	2	0	0	0	0	2	0	0	0	10	10	25	2	0	0	0	25	0
SCAF3	foram wacke-grainstone	20	5	0	0	0	5	0	5	0	0	0	0	0	5	0	0	0	20	10	3	2	0	0	5	20	0
SCAF4	disco/opere wackestone	15	2	0	15	0	0	0	0	0	2	0	0	0	0	0	0	0	10	0	50	5	0	0	0	0	0